University of Bath

UNIVERSITY OF BATH

PHD

Robust analytical methods for the detection of illicit drugs and their cutting agents

Naqi, Husain

Award date:
2019

Awarding institution:
University of Bath

[Link to publication](#)

Alternative formats

If you require this document in an alternative format, please contact:
openaccess@bath.ac.uk

University of Bath

Robust analytical methods for the detection of

illicit drugs and their cutting agents

Husain A. Naqi

A thesis submitted for the degree of Doctor of Philosophy

University of Bath

Department of Pharmacy and Pharmacology

March 2019

Acknowledgements

I dedicate this study to my late mother,

who inspired me to pursue a life in science

and to my wife for her love and faith

Abstract

Novel Psychoactive Substances (NPS) are currently a major cause of concern, in particular to drug analysts, health officials and in law enforcement. The dynamic nature of the clandestine synthesis of NPS results in many new analogues, some of them with different chemistry, in addition to the mixing of some NPS analogues in combination with other cutting agents (adulterants). This requires up-to-date robust analytical methods. All of the major classes of NPS were studied in this research project: Synthetic Cannabinoid agonists, cathinones, phenethylamines, arylcyclohexylamines and phenidates. Together this makes a total number of 341 different samples, plus their replicates. The first aim is to develop and implement spectroscopic, spectrometric and chromatographic methods for the qualitative and quantitative analysis of NPS, with a focus on the application of NMR spectroscopy in forensic chemistry. The second aim is to develop a validated quantitative NMR (q-NMR) analysis method to be employed for the quantification of MDMA/NPS mixtures and Synthetic Cannabinoids where a cross-method confirmation of ^{19}F q-NMR analysis was developed together with an analytical platform for the separation and characterization of complex mixtures of Synthetic Cannabinoids.

An extensive critical review of the literature relates to areas of illicit drug analysis and forensic chemistry with respect to major current events. Applying ^{1}H q-NMR analysis, an analytical evidence-based connection is revealed for the association of MDMA and other NPS from different night-club venues. The current status of the purity and dose of MDMA in typical tablets is established using the first reported q-NMR method with cross-method confirmation (UHPLC). Complex mixtures of arylcyclohexylamines are discussed with respect to the advantages and disadvantages of each analytical technique applied. High accuracy NMR assignments are reported with impurity profiling of AM-694, AB-CHMINACA and PX-1. Additionally, a method is developed for the analysis of molecules vaporised when Synthetic Cannabinoids are smoked.

Abbreviations

μg	microgram
^{19}F q-NMR	fluorine quantitative nuclear magnetic resonance
^{19}F-HOESY	fluorine heteronuclear Overhauser effect spectroscopy
4-MBC	4-methylbenzyl cathinone
4-MTA	4-methylthioamphetamine
5-HT	5-hydroxytryptamine
5-MeO-DIPT	5-methoxy-*N,N*-diisopropyltryptamine
5-MeO-*N*-DALT	5-methoxy-*N,N*-diallyltryptamine
ACMD	The Advisory Council on the Misuse of Drugs
ADHD	Attention Deficit Hyperactivity Disorder
AMT	α-Methyl-tryptamine
API	Active Pharmaceutical Ingredient
ATS	amphetamine-type stimulants
Binding Affinity	K_i
BZP	benzodiazepines
CB$_1$	cannabinoid receptor 1
CB$_2$	cannabinoid receptor 2
CBD	cannabidiol
CBN	cannabinol
CDC	Centers for Disease Control and Prevention
CID	collision induced dissociation
CNS	central nervous system
COSY	correlation spectroscopy
CZ	combustion zone
D	diffusion coefficient
Da	Dalton
DCM	dichloromethane
DEA	Drug Enforcement Agency
DEAT	Drug Enforcement Action Team
DEG	diethylene glycol

DEPT	distortionless enhancement by polarization transfer
DMS	dimethyl sulphone
DMT	dimethyltryptamine
DOSY	diffusion-ordered spectroscopy
EC_{50}	half maximal effective concentration
EI	electron impact
EIC	extracted ion chromatogram
EMCDDA	European Monitoring Centre for Drug and Drug Addiction
EMS	Emergency Medical Services
ESI/MS	electrospray ionization mass spectrometry
FA	formic acid
FDA	Food and Drug Administration
FFRC	fentanyl and fentanyl-related compounds
FT-IR	Fourier-transform infrared
GC/IRMS	gas chromatography isotope ratio mass spectrometry
GC-CI/MS	gas chromatography-chemical ionization mass spectrometry
GC-MS	gas chromatography-mass spectrometry
GHB	γ-hydroxybutyric acid
H2BC	heteronuclear 2-bond correlation
HCP	Health Care Professionals
HMBC	heteronuclear multiple bond correlation
HMG	Her Majesty's Government
HMP	Her Majesty's Prison
HSQC	heteronuclear single quantum coherence
Hz	Hertz
IPA	isopropyl alcohol
IR	infra-red
IS	internal standard
JWH	John W. Huffman
LC/MS	liquid chromatography mass spectrometry
LLOD	lower limit of detection
m/z	mass-to-charge ratio

MA	maleic acid
MDMA	3,4-Methylenedioxymethamphetamine
MDP2P	3,4-methylenedioxyphenyl-2-propanone
MDT	mandatory drug tests
mM	millimolar
MPA	methiopropamine
MS	multiple sclerosis
MXE	methoxetamine
MXP	methoxphenidine
NIDA	National Institute of Drug Abuse
nM	nanomolar
NMDA	N-methyl-D-aspartate
N-methyl-TFA	N-methyltrifluoroacetamide
NMR	nuclear magnetic resonance
NOESY	nuclear Overhauser spectroscopy
NPS	novel psychoactive substances
O1P	centre point of channel
PCP	1-(1-phenylcyclohexyl) piperidine
PFGSTE	pulse field gradient stimulated spin echo
PG	propylene glycol
PMA	4-methoxyamphetamine
PMMA	4-methoxymethamphetamine
ppm	part per million
PSYCHE	pure shift yielded by chirp excitation
PTSI	p-toluenesulfonyl isocyanate
QC	quality control
q-NMR	quantitative nuclear magnetic resonance
RCT	randomized controlled trials
RP	reverse phase
RSD	relative standard deviation
RSPH	Royal Society for Public Health
S/N	signal-to-noise
SCA	synthetic cannabinoid agonist

SDAT	senile dementia of the Alzheimer type
SWGDRUG	Scientific Working Group for the analysis of seized drugs
T_1	longitudinal relaxation time
TCF	2,2,2-trichloroethyl chloroformate
TFMPP	*N*-[3-(trifluoromethyl)phenyl]piperazine
THC	Δ^9-tetrahydrocannabinol
THC-COOH	tetrahydrocannabinol carboxylic acid
TIC	total ion current chromatogram
TOCSY	total correlation spectroscopy
UHPLC	ultra high-performance liquid chromatography
VWD	variable wavelength detector
WADA	World Anti-Doping Association
v/v	volume by volume

Contents

Chapter 1. General introduction and literature review

1.1 Aims and objectives

The aims of this thesis include a robust pharmaceutical analysis of illicit drugs and of their cutting agents. The topic of "a robust analysis of drugs", which was already important when these studies were designed, continues to gain in importance. Therefore, a perhaps larger than is typical number of press cuttings and WWW sites have been included to help set the scene with respect to Novel Psychoactive Substances (NPS). This topic is introduced with a review of the refereed literature also incorporating Press and Media reports.

The objectives chosen in order to achieve these aims include: a section on the challenges facing the integrity in drug testing with examples of how things go wrong even with cutting-edge analytical instruments and techniques available. The opioid crisis, currently sweeping across the USA in the form of illicit synthetic opioids of enhanced potency, is introduced as the number of reported deaths is staggeringly high. Then cannabis issues in the UK are introduced, from a perspective of harm reduction compared to legal drugs (alcohol and nicotine in tobacco) causing much more harm, and how the legal restrictions placed on cannabis have resulted in the now flourishing market in Synthetic Cannabinoid Agonists (SCA), followed by the growing problem of drugs in UK prisons with an emphasis on NPS use, especially SCA. Cocaine distribution is addressed, and then the controversy surrounding drug testing with a focus on phenethylamine and cathinone assays at music festivals.

Quantitative analytical research on phenethylamines and cathinones and their impurities using samples obtained from different night-clubs in the South West of England is presented in Chapter 2. In Chapter 3, arylcyclohexylamines, methylphenidate analogues and other NPS and their associated cutting agents are analysed. In Chapters 4 and 5, the analysis of SCAs is reported using cross-method detection and quantification of fluorinated analogues by ^{19}F q-NMR spectroscopy. A SCA smoking model has been developed. Such NPS samples were provided by the Drug Enforcement Action Team (DEAT) following seizures, including in a UK prison, Bristol. The thesis is then brought together in a general conclusions section.

1.2 General introduction

The research presented in this thesis is on the pharmaceutical analysis of drugs which are abused and their cutting agents. Apart from the abuse of prescription drugs, these compounds are known collectively as Novel Psychoactive Substances (NPS). This research spans before, during, and after the implementation of The Psychoactive Substance Act 2016 which came into effect on the 26th of May 2016. This act rendered illegal all substances that are sold by "head shops" and marketed as "legal highs", plant feeders, herbal incense or bath salts. It includes substances sold presently or any substance that might be introduced in the future.[1] It makes it an offence to produce, supply, offer to supply, possess with intent to supply, possess on custodial premises, import or export psychoactive substances; that is, any substance intended for human consumption that is capable of producing a psychoactive effect, excluding legitimate substances, such as food, alcohol, tobacco, nicotine, caffeine, and medical products from the scope of the offence, as well as controlled drugs, which continue to be regulated by The Misuse of Drugs Act 1971. The maximum sentence is 7 years imprisonment.

The Act defines psychoactive substances as "any substance that produces a psychoactive effect by stimulating or depressing the person's central nervous system (CNS), thus causing an alteration in the mental or emotional state of the individual", excluding from that alcohol, tobacco, and caffeine. This, in itself, is controversial as a number of people have criticized the law as it will drive the sale of NPS underground and may result in an increase in deaths from those substances,[2] similar to the experience found in Ireland when they banned NPS in 2010. Others believe that the Criminal Justice Act (Ireland Psychoactive Substance Act) of 2010 resulted in a significant reduction in the number of headshops and, as a result, a decline in the number of users.[3] Other UK researchers showed that the drop in the number of online headshops or vendors selling NPS on the visible web was counteracted by an increase in the number of NPS vendors selling in the UK on the dark web (cryptomarket).[4] Another area of controversy is the fact that some of the exempted drugs, such as alcohol and tobacco, kill more people annually than all the deaths from NPS combined.[5]

The driving force behind The Psychoactive Substance Act 2016 is the continuous proliferation of NPS. These are synthetic compounds that could be based on mainstream drugs, e.g. MDMA (ecstasy), amphetamine, heroin, producing psychoactive effects by acting on their corresponding CNS receptors. They are not regulated by the 1961 or 1971 United Nations Acts, thus circumventing legislation. They are marketed as bath salts, legal highs, and research chemicals.[6,7] Most of them are analogues of classical drugs with functional group modification on different positions and bioisosteric replacement of functional groups that potentially result in different biological and pharmacological properties.

According to the European Monitoring Centre for Drug and Drug Addiction (EMCDDA) more than 3.1 tons of NPS were seized in 2014 across Europe. The majority of these seizures consist of synthetic cathinones and SCAs, totalling approximately 46,730 seizures in 2013, with 101 previously unreported NPS seized in 2014 resulting in a total of 620 NPS currently being monitored.[8,9] Between the years 2008-2013, there was a seven-fold increase in the number of seizures of NPS. The high volume of seizures of cathinones and SCAs could possibly be as a result of the high demand as 8% of the youths in Europe have experienced NPS in their lifetime according to the European Commission Eurobarometer survey among youths.[10,11] Alarmingly, this differs from the staggering 65.8% of people attending the club scenes in the UK who say they have had experience with NPS.[12]

So it would appear that these are very popular among certain demographics who attend night-clubs. This trend is corroborated by our analytical findings of different types of NPS from night-club amnesty bins and police seizures. The major categories of NPS are: SCAs, cathinones, phenethylamines, tryptamines, benzodiazepines (BZP), arylcyclohexylamines, and other categories with a small number of compounds such as phenidate-type analogues, ring-substituted aminoindans and benzofuran derivatives. The fundamental difference between synthetic drugs and natural product drugs such as cocaine and heroin, is that the former are not geographically confined to a particular area that require cultivation at a particular season. All that they require for manufacture are precursors and moderate technical expertise in synthetic chemistry.

The first category of NPS to gain popularity was the phenethylamines family that acted as a stimulant. Popularised by Shulgin's book PIHKAL, where he synthesised a large number of derivatives, some of them are MDMA derivatives with qualitative assessment of each analogue on himself,[13] followed by the tryptamines[14] experimenting on different tryptamine analogues. Cathinones and SCAs were introduced illicitly in Europe at 2005 and 2008 respectively.[15-17] The use of classical drugs, such as cocaine and MDMA, is still rising in popularity, even with increased number of seizures worldwide.

Drug analysts must adapt to the challenge of a fast-changing climate of drug synthesis, with hundreds of analogues produced annually by clandestine chemists. Forensic and pharmaceutical analysis must be robust. Important parameters and criteria such as sampling, analytical technique of choice, qualitative and quantitative analysis, and validation of the methods must be addressed. The Scientific Working Group for the analysis of seized drugs (SWGDRUG) categorized analytical techniques into three categories (Table 1) to achieve the minimal requirements for the forensic analysis of seized drugs, taking into account the diminishing discriminative power of the technique that is due to the sample or the analytical technique employed. An example of this is the use of Infra-Red (IR) spectroscopic detection of samples of complex mixtures, or the use of an LC/MS method that only results in the identification of the molecular ion without the fragmentation pattern that provides structural elucidation data. In the case of using a category A (Table 1) technique, e.g. NMR spectroscopy, at least one other technique from any other category must be used. While in the case of the absence of any category A technique, three different validated methods must be used.[18] It is true that the legal drugs that were abused were pure; with illegality came impurity (cutting). Not only is the scale of the drugs abused increasing, as measured by the tonnage of seizures, but the number and chemical variety of drug analogues are also increasing. Evidence for this follows from seizures and from forensic, toxicological, and their associated analyses.

Table 1. Categories of analytical techniques used by the SWGDRUG.

Category A	Category B	Category C
Infrared Spectroscopy	Capillary Electrophoresis	Colour Tests
Mass Spectrometry	Gas Chromatography	Fluorescence Spectroscopy
Nuclear Magnetic Resonance Spectroscopy	Ion Mobility Spectrometry	Immunoassay
Raman Spectroscopy	Liquid Chromatography	Melting Point
X-Ray Diffractometry	Microcrystalline Tests	Ultraviolet Spectroscopy
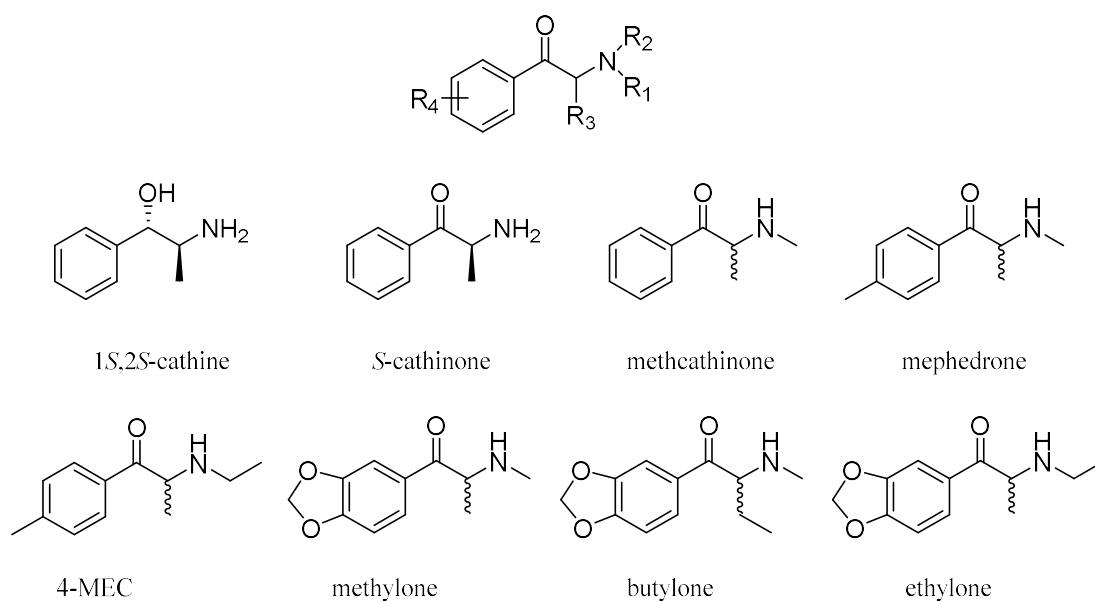
Figure 1. Core structure of cathinones and possible functional group modification, and some examples of currently abused synthetic cathinones.

Cathinones are a major group of NPS with 1.1 tons seized in 2013, a close second to SCAs (1.6 tons), and first in the number of newly reported drugs by the EMCDDA.[8] The members of the cathinones family are analogues of the natural product cathinone (Figure 1). It is found in the fresh leaves of *Catha edulis*, khat, a popular plant in East Africa and parts of the Arabian peninsula such as Yemen. The stimulant effect of khat is noticeable after chewing the leaves.[19] Initially, the stimulant effects were attributed to cathine (d-norpseudoephedrine), the first compound to be extracted from the leaves in 1930,[20] but later this was shown to be too weak to take credit for the entire stimulating effect resulting from

chewing khat leaves, and in 1975 the strong stimulant cathinone (Figure 1) was extracted

from fresh leaves as it decomposes in stored leaves.[21]

The synthesis of cathinone analogues occurred a year prior to the isolation of cathine

from khat. Methcathinone and mephedrone were synthesized at 1928 and 1929 respectively.

They were initially tested and marketed as antidepressants in the USSR and as CNS

stimulants in the USA.[16,22,23] The abuse potential of cathinones, e.g. methcathinone, was first

reported in the mid-1970s in USSR, and in the USA in the 1990s.[24] Mephedrone was first

described in Europe in 2009.[25] Since then, the drug has gained in popularity among users as

an alternative to mainstream illicit drugs, e.g. MDMA and methamphetamine. In 2010, a

cross-sectional survey of the dance-scene drug use of 2295 participants revealed that

mephedrone ranked as number six after tobacco, alcohol, cannabis, cocaine, and MDMA.[26]

However, after the UK mephedrone ban in April 2010, the purity of mephedrone suffered, as

seen in the analysis of mephedrone in South Wales amnesty bins between the 2011-2013.

Analysis by GC-MS and FT-IR showed that the purity of mephedrone declined as time

progressed supporting the conclusion that the decline in purity began with the ban of

mephedrone.[27]

Chemically, the cathinones are similar to phenethylamines, but with the addition of a

ketone at the β-position. Methylation at R1 and R3 results in methcathinone (Figure 1), while

N,*N*-dimethylation at R1 and R2 results in metamfepramone. Additionally, aromatic position-

4 methylation results in the formation of mephedrone. The bioisosteric replacement of the

aromatic methyl of mephedrone with F results in the formation of flephedrone; methylation

of R3, aromatic 4, and extending R1 into an ethyl group gives 4-methylethcathione (4-MEC).

MDMA structural similarities have been introduced, where R4 is methylenedioxy, to

introduce methylone, butylone, ethylone (Figure 1), and others each with their own

distinctive additional functional group modification.[28-30]

Phenethylamines are a group closely associated with cathinones, in fact

methylenedioxy cathinones are based on the MDMA (methylenedioxy methamphetamine)

structure (Figure 2), but the resulting cathinones pharmacologically remained as stimulants

and are not empathogenic or entactogenic (compounds that promote emotional openness),

partially due to lower inhibition of serotonin (5-HT) monoamine reuptake inhibitors.[31]

MDMA, though legally classified as a class A drug,[32] is chemically classified as a

phenethylamine. Although first synthesized by Merck in 1912 for therapeutic use, no

published data were reported by the company.[33] Furthermore, the first illicit analytical

detection of recreational use was in Chicago IL, USA, in 1972.[34]
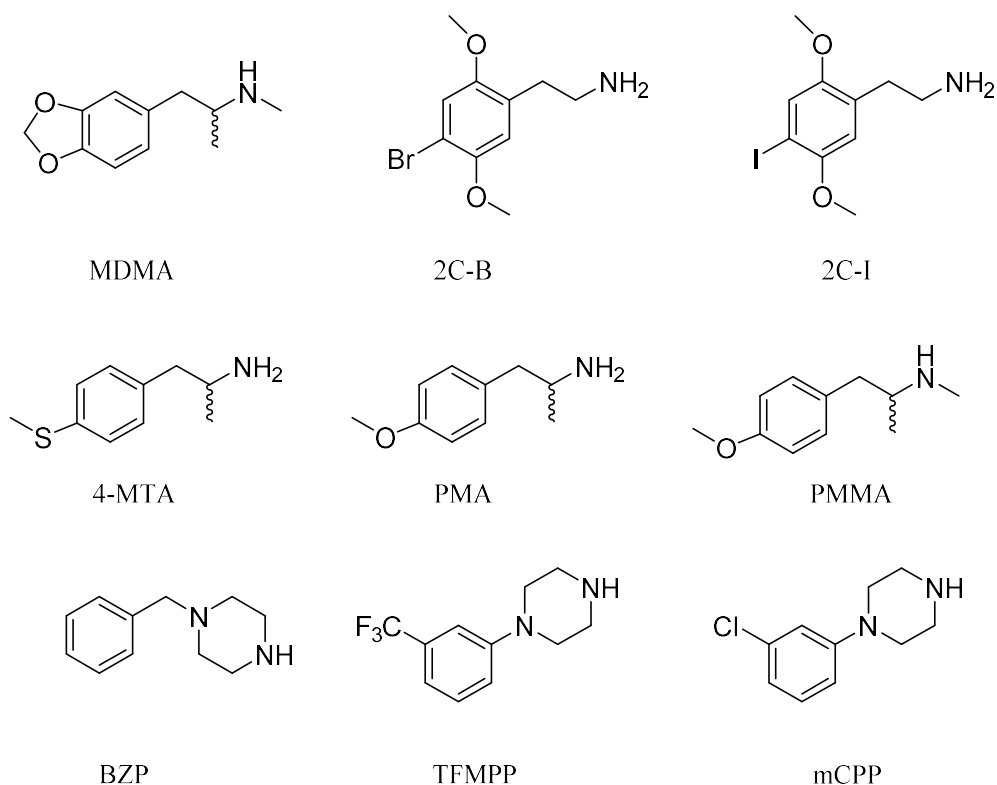
Figure 2. Abused phenethylamines and piperazines.

The purity of supplied MDMA has fluctuated over the last 23 years.[35] A European

study found that 1997 recorded the lowest purity for MDMA, then purity started rising over

1998-2004, peaking at 2004 and then dropping again.[35] One of the reasons for this drop in

purity after 2004 is the seizure of 29,100 litres of safrole and isosafrole (Figure 3), the

precursors used for piperonal synthesis, which is used for MDMA production as reported by

the World Drug Report.[36] A further crackdown on methylenedioxy precursors may also

explain the decrease in MDMA purity post-2008 when the authorities in Cambodia

confiscated 5.7 tons of safrole in one seizure in 2008; a total of 33 tons were seized in that

year alone.[37] Since then, illicit MDMA manufacturing switched to another precursor, 3,4-methylenedioxyphenyl-2-propanone, also known as the MDP2P or piperonyl methyl ketone (PMK) method. When law enforcement started focusing on this precursor, the technique of precursor of precursor was used to synthesize MDP2P from ethyl 3-[3′,4′-(methylenedioxy)phenyl]-2-methylglycidate (Figure 3).[38]

safrole   isosafrole

piperonal

$NaOC_2H_5$

ethyl α-bromopropionate

ethyl 3-[3',4'-(methylenedioxy)phenyl]-2-methylglycidate

1. MeOH/H_2O/NaOH

2. Copper/Heat

3,4-methylenedioxyphenyl-2-propanone
(PMK)
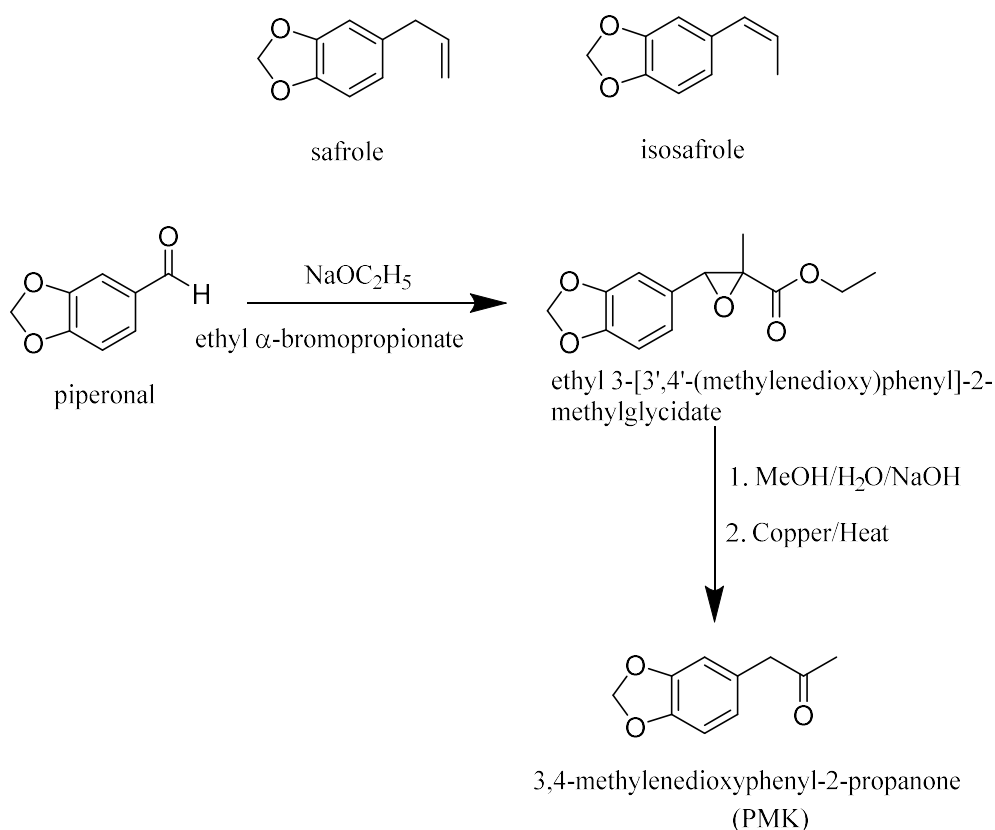
Figure 3. Natural MDMA precursors and a synthetic scheme for PMK.[38]

The 2016 EMCDDA report established that MDMA use is increasing.[39] MDMA's resurgence in European countries, measured by wastewater analysis, revealed that Belgian and Dutch cities have among the highest levels. In the UK, the downward trend of MDMA detection from 2011-2012 has now changed into statistically significant figures in the detection of MDMA seen in cities, e.g. Bristol and London (Figure 4). Additionally, this rise in the figures of MDMA detection in wastewater could be attributed to a number of factors such as availability, purity or increased demand. Additionally, Health Care Professionals (HCP), and Emergency Medical Services (EMS) need to be aware of the trends in cutting

agents, especially cutting with other psychomimetic drugs (e.g. cocaine) or NPS (cathinones and tryptamines) in order to be better equipped to handle overdose and toxicity cases.

After Shulgin's publication of the PIHKAL book revealing numerous MDMA analogues such as 2C-B and 2C-I (Figure 2),[13] there was then further development into drugs with no precedent in the scientific literature, e.g. 4-methylthioamphetamine (4-MTA), 4-methoxyamphetamine (PMA), and 4-methoxymethamphetamine (PMMA), all of which are now implicated in toxicities and fatalities.[40] The piperazine category of NPS is also associated with phenethylamines and cathinones. It was originally developed as a de-worming agent, but the stimulating effects (somehow) noted resulted in their use as anti-depressants, acting as agonists on serotonin receptors and inhibitors of the serotonin monoamine reuptake transporters.[41] The piperazine group makes 2% of the total NPS seized, in Europe in 2013.[8] A study of the UK club scene reported that 26% of people attending night-clubs had used 1-benzylpiperazine (BZP).[42] Other analogues have been identified such as TFMPP and mCPP (Figure 2).
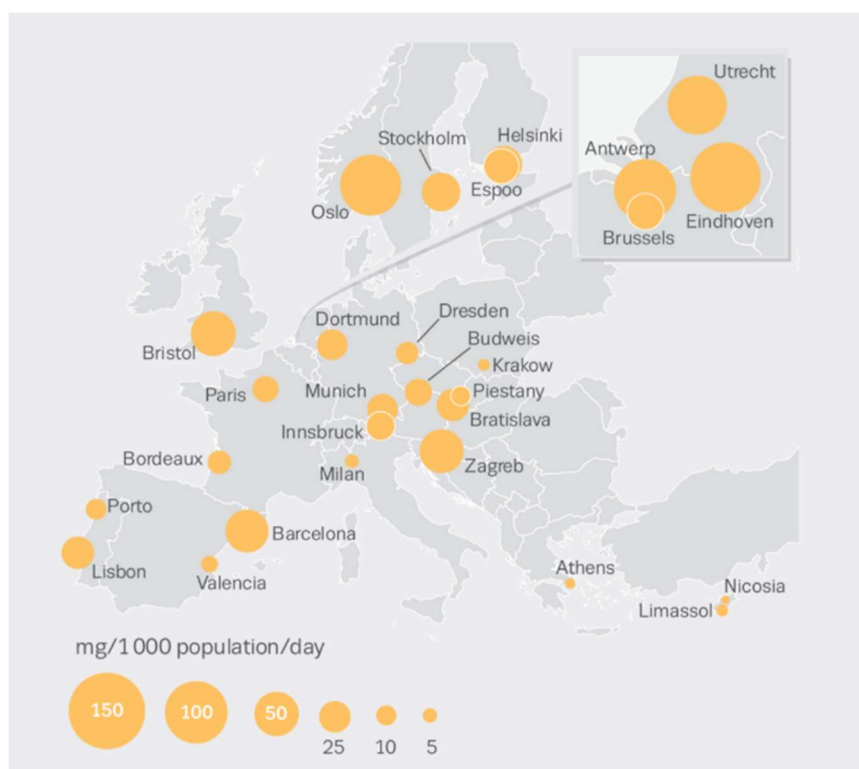
Figure 4. MDMA wastewater analysis in some major European cities.[39]
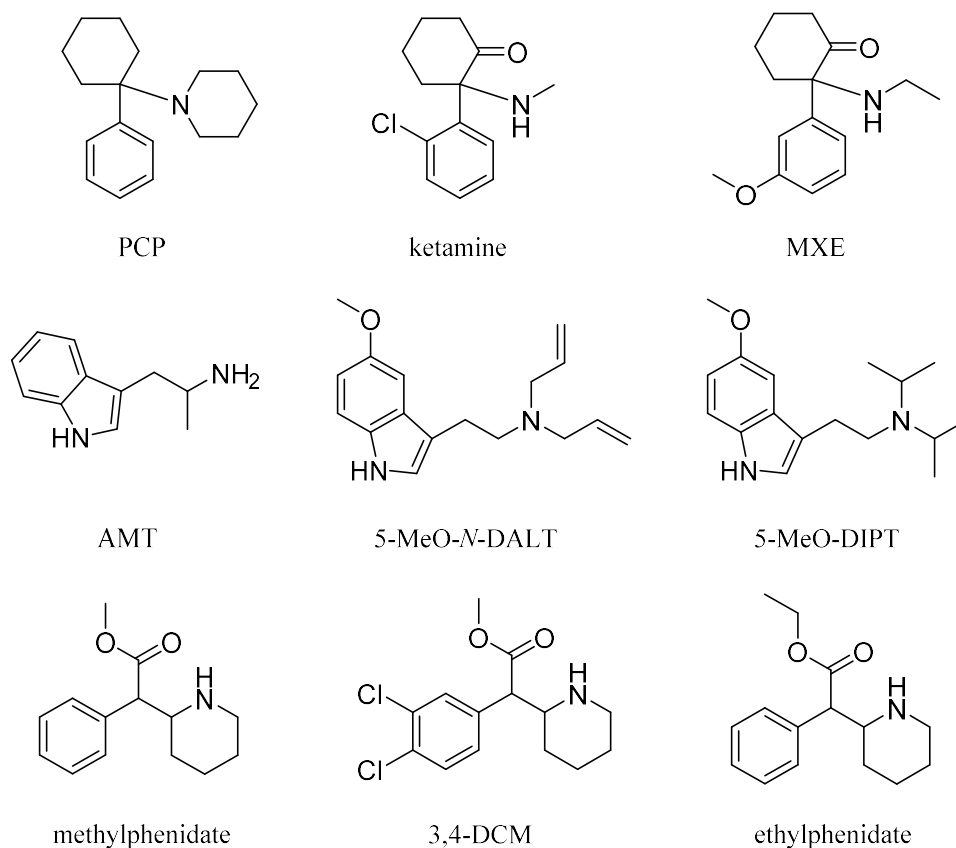
Figure 5. NPS of the arylcyclohexylamine, tryptamine, and methylphenidate classes.

Additional NPS classes include arylcyclohexylamines and tryptamines which make up 8% and 1% respectively of the amount of NPS seized, in 2013, in Europe.[8] Another NPS class is based on methylphenidate. Members of the arylcyclohexylamines includes 1-(1-phenylcyclohexyl) piperidine (PCP), 2-(2-chlorophenyl)-2-(methylamino)-cyclohexanone (ketamine), 2-(ethylamino)-2-(3-methoxyphenyl)-cyclohexanone (methoxetamine, MXE) and many others (Figure 5). The arylcyclohexylamines class exerts its dissociative sedative effect by acting on the *N*-methyl-D-aspartate (NMDA) L-glutamate sub-type receptors with variable efficacy and cross binding to other CNS receptors such as dopamine and also opioid receptors.[43,44] PCP was synthesized in 1956 at Parke-Davis, and marketed for its use in anaesthesia,[45] but it was later withdrawn by the FDA due to its reoccurring side-effects such as agitation and unusual behaviour.[43]

Medicinal ketamine was first synthesized and used in 1962 and 1965 respectively.[46] Recreational use was reported in the early 1970s[47] and, in the late 1970s, the first analytical detection in street samples was reported.[48] Soon after, reports of side-effects among ketamine abusers started to surface. Chu *et al.*, in Hong Kong, published the first findings of ketamine-induced bladder and urinary tract dysfunction,[49] which became a common side-effect and complication among ketamine abusers. Due to the dissociative effects, ketamine has been greatly side-tracked from its intended medicinal and veterinary tranquilizer uses and introduced into clubs and dance parties, thus joining MDMA and γ-hydroxybutyric acid (GHB).[50] Ketamine started gaining popularity among clubbers in the early 2000s, and as a result it was classified initially by The Misuse of Drug Act 1971 as class C and later upgraded to class B, following many reports of abuse and harm.[32]

Methoxetamine (2-(ethylamino)-2-(3-methoxyphenyl)-cyclohexanone, MXE), is an analogue of ketamine where the aromatic chlorine at position 2 is substituted with a methoxy at position 3, and the *N*-methyl extended into an ethyl. Internet chatter about MXE started appearing on the drug forum Bluelight in 2006, as chatroom members started to discuss its chemical structure and possible pharmacological effects. This was followed by its synthesis and administration by a member of the Drug Forum, which increased its popularity. Online research chemical companies showed interest and started manufacturing MXE giving free 50 mg samples, which resulted in even more online chatter among Bluelight members. This was followed by the Vice online magazine interview with a ketamine chemist which shed more light on the drug.[51,52] The analytical profile data of MXE in seized exhibits were provided by the DEA laboratories in the USA. GC/MS, IR, ^{1}H and ^{13}C NMR spectroscopic data became available.[53] MXE was initially promoted as a bladder friendly alternative to ketamine, but later, evidence of urinary tract toxicity started to emerge.[54] According to the EMCDDA MXE risk assessment report,[55] 120 intoxications were reported in member states, and of those 55 had analytical/toxicological data for the presence of MXE. Furthermore, 20 deaths due to MXE were reported by member states, in eight of these cases, MXE was the sole NPS detected; 15 of those deaths occurred in the UK.

Members of the tryptamine class are indole based NPS. They are similar chemically to the neurotransmitter serotonin (5-hydroxytryptamine, 5-HT) and differ only in the absence of hydroxy at the 5-aromatic position (Figure 5), thus acting as agonists on the 5-HT$_{2A}$ receptors, producing hallucinogenic effects.[56] Natural product tryptamines were used by the ancient Aztec civilization. The leaves of the South American plant *Psychotria viridis* contain dimethyltryptamine (DMT). Ayahuasca is a tea brew made from *Banisteriopsis caapi* and *Psychotria virdis* containing a significant amount of DMT (approximately 24 mg/100 mL).[57] Psilocybin extracted from magic mushroom (*Psilocybe spp*) is another example of natural product containing tryptamines.[57] α-Methyl-tryptamine (AMT) was used as a potential antidepressant in the USA and the Soviet Union in the 1960s, but the psychoactive effects experienced by users limited its clinical use.[57]

Later on in 1997, Shulgin's work on tryptamines in his book TIHKAL resulted in an increased popularity of this class and many analogues started appearing, e.g. 5-methoxy-*N,N*-diallyltryptamine (5-MeO-*N*-DALT) and 5-methoxy-*N,N*-diisopropyltryptamine (5-MeO-DIPT), with many modifications mostly at the aromatic position with a methoxy group, and diallyl groups at the nitrogen side-chain (Figure 5). Signs of toxicities included tachycardia, elevated blood pressure, and hyperthermia; cases of overdose started emerging. 5-MeO-DIPT was identified along with its metabolites in a fatality in Japan.[58] AMT and 5-MeO-*N*-DALT have also been identified in fatalities with high blood and urine concentrations.[58-60]

Phenidate-type NPS are all based on methylphenidate, marketed as Ritalin used for the treatment of Attention Deficit Hyperactivity Disorder (ADHD), acting as dopamine transporters reuptake inhibitors. Thus, at lower doses stimulating the CNS, enhancing cognition, vigilance and reducing tiredness.[61,62] As with any other CNS stimulant, abuse potential started emerging; side effects included psychosis and increased heart rate.[62]

NPS analogues of methylphenidate started emerging on the streets, driven by drug forums discussions and online headshops. Ethylphenidate, the ethyl ester analogue of methylphenidate, was first reported as a transesterification marker when alcohol is consumed alongside methylphenidate,[63] with first detection on the streets in the UK in 2011.[64] Its first

reported analytical detection by LC/MS/MS in fatalities appeared in 2013.[64,65] Additionally, ethylphenidate deaths were addressed in an Eastern Scotland study of 19 cases between 2013-2014, where post-mortem toxicological examination revealed that ethylphenidate, among other drugs (benzodiazepines and opiates), contributed to the deaths. In five of these cases, ethylphenidate was mentioned on the death certificates as contributing to the cause of death.[66] Other analogues started appearing on the streets, all of which have no medicinal use and are presumably intended for recreational purposes (Figure 5).[67]

Cocaine is one natural alkaloid (among many) found in the leaves of the coca plant (*Erythroxylon coca*). In Europe, cocaine is still the most popular stimulant with 3.5 million users in 2016 in people between the ages 15-64, followed by MDMA and amphetamine. Cocaine ranks second in the amounts seized after cannabis, with a value of 6.3-10.2 Billion Euros.[39,68] The purity of cocaine has been an important issue among drug analysts. Levamisole was first approved by the FDA for the treatment of colon cancer in the early 1990s, but it was withdrawn in 2000 due to several reported cases of agranulocytosis (low blood-count) and now is only used as an anthelmintic agent for veterinary uses. Levamisole has been reported as a cutting agent since 2000 by the US Drug Enforcement Agency (DEA).[69,70] The prevalence of levamisole in cocaine bricks has increased since 2005 with up to 30% of cocaine samples seized found to contain this adulterant by the end of 2008,[71] and by 2010 77% of the cocaine samples submitted for analysis in the US had levamisole in them.[72] Levamisole-cut cocaine was first described in analytical chemistry terms in Europe, in 2007, by the Italian authorities using GC/MS for the analysis.[73] In an analytical study between the years 2005-2010 of cocaine seizures in Luxembourg, the percentage of levamisole in cocaine ranged between 1.5-4.1%.[74] The possible reasons for the addition of levamisole to cocaine are mostly speculative, but some believe it to be the similar physical appearance of levamisole to cocaine making it an ideal bulking agent and/or the actions on the adrenergic system such as the inhibition of monoamine oxidase-A, thus increasing neurotransmitter concentration in the presynaptic cleft.[69, 75] There are clear and alarming

health implications from cutting with levamisole, especially the development of agranulocytosis and many incidents of necrotizing vasculitis.[69,76]

SCAs, also known by their street name spice, are the largest class of NPS measured in the number of seizures.[8] SCA are potent binders to the CB_1 and CB_2 receptors distributed throughout the CNS and immune system respectively.[77] Δ^9-Tetrahydrocannabinol (THC), the main active component of the plant *Cannabis sativa* L. (marijuana), is a partial agonist at CB_1 receptors, but not at CB_2. Due to the possible implication of CB receptors in various diseases, e.g. senile dementia of the Alzheimer type (SDAT), many compounds were synthesized to mimic the activity of THC on CB_1 receptors such as CP 47,497 synthesized by Pfizer in the 1970s and 1980s and Hebrew University HU-210 which are both structurally similar to THC (Figure 6).[78] In 1994, other CB_1 and CB_2 receptor agonists were synthesized by John W. Huffman with an indole core structure.[79] These compounds became the first generation SCAs, found in herbal blends for smoking as cigarettes, to hit the streets in 2008.[80]

As governments became aware of the situation and the threat level, the previously mentioned SCA compounds were banned, but the ban resulted in hundreds of SCA analogues being illicitly synthesized in clandestine laboratories, leading to a game of cat and mouse, where the second generation of SCA was from 2009-2012. Additional banning of these compounds resulted in the third generation (2013-present) of SCA. Most of these analogues have no precedent in the scientific literature.[81]
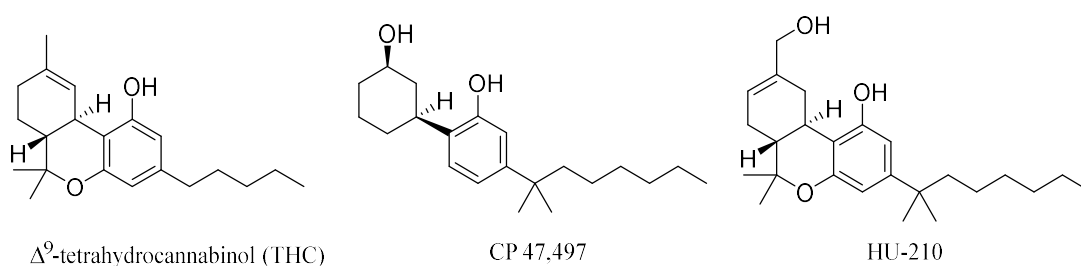
Figure 6. Classical and synthetic cannabinoid agonists (SCA)

1.3 Integrity in drug testing (Sochi and Randox Scandals)

It is a *sine qua non* that forensic and pharmaceutical analysis must be honest. Whilst there is room for a wry smile, indeed it might even be ironic that the 2014 Winter Olympics in Sochi changed people's lives, not least those who just failed to achieve an Olympic medal. Doping, the use of performance enhancing drugs, is not a new phenomenon, but has increased dramatically in the past 3 decades with shocking tales emerging from East Germany, and also the Canadian sprinter Ben Johnson doping scandal at the Seoul 1988 Olympics.[82]

The Sochi anti-doping laboratory was equipped with state-of-the-art instrumentation to analyse banned substances, with sample reception on the first floor and the upper floors containing areas for peptides, non-peptide analysis and a number of mass spectrometers, LC/MS/MS, GC/MS/MS, GC-Isotope Ratio Mass Analysis (GC/IRMS), and many others.[83] Nevertheless, the German documentary aired on Mitteldeutscher Rundfunk (MDR) broke the news on possible doping and sample tampering, the allegations also implicated the anti-doping management and high-ranking officials in a State-run doping scandal. The report included leaked documents and testimonies from athletes, who claimed that they were instructed by their coach to use performance-enhancing drugs such as oxandrolone (Anavar), and to keep clean urine samples for them to submit for analysis. This led the General Director of the World Anti-Doping Association (WADA) to initiate a full investigation.[84]

The Sochi anti-doping laboratory director Dr Grigory Rodchenkov came forward and exposed the magnitude of the scandal. He admitted to providing Russian athletes with a cocktail of banned anabolic substances to enhance their performance. Additionally, he implicated officials who swapped tainted urine samples with clean ones prepared months in advance through small holes made in the laboratory walls where the urine samples were kept, breaking the tamper proof seals. Ultimately, 100 urine samples were switched.[85] The WADA investigation, "the McLaren Report"[86] corroborated Dr Rodchenkov's story and came to the conclusion that a State-run doping system was run by Russian officials providing cover for athletes to use performance-enhancing drugs without being exposed. The report is based on eye-witness accounts, interviews, forensic analysis of samples, and documents analysis. The

report exposed tampering and doping facilitation by the Russians during the London 2012 Olympics. The report also exposed the unauthorized opening of urine samples in the tamper proof Bereg kit bottles. As a result of the investigation, a number of Russian athletes lost their medals and ultimately the Russian team were removed from top of the table ranking, and the suspension of the Russian Olympic Committee.[87,88]

Forensic drug analysts are under scrutiny most of the time. They are called upon by law enforcement, District Attorneys and judges to clarify, explain, and or testify in law courts. They are trained to the highest standards for these purposes. In the UK, drug samples that require forensic analysis are either analysed in house by the police or sent to private forensic service companies, e.g. LGC, Alere Forensics, and Randox. Nonetheless, there are cases where forensic services have totally failed to maintain professional standards.

On February 19th 2017 the story broke of two Randox Testing Services analysts doctoring the results of toxicology samples, e.g. blood, hair, and saliva, at the Manchester office. It is believed that over 484 cases could be affected from different areas in the UK as the laboratory handled cases from across the UK with the exception of alcohol testing. The manipulation of the samples was of the quality control data and not by adulterating the samples.[89] The scale of the scandal later became apparent as the laboratory handled cases for 42 Police Force throughout the UK, including the Greater Manchester Police, with 10,000 cases in question. That number will include cases of drink driving and violent crimes (murders and sexual offences). Two death cases are now being considered for appeal.[90,91] Additionally, it is believed that the retesting of 1500 samples will be required. In some cases, that will not be possible as the samples have not been well-maintained and some drugs may breakdown when stored for a long time. This will put more pressure on an already burdened criminal justice system.[91] Many criticized the current standards of the forensic system, and claimed that this decline is a direct result of the closure of HMG owned Forensic Science Service due to losses of £2 million per month. HMG is tackling the problem by planning to establish new forensic science services.[92] This follows the 2015 National Audit Office (NAO) report whose key findings included the current decline of the forensic services and the

inability of the current forensic regulators to enforce strict quality control measures on drug testing.[93]

Another example of drug analysts going rogue on the same scale of the Randox testing scandal, occurred in Amherst, Massachusetts, USA in 2013, where an analyst was found guilty of stealing drugs from the drug analysis laboratory where she worked, and that she has been doing so for the past eight years. 8000 cases that the drug analyst has worked on could be thrown out of the courts. This came after another drug analyst named Annie Dookhan, also in the State of Massachusetts, was convicted and sentenced to 3 years in prison, after falsifying, not testing, and fabricating data. This resulted in over 20000 drug convictions being overturned.[94] These are examples of how critical being a drug analyst is, the ethical and professional levels which the analyst should display, and how it can go wrong for a lot of people due to gross misconduct.

Incidents of misconduct by drug analysts in the fields of forensics and doping result in mistrust and doubts in the public eye. Drug testing services should reflect an image of reliability, honesty, and accuracy. The impact of exonerating a drug user or a doping athlete as a result of false negative or doctored results can be profound on the people directly involved or on the public in general. The impact is even worse in the case of false drug or doping convictions resulting from false positives of the test results or rogue analysts fabricating drug results, with lives and careers on the line that could be destroyed, in addition to the generated mistrust of drug services which are considered a critical tool in the armamentarium of the justice system.

There are no easy solutions to fully proof drug analysis services from errors generated in the analysis, whether they are mistakes made during the analysis (false positive or false negative) or deliberate data fabrication, but some precautions can help resolve or at least mitigate mistakes produced as a result of the misapplication of drug analysis, e.g. quality control (QC) of samples, method validation of the technique used. As for preventing misconduct, an independent external oversight body is required to ensure fairness, even honesty, in drug analysis.

1.4 The opioid crisis

Opium is the most commonly used analgesic for mild to severe pain, and in palliative care of terminal-stage cancer. Historically, it is believed that the first to grow poppies and extract opium from the seeds were the Sumerians in 3400 B.C. From the eighth century, Arabs introduced it to India and China. This was followed by widespread addiction in many areas such as Egypt, Turkey, but more noticeably in China. Another hallmark in the history of opium is the isolation of the active components from the latex of the sap of poppies (*Papaver somniferum*) by the German pharmacist F. W. A. Sertürner in 1806. He named it morphine after the Greek god of dreams, Morpheus. Besides the main component morphine, opium contains codeine, thebaine, noscapine, and papaverine (Figure 7). Due to the abuse potential of morphine, di-*O*-acetylation was investigated at Bayer in 1898, heroin (diamorphine) was synthesized as a safer alternative; this was later found to be untrue.[95] Furthermore, the first opium war occurred between England and the Quing Dynasty, 1839-1842, a result of the British East India company's efforts to import Indian opium in to China, in order to further their trade expansion in Asia, but those efforts were opposed by the then Emperor of China, Daoguang, due to the heavy toll that opium addiction was taking on the Chinese population.[96]

heroin $R^1 = R^2 = C(O)CH_3$
morphine $R^1 = R^2 = H$
codeine $R^1 = OCH_3$, $R^2 = H$

thebaine

noscapine

papaverine
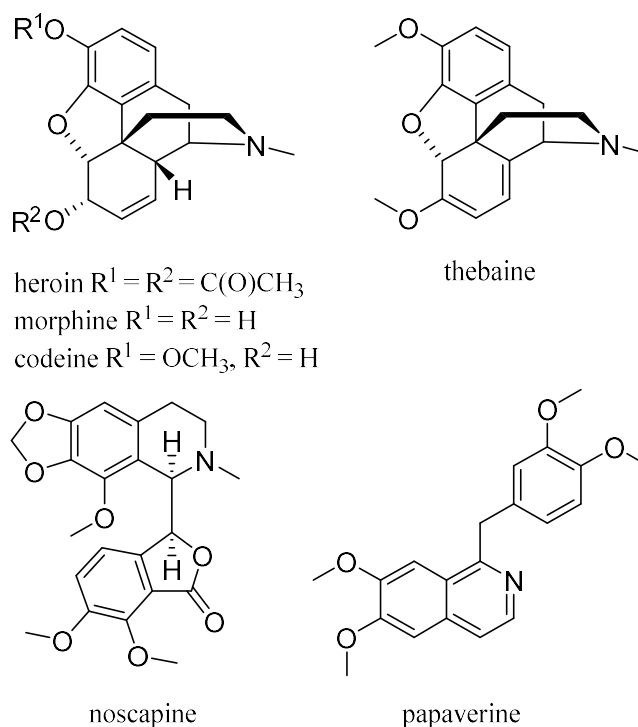
Figure 7. Compounds present in opium with the exception of semi-synthetic heroin.

The majority of heroin is produced in the Golden Crescent (Afghanistan, Iran, Pakistan) and the Golden Triangle (Myanmar, Laos and Thailand), with 90% of the world production of opium from Afghanistan alone. Furthermore, the Taliban ban on opium in the year 2000 resulted in an opium production decrease of 95% (Figure 8).[97,98]
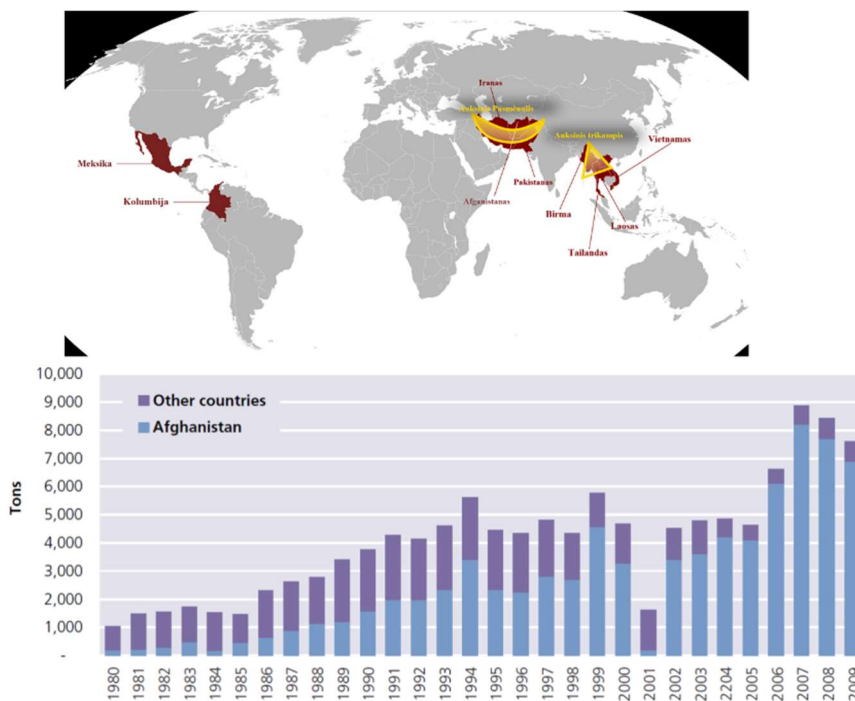
Figure 8. Global production of heroin (top) and of opium (tons) (bottom).[97]

oxycodone

fentanyl

α-methylfentanyl

carfentanil
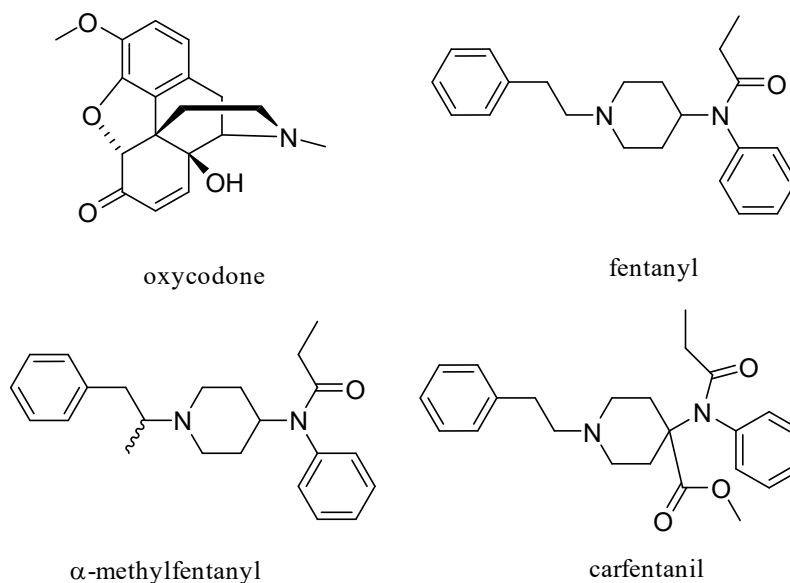
Figure 9. Prescription and synthetic opioids.

On the 26th of October 2017, President Donald Trump declared the opioid crisis a national health emergency in the USA, directing funds and personnel towards reducing the number of opioid-related deaths, with deaths from opioids exceeding deaths from car accidents and guns combined.[99] The number of deaths from opioids, including prescription (oxycodone, methadone, and hydrocodone) and non-prescription illicit opioids (heroin, fentanyl, and carfentanil) (Figure 9), has increased by four-fold since 1999 reaching 33,091 deaths in 2015 (Figure 10), and in 2017, prescription and non-prescription illicit opioid resulted in more than 47,000 deaths.[100,101]
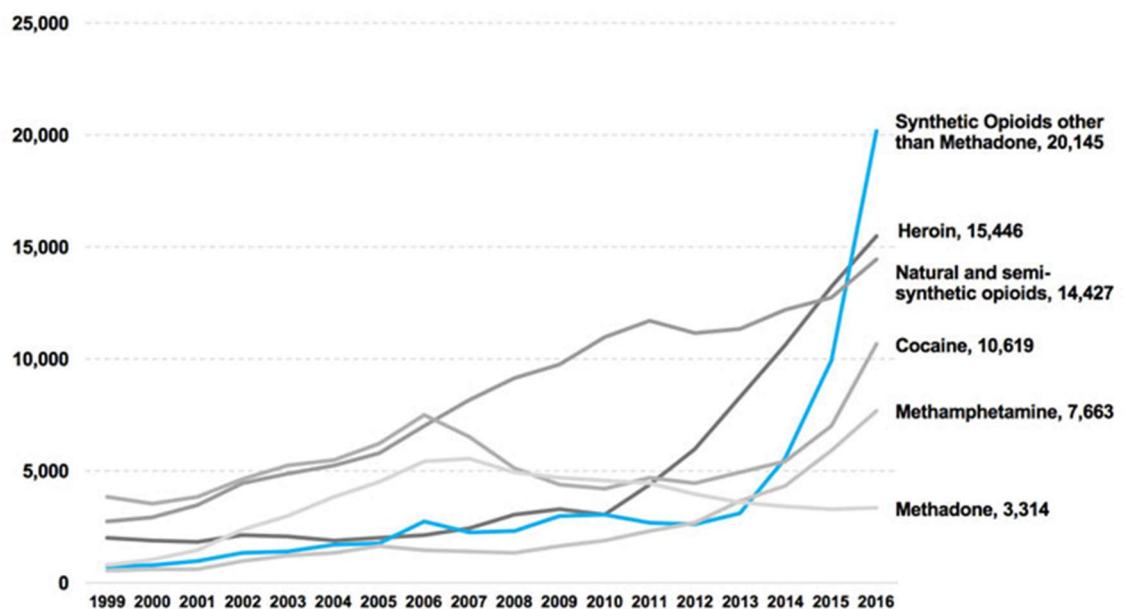
Figure 10. NIH National Institute of Drug Abuse (NIDA) report 2017.[101]

The problem is confounded by the fact that more than 289 million prescriptions are issued yearly for opioid analgesic drugs in the USA, with this trend of overprescription starting in the 1990s. With overprescription came an increase in the misuse of this class of drugs, with some demographics even using illicit heroin as a cheap and easy to obtain alternative compared to prescription opioids.[102] Some researchers believe that one of the reasons for the overprescription of opioids today is the one paragraph letter published in the *New England Journal of Medicine* in 1980, stating that out of 11,882 hospitalized patients

that received opioid preparations, only 4 showed signs of addiction, concluding that addiction is rare in patients with no history of opioid addiction.[103] However, the article only described the results in acute hospitalised patients and not patients with chronic pain who take opioid medications on a regular basis.[104] In 2017, a bibliometric analysis of the 1980 *NEJM* paper was published, revealing that it was cited 608 times, of which 439 cited it as evidence of the non-addictive nature of opioids, and 439 failed to address the fact that the study was on acute patients in emergency settings and not patients with chronic pain.[105]

According to the National Institute of Drug Abuse (NIDA) 2017 report, the sharpest increase in all of the drug deaths in the USA, in recent years, is attributed to the synthetic opioids family, e.g. fentanyl and carfentanyl (Figures 9 and 10).[101]

The first wave of synthetic opioids came in the late 1970s, known as the "China white" fentanyl crisis after the origin of the heroin and the physical appearance of the samples. Two overdose cases in Orange County, CA, USA occurred. With the limited sensitivity of the analytical instruments at the time, the identification of the component responsible for the deaths was a daunting task. The low concentration in the sample received, and the presence of two cutting agents besides heroin complicated the analysis. Nevertheless, the culprit was identified using ^{1}H NMR spectroscopy and Gas Chromatography-Chemical Ionization Mass Spectrometry (GC-CI/MS) fragmentation pattern to be α-methylfentanyl in the chloroform fraction. Its highest mass ion was at 350 m/z. ^{1}H NMR revealed that it was the citrate salt, with lactose and propionic acid in the water-soluble fraction believed to be a cutting agent and synthesis impurity respectively.[106] Toxicological examination of the overdose cases confirmed the presence of α-methylfentanyl in peripheral blood and the analytical data were a match with the analysed exhibits recovered at the scene.[107]

The current wave of fentanyl and fentanyl-related compounds (FFRCs) started in 2013, with 5000 deaths in 2014, 1100 of which occurred in Ohio.[108] Ohio State Health Services reported that, in 2016, 11 drug overdoses occurred daily.[109] In the summer of 2016, 27 people were hospitalised in Huntington West Virginia in 4 hours as a result of a batch of heroin laced with a potent unknown compound. The Centers for Disease Control and

Prevention (CDC) confirmed later that toxicological analysis revealed the presence of fentanyl and also the much more potent fentanyl analogue carfentanil.[110,111] Carfentanil (methyl 1-(2-phenylethyl)-4-(*N*-propanoylanilino)piperidine-4-carboxylate) which differs from fentanyl by the additional methyl ester at position-4 of the piperidine ring (Figure 11), has recently been implicated in a number of deaths in the USA. Carfentanil is 100-times more potent than fentanyl and 10,000-times more potent than heroin, where a dose of 20 μg could result in death.[108] Carfentanil is believed to be implicated in the 125 deaths at the Moscow theatre siege (2002) after Russian forces released an aerosol gas of fentanyl derivatives onto the terrorists to "save" the hostages. The high number of casualties is believed to be a combination of deficient medical care and the presence of two fentanyl derivatives, carfentanil and remifentanil (Figure 11) in unknown proportions. The presence of strong opioids in the released gas was confirmed by urine and clothing analysis of three British survivors, using LC/MS/MS with transition ion monitoring mode 395 m/z to 351 m/z for carfentanil, and 377 m/z to 285 m/z, and 377 m/z to 116 m/z for remifentanil.[112] The administration of multiple doses of naloxone (a potent competitive agonist at the μ opioid receptors) in heroin overdoses is highly indicative of a potent opioid and therefore higher than usual doses of naloxone were used, as seen in the Huntington West Virginia incident, where 6 of the 16 who received the naloxone antidote required multiple administrations.[113]

Even though the UK has a more strict prescription policy when it comes to opioid painkiller prescriptions, reflected in the lower number of fentanyl deaths, still the trend of FFRCs seems to have crossed the Atlantic. Here the police reported at least 60 deaths, related to heroin laced with FFRCs, mostly in the Yorkshire area.[114] The UK crime agency report stated that fentanyl and its analogues started appearing in the UK drug market in late 2016,[115] and the report emphasized the vulnerability of heroin abusers as they represented a high-risk group due to the fact that heroin is being cut with fentanyl or its analogues. It is also unclear whether the two-fold increase in the heroin-related deaths, in 2015 compared to 2012, is due to the high purity of heroin or fentanyl lacing. Additionally, in Europe, there has been a growth of fentanyl analogues such as 4-chloro-isobutylfentanyl and 4-fluoro-isobutylfentanyl

(Figure 11), responsible for three and four deaths respectively.[115] Moreover, 95 seizures of another analogue of fentanyl, acryloylfentanyl (Figure 11) have been reported. The majority of the seizures were in Sweden and Estonia with 63 serious adverse events reported.[115] Furthermore, from a toxicological point of view, the detection of fentanyl and other analogues is relatively easy. Carfentanil is more difficult to test for, due to its low levels in blood and urine and no actual limits have been established for its detection.[115]

R = Cl; 4-chloro-isobutylfentanyl
R = F; 4-fluoro-isobutylfentanyl

R = ethyl; fentanyl
R = vinyl; acryloylfentanyl

carfentanil

remifentanil
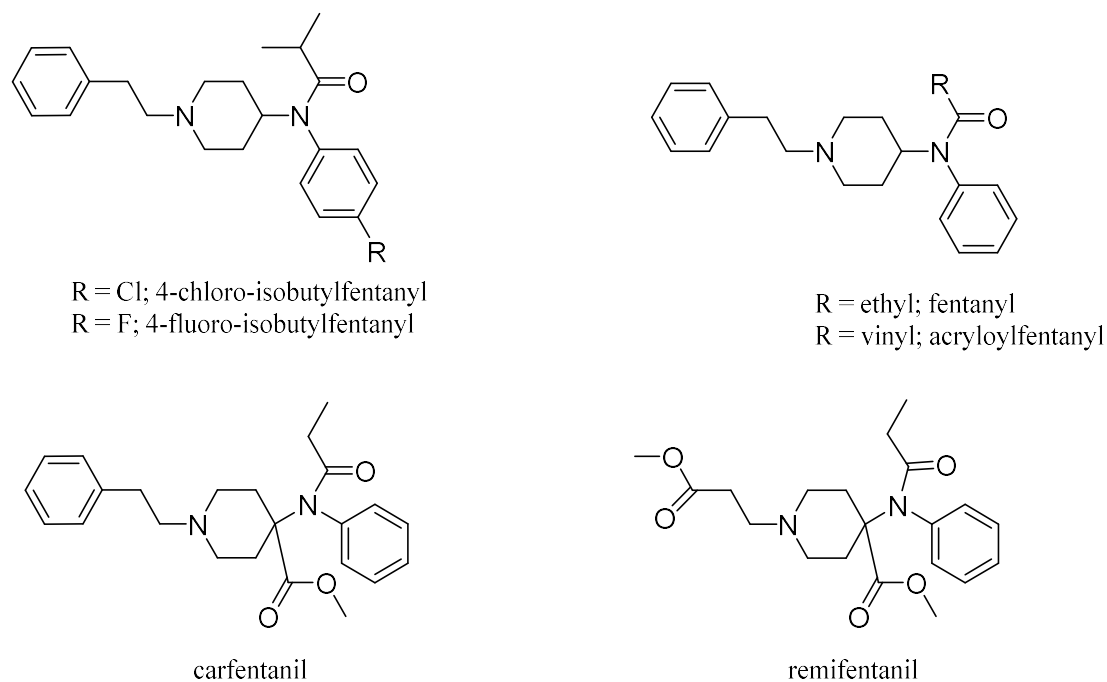
Figure 11. Illicit fentanyl analogues seized in Europe with their non-systematic nomenclature based on fentanyl which contains a tertiary propanamide.

Clandestine chemists are synthesizing analogues of fentanyl at a rate faster than they can be controlled by law enforcement agencies. The opioid epidemic is hitting the USA and has really already started spreading to Europe and other countries. Complicating the problem is the fact that fentanyl analogues are potent at microgram doses and found as cutting agents or mixing agents with mainstream drugs such as cocaine, but mostly with heroin, making it difficult for drug analysts to detect them especially in toxicological cases.

1.5 Cannabis in the UK

No longer "just a bit of weed", cannabis is now grown by the industrial-scale manufacturing of high concentration skunk also known as sinsemilla, bred to have a high concentration of THC. In August 2017, three men were charged with large-scale farming of cannabis inside a sold-on Ministry of Defence nuclear bunker near Salisbury. Approximately 4400 cannabis plants were found and the estimated amount of cannabis that could have been produced was £2M. The culprits diverted electricity to power the heating lamps to create ideal conditions for growing the cannabis plants.[116] However, there was also modern slavery, and it was certainly not a jape for those in forced labour.

The term cannabis stands for the extract of the plant *Cannabis sativa* L. in the form of leaves of marijuana or cannabis oil. Even though there are more than 60 compounds in the plant, the effects of cannabis are attributed to the compound Δ^9-THC. Other components (Figure 12) either possess weak or no activity on the cannabinoid (CB$_1$) receptors producing the psychoactive effects.
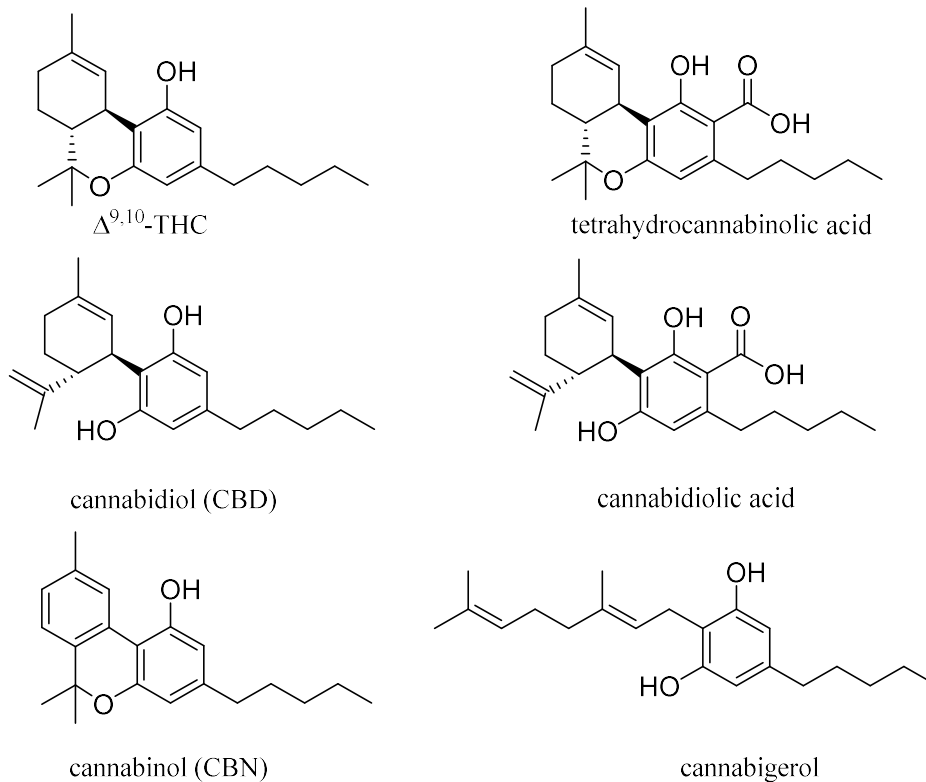
Figure 12. Δ^9-THC and its related naturally occurring analogues in cannabis.

The concentration of THC in marijuana has been increased (by horticulture) from 1% in 1973 to 9% in 2008. The main route of administration remains inhalation, some users resorting to vaporization to avoid potentially harmful pyrolysis products. Ingestion is less popular, possibly due to the irregular peak plasma concentration and delayed action of up to two hours.[117] Large randomized controlled trials (RCT) gave positive results for the use of smoked marijuana in the treatment of spasticity associated with Multiple Sclerosis (MS).[118] Medically approved marijuana such as Sativex, containing THC:CBD (cannabidiol), in the ratio 1:1, is delivered as an oromucosal (administration through the mucosa of the mouth) spray of 100 μL. It is used for the treatment of moderate to severe spasticity associated with MS which is not responsive to conventional medications.[118] It is believed that CBD potentiates the effects of THC and reduces the side effects associated with THC.[119] Illicit cannabis is believed to be the leading drug in Europe in terms of the number of users with 23.5 million users in 2016 and life-time users (at least once in their lifetime) of approximately 87.7 million among adults aged between 15-64. This is 70 million more life-time users compared to those for the most popular stimulant, cocaine. In the form of marijuana and resin, it accounts for 70% of drug seizures, with a retail value of 9.3 billion Euros. Most of the seized illicit cannabis products are either grown indoors in Europe or are shipped from Morocco; the amounts seized annually since 2009 remain the same.[39]

The legalization of marijuana has been a controversial issue for discussion throughout the past 50 years, even though it remains illegal in the UK and at the federal level in the USA. In the majority of European countries it is either illegal or decriminalised (reduction of penalties), with the exception of the Netherlands, where it remains illegal except in coffee shops i.e. for personal use. Nevertheless, restrictions were put in place to control the sales of cannabis in coffee shops, e.g. prohibition of the sales of cannabis to minors, no more than 5 grams per person is sold per day, no sales of hard drugs are permitted, and no advertisements.[120] Recently, there has been a change in policy regarding the legal status of cannabis, e.g. The Canadian Cannabis Act, implemented in August 2018, which made cannabis legal at the federal level, thus making Canada the second country in the world

to legalize cannabis after Uruguay. A decision which was aimed to combat high crime rates resulting from the sales of illicit cannabis.[121] The justification for the Canadian Act was different from the Uruguayan. It stemmed from the fact that a survey revealed that approximately half of Canadians claimed to have used cannabis even though it is illegal.[121]

On August 2nd, 1977, President Carter addressed Congress and stated that penalties for the use of any drug should not be more harmful to an individual than the use of the drug itself.[122] The harm caused by legal drugs, e.g. alcohol, and tobacco with respect to tar and nicotine, compared to cannabis is grounds for debate. Indeed, there is a clear association between alcohol and domestic violence.[123] In a paper published in *The Lancet*, Professor David Nutt and co-workers revealed that in developing a harm-score criteria for drugs of abuse, alcohol scored above all other drugs tested in harm to the individual and harm to society, much more significantly than cannabis, ketamine, and ecstasy (Figure 13).[124] These data add to the controversial problem of such legal drugs doing more harm than illegal drugs, e.g. cannabis for MS, and ketamine as a horse tranquilizer. MDMA has been found to have the potential to treat PTSD (as part of psycho- and other therapies). Indeed, MDMA was recently granted Breakthrough Status by the FDA in Phase 3 trials.[125] MDMA is also being studied as a treatment for alcoholism by Dr Ben Sessa also at Imperial College, London.[126]
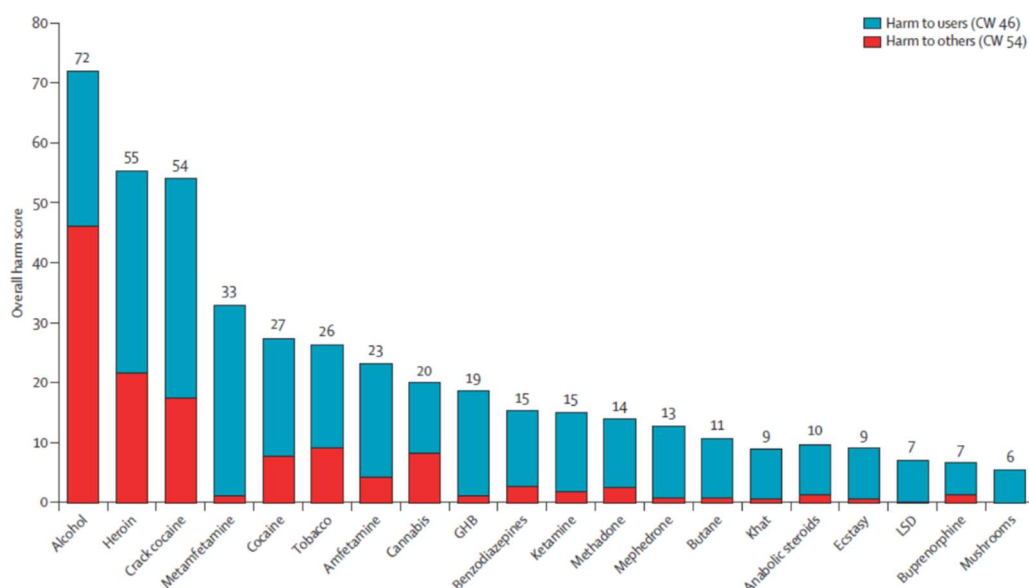
Figure 13. Harm scores to users (blue) and to others (red) of a number of drugs of abuse.[124]

[Reprinted with permission from Elsevier (*The Lancet*, **2010**, 376, 1558-1565)]

1.6 Drugs in UK prisons

In any community, drugs flourish whenever there is demand, coupled to the socio-economic level of the individuals in the community. In UK prisons, violence and anti-social behaviour as a result of drug abuse and dependence, especially mainstream illicit drugs, i.e. cocaine, heroin, amphetamines, have been well documented.[127] A systematic review of drug and alcohol abuse among male and female inmates in prisons, from the USA, UK, Ireland, and New Zealand, revealed significant variation in the percentage of prisoners' drug abuse. Males had a range between 10-48%, while females had between 30-60 % incidence of drug abuse or drug dependence. Furthermore, comparing the percentage of USA prisoners to the general population of a similar age, showed that male prisoners had a 2-10-fold increase in the incidence of drug dependence, while female prisoners had more than a 13-fold increase in drug dependence compared to the general population of a similar age.[128]

In a 2010 Policy Exchange report about combating drug misuse in the UK, the magnitude of the drug problem among prisoners was made clear. About 35% of prisoners had used drugs of abuse in prisons, with 14,000 inmates using at least once a week. The leading drug of choice among inmates was cannabis, followed by heroin, MDMA, amphetamine, and cocaine. The numbers are an improvement compared to the 2006 report conducted after surveying six UK prisons with regard to abuse of drugs in prisons, where 60% of inmates used heroin, and 70% used cannabis.[129] The annual report 2011-2012 of Her Majesty's Chief Inspector of Prisons for England and Wales reported that 29% of prisoners have a drug problem prior to their arrival in prison and 6% developed a drug problem during their time in prison. Additionally, 24% of prisoners admitted that it was easy for them to obtain drugs in prisons. Furthermore, the report also addressed the trend of diverted prescription drugs such as buprenorphine, tramadol, and gabapentin (Figure 14) that were not on the list of drugs detected by the Mandatory Drug Tests (MDT) which are conducted randomly or in the case of suspicion of drug intoxication or possession.[130] However, in the following annual report, the percentage of prisoners who developed a drug dependence in prison increased by 1%, whereas 31% stated that acquiring drugs in prison is easy. In 2013-2014 Her Majesty's Chief

Inspector of Prisons for England and Wales said that the MDT positive results declined

significantly which was not attributed to the reduction of drug use among inmates, but rather

the inability of the MDT to detect NPS including the popular SCAs (spice), e.g. "Black

Mamba". Also, the report highlighted the increase in the incidence of bullying among

prisoners, with a 38% increase in life-threatening assaults, which is believed to be primarily

due to the increased smoking of spice.[131]

| buprenorphine | tramadol | gabapentin |
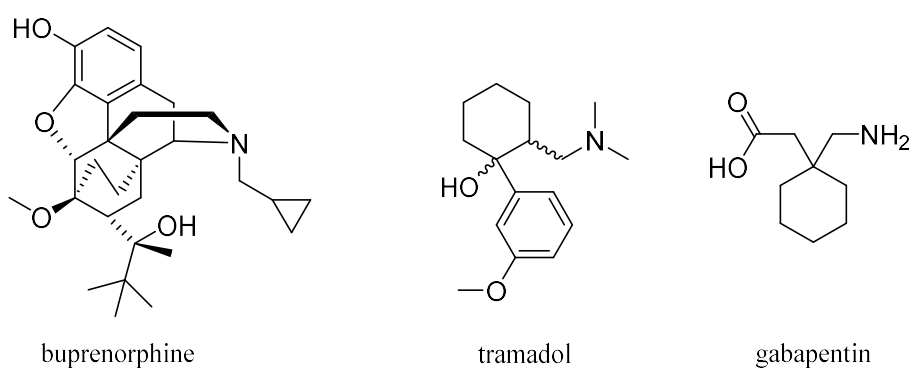
Figure 14. Commonly abused prescription drugs among prisoners.

Since 2014, the number of spice seizures has continued its dramatic increase in UK

prisons from 15 seizures in 2010 to 737 in 2014.[132] In 2016, there were increases of 27% and

31% on the previous year concerning overall assaults and life-threatening assaults

respectively.[133] Even prior to the appearance of NPS including spice, that caused analytical

difficulties to the MDT, the MDT was under fire as not being a clear representative of the

number of drug users in prisons, as there were massive discrepancies between the number of

drug users in prison surveys and the MDT results. Additionally, there is some criticism of the

MDT as being degrading to the prisoners and a violation of their human rights. Further

adding to the problem are reports of corrupt prison officers manipulating urine samples that

are destined for MDT testing.[129]

Now the UK and especially UK prisons are in the midst of a SCA (spice) crisis. The

reports of prisoners' intoxications and death as a result of the so-called legal highs in 2015,[134]

from the Prisons and Probations Ombudsman stated that, in 2012-2014, 19 deaths were

attributed to the use of legal highs and in particular to SCA brands such as "spice" and

"Black Mamba". The report added that the prisoners were using SCAs unknowingly, by

smoking spice-spiked cigarettes, or knowingly as a way of experimentation with new and

alternative drugs to cannabis. According to eyewitness accounts, at least one prisoner

collapsed after taking a cigarette from another inmate, and died later the same day. Violent

behaviour and unrest in the prison population have also been growing. Prisoners under the

influence of SCA are either being hospitalized or are attacking guards.[135] Prison authorities

are revealing that the unrest in prisons has a direct connection with prisoners' consumption of

SCA and this impact is more profound than for any other drug. Furthermore, prison guards

and prison workers have been hospitalized on different occasions in different prisons as a

result of accidently inhaling the fumes of the burnt herbal blends containing SCA.[136]

A survey conducted in 9 prisons, on 805 inmates, revealed that a third of them had

used SCA in the last month and between 50-100% had used spice at some point.[136] The report

also indicated that in particular, spice intake allows prisoners to alter their perception of time,

which is one of the problems faced by prisoners in general in that they have too much time on

their hands, and they are taking drugs due to being bored. Additionally, the report highlighted

that the emergency calls for medical help in prisons had increased by more than 50% in 2015

compared to 2011, with reports of 17 ambulance calls to a particular prison in just one day.

Moreover, deaths in prisons are on the increase. Indeed, they are at their highest since official

records began. The Prisoners' Ombudsman revealed that the number of deaths in prisons has

risen to 89 deaths in 2017, a possible result of the increase in the use of spice in prisons.[137]

One example of the amount of SCA seized is from HMP Lindholm near Doncaster,

from where it was reported that more than a kilo of NPS had been seized in one month among

other contraband. Additionally, the failure of the routine urine testing among inmates was

reported by the University of Maryland Center for Substance Abuse Research such that SCA

appeared in 33% of the urine samples submitted for analysis. The identification was made

possible by special testing as the routine drug analysis failed to identify them. Additionally, 4

prisoners in a Louisiana prison became unresponsive after overdosing on spice.[138] The drug

markets in prisons has significantly changed as evidenced by the type and amounts of drugs seized. SCA seizures in prisons increased by 400% in 2015 compared to 2014, over the same period cannabis seizures decreased by 60% compared to the previous year. It has been established that the driving force for this change was profit. SCA are sold in prisons at 3-4 times the price on the street (£100 per 1 gram), coupled with the low chance of detection compared to mainstream drugs. Furthermore, one prisoner described the situation as "it's all spice now" describing how it has taken over the popularity of heroin and even cannabis. Moreover, intoxications reported among inmates include agitation, stomach cramps, sweating, twitching, and mental and emotional alterations in behaviour. Prison guards reported many incidents of violence. One prison guard was stabbed in the face as a result of approaching a prisoner who had smoked spice and was hallucinating in the prison yard, and some reports describe the hallucinations as five times more frequent than with cannabis. SCAs are smuggled in compressed soda drinks lids, as a joint for smoking, and others use "Kinder egg" smuggled rectally also known as "plugging" to evade detection by prison guards, as there are restrictions on searching intimate areas of prisoner's bodies.[139]

Many reasons have been proposed for the spice takeover of the drug culture in prisons. Spice has started to become the preferred drug for prisoners. SCAs result in the alteration of perception and time, allowing time (apparently) to pass quicker for the users. Cannabis was the most popular drug among inmates, but due to its showing in the blood and urine analytical tests for days or weeks after consumption, because of its retention in fatty tissues (lipophilicity), there was a significantly increased chance of detection.[140] Additionally, detection limits have been established in many types of users by monitoring the tetrahydrocannabinol carboxylic acid (THC-COOH) metabolite in urine using GC/MS, showing that even after a single use, the metabolite can be detected for up to three days while, in chronic users, the THC-COOH metabolite can be detected for up to thirty days.[141] The prisoners switched to heroin which stays in the blood, urine, and saliva for a shorter time, and thus is unlikely to be detected by the MDT. The inability of MDT to detect SCA, and its potent psychoactive effects, caused the prisoners to refer to it as the "perfect drug".[139] Also,

smoking spice does not give the distinctive smell that results from smoking cannabis.[139] Perrone *et al.* conducted a study on students in southern California applying for criminal law jobs that required MDT, found that 60% of students consumed spice, this included students trying to apply to the military or who are under correctional facilities supervision, and their main reason for using spice is because it did not show on the MDT even though they preferred cannabis. The study concluded that the drug policies of the USA, such as the illegalization of marijuana on a federal level, and the large scale implementation of drug tests is causing the increase in spice and other NPS use.[140]

Many routes had been reported for the smuggling of drugs in to prisons, such as social visits which are believed to be the most common route, new inmates arriving into prisons, throwing items with weights, such as coins and car tire bolts, over the prison wall (throw-overs), corrupt prison officers, and more recently drones flying into prisons with prisoners using hooks to pull in the suspended goods. A drone carrying class B drugs, NPS and mobile phones was recently captured on CCTV at Wandsworth Prison.[139,142] Reports from other countries in Europe have also shown the spread of spice in their prisons. A Slovenian study revealed that 54.5% of inmates aged between 18-35 had used synthetic drugs, with spice being the most popular. The study also reported that at least a third of the users had experienced side-effects.[143]

For the reasons listed above and the continuous news reports from across the UK about spice incidents in prisons, it is unlikely that this problem will come to an end anytime soon. To tackle such a complex issue, a harm reduction approach is required that spreads awareness among prisoners of the dangers of SCA. Additionally, incorporating new analytical techniques into the MDT might help in the accurate detection of SCA and their metabolites, ultimately leading the prisoners to stop abusing this class of drugs (or choose to go back to cannabis).
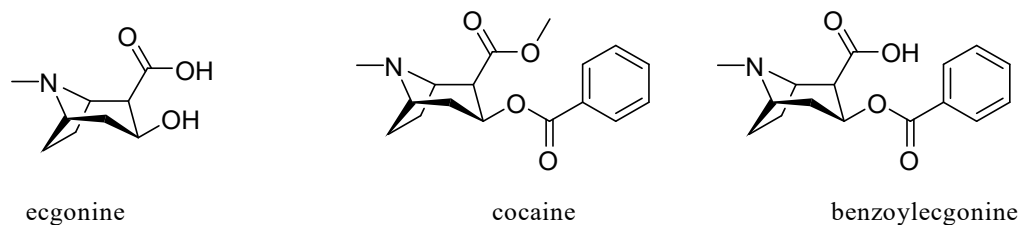
1.7 Cocaine

The high profile of cocaine in the media, its role in human suffering and cost to countries are both perceived and documented. Horrific stories of addicts, people's lives destroyed, murder, and impacts on economies are all well documented in the literature.[144,145] People outside South America became aware of cocaine with the development of industrial scale production methods related to the drug.

Cocaine is a natural product alkaloid occurring in the leaves of *Erythroxylum coca*, which is endogenous to the Andes mountains in South America that span e.g. Bolivia, Columbia, Ecuador, and Peru (Figures 15 and 16).[146] It was perceived in ancient Incan civilizations as a gift from their gods. Only the privileged would be allowed to inhale it and participate in religious ceremonies that were considered as ritualistic or for treating the ill, and it was either smoked or chewed.[147] Peruvian mummies have been discovered with coca leaves in their mouths, which reveals how established is the ancient use of this plant. After realizing its potential, the Spanish used to supply the conquered natives with coca to boost their stamina and reduce their appetite while working in silver mines.[147]

German chemists first isolated cocaine in the 1850s, and then an improvement of the extraction was made by Albert F. E. Niemann in 1859 who noted its numbing properties. These were exploited in 1884 when cocaine was used as a local and general anaesthetic, with Karl Köller claiming that discovery.[148] Cocaine had been used for the making of wine such as the Vine Mariani which is a mixture of alcohol and coca leaves extract prepared by soaking coca leaves (60 g) for ten hours in wine. The resulting drinks contained less than 50.0 mg of cocaine in two glasses. Others made soft drinks and tonics such as the famous Coca-Cola drink created in May 1886 by pharmacist Dr John S. Pemberton in Atlanta, GA, USA, with many recipes containing different amounts of cocaine. The original 1886 recipe contained coca leaves with approximately 9 mg of cocaine in a glass of Coca-Cola (with caffeine from the Kola nut of evergreen trees in the genus *Cola*), until 1903, when the fresh leaves were substituted with used ones (cocaine rapidly deteriorates in aged coca leaves). Furthermore, cocaine was found in tonic drinks that could be obtained without a prescription in the USA

until 1916. The problems of the decomposition of the leaves during shipment was overcome by Parke-Davis chemists by using on-site semi-refinement of cocaine, resulting in higher concentrations of cocaine and a cheaper price. Sigmund Freud contributed to the increased popularity of the drug when he tried it and published its stimulating mood-lifting effects.[146,148]

ecgonine   cocaine   benzoylecgonine

Figure 15. Ecgonine the natural precursor of cocaine, cocaine and its primary metabolite benzoylecgonine.


Figure 16. Cocaine growing and cultivation regions among major producing countries.[149]

Columbia and Peru are responsible for most of the cocaine exported to the USA. The extraction of cocaine is by harvesting fresh leaves that contain the highest amount of cocaine in the coca plant, followed by soaking in hexane until a thick paste is formed. Finally, salting out using hydrochloric acid and packaging of the powder, the hydrochloride salt of cocaine which can be administered by snorting or intravenous injection. On the other hand, the free base is formed by the addition of ammonia to the cocaine hydrochloride in water, followed by dissolving in ether and evaporation. Unlike the hydrochloride salt, the free base has a low melting temperature, and therefore can be smoked, but there are many safety concerns such as the flammability of remaining processing residues, e.g. ether, that caused many accidents and fatalities due to its combustion.[143,150]

Crack cocaine (the free base) is converted from the hydrochloride salt by mixing it with aqueous baking soda and heating, resulting in decarboxylation yielding lumpy rocks, that give a popping or cracking sound when smoked. This free base has a low melting point making it suitable for smoking, but in using water in the manufacturing it is without the risks associated with the residual organic solvents above.[143] Between the mid-1970s and mid-1980s the USA witnessed an explosion of cocaine on the streets. Initially, in the form of powder hydrochloride salt, reaching a peak of 25 million American users in 1985, followed by a gradual downward trend in its use. Unfortunately, the wave of crack cocaine swept across the USA with cheap prices of $5 per rock expanding the market for this previously upper-middle class drug to include minorities and marginalized groups. This expansion was coupled with unprecedented violence.[151] All forms of cocaine possess identical pharmacology, increasing dopamine indirectly by acting as inhibitors of the dopamine reuptake monoamine transporter. Pharmacokinetically, cocaine has fast absorption and distribution, with the form of drug (hydrochloride, crack) and consequently the route of administration resulting in more abuse potential for crack cocaine as a result of its more instant effect.[151,152]

United Nations drug report on cocaine (2010) revealed that there are approximately, 16-17 million cocaine users worldwide with an estimated 470 tons shipped to North America, with North America and the European Union (EU) combined making up 80% of the world

cocaine market (Figure 17).[153] The European Monitoring Centre for Drug and Drug
Addiction (EMCDDA) reported 3.5 million European users of cocaine. The drug accounts for
9% of seizures of all classes of drugs, equating to 69.4 tons estimated to be worth 5.7 billion
EUR.[39] In the UK, more than half of the class A drugs seized in 2015/2016 was cocaine.
Crack cocaine seized showed an increase of 14% in 2015/2016 compared to the previous
year.[154]
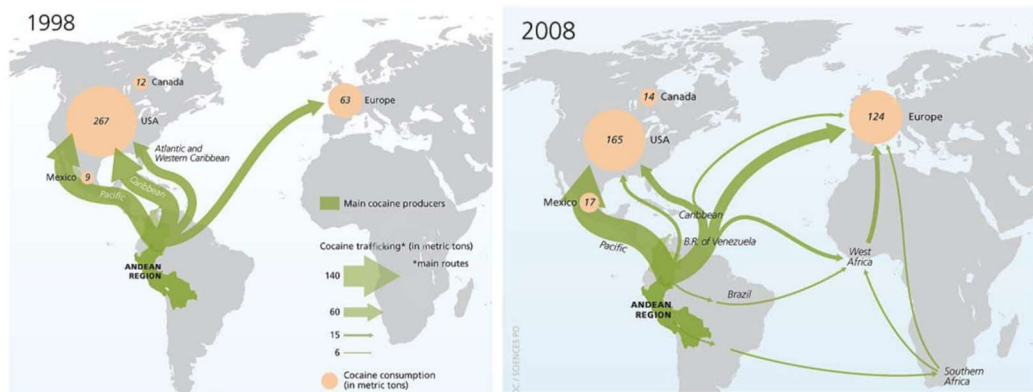
Figure 17. Quantities of South American cocaine and shipping routes to different areas
around the world.[153]

Figure 18. Cocaine seized disguised as wooden pallets.[155]

A big blow to organized crime came with the 2015 seizure of 1.4 tons of cocaine in
the port city of Valencia, Spain.[155] The most striking feature of this drug bust is not the sheer
quantity of the amount in one seizure, but the way that the drugs were concealed. The cocaine
was in the form of pallets, apparent wood pallets used for shipping and the loading of
shipments (Figure 18). Moreover, an additional amount of cocaine, compressed and moulded

in the form of BBQ charcoal briquettes, was also seized in the same shipment.[155] This is

considered one of the major seizures in Europe similar in magnitude to the 23rd of April 2015

North Sea bust of £500,000,000 worth of cocaine on board a Tanzanian registered ship by the

British Royal Navy with the aid of local and international agencies.[156] Additionally, men of

different nationalities from Britain, Peru and Dubai were arrested in connection with the

shipment that came from Colombia to be delivered to a charcoal factory which the authorities

in Spain believe to be a front for the distribution of the drugs to Europe. It is also believed

that the charcoal factory is the location where the cocaine from the pallets and compressed

charcoal briquettes was to be extracted.[157] According to the Daily Mail online, the

involvement of 6 British men might indicate that the shipment was intended to be distributed

in the UK and more specifically Liverpool.[158]

Clearly drug manufacturers and distributers are going to great lengths to smuggle

drugs in very sophisticated and clever ways to by-pass border check-points undetected. Even

though this drug bust is considered a major setback to organized crime in Europe, it will

undoubtedly cause the price of cocaine to increase and that might also influence (reduce) the

purity of the drug, for example increasing the presence of benign cutting agents such as

sugars or the more dangerous pharmaceutically active drugs e.g. benzocaine, ephedrine, and

levamisole.[70,71] Illicit drugs are well known for being cut with adulterants or cutting agents.

These agents should not be confused with excipients found in pharmaceutical preparations

that are used to bind the drug e.g. cellulose. Common cutting agents used for cocaine from

the years 1991-1996 in the UK are: sugars, paracetamol, caffeine, benzocaine, and procaine

with a mean cocaine purity of 85%.[159]

Recently, the Maritime Analysis and Operations Centre-Narcotics (MAOC-N)

conducted an operation close to the coast of Portugal where £200,000,000 worth of cocaine

weighing approximately 3.7 tons was seized aboard a tug boat. There was much media

speculation about the destination of the shipment, but officials believe that it was destined

either for Europe or the UAE.[160] Pure crystalline cocaine and its free-base crack are

continuing to arrive in the EU by the ton. Free samples are causing a rise in crack addiction.

1.8 Phenethylamines and cathinones testing at music festivals

Drug testing at music festivals is a controversial issue nowadays. The debate includes politicians, music festival organizers, drug analyst experts, harm reduction specialists, police forces, and not least of all music festivals attendees most of whom are young people. It is well known that drugs are popular and trendy at music festivals and night clubs, especially at rave scenes. One study revealed that of young people aged between 16-29 attending dance scenes, one in five intended to take drugs which might increase the pleasure of the experience.[161] By the end of 2017, organizers of six music festivals had implemented on-site drug testing including the Reading and Leeds music festivals. This number is expected to rise, though the UK biggest music festival (Glastonbury) still has a firm stance that drug use of any kind is illegal and that police officers on site will apprehend any person caught with drugs on them.[162,163] The Royal Society for Public Health (RSPH) is recommending on-site testing. It is supported by 95% of festival attendees and will help in harm reduction of the growing drug problem at music festivals. One in five of the users at the Secret Garden Party and Kendal Calling festivals chose to dispose of their drugs after receiving the results of their drugs' contents analysis.[164]

The first to implement on-site testing at music festivals was in Cambridgeshire, where the charity responsible for the testing, the Loop, coordinated with police officials, offering a 10 minutes harm reduction service to festival goers to test their drugs, with the main concern among festival organisers and goers being high strength MDMA tablets.[165] Additionally, Loop officials stated that more than 80 substances monitored are a cause of concern.[165]

Prior to on-site testing, drug analysts used to rely on amnesty bins situated at major music festivals and dance clubs for the analysis and to educate attendees in harm reduction awareness. Methods used by the forensic company TIC TAC rely on coupling FT-IR and GC/MS to create a drug database for the analysis of the disposed sample, which gave insight into some of the drugs used in such venues. However, some critics argued that these drugs are disposed of and do not represent the actual drugs of choice. Nevertheless, analyses by

Kenyon et al.[166] revealed that cocaine is the most used drug powder and that most of the tablets used are MDMA tablets.[166]

The main drive behind this trend of on-site testing is intoxications and deaths among young people in general and music festivals goers in particular. MDMA causes euphoria and excitation, but also potentially serious side-effects such as hyperthermia (increase in body temperature), rhabdomyolysis (muscle injury) and significant dehydration. The availability of high purity MDMA, combined with the use of the Dark Web to buy such MDMA make it more difficult to tackle the issue. Van Hout and Hearne[167] shed some light on the use of the Dark Web also known as online cryptomarkets such as Silk Road, Alphabay and Valhalla for the purchase of NPS and illicit drugs that can only be accessed through TOR browsers that conceal the identity of the purchasers. Their study explored the dynamics of two such online markets (Alphabay and Valhalla) in the second quarter of 2016 by searching for NPS under seven categories: cathinones, stimulants, opioids, cannabinoids, dissociative, hallucinogenic and other non-categorized drugs, revealing that the buyer is well informed regarding harm reduction and each vendor's reputation. Moreover, the study revealed a rise in demand for GABA activating substances and the poly-drug use of NPS, along with mainstream drugs such as MDMA. Although, in a sample of 50,000 individuals, only 10% buy their MDMA from the Dark Web.[168] Nevertheless, the main issue still remains as the drug buyer currently has no guarantee of the type, purity (adulteration) or the dose of the drug. Wood et al.[169] concluded in their retrospective study using the UK National Poison Information Service (NPIS) with regards to the reporting of toxicity in hospital A&E Departments, coupled with urine drug testing results, that poisoning from other stimulants such as amphetamine is not as significant as MDMA poisoning.

The UK MDMA hospitalizations and fatalities receive significant attention in the main stream media. A man died and four are in critical care in Rochdale after reportedly taking a crystalline form of MDMA known locally, according to police sources, as "Pink Champagne" or "magic".[170] Two weeks prior to the Rochdale incident, in the Sheffield area, a 22 year old student died after taking an ecstasy tablet.[171] Furthermore, a 15 year old boy

died and two others were hospitalized after taking ecstasy at a youth disco event in Plymouth.[172] These are just some fatalities and hospitalizations from late May to late June 2017. Another troubling incident is the appearance of teddy-bear shaped ecstasy tablets that could possibly attract younger people to experiment with them. Indeed, three 12 year old girls were hospitalized in Salford after taking these tablets, having been told that they were sweets.[173] Overall, in England and Wales, deaths due to ecstasy have maintained a generally increasing trend, only fluctuating minimally with the exception of the years 2010 and 2011 where, in the latter, deaths due to ecstasy dropped by 50% compared to 2009 (Figure 19).[174] One possible explanation for this drop is the 2008 seizure of enormous amounts of the MDMA precursors safrole and isosafrole (Figure 3).[37]
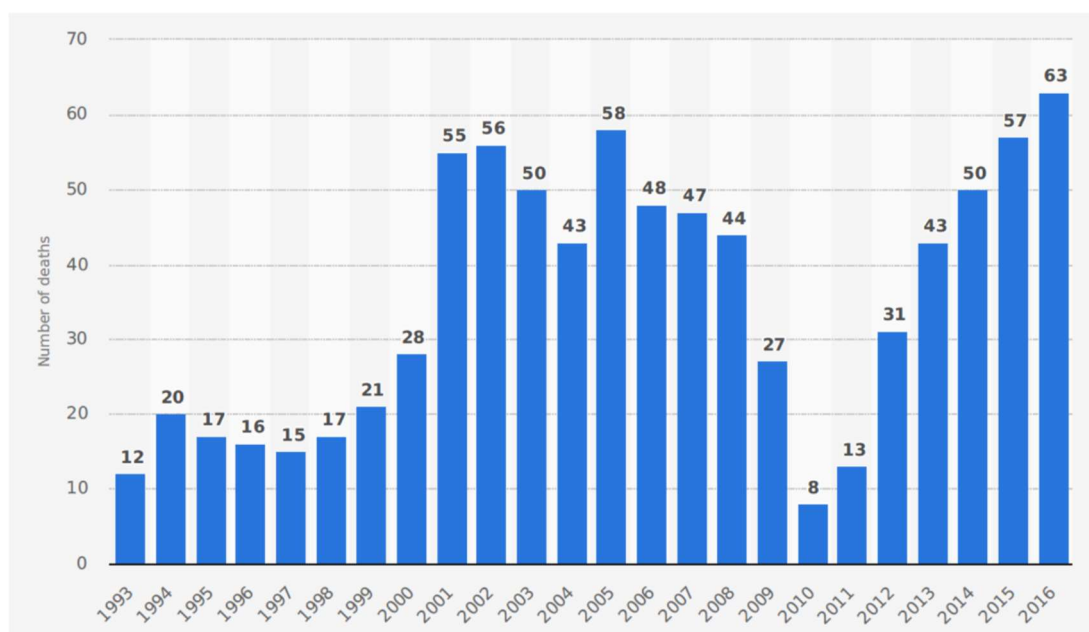
Figure 19. Number of MDMA deaths in England and Wales, 1993-2016.[174]

Even though their number is not anywhere near as high as deaths from cocaine and opioids, deaths from so-called legal highs including cathinones and phenethylamines have increased between 2004 and 2013, with a 3-fold increase in the number of deaths between 2011 and 2013.[175] A three year review over 2010-2012 of deaths and intoxications resulting from NPS found that the polydrug trend is common in fatalities involving NPS such as

mephedrone (4-methylcathinone), flephedrone, methiopropamine and many others, with mephedrone being the NPS most frequently found.[176] In 84% of the deaths, other drugs were also found, in order of decreasing frequency: alcohol, antidepressants, cocaine, amphetamines, opioids, benzodiazepines, and cannabis, with a worrying combination of stimulants such as amphetamines and cocaine which could result in serotonergic toxicity (serotonin syndrome) due to the monoamine transporter activities of those drugs. Another perhaps interesting, certainly macabre, finding of their review is that most of the deaths resulting from cathinones ingestion were from hanging.[176]

A study examining deaths among music festivals goers, using published scientific literature and news reports, found that 75% of non-traumatic deaths at music festivals are due to drug overdose.[177] A survey conducted for self-reporting NPS use on 682 attendees aged between 16-25 at electronic dance music festivals in New York (2015), found that 35% reported the use of NPS including cathinones, with methylone being the most popular cathinone and 2C-I the most popular phenethylamine NPS. The survey also highlighted the multidrug use of MDMA with other NPS and its risk factors for intoxication and possibly death.[178] In 2013, two deaths occurred at a dance music festival in New York. This triggered an investigation by the US Department of Health and Mental Hygiene (DOHMH) which identified 22 cases of intoxication, 17 of them tested positive for MDMA and other drugs, 11 of them tested positive for the cathinone methylone. Moreover, toxicological analysis on both deaths revealed MDMA in one case and MDMA plus methylone in the other.[179] The association of MDMA and cathinones has also been documented in another toxicological (blood, urine and oral fluids) study in 396 individuals at dance scene festivals in the USA, where 75% of the participants tested positive for a drug or alcohol, and of those, 36% tested positive for NPS and/or MDMA. Furthermore, methylone was the most detected drug in blood and urine samples (n = 34), while ethylone was the most detected drug in oral fluids (n = 54). Also, ethylone was implicated in deaths in nine other cases.[180,181]

The issue remains that other legal drugs such as tobacco and alcohol kill many more people than MDMA and cannabis which are illegal. Lung cancer was the leading cause of

death in the UK in 2014 with 98 deaths every day and 80,000 deaths that year attributed to smoking.[182,183] It is believed that smoking (tobacco) cost the NHS £2.7 billion in 2006, while the revenues were £8.1 billion.[184,185] Additionally, in 2015 there were 8,758 deaths related to alcohol with an estimated annual cost to the NHS of £3.5 billion.[186,187] Moreover, the socioeconomic impact of alcohol is evident in the 491,000 violent crimes recorded in the year 2015/2016 making up 40% of all violent crimes.[188] Furthermore, the increase in the consumption of alcohol is directly proportional to the incidence of cirrhosis which ranks third in the premature cause of deaths in the UK, with 1 million annual admissions to hospitals as a result of disorders caused by alcohol.[189] Professor David Nutt used various examples of legal activities that cause more annual harms and mortalities than MDMA, when he stated that horse riding caused more deaths (10 annually), more accidents (over 100 road traffic accident annually) and more injuries (350 annually). Additionally, Nutt criticised the media for eliciting fear in the public, an example of that is the reporting of all (100%) MDMA deaths each year compared to reporting 1 out of 250 deaths for paracetamol.[190]

The debate around this issue has been divided between advocates and critics. People for the on-site music festivals testing see it from a harm reduction angle and that it could deter users, in some instances, from using. Even though some data show festival goers are positive and responsive toward the testing issue as stated by The Royal Society for Public Health (RSPH) and other research,[191] other studies have shown a higher percentage (27%-42%) of people attending music festivals choosing not to use drug testing. [192] Additionally, one of the reasons that some are against such testing is purely analytical. Some argue that the on-site testing is not equipped to identify and quantify, with a high degree of safety, the drugs involved. This might result in life threatening false-negative results, or inaccurate dose quantitation, that could be problematic, e.g. in the case of high dose MDMA tablets. Furthermore, some of the techniques, e.g. reagent colour testing, may fail to identify novel compounds. The method of chipping off part of the tablet for its identification is not good practice, because illicit manufacture of drug tablets may result in a non-uniform distribution of the active drug in the tablet, potentially affecting the analytical results.

HPLC and GC used on-site at festivals and clubs will require reference standards to be used in the drug libraries for detection. This is a problem encountered in the most sophisticated drug laboratories all over the world in accurate NPS analysis.[192] Added to that, the problem of multicomponent drugs (polypharmacy) will complicate the analysis, as some of the peaks appearing in the chromatogram could overlap in closely related analogues of NPS. There is also the limitation of some analytical instrumentation such as FT-IR and near IR when used to investigate samples which are complex mixtures.

Drug testing at music festivals and night-clubs is a commendable work, that is aimed toward protecting young people from illicit drugs including NPS. Nevertheless, many drugs exist in a complex mixture of different groups of illicit drugs such as MDMA, cathinones e.g. ethylone, methylone and/or other groups of NPS. Their detection requires accurate validated techniques and instruments that can reliably identify and quantify such samples that do currently exist in music venues. Complex mixtures require techniques such as 2D NMR spectroscopy for robust analysis. Trace amounts of impurities, cutting agents, and potent drugs that exist in µg amounts require sensitive techniques such as hyphenated-MS for analysis whether qualitative or quantitative.

In the following chapters, demonstrations are given of the complexity of samples surrendered or seized from different dance venues and HMP Bristol. The analyses rely primarily on 1D/2D NMR spectroscopy and MS techniques. Identification and quantification of illicit drug samples and their frequency of coexistence with other NPS will be revealed. What is the dose of MDMA in tablets that were recently in circulation, at least in the South West of England? A q-NMR analysis method has been developed to answer this question. The method has been cross-validated with both UHPLC and UHPLC/MS.

Chapter 2. Phenethylamines and cathinones

2.1 Introduction

3,4-Methylenedioxymethamphetamine (MDMA, ecstasy) is considered to be by far the most popular of the phenethylamines in Europe, as demonstrated by the amount seized, 5.3 million tablets and 295 kg of powder in 2016.[193] This popularity is the result of many factors such as the high purity (higher than seized amphetamine and methamphetamine) and the low price of only 6-11 Euros/tablet.[193] Even though considered as a phenethylamine, the presence of the methylenedioxy group in MDMA results in altered pharmacology compared to amphetamine and methamphetamine.[31]

Cathinones are the second most popular class by seizures among NPS (after SCAs) and the leading NPS available in the powdered form.[193] They are based on the natural product *S*-cathinone, with many positions along the chemical structures that can be altered with different alkyl substituents resulting in a large number of derivatives, e.g. methylenedioxy substituents giving rise to analogues such as butylone, ethylone and methylone.[28,194] The pharmacology and dose of cathinones and MDMA are of importance, especially in the context of analytical and forensic toxicology. Cathinones elicit their action on dopamine levels either by inhibiting reuptake by pre-synaptic dopamine transporters or directly by causing the release of dopamine. This dual effect is believed to be the reason for their strong action on the user/abuser. On the other hand, MDMA works primarily on serotonin receptors (5-HT-R), but also possesses dopamine release action.[28,194] Moreover, mephedrone is a more potent inducer of locomotor activity in rodents than MDMA.[28] Therefore, taking both types of drug can lead to serious consequences such as tachycardia, hypertension, hyperthermia and dehydration.[195,196]

The association of cathinones with each other and with other NPS has been described by *Zuba et al.*[197] Using LC, GC/MS and NMR, they showed that the most common cathinones detected were 3,4-methylenedioxypyrovalerone (MDPV) and butylone, found

with piperazines. Toxicological identification of post-mortem cases showed MDMA with methylone, and MDMA with ethylone.[180,181]

Analytical techniques used for the detection and quantification of phenethylamines and cathinones depend primarily on chromatographic methods coupled to MS (UHPLC/MS and GC/MS).[9] Although considered as gold standards in the pharmaceutical industry and in forensic analysis, each technique has its limitation and drawbacks. For example, the failure of the UHPLC method in detecting impurities with no chromophore that are associated with MDMA and cathinones will affect the outcome of the analysis. Additionally, the high polarity of some of the components present in the seized samples may result in poor peak resolution and even no retention on the UHPLC column.[198] Poor ionization of some of the impurities will hinder the identification process using MS methods, while GC analysis will require derivatization to give sharp peaks in the chromatogram that are suitable for integration to achieve quantitative analysis. Moreover, a derivatizing agent is required to provide a distinctive mass ion, especially molecular ions that are at best weak due to the high energy collision (70 eV) of the Electron Impact (EI) in GC analysis. The main issue affecting chromatographic techniques is the need for an authentic reference compound for the targeted drug, which is either expensive or simply not available in the case of many NPS.

NMR spectroscopic analysis provides a great opportunity for the characterization and quantification of complex exhibits containing multiple components of NPS and illicit drugs. 1D (^{1}H, ^{13}C, DEPT) and 2D (COSY, HSQC, HMBC, H2BC, NOESY) NMR allow the definitive structural elucidation and assignment of the compounds in the mixture. Unlike MS and chromatographic techniques, NMR does not require a reference standard, a particular problem with NPS. NMR also does not require interaction with a chromatography column that could result in many drawbacks such as retention, carry-over that requires injecting a blank sample prior to the next analysis. Furthermore, the time-consuming preparation of mobile phases and chromatographic method development makes NMR a more attractive method.[198,199] With the development of high-field NMR instruments, sensitivity is improving and that is reflected in quantitative NMR experiments with lower amounts of analyte. ^{1}H

NMR is inherently quantitative, as the intensity of the signal being integrated is directly proportional to the number of protons represented by the signal, with the exception of some exchangeable protons (OH, NH, SH). This is only true when certain parameters are met such as the relaxation delay (T_1) of the signal which can be measured using an inversion recovery pulse sequence of the signals of the analyte. Leaving $5xT_1$ to recover the magnetization to 99.3% of its size will allow accurate integration for optimum quantitative results, given an appropriate number of scans to provide an acceptable signal-to-noise (S/N) ratio.[199,200]

The first q-NMR experiment was performed by Jungnickel and Forbes,[201] and also by Hollis 1963,[202] where both research groups employed the molar ratio of the integrated protons for the quantitative analysis of a number of compounds including APIs, e.g. paracetamol, phenacetin and caffeine.[199]

Another q-NMR experiment was developed and reported in 1997 by Akoka and co-workers,[203-205] known as Electronic Reference To access In vivo Concentrations (ERETIC) which does not rely on an Internal standard (IS) present in the solution, but instead uses an electronic signal of a separately calibrated real standard that is integrated into the probe during aquisition.[200,206] QUANTAS (QUANTification by Artificial Signal),[207]is another q-NMR protocol which is similar to ERETIC, but the artificial signal is integrated during processing and not acquisition.[206] Electronic methods for NMR quantification were developed due to the absence of an ideal IS, as solubility and spectral overlap has always been an issue, especially in the quantification of large molecules such as proteins.

Many reports on the increase of purity and overdose cases of MDMA have surfaced and made news headlines in some cases.[35,39,170] Most of the published literature regarding MDMA tablet analyses rely on hyphenated chromatographic techniques,[9,198,208] and no recent analysis of MDMA tablets in the UK has been published. Furthermore, no validated q-NMR method has been applied to MDMA tablets in the UK, thus warranting an investigation.

GC-FID analysis of phenethylamines and related cathinones mostly suffer from non-reproducible, broad and tailing peaks due to poor interaction with the stationary phase. This is most likely due to the compounds' high polarity as a result of the presence of an amine in

their structure. Therefore, derivatization is essential, especially for consistent integration that will result in accurate quantitation.[209,210] Additionally, depending on the derivatizing reagent used, the formation of distinctive molecular ions and fragments is helpful in confirming the identity of the target compound. This is a problem frequently encountered in NPS GC/MS analysis where the absence of a mass ion or only a weak mass ion peak will hamper definite identification of the analyte. The non-distinctive nature of other fragments, including the base peak, will negatively affect any definitive identification of the NPS analyte.

In this chapter, qualitative and quantitative analysis of multicomponent MDMA with other NPS, such as cathinones, phenethylamines, and piperazines, will illustrate the complexity of the samples with definitive identification using NMR and UHPLC/MS/MS using a HILIC column. Additionally, a cross-method validation of q-NMR using an internal standard (IS) method is used to assay different MDMA tablets seized from night-club venues in Bristol. Validation is by UHPLC and UHPLC/MS using d_5-MDMA as an IS for the latter. Furthermore, derivatization followed by GC/MS and ESI-MS analysis of selected cathinones and phenethylamines is performed using 2,2,2-trichloroethyl chloroformate. Derivatization of ethylone and 2C-B have not been published before.

2.2 Experimental

2.2.1 Chemicals and samples

NMR grade solvents D_2O 99.9%, CD_3OD 99.8%, DMSO-d_6 99.9%, and TMSP-2,2,3,3-d_4 98.0% were purchased from Cambridge Isotope Laboratories (UK, Goss Scientific). Methanol and water for UHPLC and UHPLC/MS analysis were Lichrosolve Honeywell LC/MS grade, and ethyl acetate 99.9% AcroSeal were purchased from Fisher Scientific (UK). ±-MDMA 1.0 mg/mL in methanol solution reference standard, ±-MDMA-d_5 1.0 mg/mL in methanol solution reference standard, N-[3-(trifluoromethyl)phenyl]piperazine hydrochloride (TFMPP) 99%, 1-(3-chlorophenyl)piperazine hydrochloride (m-CPP) 99%, maleic acid (MA) 99.94% and dimethyl sulphone (DMS) 99.96% are TraceCERT certified

for quantitative NMR analysis, acetanilide (99%), 2,2,2-trichloroethyl chloroformate 98%, and trifluoacetic acid (TFA) were purchased from Sigma-Aldrich (UK).

In-house reference standard MDMA was prepared by converting a seized sample into its free base, followed by purification by flash column chromatography using a mobile phase of dichloromethane (DCM) and 10% methanol, followed by HCl salt formation in aqueous hydrochloric acid (1M, one equivalent) to obtain MDMA HCl as a white powder.

Illicit samples (n = 195) were provided by the Drug Expert Action Team (DEAT), Avon and Somerset Constabulary, in sealed evidence bags containing numerous drug samples in different forms (capsules, crystals, powders, tablets and plant materials) in different packaging (small packs, magazine twists). Samples in small packs in the form of crystals and powders weighing between 50-250 mg were from different night-club venues in Bristol, while MDMA tablet weights ranged between 188-645 mg.

2.2.2 Sample preparation

For qualitative analysis, depending on the purity and complexity of the samples, between 10-30 mg were weighed using a Sartorius BP221S balance in a 1.5 mL Eppendorf tube, followed by dissolving the samples in either D_2O or CD_3OD. Samples were then vortexed until all contents were dissolved or centrifuged and the supernatant was transferred to a 5 mm NMR tube. For LC/ESI-MS analysis, a stock solution (1.0 mg/mL) of seized materials was prepared, followed by 100-fold dilution into a MS vial. For quantitative analysis, crystals and powders were weighed using a Sartorius analytical balance MC 5 followed by extraction with D_2O containing IS maleic acid (2.0 mg/mL) and 0.5% of TMSP-2,2,3,3-d_4 (1.0 mL) for NMR spectroscopic analysis.

For MDMA quantitative analysis, tablets of different sizes and shapes were photographed for documentation, followed by manual pulverization using a mortar and pestle. 10.0 mg of powder was weighed using a Sartorius analytical balance MC 5, transferring into a 7.0 mL glass screw neck specimen vial (Fisher Scientific), then extraction with D_2O (2.0 mL) containing maleic acid (1.0 mg/mL) as an NMR quantitative IS with

sonication for 30 minutes, filtration through a Sartorius Minisart® 0.2 μm filter followed by taking a final volume of 1.0 mL for NMR spectroscopic analysis. For UHPLC analysis, the sample was diluted 100-fold into a MS vial. Samples were quantified using a 6-point calibration curve 1.5, 3.1, 6.3, 12.5, 25.0, and 50.0 μg/mL prepared in UHPLC solvent. For UHPLC/ESI-MS quantitative tablet analysis, the sample was extracted with LC/MS grade water and diluted 10000-fold into a MS vial and spiked with MDMA-d_5 (500 ng/mL) as an IS. Samples were quantified using an 8-point calibration curve from 32.25, 62.50, 125.0, 250.0, 500.0, 1000, 2000, and 4000 ng/mL. Each concentration was spiked with IS MDMA-d_5 (10 μL of 25 μg/mL) to achieve a final IS concentration of 500 ng/mL. The response was calculated as the ratio of the area under the curve of the target compound to that of the IS.

The derivatization protocol is based on the work developed by Frison *et al*.,[209,210] with some modification. Prior to the analysis, samples were identified by 1D/2D NMR and ESI/MS. Seized samples (2.0 mg) of MDMA, mephedrone, and ethylone, and 10 mg of tablets containing 2C-B were placed in 1.0 mL micro reaction-vials (Sigma-Aldrich, UK), 100 μL of a 3:7 v/v mixture of derivatizing reagent 2,2,2-trichloroethyl chloroformate and ethyl acetate was added to the residue and heated to 80˚C in a reaction vial heating block for 15 min, followed by evaporating under a gentle stream of nitrogen, and finally it was reconstituted in ethyl acetate (100 μL), transferred into 200 μL polypropylene vials (Phenomenex, UK) and submitted for GC/MS and ESI-MS analyses.

2.2.3 Instrumentation

NMR spectroscopy

NMR spectra were recorded on a Bruker AVANCE III 500 MHz spectrometer, ^{1}H and ^{13}C frequencies are 500.130 and 125.758 MHz respectively. The probe was a variable temperature BBFO+ with three channels, temperature was 25˚C. Chemical shifts were referenced to 0.00 ppm for TMSP-d_4 or the HDO residual solvent peak at δ 4.76 (HDO) and are reported in ppm. Coupling constants (*J*, line-separations, absolute values) are rounded to the nearest 0.5 Hz and rationalised. Structural elucidation was achieved with 2D NMR

Correlation Spectroscopy (COSY) which shows 2-, 3- and sometimes 4-bond connection of protons as cross peaks. Heteronuclear Single Quantum Coherence (HSQC) shows direct connection between protons and their carbon, Heteronuclear 2-Bond Correlation (H2BC) which is an exclusive 2-bond experiment between protons and their neighbouring carbons, Heteronuclear Multiple Bond Correlation (HMBC) which shows 2-, 3- and rarely 4-bond couplings between protons and their neighbouring carbons, ^{15}N HMBC NMR which shows the two- and three-bond coupling of the ^{15}N to protons, NOESY (proton-proton through space interaction). NMR spectra were processed using Bruker TopSpin 3.5 and Mestralab Mnova 11.2. For quantitative ^{1}H NMR (q-NMR) analysis, the zg pulse sequence was composed of 3.18 s acquisition time, 16 scans, 50 s delay, 90° pulse angle, phase and baseline corrections were automatic while integration was performed manually.

ESI-MS infusion

Electrospray Ionization-Mass Spectrometry (ESI-MS) was conducted on a Bruker Daltonik micrOTOF in positive-ion mode on diluted samples (10 μg/mL in HPLC grade methanol). The mass accuracy of the $[M+H]^+$ and $[M+Na]^+$ ions is within 5 ppm of the required mass ion, unless otherwise stated.

UHPLC and UHPLC/ESI-MS

UHPLC calibration curve and samples quantitative analysis, was performed on a Dionex Ultimate 3000 UHPLC (Thermo Fisher Scientific, CA, USA) with a variable wave-length detector (λ = 210, 254, 280, 285 nm). Liquid chromatographic separation was performed using an Acquity UPLC BEH C18, 1.7 μM, 2.1 x 50 mm RP-column (Waters, Milford, MA, USA) with a flow rate of 0.3 mL/min, and an injection volume of 10 μL at 25°C column temperature. Mobile phase A consisted of water 0.1% TFA, mobile phase B was ACN 0.1% TFA. Gradient elution started with 1% B for 1.0 min, followed by a linear increase from 1.0 min to 100% B at 4.0 min and maintained for 1.0 min, followed by a decrease to 1% B at 5.1 min, where it was held for equilibration 2.9 min, total run time of 8.0 min. Data analysis used Bruker Data analysis 4.3, and Excel data analysis tool pack. QTOF-UHPLC-MS analysis was

conducted on a MaXis HD Quadrupole electrospray Time-of-Flight (ESI-QTOF) mass

spectrometer (Bruker Daltonik GmbH, Bremen, Germany), operated in ESI positive mode.

The QTOF was coupled to an Ultimate 3000 UHPLC (Thermo Fisher Scientific, CA, USA).

The capillary voltage was set to 4500 V, nebulizing gas at 4 bar, drying gas at 12 L/min at

220°C. The TOF scan range was from 75-1000 mass-to-charge ratio (m/z). Formic acid (FA)

0.1% was used for the mobile phase instead of TFA and the same gradient and conditions as

the UHPLC were used. For LC/MS/MS the in-source CID was set to 0.0 eV, with the

collision energy for TOF MS acquisition at 3.0 eV. The collision energy was set to a sliding

scale from 100 m/z at 14.0 eV, 500 m/z at 20.0 eV and 1000 m/z at 30.0 eV. For the analysis,

the actual collision energy was between 15.0-18.0 eV. For the HILIC UHPLC-ESI/MS

analysis, the column was a Kinetex 1.7µ 100A 100 x 2.1mm (Phenomenex, UK). Flow rate

was 0.4 mL/min, mobile phase A consisted of 50:50 ACN:water v/v with 10 mM ammonium

formate and 0.1% FA, while mobile phase B consisted of 95:5 ACN:water v/v with 10 mM

ammonium formate and 0.1% FA. Gradient elution started with 100% B until 4.0 min,

followed by a decrease to 0% B between 4.0-6.0 min and maintained until 8.0 min. followed

by an increase to 100% B from 8.0-8.2 min, followed by an equilibration for 4.8 min with a

total run time of 13.0 min.

GC/MS

Derivatized and non-derivatized samples were run on a Shimadzu GC-2010 GC-FID/MS

under the following conditions: full-scan mode 50-500 m/z, split mode ratio 1:20, with He as

the carrier gas with a flow rate of 40.0 mL/min. BPX-5 column (30 m x 0.25 mm, 0.25 µm

thickness) was used with the starting (0.5 min) oven temperature 50°C increased to 200°C at

30°C/min, then to 280°C at 10°C/min, and maintained for 7.5 minutes with a total run time of

21 min, except for ethylone where the temperature was maintained at 280°C for 21.5 min

with a total run time of 35 min.

Statistical analysis

Excel data analysis tool pack was used for the statistical analysis, using Anova single- and two-factor analysis for obtaining the p values.

2.3 Results and discussion

2.3.1 Coexistence of MDMA with Novel Psychoactive Substances (NPS)

In this study the association (formulation) of MDMA with other NPS will be presented, using spectroscopic and spectrometric assays. The complexity of the samples will be revealed with structural elucidation (1D/2D NMR and UHPLC/ESI-MS) and quantification using a fast, simple and accurate ^{1}H q-NMR of each of the components without resorting to tedious preparation and method development assays. Analysis of 195 seized samples, obtained through DEAT in the years 2015-2016, revealed 174 MDMA samples and a further 21 MDMA mixtures in different combinations (Figure 20). High dose MDMA is already a health concern; to find it associated with stimulant cathinones and other NPS is alarming.[169,211]
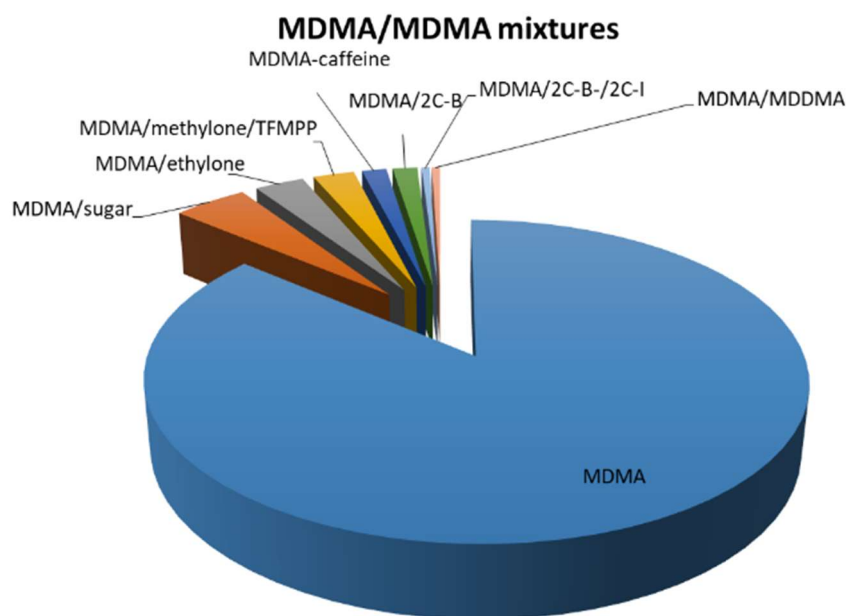

Figure 20. Pie chart revealing the proportion of MDMA and its association with other NPS and cutting agents (in n = 195 samples) using both NMR and ESI-MS analysis.

Samples of MDMA/ethylone mixtures in different ratios were identified and quantified using a combination of 1D/2D NMR and UHPLC/ESI-MS. 18 non-coinciding peaks were found in the ^{1}H NMR (see Table 2 and Figure 21).
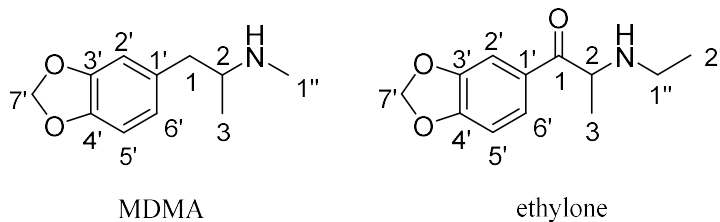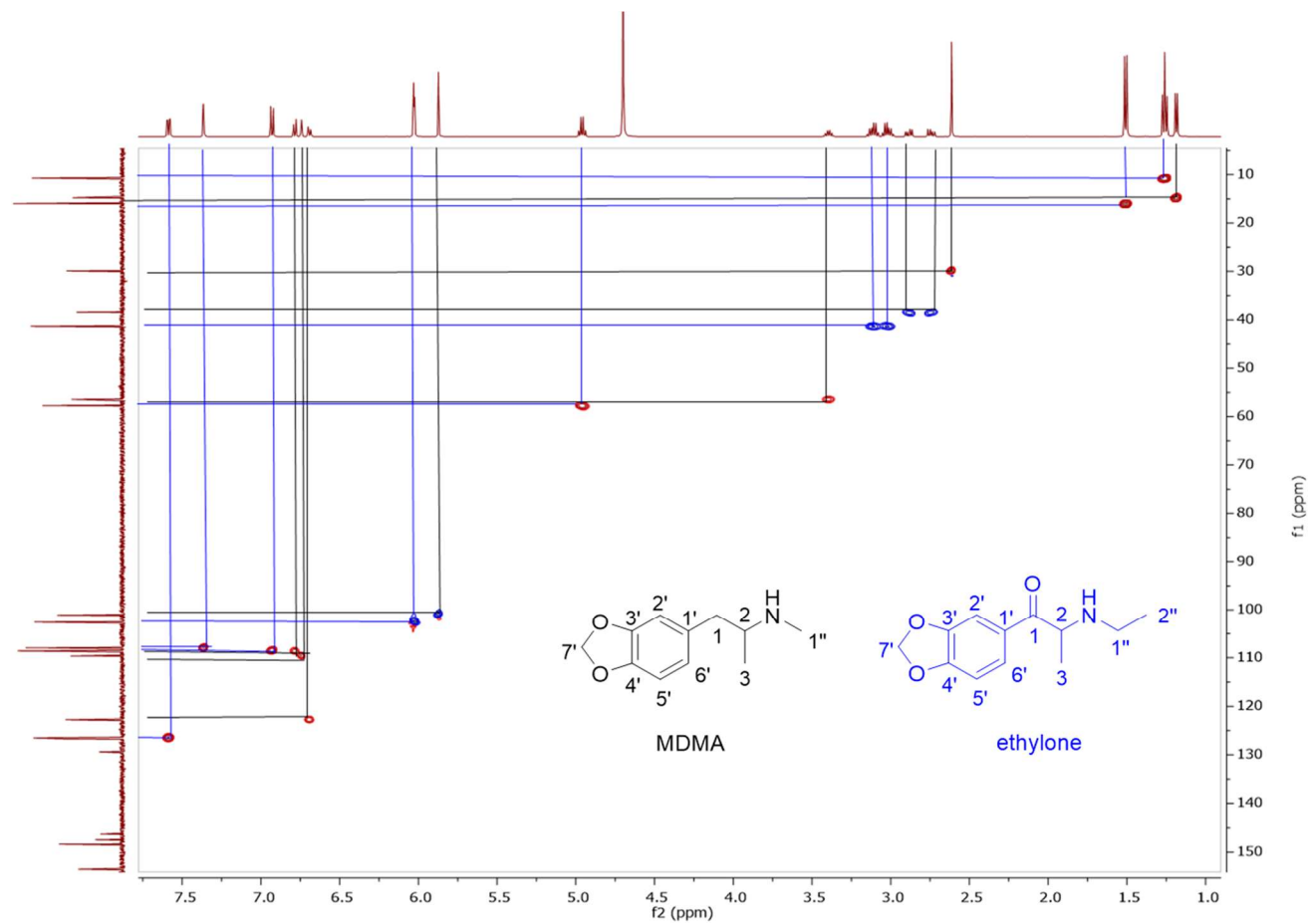

MDMA   ethylone

Table 2. ^{1}H and ^{13}C NMR (in D_2O) assignments of one of the MDMA plus ethylone mixtures.

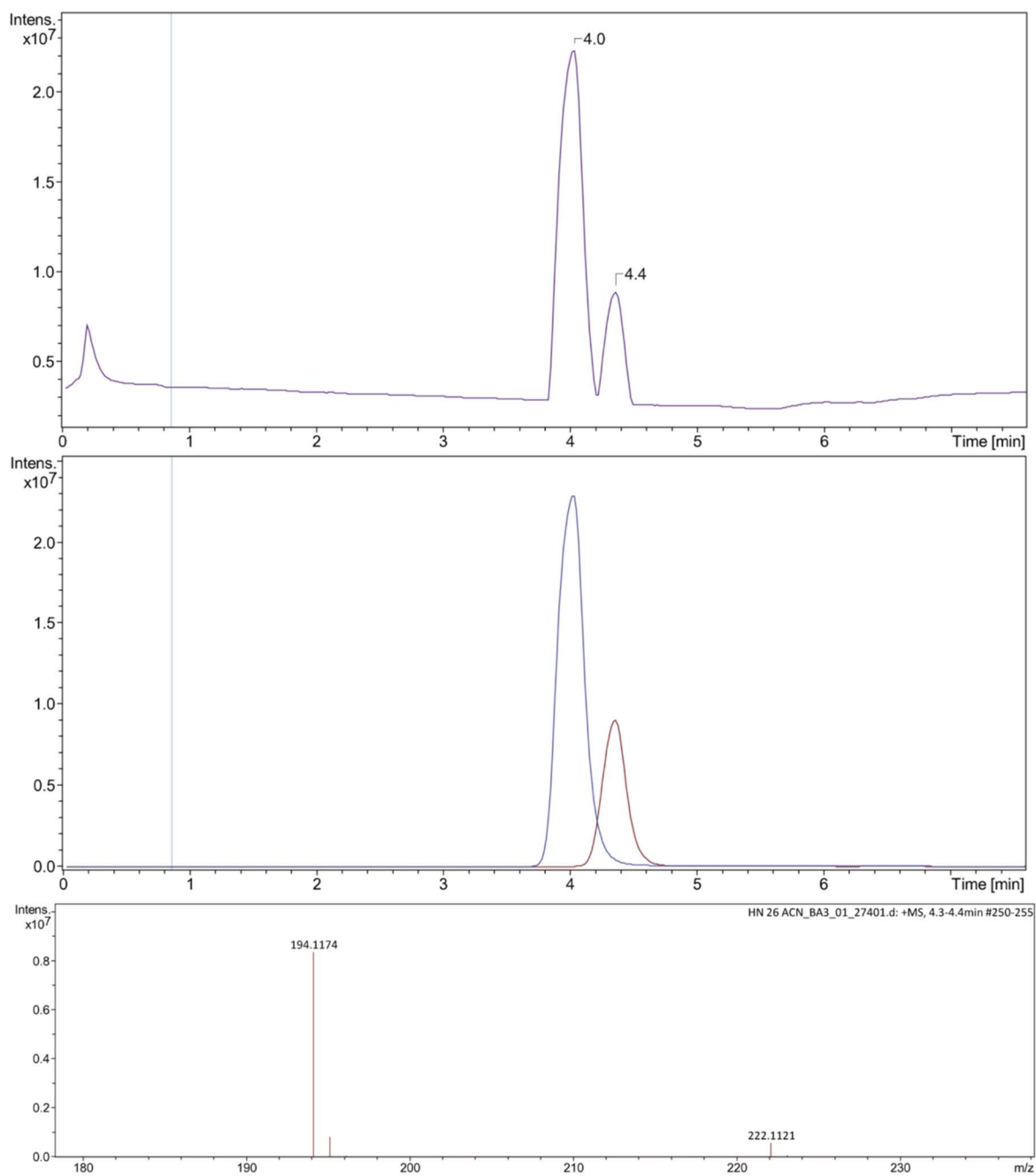| Position	MDMA		ethylone	
	[13]C	[1]H	[13]C	[1]H
1	38.4	2.75 1H, dd (14.0, 7.0) 2.89 1H, dd (14.0, 7.0)	195.3	-
2	56.4	3.39 1H, sextet (7.0)	57.7	4.96 1H, q (7.0)
3	14.8	1.19 3H, d (7.0)	16.0	1.51 3H, d (7.0)
1'	129.4	-	126.7	-
2'	109.6	6.75 1H, d (1.5)	107.9	7.38 1H, d (2.0)
3'	147.4	-	148.4	-
4'	146.2	-	153.5	-
5'	108.6	6.79 1H, d (8.0)	108.6	6.94 1H, d (8.0)
6'	122.8	6.69 1H, dd (8.0, 1.5)	126.5	7.59 1H, dd (8.0, 2.0)
7'	101.0	5.88 2H, s	102.6	6.03 1H, d (2.0), 6.04 1H, d (2.0) (AB)
1"	29.9	2.61 3H, s	41.4	3.02 1H, dq (12.5, 7.5) 3.11 1H, dq (12.5, 7.5)
2"	-	-	10.7	1.25 3H, t (7.5)
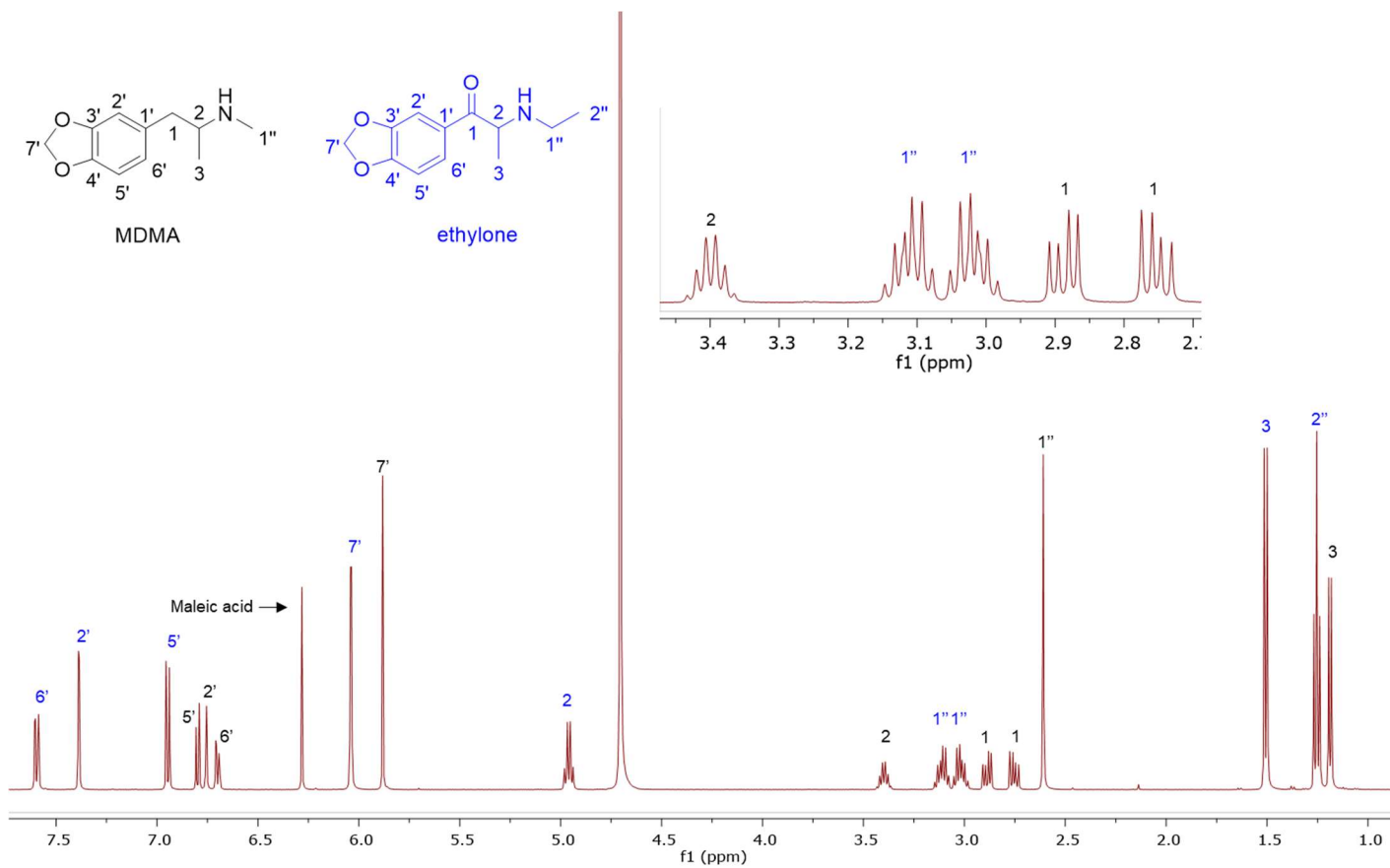
Figure 21. ^{1}H NMR (500MHz in D$_2$O) of MDMA/ethylone mixture

with MA as a quantitative IS.

Figure 22. HSQC of MDMA (black lines)/ethylone (blue lines) mixture,

the blue cross peaks indicate methylene protons, the red cross peaks indicate methyl and methine.

Two distinctive NMR spectroscopic features were observed between the 2 compounds in the mixture. The first is the quartet at 4.96 ppm of ethylone (β-ketone MDEA) at the α-position (H2), and the other is the chemical shift of the signals for the methylenedioxy, which in MDMA occurred as a singlet at 5.88 ppm. In ethylone its chemical shift was further downfield at 6.04 ppm with an apparent dd splitting pattern (AB system). In fact the signal is two doublets with a particularly small ^2J *geminal* value.[212] This separation of the two methylene proton signals can be interpreted as an effect of the (somewhat distant) chiral centre transmitted through the benzoyl carbonyl functional group. It is not seen in the MDMA ^{1}H NMR spectrum. HSQC analysis 2D dispersive powers allowed definitive structural assignments (Figure 22). In the LC/ESI-MS analysis of sample HN26, using a HILIC column allowed chromatographic base-line separation of the two components and molecular ion identification. Retention times for ethylone and MDMA were 4.0 min and 4.4 min respectively. The found $[M+H]^+$ for MDMA 194.1174 and ethylone 222.1121, for the required $C_{11}H_{16}NO_2$ 194.1175 (MDMA) and $C_{12}H_{16}NO_3$ 222.1124 (ethylone) (Figure 23). The analysis of high polarity cathinones and phenethylamines was efficient on a HILIC column.

Figure 23. Sample HN26 analysis on a HILIC column (top) Base Peak Chromatogram

(BPC), (middle) Extracted Ion Chromatogram (EIC), and (bottom) MS spectrum.
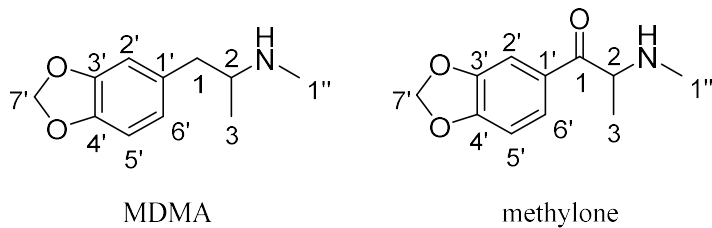
MDMA　　　　　　　　methylone

Table 3. ^{1}H and ^{13}C NMR (in D_2O) assignments of one of the MDMA/methylone mixtures.

	MDMA		methylone	
Position	[13]C	[1]H	[13]C	[1]H
1	38.4	2.73 1H, dd (14.0, 8.0) 2.87 1H, dd (14.0, 6.5)	195.2	-
2	56.4	3.39 1H, overlap with TFMPP 1′,2′	59.3	4.91 1H, q (7.0)
3	14.7	1.18 3H, d (6.5)	15.7	1.51 3H, d (7.0)
1′	129.3	-	126.6	-
2′	109.6	6.75 1H, d (2.0)	107.8	7.37 1H, d (2.0)
3′	147.4	-	148.3	-
4′	146.2	-	153.4	-
5′	108.6	6.79 1H, d (8.0)	108.5	6.94 1H, d (8.5)
6′	122.7	6.69 1H dd (8.0, 2.0)	126.5	7.58 1H, dd (8.5, 2.0)
7′	101.0	5.88 2H, s	102.5	6.03 1H, d (2.0), 6.04 1H, d (2.0), (AB)
1″	29.9	2.60 3H, s	30.9	2.69 3H, s
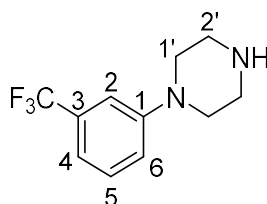
Table 4. ^{1}H, ^{19}F and ^{13}C NMR (in D_2O) assignments of TFMPP in the mixture.

| Position	[13]C	[1]H/[19]F
1	149.8	-
2	113.6, q ([3]J_{C-F} 3.5)	7.29 1H, t (2.5)
3	130.9, q ([2]J_{C-F} 32.0)	-
4	118.2, q ([3]J_{C-F} 3.5)	7.24 1H, dd (8.0, 2.5)
5	130.1	7.40 1H, t (8.0)
6	120.6	7.22 1H, dd (8.0, 2.5)
CF_3	125.1, q ([1]J_{C-F} 271.5)	-
1′	46.2	3.40-3.45 4H, overlapped with MDMA 2
2′	42.9	3.33-3.35 4H, overlapped with MDMA 2
[19]F observe		-62.50, s

Five samples containing a mixture of MDMA with methylone and trifluoromethylphenylpiperazine (TFMPP) in different ratios, from Bristol Police amnesty bins, were identified and characterized using NMR spectroscopy (Tables 3 and 4, and Figure 24) and ESI-MS. In this mixture, HSQC allowed assignment of overlapping proton signals by connectivity to their corresponding carbon resonances. For example, the 8 protons of piperazine (TFMPP) overlapped with the stereogenic centre methine sextet of MDMA at 3.39 ppm. However, they were assigned as (1′) 3.40-3.45 ppm 4H, m, and (2′) 3.33-3.35 ppm 4H, m in an authentic sample of TFMPP. COSY enabled the extraction of the coupled piperazine protons from the cross peaks. Another diagnostic feature of methylone is the proton chemical shift and coupling of the methine stereogenic centre quartet at 4.91 ppm and the ketone carbonyl at 195.2 ppm. HSQC and DEPT allowed the assignment, with high confidence, of the two closely placed signals of methylone in ^{13}C spectra of quaternary 1′ (126.6 ppm) and 6′ (126.5 ppm). ^{19}F-HOESY experiment allowed the differentiation between H4 and H6 of aromatic protons via their through-space interactions with the trifluoro group. HMBC allowed the differentiation of TFMPP protons 1′ and 2′ through 1′ connection to C1 quaternary carbon at 149.8 ppm. Distinctive ^{13}C splitting of the carbons one, two, and three bonds away $^1J_{C-F}$ 271.5, $^2J_{C-F}$ 32.0, and $^3J_{C-F}$ 3.5 Hz were observed (Table 4, Figure 25). Due to the low ratio of TFMPP in the mixture, the ^{13}C results were obtained from an authentic sample and compared with the mixture in the sample. NMR and MS were corroborated using authentic MDMA, methylone, and TFMPP.

LC/MS/MS analysis revealed the mass ions and distinctive fragmentation pattern for each component in the mixture. [M+H]$^+$ MDMA 194.1177 required for $C_{11}H_{16}NO_2$ 194.1175, methylone [M+H]$^+$ 208.0968 required for $C_{11}H_{14}NO_3$ 208.0968, and [M+H]$^+$ TFMPP 231.1108 required for $C_{11}H_{14}N_2F_3$ 231.1103 (Figure 26). In MDMA, loss of the methylamine from [M+H]$^+$ resulted in the formation of 163.0757 ion, and the formation of 1,3-dioxole-5-yl methylium ion at 135.0440, while the 133.0647 resulted from the loss of O=CH$_2$ of the methylenedioxy moiety, the 58.0652 fragment is the iminium ion. Methylone fragmentation is typical of cathinones with a methylenedioxy group.[213] Loss of water (190.0863), then loss

of methylamine from the parent molecular ion resulting in the 177.0544 ion, while the loss of

the methylenedioxy moiety gave rise to 160.0758 ion. On the other hand, the MS/MS trace of

TFMPP was less informative with only one fragment resulting from the opening of the

piperazine ring and loss of C_2H_5N.[213-215]
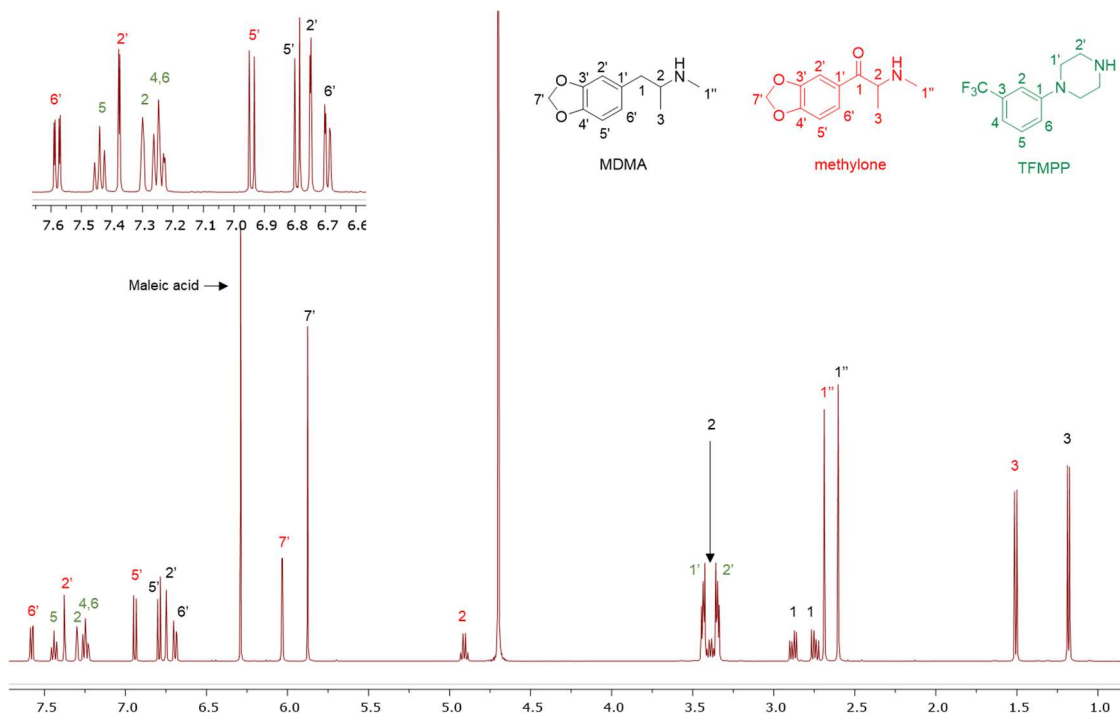
Figure 24. ^{1}H NMR (in D_2O) of a 3-component mixture, with MA as quantitative IS, and an

expansion of the aromatic area showing resolved protons of all components.
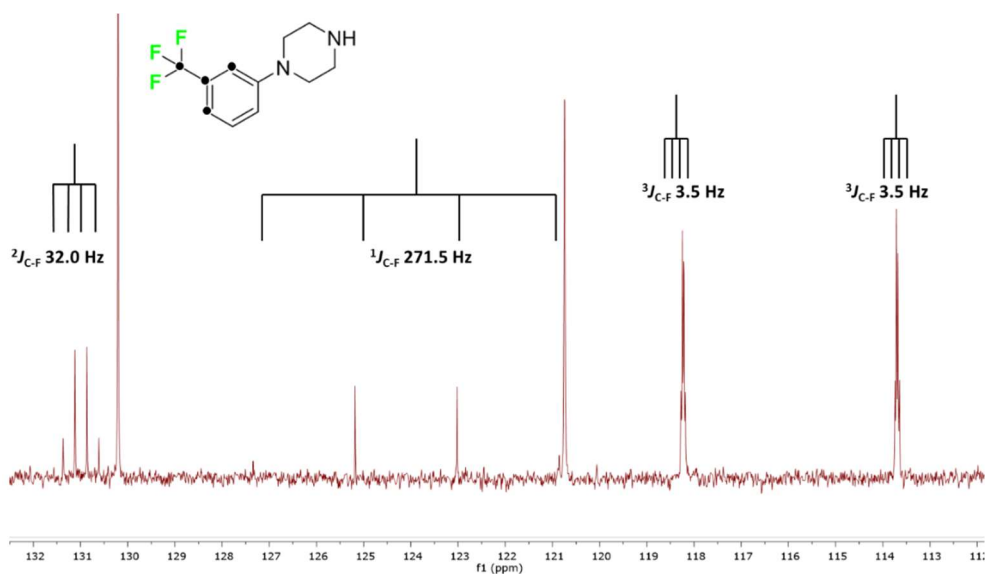
Figure 25. ^{13}C NMR spectra (in D_2O) of an authentic sample of TFMPP showing the fluorine

coupling effect on sequential carbon atoms.
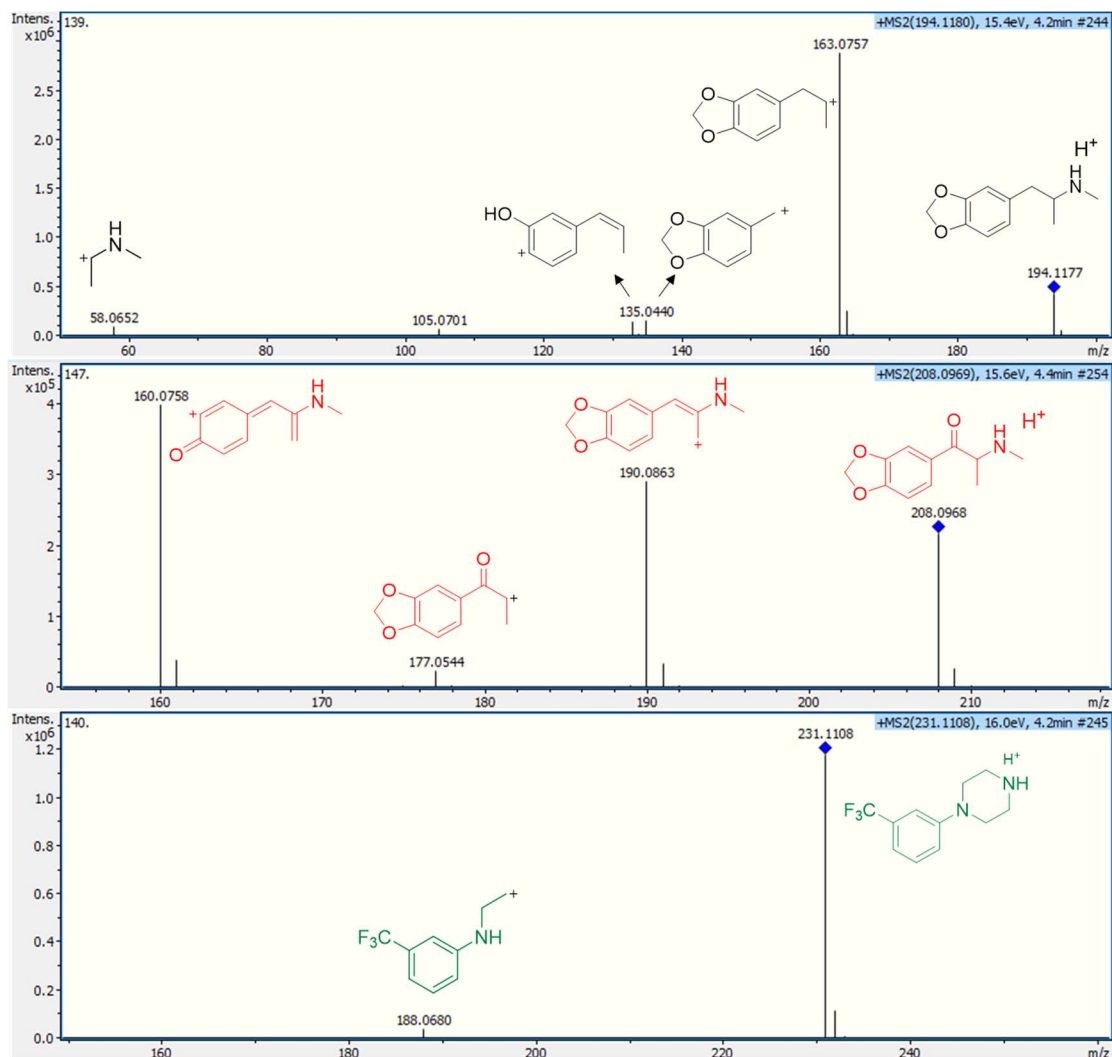
Figure 26. MS/MS fragmentation of (top) MDMA, (middle) methylone, (bottom) TFMPP.

^{1}H q-NMR of MDMA/ethylone mixtures and MDMA/methylone/TFMPP mixtures using maleic acid (MA) as an IS resonating at $\delta = 6.38$ ppm was performed (Table 5). MA is an ideal IS due to its simple resonance signal (singlet), non-overlapping peak, high purity (99.96%) and high solubility in D_2O. An inversion recovery NMR experiment of MDMA, methylone and TFMPP in the mixture was performed to establish the relaxation time (T_1) of the signals selected for quantification, to satisfy the parameter of adequate relaxation delay. This was found by experiment to be between 1.5-4.4 s, adopting at least $5 \times T_1$ to ensure complete relaxation of the signals between pulses.[199,200] Additionally, no more than 10.0 mg of sample was used for quantitative NMR analysis in D_2O as the high salt concentration

affected the broadness of the peaks by affecting the shimming. The reported amounts are in

mg employing equation (1) that uses compound-specific information:

$$m(x) = P(std) \cdot \frac{Mw(x)}{Mw(std)} \cdot \frac{A(x)}{A(std)} \cdot m(std) \cdot \frac{N(std)}{N(x)} \quad (1)$$

where (x) is the analyte and (std) is the IS, (m) is the mass in mg, (P) is the purity, (Mw) is

the molecular weight in g/mol, (A) is the integral value of the resonance being investigated,

and (N) is the number of protons represented by the signal.[198,216]

Table 5. Replicates of ^{1}H q-NMR analysis of 6 different mixtures of NPS with MDMA.

Sample name	Components identified	mg/10 mg of sample ± SD	RSD %
HN26 n = 6	MDMA	1.99 ± 0.2	6.4
	ethylone	6.54 ± 0.1	0.9
HN31 n = 6	MDMA	5.01 ± 0.1	0.3
	ethylone	3.40 ± 0.2	5.5
HN48 n = 3	MDMA	5.85 ± 0.1	1.2
	ethylone	2.94 ± 0.3	11.0
HN153T n = 6	MDMA	3.22 ± 0.2	5.6
	methylone	2.31 ± 0.2	7.2
	TFMPP	2.50 ± 0.1	3.8
HN154 n = 6	MDMA	7.42 ± 0.3	4.2
	ethylone	0.71 ± 0.1	5.1
HN157 n = 6	MDMA	7.08 ± 0.2	2.4
	methylone	0.53 ± 0.1	8.2
	TFMPP	0.18 ± 0.1	7.5

In this study, quantitative analysis of different selected samples of MDMA/NPS

powder and crystal mixtures was achieved, with simple extraction using D_2O containing MA

(2.0 mg/mL) as an IS (Table 5). Initially the samples were identified and characterized using

1D/2D NMR and LC-ESI/MS. Structural elucidation allowed the selection of signals for

quantification of each component with high confidence. The amounts of MA and TMSP-d_4

were fixed throughout the analyses. The MA olefinic signal (at $\delta = 6.38$ ppm) was used for

quantification. It is well separated from the rest of the components in the mixture, even the

methylenedioxy peaks of MDMA, ethylone and methylone, and was normalized to the value

of 1.00. TMSP-d_4 not only allowed the referencing of the NMR spectra to 0.00 ppm, but also

was used to monitor the ratio of MA/TMSP in case of any impurity appearing beneath the

MA peak, especially any cutting agents in the maleate form.

In all the mixtures, all the signals of MDMA were available for integration with the

exception of the chiral centre signal (2) at 3.39 ppm, where in MDMA/ethylone mixture an

unknown impurity resulted in a significantly higher integration value compared to the rest of the signals. In the MDMA/methylone/TFMPP mixtures, the same signal overlapped with the 1′ and 2′ of TFMPP piperazine ring, whose signals were also excluded from the integration/quantitation analyses. Ethylone signals for integration depended on the signal to noise (S/N) ratio. In samples HN26, 31 and 48 all the signals were of an appropriate S/N, while in sample HN154, low S/N allowed only the aromatics and methylenedioxy signal (7′) to be integrated. The rest of the signals were too close in proximity to MDMA signals. In methylone spectra, each signal was used for quantitation except the 1″ methylamine signal at 2.69 ppm due to its close proximity with the ^{13}C satellite signals of 1″ and 1 of MDMA.

The Relative Standard Deviation (RSD%) is affected by the non-uniformity of the original sample, and even though homogenization was carried out on the powder material some components comprising less than 30% of the sample, and especially less than 10% of the sample, resulted in more than 5% RSD.[217] An example of this is the minor components of sample HN157, TFMPP and methylone compared to the major component MDMA (Table 5, Figure 27). Furthermore, the total composition of the samples is between 77.9%-87.9%. This is possibly due to the presence of insoluble materials, moisture in the sample, and even an excess of the salt to drug ratio in illicit drug samples as explained by Hays, in which salt and water content have influenced the purity of the samples under investigation by ^{1}H NMR.[198] Two important parameters were taken into consideration: the S/N ratio was more than 150, and the integration. The latter is believed to be the most significant parameter for error introduction because of it being operator dependent. Therefore, consistency in integration across all the samples is crucial for obtaining accurate quantitative results.[218,219]
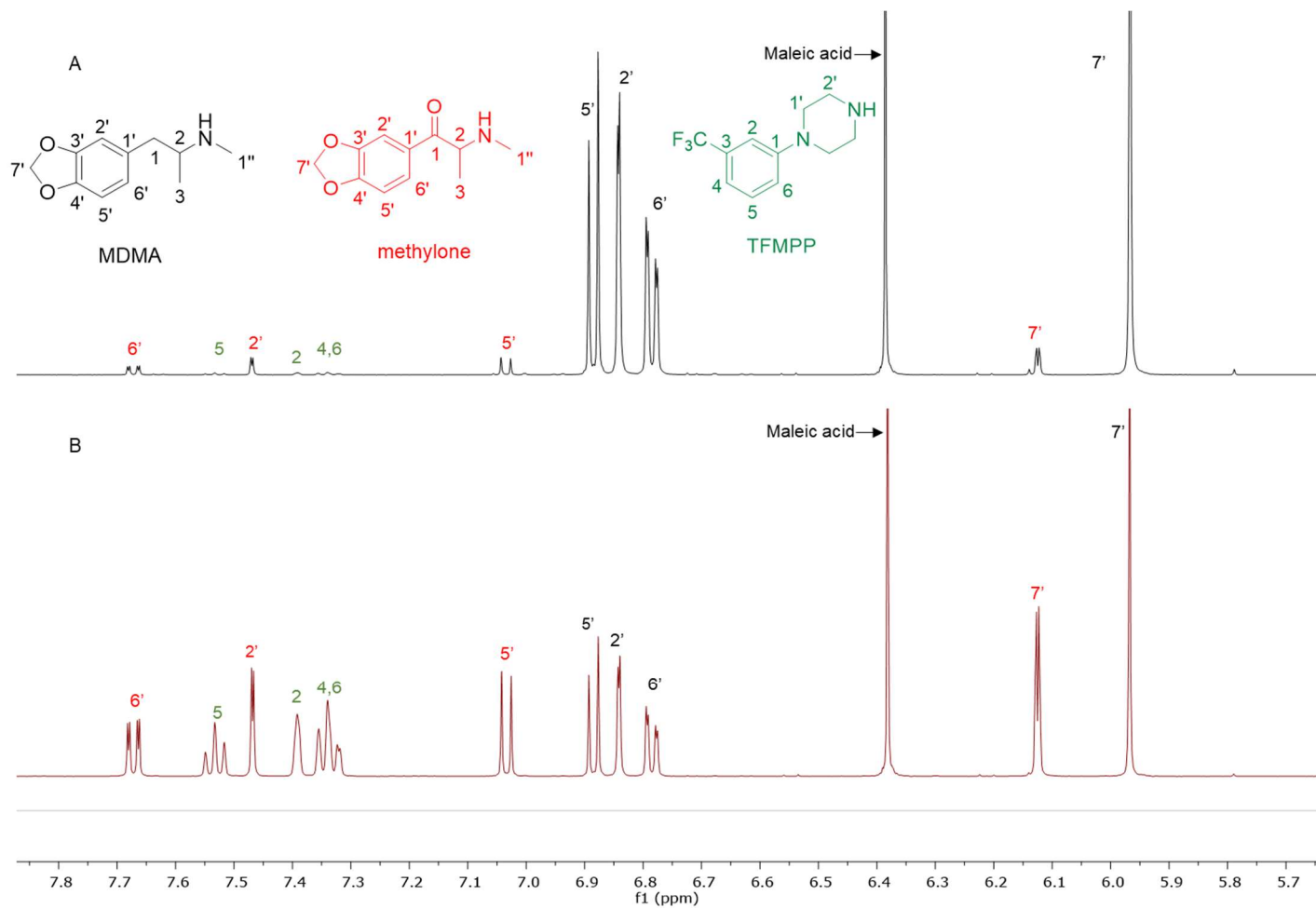
Figure 27. Spectra of ^{1}H NMR (in D_2O) between 5.70-7.80 ppm of (A) sample HN157 and

(B) sample HN153T, revealing significant differences in the ratio of each component.

A fast (15 min), accurate and reproducible ^{1}H q-NMR analysis was performed on many samples (n = 33) containing complex mixtures of MDMA and NPS. The extraction step with D_2O was compatible with all the components present in their salt form due to their high water solubility. NMR allowed the separation of the majority of peaks, the few overlapping signals were excluded from the analysis. The RSD% affected the minor components (less than 10%) in the samples possibly due to the non-uniformity of the samples. This q-NMR analysis was suitable for an NPS that has no reference standard available for chromatographic analysis. The analysis results revealed a mixing-trend rather than cutting of MDMA with NPS in different ratios. Mixing is perhaps experimentation to increase the pharmacological effect. Cutting is dilution to increase profit. It is outside the scope of this analytical research to determine how such samples are marketed when 2 (or more) illicit compounds are mixed.

MDMA is also found mixed or contaminated with its dimethyl analogue, *N,N*-dimethyl-3,4-methylenedioxyamphetamine (MDDMA), reported to be found in MDMA samples synthesized through a nitropropene and reductive amination route.[220] Due to the similar chemical structures, and therefore similar magnetic environments, the NMR spectra displayed multiple overlapping signals especially in the aromatic region and the methylene protons resonating at 2.73-3.10 ppm. The distinctive appearance of the stereogenic centre methine 3.58-3.64 ppm (Figure 28), integrals, 2D NMR (COSY and HSQC), and ESI-MS were all key diagnostic signals in the identification process. In addition to the 194.1194 [M+H]$^+$ for MDMA, the 208.1326 for the required $C_{12}H_{18}NO_2$ 208.1332 and its ^{13}C isotopomer at 209.1364 give rise to numerous possibilities of common molecular formulae for associated NPS and MDMA analogues. Such compounds as 3,4-methylenedioxy-*N*-methyl-butanphenamine, also known as MBDB ($C_{12}H_{17}NO_2$), 3,4-MDMA methylene analogue ($C_{12}H_{17}NO_2$) and 3,4-methylenedioxy-*N*-ethylamphetamine also known as MDEA ($C_{12}H_{17}NO_2$) are shown in Figure 29. A total of 7 protons, 2 x *N*-CH$_3$ plus one CH from the methylene overlapped with one of the MDMA methylene doublet of doublets at 2.78. MDDMA comprises 10% of the sample. The NMR spectra and MS acquired [M+H]$^+$ are confirmed by comparison with the SWGDRUG monographs.[221]
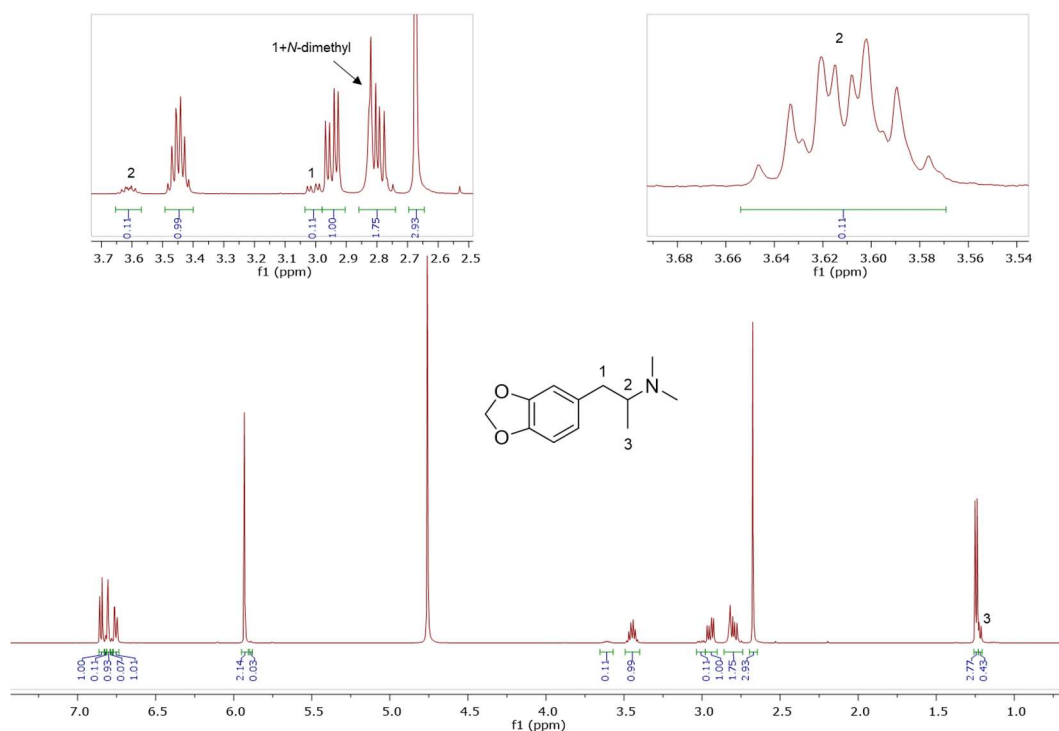
Figure 28. ^{1}H NMR (in D_2O) of sample HN165 containing MDDMA impurity with expansions revealing signals for positions 1, 2 and *N*-dimethyl.
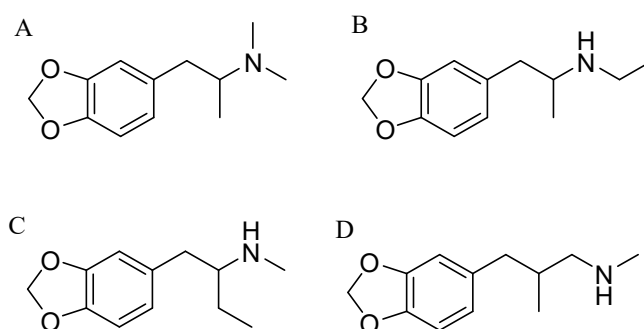
Figure 29. Analogues with the same molecular formula $C_{12}H_{17}NO_2$ (A) MDDMA, (B) MDEA, (C) MDBD, (D) MDMA methylene homologue (phenylpropylamine).

4-Bromo-2,5-dimethoxyphenethylamine (2C-B) has been identified in combination with MDMA (83% 2C-B, 17% MDMA as molar ratios) as a ground-up orange tablet supplied in a small plastic packet. First synthesized by Shulgin in the mid-1970s,[13] the 2C-B pharmacological profile is similar to that of MDMA in that it primarily inhibits 5-HT transporters. It also has less potency for dopamine and noradrenalin transporters. There has been a report of tablets sold as MDMA, but rather containing other psychoactive drugs:

MDA, TFMPP, 2C-B, caffeine.[222] This supports the argument that people have probably

consumed 2C-B unknowingly.
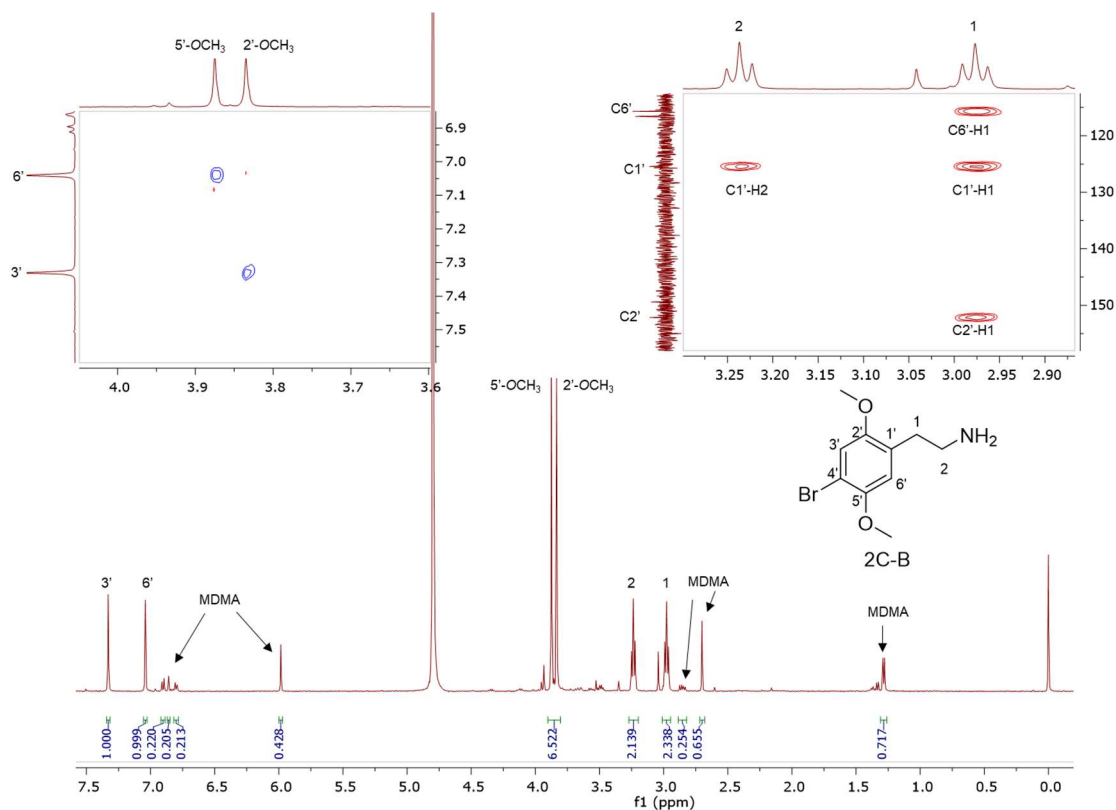
**Figure 30.** [1]NMR (in D_2O) of 2C-B and MDMA mixture with TMSP 0.00 ppm,

(top right) expansion of the HMBC spectra showing key HMBC connectivities,

(top left) expansion of NOESY spectra revealing key NOE cross-peak connectivities.

NMR analysis (Figure 30) (500 MHz in D_2O) showed: (C1) [13]C δ = 27.9 [1]H δ = 2.98,

2H, t 7.0 Hz, (C2) [13]C δ = 39.4, [1]H δ = 3.23, 2H, t 7.0 Hz, (C1') [13]C δ = 125.4, (C2') [13]C δ =

152.2, (C3') [13]C δ = 116.6, [1]H δ = 7.33, 1H, s, (C4') [13]C δ = 109.7, (C5') [13]C δ = 149.4, (C6')

[13]C δ = 115.7, [1]H δ = 7.04, 1H, s, (2'-OCH$_3$) [13]C δ = 56.2, [1]H δ = 3.83, 3H, s, (5'-OCH$_3$) [13]C δ

= 57.0, [1]H δ = 3.88, 3H, s. The analysis revealed two *p*-aromatic proton singlets and two

methoxy signals at 3.83 and 3.88 ppm. These two aromatic singlets confirmed that this is the

2,4,5-trisubstitution pattern of the phenylethylamine. Accurate assignment of all the ^{1}H and

[13]C signals was established via HMBC and 2D Nuclear Overhauser Effect Spectroscopy

(NOESY) (Figure 30), where the protons at position 1 had an HMBC connection to the

aromatic carbons C1′, C2′ and C6′, and NOESY connectivity to the aromatic proton at 6′.

Other key NOE connectivities are 2′-OCH$_3$ to H3′ and 5′-OCH$_3$ to H6′, while other key HMBC connectivities include 5′-OCH$_3$ protons to the 5′-quaternary carbon and 2′-OCH$_3$ protons to the 2′-quaternary carbon. Additional analytical confirmation of the presence of a bromine substituent and not iodine (2C-I) or chlorine (2C-C) is [M+H]$^+$ 260.0265 for C$_{10}$H$_{15}$^{79}BrNO$_2$ requires 260.0286, 262.0245 for C$_{10}$H$_{15}$^{81}BrNO$_2$ requires 262.0260 (ratio 1:1 and both within 6 ppm) (Figure 31), in addition to the [M+H]$^+$ for MDMA 194.1173 for C$_{11}$H$_{16}$NO$_2$ requires 194.1181. These findings are consistent with work reported by Kanai *et al*.[223]
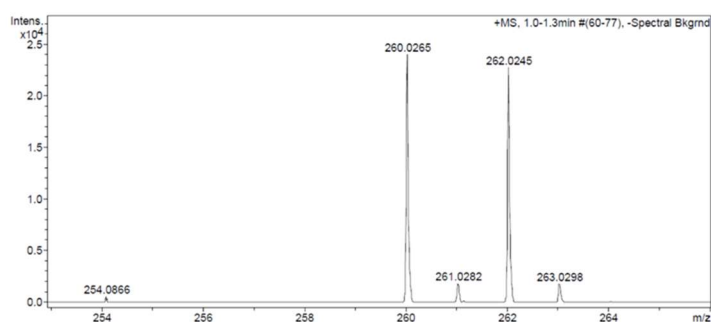
Figure 31. ESI-MS loop injection of the mixture showing the diagnostic ^{79}Br:^{81}Br isotopic ratio of 1:1.

2C-I, the iodo analogue of the 2C family, was detected in sample HN144, a blue powder, in combination with 2C-B and MDMA with a molar percentage of 50% 2C-I, 41% 2C-B and 9% MDMA. The ESI-MS analysis revealed 2C-I [M+H]$^+$ 308.0130 for C$_{10}$H$_{15}$INO$_2$ requires 308.0147 (within 6 ppm). 2C-B [M+H]$^+$ 260.0264 for C$_{10}$H$_{15}$^{79}BrNO$_2$ requires 260.0286 (within 6 ppm), and [M+H]$^+$ 262.0253 for C$_{10}$H$_{15}$^{81}BrNO$_2$ requires 262.0260 (within 6 ppm) (ratio 1:1). The ^{1}H NMR of 2C-I and 2C-B overlapped with the exception of the aromatic signals, where the presence of the iodo substituent at the *para*-aromatic position resulted in a greater chemical shift difference in the ^{1}H spectra between the *ortho*- (3′) (7.49 ppm) and the *meta*- (6′) (7.00 ppm) protons compared with that found in 2C-B (Figure 32). This difference is of diagnostic value in determining the type of substituent in the NPS 2C family by ^{1}H NMR spectroscopy.
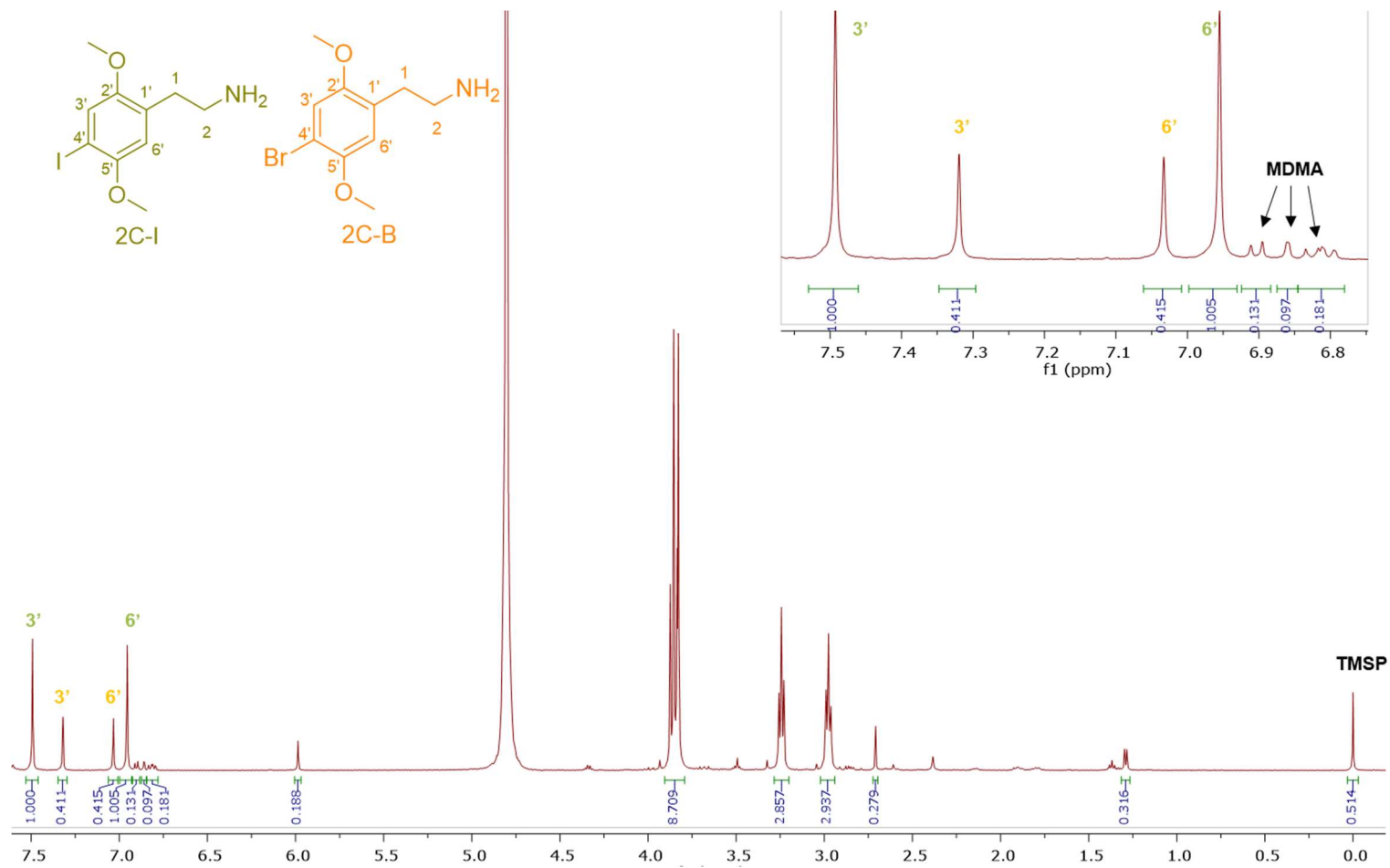
Figure 32. ^{1}H NMR (in D$_2$O) spectra of sample HN144 containing 2C-I, 2C-B, and MDMA with expansion of the aromatic region between 6.80-7.55 ppm.

Samples from Bristol night-clubs included high purity MDMA powders and crystals. Nevertheless, this analysis revealed multiple components of the cathinone and phenethylamine families mixed with MDMA. Even the selling of NPS samples, presumably as MDMA (ecstasy), but with MDMA only as the cutting agent, e.g. 9% molar ratio in 50% 2C-I and 41% 2C-B, increasing the likelihood of toxicity. 1D/2D NMR and ESI-MS/MS provided high confidence analytical characterization and quantification of complex mixtures. The use of a HILIC column which is designed for high polarity compounds, such as amino acids, proved useful for the analysis of these samples. Additionally, MS/MS analysis revealed distinctive fragments of compounds in the mixture. ^{1}H q-NMR using the MA IS method was applied successfully to complex samples of MDMA cut with other NPS of closely similar structures. This analysis provides some insight for law enforcement agencies, drug analysts, emergency first responders to any overdose situation in night-club venues, and for users where accurate knowledge of drug content could help reduce harm.

**2.3.2 A cross-method validated ^{1}H q-NMR analysis for the quantification of seized MDMA (ecstasy) tablets**

3,4-Methylenedioxymethamphetamine (MDMA) is a psychoactive drug popular among youths especially those attending night-club venues due to its stimulating and empathogenic effects.[224] The dose of MDMA in illicit tablets has fluctuated during the past decade, but currently it is at an all-time high as reported by the EMCDDA[39] and in our analysis. There are many reports of intoxications and even some fatalities especially among young adults attending night-clubs and music festivals.[180,181] Adverse effects have been reported with the use/abuse of MDMA, with most of the intoxications and fatalities attributed to hypertension, kidney dysfunction, rhabdomyolysis, muscle tension, hyperthermia and dehydration.[195,196] Most of the analytical methods used for the quantification of MDMA tablets are chromatographic techniques that may be coupled to MS.[9] Even though chromatography is the gold standard in industrial and forensic laboratories for quantitative analysis, it suffers from disadvantages.[198] Lengthy method development and preparation of mobile phases are time consuming. Furthermore, UHPLC is unable to detect impurities that have no chromophore or are adulterated with high polarity excipients such as glycerol and sugars. Another disadvantage is the poor ionization of such excipients in MS analysis. GC/MS analysis suffers from the absence of or only weak mass ion, and requires derivatization for Amphetamine-type Stimulants (ATS) in order to achieve accurate quantitative results.[209] On the other hand, NMR requires no solvent preparation and will detect organic impurities, even ones not possessing a chromophore, no method development and no stationary phase (column) for the compounds to interact with.[198,199] NMR allows a simultaneous structure elucidation and quantification of the targeted analyte in a relatively fast time compared to various different chromatographic techniques.

In this study, 26 tablets belonging to 11 different brands of seized MDMA tablets were quantified using ^{1}H q-NMR and cross-method validated using UHPLC equipped with a variable wavelength detector (VWD) and UHPLC/MS using MDMA-d$_5$ as an internal standard (Table 6). Equation 2 used for ^{1}H q-NMR tablet quantitation is:

$$\mathbf{m(x)} = \mathbf{P(std)}.\frac{Mw(x)}{Mw(std)}.\frac{A(x)}{A(std)}.\mathbf{m(std)}.\frac{N(std)}{N(x)}.\frac{m(tablet)}{m(sample\ used)} \quad \textbf{(2)}$$

where (x) is the analyte and (std) is the IS, (m) is the mass in mg, (P) is the purity, (Mw) is the molecular weight in g/mol, (A) is the integral value of the resonance being investigated, (N) is the number of protons represented by the signal, m(tablet) is the mass of the tablet in mg while m(sample used) is the mass of the extracted sample, e.g. ~10.00 mg.[198,216]

Table 6. NMR and UHPLC quantitative results of seized MDMA tablets.

No	MDMA tablet	Sample	Weight (mg)	UHPLC MDMA dose (mg) ± SD	UHPLC RSD %	NMR MDMA dose (mg) ± SD	NMR RSD %
1		a	468.77	82.80 ± 3.0	3.6	89.08 ± 0.5	0.6
		b	494.71	108.65 ± 0.9	0.8	105.26 ± 0.9	0.8
		c	486.26	93.99 ± 1.7	1.8	97.16 ± 0.8	0.8
2		a	449.57	69.76 ± 1.0	1.4	76.24 ± 0.3	0.4
		b	449.11	75.64 ± 1.1	1.5	81.54 ± 0.3	0.4
		c	443.17	72.94 ± 2.2	3.1	75.00 ± 1.1	1.5
3		a	520.37	121.13 ± 0.6	0.5	121.24 ± 0.7	0.6
		b	477.08	113.26 ± 0.4	0.3	112.66 ± 0.5	0.4
		c	501.74	94.38 ± 0.6	0.6	92.58 ± 0.8	0.9
4		a	512.73	160.55 ± 0.8	0.5	164.21 ± 0.4	0.3
		b	481.95	150.27 ± 2.4	1.6	151.92 ± 2.1	1.4
		c	496.73	160.01 ± 0.5	0.3	165.13 ± 0.5	0.3
5		a	513.82	162.88 ± 3.0	1.8	163.45 ± 0.3	0.2
		b	520.66	160.95 ± 3.6	2.2	165.10 ± 0.9	0.5
		c	514.93	166.54 ± 1.5	0.9	171.55 ± 1.4	0.8
6		a	325.00	89.45 ± 0.2	0.2	89.08 ± 1.2	1.4
7		a	233.1	87.79 ± 0.6	0.6	90.98 ± 0.2	0.2
8		a	211.12	85.63 ± 0.1	0.1	88.36 ± 0.7	0.8
		b	209.21	83.31 ± 0.3	0.4	84.18 ± 0.3	0.4
		c	187.27	78.38 ± 0.8	1.0	81.55 ± 0.5	0.6
9		a	503.50	147.70 ± 2.0	1.3	151.77 ± 3.2	2.1
		b	468.77	139.74 ± 1.7	1.2	144.66 ± 1.4	1.0
		c	476.81	155.02 ± 3.2	2.1	153.75 ± 1.2	0.8
10		a	644.70	87.13 ± 0.9	1.0	95.08 ± 0.4	0.5
11		a	273.54	85.34 ± 1.8	2.2	87.39 ± 0.7	0.8
		b	288.10	91.57 ± 0.7	0.8	88.59 ± 1.5	1.7

For UHPLC analysis, the non-specific (in terms of analyte) UV wavelength of 210 nm was selected to detect impurities present in tablets. Both UHPLC using UV and UHPLC/MS quantification were determined first by determining the % of MDMA, followed by calculating the MDMA content using equations 3 and 4:[225]

$$\text{MDMA\%} = \frac{\text{concentration of sample (µg/mL) .dilution factor .volume used (mL) .100\%}}{\text{weight of sample (µg)}} \quad (3)$$

$$\text{mg of MDMA} = \frac{\text{MDMA\% .weight of tablet in mg}}{100} \quad (4)$$

A single extraction, using D_2O for NMR analysis and H_2O for UHPLC and UHPLC/MS analysis, was employed. This has been deemed sufficient with 100% recovery according to the literature.[225,226] Additionally, numerous tablets were qualitatively analysed for cutting agents and types of excipients using NMR. The UHPLC method gave a good linearity by plotting the concentration (µg/mL) against UV response (Figure 33). Using TFA provided a better buffering capacity for MDMA, with good peak resolution and no peak tailing compared to using FA with UV detection (Figure 33).
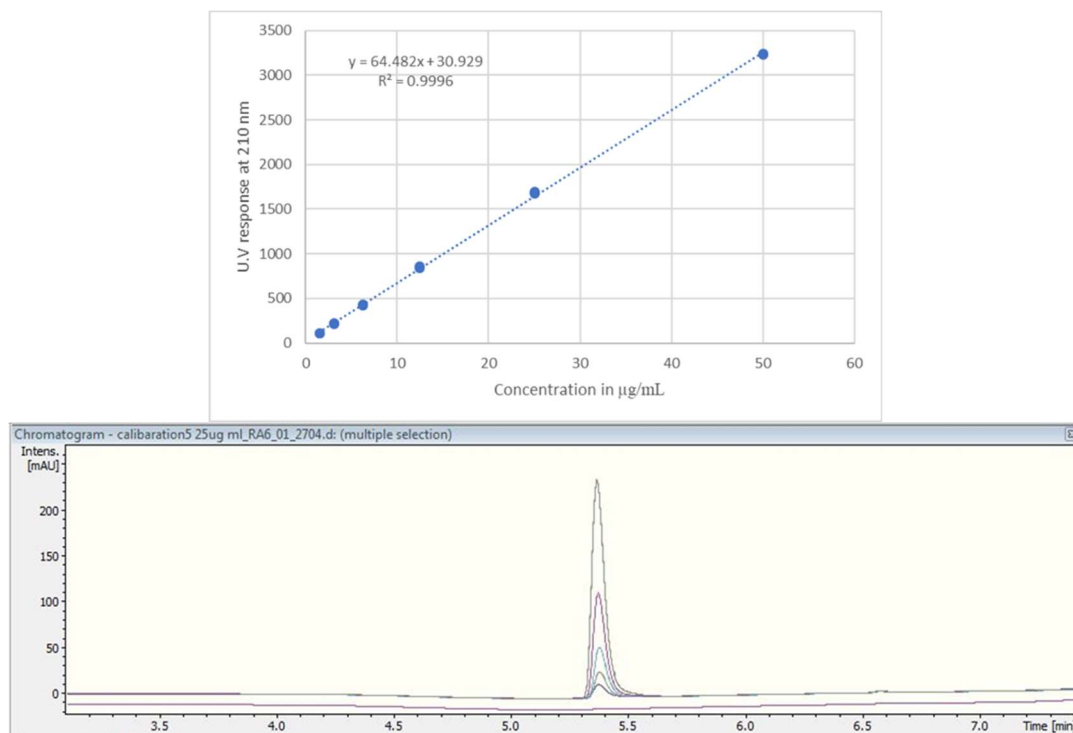
Figure 33. (Top) calibration curve of MDMA between 1.5-50 µg/mL, $R^2 = 0.9996$, (bottom) UV chromatogram MDMA RT = 5.4 min of the calibration curve concentrations.

For UHPLC/MS, two tablets from the red UPS brand were selected for comparative analysis (Table 7). The calibration curve was run in triplicate, and gave a good linearity by plotting the concentration (ng/mL) against response ratio of MDMA to MDMA-d_5 (Figure 34). The Extracted Ion Chromatograms (EIC) (Figures 35) and spectra (Figure 36) of the molecular ions of both MDMA and MDMA-d_5 were used for quantification. Using a deuterated analogue as an IS is optimal, due to it satisfying the IS criteria by having the same chromatography yet with a different mass ion, no possibility of it existing in the targeted analyte, and possessing similar ionization in ESI-MS.[227,228] Furthermore, the RSD% across all methods gave a good RSD% of an acceptable value lower than 5% for powdered samples as set out by the European Network of Forensic Science Institute,[217] with the exception of one sample 4b using UHPLC/MS analysis. The results of the UHPLC and NMR analyses were comparable. Additionally, using ANOVA single factor analysis of the three methods (NMR, UHPLC, and UHPLC/MS), there is no significant statistical difference ($p > 0.05$) (Table 7).

Table 7. UHPLC, NMR and UHPLC/MS quantitative results of MDMA tablet number 4.

No		UHPLC			NMR		UHPLC/MS	
4	Entry	Weight mg	MDMA dose (mg) ± SD	RSD %	MDMA dose (mg) ± SD	RSD %	MDMA dose (mg) ± SD	RSD %
	a	512.73	160.55 ± 0.8	0.5	164.21 ± 0.4	0.3	161.07 ± 4.7	2.9
	b	481.95	150.27 ± 2.4	1.6	151.92 ± 2.1	1.4	153.80 ± 8.6	5.6
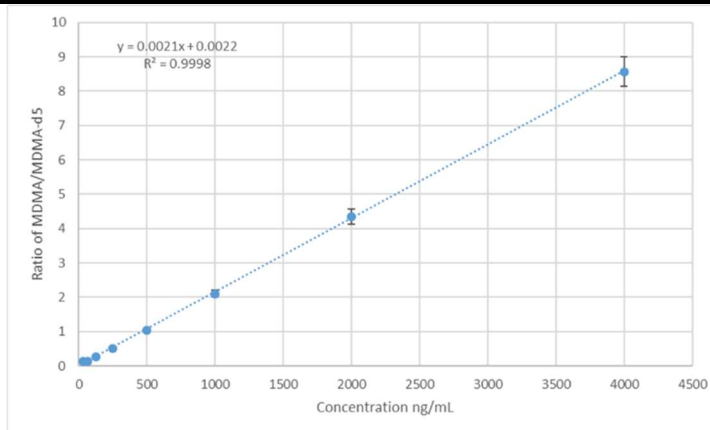
Figure 34. Calibration curve of MDMA range between 31.25-4000 ng/mL, response was calculated as the ratio of the area under the curve (EIC) of MDMA to that of IS (MDMA-d_5), $R^2 = 0.9998$.
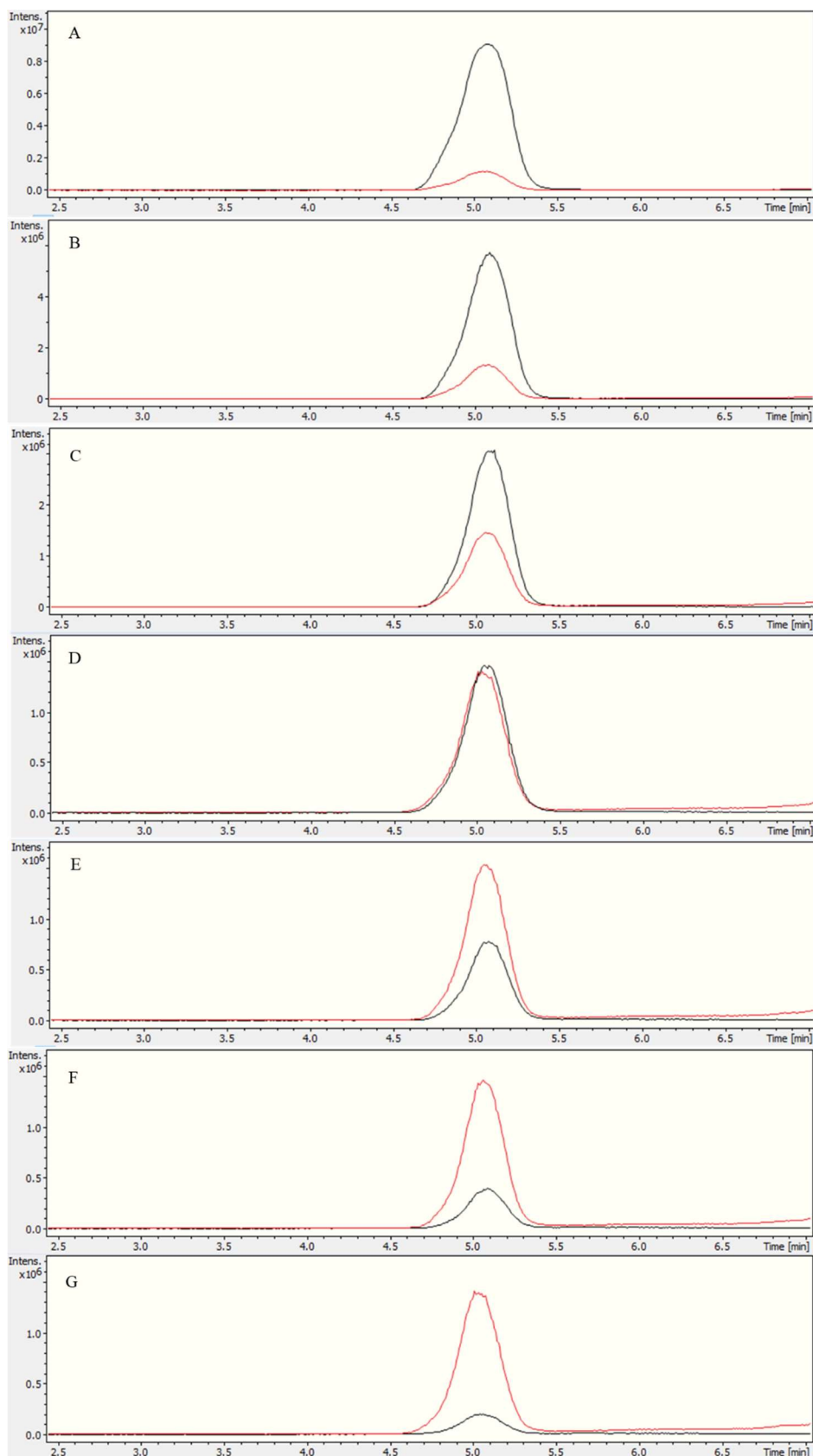
Figure 35. EIC calibration curve of MDMA (black) using 500 ng/mL d$_5$-MDMA (red) at

(A) 4.000 µg/mL, (B) 2.000 µg/mL, (C) 1.000 µg/mL, (D) 500.0 ng/mL, (E) 250.0 ng/mL,

(F) 125.0 ng/mL, and (G) 62.50 ng/mL.
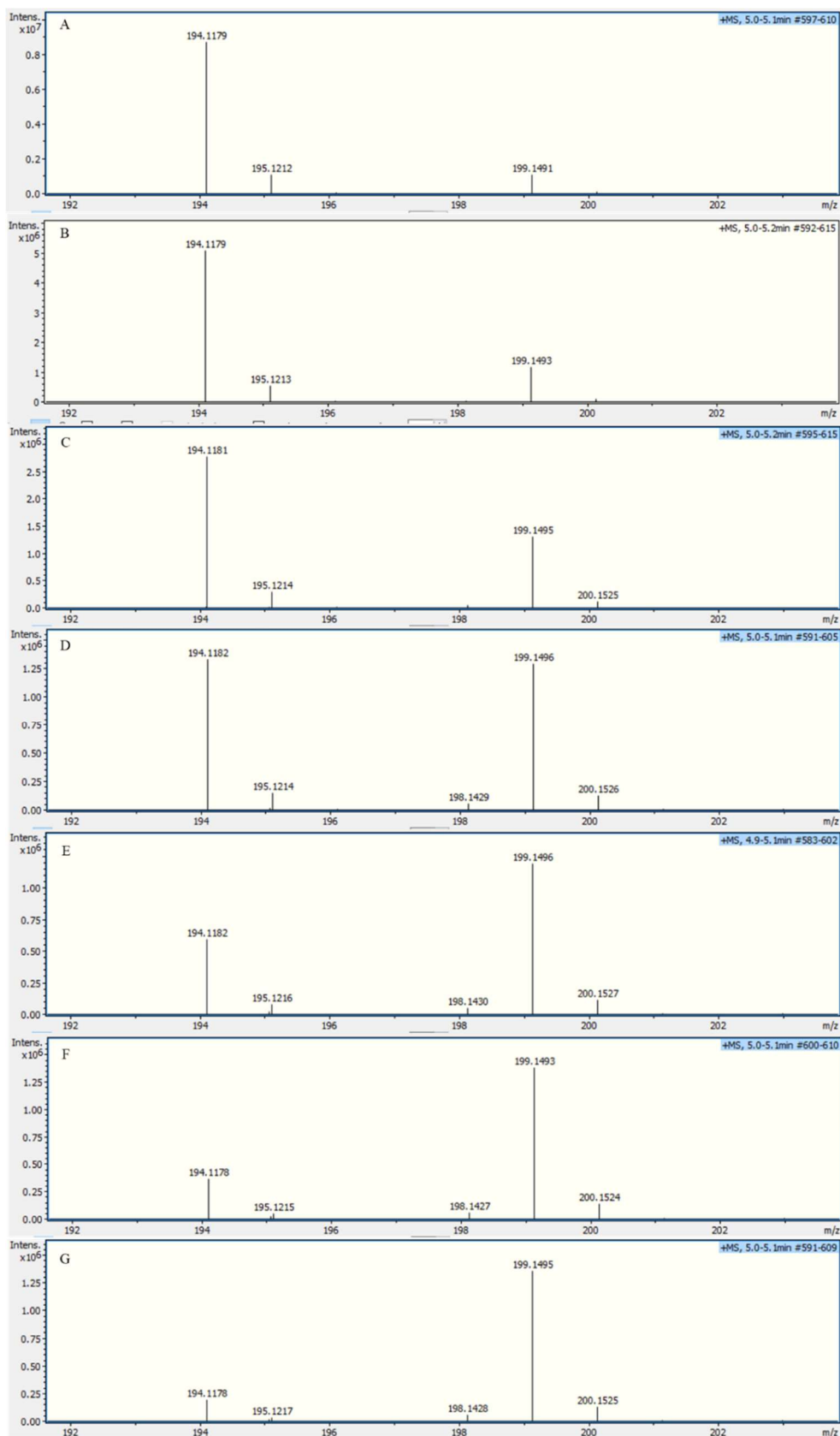
Figure 36. Compound spectra of the EIC calibration curve of MDMA (194 [M+H]$^+$) using 500 ng/mL MDMA-d$_5$ (199 [M+H]$^+$) as IS at (A) 4.000 µg/mL, (B) 2.000 µg/mL, (C) 1.000 µg/mL, (D) 500.0 ng/mL, (E) 250.0 ng/mL, (F) 125.0 ng/mL, and (G) 62.50 ng/mL.

MA was selected as a quantitative IS due to its high solubility in D_2O, simplicity of the olefinic signal (singlet), non-overlapping signal at $\delta = 6.38$ ppm. Due to the hygroscopic nature of MA, the purity was checked against high purity DMS in D_2O and acetanilide in DMSO-d_6. TMSP-d_4 was used for referencing at 0.00 ppm using a fixed concentration of 0.5%. This allowed the use of the ratio of MA/TMSP-d_4 to check for any impurities that might be under the MA peak, such as drugs in the maleate salt form.

Prior to commencing the analysis, an inversion-recovery experiment was carried out to establish the time it takes the signals of MDMA to relax which ranged between 2-4 s. For MA and DMS, the relaxation times were 6.1 s and 2.9 s respectively.[229] Based on these T_1 values, the relaxation delay of the pulse sequence was set to achieve at least 5xT_1 for almost complete relaxation.[199,200]

Quantitative analysis revealed variations between different brands of MDMA tablets and within the same brand. Most of the doses quantified are significantly more than the average doses of MDMA recorded up to the year 2000 (50-80 mg).[230] Additionally, many tablets, especially tablets number 4 and 5, contain from double to more than double the dose of MDMA required to produce a physiological effect (70 mg or between 1-2 mg/kg).[196,231] ^{1}H q-NMR allowed not only the quantification of the dose of MDMA, but also facilitated both detection and quantification of any protonated impurities present in the tablets. Caffeine was detected and quantified in tablets 11 a and b, containing 16.72 mg and 17.93 mg respectively with an RSD lower than 3%. Caffeine signals N-methyl 10, N-methyl 14 and aromatic 8 were used for quantification,[232] while N-methyl 12 was not integrated due to its close proximity to the methine at position 2 of MDMA (Figure 37). UHPLC using UV resulted in a broad peak at 4.7 min for caffeine, and the MS analysis showed a weak $[M+H]^+$ at 195.0874 m/z, required for $C_8H_{11}N_4O_2$ 195.0876 (Figure 37). The reason behind the poor UHPLC peak shape (tailing and broadening) is the pK_a of caffeine at the acidic pH of the mobile phase, while the weak molecular ion in MS analysis is the result of the 10000-fold dilution of the analyte to put it in the range of the calibration curve, and not to saturate the MS detector at higher concentrations (>5.0 µg/mL for MDMA).
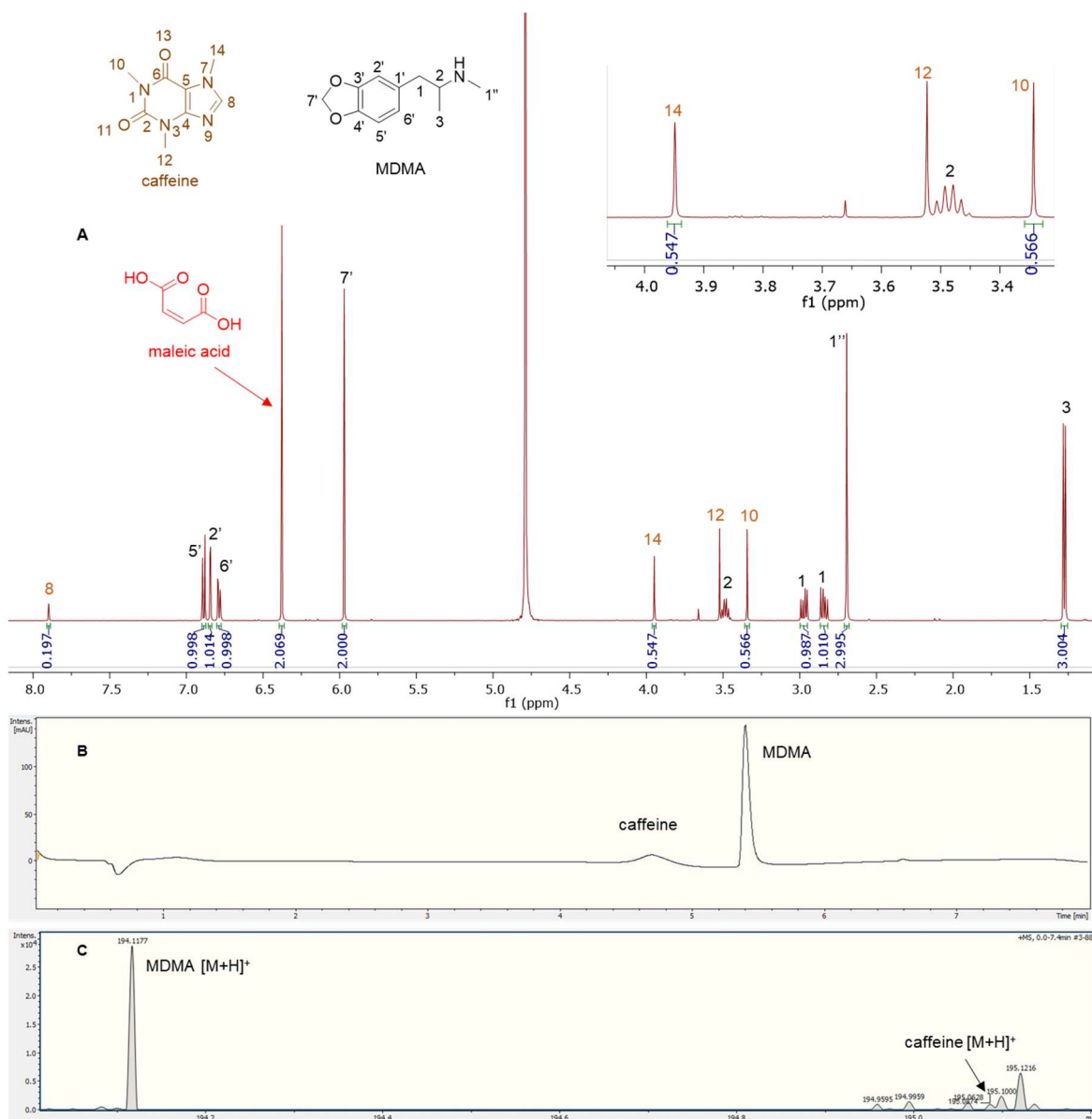
Figure 37. (A) ^{1}H NMR (in D$_2$O) of tablet 11a showing the caffeine peaks with expansion of the region between 3.4-4.5 ppm, (B) UHPLC of sample 11a showing a broad peak for caffeine at RT= 4.7 min, (C) MS trace of sample 11a showing MDMA molecular ion and caffeine low intensity molecular ion at 195.0874.

Conclusions

In this study, a cross-method validation of ^{1}H q-NMR to analyse seized MDMA tablets is described. ^{1}H q-NMR proved its versatility in the identification and quantification of MDMA as well as cutting agents, with less sample handling (no serial dilution) and better precision (RSD%) compared to chromatographic and MS-based techniques. NMR analysis provided a fast, reproducible quantification without the use of a reference standard of the analyte under

investigation. MA is a suitable NMR quantitative internal standard due to its high solubility, simplicity of the peak and non-overlapping signal. Identification of tablets containing more than double the dose of MDMA is a cause of concern to the public. It is of value to law enforcement officials and health workers. Comparative analysis with chromatographic and MS-based methods further corroborated the results of ^{1}H q-NMR. When certain parameters are carefully optimized and considered such as the relaxation delay, number of scans, and S/N, NMR possesses the accuracy and reliability in the quantitative analysis of MDMA in seized tablets with results comparable to other gold standard techniques, e.g. GC and LC.

2.3.3 GC/MS and ESI-MS analytical studies of selected derivatized phenethylamines and cathinones

In this study, selected phenethylamines (MDMA and 2C-B) and cathinones (ethylone and mephedrone) were analysed non-derivatized and derivatized using 2,2,2-trichloroethyl chloroformate (TCF) to produce the carbamate derivative of the drugs selected, resulting in altered volatility and decreased polarity, thus enhancing the interaction of the compounds with the non-polar stationary phase (BPX-5 low polarity column). Differences in the mass ions detected, retention time and peak resolution are discussed. Additionally, isotopic analytical data on two drugs (ethylone and 2C-B) are provided for the first time.

Simultaneous derivatization of a seized sample containing mephedrone and 2C-B was successful, non-derivatized mephedrone RT = 10.1 min on a BPX-5 column using the temperature ramp described (Experimental). On the other hand, the carbamate derivative of mephedrone has an RT = 16.5 min (Figure 38), as a result of the alteration of polarity and volatility.[209] The Electron Impact (EI) MS spectrum of non-derivatized mephedrone suffered from an absent or a weak molecular ion at 177-178 m/z, with 119 m/z and 58 m/z (base peak) resulting from the 4-methylbenzoyl cation, and formation of the iminium ion found in *N*-methylated phenethylamines respectively. This iminium ion is typical of phenethylamines, and thus does not provide enough evidence for unambiguous detection using GC/MS.[209,233]
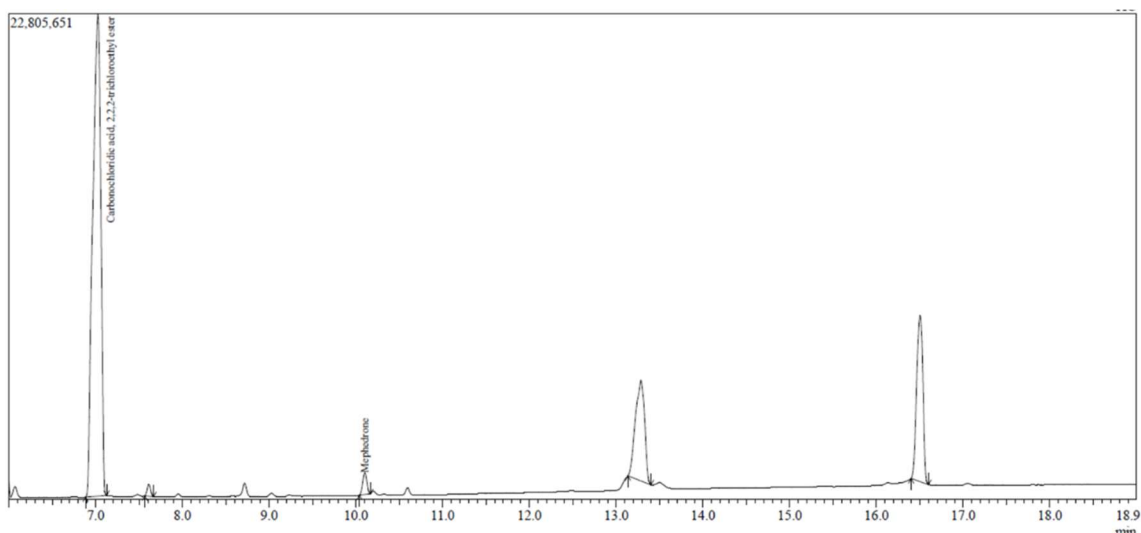
Figure 38. GC Total Ion Chromatogram (TIC) of non-derivatized mephedrone 10.1 min, TCF-derivatized 2C-B 13.3 min, and TCF- derivatized mephedrone 16.5 min.

The mephedrone carbamate derivative resulted in a distinctive mass ion formed due to the isotopic ratio distribution of three chlorine atoms in the derivative, displaying: 27:27:9:1, seen for the mass ions in low abundance at 351:353:355:357, while the loss of 1 chlorine results in the formation of the 316:318:320 weak ions (Figure 39). The base-peak cluster at 232:234:236:238 is the result of the 2,2,2-trichloroethyl *N*-ethyl-*N*-methyl carbamate fragment ion. The mephedrone derivative was also infused into the ESI-MS to obtain HR-MS on the molecular ion (Figure 40), giving $[M+H]^+$ 352.0278 required for $C_{14}H_{17}NO_3{}^{35}Cl_3$ 352.0268, 354.0247 required for $C_{14}H_{17}NO_3{}^{35}Cl_2{}^{37}Cl$ 354.0240, 356.0214 required for $C_{14}H_{17}NO_3{}^{35}Cl{}^{37}Cl_2$ 356.0214, 358.0185 required for $C_{14}H_{17}NO_3{}^{37}Cl_3$ 358.0192. The fragmentation pattern fits the distinctive pattern ratio of an analyte containing three chlorine isotopes.[234]

Non-derivatized 2C-B resulted in a broad peak at 13.1 min, a difference of 0.2 min from the 2C-B TCF derivative (13.3 min), which was surprising given the structural alteration that has a significant impact on the polarity of Amphetamine-type Stimulants (ATS), and comparing it to mephedrone, where the derivative differed in RT by 6.4 min (Figure 38). Nevertheless, Kanai *et al.* reported only small changes in RT with 2C-B of 1.3 min using trifluoroacetic anhydride as the derivatizing agent.[223]
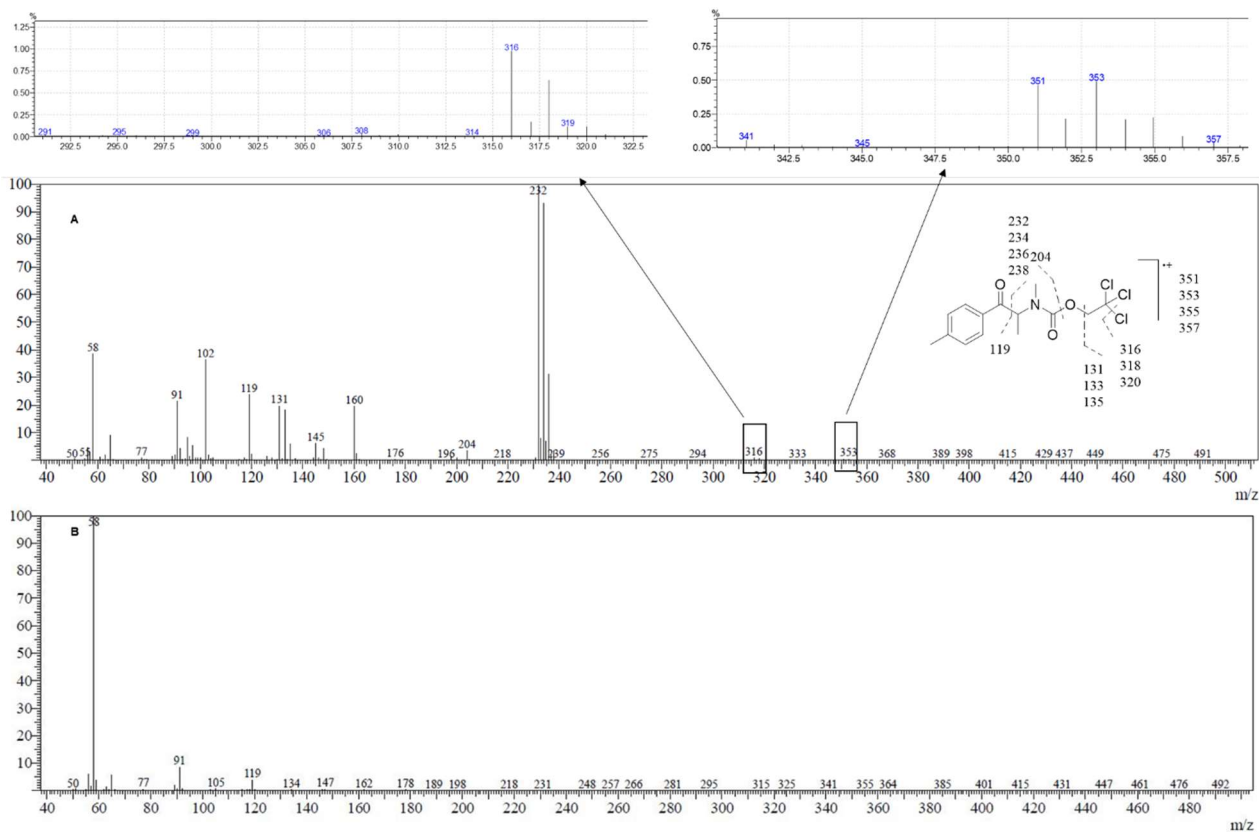
Figure 39. (A) EI-MS of mephedrone carbamate derivative showing its fragmentation pattern

with expansion of mass ion at 353 m/z and fragment at 316 m/z,

(B) EI-MS of non-derivatized mephedrone showing base-peak fragment at 58 m/z.
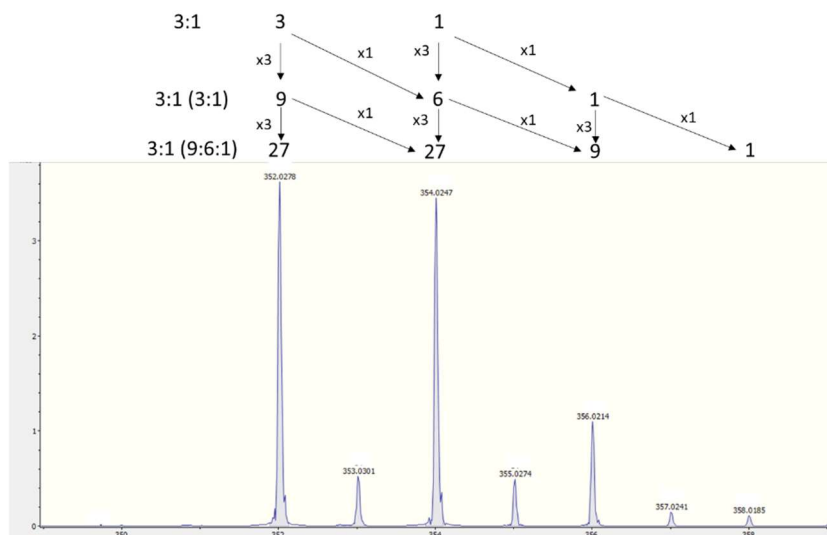
Figure 40. ESI-MS of mephedrone carbamate derivative showing the [M+H]$^+$ with a ratio of

27:27:9:1 containing three chlorine isotopes.

For non-derivatized 2C-B, the molecular ion at 259/261 m/z was identified, as well as loss of part of ethylamine at 230/232 and the loss of the entire ethylamine moiety (-44) at 215/217 (Figure 41). The rest of the fragments are less distinctive as they lack the 4-bromo substituent such as 121, 105 and 77, which are common in phenethylamine analogues.[235]
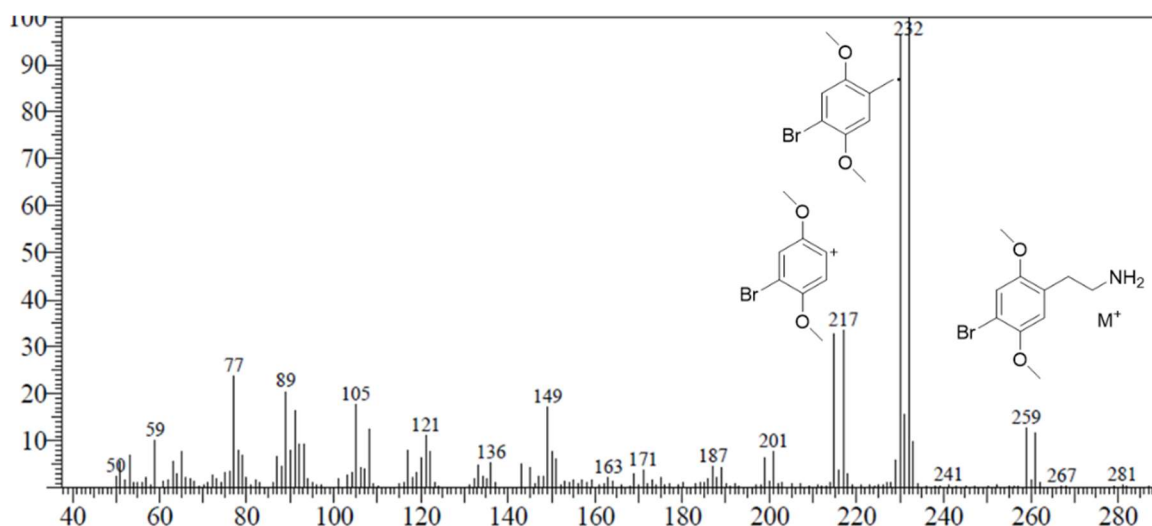
Figure 41. EI-MS of non-derivatized 2C-B.

Additionally, due to the broad peak and low intensity mass ion detected for 2C-B, further corroboration is required especially from a spectrometric point of view. 2C-B TCF derivative gave a distinctive isotopic pattern of one bromine and three chlorine isotopes with multiple isotopic clusters (Figure 42). Molecular ions at 433:435:437:439:441 are the result of the combination of three chlorine atoms and 1 bromine atom, giving rise to the complex isotopic pattern in the ratio of 27:54:36:10:1, explained using the following calculations:

For 2 Cl atoms 3:1 a:b

$(3a + 1b)^2 = 9a^2 + 3ab + 3ab + 1b^2$

$= 9a^2 + 6ab + 1b^2$

For 3 Cl atoms (3:1 a:b)

$(3a + 1b) (9a^2 + 6ab + b^2) = 27a^3 + 18a^2b + 3ab^2 + 9a^2b + 6ab^2 + 1b^3$

$= 27 a^3 + 27 a^2b + 9ab^2 + 1b^3$

For an added 1 Br (1:1 a:b) $^{79}Br:^{81}Br$ ratio 1:1

$(27a^3 + 27a^2b + 9ab^2 + 1b^3) (1a + 1b) = 27a^4 + 54 a^3b + 36 a^2b^2 + 10ab^3 + 1b^4$
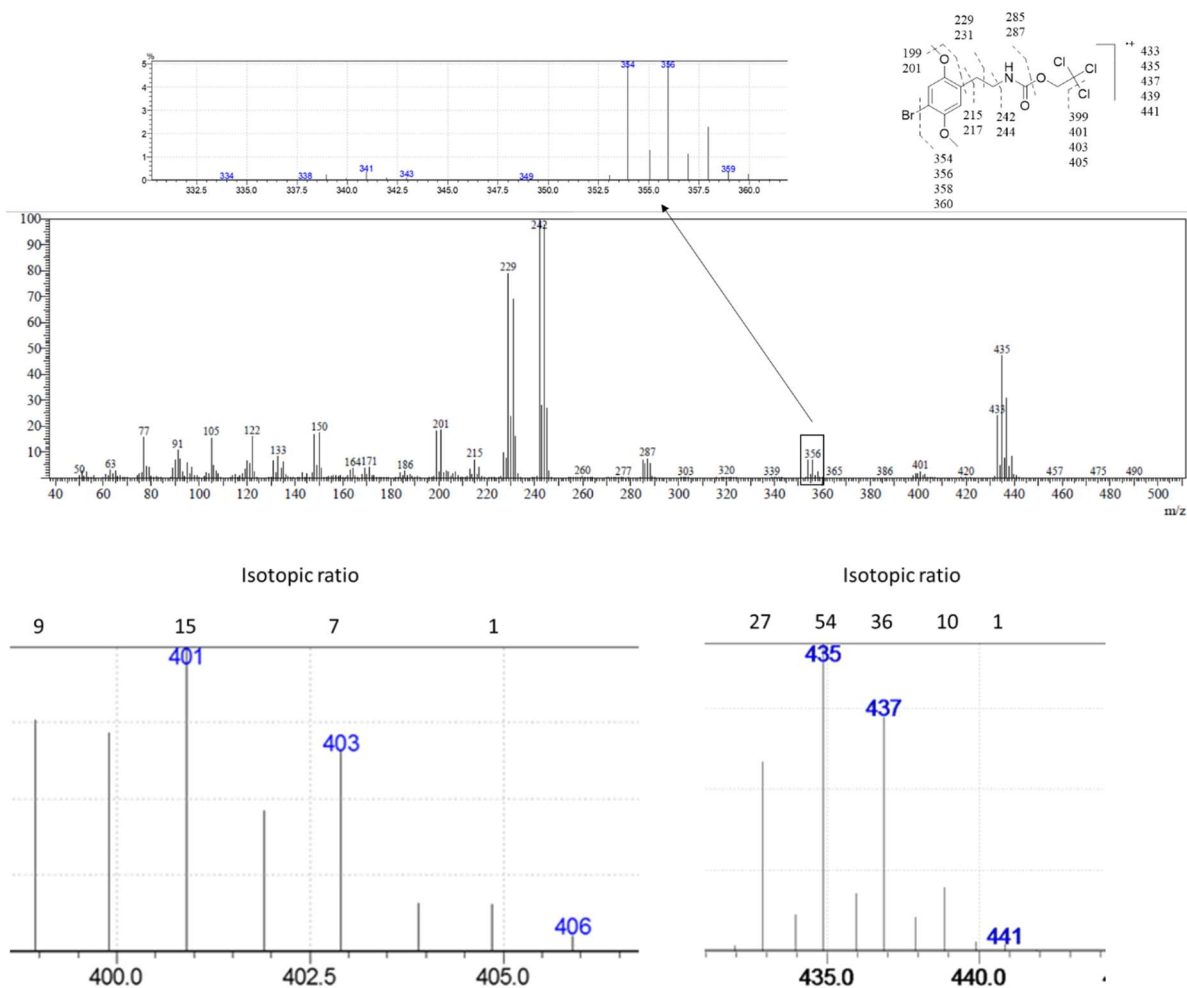
Figure 42. EI-MS of carbamate derivative of 2C-B showing the region of the spectrum between 50-500 m/z, the proposed fragmentation pathway, and expansions of isotopic fragments and clusters showing the isotopic ratio of distribution of the molecular ion at 433 m/z and the fragment at 399 m/z.

The cluster fragments at 399:401:403:405 are the result of loss of one chlorine from the molecular ion (Figure 42), while the 354:356:358:360 cluster is the result of 4-bromo substituent loss giving the isotopic ratio of 3 chlorines (Figure 42). Additional fragmentations can be observed in Figure 42, especially the base peak (100% abundancy) resulting from the loss of the entire 2,2,2-trichloroethyl carbamate part. All of these complex isotopic signatures give a definitive identification to the compound with valuable structural elucidation information. The analysis could not be compared to the literature as none exists, nevertheless it is in line with the work of Frison *et al.* on a similar compound (bk-2C-B).[210]

Accurate mass was acquired using ESI-MS for all the isotopic fragments of the molecular ion starting with 433.9301 (51% abundance) required for $C_{13}H_{16}NO_4{}^{79}Br^{35}Cl_3$ 433.9322, 435.9285 (100% abundance) required for $C_{13}H_{16}NO_4{}^{81}Br^{35}Cl_3$ 435.9302, and required for $C_{13}H_{16}NO_4{}^{79}Br^{35}Cl_2{}^{37}Cl$ 435.9293, 437.9258 required for $C_{13}H_{16}NO_4{}^{81}Br^{35}Cl_2{}^{37}Cl$ 437.9272, and required for $C_{13}H_{16}NO_4{}^{79}Br^{35}Cl^{37}Cl_2$ 437.9263, 439.9258 required for $C_{13}H_{16}NO_4{}^{81}Br^{35}Cl^{37}Cl_2$ 439.9243, and required for $C_{13}H_{16}NO_4{}^{79}Br^{37}Cl_3$ 439.9234, found 441.9198 required for $C_{13}H_{16}NO_4{}^{81}Br^{37}Cl_3$ 441.9213.

The RT of non-derivatized MDMA was 10.6 min. The EI spectrum gave a very weak mass ion at 193, as well as a very weak signal (163) for the loss of methylamine (Figure 43). This is different from the ESI-MS/MS results (Figure 26), where a strong $[M+H]^+$ at 194 m/z and a base peak for the loss of methylamine (163 m/z) were observed. Of the other fragments shown in the EI spectrum, the only prominent signal is the base peak at 58 for the iminium ion, which is common among phenethylamines and cathinones.[236] However, the TCF derivative of MDMA resulted in a RT = 18.5 min, a significant increase in RT compared to the non-derivatized MDMA (Figure 43). This is a result of the increase of molecular weight, and alteration of polarity and volatility, due to the formation of the carbamate derivative.[237]

In the EI spectrum 50-500 m/z scan, the MDMA TCF-carbamate derivative resulted in an intense mass ion at 367 m/z, showing the clear isotopic distribution of substitution with three chlorine atoms (Figure 43C). A low intensity fragment from the loss of one chlorine is visible at 332 m/z, and a base peak at 232 m/z which is the result of the loss of trichloroethyl-(methyl)carbamate, similar to the mephedrone derivative base-peak fragment (Figure 39A).

For an enhanced analytical specificity, the derivative was infused in the positive-ion mode loop-injection into ESI-MS, resulting in the detection of the $[M+H]^+$ found at 368.0241 required for $C_{14}H_{17}NO_4{}^{35}Cl_3$ 368.0217 (within 6.5 ppm), found 370.0189 required for $C_{14}H_{17}NO_4{}^{35}Cl_2{}^{37}Cl$ 370.0189, found 372.0156 required for $C_{14}H_{17}NO_4{}^{35}Cl^{37}Cl_2$ 372.0163, found 374.0155 required for $C_{14}H_{17}NO_4{}^{37}Cl_3$ 374.0142 (Figure 43). Moreover, traces of ketamine and ethylone of less than 2% were confirmed by GC/MS and ESI-MS, possibly due to cross-contamination of the sample rather than the presence of cutting agents.
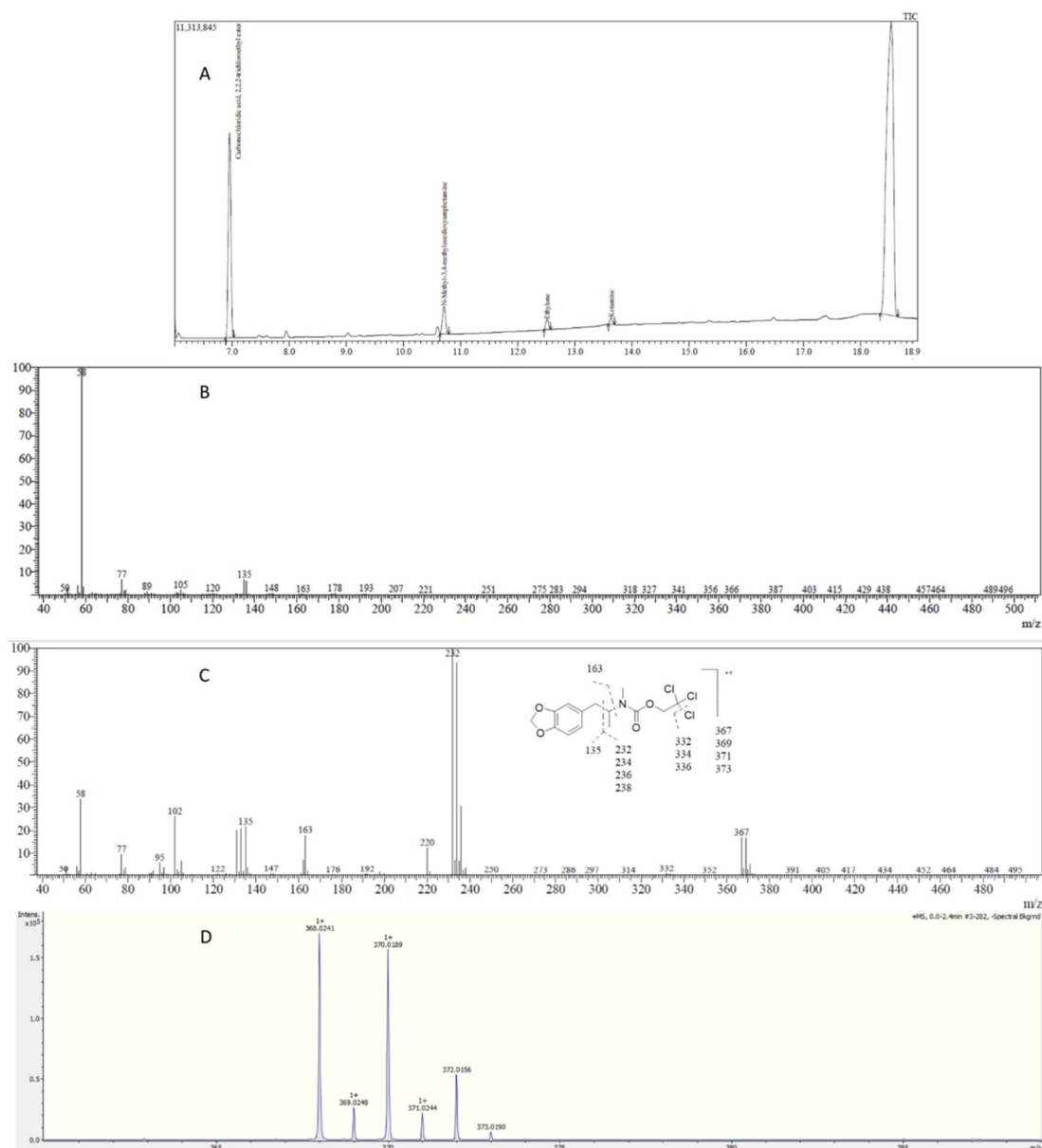
Figure 43. (A) TIC of non-derivatized MDMA RT 10.6 min, and MDMA TCF-carbamate RT 18.5 min, (B) EI spectrum of non-derivatized MDMA showing base peak at 58 m/z, (C) EI spectrum of MDMA carbamate with proposed structural fragmentation showing the M$^+$ isotopic cluster at 367 and base-peak cluster at 232, (D) ESI-MS loop-infusion of MDMA carbamate derivative showing the [M+H]$^+$ cluster in the isotopic ratio of 27:27:9:1.

Ethylone was the least polar of the seized drugs being derivatized, due to the presence of an *N*-ethyl group. This resulted in a RT = 12.5 min. Derivatization resulted in a significant change in polarity, with RT increasing to 21.1 min. The standard run therefore needed to be extended beyond 20.0 min as explained in the Experimental/Instrumentation

section 2.2.3. The EI-MS 50-500 m/z scan of non-derivatized ethylone gave a weak mass ion at 222 m/z and also a weak 149 m/z for the loss of the diethylamine radical. The base peak at 72 m/z is the result of the formation of an iminium ion, a common base-peak in cathinones.[213]

Even though the carbamate derivative of ethylone gave a weak signal for the mass ion at 396 m/z, the base-peak cluster (246:248:250:252) with an isotopic ratio arising from three chlorine atoms (27:27:9:1) corresponds to the formation of 2,2,2-trichloroethyl *N,N*-diethyl carbamate fragment ion (Figure 44 top) by acyl cleavage. This differs from the mephedrone base-peak cluster at 232 m/z, that corresponds to 2,2,2-trichloroethyl *N*-ethyl-*N*-methyl carbamate fragment ion. The 246 m/z base peak was distinctive enough to provide some evidence that the TIC peak at 21.1 min belongs to the ethylone carbamate derivative. Moreover, infusion of the derivative into ESI-MS positive-mode loop injection resulted in the detection of the molecular ion providing HR-MS molecular ion identification: found $[M+H]^+$ 396.0176 required for $C_{15}H_{17}NO_5{}^{35}Cl_3$ 396.0168, found 398.0134 required for $C_{15}H_{17}NO_5{}^{35}Cl_2{}^{37}Cl$ 398.0139, found 400.0114 required for $C_{15}H_{17}NO_5{}^{35}Cl^{37}Cl_2$ 400.0107, found 402.0059 required for $C_{15}H_{17}NO_5{}^{37}Cl_3$ 402.0078 (Figure 44).
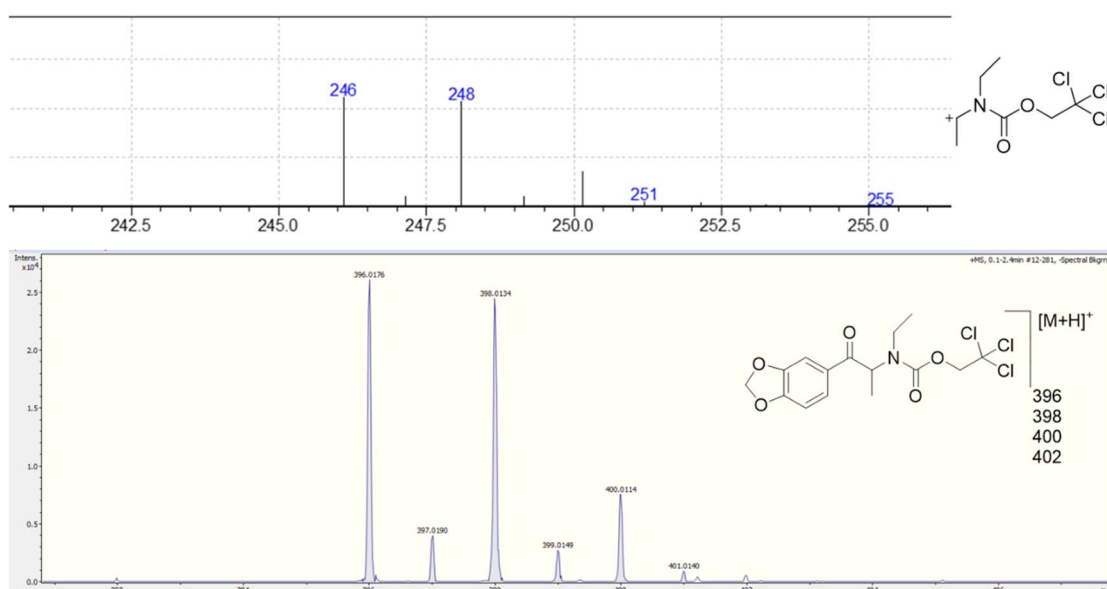
Figure 44. (Top) EI-MS base peak cluster arising from ethylone carbamate derivative, (bottom) ESI-MS infusion in the positive-ion mode of ethylone carbamate derivative showing the M+H$^+$ with its isotopic distribution.

2.4 Conclusions

In this Chapter, an analytical description of the association of phenethylamines, in particular MDMA, with other NPS using 1D/2D NMR and MS is given. 2D NMR was crucial in the identification and structural-elucidation process due to its 2D dispersive advantages, while LC-ESI/MS/MS allowed observation of the molecular ion, as well as distinctive fragmentation patterns of drugs even in mixtures. The use of a HILIC column, which was developed to analyse polar components such as amino acids, proved useful for the analysis of phenethylamines and cathinones. ^{1}H q-NMR using MA as the IS allowed the quantification of multicomponent drug samples (in powders) without resorting to chromatographic methods that require a reference standard and lengthy preparation steps.

^{1}H q-NMR for the analysis of seized ecstasy tablets allowed fast, robust, precise analysis of a variety of MDMA tablets, using MA as the IS. Furthermore, this method allowed simultaneous quantification as well as detection of organic impurities/cutting agents present in the tablets that were not detected by UHPLC/MS, such as caffeine. Moreover, the finding of MDMA tablets containing double the typical dose is alarming and a cause of concern with respect to potential harm.

Chromatographic and mass spectrometric analytical studies of phenethylamines and cathinones allowed the examination of the altered polarity and increase in molecular weight of the compounds after converting them into their carbamate derivatives, and the impact on chromatographic behaviour. Moreover, the incorporation of three chlorine atoms resulted in a highly specific molecular ion observed in the ESI-MS, as well as distinctive fragmentation patterns in the EI-MS with complex yet discernible isotopic clusters. Finally, MDMA is the most popular drug from night-club seizures. It was found in high purity. However, examples of mixing of MDMA with other pharmacologically more potent NPS were observed, thus possibly increasing the likelihood of toxicity or even death to users. This is a challenge to law enforcement, emergency room medical personnel, and drug analysts.

In the next chapter, a more spectroscopically complex NPS class and further complex mixtures are analysed, revealing how challenging analytical studies of street samples can be.

Chapter 3. Analytical characterization of seized arylcyclohexylamines and phenidates

3.1 Introduction

The arylcyclohexylamine family of NPS is based on the chemical structures of 1-(1-phenylcyclohexyl)piperidine (PCP) and ketamine (Figure 45) which exert their effects through NMDA L-Glutamate receptors, but their NPS analogues have other CNS receptor cross-reactivities whilst retaining their dissociative properties similar to ketamine.[43,44,238] This group, along with tryptamines, makes up only 8% and 2% respectively of total NPS seized in 2013.[8] Nevertheless, there are many arylcyclohexylamine-associated reports of dependence, intoxications and deaths.[239-241] The first two such UK analytical detections were reported in 2012 in six individuals reporting mainly signs of tachycardia, hypertension and cerebral toxicity.[239,240] GC/MS confirmed the detection of 2-(3-methoxyphenyl)-2-(ethylamino)cyclohexanone (MXE) in all these six intoxication cases, while one case also had two other NPS both belonging to the benzofuran family.[239] Furthermore, with respect to deaths in the UK due to MXE, toxicological reports stated that MXE was solely responsible in 90% of cases.[241] MXE is promoted through internet vendors as a research chemical.
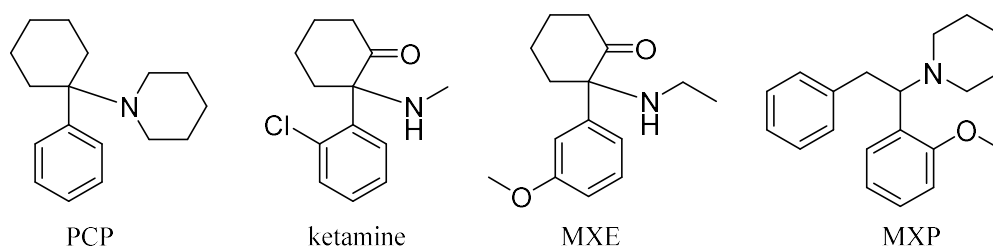
Figure 45. Classic arylcyclohexylamines and their NPS research chemicals.

The synthesis of MXE has been described by Hays *et al.*[53] in a four-step reaction scheme starting with a cyclopentyl Grignard reaction with 3-methoxybenzonitrile to form 3-methoxyphenyl cyclopentyl ketone, followed by α-bromination, reacting the product with ethylamine to form a Schiff base, and finally heating the tertiary alcohol imine for thermal rearrangement to form the desired cyclohexanone, MXE (Figure 46).
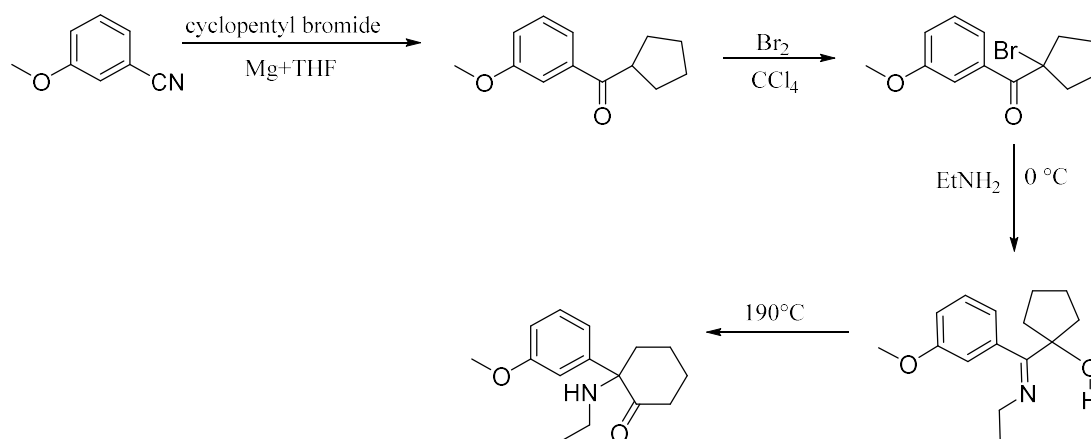
Figure 46. Synthetic scheme of MXE.

Methoxphenidine (MXP) (Figure 45) is an NPS classified in the family of arylcyclohexylamine dissociative drugs (Figure 45). Analogues of MXP circulating among internet vendors include regioisomers such as 3-MXP and 4-MXP, based on the position of the methoxy group on the aromatic ring. Analytical characterization of MXP has been described by McLaughlin *et al.*[242] Furthermore, intoxications and deaths associated with MXP have been reported.[242] Ketamine is usually not adulterated, but night-clubs' amnesty bin analysis revealed that ketamine is being cut with caffeine.[166] Nevertheless, no description of the mixing of arylcyclohexylamines with each other or with other cutting agents has been reported, thus warranting an analytical study on such street samples.

Phenidate-type NPS are based on the ADHD drug methylphenidate (Ritalin), with many analogues based on the methylphenidate structure. The most common analogue is ethylphenidate, with online drug forums chatter contributing to the increased popularity of this drug.[64] Both methylphenidate and ethylphenidate are psychostimulants, mainly acting through the potent inhibition of dopamine and (nor)adrenalin reuptake.[61] The first analytical characterization of ethylphenidate was reported by Casale and Hays in 2011,[243] using GC/MS, FT-IR and NMR of both the free base and the hydrochloride salt in CDCl3. The first analytical post-mortem detection in Europe was reported by Krueger *et al*. in 2014,[65] using LC/MS/MS and GC/MS. The authors believe that the levels of ethylphenidate were not in the lethal range, but they contributed to death which was caused by the intake of other drugs.

However, in 2015 Parks *et al.*[66] reported that in Eastern Scotland there were 19 cases where post-mortem toxicological examination revealed that ethylphenidate among other drugs (benzodiazepines and opiates) contributed to death; in 5 of them, ethylphenidate was mentioned on the death certificates as contributing to the cause of death. Identification of street samples of ethylphenidate are lacking in the literature, especially in the context of the analysis of mixtures of multiple components. This is an avenue worth exploring.

In this chapter, analytical studies of Bristol night-club amnesty bins and police seizures from different locations in the South West of England of arylcyclohexylamines and phenidate-based NPS are demonstrated. Furthermore, some of the samples are found to be complex four- and five-component mixtures of NPS, other illicit drugs, active pharmaceutical ingredients (APIs) as cutting agents, and impurities. Analysis utilized 1D/2D NMR spectroscopy and LC-ESI/MS/MS. LC/MS on a C-18 column is used for the analysis of arylcyclohexylamines and phenidate-based multi-component complex samples.

3.2 Experimental

3.2.1 Chemicals and samples

NMR grade solvents D_2O 99.9%, $CDCl_3$ 99.8%, and TMSP-2,2,3,3-D_4 98.0% were purchased from Cambridge Isotope Laboratories (Goss Scientific, UK). Methanol and water for UHPLC and UHPLC/MS analysis were Lichrosolve Honeywell LC/MS grade purchased from Fisher Scientific (UK). Maleic acid (MA) 99.94% is TraceCERT certified for quantitative NMR analysis purchased from Sigma-Aldrich (UK). Methoxetamine (MXE) hydrochloride 98.3% and 5-methoxy-*N*,*N*-diallyltryptamine (5-MeO-*N*-DALT) 99.5% were purchased from LGC (Teddington, UK).

Samples (collected in 2015-2016) in the form of creamy coloured powders, crystals, orange coloured tablet fragments, and magazine twists and wraps, weighing between 50-150 mg, were obtained from the Drug Expert Action Team (DEAT) of the Avon and Somerset Constabulary from seizures and amnesty bins in 3 different areas of the South West of England.

3.2.2 Sample preparation

For qualitative analysis, depending on the purity and complexity of the samples, between 10-50 mg were weighed using a Sartorius BP221S balance in 1.5 mL Eppendorf tubes, followed by dissolving the samples in D_2O, CD_3OD or $CDCl_3$. Samples were vortexed or centrifuged and the supernatant was transferred in to a 5 mm NMR tube. For NMR quantitative analysis, samples (11.0 mg) were weighed using a Sartorius analytical balance MC5 extracted with D_2O containing IS MA (3.0 mg/mL). For LC/ESI-MS analysis, a stock solution (1.0 mg/mL) of seized materials was prepared, followed by 100-fold dilution into a MS vial. Conversion of the MXE and ketamine salt samples into their respective free-bases was achieved using drops of concentrated aqueous ammonia, followed by extraction with $CHCl_3$, drying ($MgSO_4$) and then concentration under vacuum.

3.2.3 Instrumentation

NMR spectroscopy

NMR spectra were recorded as detailed in chapter 2, section 2.2.3 instrumentation.

ESI-MS infusion

Electrospray Ionization-Mass Spectrometry (ESI-MS) was conducted as detailed in chapter 2, section 2.2.3 instrumentation.

UHPLC/ESI-MS

Liquid chromatography was performed using an Acquity UPLC BEH C18, 1.7 µM, 2.1 x 50 mm RP-column (Waters, Milford, MA, USA) with an a injection volume of 10 µL at 25°C. Mobile phase A consisted of water 0.1% formic acid v/v, and mobile phase B consisted of acetonitrile 0.1% formic acid v/v. Two methods were used for the UHPLC separation of components. Gradient 1 flow rate 0.3 mL/min, elution started with 1% B for 1.0 min, followed by a linear increase from 1.0 min to 100% B at 8.0 min and maintained for 2.0 min, followed by a decrease to 1% B at from 10.0 to 10.1 min, where it was held for equilibration

for 2.9 min, total run time 13.0 min. Gradient 2 flow rate 0.4 mL/min, elution started with 1%

B for 2.0 min, followed by a linear increase from 2.0 to 100% B at 5.0 and maintained for 3

min, followed by decrease to 1% B at 8.1 where it was held for equilibration for 3.9 min, total

run time 12.0 min. Mass spectra were obtained using ESI-MS micrOTOF from Bruker

Daltonik with positive-ion mode on diluted samples (10 μg/mL in HPLC grade methanol

from a stock solution of 5 mg/mL). The mass accuracy of $[M+H]^+$ and $[M+Na]^+$ is within 5

ppm of the required mass, unless otherwise stated. The QTOF-UHPLC LC-MS analysis was

conducted using a MaXis HD electrospray Quadrupole Time-of-Flight (ESI-QTOF) mass

spectrometer (Bruker Daltonik GmbH, Bremen, Germany), operated in ESI positive-ion

mode. The QTOF was coupled to an Ultimate 3000 UHPLC (Thermo Fisher Scientific, CA,

USA). The capillary voltage was set to 4500 V, nebulizing gas at 4 bar, drying gas at 12

L/min at 220°C. The TOF scan range was from 75-1000 mass-to-charge ratio (m/z). For

LC/MS/MS capabilities, the in-source CID was set to 0.0 eV, with the collision energy for

TOF MS acquisition at 3.0 eV. The collision energy was set on a sliding scale from 100 m/z

at 14.0 eV, 500 m/z at 20.0 eV, and 1000 m/z at 30.0 eV. For the analytes the actual collision

energy was between 15.0-18.0 eV. The MS instrument was calibrated using a range of

sodium formate clusters introduced by 10 μL loop-injection prior to the chromatographic run.

The mass calibrant solution consisted of 3 parts of 1 M aqueous NaOH to 97 parts of 50:50

water:isopropanol with 0.2% formic acid (v/v) and was used to calibrate the instrument

within 1 ppm mass error standard deviation. Ions were detected as $[M+H]^+$ ion with a mass-

to-charge (m/z) ratio within 5 ppm, respectively. Data processing was performed using the

Data Analysis software version 4.3 (Bruker Daltonik GmbH, Bremen, Germany).

3.3 Results and discussion

3.3.1 Analytical studies of seized arylcyclohexylamine complex mixtures

A total of 26 samples were found containing ketamine or MXE, in addition to samples

containing ketamine and/or MXE mixed with cutting agents (Table 8) (Figure 47).

Table 8. Arylcyclohexylamine samples identified using NMR and ESI-MS.

Description of sample	Quantity
ketamine	9
ketamine-creatine	2
ketamine-MXE-MXP-creatine-DMS	5
ketamine-procaine-creatine	1
MXE	7
MXE-creatine	2
Total	26

Figure 47. Magazine twists containing combinations of different

cutting agents and NPS associated with ketamine or MXE.

NMR analysis of sample HN76 revealed ketamine and the cutting agent creatine, deduced from 2 proton singlets at 3.02 and 3.92, and ^{13}C NMR data for 4 carbons, 2 of them quaternaries. HSQC revealed the singlet at 3.02 ppm is a methyl group with corresponding carbon at 36.9 and the 3.92 singlet is a methylene corresponding to its carbon at 53.8 ppm with no correlation in COSY, but the HMBC revealed methylene carbon coupling to the methyl and vice versa. Moreover, the sample was converted into the free base to obtain a better resolution in the aromatic region compared to the salt in D_2O showing a multiplet of 3 protons and a distorted doublet of doublets (Table 9 and Figures 48 and 49). Hays *et al.*[53] published the first analytical characterization of ketamine. However, there the signals at 1′

and 2′ were transposed. They have been re-assigned in this study, using HMBC (in D_2O) that showed connection of 1′ carbon at 127.2 ppm to the one of H3 protons at 1.90-1.94 ppm, thus warranting a complete assignment of the compound with creatine impurity present.
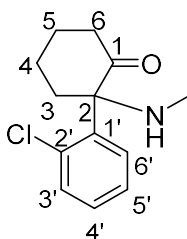
Table 9. ^1H and ^{13}C NMR ketamine assignments of sample HN76.

Position	Ketamine free base (in CDCl₃)		Ketamine salt (in D₂O)	
	^{13}C	^1H	^{13}C	^1H
1	208.9	-	211.4	-
2	70.1	-	72.5	-
3	38.6	1.73-1.74 1H, m	36.0	1.90-1.94 1H, m
		2.73-2.79 1H, m		3.34 1H, dd (13.5, 2.5)
4	21.8	1.69-1.75 2H, m	21.1	1.72-1.78 1H, m, 1.86-1.90 1H, m
5	27.9	1.78-1.85 1H, m, 1.98-2.09 1H, m	30.1	1.78-1.83 1H, m, 2.10-2.18 1H, m
6	39.5	2.46 1H, ddd (13.5, 8.5, 5.5),	39.4	2.56-2.69 2H, m
		2.49 1H, ddd (13.5, 7.5, 5.5)		
N-CH₃	29.1	2.10 3H, s	36.9	2.42 3H, s
1′	133.7	-	127.2	-
2′	137.9	-	134.1	-
3′	131.2	7.36 1H, dd (8.0, 1.5)	128.4	7.59-7.64 1H, m overlapped
4′	128.6	7.23 1H, td (8.0, 1.5)	132.6	7.59-7.64 1H, m overlapped
5′	126.5	7.31 1H, td (8.0, 1.5)	131.9	7.59-7.64 1H, m overlapped
6′	129.3	7.54 1H, dd (8.0, 1.5)	131.7	7.88 1H, dd (6.5, 3.0)
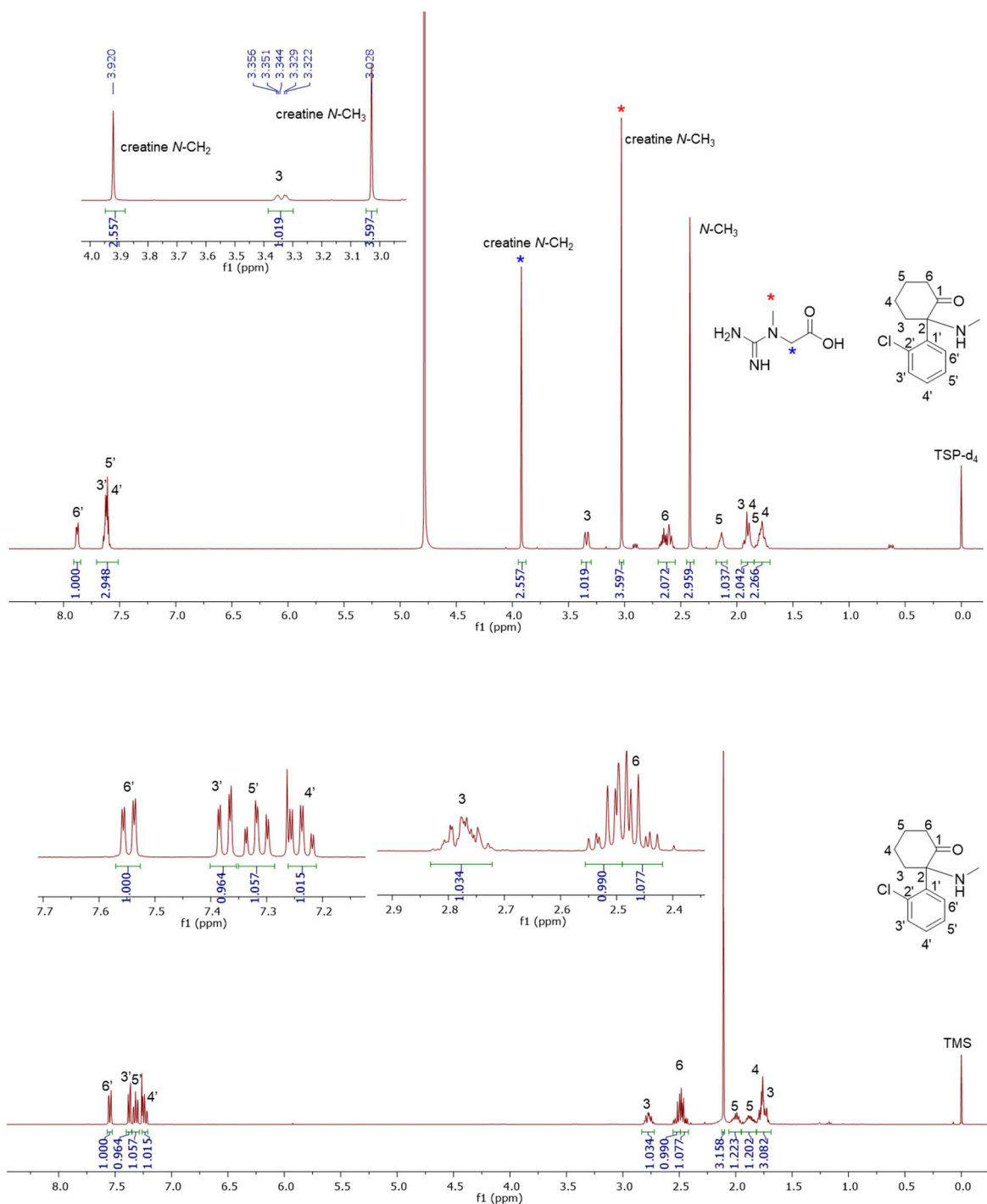
Figure 48. (Top) ^{1}H NMR (in D$_2$O) of sample HN76 containing ketamine salt and creatine with expansion of the two creatine signals, (bottom) ketamine free-base (in CDCl$_3$) with expansion of the 2.4-2.9 ppm region and expansion of the aromatic region showing the 1,2-disubstituted aromatic pattern.
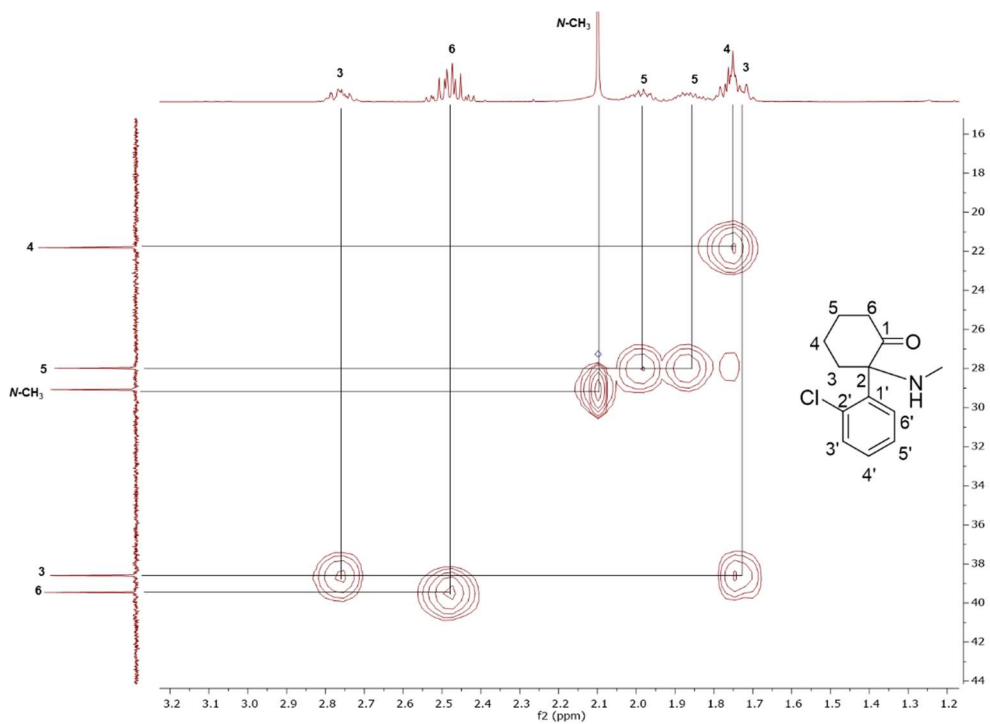
Figure 49. HSQC expansion (1.2-3.2 ppm and 16-44 ppm) of ketamine free-base (in CDCl$_3$).
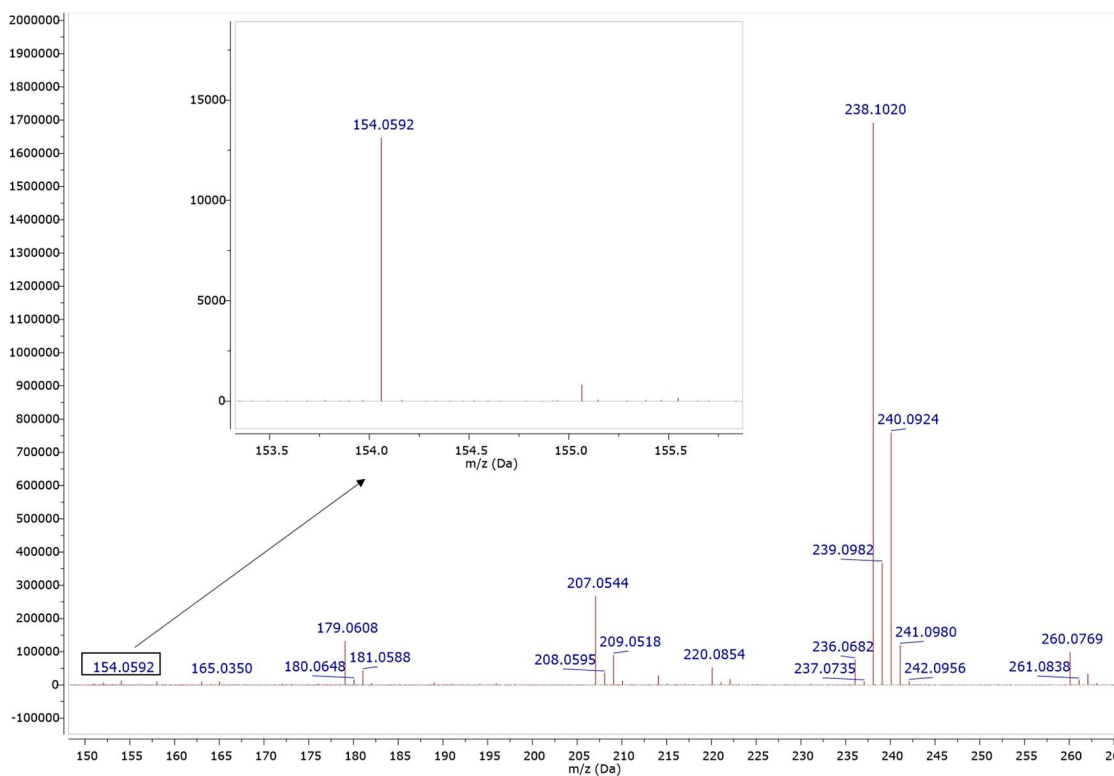
Figure 50. ESI-MS loop injection in the positive-ion mode of a ketamine/creatine mixture with an expansion (inset) of the [M+Na]$^+$ for creatine 154.0592.

ESI-MS analysis of sample HN76 detected the cutting agent creatine, found $[M+Na]^+$ 154.0592 required for $C_4H_9N_3O_2Na$ 154.0586. Even though the abundancy of the mass ion detected was significantly low due to the poor ionization of creatine, the mass accuracy was within the acceptable 5 ppm error (Figure 50). Creatine impurity was easily isolated by separation of the water fraction against chloroform, after converting ketamine into the free base using drops of aqueous ammonia. Furthermore, creatine is a cheap and widely available supplement product in health shops, with a physical appearance that resembles a ketamine salt making it a suitable cutting agent.

Analysis of sample HN209 revealed (molar ratios) ketamine (80%) with creatine (16%) and procaine (4%) as cutting agents (Figure 51). Procaine has been reported as a cutting agent in cocaine,[244] but to the best of our knowledge it has not been reported before as a cutting agent for ketamine. The ^1H and ^{13}C NMR data in this mixture were all consistent with ketamine and creatine. In addition, NMR analysis of the mixture allowed the structural elucidation and assignment of procaine (500 MHz in D_2O) (C1) ^{13}C δ = 168.7, (C1″) ^{13}C δ = 116.5, (C2″,6″) ^{13}C δ = 131.9 ^1H δ = 7.84, 2H, d 8.5 Hz, (C3″,5″) ^{13}C δ = 114.6 ^1H δ = 6.83, 2H, d 8.5 Hz, (C4″) ^{13}C δ = 153.0, (C1′) ^{13}C δ = 59.0 ^1H δ = 4.65, 2H, t 5.0 Hz, (C2′) ^{13}C δ = 50.4 ^1H δ = 3.66, 2H, t 5.0 Hz, (C1‴) ^{13}C δ = 48.4 ^1H δ = ~3.40, 4H (overlapped with 1H of ketamine H3), (2‴) ^{13}C δ = 8.3 ^1H δ = 1.38, 6H, t 7.5 Hz. ESI-MS analysis of the mixture revealed the molecular ions of ketamine with the isotopic ratio of 3:1 of 1 chlorine atom, found $[M+H]^+$ 238.1033 for $C_{13}H_{17}NO^{35}Cl$ requires 238.0993 (within 17 ppm), found 240.0957 for $C_{13}H_{17}NO^{37}Cl$ requires 240.0963, as well as procaine found 237.1605, $C_{13}H_{21}N_2O_2$ requires 237.1597. Furthermore, creatine was not detected in this mixture (sample HN209) by ESI-MS loop injection, possibly due to its poor ionization and low amount in the mixture (16%). Nevertheless, NMR allowed the detection and quantification of creatine in this mixture.
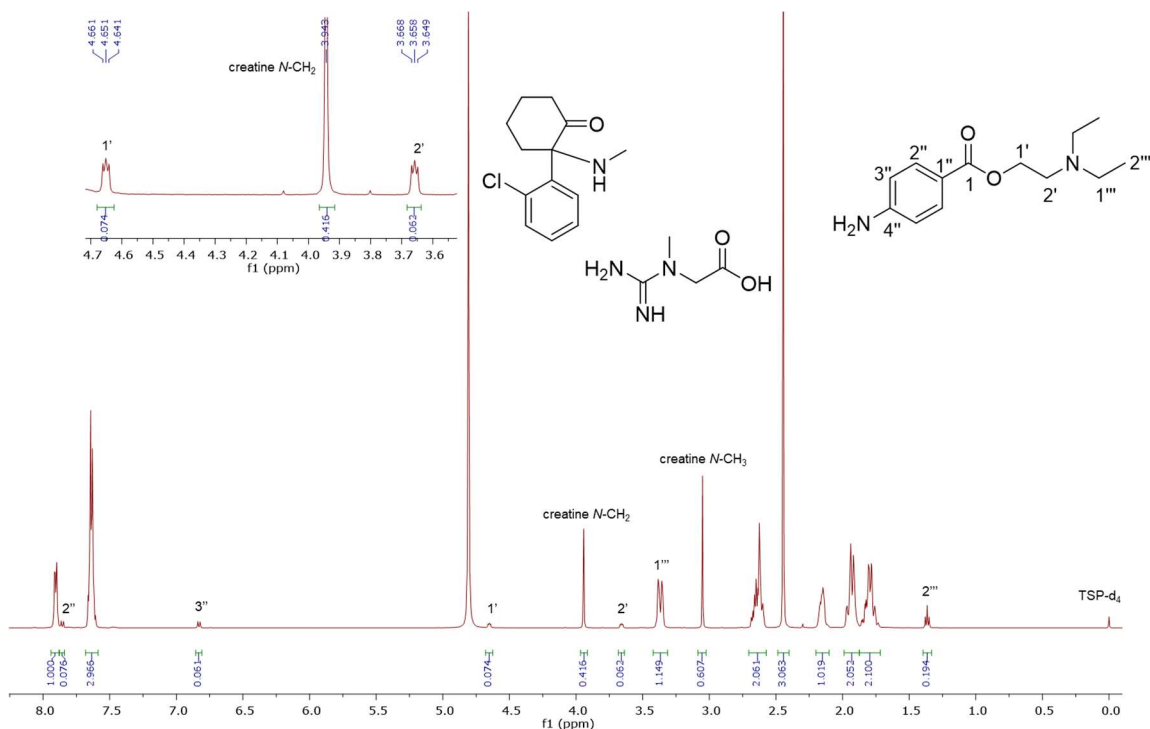
Figure 51. ^{1}H NMR (in D$_2$O) of ketamine salt cut with creatine and procaine (peaks assigned).

MXE samples (50-100 mg) were found in folded, cut-out magazine papers, obtained from Bristol police seizures. NMR analysis (in D$_2$O) of sample HNSE89 revealed the absence of the 1,2-disubstitution pattern of the ketamine aromatic ring in favour of the 1,3-pattern, together with the methoxy singlet at 3.87 ppm, and the methyl (1.17 ppm) coupling (from COSY analysis) to the *N*-methylene of the *N*-ethyl at 2.56 ppm and at 2.90 ppm, split presumably due to the chiral centre (Figure 52 and Table 10). This structural assignment was confirmed by MS analysis which showed the molecular ion of MXE [M+H]$^+$ 248.1673 for C$_{15}$H$_{22}$NO$_2$ requires 248.1645 (within 11 ppm) and [M+Na]$^+$ of 270.1452 for C$_{15}$H$_{21}$NO$_2$Na requires 270.1469 (within 7 ppm), and the cutting agent creatine 154.0603 incorporating Na$^+$ for C$_4$H$_9$N$_3$O$_2$Na requires 154.0586 (within 11 ppm). As above in cutting ketamine, creatine was detected as the adulterant (41%); two singlets in the ^{1}H NMR (in D$_2$O) at 3.04 and 3.93 ppm correspond to the methyl and methylene groups respectively. The 4 signals in the ^{13}C NMR are assigned to the methyl (36.9) and methylene (53.8) and quaternary carbons at 157.1 (guanidine C=N) and at 174.6 (COOH) ppm. ^{1}H and ^{13}C assignments of creatine in both ketamine and MXE samples were validated against an authentic sample of creatine.
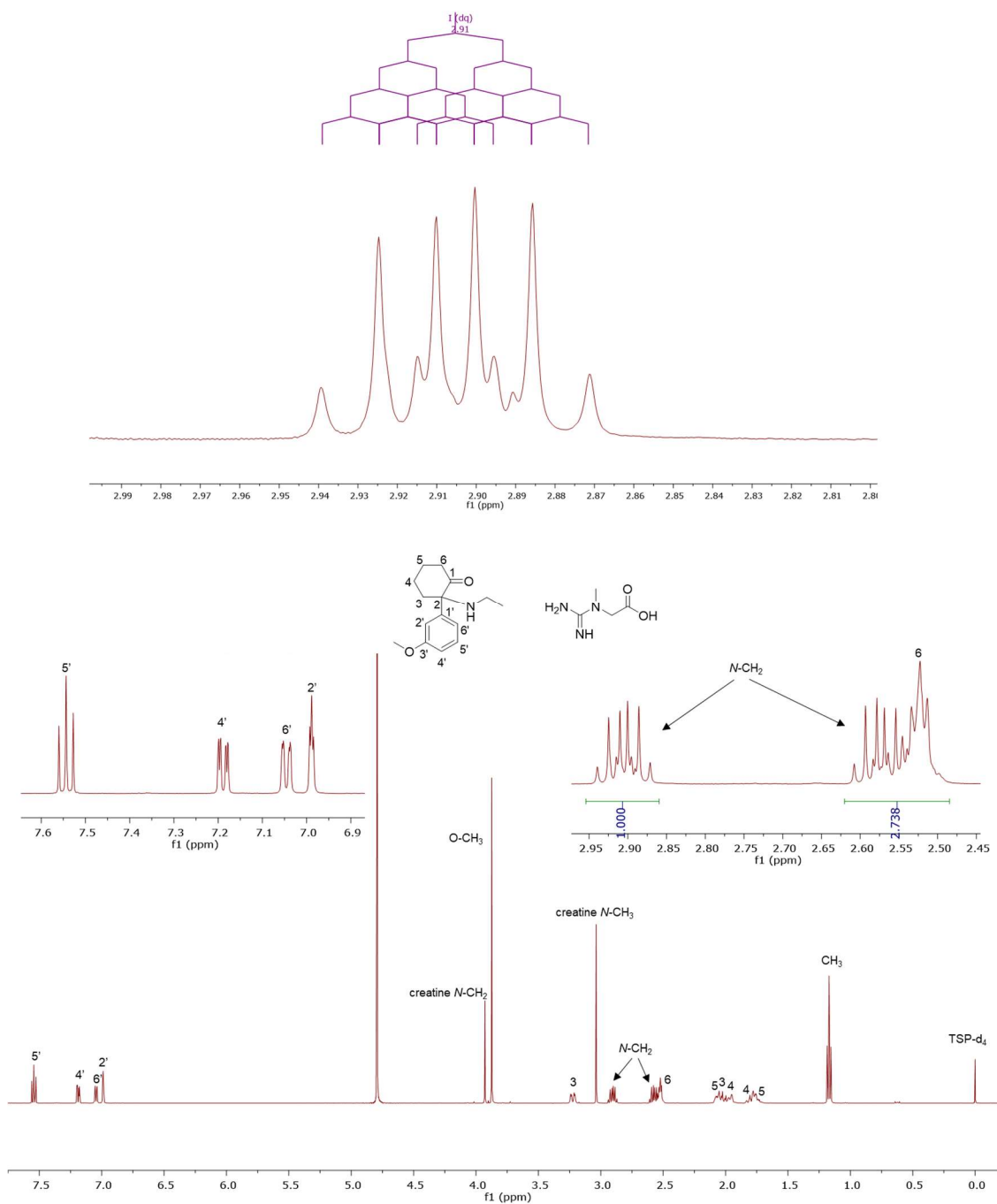
Figure 52. (Bottom) ^{1}H NMR (in D$_2$O) of sample HNSE 89 containing MXE (59%) and creatine (41%) with (inset) expansions of 2.45-2.95 and the aromatic region showing the 1,3-disubstitution pattern, (top) expansion of one of the MXE *N*-ethyl doublet of quartets (dq) *J* splitting tree of *geminal* $^2J_{HH}$ of 14.5 Hz and *vicinal* $^3J_{HH}$ 7.5 Hz at 2.90 ppm.
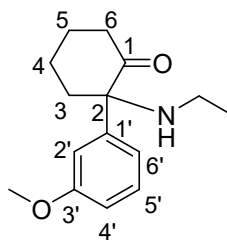
Table 10. ^{1}H and ^{13}C NMR assignments of MXE salt in D_2O.

Position	^{13}C	^{1}H
1	209.0	-
2	72.0	-
3	32.4	1.98-2.05 1H, m, 3.22 1H, ddd (14.0, 6.0, 3.0)
4	21.1	1.78-1.83 1H, m, 1.95-1.98 1H, m
5	27.3	1.73-1.78 1H, m, 2.06-2.09 1H, m
6	38.9	2.52 2H, t (6.0)
N-CH$_2$	37.1	2.57 1H, dq (14.5, 7.5), 2.90 1H, dq (14.5, 7.5)
N-CH$_2$-**CH$_3$**	10.6	1.17 3H, t (7.5)
1′	131.1	-
2′	114.1	6.99 1H, t (2.0)
3′	160.0	-
4′	115.9	7.19 1H, dd (8.0, 2.0)
5′	131.3	7.54 1H, t (8.0)
6′	120.8	7.05 1H, dd (8.0, 2.0)
O-CH$_3$	55.6	3.87 3H, s

HSQC allowed the assignment of the protons in the multiplets of the cyclohexanone to their corresponding carbons especially at positions 3, 4, and 5 as well as the aromatic protons (Figure 53). The aromatic protons signals at H4′ and H6′ were assigned by the HMBC relationship of C3′ to H4′. Furthermore, H5′ and H2′ had HMBC connectivities to C3′, while H6′ had no connectivity to C3′ as expected with a *para*-proton. Moreover, the HMBC relationship of C2 to H6′ and H2′ support the proton assignments in the aromatic region, H4′ has no such correlation. H2′ was a triplet from two *meta*-couplings to H4′ and H6′, ^4J = 2.0 Hz, but there was no additional *meta*-coupling between H4′ and H6′ which were both dd (Table 10). Unusually, the order of resonance of H4′ (7.19 ppm) and H6′ (7.05 ppm) is inverted in the ^{13}C NMR data, C4′ (115.9 ppm) and C6′ (120.8 ppm). The Heteronuclear 2-bond correlation (H2BC) experiment is an exclusive 2-bond coupling experiment that aids in the accurate assignment of the cyclohexanone and also the aromatic signals. This helps to

solve the issue of missing 2-bond connections in HMBC data. Nevertheless, for accurate assignment of these signals both HMBC and H2BC need to be employed. H2BC of the aromatic region revealed 2-bond connection of C3'-H2', C4'-H5' and C6'-H5' confirming the carbon and proton assignments. Combining HSQC data (Figure 53) with HMBC (Figure 54) and H2BC allowed the unambiguous assignments around the cyclohexanone ring where H6 has 2-bond and 3-bond connections with C5 and C4 respectively. In the H2BC experiment, only the cross-peak for the 2-bond connection C5-H6 showed on the diagonal. ESI-MS analysis revealed the molecular ion of the cutting agent creatine 154.0603 incorporating Na^+ within 7 ppm of the required 154.0592 for $C_4H_9N_3O_2Na$. MXE MS resulted in the $[M+H]^+$ of 248.1673 requiring 248.1650 for $C_{15}H_{22}NO_2$ (within 10 ppm) and $[M+Na]^+$ of 270.1452, requiring $C_{15}H_{21}NO_2Na$ 270.1469 (within 7 ppm). Moreover, the MXE single crystal structure was obtained (Figure 55) with data given in Appendix 1.
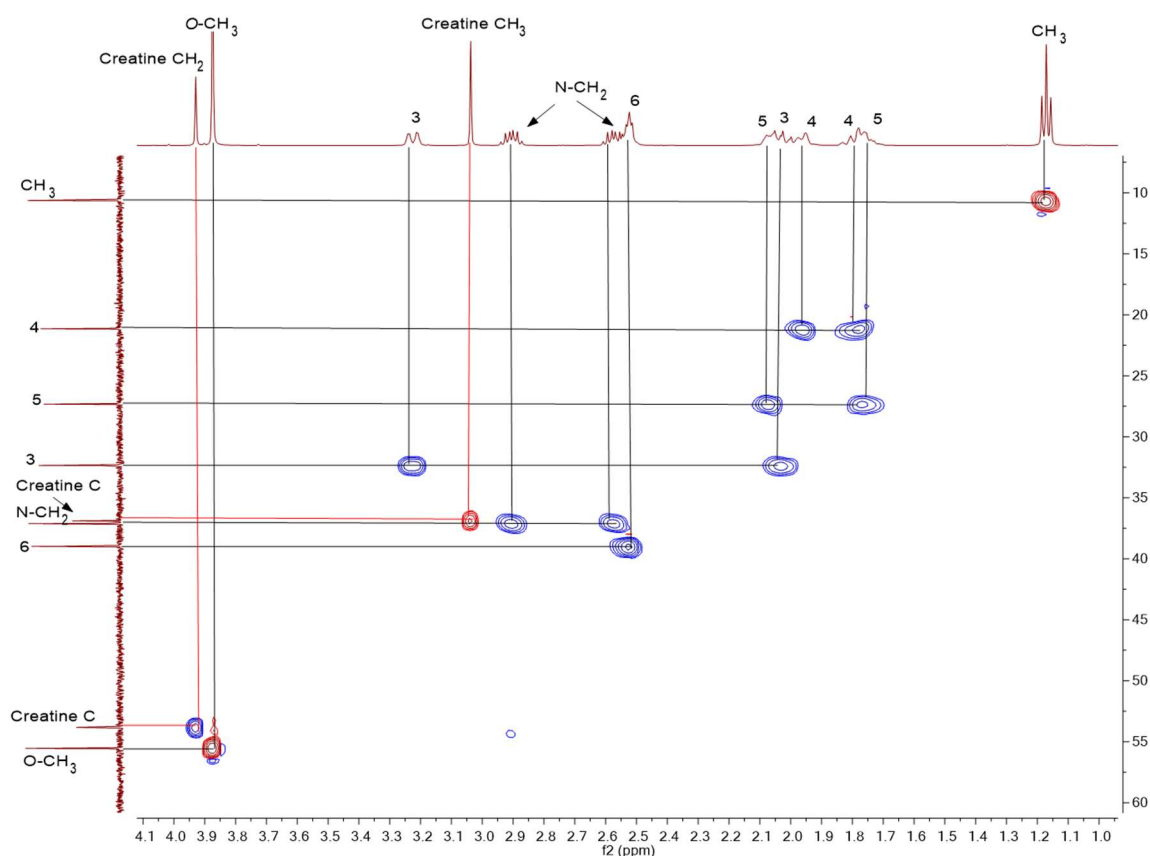
Figure 53. HSQC spectra of MXE/creatine mixture between 1.0-4.1 ppm and 10.0-60.0 ppm, red lines show creatine ^{1}H to ^{13}C 1-bond correlation, black lines show MXE ^{1}H to ^{13}C 1-bond correlation, red cross-peaks for methyls (and any methines), blue cross-peaks for methylenes.
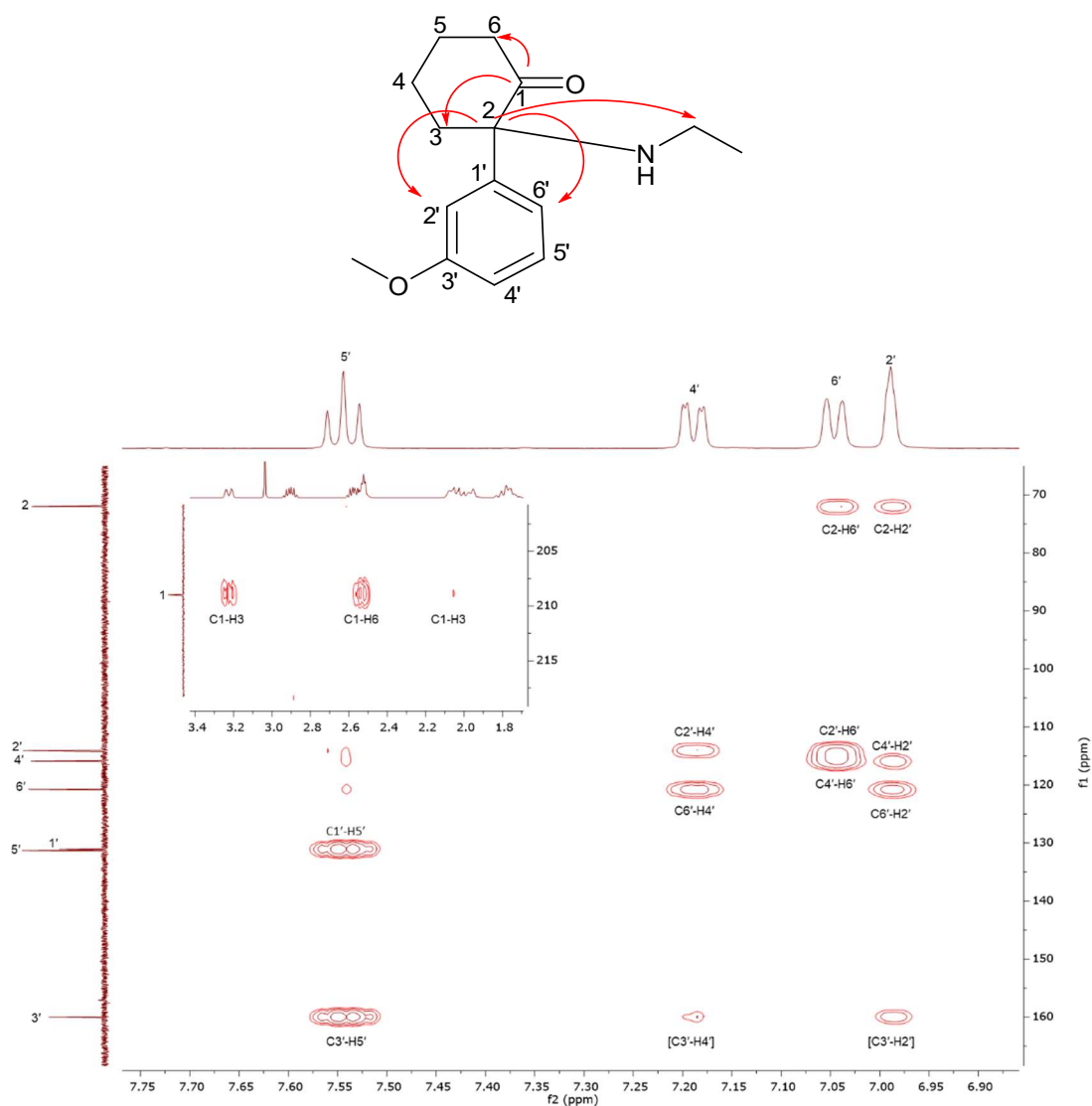
Figure 54. HMBC spectra showing key connectivities in MXE.
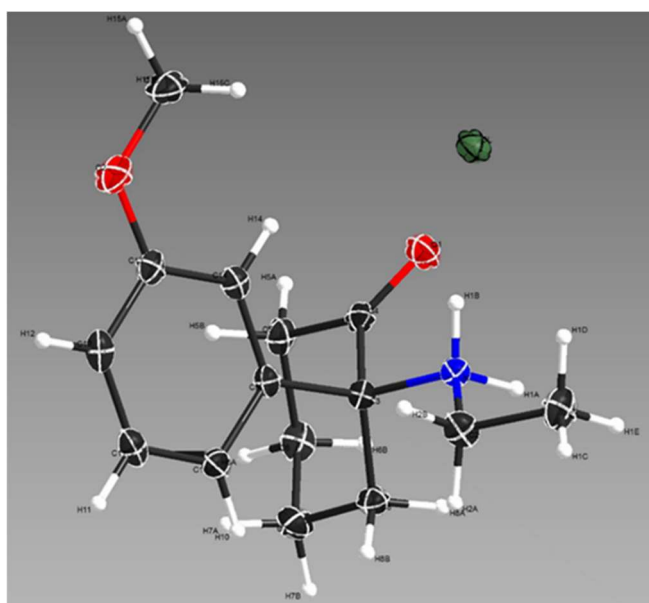
Figure 55. X-ray structure of MXE.

More complex mixtures of arylcyclohexylamines and cutting agents were identified in a cream coloured powder wrapped in a magazine paper (samples HN163 and HN200). These were analysed using a combination of 1D/2D NMR, ESI-MS and UHPLC/ESI-MS. NMR analysis of sample HN163 revealed ketamine 58%, MXE 2%, and MXP 1%, as the main psychoactive compounds present, in addition to creatine 5% and dimethyl sulfone (DMS) 34% as molar ratios (Figure 56), which were calculated using non-overlapping signals at 2.89, 2.40, and 2.61 ppm for ketamine, 1.14, 3.84, 7.00, and 7.70 ppm for MXE, 3.00 and 3.90 ppm for creatine, 6.90 and 7.40 ppm for MXP, and 3.12 for DMS, where HSQC revealed the singlet at ^{1}H δ = 3.12 ppm, ^{13}C δ = 41.6 ppm representing 2x methyls. MXP NMR data are consistent with the DEA SWGDRUG monograph collection.[245]

UHPLC/MS analysis using gradient 1 showed RT = 5.5 min [M+H]$^+$ for ketamine as the major component of the mixture 238.0997 for $C_{13}H_{17}NO^{35}Cl$ requires 238.0993, 240.0968 for $C_{13}H_{17}NO^{37}Cl$ requires 240.0963; RT = 5.8 min MXE [M+H]$^+$ 248.1649 for $C_{15}H_{22}NO_2$ requires 248.1645; RT = 6.9 min MXP [M+H]$^+$ 296.2012 for $C_{20}H_{26}NO$ requires 296.2008. As for creatine, its high polarity prevented its retention on a C18 column. Nevertheless, infusion of the sample into the MS using the loop-injection method allowed the detection of [M+Na]$^+$ 154.0581 for $C_4H_9N_3O_2Na$ requires 154.0586. Moreover, DMS was not detected using LC/MS even though it is present in 34% according to ^{1}H NMR, a problem encountered for small molecules that have poor ionization and no chromophore. Furthermore, a trace amount of a cathinone was detected on the UHPLC/ESI-MS spectrum in a green coloured peak (Figure 57) at 6.3 min with [M+H]$^+$ 254.1540 for $C_{17}H_{20}NO$ requires 254.1539, analysed as trace amounts (< 0.1%) of methylbenzyl cathinone; the only one reported is the 4-methylbenzyl cathinone also known as benzedrone/4-MBC.[246] MS/MS analysis allowed the confirmation of the structure according to the proposed fragmentation (Figure 58). Even though MXP was detected unambiguously, complete NMR spectroscopic characterization was not possible due to some of the piperidine signals overlapping with cyclohexanone signals in both ketamine and MXE.
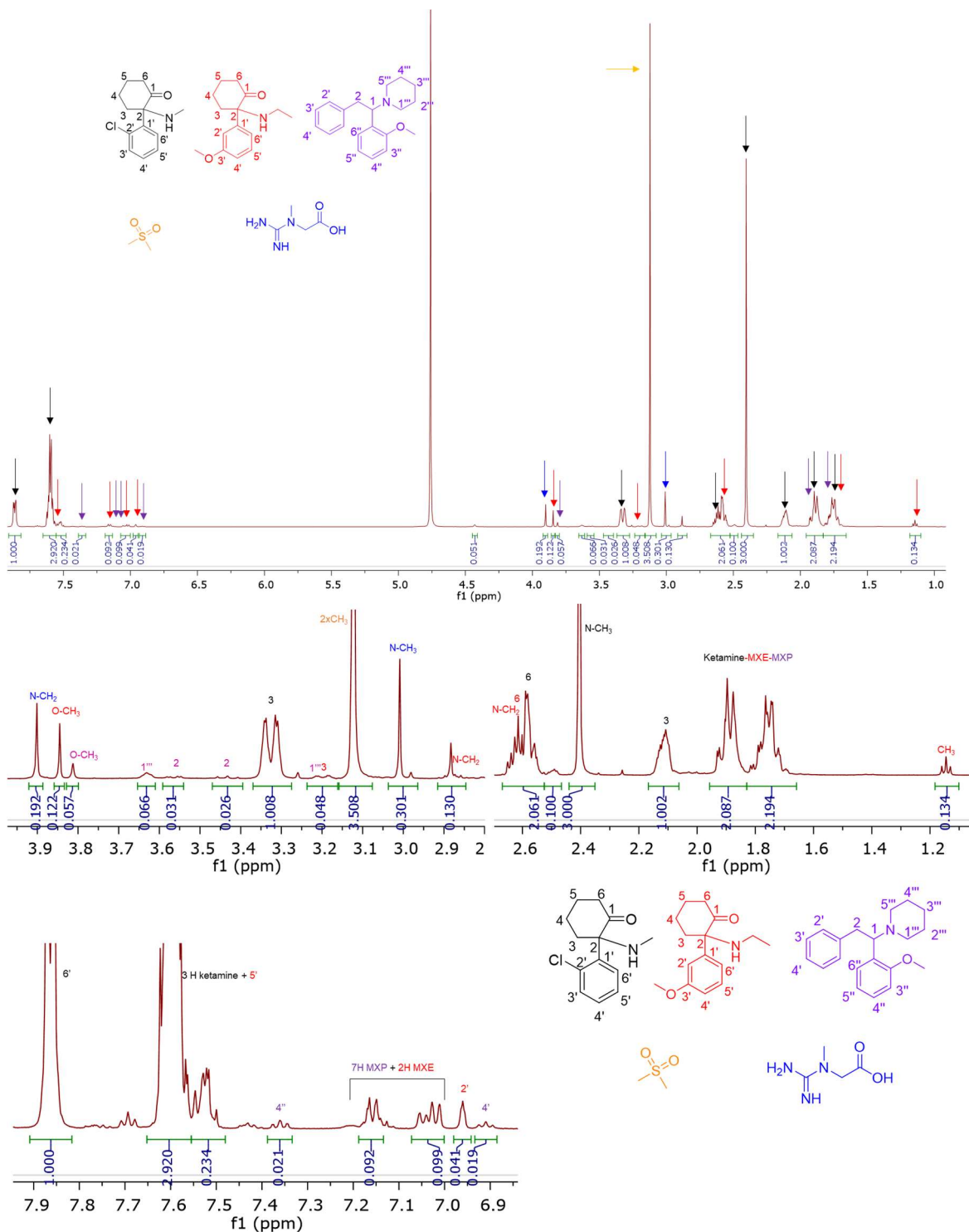
Figure 56. ^{1}H NMR (in D_2O) of sample HN163 containing ketamine, MXE, MXP, creatine and DMS, (top) ^{1}H spectrum of the 5-component mixture, (bottom) expansions of all regions with assignments.
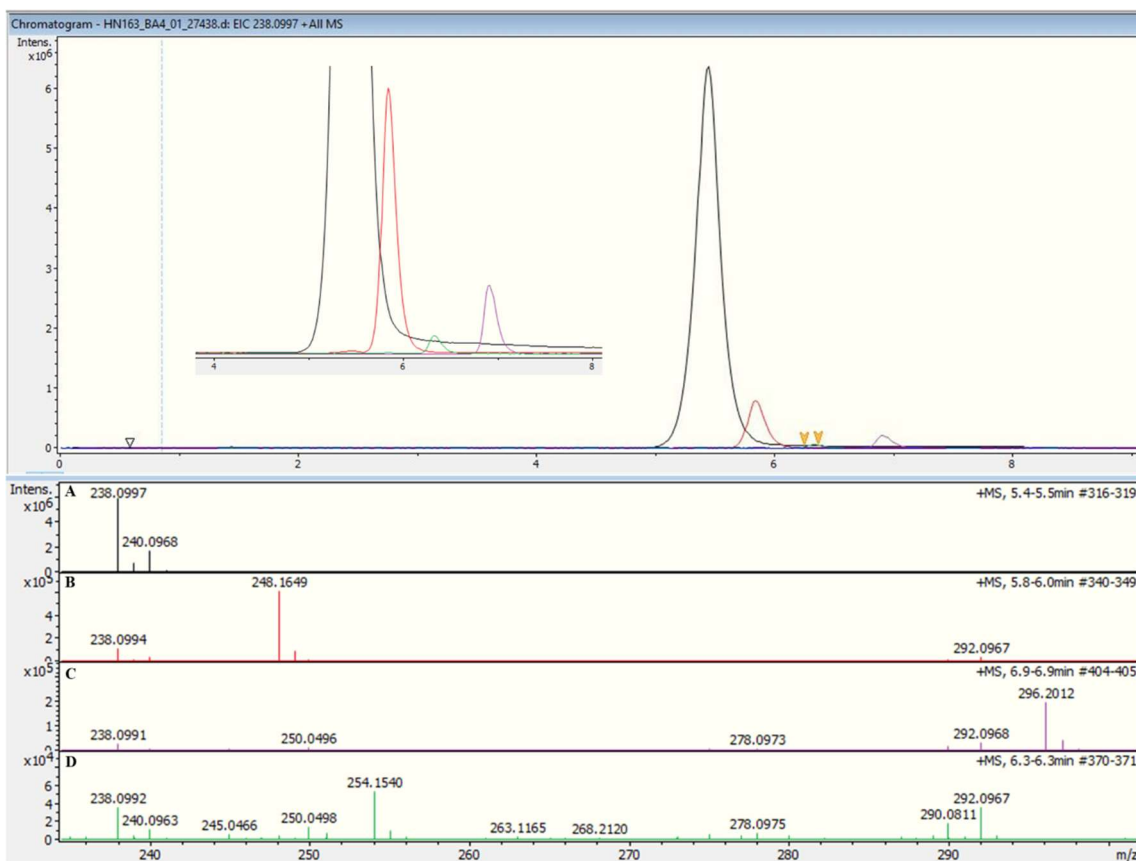
Figure 57. UHPLC/ESI-MS of sample HN163 showing (top) EIC of the 4 active components with expansion showing 4-MBC (green peak RT = 6.3 min), (bottom) ESI-MS spectra of (A) ketamine, (B) MXE, (C) MXP, (D) 4-MBC.

MS/MS analysis revealed the characteristic fragmentation pattern for each component in the mixture (Figures 58 and 59). Ketamine ESI-MS/MS fragmentation was distinctive due to the presence of a chlorine atom in all fragments giving the characteristic 3:1 ratio two mass ions. Unlike the GC/MS analysis of ketamine that suffered from an absent or weak molecular ion,[53] ESI-MS/MS resulted in a clear molecular ion that underwent two pathways of fragmentation. The first resulted from the loss of water (220.0891 m/z), and the second from the loss of methylamine (207.0575 m/z). 179.0624 m/z and 125.0155 m/z fragments result from the opening of the cyclohexanone ring and formation of 2-chlorobenzyl ion respectively. 4-MBC formed two fragments, 134.0970 m/z and 91.0545 m/z resulting from the formation of N-benzylethylamine ion and tropylium ion ($C_7H_7^+$). In MXP, in addition to the [M+H]$^+$ at 296.2012, fragments result from the loss of the piperidine ring at

211.1120 m/z (base peak) and the formation of piperidinium ion 86.0967 m/z, 193.1014 m/z results from the formation of a (2-phenylethylidene)cyclohexa-2,4-dien-1-ylidene)methylium ion, while 183.1170 m/z results from the formation of 1-(cyclohexa-2,5-dienyl)-2-phenyl-ethan-1-ylium ion. The proposed fragmentation of MXP has a similar pattern to the parent compound diphenidine and as in McLaughlin et al.[242] who published an in depth analysis of MXP analogues differing only in the methoxy position on the aromatic ring.
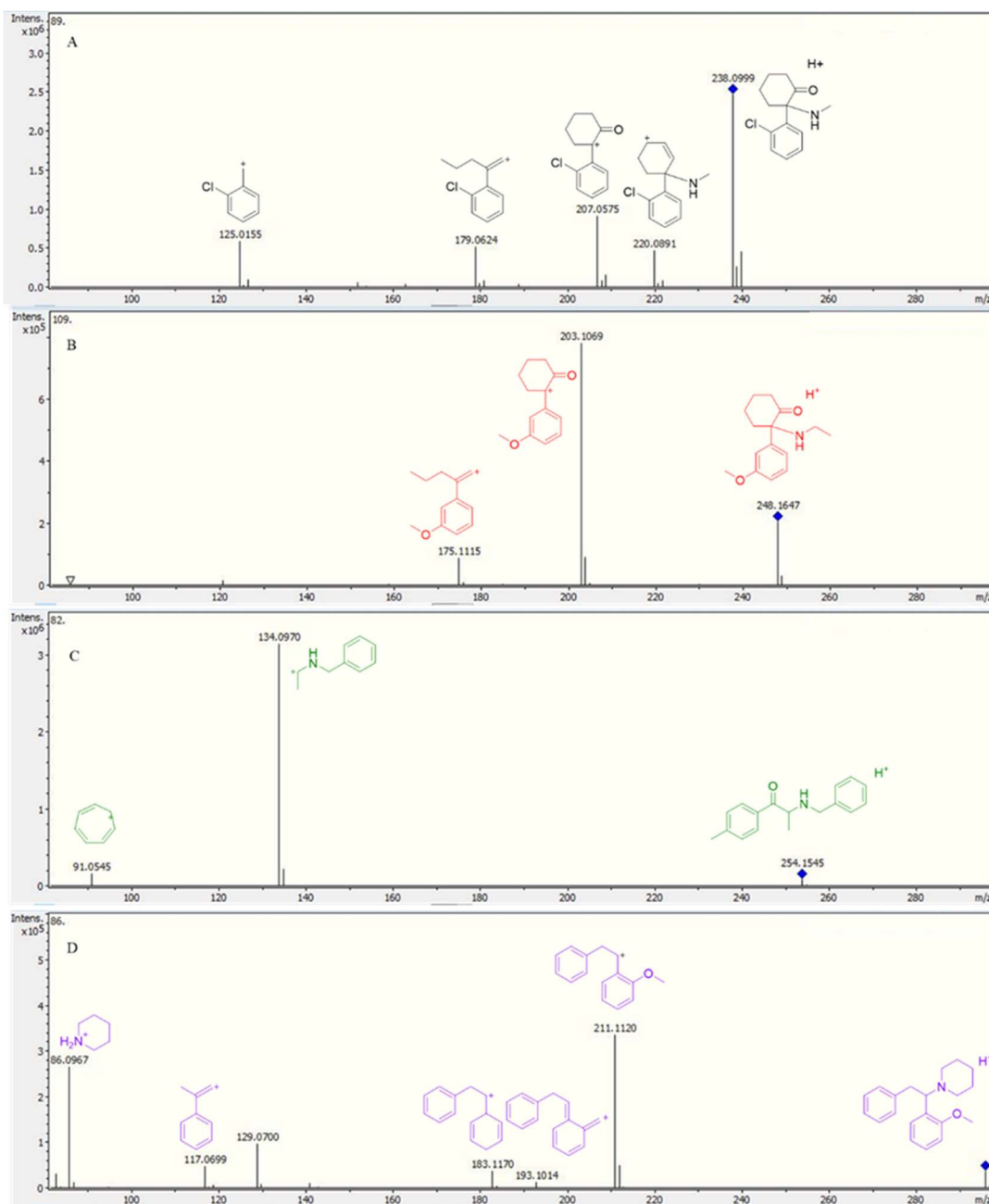
Figure 58. MS/MS spectrum of sample HN163 showing molecular ions and assigned fragments for (A) ketamine, (B) MXE, (C) 4-MBC, and (D) MXP.
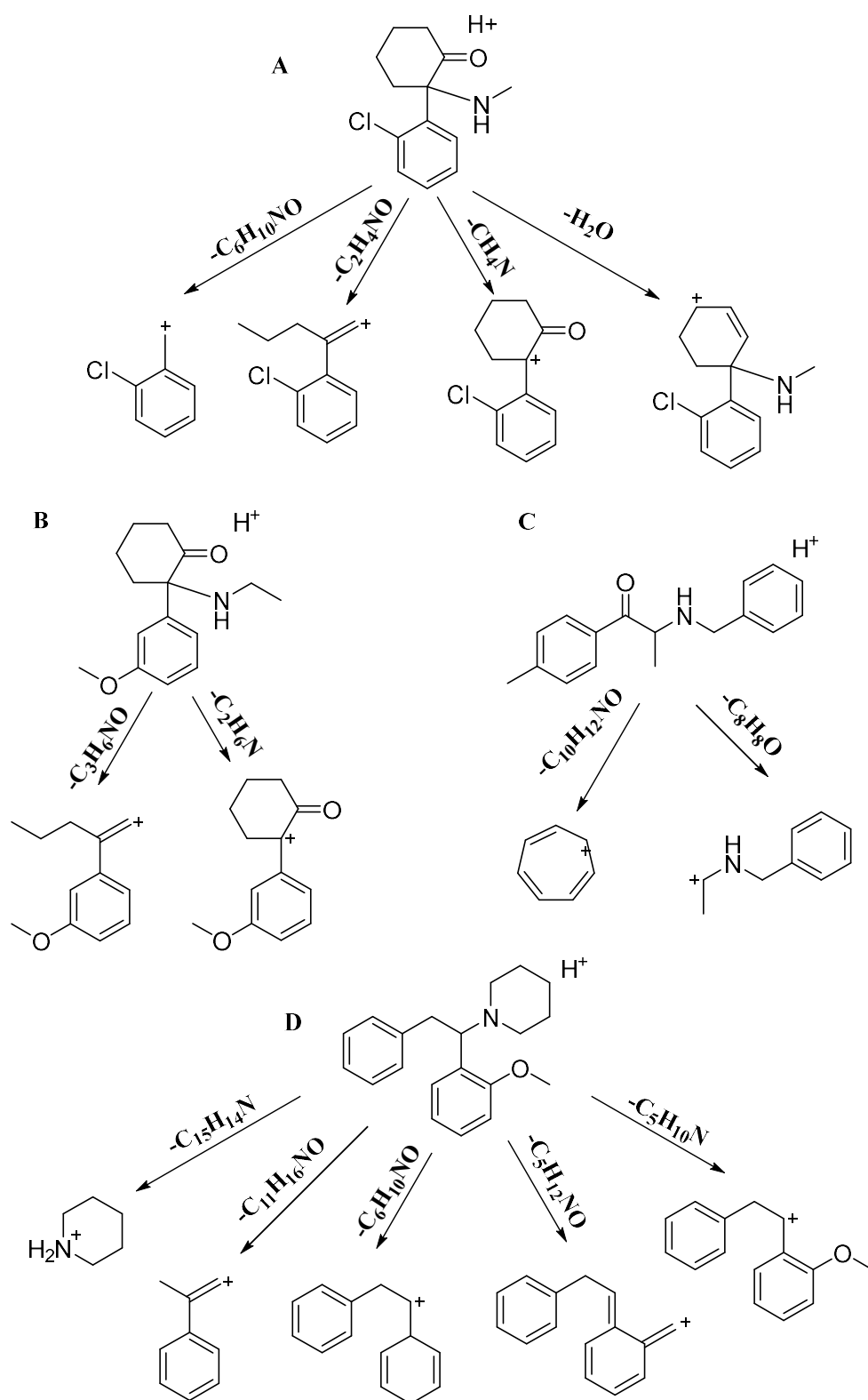
Figure 59. Proposed fragmentations for (A) ketamine, (B) MXE, (C) 4-MBC, and (D) MXP.

Sample HN163 provides a good example of the various analytical advantages and disadvantages of NMR, UHPLC and ESI-MS. NMR allowed the assignments of all the five components and the calculation of their molar ratios. Creatine, which suffered from low ionization and poor retention on the C18 column, was unambiguously characterized in the NMR, as was DMS which could not be detected using UHPLC/ESI-MS, possibly due to its poor ionization and the absence of a chromophore. On the other hand, NMR failed to detect trace impurities present in the sample such as 4-MBC, which was only detected using UHPLC/ESI-MS and its MS/MS fragmentation is proposed. DMS has been found used in cutting methamphetamine analysed in the USA, thus care must be taken if considering using it as an IS for q-NMR.[198]

Sample HN200 NMR and UHPLC/ESI-MS/MS analysis revealed similar components to sample HN163 analysis with the absence of DMS and the presence of MDMA (Figure 60). Resolved signals for each component in the mixture allowed the calculation of the percentage (molar ratio) of each component in the sample: ketamine 85%, creatine 8%, MXE 4%, MXP 2%, and MDMA 1%. A trace amount of 4-MBC was also detected using UHPLC/ESI-MS/MS. The presence of MDMA in only 1% is possibly a result of cross-contamination that may have occurred during manufacturing rather than any intentional cutting of the ketamine.
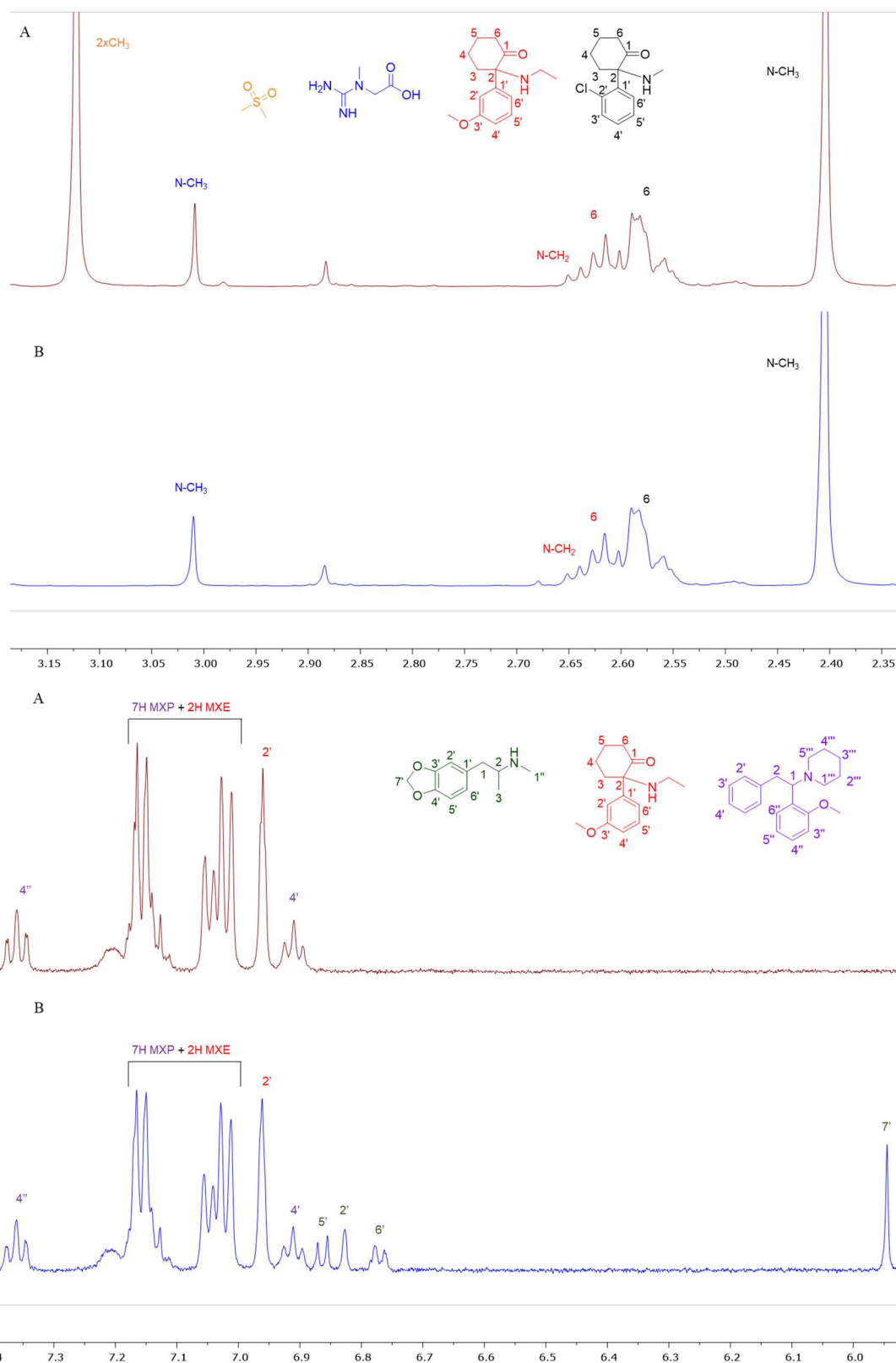
Figure 60. ¹H NMR stacked spectra expansion of (A) sample HN163 and (B) sample HN200

between 2.35-3.15 ppm revealing the absence of DMS in HN200; expansions 5.5-7.4 ppm

show the presence of MDMA aromatic (6.75-6.88 ppm) and methylenedioxy (5.94 ppm)

peaks in HN200 which are absent in HN163.

MXE and ethylphenidate are frequently encountered NPS in drug analysis laboratories due to their popularity especially in dance scene events because of their stimulating and dissociative effects. Each is associated with cases of intoxications and fatalities.[66,240,241] NMR is not usually available in forensic drug analysis laboratories, for technical and financial reasons, and most drug analysis laboratories rely on chromatographic techniques coupled to MS, whether it is soft ionization ESI-MS or CI or EI, each with its own set of advantages and disadvantages.[9] MXE and ethylphenidate are structural isomers having the formula $C_{15}H_{21}NO_2$, their molecular ions are indistinguishable by ESI-MS, and the EI in GC/MS analysis will result in no or only a weak molecular ion. However, Collision Induced Dissociation (CID) using ESI-MS/MS allows the detection of the molecular ions as well as distinctive fragmentation for each component.
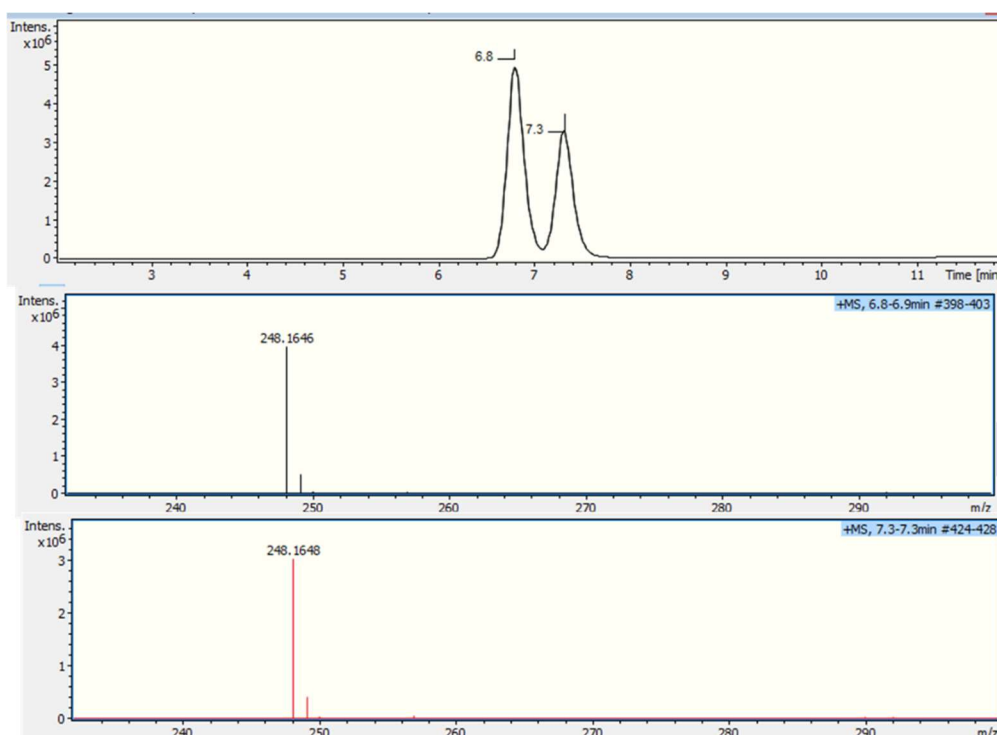
Figure 61. (Top) TIC and (bottom) MS spectra of a spiked sample of MXE (black) and ethylphenidate (red).

UHPLC/MS resulted in two base-line resolved peaks at 6.8 min for MXE and 7.3 min for ethylphenidate (Figure 61) having similar $[M+H]^+$ found 248.1646 and 248.1648 respectively within 5 ppm for both MXE and ethylphenidate, $C_{15}H_{22}NO_2$ requiring 248.1645.

On the other hand, the MS/MS spectrum showed a distinctive fragmentation for both MXE and ethylphenidate. MXE fragmentation is similar to ketamine, with the loss of ethylamine instead of methylamine in ketamine, opening of the cyclohexanone ring, and the formation of 3-methoxybenzyl cation (Figure 62). On the other hand, ethylphenidate showed more stability of its molecular ion fragmenting only to the piperidine cation ($C_5H_{10}N^+$). Furthermore, the GC/MS spectra of both compounds show weak or even not detectable molecular ions,[53,243] while the UHPLC/ESI-MS/MS resulted in a good intensity molecular ion and sufficiently distinctive fragmentation pattern to allow structural information to be deduced.
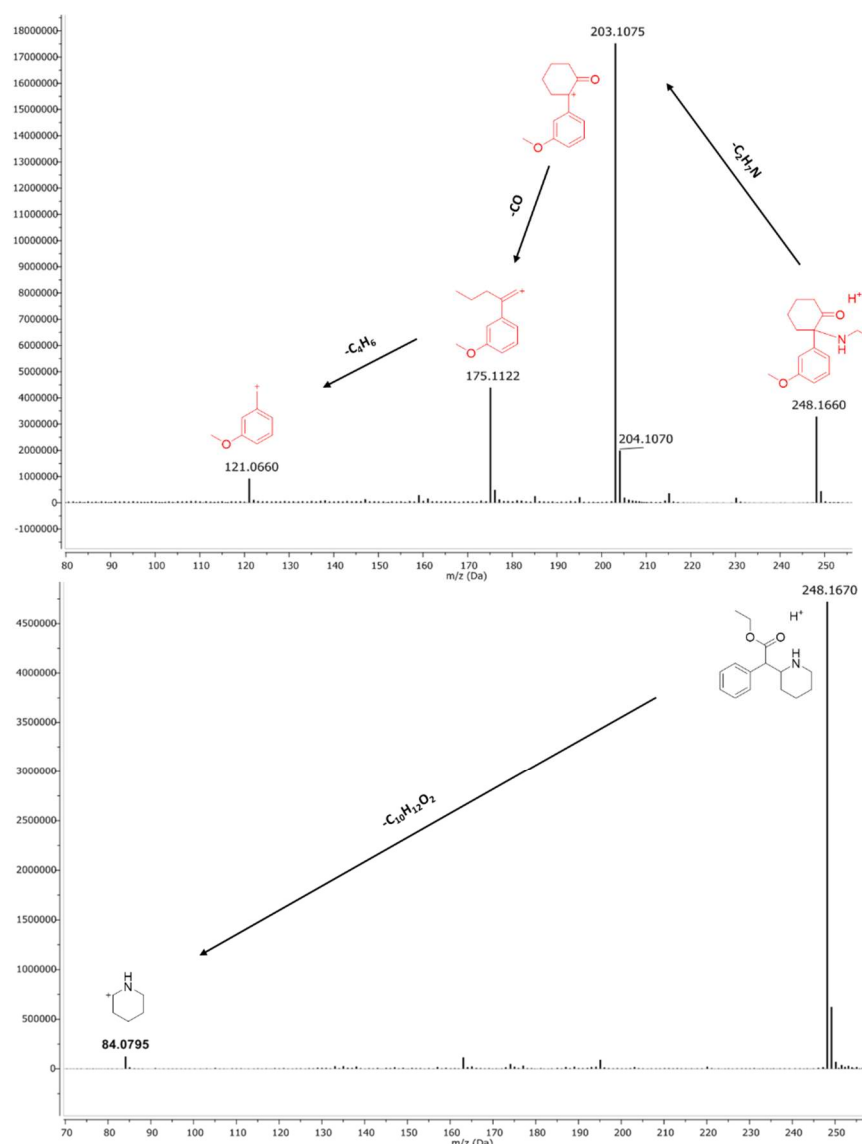
Figure 62. MS/MS spectra of (top) MXE, and (bottom) ethylphenidate with their proposed fragmentation pathways.

3.3.2 Analytical characterization of complex phenidate-based NPS

Analysis of 330 samples revealed 7 ethylphenidate-associated NPS with 2 samples of complex mixtures. "Charles" 4-component mixture was analysed by 1D/2D NMR spectroscopy and ESI-MS revealing methiopropamine (MPA), a methamphetamine thiophene analogue, benzocaine and mannitol as well as ethylphenidate. Quantitative ^{1}H NMR in D_2O on a sample (11.00 mg) was performed (n = 4) using MA (3.00 mg) as an IS revealing: MPA (2.81±0.04 mg RSD = 1.46%), benzocaine (2.87±0.02 mg RSD = 0.79%), ethylphenidate (1.48±0.05 mg RSD = 3.23%), and mannitol (2.63±0.03 mg RSD = 1.15%) after normalizing the N-methyl of MPA (1″) to 3.00, quantified using signals from each compound: MPA (1′, 1″, 2′), ethylphenidate (1‴, 6″$_{ax}$, 5″, 4″), benzocaine (2′, 6′, 1), and mannitol (1, 3). The calculated purity of the sample was 89%, small amounts of insoluble materials in addition to the water content of illicit samples could account for that purity value. 1D/2D NMR allowed the complete characterization of the 4-component sample (Tables 11 and 12, Figure 63).
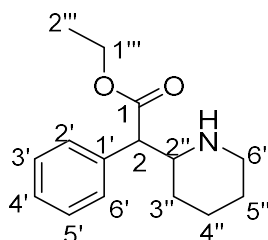
Table 11. ^{1}H and ^{13}C NMR (in D_2O) assignments of ethylphenidate in the "Charles" mixture.

Position	^{13}C	^{1}H
1	172.8	-
2	53.8	4.00 1H, d (9.0)
1‴	63.0	4.18-4.28 2H, m
2‴	13.0	1.19 3H, t (7.0)
2″	57.9	3.83-3.84 1H, m
3″	26.2	1.39-1.47 1H, m, 1.62-1.67 1H, m
4″	21.3	1.39-1.47 1H, m, 1.79-1.83 1H, m
5″	21.8	1.58-1.67 1H, m, 1.79-1.91 1H, m
6″	45.6	3.09 1H, td (13.0, 3.5), 3.47 1H, dt (13.0, 3.5)
1′	133.3	-
2′,6′	128.6	7.34 2H, dd (5.0, 3.5)
3′,5′	129.5	7.45-7.51 2H, m overlapped with 4′
4′	128.8	7.45-7.51 1H, m overlapped with 3′,5′
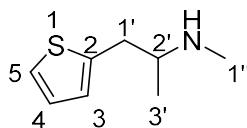
Table 12. ^{1}H and ^{13}C NMR (in D_2O) assignments of MPA salt in the "Charles" mixture.

Position	^{13}C	^{1}H
2	137.1	-
3	127.6	7.05 1H, dd (3.5, 1.5)
4	127.6	7.08 1H, dd (5.5, 3.5)
5	125.7	7.41 1H, dd (5.5, 1.5)
1′	32.7	3.23 1H, dd (15.0, 6.5), 3.27 1H, dd (15.0, 6.5)
2′	56.3	3.56 sextet (6.5)
3′	14.9	1.36 3H, d (6.5)
1″	29.9	2.72 3H, s

NMR of cutting agent benzocaine (500 MHz in D_2O) (C1) ^{13}C δ = 169.0, (C1′) ^{13}C δ = 118.9, (2′,6′) ^{13}C δ = 131.5 ^{1}H δ = 7.86, 2H, d 7.0 Hz, (C3′,5′) ^{13}C δ = 114.7 ^{1}H δ = 6.83, 2H, d 7.0 Hz, (C4′) ^{13}C δ = 139.0, (C1″) ^{13}C δ = 61.7 ^{1}H δ = 4.33, 2H, q 7.0 Hz, (C2″) ^{13}C δ = 13.5 ^{1}H δ = 1.37 3H overlapped with α-(3′)-methyl of MPA. The first analytical profile of MPA was published by Casale and Hays,[247] the NMR of MPA HCl salt in $CDCl_3$, but this research has shown that D_2O resulted in more spectral information in terms of coupling. Additionally, D_2O was the deuterated solvent of choice for the analysis of such complex samples containing different components of varying polarity. The CH_2 (1′) of MPA occurred as two closely resonating doublets of doublets, overlapping and appearing as an apparent septet. Even though the methyl of benzocaine overlapped with the methyl of methiopropamine (MPA), it was possible to extract cross-peak connectivity with the CH_2 quartet at 4.33 ppm of benzocaine using COSY. Moreover, a fourth component in the mixture was mannitol, included as a cutting agent, with 3 carbon and 4 proton signals due to the symmetry of mannitol at: (1) 63.2 ppm, 3.68 ppm 2H, dd 12.0 (*gem*), 6.0 Hz, 3.87 ppm, 2H, dd, 12.0 (*gem*), 2.5 Hz; (2) 70.8 ppm, 3.77 ppm 2H, ddd 8.5, 6.0, 2.5 Hz; (3) 69.2 ppm, 3.81 ppm 2H, d 8.5 Hz (Figure 63). The spectra were confirmed by coincidence with the ^{1}H and ^{13}C NMR data of authentic mannitol.
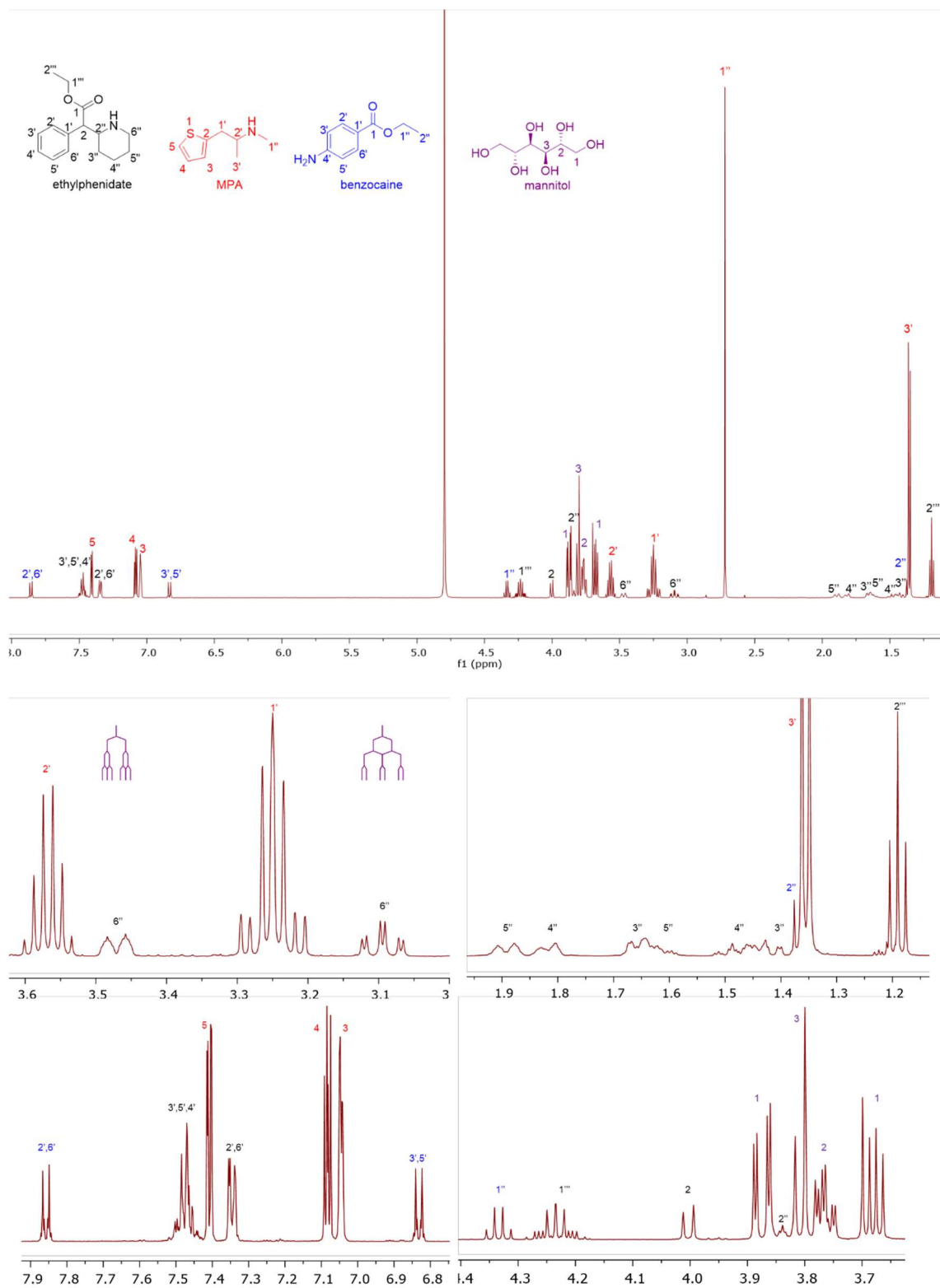
Figure 63. ^{1}H NMR (in D$_2$O) assignments of ethylphenidate, MPA, benzocaine, and mannitol in the "Charles" mixture with expansions of each segment of the spectra.

Not withstanding the complexity of the mixture, UHPLC/ESI-MS resulted in obtaining the molecular ions of all four components (Figure 64) in the "Charles" mixture. The different polarities and ionization of the components in the mixture was a challenge: ethylphenidate RT = 5.5 min, found $[M+H]^+$ 248.1646 for $C_{15}H_{22}NO_2$ requires 248.1645, benzocaine RT = 5.8 min, found $[M+H]^+$ 166.0860 for $C_9H_{12}NO_2$ requires 166.0862, MPA salt RT = 0.5 min found $[M+H]^+$ 156.0843 for $C_8H_{14}NS$ requires 156.0841. MPA salt's high polarity caused it to have a retention time RT = 0.5 min, while (at RT = 0.6 min) mannitol's poor ionization in the positive-ion mode using gradient 1 resulted in a low intensity mass ion. Additionally, the high polarity of mannitol and an absence of a chromophore makes it a poor candidate for UHPLC analysis on a C18 column (Figure 64 top and A). For mannitol, the sample was infused in a loop injection positive-ion mode and resulted in found $[M+Na]^+$ 205.0681 for $C_6H_{14}O_6Na$ requires 205.0682.
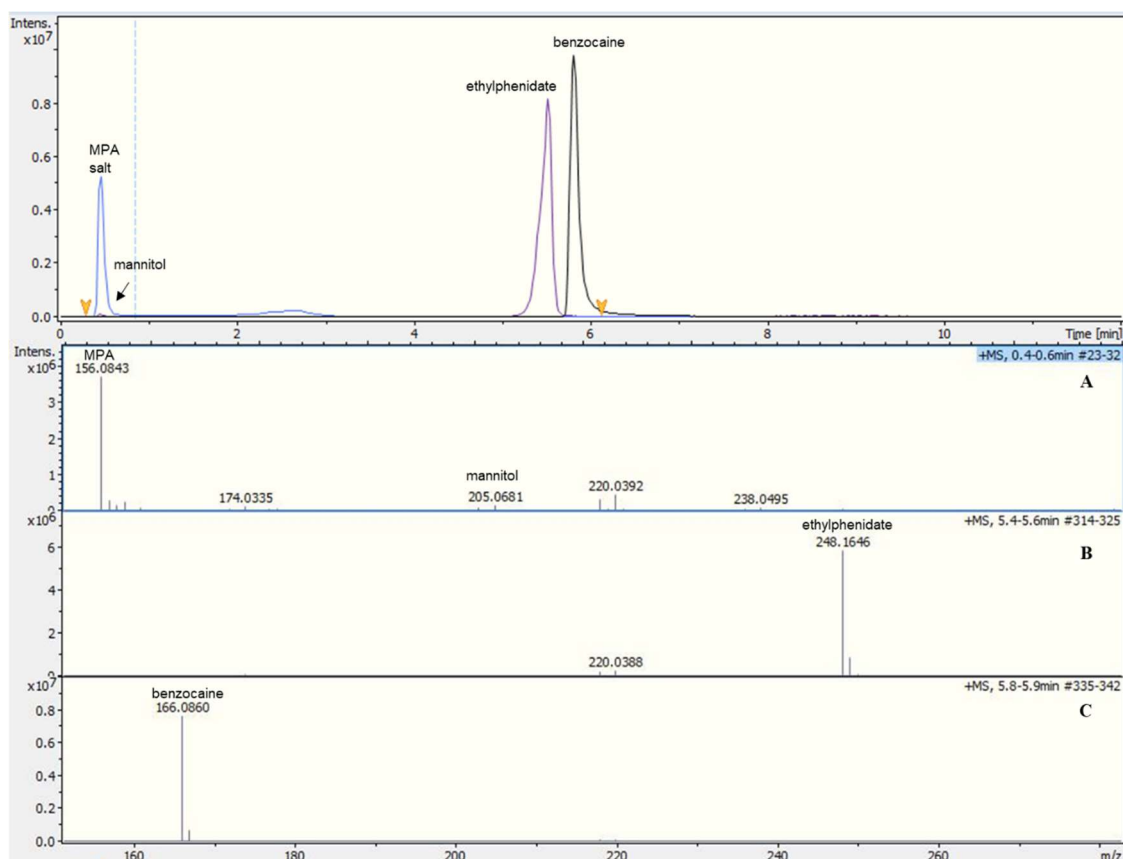
Figure 64. (Top) TIC of "Charles" mixture showing RT of MPA, mannitol, ethylphenidate and benzocaine, MS spectra of (A) MPA and mannitol, (B) ethylphenidate, (C) benzocaine.

The second mixture (sample HN181) contained ethylphenidate, methiopropamine (MPA) and 5-methoxy-*N*,*N*-diallyltryptamine (5-MeO-*N*-DALT) (Table 13 and Figures 65 and 66). The mixture was identified by having three different spin systems in the COSY and the HSQC-TOCSY experiments. The latter relates a specific proton spin system to its corresponding carbon signals, with the multiplets between 1.39-1.47, 1.58-1.67, 1.80-1.91 ppm and CH_2-*N* at 3.09 and 3.47 ppm indicating the presence of a piperidine ring as found in ethylphenidate. Separately, the sharp singlet at 3.90 ppm integrating for 3H is diagnostic for the presence of a methoxy group. Additionally, full assignments of the mixture and separation of overlapped peaks followed from COSY NMR. Quantification showed ethylphenidate and MPA both were 40% and 5-MeO-*N*-DALT was 20%. The NMR shifts of ethylphenidate (Table 11) and MPA (Table 12) are similar to those in the "Charles" mixture (above). Due to the low solubility of tryptamines in D_2O, extraction of the mixture with $CDCl_3$ resulted in distinctive spectra for 5-MeO-*N*-DALT, with the alkene signal of H2″ now resonating at 6.16 ppm as a doublet of doublet of triplets (ddt) with 3 *J* values of 17.0 Hz *trans-E*-coupling, 10.0 Hz *cis-Z*-coupling and 7.0 Hz coupling to the two methylene protons (Figure 67). Furthermore, in $CDCl_3$, H3″ signals appeared as two doublet of doublets (dd), with 2 *J* values, the first signal has a 17.0 Hz *trans-E*-coupling and a $^2J_{gem}$ terminal alkene of 1.0 Hz, the second signal has a 10.0 Hz *cis-Z*-coupling and a $^2J_{gem}$ terminal alkene of 1.0 Hz.

Using gradient 2, UHPLC/ESI-MS/MS analysis of the mixture resulted in three base-line resolved peaks in the EIC at 1.5, 6.9, and 7.4 min for MPA, 5-MeO-*N*-DALT, and ethylphenidate respectively, with MPA and ethylphenidate giving the same molecular ions and fragmentation patterns to those previously observed in the analysis of the "Charles" sample. 5-MeO-*N*-DALT was detected, found $[M+H]^+$ 271.1808 for $C_{17}H_{23}N_2O$ requires 271.1804, with an MS/MS fragmentation pathway that resulted in a base peak of the iminium ion formation at 110 m/z from α-position bond cleavage. Nevertheless, the small (C_3) allyl fragment could not be observed due to the scan range being between 50-500 m/z. The 174 m/z fragment is the result of the formation of 5-methoxyindole ethyl ion with the formula $C_{11}H_{12}NO^+$ (Figure 68). The HR-MS data are consistent with the work of Brandt *et al.*[248]
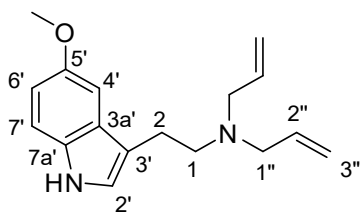
Table 13. ^{1}H and ^{13}C NMR (in D$_2$O) assignments of 5-MeO-*N*-DALT in the 3-component mixture (sample HN181).

position	^{13}C	^{1}H
1	51.5	3.48 2H, overlapped with 6″ ethylphenidate
2	19.7	3.23-3.27 2H, overlapped 1′ MPA
2′	125.1	7.32 1H s
3′	113.0	-
3a′	131.4	-
4′	100.5	7.16 1H, d (2.5)
5′	153.0	-
6′	108.2	6.96 1H, dd (8.5, 2.5)
7′	111.9	7.48 1H, overlapped with 3x H of ethylphenidate
7a′	143.7	-
O-CH$_3$	56.1	3.90 3H, s
1″	55.0	3.83 4H, d (7.0)
2″	125.5	5.90 2H, ddt (17.0, 10.0, 7.0)
3″	126.5	5.60 2H, d (17.0), 5.62 2H, d (10.0)
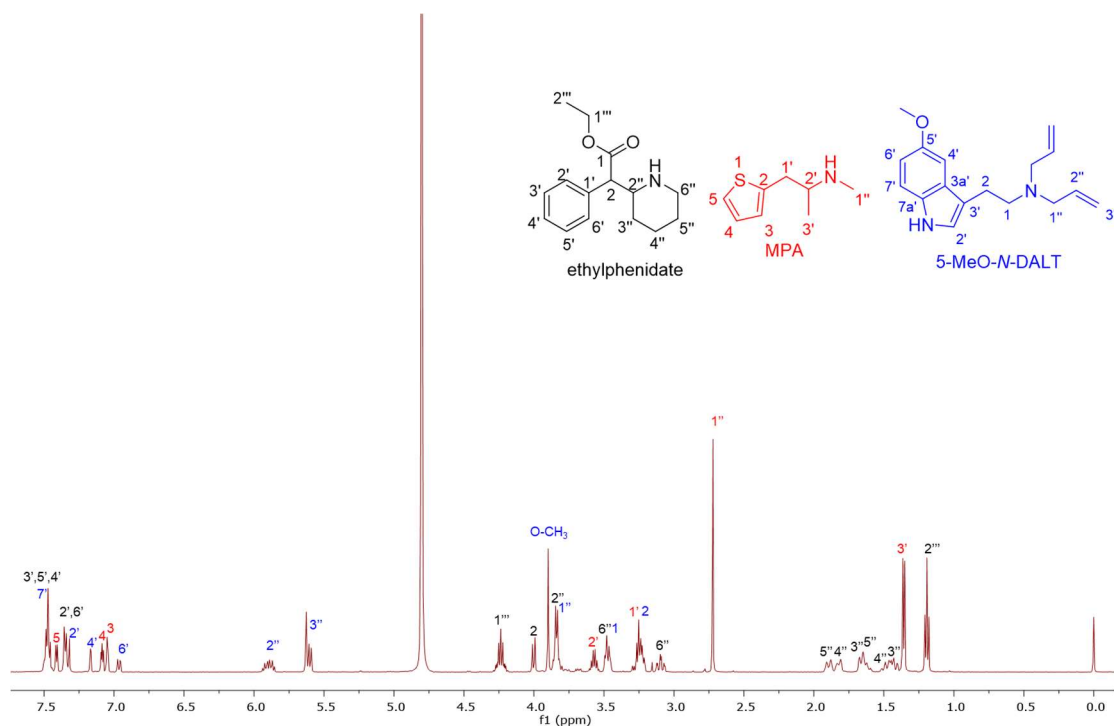
Figure 65. ^{1}H NMR (in D$_2$O) assignments of sample HN181.
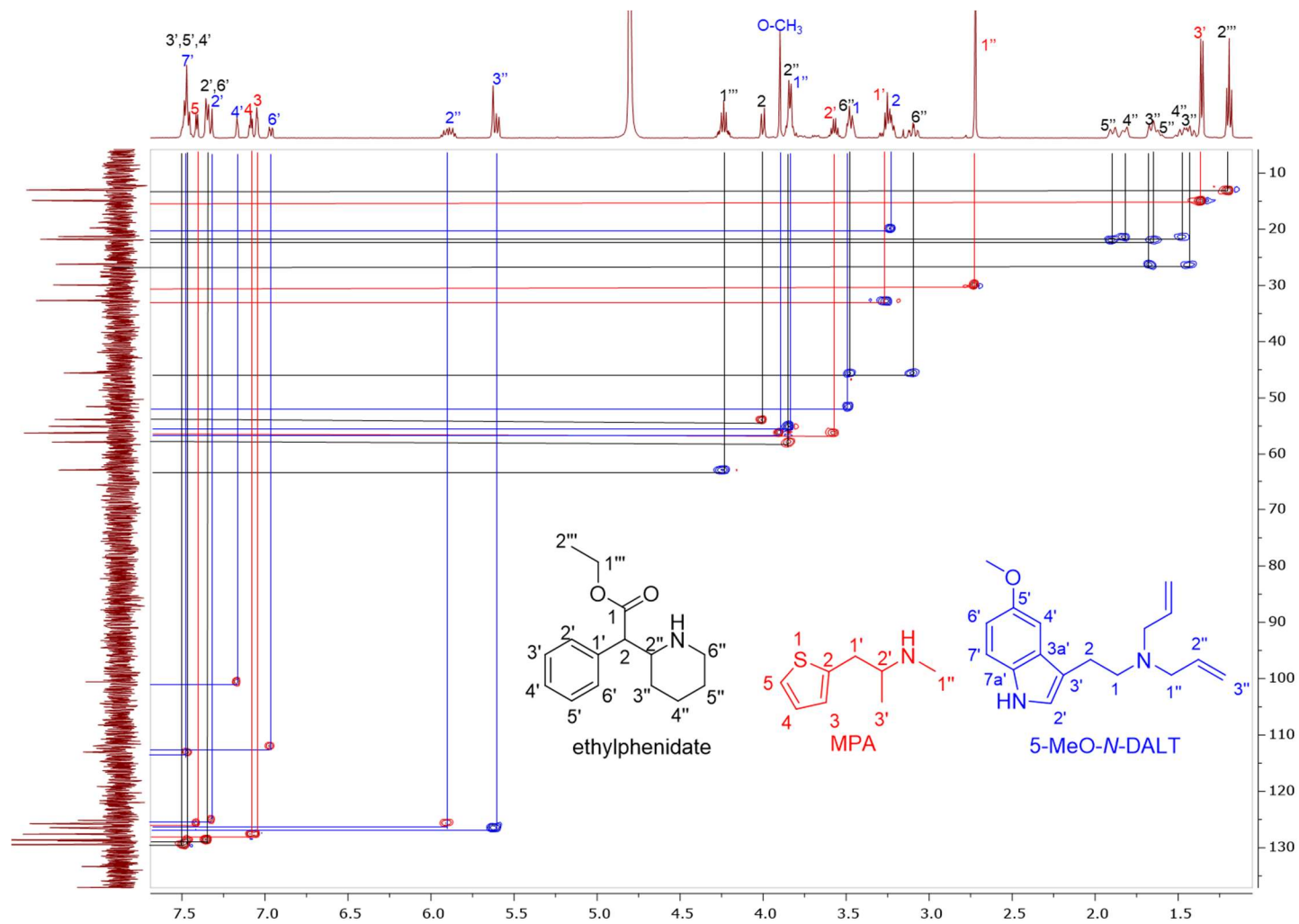
Figure 66. HSQC (in D$_2$O) assignments of all three components in the mixture in HN181.
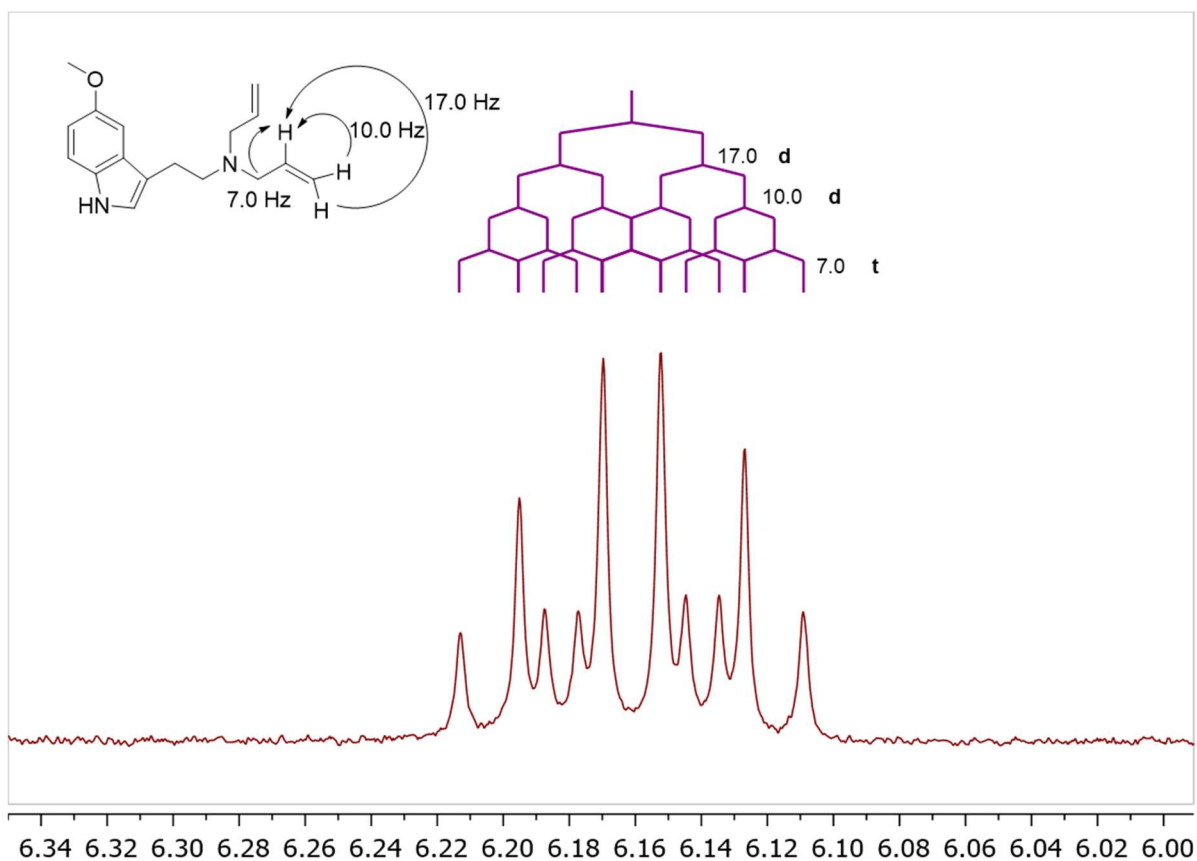
Figure 67. ^{1}H NMR (in CDCl$_3$) expansion of *N*-allyl H2″ of 5-MeO-*N*-DALT showing the

ddt splitting pattern.

5-MeO-*N*-DALT is based on earlier NPS, α-methyl- and ethyl-tryptamines, that were

developed in the 1960s as antidepressants, but abandoned due to their side effects.[57] Later, in

1997, they were popularized by Shulgin along with many other tryptamines.[14] The number of

tryptamine NPS has since increased dramatically, driven by the internet and sold as research

chemicals before being banned in the 2016 NPS Act. Nevertheless, they constituted 2% of

seized NPS in 2016 according to EMCDDA.[193]
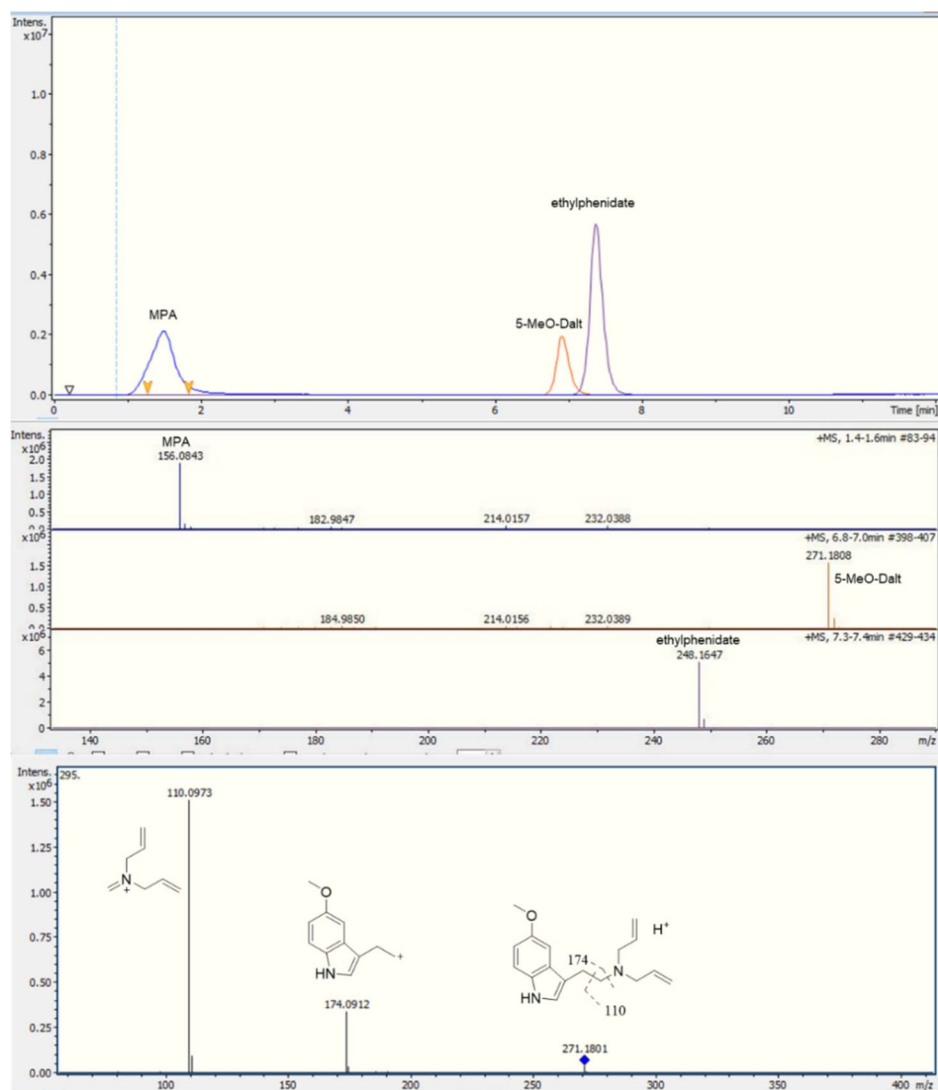
Figure 68. Sample HN181 (top) EIC, (middle) MS spectra of the three components in the mixture, (bottom) MS/MS spectrum and proposed fragmentation of 5-MeO-*N*-DALT.

α-Methyl-tryptamine was identified in seized samples using 1D/2D NMR and ESI-MS. Its NMR analysis (Figure 69) (400 MHz in CDCl₃) showed: (C2) ^{13}C δ = 122.5 ^{1}H δ = 7.01, 1H, br s, (C3) ^{13}C δ = 113.6, (C3a) ^{13}C δ = 127.7, (C4) ^{13}C δ = 119.0 ^{1}H δ = 7.63, 1H dd 7.0, 1.0 Hz, (C5) ^{13}C δ = 119.2 ^{1}H δ = 7.13, 1H td 7.0, 1.0 Hz, (C6) ^{13}C δ = 121.8 ^{1}H δ = 7.20 1H td 7.0, 1.0 Hz, (C7) ^{13}C δ = 111.1 ^{1}H δ = 7.35 1H dt 7.0, 1.0 Hz, (7a) ^{13}C δ = 136.4, (1′) ^{13}C δ = 36.0 ^{1}H δ = 2.68, 1H, ddd 14.0, 8.5, 1.0 Hz, 2.91 1H, ddd 14.0, 5.0, 1.0 Hz, (2′) ^{13}C δ = 47.3 ^{1}H δ = 3.28-3.36, 1H, m, (3′) ^{13}C δ = 23.7 ^{1}H δ = 1.20, 3H, d 8.0 Hz, indole amine ^{1}H δ = 8.54, 1H, br s, primary amine ^{1}H δ = 1.32, 2H, s. These NMR data are an improvement over published data by showing the 4-bond (1 Hz) coupling of the two methylene protons (1′)

possessing benzylic coupling to the indole proton on C2.[249] ESI-MS showed [M+H]$^+$ 175.1242 for $C_{11}H_{15}N_2$ requires 175.1235, and the base peak (-NH$_3$) found 158.1005 for $C_{11}H_{12}N$ requires 158.0969.
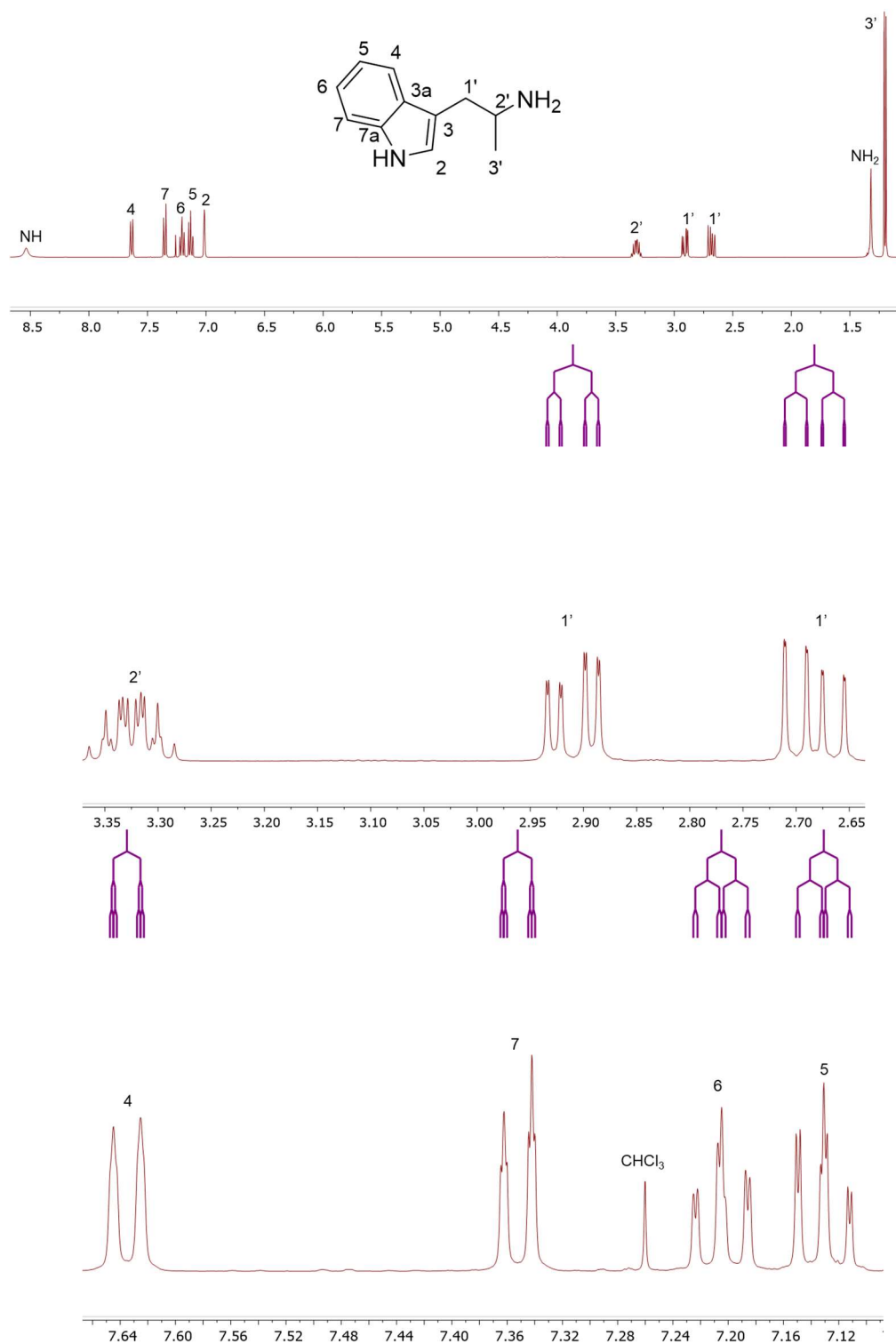
Figure 69. ^{1}H NMR (in CDCl$_3$) of α-methyl-tryptamine assignments, with expansion of 2.65-3.35 ppm and the aromatic region, with splitting trees of the *J* coupling pattern.

3.4 Conclusions

Ketamine and MXE were found in pure form and in combination with other NPS and cutting agents. Indeed, arylcyclohexylamines were the most extensively cut category of the NPS analysed. Multiple adulterants have been identified ranging from simple cutting agents such as DMS and creatine, to the pharmacologically active dissociative agent (MXP) and a stimulant cathinone (4-MBC). Such complex samples are not suitable for analysis using only one single method. Here it has been demonstrated that there are limitations to each individual analytical method in tackling such complex mixtures. By NMR it was possible to calculate the ratios of multiple components and detect compounds with no chromophore and poor ionization, e.g. DMS, creatine, although NMR suffers from somewhat low sensitivity. On the other hand, the high sensitivity of MS allowed the detection of 4-MBC, present at a level below the Lower Limit of Detection (LLOD) of NMR. The poor ionization of the UHPLC method was overcome, in some instances, by directly infusing (the loop-injection method) the sample into the HR-MS, thus by-passing any column interactions. Unlike the rapid analysis and quantification of each component by NMR spectroscopy, UHPLC required method development for the separation of multi-component mixtures.

Quantitative ^{1}H NMR analysis (q-NMR) allowed the quantification of a complex ethylphenidate-based NPS mixture using MA as an IS which provided a non-overlapping singlet peak at $\delta = 6.38$ ppm, suitable for integration. Such a mixture of ethylphenidate, MPA and benzocaine was identified. It also contained a high polarity component (mannitol) that was impossible to quantify using a C18 column. However, mannitol was quantified by q-NMR spectroscopy. Two tryptamine NPSs have been identified. One in a mixture (5-MeO-*N*-DALT) and one as a pure sample (α-methyl-tryptamine), with improved spectroscopic data provided for both.

The association of psychoactive compounds requires monitoring and careful analysis. Such complex mixtures have not been described in the refereed literature, thus warranting an analytical investigation that may be helpful to drug analysts and health-care professionals (HCP) who are in direct contact with such samples and users/abusers.

Chapter 4. Chemical characterization of 2ⁿᵈ and 3ʳᵈ generation seized Synthetic Cannabinoid Agonists and their impurities

4.1 Introduction

Considered one of the first plants to be used for recreational, therapeutic, and ceremonial purposes, cannabis use stretches back nearly 5000 years.[250] Ancient Chinese civilizations have a well-documented record of the use of cannabis. Patients described physiological effects ranging from relief of pain to interacting with the spirits (getting high).[251] It was relatively recently (1930s-1940s) when the components responsible for the effects of cannabis, cannabinol (CBN), cannabidiol (CBD) and Δ^9-tetrahydrocannabinol (THC), were discovered (in that order). The endogenous cannabinoid receptors CB_1 and CB_2 were discovered and isolated/cloned in the late 1980s and early 1990s.[250]

The cannabinoid receptor system is of interest in many pathological conditions.[252] The cannabinoid receptors CB_1 and CB_2 are named after their amino acid sequences and tissue distribution, being the target for treatments particularly for neurological conditions such as Parkinson's disease, Alzheimer's disease, and Multiple Sclerosis (MS).[78,252] THC, CBD, and CBN, found in *Cannabis sativa* L. (marijuana), are the main natural phytoproduct cannabinoids. In particular, THC acts on CB_1 receptors as a partial agonist, producing psychoactive effects (EC_{50} = 170 nM[78] and 250 nM[253]).

A number of synthetic cannabinoids, that act on the same receptors as the natural product cannabinoids, do so with much higher potency on both receptor subtypes. They have been further developed, e.g. the Hebrew University compound HU-210, Pfizer compounds CP 47,497 and CP 59,540.[252] Additionally, in the early 1990s, John W. Huffman from Clemson University synthesized a series of synthetic cannabinoid agonists (SCAs) with a core structure of naphthoylindole, most notably JWH-018 (Figure 70) which, along with CP 47,497, constituted the first wave of illicitly synthesized SCAs that started emerging on the streets in 2008, with the help of internet vendors that promoted these compounds as apparent research chemicals, herbal incense and so called legal highs, at least before the 2016

Psychoactive Substance Act.[79,80,254] These SCAs are still known by the street name "spice" due to the first brands promoted over the internet and sold on the street (spice and K2). They were sold in the form of herbal blends of potpourri, Damiana (*Turnera diffusa*), Marshmallow plant (*Althaea officinalis*) and other herbal blends soaked or sprayed with the SCA.
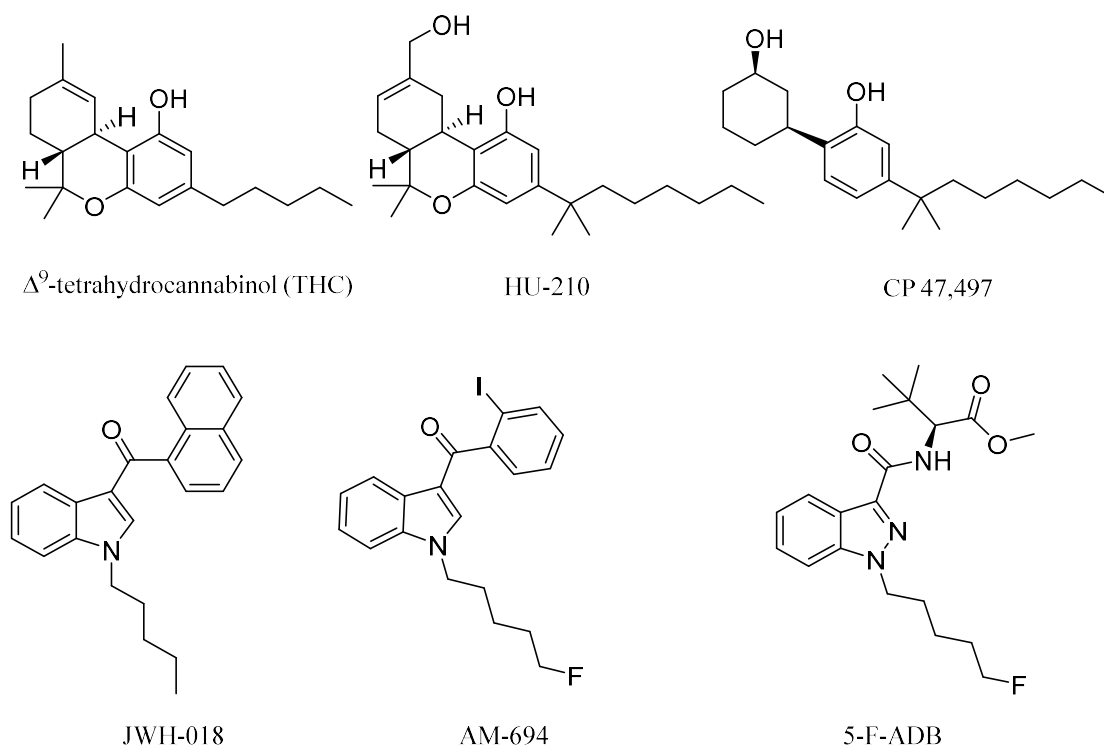
Figure 70. A natural phytocannabinoid and five SCAs.

Later SCAs, illicitly manufactured, retained the indole core, but with modifications to the head, tail and linker moieties (Figure 71) using different functional groups, resulting in hundreds of compounds in the second generation of SCAs, that were also based on medicinal chemistry compounds, some of which are based on the AM series developed by Prof. Alex Makriyannis at the University of Connecticut, CT, USA.[255] Continuous banning of SCAs by Governments worldwide resulted in them being developed into compounds that possess the indazole core structure instead of the indole, and amino acids such as alanine and phenylalanine in the head components, replacing the naphthalene and substituted aromatic moiety. Most of these newer generation SCAs are novel compounds.[78]
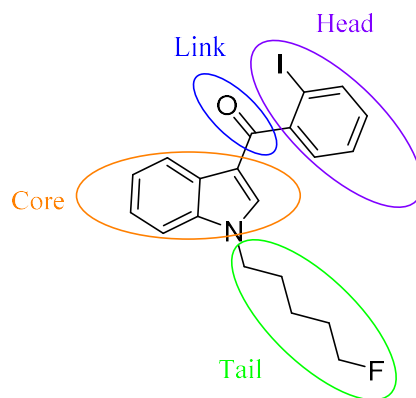
Figure 71. Regions of functional group modifications in the structure of SCAs.

Synthesis of third generation indole and indazole based SCAs has been described by Banister *et al*.[78,253] For indazole based SCAs, indazole-3-carboxylic acid was Fisher esterified using concentrated sulfuric acid to form indazole 3-carboxylates which were deprotonated with potassium *tert*-butoxide and then *N*-alkylated with 4-fluorobenzyl bromide or 5-fluoro-pentyl bromide to create a 1-indazole tail with different substituents. This was followed by conversion into the free acid and amino acid coupling to yield the final compound (Figure 72).[253]
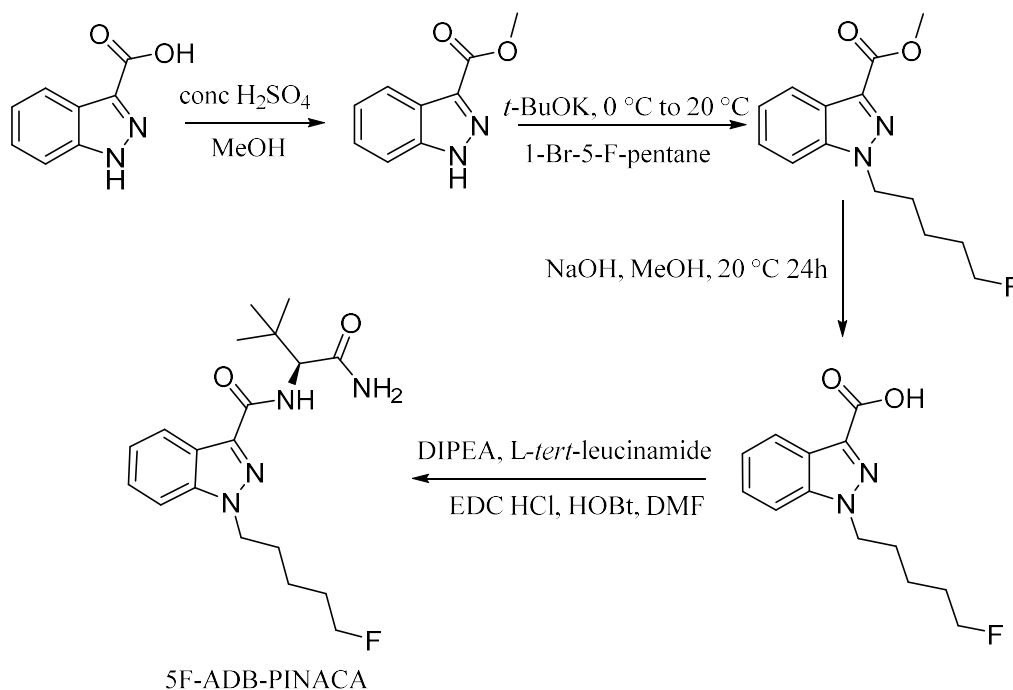
Figure 72. Synthetic scheme for indazole-based SCA 5F-ADB-PINACA.

The use of enantiomerically pure amino acids such as L-valine amide, L-phenylalanine and L-*tert*-leucinamide will result in a final product with an *S*-chirality. Nevertheless, recent analytical chiral separation using a CHIRALPAK column revealed that out of 10 samples of herbal blends bought from the internet two contained 20% of the *R*-enantiomer.[256] Reports about the pharmacology of recently identified SCAs are scarce. In vivo based studies consistently confirmed that these are full agonists at the CB_1 receptor and, unlike THC, they possess significant CB_2 potencies. Examples are PB-22 and 5F-PB-22 that with EC_{50} of 5.1 and 2.8 nM respectively, are approximately 50-fold to 90-fold more potent than THC (EC_{50} = 250 nM).[253] Moreover, various intoxications and fatalities have been reported for SCAs with toxicological post-mortem analysis revealing 3rd generation SCAs, e.g. 5F-ADB, MDMB-CHMICA, and 5F-PB-22.[257-259] Coupling these toxicological findings with the fact that SCAs have been dominating the number of seizures of NPS across Europe,[260] makes SCAs currently the most dangerous class of NPS.

In this Chapter, four themes of SCAs in herbal blends will be considered. First is the analysis of herbal blends containing SCAs with impurities showing qualitative assessment of herbal blend package contents. This is necessary and important due to the lack of literature data on the impurities associated with SCAs in the herbal form. Additionally, analysis of a liquid form SCA for Electronic cigarettes (E-cigarettes) will reveal the type of SCA and its NMR profile as well as any impurities present. The second theme is the analysis of herbal blends seized from UK prisons. Even though there are many reports of SCAs taking over UK prisons in the mainstream media, no analytical findings of such have been published in the literature. The third study will be the first application and evaluation of 2D Diffusion Ordered Spectroscopy (DOSY) on different seized samples containing mixtures of SCAs in herbal blends. Finally, an analytical protocol will be presented for the separation and characterization of the contents of K2 herbal blend samples containing a six-component complex mixture of closely related SCAs and impurities, using NMR, UHPLC/ESI-MS/MS, and flash column chromatography. Such an approach has not been reported before to physically separate such a complex mixture of SCAs dispersed in a herbal matrix.

4.2 Experimental

4.2.1 Chemicals and sample preparation

All extraction solvents (methanol, chloroform, and acetonitrile) 99.9% anhydrous, were purchased from Fisher Scientific (UK) or ACROS Organics (UK). Deuterated solvent ($CDCl_3$) was purchased from Cambridge Isotopes Laboratories (Goss Scientific, UK). DMS NMR internal standard was purchased from Sigma-Aldrich (UK). Herbal-blend samples were provided by the Drug Enforcement Action Team (DEAT), the Avon and Somerset Constabulary, from recent seizures (2016-2018). The samples were in the form of herbal blends (1.0-3.0 g) as commercially packaged brands (K2 black edition, Exodus, Loco Elite, Joker, Extinction), and in vials containing liquid (Kronic Juice). Prison samples were provided in sealed evidence bags containing herbal blends. They ranged from 10.0 mg in small paper twists to 9.0 g herbal blends in a nylon bag.

Samples were weighed using a SE2F Sartorius analytical balance. Herbal blends were extracted with $CHCl_3$ (2 x 20-30 mL) with sonication (30 min), centrifuged, removal of the supernatant extract, and the pellet (plant material) was discarded. Then the extract was evaporated to dryness under reduced pressure and reconstituted in $CDCl_3$ (0.6-1.0 mL) for NMR analysis, or reconstituted in methanol and diluted 100-fold for UHPLC-ESI/MS analysis.

4.2.2 Instrumentation

NMR spectroscopy

NMR spectra were recorded on a Bruker AVANCE III 500 MHz spectrometer, ^{1}H, ^{13}C, and ^{19}F frequencies are 500.130, 125.758, and 470.592 MHz respectively. The probe was a variable temperature BBFO+ with three channels, temperature was 25˚C. Alternatively, NMR spectra were recorded on a Bruker 400 MHz spectrometer, ^{1}H and ^{13}C frequencies are 400.130 and 100.613 MHz respectively. Chemical shifts were referenced to 0.0 ppm for TMS or the residual (protio) solvent peak for chloroform (7.26) and are reported in ppm. Coupling constants (*J*, line-separations, absolute values) are rounded to the nearest 0.5 Hz. Structural

elucidation was achieved with 2D NMR COSY, HSQC, H2BC, HMBC, DOSY, TOCSY-HSQC, and ^{15}N-HMBC NMR shows the two-and three-bond coupling of the ^{15}N to ^{1}H. ^{15}N-HSQC shows protons directly attached to the nitrogen and ^{19}F-HOESY is similar to the NOESY (proton-proton through-space interaction) experiment, but with the through-space interaction between a heteroatom (^{19}F in this case) and ^{1}H. DOSY NMR experiment pulse sequence is a bipolar gradient pulse (BPP)-longitudinal eddy current delay (LED) 2 spoil gradients (ledbpgp2s1d), 4 scans, acquisition time 3.0 s, delay (D1) 4.0 s with gradient strength (gpz6) incremented from 2% to 95%, gradient length (p30) 1500 µs, total run time was 19.3 min. NMR spectra were processed using Bruker TopSpin 3.5 and Mestralab Mnova 11.2.

UHPLC/ESI-MS/MS and flash column chromatography

The QTOF-UHPLC-MS analysis was conducted using a MaXis HD Quadrupole electrospray ionization Time-of-Flight (ESI-QTOF) mass spectrometer (MS) (Bruker Daltonik GmbH, Bremen, Germany), operated in ESI positive mode. The QTOF was coupled to an Ultimate 3000 UHPLC (Thermo Fisher Scientific, California, USA). The capillary voltage was set to 4500 V, nebulizing gas at 4 bar, drying gas at 12 L/min at 220°C. The TOF scan range was from 75-1000 mass-to-charge ratio (m/z). For LC/MS/MS capabilities, the in-source CID was set to 0.0 eV, with the collision energy for TOF MS acquisition at 3.0 eV. The collision energy was set to a sliding scale from 100 m/z at 14.0 eV, 500 m/z at 20.0 eV and 1000 m/z at 30.0 eV. For the analytes, the actual collision energy was between 15.0–18.0 eV. Liquid chromatography separation was performed using an Acquity UPLC BEH C18, 1.7 µM, 2.1 x 50 mm RP-column (Waters, Milford, USA) with a flow rate of 0.4 mL/min, and an injection volume of 10 µL at 40°C column temperature. Mobile phase A consisted of LC/MS grade water 0.1% formic acid v/v, mobile phase B consisted of acetonitrile 0.1% formic acid v/v. For Gradient 1 starting with 1% B for 2 min followed by a linear increase from 2.0 min to 100% B at 5.0 min, held for 3 min, followed by return to 1% B at 8.1 min, where it was held for equilibration for 3.9 min, total run time of 12.0 min. For gradient 2, starting with 1% B

for 2 min followed by a linear increase from 2.0 min to 100% B at 10.0 min, held for 3 min followed by return to 1% B at 13.1 min, where it was held for equilibration for 2.9 min, total run time of 16.0 min. Data analysis used Bruker data analysis 4.3.

Flash column chromatography was performed on a Teledyn Combiflash with RediSep normal phase columns 12.0 g (Lincoln, NE, USA) using hexane (A)/ethyl acetate (B) as the mobile phase. Samples were loaded using the liquid loading method, by dissolving the extract in $CHCl_3$ (2.0 mL), using two gradients. Gradient 1 (flow rate 18 mL/min) started with 0% B for 2.3 min, followed by an increase to 18% B at 8 min, held for 0.5 min, followed by an increase to 37% B at 14 min, then by a linear increase to 100% B at 34 min, total run time of 40 min. Gradient 2 (flow rate 22 mL/min) started with 0 % B for 2 min followed by a linear increase to 25% B at 8 min, held for 1 min and increased to 33% B at 11 min and held for 1 min, followed by an increase to 38% B at 14 min and held for 2 min, followed by an increase to 59% B at 18 min held for 2 min followed by a linear increase to 100% B at 35 min, total run time 35 min. Fraction collection was performed by monitoring at λ = 254 and 280 nm.

4.3 Results and discussion

4.3.1 Qualitative analysis of 2016/2017 seized herbal blends

All of the SCA seizures analysed were in herbal blend forms. Samples were received in marked evidence bags from DEAT in the summers of 2016 and 2017. These samples consisted of 61 samples of herbal blends in 7 brands such as Exodus, Extinction, Joker, K2, Kronic, Insane Joker and Loco elite (Figure 73).

Mislabelling was identified in all of the brands analysed, e.g. the brands "K2", "Insane Joker", and "Exodus". Some brands labelled one compound correctly in addition to incorrect ones, e.g. "Extinction" was labelled to contain both *N*-(adamantan-1-yl)-1-(5-fluoropentyl)-1H-indazole-3-carboxamide (5F-AKB48) and quinolin-8-yl 1-(5-fluoropentyl)-1H-indole-3-carboxylate (5F-PB-22), but found to contain only 5F-PB-22 in 2017 seizure samples and none of the compounds on the label in the 2016 seizure samples. Some brands such as "Kronic juice" and "LOCO elite" had no chemical compound labelling. This is particularly problematic for the user, where s/he cannot be certain of the SCA they are consuming. As each SCA has its own pharmacological profile, that could lead to serious side effects. This can have toxic, even fatal consequences. Furthermore, mislabelling has been reported by Frinculescu *et al.*[261] following from using GC and LC/MS analysis. However, there has been no report on the impurities associated with SCAs.

The carrier plant material was either Damiana (*Turnera diffusa*) or Marshmallow plant (*Althaea officinalis*), which were compared morphologically to purchased authentic herbal reference materials. The most common SCA identified (Table 14) was 5F-ADB, which will be discussed in detail in the following sections of this chapter. 5F-ADB was also found associated with other SCAs such as 5F-PB-22, MMB-2201, MDMB-CHMICA, 5F-AKB48, and PX-1 amide and its corresponding acid (Figure 73). In this section, chemical profiling of herbal blends containing SCAs seized in the South West of England was carried out using NMR spectroscopy and LC/ESI-MS/MS techniques. Identification of the main SCA and any impurities present used chromatographic and spectroscopic techniques for the separation and characterization of such components in a complex herbal matrix.
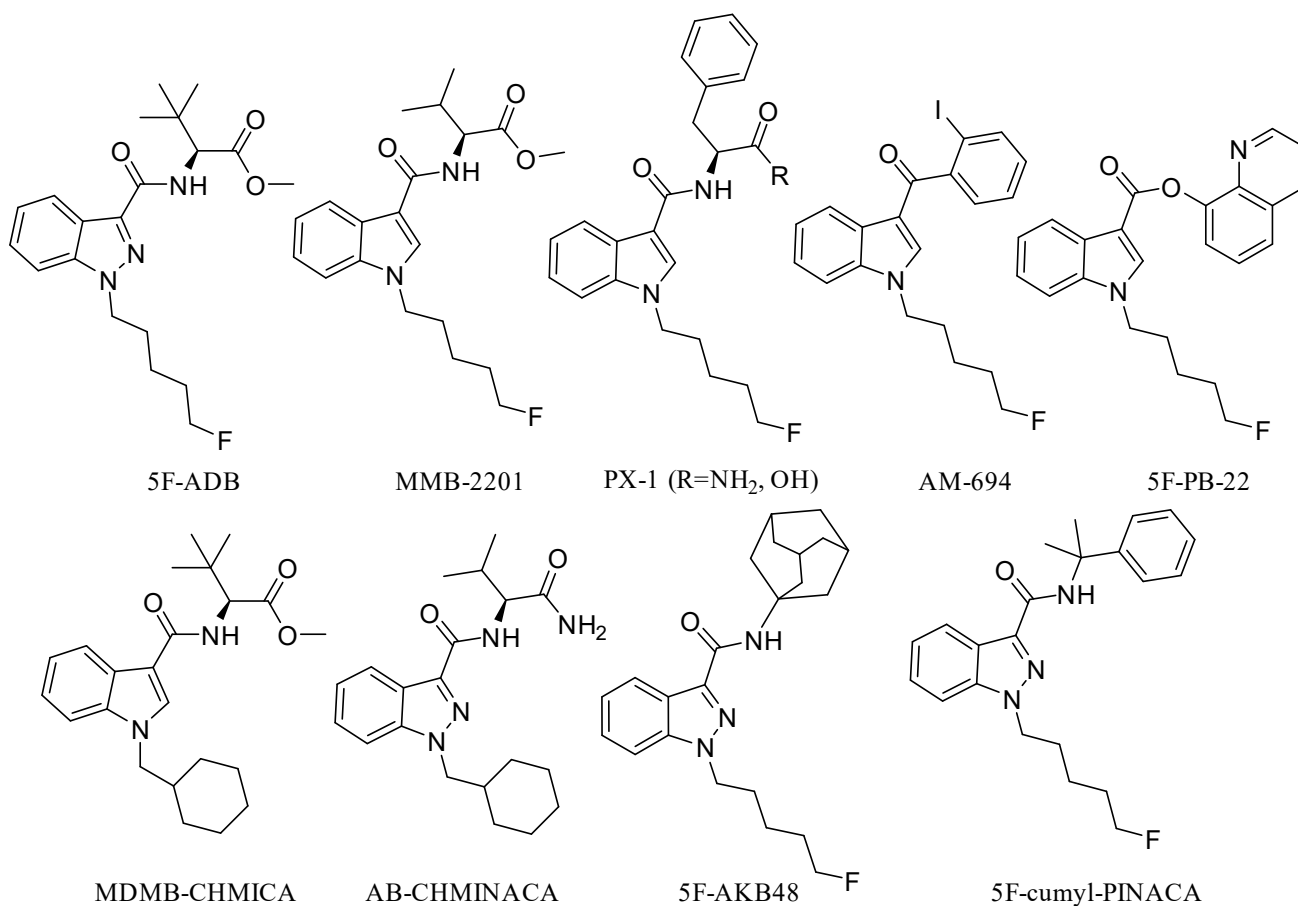
Figure 73. (Above) Examples of herbal blend sample brands containing these SCAs (below).

5F-ADB   MMB-2201   PX-1 (R=NH$_2$, OH)   AM-694   5F-PB-22

MDMB-CHMICA   AB-CHMINACA   5F-AKB48   5F-cumyl-PINACA

Table 14. Results of the qualitative analysis of 2016/2017 seized herbal blend samples

(Damiana) using NMR and ESI-MS.

Entry	Sample name/year of seizure	SCAs detected
1	HN Exod 1/2016	5F-ADB
2	HN Exod 2/2016	5F-ADB
3	HN Exod 3/2016	5F-ADB
4	HN Exod 4/2016	5F-ADB
5	HN Exod 5/2016	5F-ADB
6	HN Exod 6/2016	5F-ADB
7	HN Exod 7/2016	5F-ADB
8	HN Exod 8/2016	5F-ADB
9	HN Exod 9/2016	5F-ADB
10	HN Exod 10/2016	5F-ADB
11	HN Exod 11/2016	5F-ADB
12	HN Exod 12/2016	5F-ADB
13	HN Exod 13/2016	5F-ADB
14	HN Exod 14/2016	5F-ADB
15	HN Exod 15/2016	5F-ADB
16	HN Exod 16/2016	5F-ADB
17	HN Ext 1/2016	AB-CHMINACA
18	HN Ext 2/2016	AB-CHMINACA
18	HN Ext 3/2016	AB-CHMINACA
19	HN Ext 4/2016	AB-CHMINACA
20	HN Loc 1/2016	AM-694
21	HN Loc 2/2016	AM-694
22	HN Loc 3/2016	AM-694
23	HN Loc 4/2016	AM-694
24	HN K2/ 1/2016	5F-ADB, 5F-PB-22, MDMB-CHMICA, 5F-AKB-48, PX1, PX1 acid
25	HN K2/ 2/2016	5F-ADB, 5F-PB-22, MDMB-CHMICA, 5F-AKB-48, PX1, PX1 acid
26	HN K2/ 3/2016	5F-ADB, 5F-PB-22, MDMB-CHMICA, 5F-AKB-48, PX1, PX1 acid
27	HN K2/ 4/2016	5F-ADB, 5F-PB-22, MDMB-CHMICA, 5F-AKB-48, PX1, PX1 acid
28	HN K2/ 5/2016	5F-ADB, 5F-PB-22, MDMB-CHMICA, 5F-AKB-48, PX1, PX1 acid
29	HN K2/ 6/2016	5F-ADB, 5F-PB-22, MDMB-CHMICA, 5F-AKB-48, PX1, PX1 acid
30	HN K2/ 7/2016	5F-ADB, 5F-PB-22, MDMB-CHMICA, 5F-AKB-48, PX1, PX1 acid
31	HN K2/ 8/2016	5F-ADB, 5F-PB-22, MDMB-CHMICA, 5F-AKB-48, PX1, PX1 acid
32	HN Jok 1/2016	5F-ADB, MMB-2201
33	HN Jok 2/2016	5F-ADB, MMB-2201
34	HN Jok 3/2016	5F-ADB, MMB-2201
35	HN Jok 4/2016	5F-ADB, MMB-2201
36	HN Jok 5/2016	5F-ADB, MMB-2201
37	HN Jok 6/2016	5F-ADB, MMB-2201
38	HN Exod 1/2017	5F-ADB
39	HN Exod 2/2017	5F-ADB
40	HN Exod 3/2017	5F-ADB
41	HN Exod 4/2017	5F-ADB
42	HN Exod 5/2017	5F-ADB
43	HN Exod 6/2017	5F-ADB
44	HN Exod 7/2017	5F-ADB
45	HN Exod 8/2017	5F-ADB
46	HN Injok 1/2017	MDMB-CHMICA
47	HN Injok 2/2017	MDMB-CHMICA
48	HN Jok 1/2017	5F-ADB, MMB-2201
49	HN Jok 2/2017	5F-ADB, MMB-2201
50	HN Ext 1/2017	5F-PB-22
51	HN Ext 2/2017	AB-CHMINACA
52	HN Ext 3/2017	5F-PB-22
53	HNK2/ 1/2017	5F-ADB, 5F-PB-22, MDMB-CHMICA, 5F-AKB-48, PX1, PX1 acid
54	HNK2/ 2/2017	5F-ADB, 5F-PB-22, MDMB-CHMICA, 5F-AKB-48, PX1, PX1 acid
56	HNK2/ 3/2017	5F-ADB, 5F-PB-22, MDMB-CHMICA, 5F-AKB-48, PX1
57	HNK2/ 4/2017	5F-ADB, 5F-PB-22, MDMB-CHMICA, 5F-AKB-48, PX1, PX1 acid
58	HNK2/ 5/2017	5F-ADB, 5F-PB-22, MDMB-CHMICA, 5F-AKB-48, PX1, PX1 acid
59	HNK2/ 6/2017	5F-ADB, 5F-PB-22, MDMB-CHMICA, 5F-AKB-48, PX1
60	HNK2/ 7/2017	5F-ADB, 5F-PB-22, MDMB-CHMICA, 5F-AKB-48, PX1
61	HN Kroinic J/2017	5F-Cumyl-PINACA
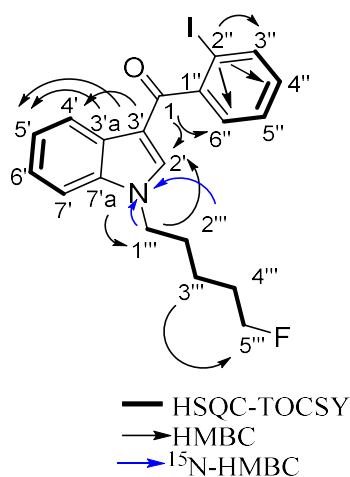
Table 15. NMR data of AM-694 with key connections shown in the figure.

Position	^{13}C	$^{1}H/^{19}F$
1	190.4	-
2'	137.1	7.31 1H, s
3'	114.5	-
3'a	125.7	-
4'	121.8	8.34 1H, d (9.0)
5'	122.0	7.33-7.34 1H, overlapped m
6'	122.7	7.34-7.35 1H, overlapped m
7'	109.0	7.37-7.39 1H, overlapped m
7'a	136.1	-
1"	145.3	-
2"	91.6	-
3"	138.5	7.92 1H, dd (7.5, 1.5)
4"	129.5	7.16 1H, td (7.5, 1.5)
5"	126.8	7.44 1H, td (7.5, 1.5)
6"	127.0	7.39-7.40 1H, m overlapped
1'''	46.1	4.13 2H, t (7.0)
2'''	28.4	1.90 2H, quintet (7.0)
3'''	21.7, d ($^{3}J_{CF}$ 5.0)	1.42-1.48 2H, m
4'''	28.8, d ($^{2}J_{CF}$ 19.0)	1.69 2H, doublet of quintets ($^{3}J_{HF}$ 26.0, $^{3}J_{HH}$ 6.0)
5'''	82.6, d ($^{1}J_{CF}$ 164.5)	4.41 2H dt ($^{2}J_{HF}$ 47.5, $^{3}J_{HH}$ 6.0)
5-F	-	-218.6 tt ($^{2}J_{HF}$ 47.5, $^{3}J_{HF}$ 26.0)

Analysis of 4 "Loco elite" herbal blend samples by NMR and LC/ESI-MS/MS revealed the presence of AM-694, 1-[(5-fluoropentyl)-1H-indol-3-yl]-(2-iodophenyl) methanone, a 2nd generation SCA which was developed by Makriyannis and Deng[255] along with analogues, the AM series. AM-694 affinity (K_i) for CB$_1$ receptors ($K_i = 0.08$ nM) is 500-times that of THC ($K_i = 40$ nM),[255] thus greatly increasing the chance for intoxication. Nakajima *et al*.[262] published the first analytical characterization of synthetic AM-694 along with 4 other benzoyl indoles bought through the internet in Tokyo. However, their AM-694 NMR assignments have ambiguities warranting further investigation (Table 15 and Figure 74).
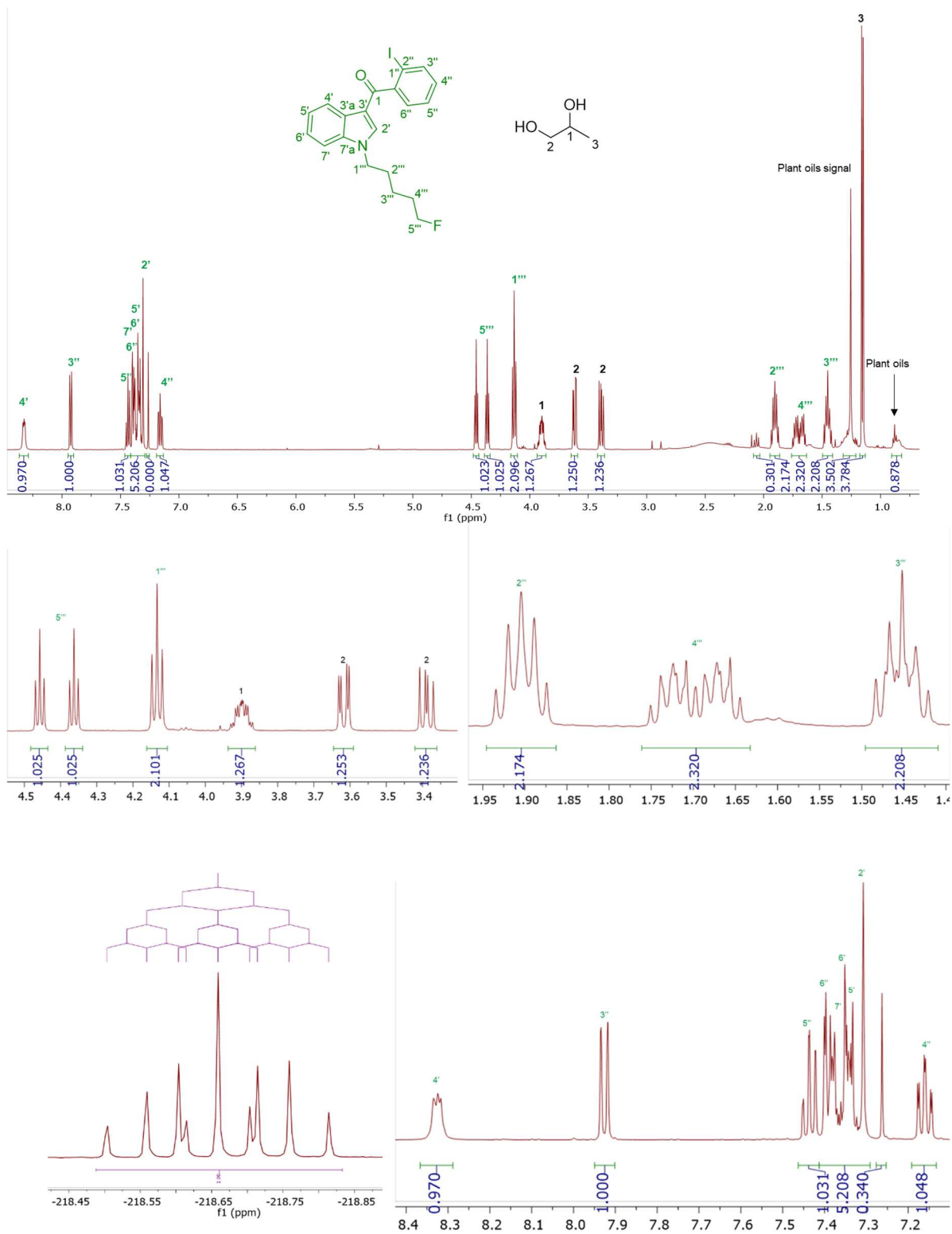
Figure 74. ^{1}H NMR spectra in CDCl$_3$ of a sample of HN Loc, containing AM-694 and propylene glycol, with expansions of all areas in the spectra and ^{19}F proton coupled spectra showing the fluorine signal of a triplet of triplets at -218.6 ppm.

Extraction of ~300 mg of herbal blend (HN Loc sample) containing AM-694 with CDCl$_3$ followed by 1D/2D NMR spectroscopic analysis resulted in 20 carbon signals including 6 quaternary carbons, including the carbonyl at δ 190.4 ppm. 3 different spin systems were identified: 2 separate aromatic systems, with 9 aromatic proton signals with separate HSQC-TOCSY correlations consistent with the presence of 2 separate aromatic rings, one of which is a singlet at δ 7.31 (2′) with ^{15}N-HMBC connection to the indole nitrogen. The third spin system was identified by HSQC-TOCSY as 5-fluoropentyl, with 5 signals integrating for 10 protons (Figures 75 and 76). ^{15}N-HMBC 2-bond connection is to 1‴ downfield at δ 4.13 and the 3-bond connection is to 2‴ at δ 1.90. The electronegative effect of the fluorine substituent is observed on the methylene signal at 5‴ δ 4.41 ppm assigned as a doublet of triplets $^2J_{HF}$ 47.5 and $^3J_{HH}$ 6.0 Hz rather than as in Nakajima *et al.*[262] of two triplets, substantiated by ^{19}F-HOESY connection of the fluorine to the mid-point of the two triplets. ^{19}F-HMBC showed connection to the methylene signals 5‴ and 4‴. Other key correlations include COSY connections of H5′ to H4′, and H6′ to H7′, with NOESY contact between H1‴ and H7′ of the indole. Distinctive fluorine coupling was observed at δ -218.6 (tt $^2J_{HF}$ 47.5, $^3J_{HF}$ 27.5 Hz). Furthermore, propylene glycol (PG) was identified at 50-60% in 4 samples of HN Loc brand, with the methyl doublet at 1.55 ppm, 2 doublets of doublets at 3.39 and 3.62 ppm (11.0 Hz *geminal* and 8.0 Hz *vicinal* couplings), and a methine multiplet 3.87-3.93 ppm. The NMR spectroscopic findings were confirmed with authentic propylene glycol which is believed to have been added to the herbal blends to help in the volatilization of the SCA.[263]

In control experiments, both Damiana and marshmallow blank herbal materials were extracted under identical conditions to the above HNLoc sample. The resulting ^{1}H NMR spectra showed equivalent signals at 0.88 and 1.25 ppm assigned to the long chain plant oils, as seen in Figure 74.
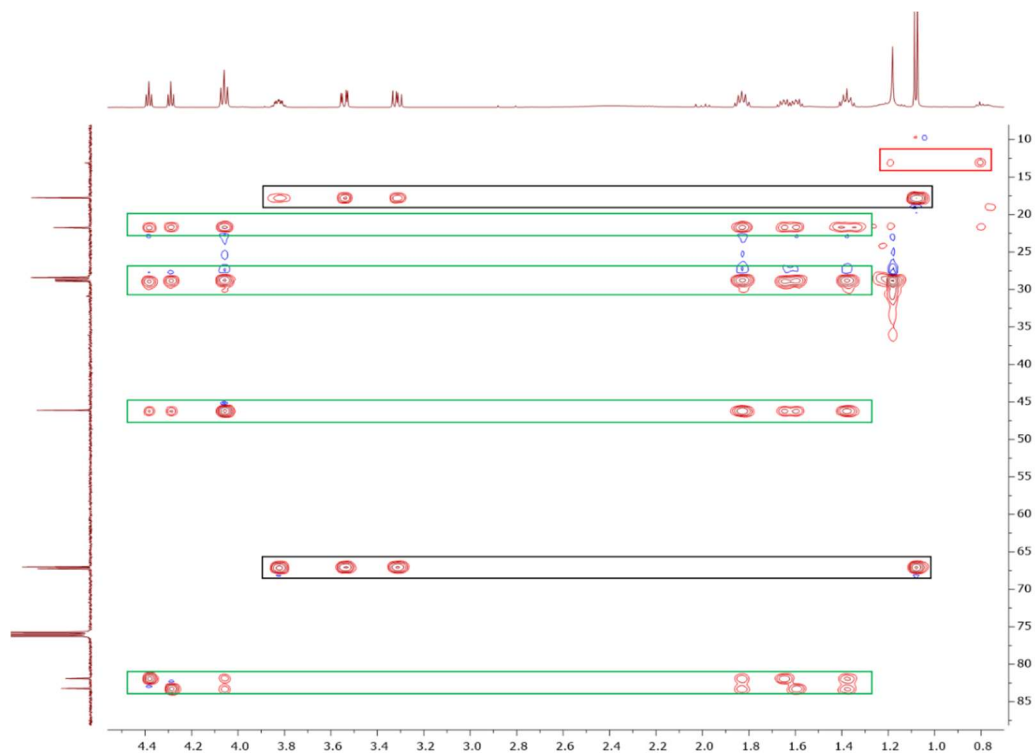
Figure 75. Expansion of HSQC-TOCSY 2D spectra of sample HN Loc showing ^{1}H-^{13}C spin systems of three different components, (green) AM-694 5-fluoropentyl tail, (red) plant oils, (black) propylene glycol.
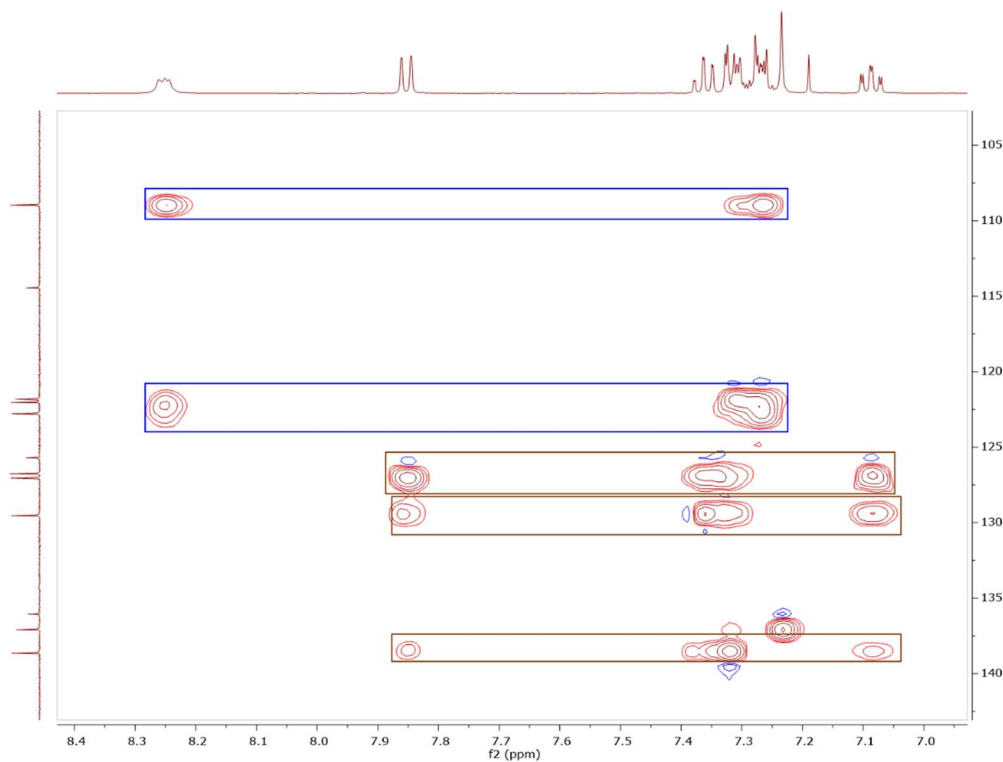
Figure 76. Aromatic expansion of HSQC-TOCSY 2D spectra of sample HN Loc showing ^{1}H-^{13}C spin systems of (blue) indole and (brown) iodophenyl.

146

LC/ESI-MS/MS analysis of the content of the Loco elite herbal blend showed only AM-694 RT 7.0 min found molecular ion 436.0576 for $C_{20}H_{20}NOFI$ requires 436.0568. Additionally, MS/MS analysis revealed a strong molecular ion peak with loss of iodine at 309 m/z and the loss of the indole 5-fluoropentyl moiety and the formation of the iodobenzoyl ion at 230 (Figure 77). The MS/MS spectrum shows significantly fewer fragments than the EI-GC/MS trace of Nakajima *et al.*[262] with a stronger molecular ion peak (100% abundancy). However, LC/MS analysis failed to detect propylene glycol due to the absence of a chromophore and its poor ionization. In order to confirm the NMR analysis and to adhere to the guidelines of the SWGDRUG requiring two methods for the confirmation of detection, propylene glycol was derivatized using *p*-toluenesulfonyl isocyanate (PTSI).
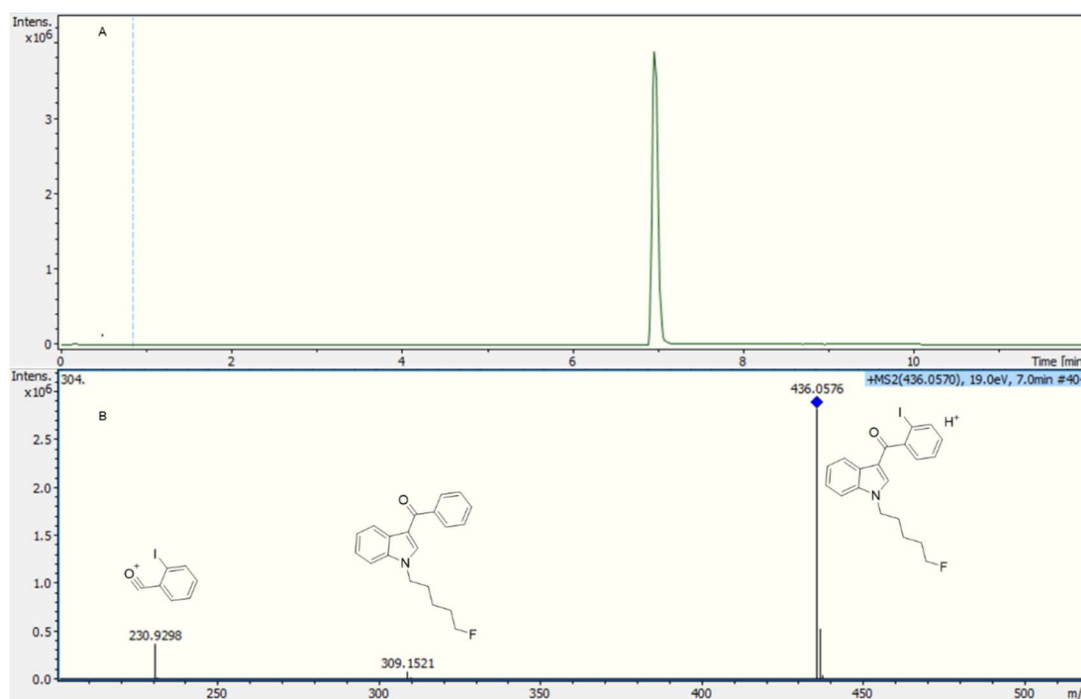
Figure 77. (A) EIC of AM-694 in sample HN Loc RT 7.0 min,

(B) CID MS/MS spectrum of AM-694.

PTSI was used successfully for the derivatization of propylene glycol and diethylene glycol (DEG) in pharmaceutical products followed by HPLC detection at 227 nm.[264] This literature method for derivatization was used with minor alterations. The main reason for choosing PTSI is the high capacity of the isocyanate moiety to undergo nucleophilic attack by

the primary and secondary alcohols of propylene glycol. Also, the reaction is relatively fast

for derivatization, 10 min at only 20 ˚C (Figure 78).
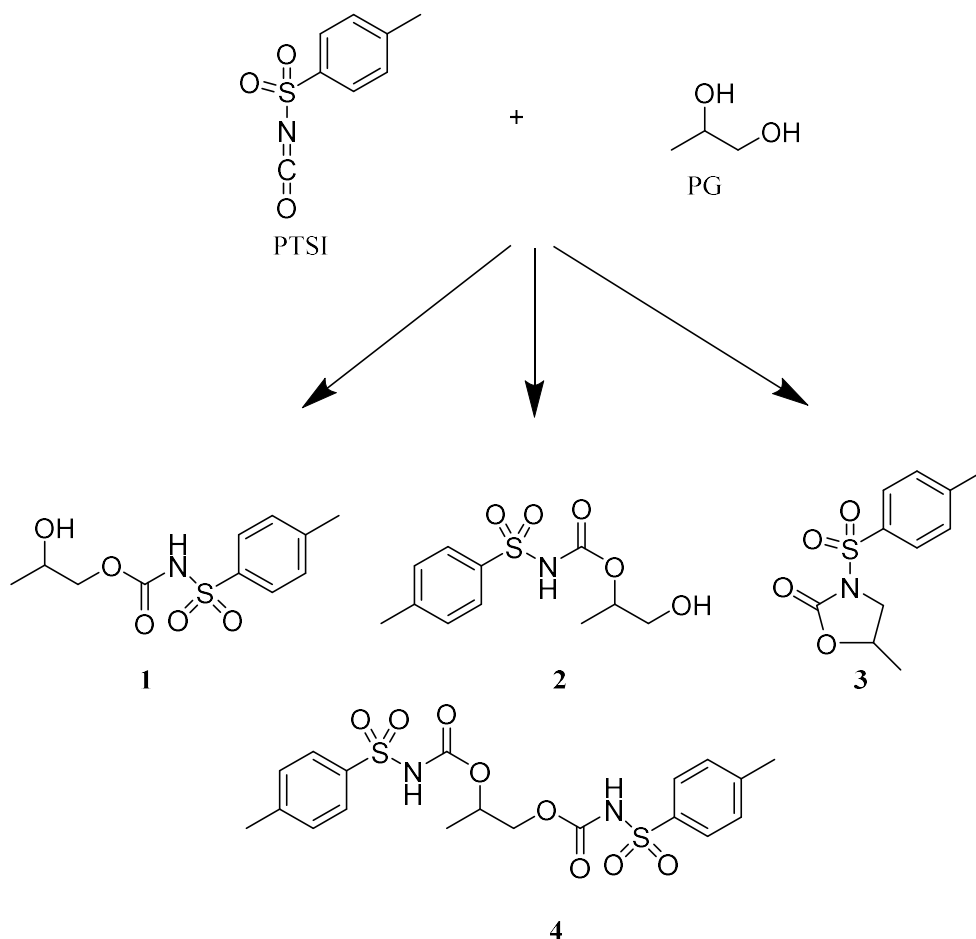
Figure 78. Derivatization products of propylene glycol showing adducts formed as detected

by LC/ESI-MS.

LC/ESI-MS analysis after derivatization resulted in the detection of multiple

molecular ions for the propylene glycol derivatives, plus the AM-694 molecular ion. At an

RT of 5.8 min, two propylene glycol derivatization products overlapped. The first molecular

ion resulting from the derivatization of the primary or secondary alcohol (derivatives 1 and

2)**,** both having $[M+H]^+$ 274 m/z, the found $[M+H]^+$ 274.0733 for $C_{11}H_{16}NO_5S$ requiring

274.0743, and derivative 3, which is the result of nucleophilic addition of an alcohol to the

isocyanate moiety, followed by cyclization which occurs with loss of water, found $[M+H]^+$

256.0622 for $C_{11}H_{16}NO_5S$ requiring 256.0638. Moreover, $[M+H]^+$ RT 6.5 min resulting from the derivatization of both the primary and secondary alcohols of propylene glycol found 471.0876 (derivative 4) for $C_{19}H_{23}N_2O_8S_2$ requiring 471.0890. In addition, a protonated dimer at 941.1652 for $C_{38}H_{45}N_8O_{16}S_4$ requires 941.1707 (within 6 ppm of mass accuracy). Furthermore, AM-694 was detected at RT 7.0 min with the found molecular ion 436.0580 for $C_{20}H_{20}NOFI$ requiring 436.0568, and its protonated dimer at 871.1048 for $C_{40}H_{39}N_2O_2F_2I_2$ requiring 871.1063 (Figure 79).
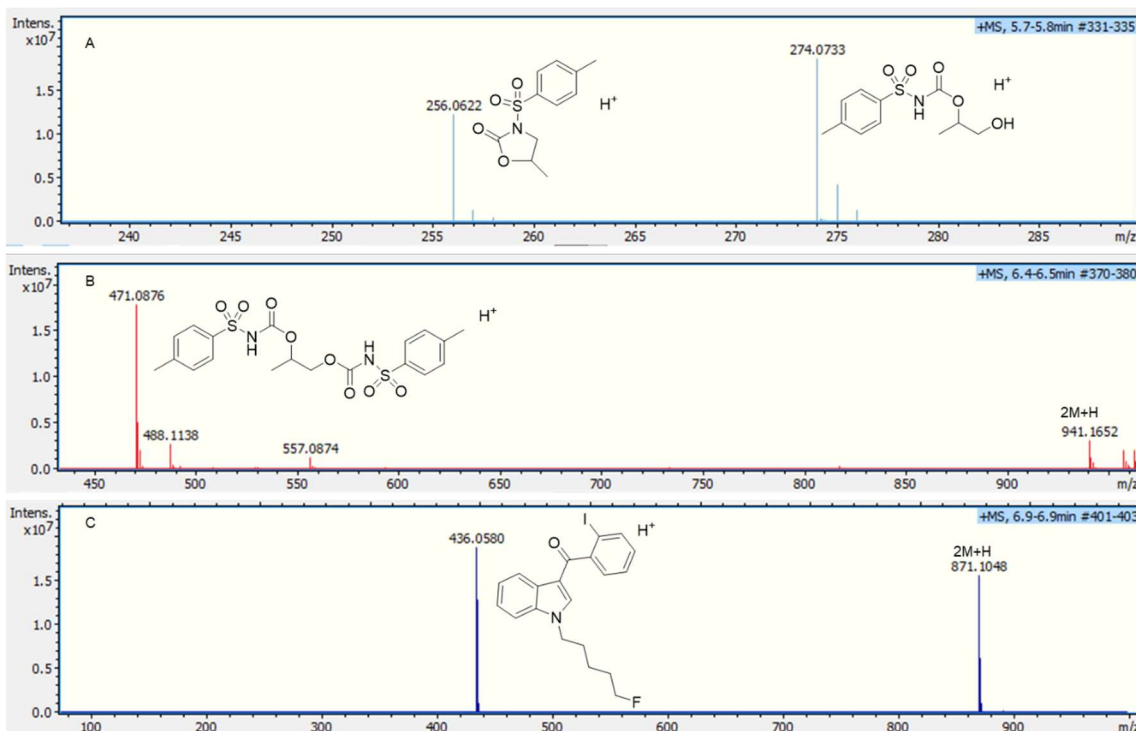
Figure 79. MS spectra of (A) derivatives 1 and 3, (B) derivative 4, (C) AM-694.

The results of the sample derivatization were compared to the derivatization of authentic propylene glycol resulting in the formation of the same PTSI adducts. More in depth MS/MS analysis of the derivatives formed is beyond the scope of this research, as the aim was to detect propylene glycol by LC/ESI-MS analysis. Derivatization of sample HN Loc allowed the detection of four propylene glycol derivatives, thus confirming the presence of propylene glycol mixed with AM-694. These LC/ESI-MS results confirmed the NMR findings. In addition, the single crystal X-ray structure of AM-694 was obtained (Figure 80) and its data are reported in Appendix 2.
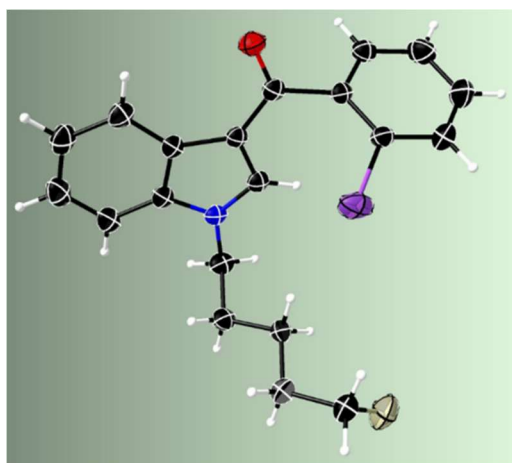
Figure 80. X-ray structure of AM-694.

NMR and LC/ESI-MS/MS analysis of the contents of a herbal blend package labelled "Extinction", seized in 2016, showed AB-CHMINACA (*N*-(1-amino-3-methyl-1-oxobutan-2-yl)-1-(cyclohexylmethyl)-1*H*-indazole-3-carboxamide), even though the "Extinction" packet is labelled 5F-AKB-48 and 5F-PB-22. AB-CHMINACA and other indazoles were developed by Pfizer for medicinal applications.[265] Langer *et al*.[266] published the NMR of AB-CHMINACA in CD$_3$OD, but there are no ^{15}N data for the compound and no mention of the impurities present in the sample which is one of the aims of this research, thus warranting full NMR assignments in CDCl$_3$. Analysis of the crude extract revealed the excipients present such as propylene glycol (PG) and isopropyl alcohol (IPA). Also, the presence of plant oil signals between 0.8-1.3 ppm obscure the isopropyl, 3‴, and 5‴ peaks of AB-CHMINACA. Further purification is therefore required for definitive characterization by NMR.

"Extinction" plant material (1.3 g) was extracted with CHCl$_3$ (2 x 25 ml) with sonication for 30 min each time. The extract was passed through a 0.25 μm syringe filter. The filtrate was evaporated to dryness under reduced pressure yielding ~190 mg of a pale yellow residue. This was dissolved in DCM (1 mL) and loaded onto a silica column (8 g) with n-hexane: ethyl acetate mobile phase using gradient 1. The ^{1}H and ^{13}C NMR analysis revealed 28 protons and 20 carbon signals respectively (Table 16 and Figure 81), with 3 spin systems of indazole, *N*-cyclohexylmethyl, and isopropyl separated by HSQC-TOCSY NMR. Key 2D NOESY correlations are shown on the structure in Table 16. Spectroscopic identification of

PG and IPA was confirmed by comparison with the data obtained from authentic samples. Differentiation between the methyls of propylene glycol and isopropyl alcohol was achieved using COSY NMR. Moreover, different "Extinction" packages showed qualitative differences in the SCA present. 2 samples of "Extinction" seized in 2017 contained 5F-PB-22 rather than AB-CHMINACA; 5F-PB-22 will be described below in section 4.3.4.

2D NOESY - - - ➤
HSQC-TOCSY ▬▬
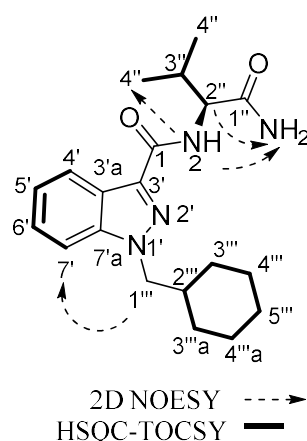
Table 16. NMR data of *N*-(1-amino-3-methyl-1-oxobutan-2-yl)-1-(cyclohexylmethyl)-1*H*-indazole-3-carboxamide (AB-CHMINACA) in CDCl$_3$.

Position	^{13}C/^{15}N	^{1}H	HMBC
1	163.0	-	2, 2″
2 (NH)	80.38	7.58 1H, d (9.0)	-
1″	174.1	-	NH$_2$, 2, 2″, 3″
2″	57.8	4.67 1H, dd (9.0, 7.0)	NH$_2$, 3″, 4″
3″	31.0	2.391 1H, octet (7.0)	2, 2″, 4″
4″	18.4, 19.5	1.06 3H, d (7.0), 1.08 3H, d (7.0)	2″, 3″
(NH$_2$)	75.4	6.18 1H, s, 6.99 1H, s	-
1′(N)	159.9	-	-
2′(N)	289.9	-	-
3′	136.4	-	4′
3′a	122.7	-	4′, 5′, 7′
4′	122.4	8.26 1H, d (8.0)	5′, 6′
5′	122.6	7.22 1H, td (8.0, 1.5)	4′, 6′, 7′
6′	126.6	7.34-7.37 1H, overlapped 7′	5′, 7′, 4′
7′	109.6	7.37-7.40 1H, overlapped 6′	5′, 6′
7′a	141.4	-	4′, 7′, 1‴
1‴	55.7	4.17 1H, d (7.0)	2‴
2‴	38.7	1.95-2.03 1H, m	1‴, 3‴, 3‴a
3‴	30.9	0.94-1.04 2H, m	cyclohexyl ring
3‴a	30.8	1.53-1.60 2H, m	cyclohexyl ring
4‴	25.5	1.11-1.22 2H, m overlapped	cyclohexyl ring
4‴a	25.6	1.57-1.70 2H, m overlapped	cyclohexyl ring
5‴	26.2	1.11-1.22 1H, m overlapped 1.57-1.70 1H, m overlapped	cyclohexyl ring

^{15}N-HMBC 2D analysis of AB-CHMINACA revealed all the connectivities between protons 2- and 3-bonds away from the nitrogen, and ^{15}N-HSQC those directly attached to

151

nitrogen (Figure 82). CDCl$_3$ was chosen due to the solubility of the compound in it and to preserve the exchangeable protons. [15]N spectra were referenced to nitromethane (380 ppm). ^{15}N-HMBC showed 2- and 3-bond connectivities of protons 3″ and 2″ respectively to N2 of the secondary amide, methylene protons (1‴) have 2- and 3-bond connectivities with N1′ and N2′ respectively of the indazole ring.

Figure 81. ^{1}H NMR (in CDCl$_3$) of (A) a crude extract of "Extinction" herbal blend containing AB-CHMINACA with expansion of areas containing impurities PG and IPA, (B) purified extract showing expansions and all proton assignments.

Figure 82. (A) ^{15}N HBMC of AB-CHMINACA showing 2- and 3-bond connectivities of protons to the nitrogens, (B) ^{15}N HSQC showing protons directly attached to the nitrogens.

Additionally, a weak 4-bond connection can be seen for the proton of the secondary amide at 7.58 ppm with the N2′ of the indazole ring. ^{15}N-HSQC showed direct connection of the two protons of the primary amide at 6.18 and 6.99 ppm with their nitrogen atom and of the secondary amide with its nitrogen atom (N2) (Figure 82).

LC/ESI-MS/MS analysis results are in accordance with the extensive MS/MS analysis reported by Langer et al.[266] In the current work, an RT of 6.9 min gave [M+H]$^+$ of 357.2297 for $C_{20}H_{29}N_4O_2$ requires 357.2285. MS/MS fragmentation is described in Figure 83, where the most abundant fragment (312 m/z) resulted from the loss of 17 (-NH$_3$) and then 28 (-CO) Da from the protonated molecular ion, and the interaction of the lone pair of N2′ with that cation to form the tricycle. A further loss of 71 Da (-C$_4$H$_9$N) gave the 241 m/z ion.
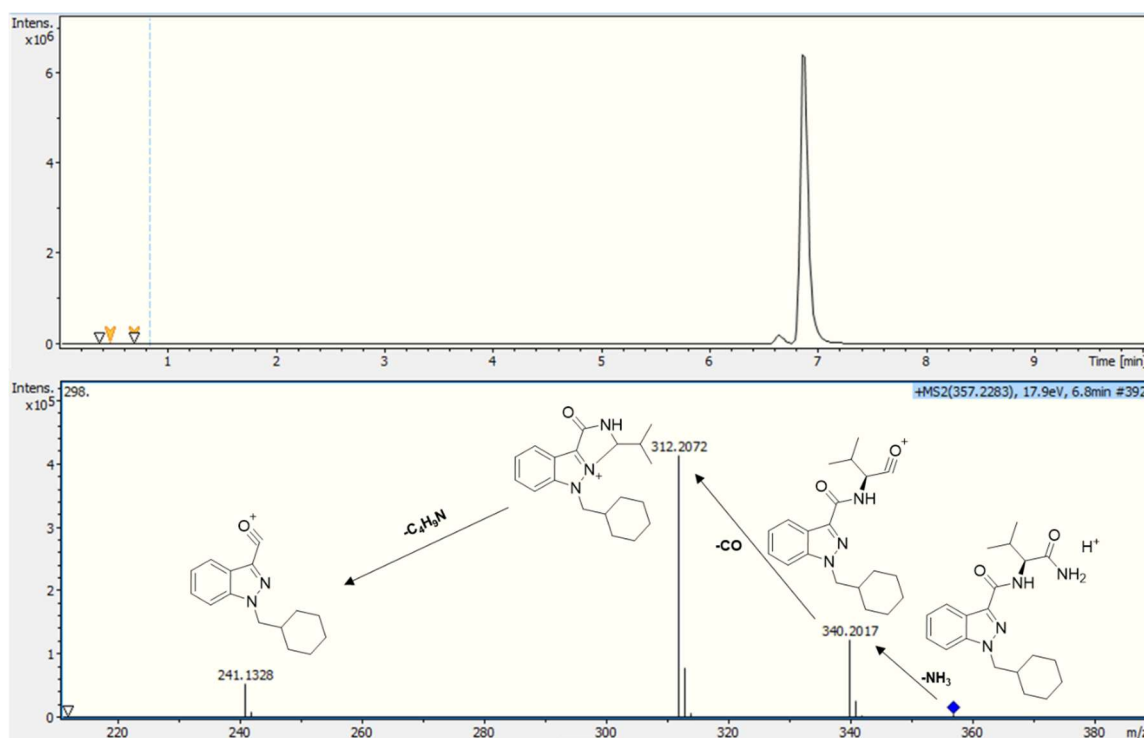
Figure 83. (Top) TIC of herbal blend sample containing AB-CHMINACA RT = 6.9 min, (bottom) MS/MS spectrum of the protonated molecular ion and its fragments.

154

Shortly after the emergence of indole and indazole carboxamide SCAs, the 2015 EMCDDA report[267] stated that cumyl analogues (2-phenylpropan-2-yl), which just like AM-694 are based on a patent by Bowden and Williamson,[268] started to be detected as seizures were reported from different European countries.[267] NMR characterization of 5F-cumyl-PINACA in a E-cigarette liquid labelled "Kronic Juice" (Figure 84) has been analysed.

Figure 84. E-cigarette vial containing SCA 5F-cumyl-PINACA.

Direct extraction of the contents of the liquid showed the presence of propylene glycol and ethyl acetate among other unknown peaks that are possibly from compounds added as flavouring agents. Moreover, as propylene glycol is a humectant, a substantial amount of water is seen in the NMR spectra of the crude extract, adding to the high ratio of the excipients to SCA. Purification using flash column chromatography was required for a full characterization of 5F-cumyl-PINACA (Table 17 and Figure 85).

Analysis of the crude extract showed the presence of propylene glycol as the main constituent in E-cigarettes along with other solvents, e.g. ethyl acetate, which are listed among many other components in E-cigarettes, e.g. nicotine, formaldehyde, limonene.[269] In general, the NMR of 5F-cumyl-PINACA is similar to SCAs that possess a 5-fluoropentyl tail and an indazole or indole core structure. The most distinctive feature is the presence of the 6H singlet at 1.87 ppm for the 2 x Me (H4) in the cumyl moiety together with the 5H for the cumyl phenyl ring in the head component of the SCA.

```
            key HMBC
- - - - ▸   key NOESY
            ¹⁹F-HMBC
```
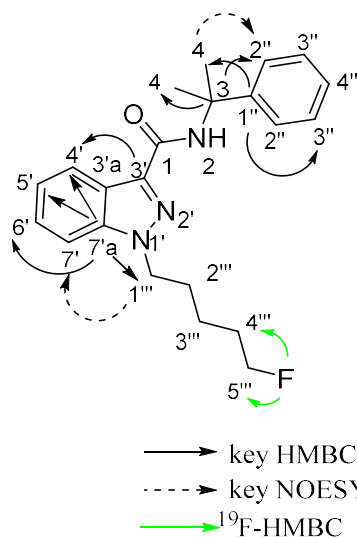
Table 17. NMR (in CDCl$_3$) data of 1-(5-fluoropentyl)-*N*-(2-phenylpropan-2-yl)-1*H*-indazole-

3-carboxamide (5F-cumyl-PINACA) with key connections shown.

Position	^{13}C/^{15}N	^{1}H/^{19}F
1	161.8	-
2 (NH)	97.9	7.36-7.40 1H, overlapped with 6′ and 7′
3	55.8	-
4	29.6	1.87 6H, s
1″	147.2	
2″	124.8	7.52 2H, dd (7.5, 2.0)
3″	128.4	7.35 2H, td (7.5, 2.0)
4″	126.6	7.19-7.24 1H, m overlapped with 5′
3′	137.9	-
3′a	122.8	-
4′	123.2	8.33 1H, dd (8.0, 2.0)
5′	122.4	7.19-7.24 1H, overlapped with 4″
6′	126.7	7.36-7.40 1H, overlapped 7′ and NH
7′	109.0	7.36-7.40 1H, overlapped with 6′ and NH
7′a	140.9	-
1‴	49.1	4.10 2H, t (7.0)
2‴	29.4	2.01 2H, quintet (7.0)
3‴	22.7, d ($^3J_{CF}$ 5.0)	1.45-1.52 2H, m
4‴	25.5, d ($^2J_{CF}$ 19.0)	1.75 2H, doublet of quintets ($^3J_{HF}$ 27.0, $^3J_{HH}$ 7.5)
5‴	83.7, d ($^1J_{CF}$ 165.0)	4.51 2H, dt ($^2J_{HF}$ 47.5, $^3J_{HH}$ 6.0)
F		-218.6 tt ($^2J_{HF}$ 47.5, $^3J_{HF}$ 27.0)
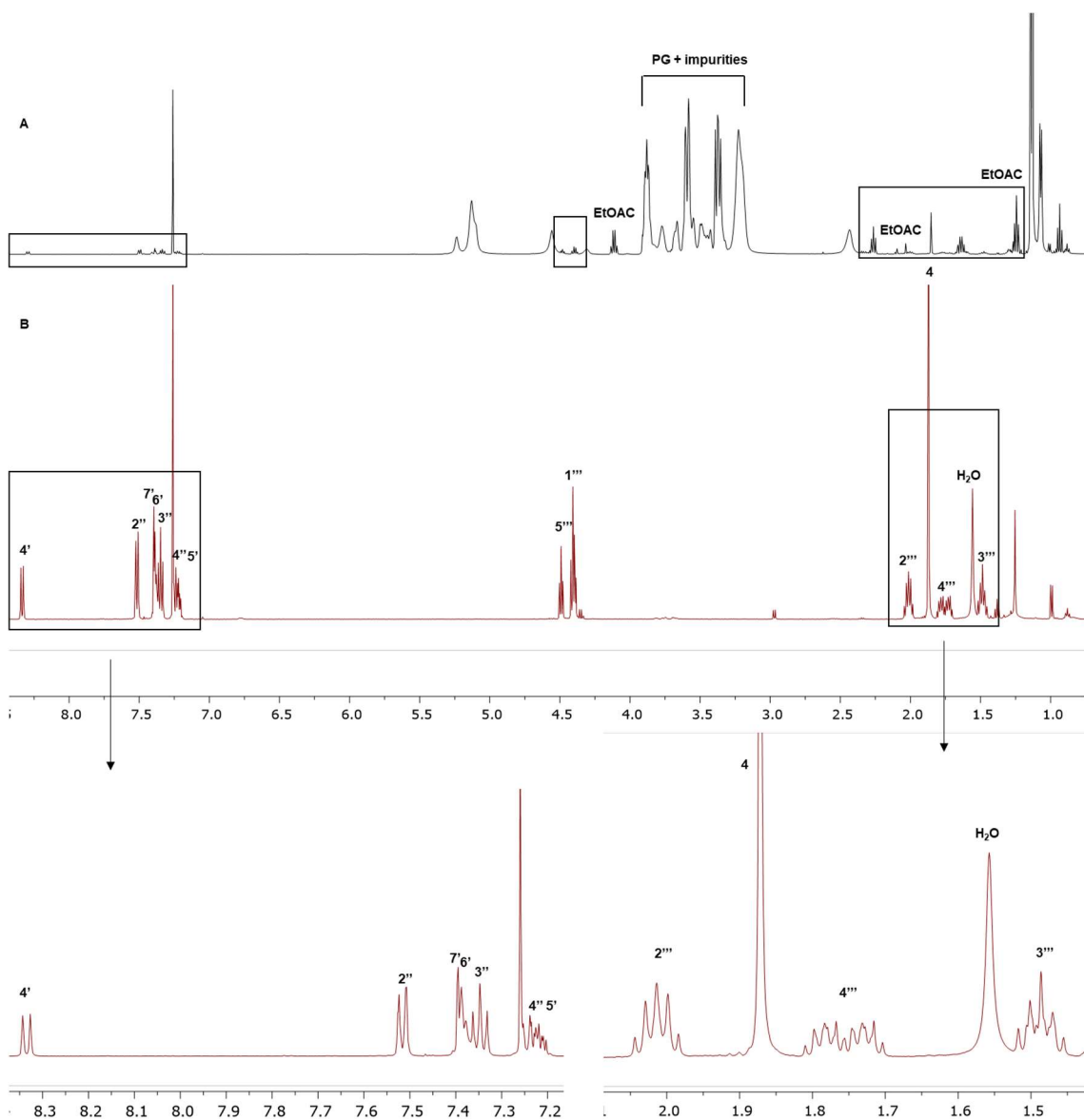
Figure 85. ^{1}H NMR spectra in CDCl$_3$ of (A) crude extract from E-cigarette liquid showing excipients and impurities present in high ratio compared to the 5F-cumyl-PINACA, (B) purified extract showing assignments of 5F-cumyl-PINACA with expansions.

^{19}F-HMBC revealed 2- and 3-bonds coupling of the fluorine to the protons of 5‴ and 4‴ respectively on the 5-fluoropentyl chain, further confirming the presence of such a 5-fluoropentyl tail (Figure 86). Moreover, infusing 100 μL E-cigarette liquid in 900 μL of MeOH into the ESI-MS resulted in the detection of the protonated [M+H]$^+$ 368.2161 for C$_{22}$H$_{27}$N$_3$OF requiring 368.2132 (within 8 ppm) and sodiated [M+Na]$^+$ 390.1970 for C$_{22}$H$_{26}$N$_3$OFNa requiring 390.1952.
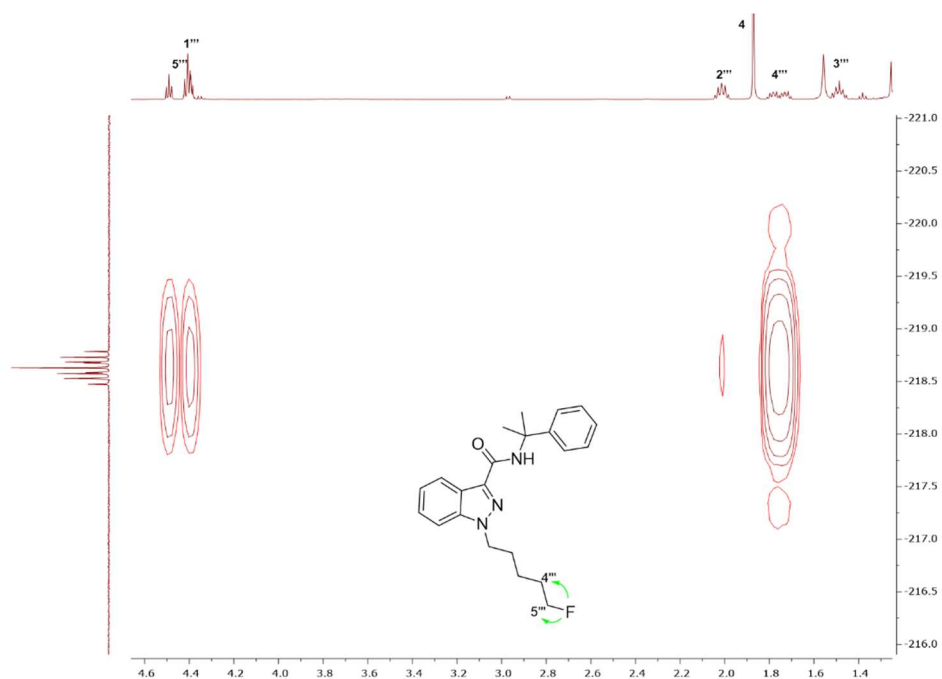
Figure 86. ^{19}F-HMBC of 5F-cumyl-PINACA showing 2- and 3-bond long range coupling of 5''' and 4''' to fluorine (where half of the 5''' signal is overlapped by the 1''' signal).

Conclusions

In this study, the analytical characterization of 61 herbal blend samples seized in 2016/2017 has been reported which can give drug analysts and law enforcement agents an idea of the SCA market after the 2016 Psychoactive Substances Act. Moreover, analysis of the excipients and impurities such as propylene glycol and isopropyl alcohol in SCA herbal blends may help in flagging large shipments of such excipients as possibly being intended for illicit purposes. Although it is true that they are both common organic solvents or coolants. NMR characterization of AM-694 is shown with high confidence removing any existing spectroscopic ambiguity. Full NMR characterization of AB-CHMINACA providing ^{15}N spectroscopic data which have not been published before, and also the identification of the impurities present in the samples are reported for the first time. Derivatization of PG present in SCA/plant matrices using PTSI allowed the compound previously undetectable on LC/ESI-MS to be detected with the formation of four adducts, confirming the NMR findings. Finally, analysis of an E-cigarette liquid allowed the identification of a recently introduced class of SCA, 5F-cumyl-PINACA with its detailed characterization using NMR spectroscopy and ESI-MS.

4.3.2 Analysis of prison samples

In Chapter 1.6 a detailed review is given of how the drug culture in prisons is changing and that SCAs are taking over, with wide spread violence and intoxications.[131-133] The Mandatory Drug Test (MDT) is failing to detect SCA.[131] In this study, an analysis of 30 UK prison (HMP) samples in the herbal form is presented using NMR spectroscopy and LC/ESI-MS/MS. The contents of the samples were examined. Samples were not packaged in attractive packages of brands, but found in different forms (Figure 87) from e.g. newspaper twists, to nylon bags, with weights (car tyre bolts or copper coins) in them for "throw overs" (with respect to prison walls). Whilst this Thesis was nearing completion, March 25th 2019, the BBC and other media reported the use of three eviscerated rats for spice and other drug delivery in HMP Guys Marsh, in Shaftesbury, Dorset. A Prison Officer commented that dead pigeons had been used previously, but using rats was new.[270]
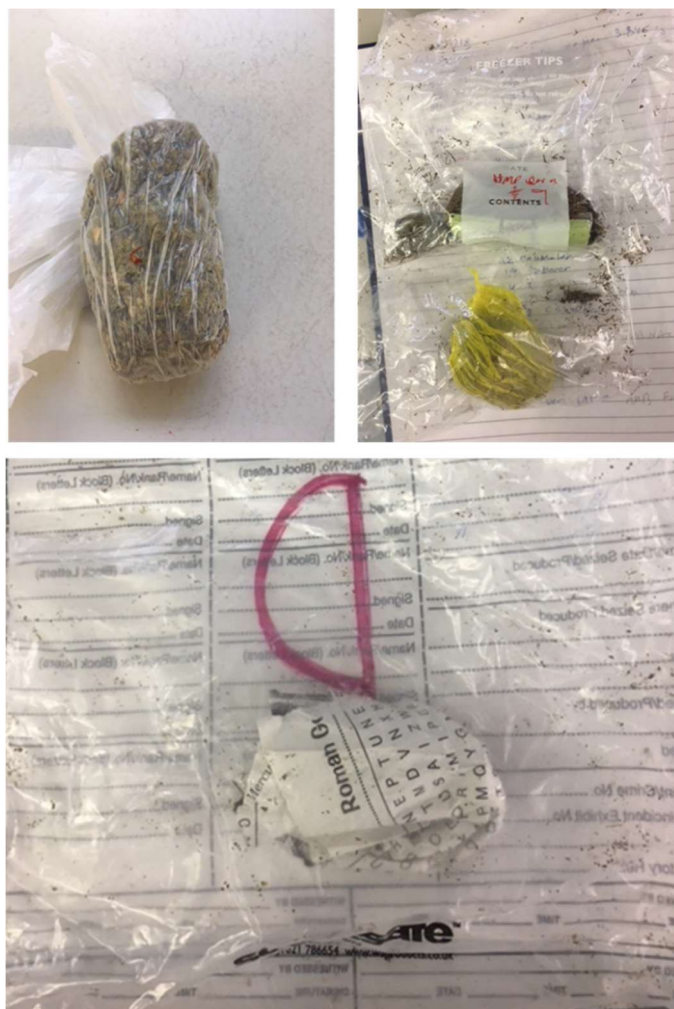
Figure 87. Examples of the seized samples from HMP.

As with the analysis of herbal blends in packaged brands, 5F-ADB was the most commonly seized SCA (11 samples identified), followed by cannabis (10 samples identified), AMB-FUBINACA (4 samples identified), 2 samples of SCA mixtures identified and 3 samples that had the appearance of tobacco (Figure 88).
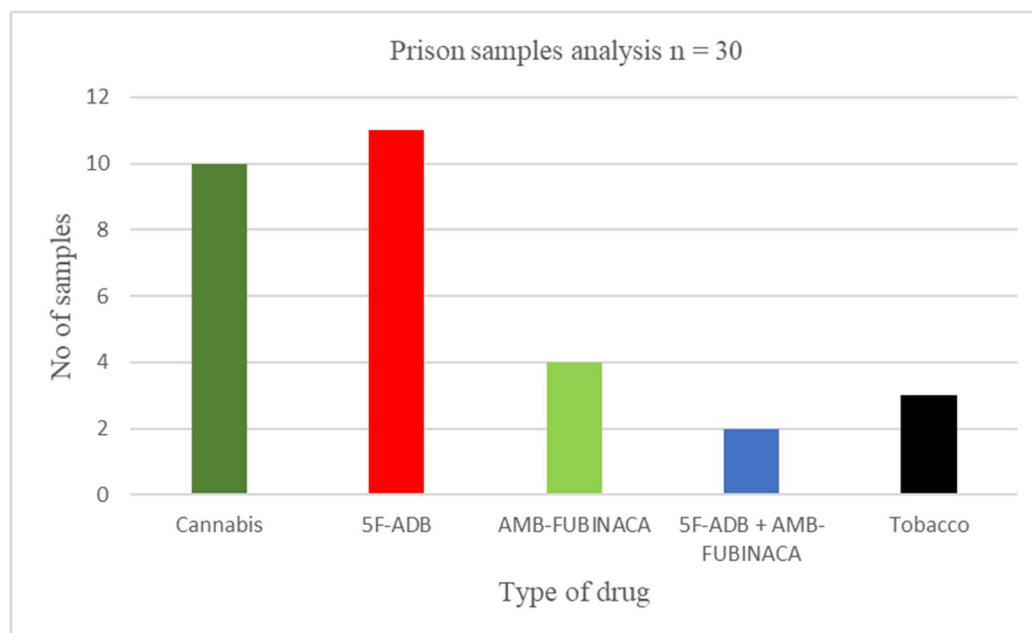
Figure 88. Analysis of HMP seized (2018) drugs.

Even though the sample size is not large enough (n = 30) to give a conclusive answer about the most common drug in HMP, these analytical findings put SCAs at the top of the most common drugs in this particular prison in 2018, which differs from the previous trend of having cannabis as the number one drug of choice among prisoners.[129] Furthermore, these findings of SCA compared to cannabis in the ratio of 2:1 in these prison samples are in accordance with a recently published Government report[134] of the increase in SCA in prisons. Nevertheless, no analytical findings have been published on the purity of SCAs in prisons.

ESI-MS was used as the preliminary analytical tool for its speed, sensitivity, and the minimal sample preparation required for profiling the HMP drug samples, and for any unknown components or any ambiguities. The samples were then further analysed by NMR and LC/ESI-MS/MS.

Confirmation of the identification of cannabis and tobacco depends on the identification of the molecular ion of THC found 315.2327 m/z for $C_{21}H_{31}O_2$ requires 315.2318 and its related phytocannabinoids such as CBN found 311.2008 m/z for $C_{21}H_{27}O_2$ requires 311.2008, and of nicotine 163.1249 m/z found $[M+H]^+$ for $C_{10}H_{15}N_2$ requiring 163.1229 (within 12 ppm) in the herbal blends (Figure 89). Furthermore, morphological examination of the plant material before ESI-MS analysis gave an idea of the type of herbal material. No SCA was found in combination with THC or nicotine.
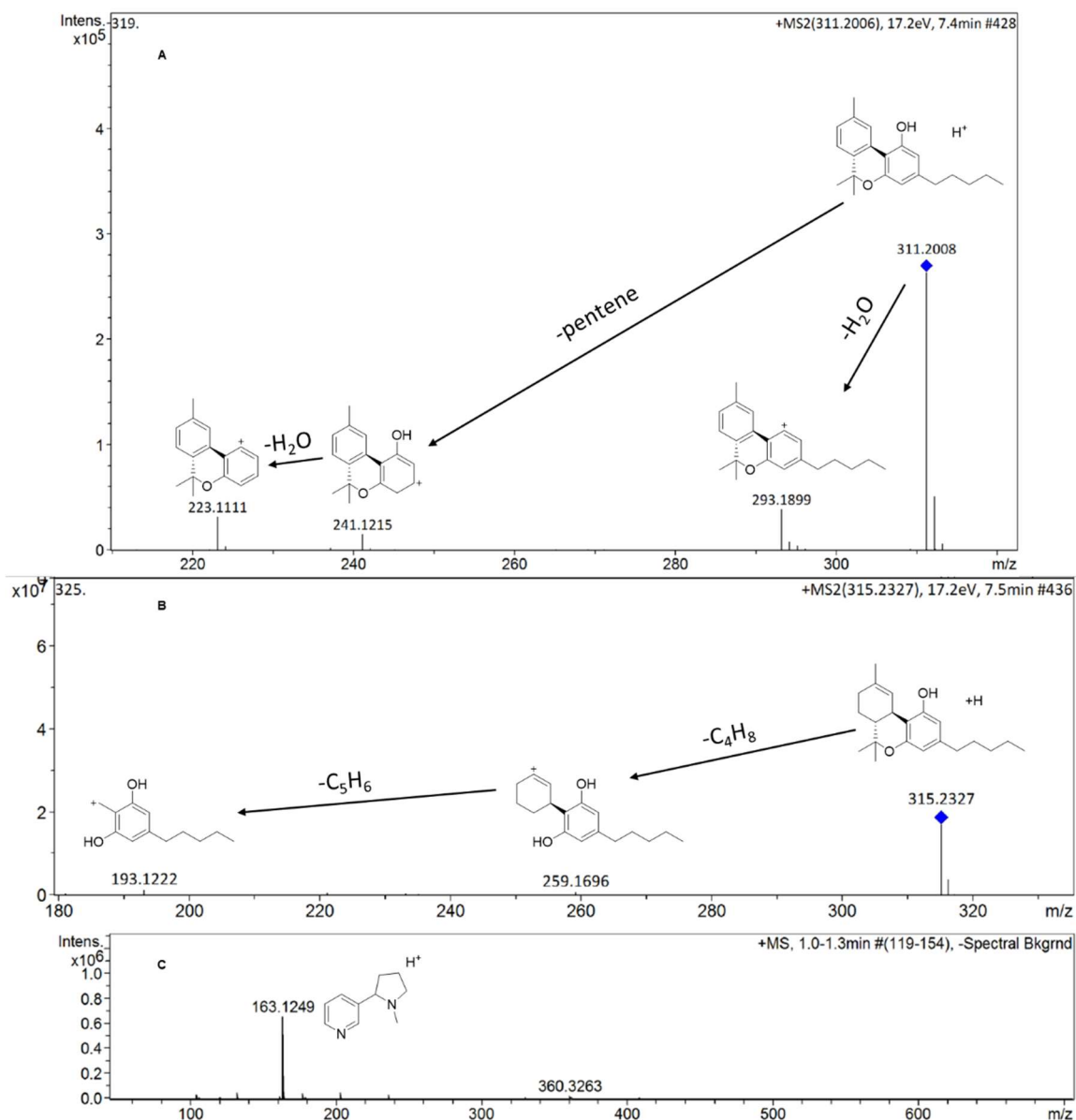
Figure 89. MS/MS spectra of a cannabis sample (HMP14) showing different phytocannabinoids, (A) CBN, (B) THC, and their fragments assigned, (C) ESI-MS of tobacco showing nicotine $[M+H]^+$.

161

AMB-FUBINACA, an NPS inspired by the Pfizer patent of similar SCAs, e.g. AB-FUBINACA, ADB-FUBINACA and AB-CHMINACA,[265] with an indazole carboxamide motif (Figure 90), has been identified in prison samples. However, AMB-FUBINACA is among recent SCA with a substitution of a carboxamide to carbonylvalinate methyl ester, where the modifications are made by clandestine chemists presumably in order to evade laws passed (perhaps more specifically) against parent compounds. This cycle of the introduction of SCA, Government banning, followed by the introduction of a new SCA product has resulted in hundreds of SCA analogues in the clandestine drugs market.

The *para*-fluorobenzyl SCA analogues are introduced to replace the SCA analogues possessing the 5-fluoropentyl chain, of which many have been banned.[271] These *para*-fluorobenzyl SCAs possess high potencies at the CB_1 receptor, similar to the 5-fluoropentyl chain SCAs, e.g. AB-FUBINACA EC_{50} = 1.8 nM and ADB-FUBINACA EC_{50} = 1.2 nM.[78,271]
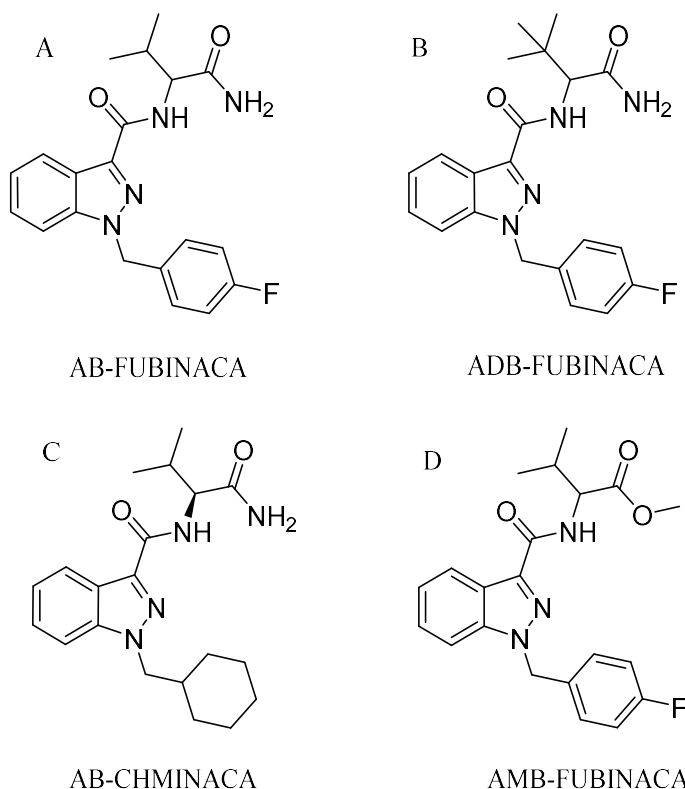
Figure 90. Pfizer indazoles A, B, and C, and D a clandestine SCA ester.

Analysis of the crude herbal blend samples containing AMB-FUBINACA revealed no excipients such as isopropyl alcohol and propylene glycol. 2 samples (HMP 11 and 15) were combined and extracted with chloroform, followed by NMR spectroscopic characterization (Table 18), using 2 different solvents CDCl$_3$ (Figure 91) and DMSO-d$_6$, in order to compare the findings with the published work of Shevyrin *et al.*[272] Spectroscopic data have also been obtained on the effect of fluorine on neighbouring protons and carbons in the 4-fluorobenzyl moiety.

^{1}H NMR, in CDCl$_3$ and in DMSO-d$_6$, showed a clearer definition of 3″ assigned as a doublet of septets and an octet respectively rather than a multiplet.[272] These multiplicities were due to the coupling to the isopropyl signals (7.0 Hz) and methine 2″ (5.0 Hz) in CDCl$_3$. In DMSO-d$_6$, the octet resulted from the coupling to the isopropyl signals and methine 2″ with the same coupling constant (7.0 Hz). NMR showed the inequivalence of the isopropyl methyls, having 2 separate ^{1}H and ^{13}C signals compared to compounds (e.g. 5F-ADB) (Figure 73) with an even bulkier group such as the *tert*-butyl which showed equivalent methyl signals. This effect was interpreted by Shevyrin *et al.*[272] as a result of the less bulkier group (isopropyl) having to adapt to hindered rotation in the conformation, with respect to the valine chiral centre. The bulkier *tert*-butyl group did not show this magnetic inequivalence. An additional NMR finding (in CDCl$_3$) is 2″ assigned as a doublet of doublets, due to coupling to the proton of the secondary amide (9.0 Hz) and also to 3″ (5.0 Hz). Furthermore, differentiation between the ^{1}H NMR signals for 5′ and 6′ of the indazole is by their HMBC connectivities to the downfield quaternary carbons 3′a and 7′a respectively.
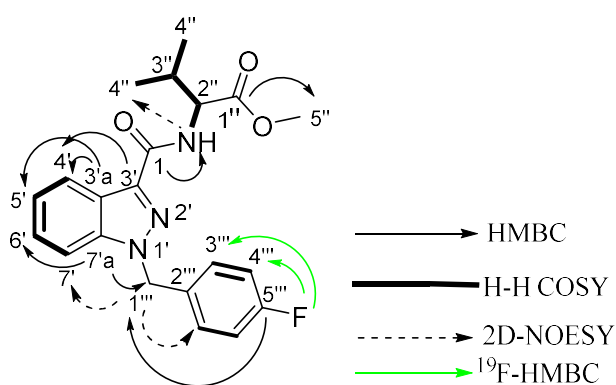
Table 18. NMR data of methyl (2*S*)-2-(1-[(4-fluorophenyl)methyl]-1H-indazol-3-yl

formamido)-3-methylbutanoate (AMB-FUBINACA) with key connectivities shown in the

(above) figure.

in CDCl₃		
Position	**¹³C**	**¹H/¹⁹F**
1	162.3	-
1″	171.5	-
2″	55.8	4.81 1H, dd (9.0, 5.0)
3″	30.6	2.32 1H, doublet of septets (5.0, 7.0)
4″	17.1, 18.1	1.04 3H, d (7.0) 1.10 3H, d (7.0)
5″	51.1	3.78 3H, s
3′	138.2	-
3′a	123.3	-
4′	121.8	8.37 1H, dd (8.0, 1.0)
5′	122.0	7.26 1H, overlapped with CHCl₃
6′	127.1	7.36 1H, td (7.0, 1.0)
7′	109.0	7.27-7.31 1H, m
7′a	139.7	-
1‴	51.9	5.59 2H, s
2‴	131.7, d ($^4J_{CF}$ 3.0)	-
3‴	128.9, d ($^3J_{CF}$ 8.0)	7.20 2H, dd (8.5, 5.0)
4‴	115.8, d ($^2J_{CF}$ 22.0)	7.00 2H, t (8.5)
5‴	162.4, d ($^1J_{CF}$ 247.0)	-
5‴-F	-	-113.98 tt ($^3J_{HF}$ 8.5, $^4J_{HF}$ 5.0)
NH		7.50 1H, br d (9.0)

in DMSO		
Position	**¹³C**	**¹H/¹⁹F**
1	161.8	-
1″	171.9	-
2″	57.3	4.42 1H, dd (8.0, 7.0)
3″	29.7	2.26 1H, octet (7.0)
4″	18.7, 19.0	0.95 3H, d (7.0) 0.97 3H, d (7.0)
5″	51.8	3.68 3H, s
3′	136.8	-
3′a	122.3	-
4′	121.6	8.14 1H, d (8.0)
5′	122.7	7.29 1H, t (8.0)
6′	126.9	7.46 1H, t (8.0)
7′	110.5	7.79 1H, d (8.0)
7′a	140.4	-
1‴	51.5	5.78 2H, t (2.0)
2‴	132.9, d ($^4J_{CF}$ 3.0)	-
3‴	129.4, d ($^3J_{CF}$ 8.0)	7.34 2H, ddt (8.5, 5.5, 2.0)
4‴	115.4, d ($^2J_{CF}$ 21.5)	7.17 2H, t (8.5)
5‴	162.5, d ($^1J_{CF}$ 244.0)	-
5‴-F		-115.18 tt ($^3J_{HF}$ 8.5, $^4J_{HF}$ 5.5)
NH		8.20 1H, d (8.0)
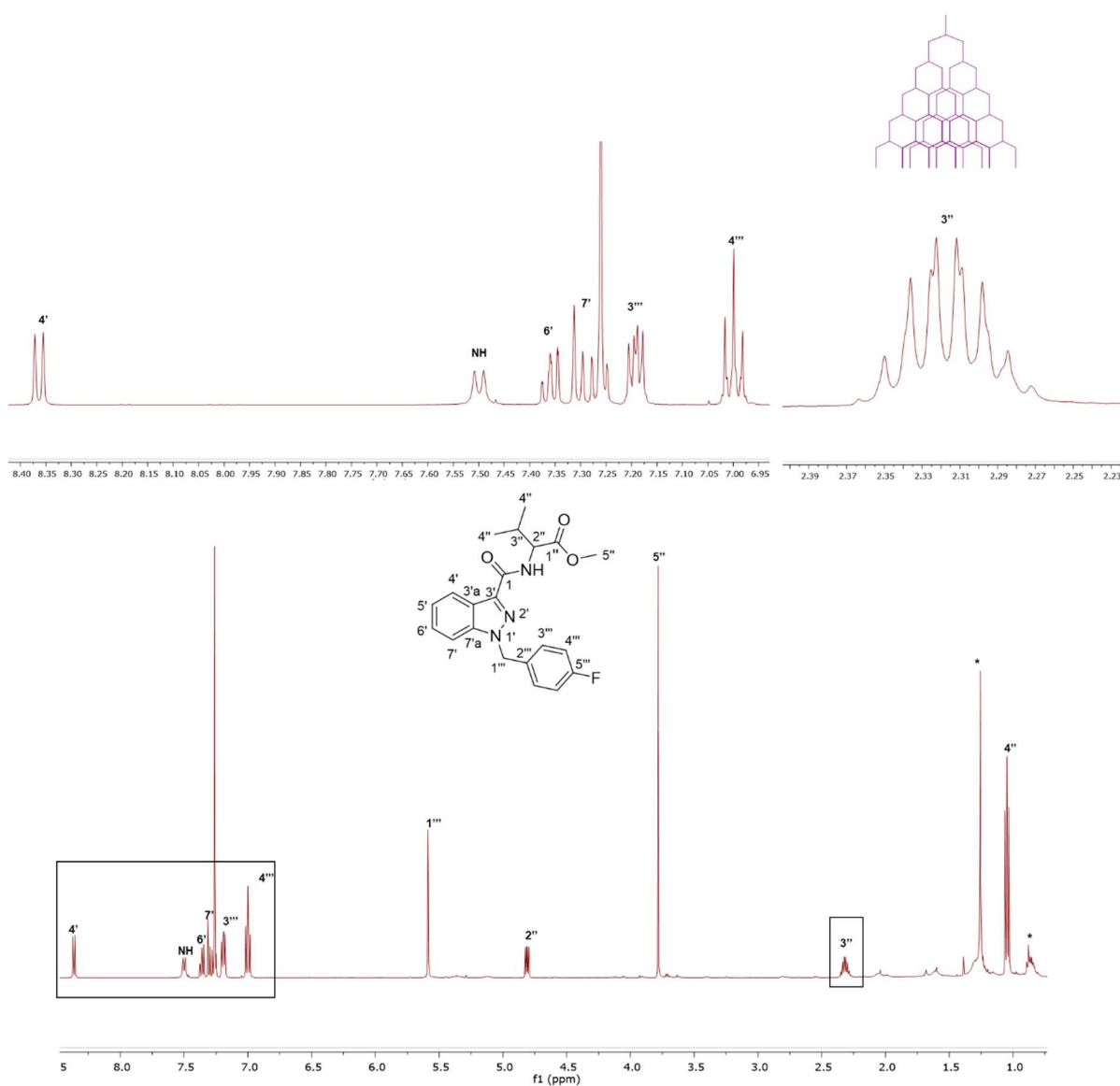
Figure 91. ^{1}H NMR spectra in CDCl$_3$ of a crude extract of a herbal blend containing AMB-FUBINACA, with expansions of proton 3″ showing the splitting pattern of a doublet of septets, and the aromatic region. * Denotes plant oil lipid-chain signals.

The effect of the fluorine substituent on the aromatic ring (4-fluorobenzyl) is clear in both ^{1}H and ^{13}C NMR data (Table 18). Aromatic ^{19}F to ^{13}C nuclei couplings (in CDCl$_3$) have been observed at position 2‴ of 4-bond coupling (3.0 Hz) and to 5‴ of a large 1-bond coupling (247.0 Hz). The 3-bond fluorine coupling to 4‴ protons of 8.5 Hz resulted in a triplet at 7.00 ppm due to a similar coupling of 8.5 Hz from 3‴. The effect of the fluorine on ^{13}C of 4‴ resulted in a 2-bond C-F coupling of 22.0 Hz. For 3‴, the H-F 4-bond coupling

constant was 5.0 Hz and the C-F 3-bond coupling constant was 8.0 Hz (Figure 92). Similar aromatic fluorine coupling values have been reported for the cathinone flephedrone, which is an analogue of mephedrone with a *para*-fluorine substituent instead of the *para*-methyl group. In flephedrone, $^3J_{HF}$ and $^4J_{HF}$ coupling constants were 8.4 and 5.2 Hz respectively, and in ^{13}C the $^1J_{CF}$, $^2J_{CF}$, $^3J_{CF}$, and $^4J_{CF}$ were 255, 22, 10 and 3 Hz respectively.[30]
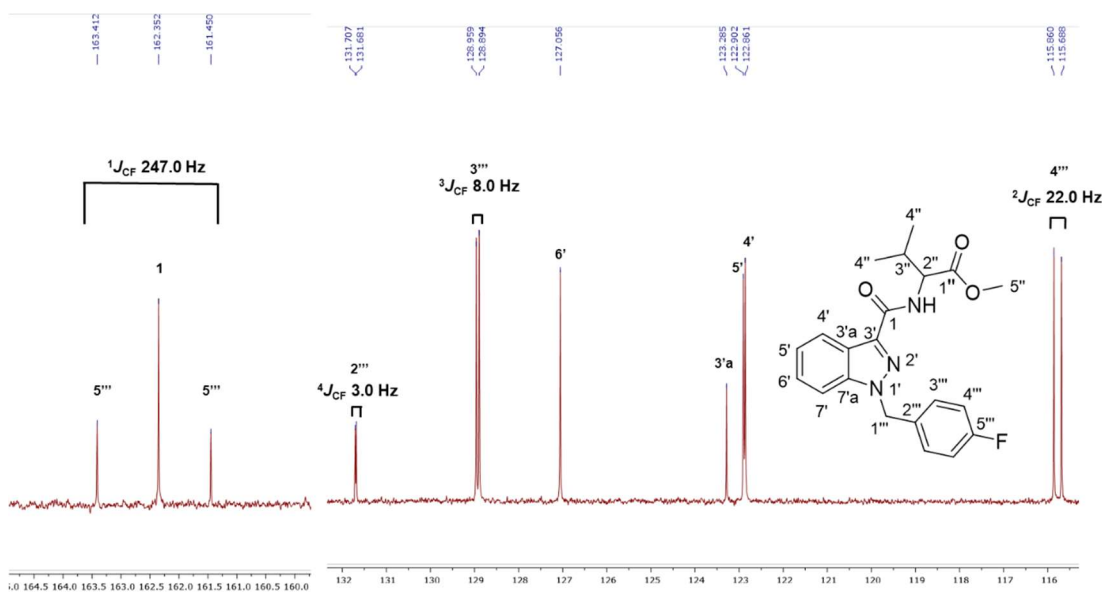
Figure 92. ^{13}C NMR spectra in CDCl$_3$ showing the fluorine coupling effects on different ^{13}C nuclei in the fluorobenzyl moiety of AMB-FUBINACA.

^{1}H coupling effects of the fluorine substituent have also been studied using ^{1}H-^{19}F decoupled NMR and pure shift NMR. The ^{1}H-^{19}F decoupled spectrum is a normal proton acquisition NMR, but with no fluorine coupling to the protons. For the pure shift NMR experiment, a Pure Shift Yielded by Chirp Excitation (PSYCHE) was used.[273] Pure shift experiments are generally used to simplify ^{1}H NMR spectra, that contain many multiplets, via broadband homodecoupling (Figure 93).

166
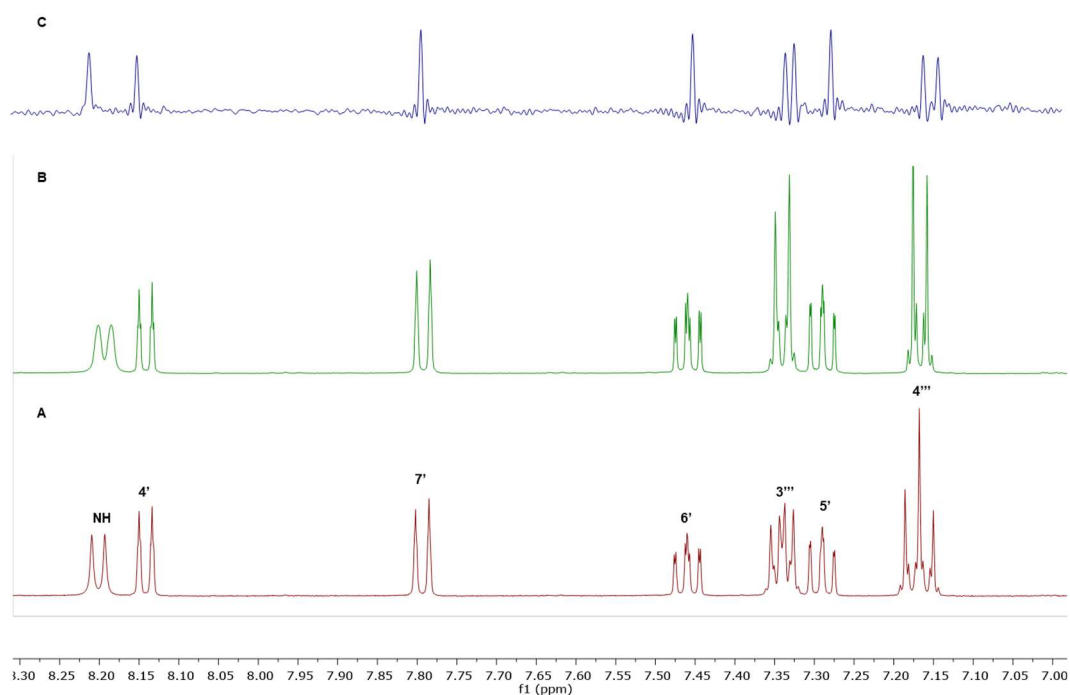
Figure 93. NMR stacked spectra of AMB-FUBINACA in DMSO-d$_6$

(A) ^{1}H NMR, (B) ^{19}F decoupled ^{1}H spectra, (C) PSYCHE pure shift spectra.

ortho-Coupling constant (*J*) of protons to fluorine in an aromatic system is typically 8.0 Hz as described by Williams and Fleming (6-11 Hz),[274] which can be seen in the coupling pattern of proton 4‴, an apparent triplet of *J* = 8.5 Hz as a result of *ortho*-coupling to 3‴ and also to F with an equal coupling constant. 3‴ necessarily has this *ortho*-coupling (8.5 Hz) to 4‴ with a 5.5 Hz 4-bond coupling to fluorine as can be seen in Figure 93A. Moreover, in the ^{19}F-decoupled ^{1}H NMR spectra (Figure 93B), where the fluorine coupling is removed, protons signals 3‴ and 4‴ both become non first-order signals with side bands resulting from the many energy levels in the AABB system.[274] The O2P (centre point of fluorine channel) must be well defined with the exact chemical shift of the fluorine atom (-113.98 ppm) to achieve optimum fluorine decoupling, and thus a simplification in the spectra. Pure shift NMR (in DMSO-d$_6$) resulted in removing all the H-H coupling leaving the fluorine coupling of 8.5 Hz for 4‴ and 5.5 Hz for 3‴ (Figure 93C).

Analysis of a prison sample (HMP15) containing a mixture of AMB-FUBINACA and 5F-ADB, using LC/ESI-MS/MS, resulted in base-line separation in the chromatogram using gradient 2, with molecular ion confirmation and a distinctive fragmentation pattern for each SCA in the mixture (Figure 94).
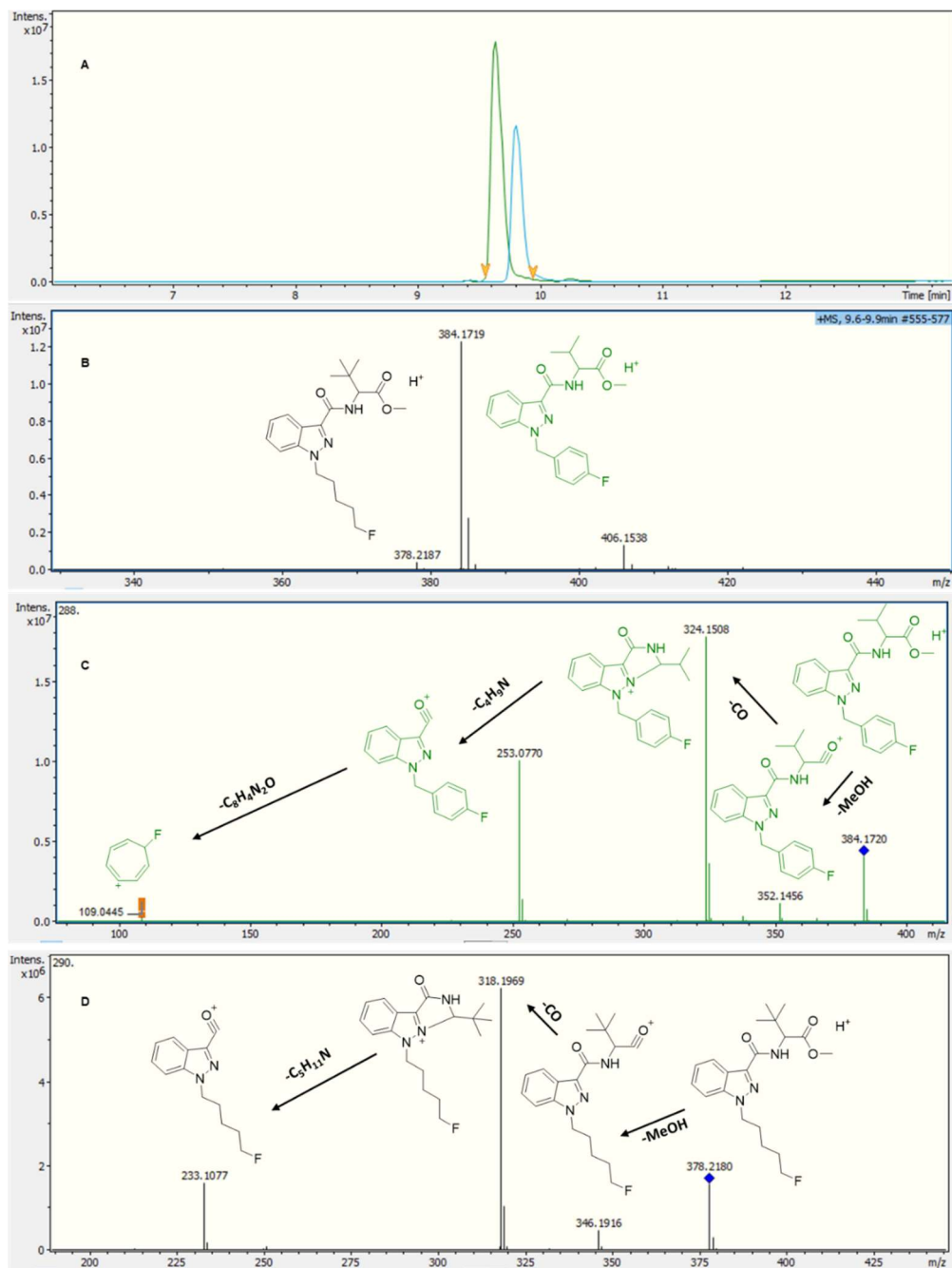
Figure 94. LC/ESI-MS/MS analysis of a mixture of a herbal blend containing AMB-FUBINACA and 5F-ADB showing (A) EIC with AMB-FUBINACA RT 9.6 min (green) and 5F-ADB 9.8 min (blue), (B) HRMS showing both molecular ions, proposed MS/MS fragmentation pattern assignments for (C) AMB-FUBINACA and (D) 5F-ADB.

LC/ESI/MS analysis resulted in AMB-FUBINACA RT 9.6 min found [M+H]$^+$ 384.1719 for $C_{21}H_{23}N_3O_3F$ requiring 384.1717, and 5F-ADB RT 9.8 min found [M+H]$^+$ 378.2187 for $C_{20}H_{29}N_3O_3F$ requiring 378.2187 (Figure 94 A and B). Collision Induced Dissociation (CID) using MS/MS resulted in a similar initial fragmentation pattern starting with the loss of methoxy from the [M+H]$^+$ and the subsequent loss of CO resulting in a base peak of 324.1508 for AMB-FUBINACA and 318.1969 for 5F-ADB (Figure 94 C and D). Both base peaks are the result of the interaction of the cation with indazole N2′ lone pair for the cyclization.[272] Another characteristic fragment in indazole based SCAs is the indazoleacylium ion,[266,272] with a 5-fluoropentyl tail at 233.1077 for 5F-ADB, and 253.0770 for AMB-FUBINACA with its 4-fluorobenzyl moiety. The latter also has the distinctive fluorotropylium ion $C_7H_6F^+$.[272] Pharmacological data are not available for 5F-ADB and AMB-FUBINACA, but similar analogues are found to have a binding affinity for CB_1 K_i = 0.78 nM for AB-CHMINACA (THC K_i = 40 nM) and EC_{50} between 0.24-1.8 nM for 5F-ADB-PINACA and AB-FUBINACA (THC EC_{50} = 170 nM).[78,275]

In this study, analysis of prison herbal blend samples revealed that SCAs are popular in this particular prison, with mixtures of potent SCA such as AMB-FUBINACA and 5F-ADB giving a high chance of intoxication even extending to the possibility of a lethal outcome. ESI-MS was used as the primary analytical tool for the fast qualitative analysis of prison samples. Full NMR characterization of AMB-FUBINACA has been presented above together with a detailed spectroscopic study of the effect of the fluorine of the 4-fluorobenzyl moiety on the ^{13}C and ^1H nuclei, the latter using a combination of a ^{19}F-decoupled ^1H experiment and pure shift NMR. LC/ESI-MS/MS characterization of a mixture of AMB-FUBINACA and 5F-ADB resulted in base-line resolution, molecular ion confirmation, and CID fragmentation assignment for both components. This is the first analytical study of the drug situation in an HMP that provides scientific data related to the growing trend of SCA use in UK prisons. It should aid drug analysts in monitoring the illicit drugs which are present.

4.3.3 2D DOSY NMR analysis of SCA mixtures in seized herbal blends

As seen in the previous two sections of this chapter, SCA in herbal blends exist in complex mixtures with multiple components such as other SCA, together with excipients such as propylene glycol and isopropyl alcohol, and matrix components from the carrier plant material. This results in complex spectra that require detailed analysis. DOSY NMR experiments rely on the diffusion rate to separate each component in the mixture, diffusion coefficient $D = log(m^2/s)$. Each D value depends on several compound specific, solvent, and instrumentation parameters such as molecular weight, shape, charge, viscosity and probe temperature.[276] In a typical DOSY experiment, the 2D experiment is preceded by several consecutive Pulse Field Gradient (PFG) Stimulated Spin Echo (STE) 1D experiments, followed by dispersion into the 2nd dimension where the horizontal axis shows the ^{1}H spectra and the vertical axis reveals the values of the diffusion coefficient. Ideally, this will result in all the chemical shift cross peaks of the same compound aligning, and the value of D is thus obtained.[276]

The first DOSY pulse sequence application was in 1965.[277] Ever since, there has been an expansion of the original pulse sequence into numerous DOSY experiments. The range of applications has widened now including the interactions of API and excipients and the analysis of counterfeit tablets.[278,279] Another application of 2D DOSY NMR on illicit drug samples was by Balayssac *et al*. in 2014,[280] who described the analytical separation of heroin and its adulterants/contaminants (caffeine, noscapine, acetylmorphine).

In this analysis, four seized brands containing SCAs were investigated using 2D DOSY NMR. Prior to the 2D DOSY experiments, the samples were profiled using 1D/2D NMR and LC/ESI-MS/MS. All the samples, HN Loc3, HN EXT2, HN EXT3, HN JOK5, were subjected to the same extraction conditions, where herbal blends (50.0 mg) were extracted with $CHCl_3$ (2 x 2.0 mL) with sonication, followed by filtration into a 25.0 mL round-bottom flask where the filtrate was evaporated. The residue was redissolved in $CDCl_3$ (1.0 mL) and transferred into an NMR tube for analysis. 2D DOSY NMR analysis of sample HN Loc3 revealed 3 resolved aligned cross-peaks (Figure 95).
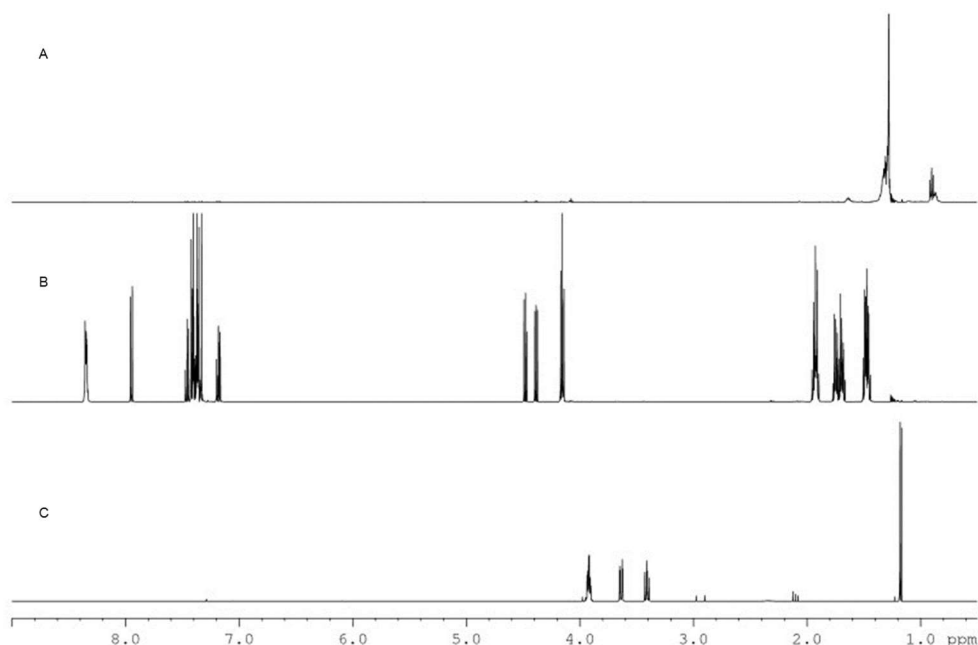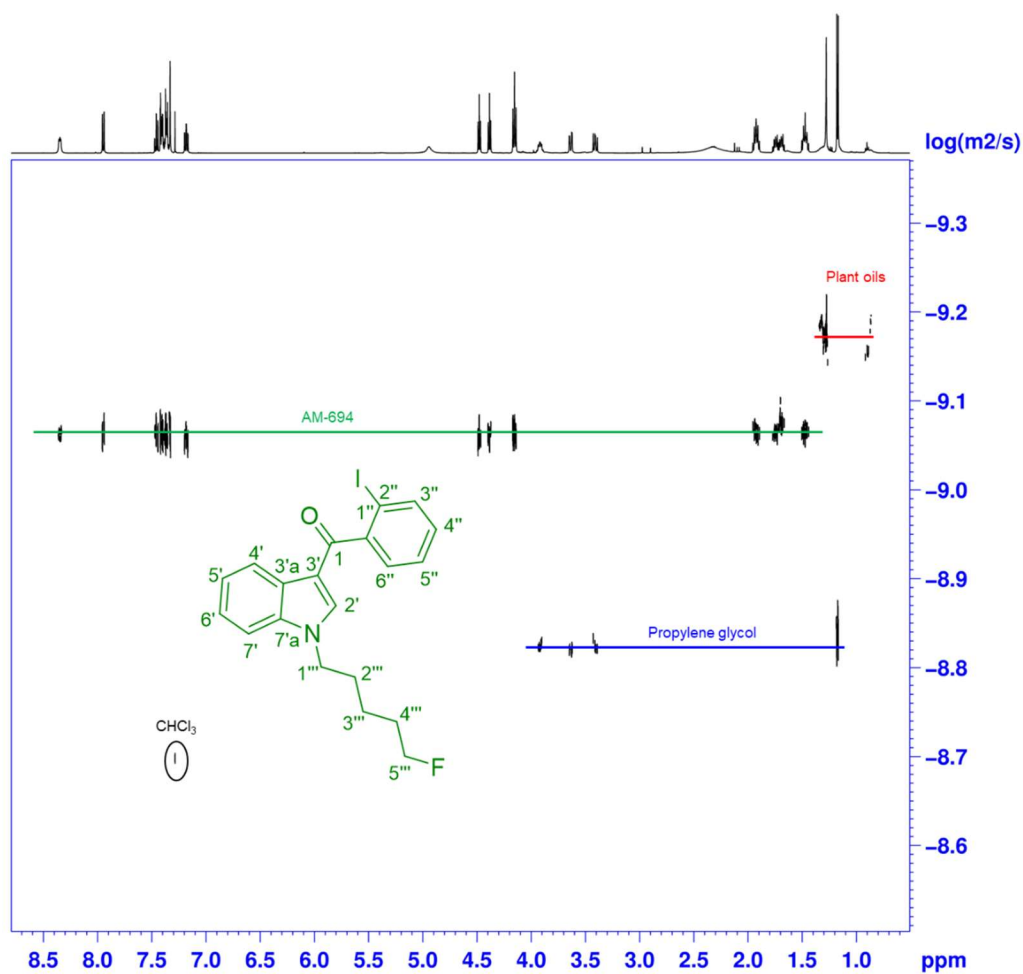
Figure 95. (Top) 2D DOSY NMR of HN Loc3 showing the alignment of the three components in the mixture, (bottom) extracted slices of 2D DOSY of the three components; (A) plant oils, (B) AM-694, (C) propylene glycol showing excellent separation by D.

2D DOSY revealed clear high-resolution separation of the 4 components in the sample, AM-694, propylene glycol, plant fatty acids, and the residual chloroform peak. Plant fatty acids signals at 0.88 and 1.25 ppm are the result of the extraction of the carrier material Damiana (*Turnera diffusa*) with $CHCl_3$. Propylene glycol has been added to the herbal blend during illicit manufacture to act as a vehicle in the delivery of SCA, where it is hygroscopic and lipophilic and helps in producing thicker smoke.[263] The diffusion coefficient is inversely proportional to the molecular weight of the compound, solvents with small molecular weights resulted in high diffusion coefficients. Propylene glycol resulted in a diffusion coefficient D value of -8.82 $\log(m^2/s)$ with all peaks aligned. Similar alignment was observed for all the peaks of the SCA present in the sample AM-694 D -9.06 $\log(m^2/s)$, and the lowest D value of -9.17 $\log(m^2/s)$ is for the plant oil lipid-chain signals These are presumably C16 and C18 chain and therefore the heaviest molecules. Furthermore, analysis of 4 additional samples of the same brand (HN Loc1, 2, 4 and 5) revealed a similar composition.

DOSY analysis of sample HN EXT2 and HN EXT3 resulted in a similar outcome in terms of separation, but the type of SCA was different in each of the packages. In HN EXT2, AB-CHMINACA was present, D value -9.14 $\log(m^2/s)$, on the other hand in sample HN EXT3, 5F-PB-22 was detected, D value of -9.23 $\log(m^2/s)$. 2D DOSY confirmed the 1D/2D NMR (^1H, ^{13}C, HSQC, HMBC) qualitative differences between packs of the same brand (Extinction), where the 2016 seized samples contained AB-CHMINACA. However, the 2017 seizures contained 5F-PB-22. Sample HN JOK5 was analysed by 2D DOSY. Preliminary 1D/2D NMR analysis revealed the presence of 5F-ADB, and its indole isopropyl analogue MMB-2201. 2D-DOSY revealed the 2 components along with propylene glycol and plant oils (Figure 96 A). The two SCAs are only 15 g/mol apart, making the cross peaks separation in the 2 D-DOSY spectra less obvious compared to the previous samples. However, expansion of the area between 0.6-4.0 ppm showed different alignments of the signals which can be seen in the methyl ester signals of both compounds, with *tert*-butyl for 5F-ADB, and with isopropyl in the case of MMB-2201 which has a slightly higher D value -9.09 $\log(m^2/s)$ compared to the 5F-ADB D value of -9.12 $\log(m^2/s)$ (Figure 96 B).
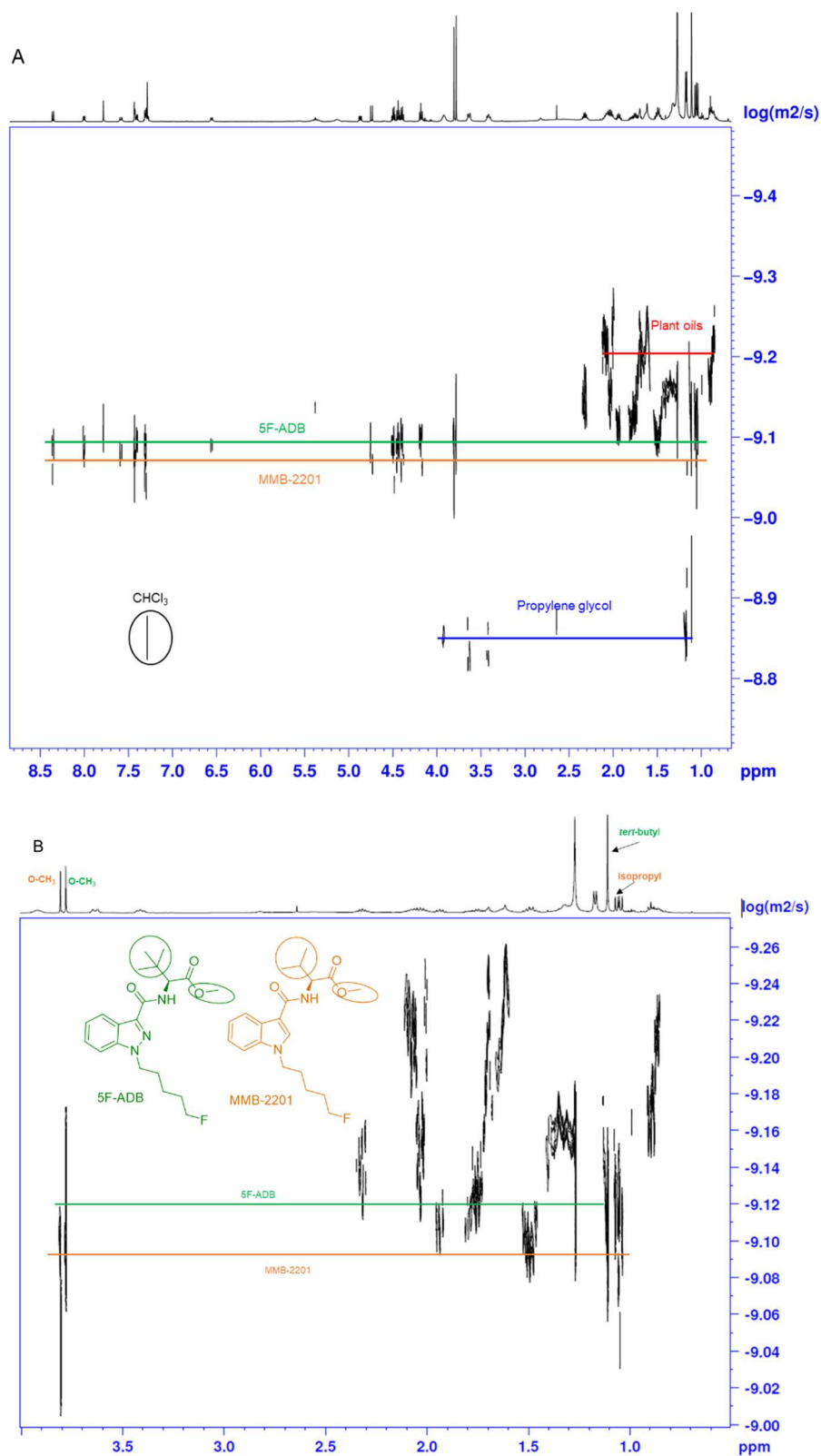
Figure 96. (A) 2D DOSY NMR of sample HN Jok5 showing alignment of the 4 components,

(B) expansion of 2D DOSY showing the alignment of the cross peak of a methyl ester (at

3.75 ppm) with the *tert*-butyl of 5F-ADB, and of a different methyl ester (at 3.81 ppm) with

the isopropyl of MMB-2201.

2D-DOSY allowed the separation of the composition of different herbal blends containing SCAs, based on their diffusion coefficient. Samples HN Loc3, Ext2 and Ext3 showed good separation for all the components present, AM-694, AB-CHMINACA, and 5F-PB-22 respectively and the excipient present (propylene glycol), and extraction by-products (plant oils). However, sample HN JOK5 containing similar SCAs, 5F-ADB and MMB-2201, cannot be definitively separated due to their close molecular weights 377.5 and 362.5 Da respectively, and due to their similar shape. Similar findings were reported by Balayssac *et al*.[280] where heroin and noscapine could not be separated by 2D-DOSY. Even so, the herbal blend samples were characterized by 1D/2D NMR (^{1}H, ^{13}C, HSQC, HMBC), additional corroboration and enhanced resolution were achieved by dispersing the signal into the second dimension in the 2D-DOSY experiment (Figures 95 and 96). Taken together, this resulted in the improved profiling of impurities in these complex mixtures.

4.3.4 Chemical characterization and separation of the contents of K2 herbal blends complex samples

Ever since the first samples of herbal blend containing SCA hit the streets in the form of dubious brands such as "K2" and "spice" in 2008,[80] the K2 and spice brand names have become the definition of the SCA category used by manufacturers, users, law enforcement agencies and drug analysts. The first generation SCA found in the earlier "K2" brand (CP 47,497 and JWH-018) are no longer found. Rather, they have been replaced with 2nd and 3rd generation indoles and indazoles with different tail and head-component modifications. Herbal blend samples with more than one SCA present are not unheard of. Reports of the JWH (John W. Huffman) and AM (Alexander Makriyannis) series of 3-component mixtures were reported in 2012 following analysis by chromatography and MS (Figure 97).[281] Logan *et al*.[282] analysed the contents of herbal blends seized in the USA using GC and LC/MS and found that the "K2" blend contained different analogues of the JWH series in 3-component mixtures (Figure 97) based around 3-(*N*-alkylindolyl)-1-naphthyl ketone.
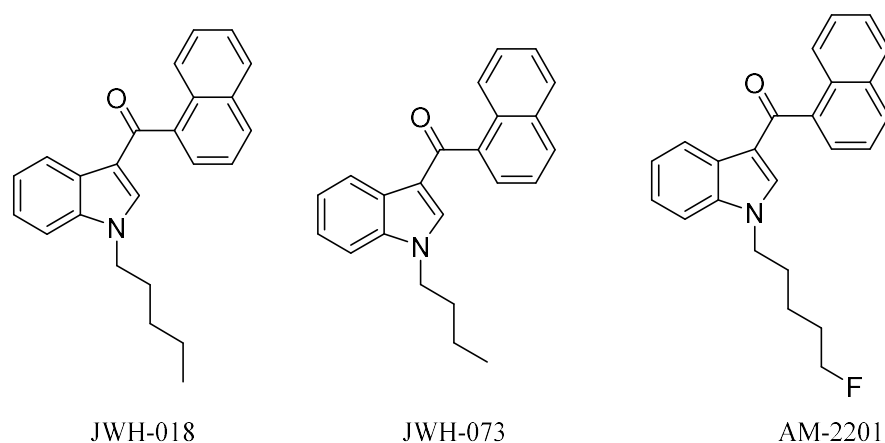
Figure 97. JWH and AM series SCA that were in "K2" samples between 2008-2013.

Nowadays, both the 1st and 2nd generation SCAs have been replaced with carboxamide indoles and indazoles, and recently a methyl ester was found to replace the primary amide. The current analogues of the 2nd and 3rd generations are in most cases fluorinated. The presence of multiple amides in their structures makes them more polar than the JWH or the AM series, thus requiring alternative methods for separation and analytical characterization. Separation of analogues of the CP and JWH series of SCAs was performed by Reverse Phase (RP) flash column chromatography.[283] In this study, an analytical platform for the detection, separation and characterization of closely related 3rd generation SCAs in six-component mixtures is described. These "K2" samples include a possible reaction impurity (Figure 98). Analysis used combination of UHPLC/ESI-MS/MS, flash column chromatography, and 2D NMR spectroscopy.

The contents of herbal blend K2 analysed by LC/TOF-ESI-MS revealed six base-line resolved peaks on the chromatogram (Figure 99). Five of them are SCA and one, **2** PX1 acid, is a possible reaction precursor for the synthesis of the amide **1** (Figure 98). All mass ions detected in the TOF are within 2.0 ppm mass accuracy (Table 19). Additionally, the ^{13}C isotopomer of **6** (385.2481) is within 2.3 ppm of **5** $[M+H]^+$ of 385.2490 resulting in a repeating overlapping peak at 7.5 min in the EIC, due to the software not being able to differentiate between them. The presence of hydrophobic components, e.g. cyclohexylmethyl in **5** and

adamantyl in **6**, caused them to be retained longer on the column compared to the other components in the mixture (Figure 99).

PX-1

1

PX-1 acid

2

5F-PB-22

3

5F-ADB

4

MDMB-CHMICA

5

5F-AKB48

6
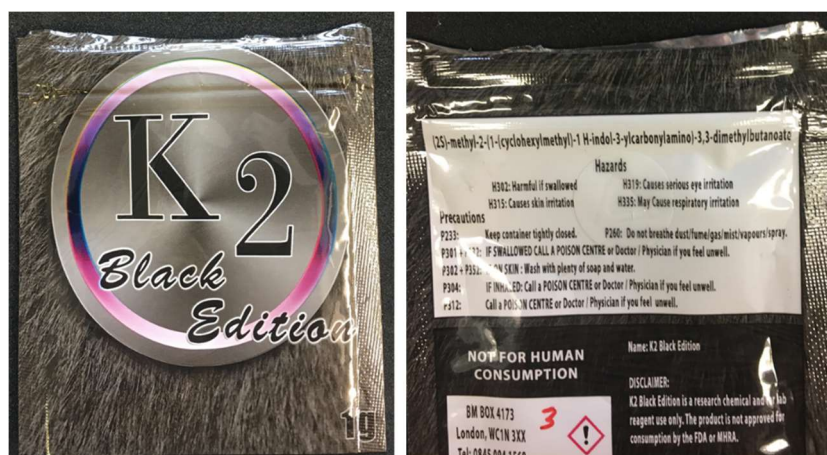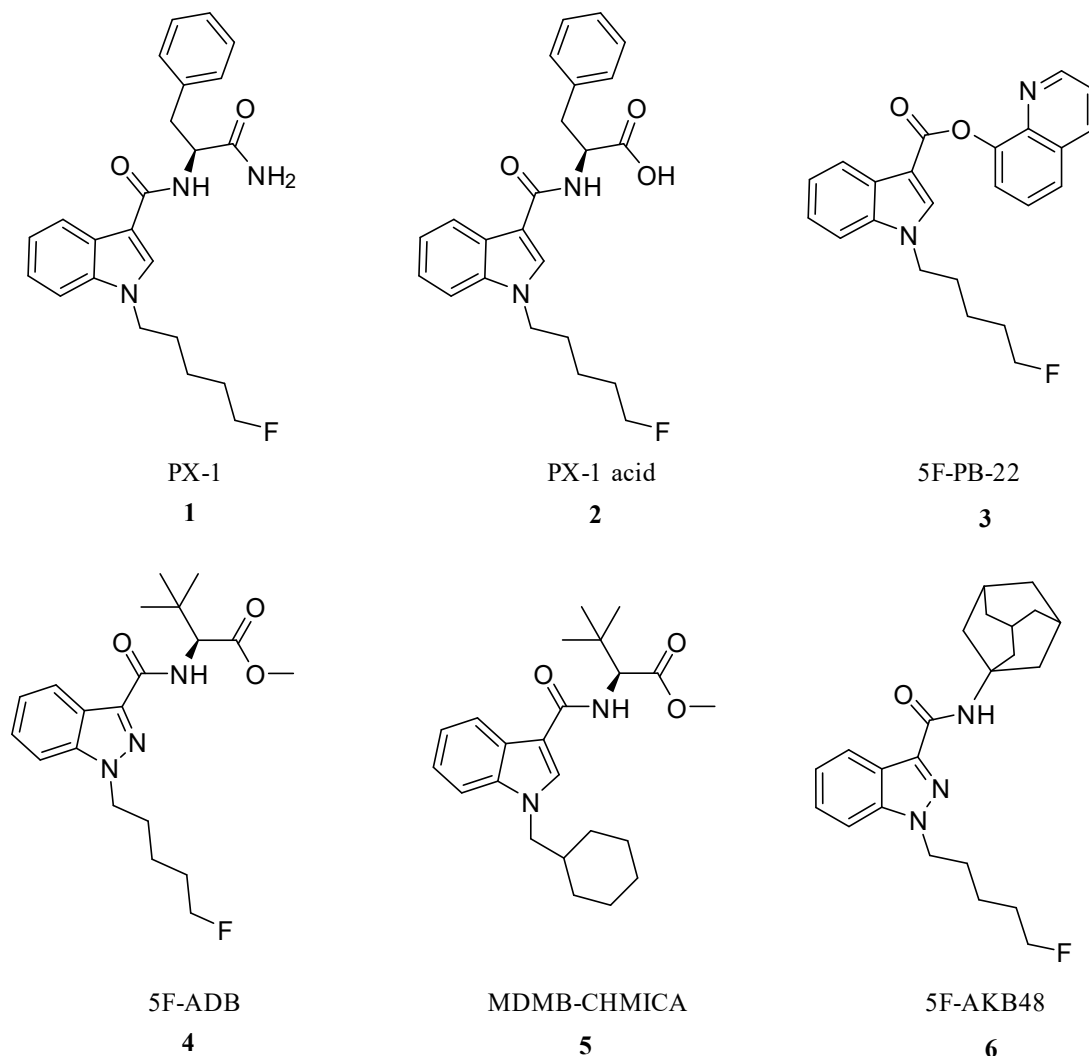
Figure 98. (Top) SCAs found in K2 herbal blend, (bottom) K2 herbal blend package accurately labelled to contain MDMB-CHMICA (2*S*)-methyl-2-(1-(cyclohexylmethyl)-1H-indole-3-carbonylamino)-3,3-dimethylbutanoate.
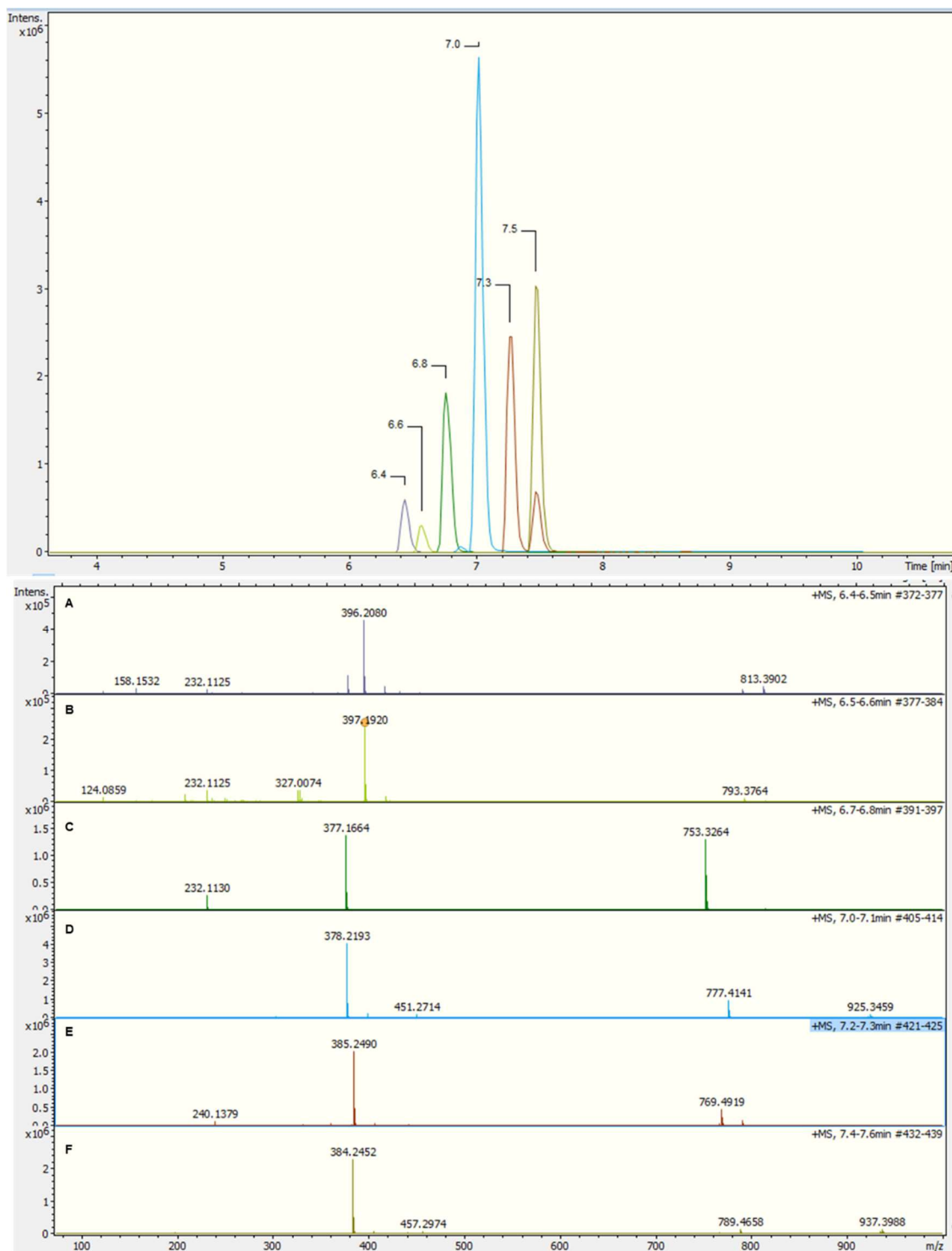
Figure 99. (Top) EIC of K2 mixture analysis separating the six components **1-6**, compound **1** RT 6.4 min, **2** RT 6.6 min, **3** RT 6.8 min, **4** RT 7.0 min, **5** RT 7.3 min, **6** RT 7.5 min, (bottom) ESI-MS spectrum showing molecular ions in the form of [M+H]⁺, protonated and [M+Na]⁺ dimers of compounds (A) **1**, (B) **2**, (C) **3**, (D) **4**, (E) **5**, (F) **6**.

Table 19. LC/ESI-MS data of compounds **1-6** in "K2" herbal blend.

Compound	Molecular formula	RT (min)	Measured m/z (found)	Theoretical m/z (required)	Error (ppm)
1	$C_{23}H_{26}FN_3O_2$	6.4	396.2080	396.2081	-0.25
2	$C_{23}H_{25}FN_2O_3$	6.6	397.1920	397.1922	-0.50
3	$C_{23}H_{21}FN_2O_2$	6.8	377.1664	377.1659	1.32
4	$C_{20}H_{28}FN_3O_3$	7.0	378.2193	378.2187	1.58
5	$C_{23}H_{32}N_2O_3$	7.3	385.2490	385.2485	1.29
6	$C_{23}H_{30}FN_3O$	7.5	384.2452	384.2445	1.82

Furthermore, the 50-1000 m/z scan range allowed the detection of: sodiated dimer of **1** $[2M+Na]^+$ at 813.3902 for $C_{46}H_{52}F_2N_6O_4Na$ requires 813.3910, protonated dimer of **2** $[2M+H]^+$ at 793.3764 for $C_{46}H_{51}F_2N_4O_6$ requires 793.3771, protonated dimer $[2M+H]^+$ of **3** at 753.3264 for $C_{46}H_{43}F_2N_4O_4$ requires 753.3246, sodiated dimer of **4** $[2M+Na]^+$ at 777.4141 for $C_{40}H_{56}F_2N_6O_6Na$ requires 777.4121, protonated dimer of **5** $[2M+H]^+$ at 769.4919 for $C_{46}H_{65}N_4O_6$ requires 769.4898, and sodiated dimer of **6** $[2M+Na]^+$ at 789.4658 for $C_{46}H_{60}F_2N_6O_6Na$ requires 789.4638 (Figure 99).

LC/MS/MS showed a unique fragmentation pattern for each component in the mixture providing valuable structural information. Amide **1** and its corresponding carboxylic acid **2** exhibited similar fragmentation patterns. In amide **1**, the 379 m/z fragment results from the loss of ammonia (-17 Da) from the molecular ion, and in carboxylic acid **2**, the 379 m/z fragment results from the loss of water (-18 Da). The 144 m/z fragment is the formation of an indoleacylium ion (Figure 100 A, B). In compound **3**, the loss of the 8-quinolinyl ester from 5F-PB-22 provided a diagnostic MS signature (fragment at 144 m/z). Additionally, all terminally fluorinated pentyl indoles (**1**, **2**, and **3**) formed 232 m/z base-peak fragments that correspond to the indoleacylium ion with the 5-fluoropentyl side chain resulting from C-N cleavage at the secondary amide in **1** and **2**, and acyl cleavage at the 8-quinolinyl ester in **3** (Figure 100 A-C).
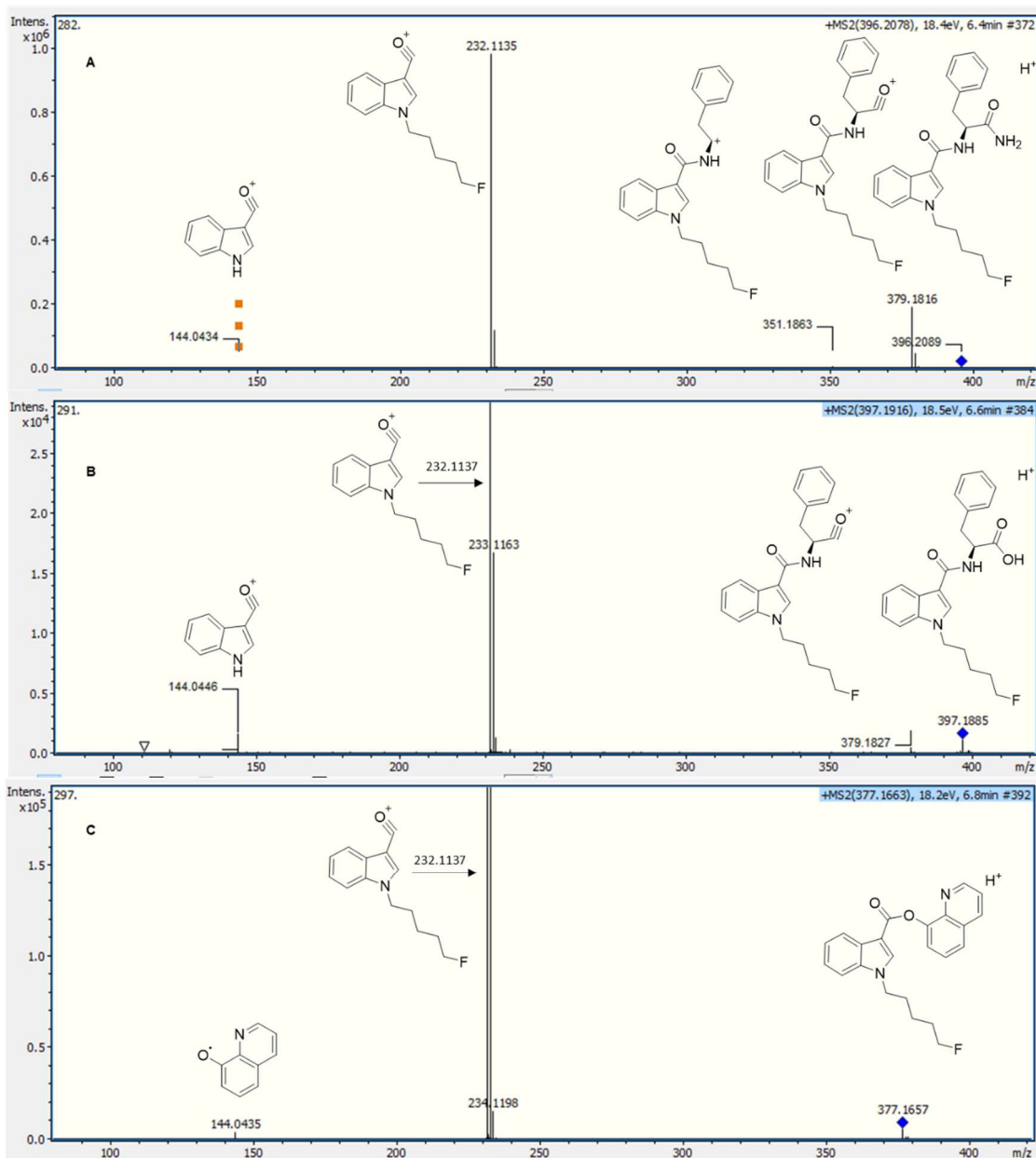
Figure 100. MS/MS proposed fragmentation and assignments of (A) amide **1**, (B) acid **2**, (C) ester **3**.

A characteristic base-peak fragment for compounds **4** and **6** is 233 m/z indazoleacylium ion with 5-fluoropentyl side chain, which helps to differentiate fluorinated SCA with 3-carbonyindazole from the indoles (Figure 101 A and C). Moreover, compound **4** 318 m/z fragment is the result of the lone pair of N2′ of the indazole interacting with the formed cation, as seen in AMB-FUBINACA (Figure 94) and AB-CHMINACA (Figure 83). Compound **5** resulted in the formation of the most prominent ion at 240.1387 resulting from

the indoleacylium ion with a cyclohexylmethyl substituent (Figure 101 B). Compound **6**

MS/MS profile showed a distinctive adamantyl loss at 135.1157 m/z (Figure 101 C). MS/MS

data for compounds **3**,[272,284] **4**,[272] **5**,[266] **6**,[266] were corroborated by comparison with their

respective literature. No ESI-MS/MS data are reported in the literature for compounds **1** and

2, although compound **1** has some GC/MS data in a SWGDRUG monograph.[285]
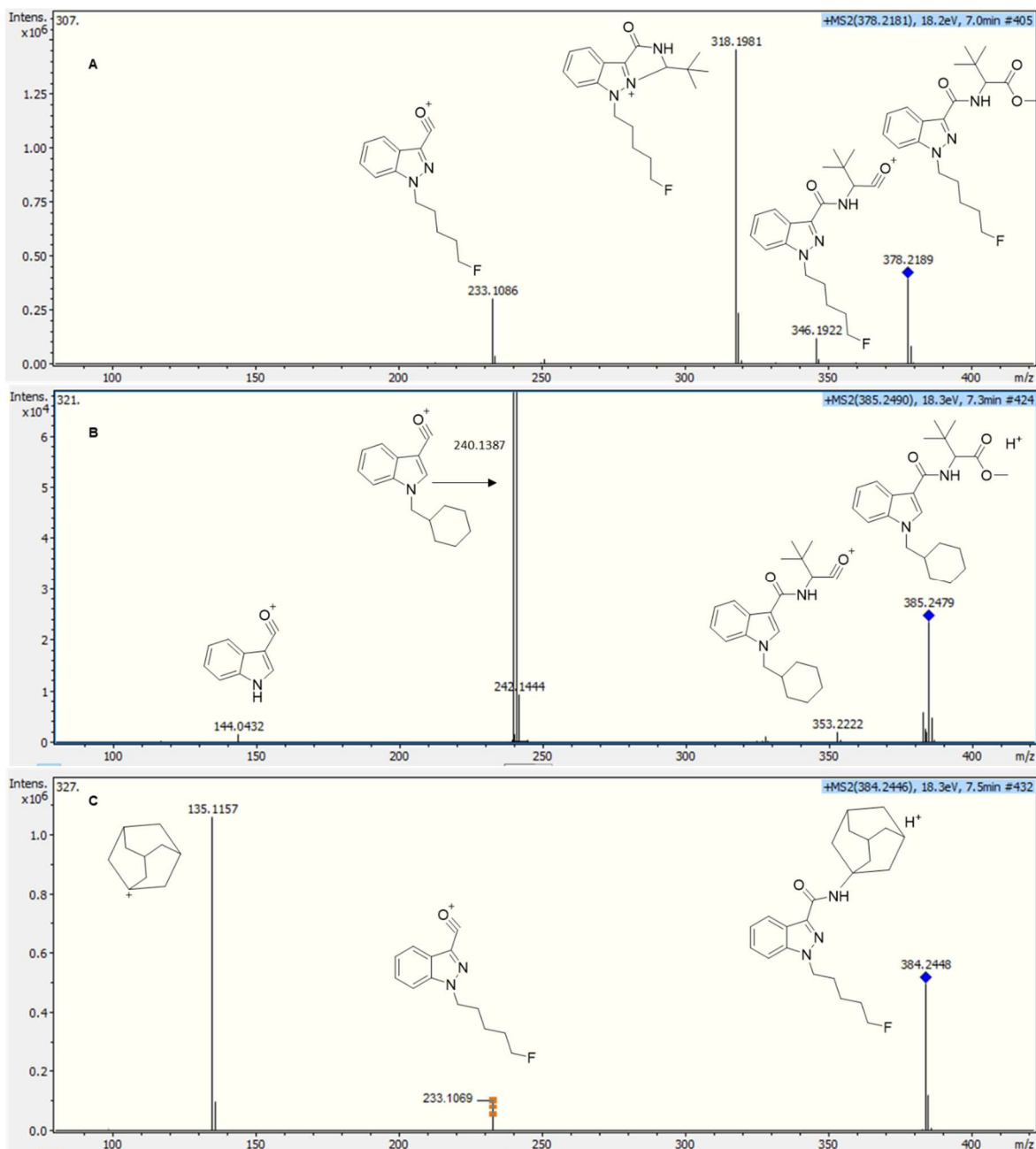
Figure 101. MS/MS proposed fragmentation and assignments of (A) indazole-ester **4**,

(B) indole-ester **5**, (C) indazole-*N*-adamantyl amide **6**.
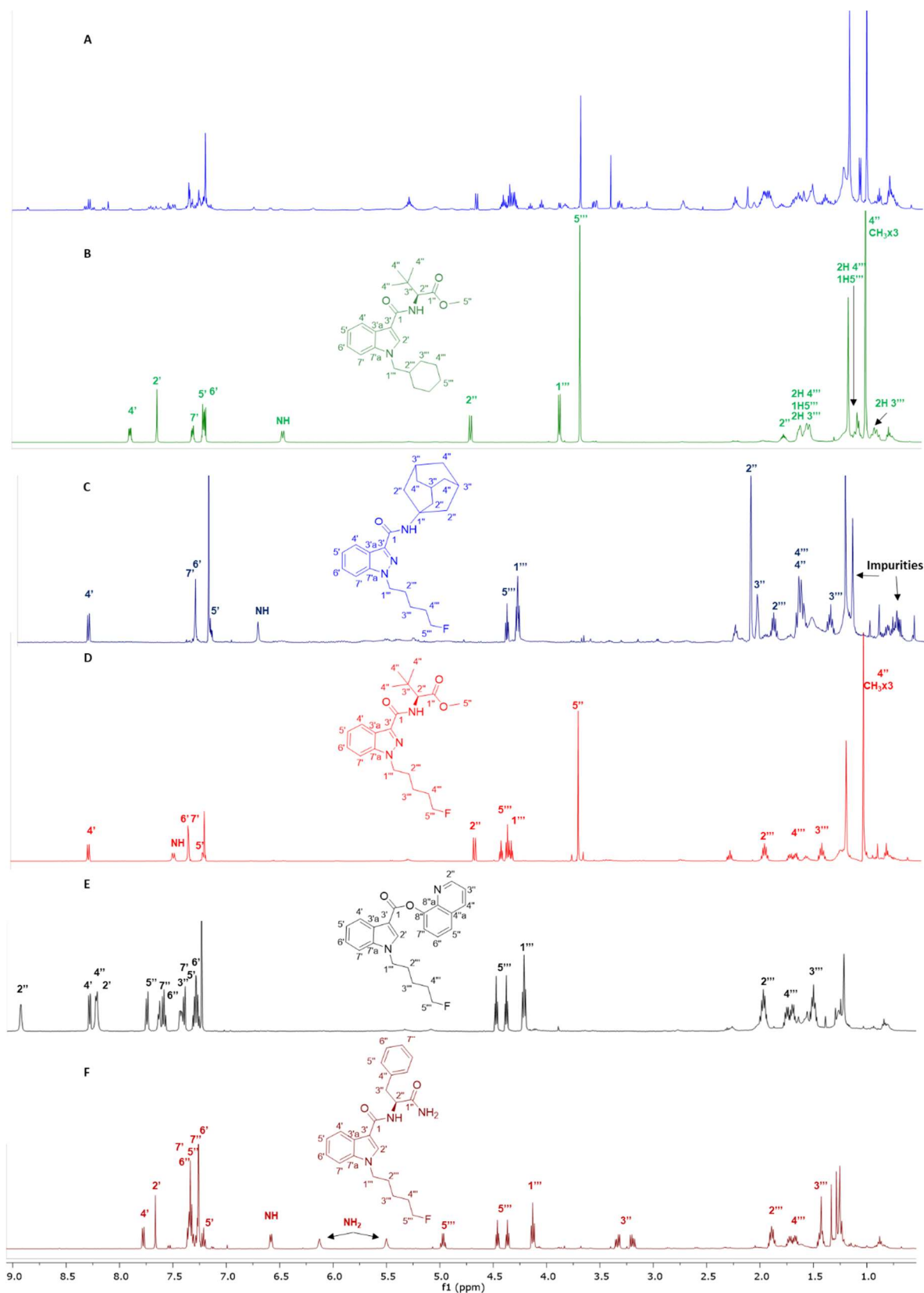
Figure 102. ^{1}H NMR in CDCl$_3$ stacked spectra of "K2":

(A) crude extract, (B) **5**, (C) **6**, (D) **4**, (E) **3**, (F) **1**.

1D/2D NMR of the crude extract (Figure 102A), resulted in complex ^{1}H NMR spectra, especially in the area of the spectra between 0.9-2.0 ppm and 4.0-4.5 due to the presence of the 5-fluoropentyl in 4 of the compounds in the mixture. The ^{19}F proton-coupled NMR spectrum revealed overlapping signals between -218 and -220 ppm, and inverse gated decoupled spectra revealed three signals in the range of the fluoropentyl signal. Nevertheless, candidate signals for integration in the ^{1}H NMR were identified for each compound, and used to calculate the molar ratio of each component in the herbal blend in one sample. These were for compound **1** using methylene protons at position 3″ 11%, compound **3** using the quinoline signal 2″ 6%, compound **4** using chiral centre signal 2″ 23%, for compound **5** using the indole 4′ signal and chiral centre signal at 2″ 7%, for compound **6** the indazole 4′ signal 9%. Moreover, the major component was propylene glycol 44%, possibly added as a vehicle for the vaporization of the SCA. However, compound **2** could not be detected by NMR as it was most likely in a concentration lower than the Lower Limit of Detection (LLOD) of the 500 MHz NMR instrument. Some of the analysed "K2" packages contained no propylene glycol.

Flash column chromatography was employed for the separation of each of the detectable components using hexane/ethyl acetate as the mobile phase. Gradient 1 allowed the separation of components, except compounds **4** and **5**. Compound **1** was separated in small amounts (~5.0 mg). Another sample was subjected to the same extraction procedure followed by flash column chromatography using gradient 2 (flow rate 22 mL/min), which allowed the separation of compounds **4** and **5**, ^{1}H NMR spectra are shown in Figure 102. Flash column chromatography has been previously applied to the isolation of SCA from herbal materials,[283] but no separation of a closely related complex mixture has been reported. For PX1 (acid and amide), no assignment data have been found in the literature from detailed searches using Web of Science and Scifinder, only a SWGDRUG monograph with no spectroscopic assignments.[285] PX1 (compound **1**) proton 5″ had NOE contact with 3″ methylene protons and 2″ methine of the phenylalanine amide moiety. Furthermore, 2″ had NOE contact with the two protons of the primary amide, and 5″ carbon resulted in a 3-bond HMBC connectivity with methylene 3″ diastereotopic protons (Table 20).

PX-1 **1**   - - - ▸ 2D NOESY   5F-PB-22 **3**
                    ──── ▸ HMBC
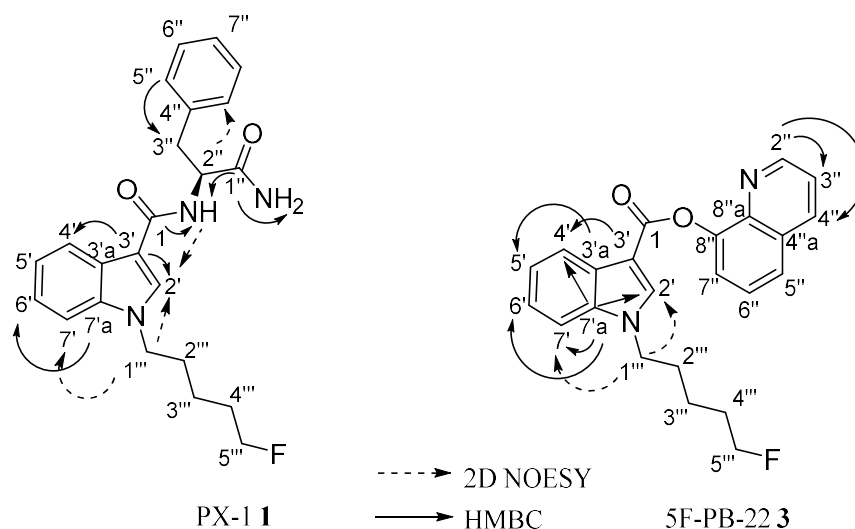
Table 20 NMR data of compounds **1** and **3** in CDCl₃.

Position	PX-1 1		5F-PB-22 3	
	¹³C	¹H/¹⁹F	¹³C	¹H/¹⁹F
1	165.1	-	163.1	-
2′	131.6	7.67 1H, s	135.7	8.16-8.18 1H, s overlapped with 4″
3′	110.1	-	106.0	-
3′a	125.4	-	127.4	-
4′	120.3	7.78 1H, dd (7.5, 1.0)	122.1	8.24 1H, dd (7.5, 2.0)
5′	121.6	7.21 1H, td (7.5, 1.0)	123.0	7.21-7.28 1H, m
6′	122.7	7.23-7.30 1H, m overlapped	122.2	7.21-7.28 1H, m
7′	110.2	7.35 1H, overlapped	109.9	7.35 1H, d (8.0)
7′a	136.5	-	136.7	-
1″	173.6	-	-	-
2″	54.0	4.97 1H, d (7.5)	150.3	8.88 1H, dd (4.5, 1.5)
3″	38.2	3.19 1H, dd (14.0, 7.5) 3.34 1H, dd (14.0, 6.5)	121.6	7.38 1H, dd (8.0, 4.5)
4″	136.8	-	136.3	8.16-8.18 1H, m overlapped with 2′
4″a	-	-	129.6	-
5″	129.5	7.31-7.35 1H, m overlapped	125.5	7.70 1H, d (8.0)
6″	128.8	7.31-7.35 1H, m overlapped	126.5	7.54 1H, t (8.0)
7″	127.1	7.23-7.30 1H, m overlapped	122.3	7.59 1H, d (8.0)
8″	-	-	147.5	-
8″a	-	-	140.2	-
1‴	46.6	4.13 2H, t (7.0)	47.1	4.18 2H, t (7.0)
2‴	29.6	1.90 2H, quintet (7.0)	29.8, d ($^4J_{CF}$ 2.7)	1.94 2H, quintet (7.0)
3‴	22.7, d ($^3J_{CF}$ 6.5)	1.39-1.47 2H, m	22.8, d ($^3J_{CF}$ 5.0)	1.43-1.5 2H, m
4‴	29.8, d ($^2J_{CF}$ 24.0)	1.70 2H, d quintets (26.0, 6.0)	30.0, d ($^2J_{CF}$ 20.0)	1.70 2H, d quintets (27.0, 6.0)
5‴	83.5, d ($^1J_{CF}$ 165.5)	4.41 2H, dt (47.0, 6.0)	83.6, d ($^1J_{CF}$ 164.5)	4.39 2H, dt (47.5, 6.0)
F (5‴)	-	-218.54, tt ($^2J_{HF}$ 47.0, $^3J_{HF}$ 26.0)	-	-218.54, tt ($^2J_{HF}$ 47.5, $^3J_{HF}$ 27.0)
NH	-	6.56 1H, d (7.5)	-	-
NH₂	-	5.46 1H, br s, 6.10 1H, br s	-	-

Similar spectroscopic findings to other SCAs with a 5-fluoropentyl moiety are seen in compound **1**, such as the 5‴ methylene at 4.41 ppm with a large 2-bond alkyl fluoride coupling $^2J_{HF}$ of 44.5 Hz and 3-bond coupling $^3J_{HF}$ to 4‴ of 26.0 Hz, 1‴ methylene triplet at 4.13 ppm, in addition to methylenes of 2‴, 3‴ and 4‴ (Figure 103). For compound **3**, assignment of the 5-fluoropentyl tail is similar to that in compound **1** and other fluoroalkyl analogues.
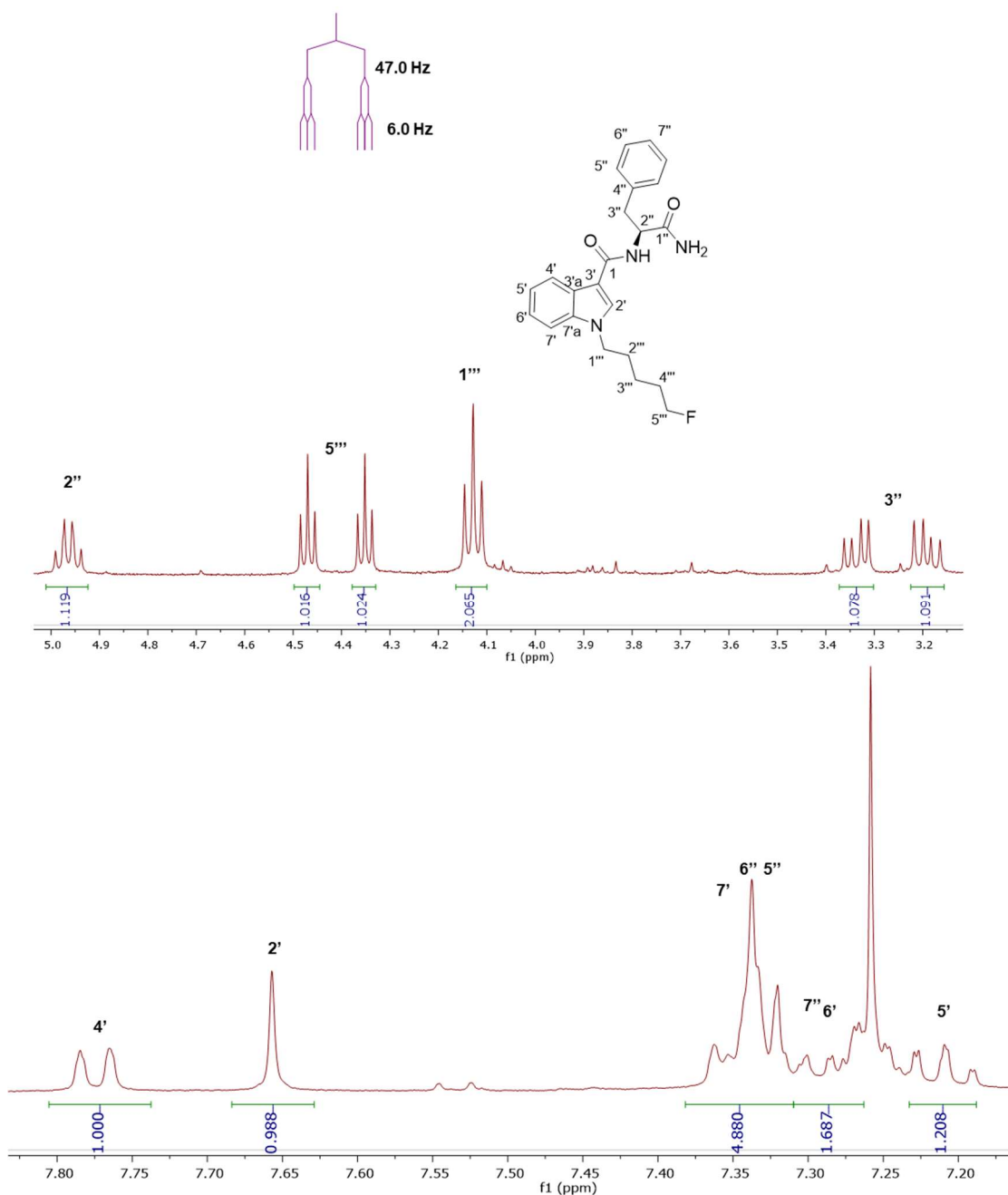
Figure 103. ^{1}H NMR (in CDCl$_3$) of compound **1** assignments with expansions of (top) 3.2-5.0 ppm, (bottom) 7.2-7.8 ppm aromatic region.

The presence of the 8-quinolinyl aromatic system resulted in a complex aromatic region. Proton 2″ of the quinoline ring at 8.88 ppm was the most downfield signal due to the electronegativity of the N heteroatom. There were also smaller *ortho-* and *meta*-coupling constants 4.5, 1.5 Hz respectively. Moreover, overlapping protons of indole (2′) and quinoline (4″) resulted in a multiplet at 8.16-8.18. A multiplet at 7.21-7.28 is the result of indole protons 5′ and 6′ overlapping (Table 20 and Figure 104). Furthermore, HMBC connectivity of C2″ at 150.3 ppm to 3″ and 4″, and 2D NOESY contact of 1‴ to indole protons (2′) and (7′) helped in assigning multiplets, thus obtaining an unambiguous confirmation of the structure.[284]
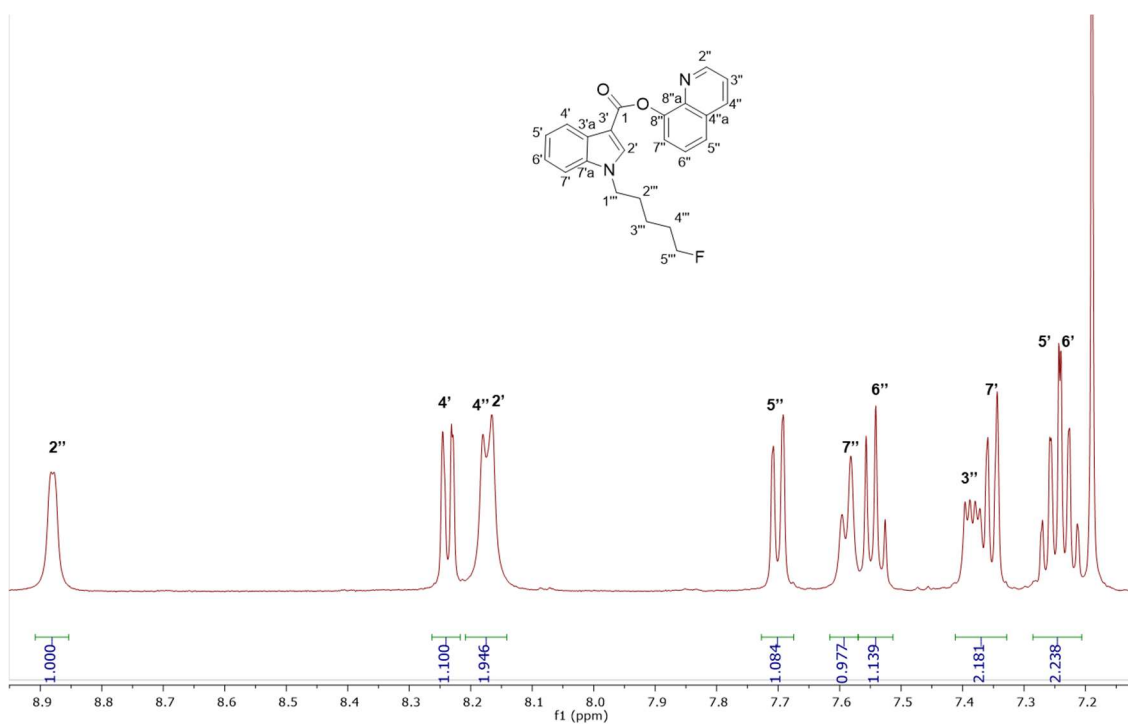
Figure 104. ^{1}H NMR of compound **3** aromatic region expansion with assigned protons.

Confirmation of the proposed structures of compounds **4** and **5** was established using 1D/2D NMR and comparison with the literature (Table 21).[266,272,286] Both compounds belong to the recent methoxycarbonyl alkyl analogues that replaced the carboxamide. Compounds **4** and **5** both possess a *tert*-butyl group giving a 9H proton singlet ~1.0 ppm, and the chiral centre proton 2″ at ~4.7 ppm, in addition to the methoxy group at ~3.8 ppm.
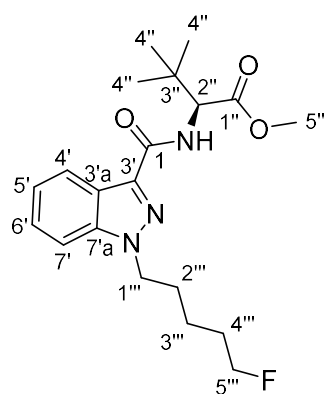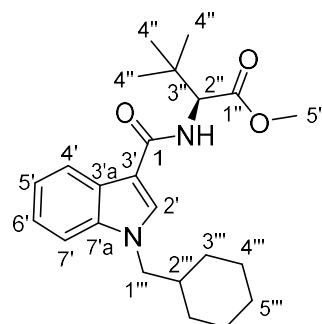
5F-ADB **4**   MDMB-CHMICA **5**

Table 21. NMR data of compounds **4** and **5** in CDCl₃.

Position	5F-ADB 4 ^{13}C	5F-ADB 4 ^{1}H/^{19}F	MDMB-CHMICA 5 ^{13}C	MDMB-CHMICA 5 ^{1}H/^{19}F
1	162.3	-	164.8	-
1″	172.2	-	172.7	-
2″	59.5	4.73 1H, d (9.5)	59.7	4.78 1H, d (9.0)
3″	35.0	-	35.1	-
4″	26.7	1.08 9H, s	26.8	1.10 9H, s
5″	51.8	3.75 3H, s	51.8	3.78 3H, s
2′	-	-	132.7	7.72 1H, s
3′	136.8	-	110.3	-
3′a	122.9	-	125.2	-
4′	122.8	8.34 1H, d (8.0)	119.9	7.97-8.00 1H, m
5′	122.6	7.24-7.26 1H, m overlapped with CHCl₃	122.4	7.26-7.29 1H, overlapped with 6′
6′	126.8	7.39-7.40 1H, m overlapped with 7′	121.6	7.26-7.29 1H, overlapped with 5′
7′	109.1	7.39-7.40 1H, m overlapped with 6′	110.7	7.36-7.40 1H, m
7′a	140.8	-	137.0	-
1‴	49.2	4.40 2H, t (7.0)	53.8	3.94 2H, d (7.0)
2‴	29.3	2.00 2H, quintet (7.0)	38.5	1.85 1H, ttt (11.5, 7.0, 3.5)
3‴	22.7, d ($^3J_{CF}$ 5.5)	1.43-1.49 2H, m	30.97, 30.99	0.94-1.03 2H, m, 1.58-1.67 2H, m
4‴	29.9, d ($^2J_{CF}$ 19.5)	1.76 2H, d quintet (26.5, 6.0)	25.6	1.12-1.21 2H, m, 1.59-1.71 2H, m
5‴	83.7, d ($^1J_{CF}$ 165.0)	4.42 2H, dt ($^2J_{HF}$ 47.0, $^3J_{HH}$ 6.0)	26.2	1.12-1.21 1H, m, 1.58-1.67 1H, m
5‴-F	-	-218.6 tt ($^2J_{HF}$ 47.0, $^3J_{HF}$ 26.5)	-	-
NH	-	7.54 1H, d (9.5)	-	6.56 1H, d (9.0)

Indazole **4** has a 4 proton aromatic system (Figure 105), on the other hand **5** has the 5 proton aromatic system of the mono-substituted indole. In the ^{13}C spectra, differentiation between indazole and indole analogues can easily be achieved by comparison of the 3′ carbon chemical shift, where in **4** the electron withdrawing effect of the second nitrogen in the indazole ring on 3′ causes it to resonate at 136.8 ppm compared to 110.3 ppm in indole **5**, a significantly higher (downfield) chemical shift.
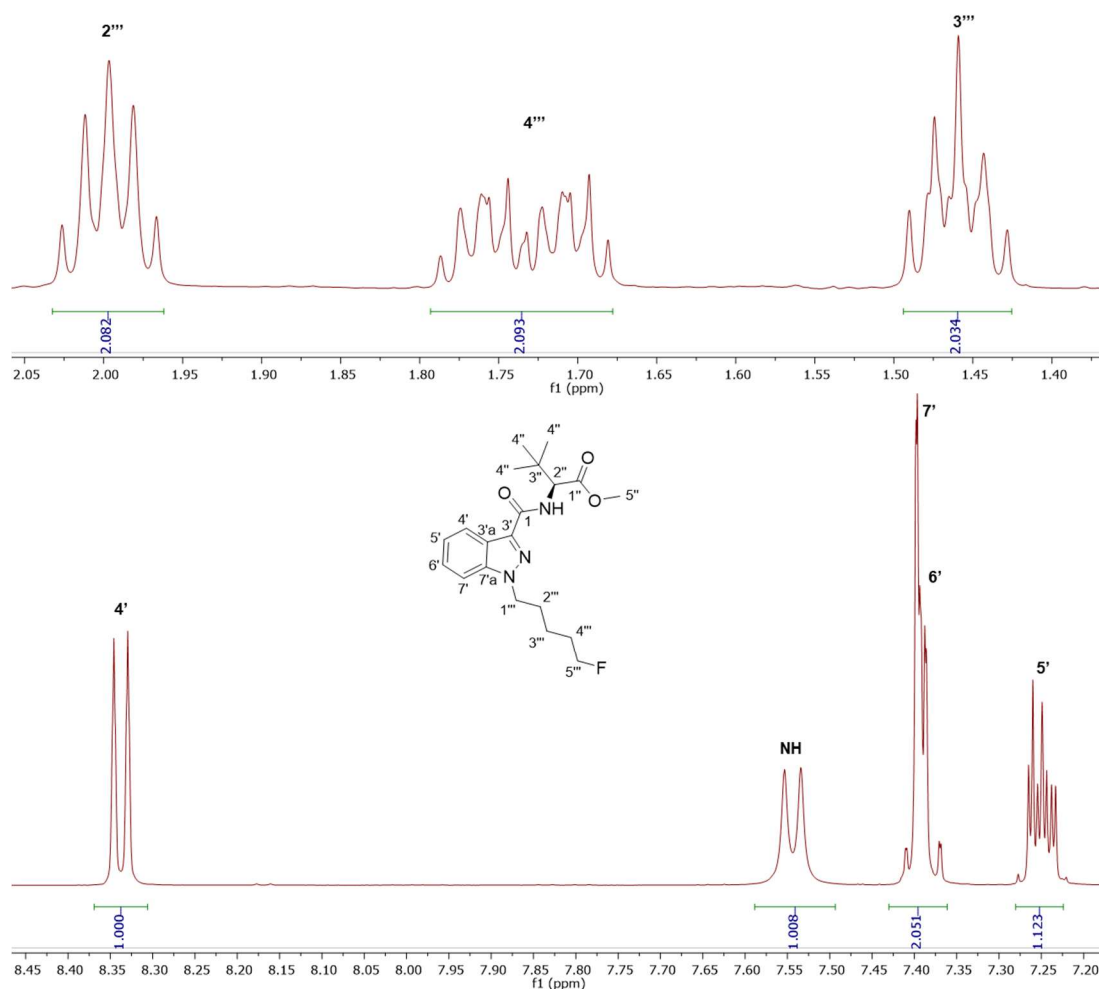
Figure 105. Compound **4** [1]H expansion of (top) the spectrum between 1.4-2.0 ppm, (bottom) aromatic region between 7.2-8.4 ppm with assigned protons.

Indazole **4** is substituted with the *N*-5-fluoropentyl moiety similar to other SCA analogues. In indole **5**, the fluoroalkyl moiety has been replaced with a cyclohexylmethyl, which resulted in multiple multiplets of methylene protons between 0.95-1.73 ppm, and the methine signal for 2‴ (Figure 106), which Shevyrin *et al.*[272] assigned as a multiplet on a 400 MHz spectrometer in a similar compound (MDMB-CHMINACA). In this study, 2‴ of indole **5** appears as a triplet of triplet of triplets, resulting from 3 different J_{HH} coupling. Coupling of 2‴ to 1‴ methylene resulted in a typical averaged $^3J = 7.0$ Hz, with $^3J_{ax,ax}$ to 3‴ of 11.5 Hz (large), and also $^3J_{ax,eq}$ to 3‴ of 3.5 Hz (small) (Figure 106), thus fixing the 1‴ substituent in the equatorial position as 2‴ methine must be axial. ^{13}C signals of the two methylene 3‴

appear at slightly different chemical shifts 30.97 and 30.99 ppm, a possible effect of the distant chiral centre on the rotation of the cyclohexylmethyl moiety. The data are confirmed by comparison to the work of Langer *et al.*[266]
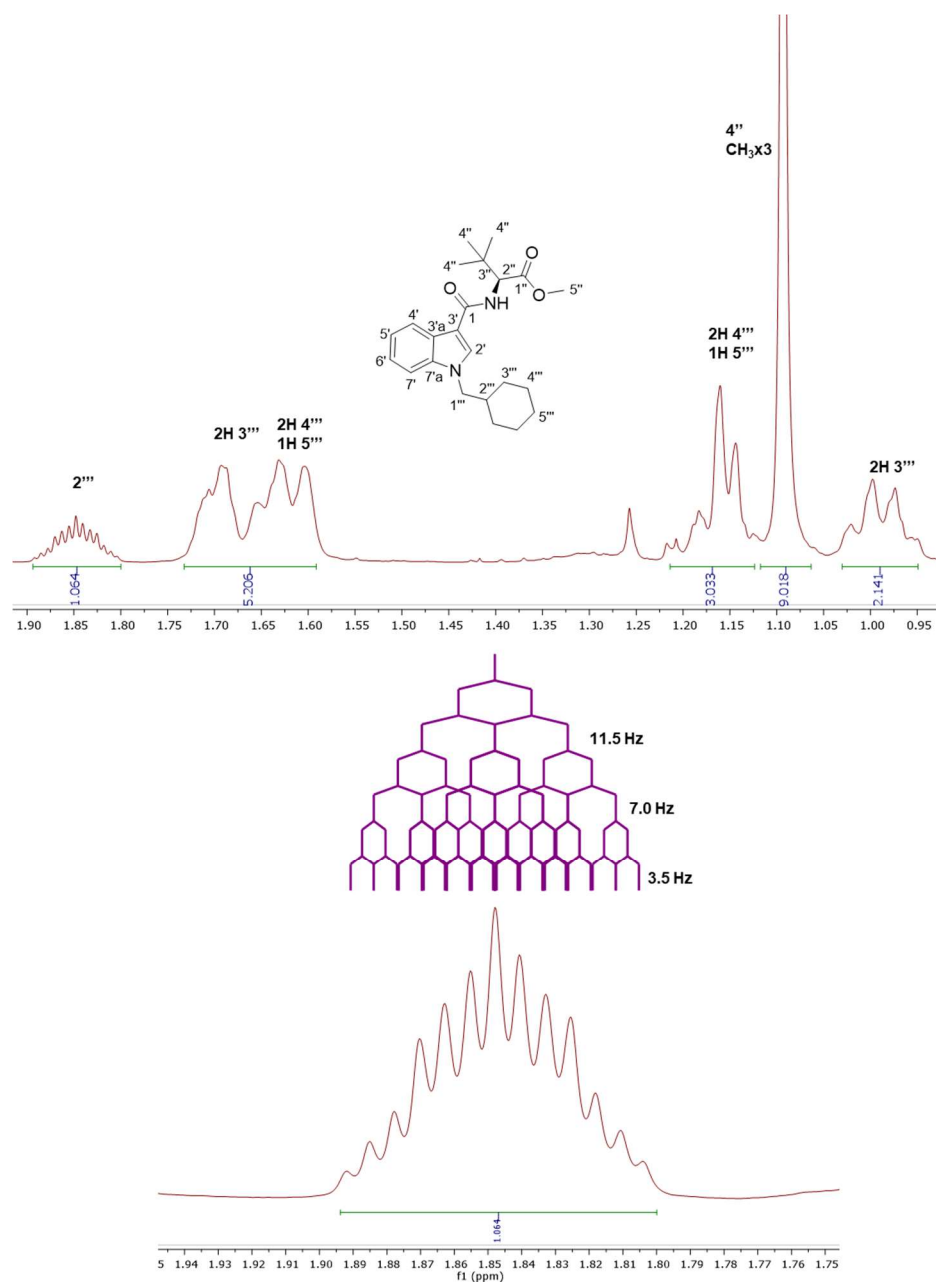
Figure 106. Compound **5** ^{1}H NMR expansion of (top) 0.9-1.9 ppm showing multiplets assignments, (bottom) expansion of exquisitely resolved 2‴ at 1.85 of ttt.

Compound **6** 5F-AKB48 is the indazole 5-fluoropentyl analogue, of indole STS-135. They can be easily differentiated using TOF-ESI-MS and NMR. The NMR assignments of the indazole ring are similar to those of compound **4**, and the 5-fluoropentyl tail has similar

assignments to that moiety found in compounds **1**, **3**, and **4**. The presence of the *N*-adamantyl

substituent in the head component resulted in 3 multiplets in the aliphatic region with 15

protons (Table 22), with 6H of 4″ overlapping with 4‴ of the 5-fluoropentyl tail. ^{19}F NMR

revealed the fluorine chemical shift at -218.5 ppm with the triplet of triplets coupling

constants of 46.5 Hz ($^2J_{HF}$) and 25.5 Hz ($^3J_{HF}$), similar to that observed in SCAs substituted

with a 5-fluoropentyl chain. The assignments are confirmed by comparison with the literature

for compound **6**.[287]
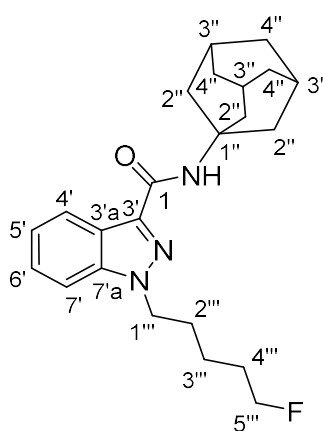
5F-AKB48 **6**

Table 22. NMR data of compound **6** in CDCl$_3$.

Position	^{13}C	^{1}H/^{19}F
1	162.0	-
1″	51.8	-
2″	41.9	2.12-2.15 6H, m
3″	29.6	2.07 3H, br s
4″	36.5	1.61-1.72 6H overlapped with 4‴
3′	138.2	-
3′a	140.3	-
4′	123.2	8.31 1H, d (8.0)
5′	122.4	7.15-7.26 1H, overlapped with CHCl$_3$
6′	126.6	7.30-7.32 1H, overlapped with 7′
7′	109.0	7.30-7.32 1H, overlapped with 6′
7′a	140.8	-
1‴	49.0	4.29-4.33 2H, overlapped with 5‴
2‴	29.4	1.92 2H, quintet (7.0)
3‴	22.7, d ($^3J_{CF}$ 5.0)	1.36-1.42 2H, m
4‴	29.9, d ($^2J_{CF}$ 19.5)	1.61-1.72 2H, overlapped with 4″
5‴	83.7, d ($^1J_{CF}$ 165.0)	4.29-4.33 2H, overlapped with 1‴
5‴-F	-	-218.56 tt ($^2J_{HF}$ 46.5, $^3J_{HF}$ 25.5)
NH		6.70 1H, br s

Many of the six separated components have been implicated in deaths or intoxications in toxicological reports.[257,258] Compound **3** was found in post-mortem toxicological samples in 4 deaths in the USA in 2013, compound **4** was implicated in 10 deaths in Japan in 2014.[259,288] Compound **5** and its metabolites were found in a post-mortem case in Germany in 2018.[289]

In this study, an analytical platform composed of LC/TOF-ESI-MS/MS, flash column chromatography and 1D/2D NMR spectroscopy is presented for the separation and characterization of complex mixtures of 5 closely related SCAs. The changing contents of "K2" are now a recent 3rd generation SCA with higher potency than the previous JWH and AM series compounds that used to be associated with "K2" and "spice" herbal blends. The NMR assignments and LC-ESI-MS/MS for PX-1 (compound **1**) are presented for the first time. Identification of PX-1 acid (compound **2**) impurity, a possible starting material or by-product of the amide **1** synthesis is also described. Additional NMR spectroscopic data for compounds **3-5** have been obtained, and a flash column chromatography method has been developed for the separation of these 5 closely related 3rd generation SCAs.

4.4 Conclusions

A combination of NMR spectroscopy and LC/TOF-ESI-MS/MS is a powerful approach for the profiling of unknown herbal blend samples containing 2nd and 3rd generation SCAs. Applying these analytical techniques allowed the characterization of the SCAs and the impurities in the samples (propylene glycol, isopropyl alcohol, and ethyl acetate). Analysis of the packaged brands revealed that 5F-ADB is the most common SCA present and it is found together with different types of SCAs. Qualitative differences have been demonstrated between brands seized in different years e.g. Extinction contained AB-CHMINACA in 2016 seizures, in 2017 it contained 5F-PB-22. This is an indication of how the illicit market in SCA is dynamic. Mislabelling or no labelling of packaged SCAs is seen in some of the brands. This is of importance to the drug user, as each type has different potency and this could have dangerous consequences. NMR characterization is described for AM-694 with

successful derivatization of the propylene glycol, found in the samples with AM-694, followed by detection via LC-ESI/MS analysis. For AB-CHMINACA, NMR characterization with additional ^{15}N-NMR data are provided for the first time.

Analytical characterization of HMP SCA samples revealed that SCAs are more popular than cannabis with combinations of potent SCAs such as 5F-ADB and AMB-FUBINACA in some samples, that could explain the reports of intoxications in prisons in the UK. 2D DOSY NMR spectroscopy is a powerful analytical technique in separating complex mixtures according to their diffusion coefficient (D). This has been successfully applied to samples containing SCAs and impurities resulting in excellent separations where there are sufficient differences in molecular weight between the analytes.

An analytical platform is provided that consists of LC/TOF-ESI-MS/MS, flash column chromatography and NMR for the separation of a closely related complex mixture of 3rd generation SCAs. UHPLC/TOF-ESI/MS analysis allowed base-line resolution of all six components in under 8 min, and molecular ions confirmation, with identification of a possible PX-1 impurity (compound **2**) with MS/MS analysis confirming the proposed structure. Flash column chromatography using 2 gradients allowed the separation and purification of SCAs in the mixture on a practical scale (mg). Final confirmation of the identity of each component, with the exception of compound **2**, was achieved by 1D/2D NMR with PX-1 NMR assignments for the first time. The contents of "K2" herbal blends keep on changing, where five years ago they were made up of 1st and 2nd generation SCAs (JWH and AM series), this analysis now shows the presence of multiple SCAs of the 3rd generation with higher potencies than the previous generations. Therefore, these qualitative and quantitative SCA analyses provide scientific evidence in support of what is being observed in city centres and in HMP, namely zombification and epidemics of spice abuse, the latter leading to dangerous combinations of intoxication and violence. Some of these 3rd generation SCAs have already been implicated in various deaths.[259,288,289]

In the following chapter, analytical areas rarely tackled of SCAs such as quantitative analysis of SCAs in herbal blends and combustion analysis are explored.

Chapter 5. Quantitative and combustion analysis of Synthetic Cannabinoid Agonists

5.1 Introduction

Synthetic Cannabinoid Agonists (SCAs), also known by their street name as spice, are potent binders to the CB_1 and CB_2 receptors distributed throughout the central nervous system (CNS) and immune system respectively, producing psychoactive effects similar to, and in most cases more potent than, the mainstream drugs they are trying to mimic, e.g. Δ^9–tetrahydrocannabinol (THC).[78] Unlike Δ^9-THC, a partial agonist with low affinity at the Cannabinoid receptor 1 (CB_1), SCAs are full agonists with high affinity binding to CB_1 and moreover they also possess CB_2 receptor affinity.[78] These pharmacological characteristics result in drug users/abusers having severe psychiatric episodes, not present with traditional cannabis smoking. These effects are described as the "cannabinoids tetrad" which are hypothermia, analgesia, catalepsy, and locomotor activities, leading to symptoms ranging from excited delirium to kidney damage.[290]

According to the European Monitoring Centre for Drug and Drug Addiction (EMCDDA), SCAs represent the largest class of NPS, with estimated seizures weighing more than 2.3 tonnes in 2015.[291] In 2008, the first generation of synthetic cannabinoids hit the streets,[80] such as the Pfizer compound, CP 47,497 and John W. Huffman JWH-018 (Figure 107), which were designed and developed as medicinal chemistry compounds, intended to exploit the pathological implications of the CB receptors in many diseases, but side-tracked to the illicit clandestine designer-drugs market.[79,253] The following generations of SCA were based initially on JWH-018, but later evolved into a variation of indazoles (5F-ADB), with fluoroalkyls and quinoline (5F-PB22), and amides (PX-1) integrated into their structures, replacing the naphthoylindole and *N*-pentyl tail of JWH-018.[262,286] This continuous change in substituents makes them into a moving target posing many analytical challenges.

The Korean National Forensic services reported that from 2008-2010, most of the SCA seized were first generation non-fluorinated compounds,[292] e.g. JWH-018, CP 47,497, and UR-144 (Figure 107). In 2012, fluorinated analogues started emerging such as XLR-11, a

fluoropentyl analogue of UR-144, and by 2013 approximately 90% of SCAs seized were fluorinated.[292] It is believed that the growing trend in the bioisosteric fluorine introduction into SCA was inspired by a Makriyannis patent,[255] where he demonstrated a much higher potency of AM-2201 compared to non-fluorinated analogues, e.g. JWH-018. Initially, AM-2201 was identified in herbal blends, and it escalated into many SCA with no precedent in the scientific literature, e.g. 5F-ADB-PINACA, 5F-AB-PICA, and 5F-PB-22.[253] Furthermore, besides the enhanced potency of fluorinated analogues, the addition of a fluorine substituent was intended to circumvent legal restrictions imposed on previous classes of SCA.[253,271]
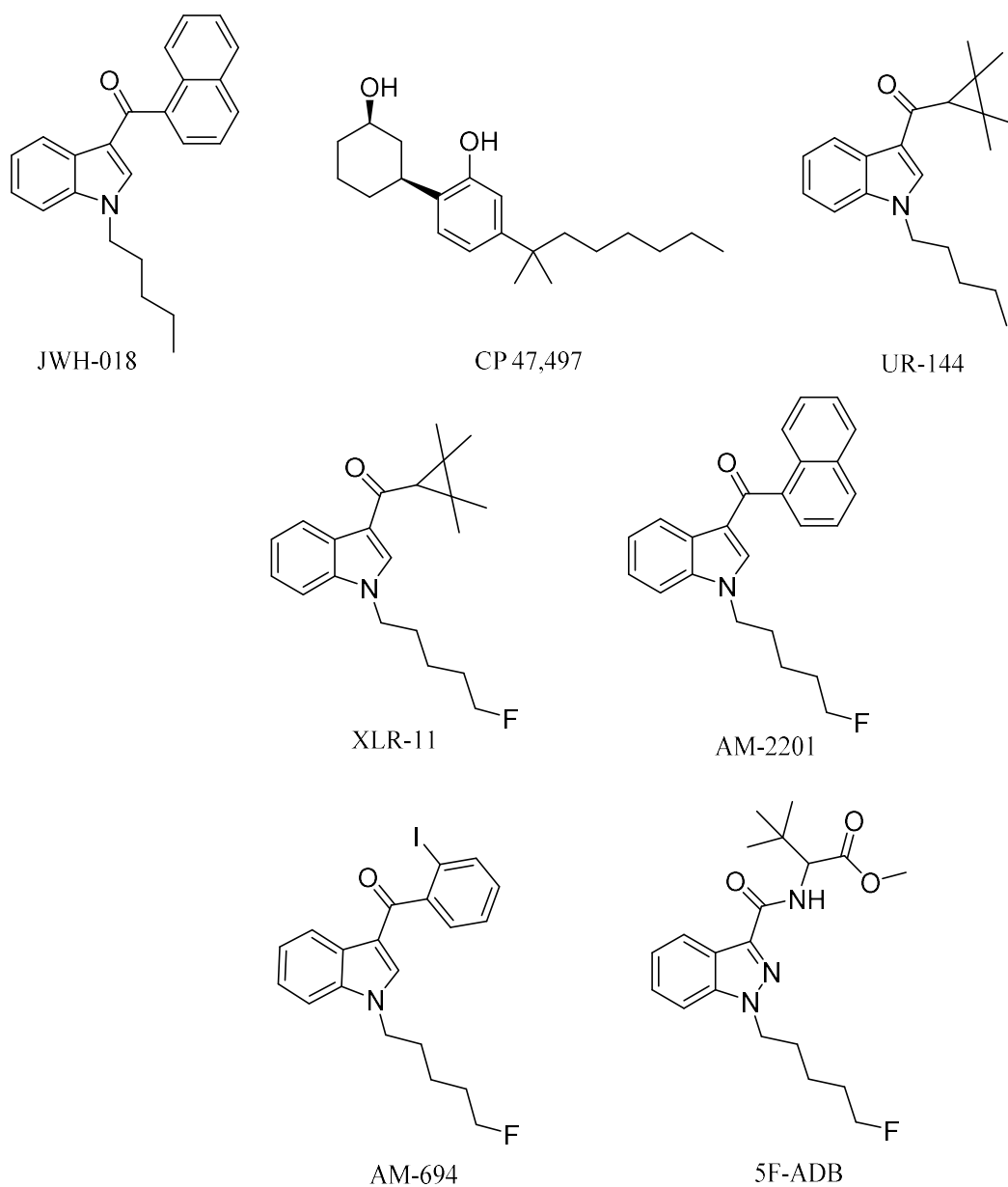
Figure 107. 1st, 2nd, and 3rd generation SCAs.

Proton Nuclear Magnetic Resonance (^{1}H-NMR) is inherently quantitative, as the integrated functional group signals are directly proportional to the number of spins generated by the signals in question. Nevertheless, NMR is only quantitative if the appropriate acquisition and processing parameters are determined by experiment and then implemented. Early applications of quantitative NMR (q-NMR) required considerably large amounts of sample and IS because they were low-field instruments. The development of high-field NMR spectrometers allowed for improved sensitivity meaning that impurities could be quantified at less than 0.1%, demonstrating that NMR is comparable with chromatographic methods for quantitative analysis.[200,218] NMR has more advantages than other analytical approaches such as those that are chromatography based. NMR does not require the use of a high purity reference standard for the construction of the required calibration curve. Such a standard is expensive and most of the time unavailable, especially for newer, more recently identified SCAs.[198] NMR also has the advantage of less sample preparation being required. No serial dilution is required to run the sample and no mobile phase has to be prepared. Additionally, there is no interaction with a column which requires blank samples to be run in order to avoid carry-over that could affect the analysis. Furthermore, NMR is not subject to problems from small compounds and impurities with no chromophore or a different UV response which pose challenges to chromatographic and UV methods.[198,199]

Quantitative analysis of SCA in herbal blends has been reported using different analytical techniques, mostly chromatography and MS-based.[9] GC/MS showed qualitative and quantitative variations among SCA in herbal-blend brands in 2014.[261] ^{1}H q-NMR reports on SCA quantitation are scarce. Techniques have been reported on purchased herbal blends containing SCA using MA as an internal standard.[293] Dunn *et al*.[294] evaluated the extraction efficiency of the major solvents e.g. chloroform, acetone, acetonitrile and methanol, using ^{1}H q-NMR with 1,3,5-trimethoxybenzene as an internal standard and GC/MS on seized herbal blends and in-house preparations, and found no significant difference across different solvents.[294]

The ^{19}F nucleus is an attractive target for q-NMR spectroscopy, mainly due to the sensitivity of the nucleus (88% of ^{1}H) and its natural abundancy of 100%.[295] Additionally, the wide range of chemical shift (500 ppm) and the absence of fluorinated impurities will reduce the chance of overlapping signals and less background noise.[296] ^{19}F q-NMR has been applied to analyse Active Pharmaceutical Ingredients (API).[297] Nevertheless, for quantitative results more parameters have to be addressed compared to ^{1}H q-NMR,[296] e.g. equal excitation for the signals across the entire spectral width must be achieved, otherwise the integration values will suffer which in turn affects the analytical results. This is achieved by setting the centre point of the spectrum (O1P) midway between the signal of the internal standard and the compound, 90° pulse angle followed by sufficient relaxation (relaxation delay) $5xT_1$ to recover the magnetization to 99.3% of its size. This parameter is also applicable to ^{1}H q-NMR, decoupling the ^{1}H signals during ^{19}F acquisition will result in NOE enhancement which can be overcome by inverse gated decoupling ^{19}F NMR.[296]

The main area of SCA analysis involves the characterization and quantification using GC-and LC-hyphenated techniques of seized powders or often herbal blends containing SCAs and toxicological samples, the latter relies on MS techniques. Analytical methods that can be applied to a crude sample are of great value to drug analysts, but due to the fact that SCAs in herbal blends are mostly smoked, analytical studies of combustion are required.[298] Simulation of smoking is challenging for a number of reasons, mainly the temperature and the flow rate. Temperature in cigarette smoking can routinely reach 700 °C and even goes up 900 °C at some hot spots.[299] Potentially toxic pyrolysis compounds are released from herbal materials when temperatures exceed 200 °C which is the case in cigarette smoking. Such toxic compounds include toluene, benzene and naphthalene.[300] The presence of several nitrogen atoms in the majority of SCAs could potentially result in a number of chemically variable combustion products due to the thermal lability of C-N bonds. For an accurate simulation of the smoking process, a flow rate of 30 L/min needs to be maintained.[301]

The first SCA pyrolysis analysis was performed on UR-144, an indole tetramethyl-cyclopropyl using LC/MS/MS.[302] Raso and Bell[303] performed GC/MS analysis, revealing

pyrolysis products of first generation (JWH-018, JWH-073) and second generation (AM-694) SCA using an in-house built pyrolysis device comprised of a quartz tube inserted into a round-bottom flask, where the sample is combusted using a blow torch, revealing common and distinctive fragments for each type of SCA, e.g. naphthalene for the JWH family and cinnolineamine for the inadzole family. The authors also acknowledged the problem of maintaining a stable temperature.[303] Kevin *et al.*[304] by-passed the issue of fluctuating temperature by conducting a temperature controlled study on six carboxamide type SCA at 200, 400, 600, and 800 °C using a pyro-probe coupled to a GC/MS, thus creating temperature-controlled pyrolysis conditions where the degradants were analysed at each temperature.[304] In this chapter, a focus on the simulation of smoking is the aim rather than pyrolysis at high temperatures coupled to anaerobic conditions.

The increased frequency of the discovery of fluorinated SCAs is exploited, and a confirmed ^{19}F q-NMR spectroscopic method is implemented for the first time to quantify fluorinated SCAs, e.g. 5-F-ADB and AM-694 (Figure 107) in herbal blends recently seized in the South West of England. The technique was compared to ^{1}H q-NMR and UHPLC for accuracy and was shown to be in good agreement. Moreover, quantitative differences between sample batches are discussed. Investigation of the acquisition parameters associated with ^{19}F q-NMR will help drug analysts to run a fast and robust quantitative analysis for fluorinated (illicit) drugs with minimal background interference and signal overlap.

Additionally, work on the combustion and degradation products is an area that requires further investigation due to the generation of potentially harmful products with possible alteration in the target receptor or the affinity for that receptor of the new compounds resulting from such exposure to high temperatures. In this study, a SCA smoking model was designed and constructed. It was then employed for the analysis of different SCAs and the detection of their combustion products. The resulting combustion products may help drug analysts to uncover markers for SCA smoking that will facilitate toxicological drug detection.

5.2 Experimental

5.2.1 Chemicals and sample preparation

All extraction solvents 99.9% anhydrous (chloroform, methanol, and acetonitrile), were purchased from Fisher Scientific (UK) and ACROS Organics (UK). Deuterated solvents (CDCl$_3$, CD$_3$OD, and CD$_3$CN) were purchased from Cambridge Isotope Laboratories (Goss Scientific, UK). NMR internal standards (IS) 2-chloro-4-fluorotoluene, dimethyl sulfone (DMS), and maleic acid (MA) are TraceCERT certified reference materials purchased from Sigma-Aldrich (UK). [1-(5-Fluoropentyl)-1H-indol-3-yl](2-iodophenyl)-methanone (AM-694) 10.0 mg, *N*-(1-adamantyl)-1-(5-fluoropentyl)-1H-indazole-3-carboxamide) (5F-AKB-48) 1.0 mg/mL in a 1.0 mL vial, and (1-pentyl-1H-indol-3-yl)-1-naphthalenyl-methanone (JWH-018) 100 µg/mL in a 1.0 mL vial were purchased from LGC (Teddington, UK). *N*-Methyltrifluoroacetamide (*N*-methyl-TFA) >98.0% was purchased from Tokyo Chemical Industry (TCI, Tokyo, Japan). Herbal-blend samples were provided by the DEAT, the Avon and Somerset Constabulary, from recent (2016-2018) seizures. The samples were in the form of herbal blends (1.0-3.0 g) as commercially packaged brands (Exodus, Loco Elite). *Turnera diffusa* (Damiana) dried herb (illicit-drug free) was purchased from Spiceworks (Hereford, UK).

IS, reference standards, and samples were weighed using a SE2F Sartorius analytical balance, between 1.0-2.0 mg/mL of IS was used. Preliminary analysis of non-homogenized herbal blend samples yielded large variations in the contents of the plant materials between samples tested by NMR. Therefore, two approaches were employed for the homogenization of the samples. Either they were ground to a fine powder with 100 grit sandpaper,[282] or they were frozen in liquid nitrogen, followed by grinding to a fine powder using a mortar and pestle. For sample preparation for UHPLC and NMR analysis, homogenized plant materials (100 mg) were extracted with methanol (2 x 4.0 mL) with sonication (30 min), centrifuged, and then the supernatant extract was decanted and the pellet (plant material) discarded. The extract was then evaporated to dryness under reduced pressure and reconstituted in deuterated solvent (1.0 mL) containing IS (DMS, MA or 2-chloro-4-fluorotoluene) for NMR

spectroscopic analysis. For UHPLC analysis, samples were diluted 100-fold to bring them within the calibration range and spiked with IS JWH-018 in the case of AM-694 quantitation, and 5F-AKB48 in the case of 5F-ADB quantitation (IS at 10.0 µg/mL). Data analysis was conducted using the Microsoft Excel data analysis tool pack.

AM-694 was quantified using a 7-point calibration curve between 1.25-80 µg/mL with JWH-018 as IS, and 5F-ADB using a 6-point calibration curve between 1.25-40 µg/mL with 5F-AKB48 as IS, both were prepared in UHPLC solvent. The response was calculated as the ratio of the area under the curve of the compounds to that of the respective IS.

5.2.2 Instrumentation

NMR spectroscopy

NMR spectra were recorded on a Bruker AVANCE III 500 MHz spectrometer. ^{1}H, ^{13}C, and ^{19}F frequencies are 500.130, 125.758, and 470.592 MHz respectively. The probe was a variable temperature BBFO+ with three channels, temperature was 25˚C. Chemical shifts were referenced to 0.0 ppm for TMS or residual solvent peaks and are reported in ppm. Coupling constants (*J*, line-separations, absolute values) are rounded to the nearest 0.5 Hz. Structural elucidation was achieved with the use of 2D NMR spectroscopy. An Inversion recovery pulse sequence was performed to measure the longitudinal relaxation time T_1 for the 2-chloro-4-fluorotoluene IS and 5F-ADB. The T_1 relaxation delay for the IS signal for ^{1}H quantification for H5 (^{1}H δ = 6.98 1H, td 8.5, 2.5 Hz) was 5.7s, and T_1 for the indazole 5F-ADB ranged from 2.9-3.5s. For quantitative ^{1}H NMR analysis, the pulse sequence was composed of 64k data points, acquisition time of 3.18s, 16 scans, 50s delay, 90° pulse angle, phase and baseline corrections were done automatically while integration was performed manually. ^{19}F q-NMR proton coupled and inverse gated pulse sequence used a sweep of 241.51 ppm, O1P -168 ppm, 6k point counts, acquisition time 0.7s, 16 scans, delay 30s, 90° pulse angle, phase and baseline correction and integration were performed manually. NMR spectra were processed using Bruker TopSpin 3.5 and Mestralab Mnova 11.2.

UHPLC quantitation, UHPLC/TOF-ESI-MS and GC/MS

UHPLC calibration curve construction and sample quantitative analysis were performed on a Dionex Ultimate 3000 UHPLC (Thermo Fisher Scientific, California, USA) with a variable wavelength detector (λ = 254, 280, 298 nm). Liquid chromatography separation was performed using an Acquity UPLC BEH C18, 1.7 µM, 2.1 x 50 mm RP-column (Waters, Milford, Massachusetts, USA) with a flow rate of 0.4 mL/min, and an injection volume of 10 µL at a column temperature of 40°C.

Mobile phase A consisted of LC/MS grade water 0.1% TFA v/v; mobile phase B consisted of acetonitrile 0.1% TFA v/v. For AM-694 and 5F-ADB calibration curves and quantitation the following gradient 1 was used, the solvent gradient started from 1% B for 2.0 min followed by a linear increase from 2.1 min to 100% B at 5.0 min, held for 3 min, followed by a return to 1% B at 8.1 min, where it was held for 3.9 min for equilibration, giving a total run time of 12.0 min. For 5F-ADB purity determination, the flow rate was 0.4 mL/min, column temperature 25.0 °C. Gradient 2 started with 10% B until 3.0 min, followed by a linear increase to 100% B at 20.0 min, held for 4.0 min, followed by a return to 10% B at 24.1 min where it was held for 10.9 min with a total run time of 35.0 min. Data analysis used Bruker data and quant analysis 4.3 package.

For the combustion analysis using UHPLC/TOF-ESI-MS, the QTOF and MS parameters are reported in section 4.2.2, but with the following gradient 3 and mobile phases: mobile phase A consisted of LC/MS grade water 0.1% FA v/v; mobile phase B consisted of acetonitrile 0.1% FA v/v. Solvent gradient started from 1% B for 2 min followed by a linear increase from 2.1 min to 100% B at 9.0 min, held for 3 min, followed by a return to 1% B at 12.1 min, where it was held for 2.9 min for equilibration, giving a total run time of 15.0 min.

GC/MS analysis of SCA combustion was achieved on a Thermofisher ISQ series GC/MS. Full scan mode 50-650 m/z, injection volume splitless 1 µL, with He as the carrier gas, flow rate 12.0 mL/min. HP-1 column was used (30 m x 0.18 mm, 0.18 µm thickness) Temperature gradient started at 80°C, it was increased to 320°C at 20°C/min, then maintained for 3.0 min with a total run time of 15.0 min. Data analysis used Xcalibur software.

SCA smoking simulation apparatus

The smoking model is a two-stage trap rig (Figure 108), constructed in-house using two 250 mL gas washing bottles Lenz® (VWR, UK), filled to the midpoint with 8 mm glass beads (VWR, UK) to increase the surface area. The gas washing bottles heads were without filters, with traps placed in a dry ice/acetone slush-bath allowing the efficient trapping of the volatiles. A Quartz tube 8 mm OD x ID 6 mm was purchased from Almath crucibles (Suffolk, UK) where the SCA cigarettes were inserted. The traps were connected to a GAST G626X pump (General Electric, USA), the pump dial was used to control the flow rate which was measured using a Copley® DFM 2000 flow regulator (Nottingham, UK). The flow rate was set between 28-30 L/min and the temperature was monitored using a TENMA thermocouple. SCA doped herb (200 mg) was rolled into a cigarette and inserted into the Quartz tube followed by lighting it with a cigarette lighter.

A

B

C
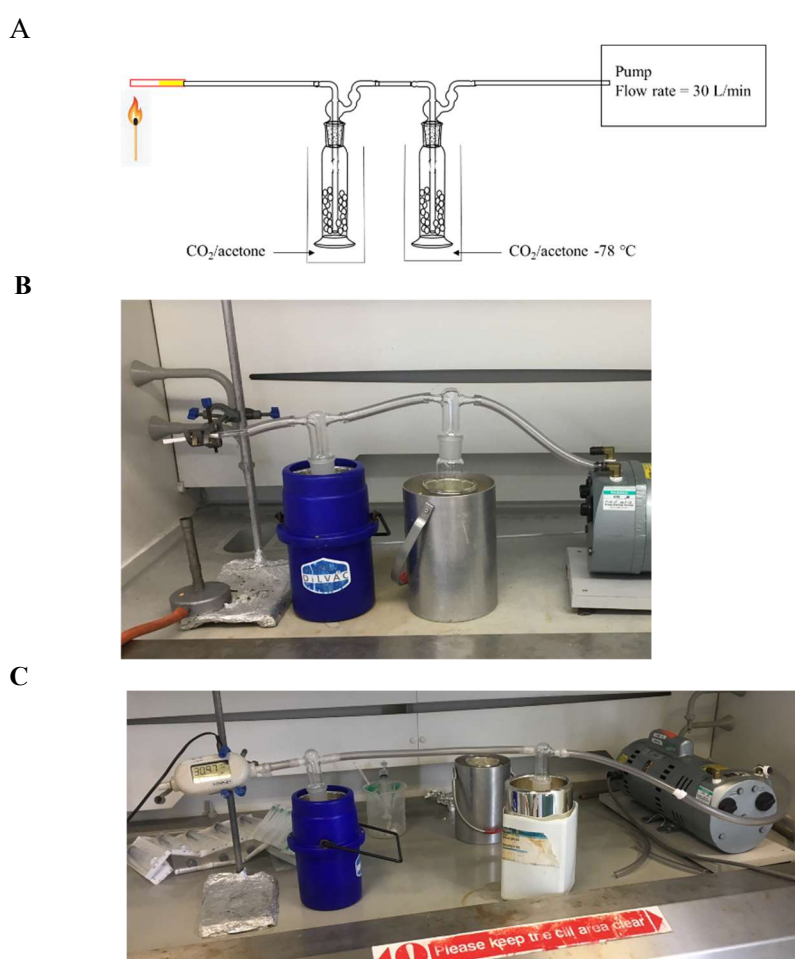
Figure 108. In-house constructed SCA smoking simulation model: (A) graphic, (B) cigarette inserted into the Quartz tube, (C) Copley flow rate meter in position.

5.3 Results and discussion

5F-ADB reference material was extracted from a seized sample (1.3 g) with $CHCl_3$ (2x 25.0 ml) with sonication for 30 min each time. The combined extracts were passed through a 0.25 µm syringe filter. The filtrate was evaporated to dryness under reduced pressure yielding ~90 mg of residue which was purified by flash-column normal phase silica chromatography using gradient 1 (section 4.2.2), followed by semi-preparative RP HPLC, resulting in pure 5F-ADB (38.0 mg). Purity and confirmation of the structure were obtained by two analytical UHPLC methods (gradients 1 and 2 on a C18 column), NMR and also HRMS (Figure 109).

^{1}H NMR (500 MHz in CD_3OD): δ 8.21 (4′) (1H, dd J = 8.0, 2.0 Hz), 7.83 (NH) (1H, br d J = 9.5 Hz), 7.64 (7′) (1H, dd J = 8.5, 1.5 Hz), 7.46 (6′) (1H, td J = 8.5, 1.5 Hz), 7.29 (5′) (1H, td J = 8.5, 2.0 Hz), 4.62 (2″) (1H, d J = 9.5 Hz), 4.52 (1‴) (2H, t J = 7.5 Hz), 4.40 (5‴) (2H, dt J = 47.5, 6.0 Hz), 3.78 (5″) (3H, s), 2.01 (2‴) (2H, quintet J = 7.5 Hz), 1.73 (4‴) (2H, d quintet J = 26.0, 6.0 Hz), 1.41-1.47 (3‴) (2H, m), 1.10 (4″) (9H, s).

^{13}C NMR (125.8 MHz in CD_3OD): δ 173.1 (1″), 164.2 (1), 142.5 (7′a), 137.3 (3′), 126.8 (6′), 124.0 (5′), 123.9 (3′a), 123.0 (4′), 111.1 (7′), 84.7 (5‴, d $^1J_{CF}$ = 164.0 Hz), 61.3 (2″), 52.5 (5″), 50.2 (1‴), 35.8 (3″), 31.0 (4‴, d $^2J_{CF}$ = 19.5 Hz), 30.4 (2‴), 27.1 (4″), 23.7 (3‴ d, $^3J_{CF}$ = 5.5 Hz); ^{19}F observe δ -220.3 (5‴F, tt $^2J_{HF}$ = 47.5, $^3J_{HF}$ = 26.0 Hz). HRMS found [M+H]$^+$ 378.2193 for $C_{20}H_{29}FN_3O_3$ requiring 378.2187, found [M+Na]$^+$ 400.2010 for $C_{20}H_{28}FN_3O_3Na$ requiring 400.2006 (Figure 109).
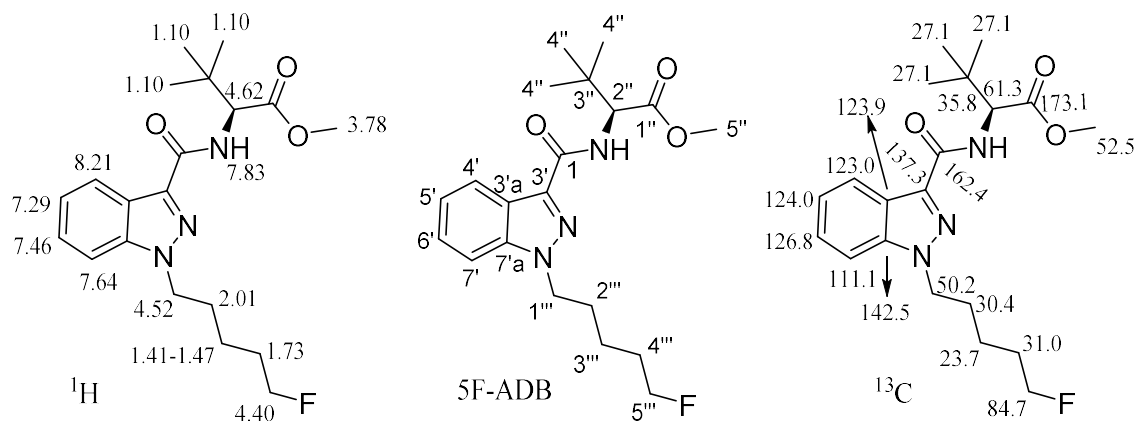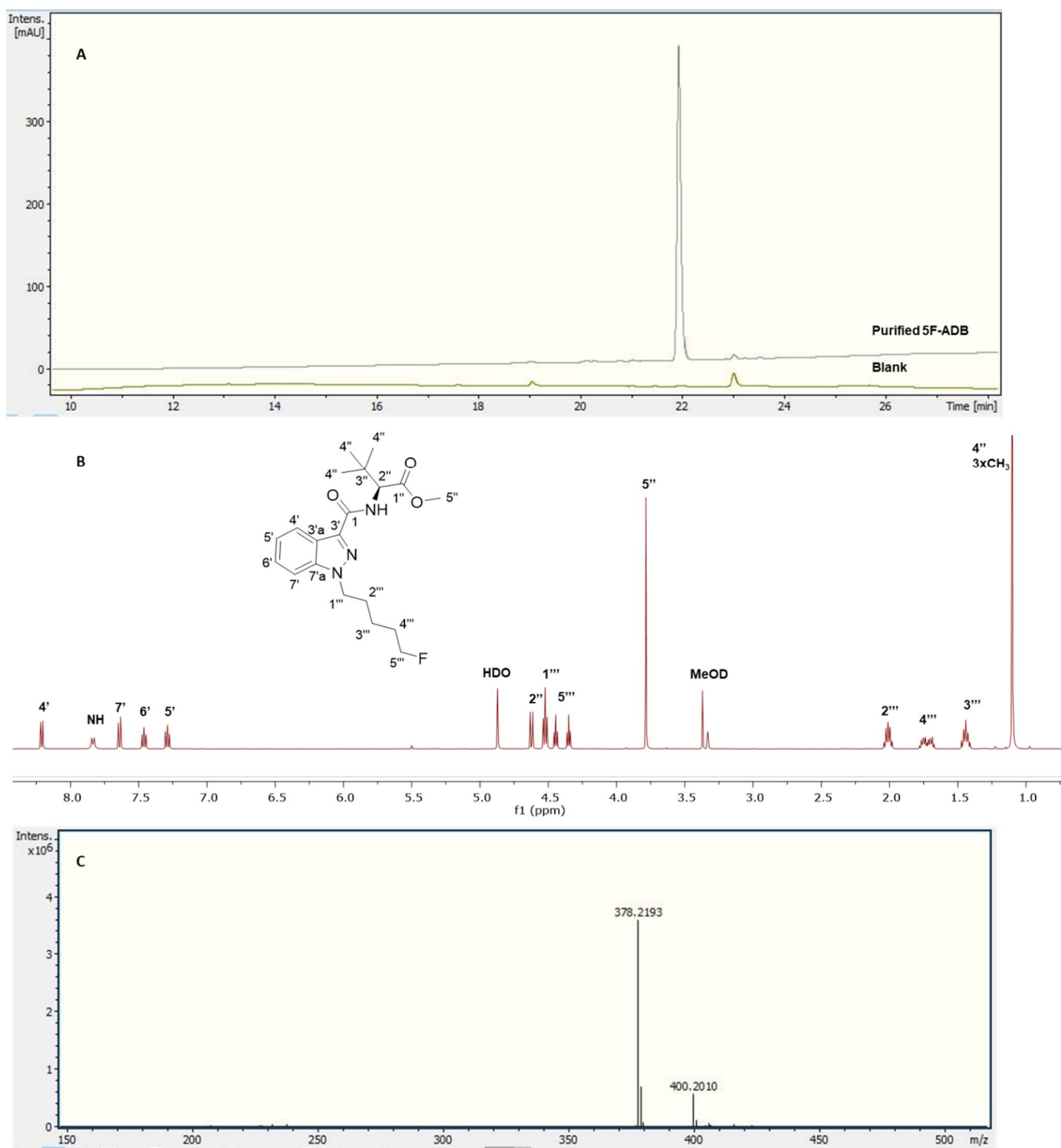
Figure 109. Analytical purity of 5F-ADB as tested by (A) UHPLC RT = 22.0 min, (B) ^{1}H-

NMR in CD$_3$OD with assignments, (C) HRMS showing [M+H]$^+$ and [M+Na]$^+$.

5.3.1 ^{19}F and ^{1}H quantitative NMR analyses of fluorinated SCA in seized herbal blends

5F-ADB

N-[[1-(5-Fluoropentyl)-1H-indazol-3-yl]carbonyl]-3-methyl-L-valine methyl ester (5F-ADB) was identified in seized herbal blend samples named "Exodus". Identification was achieved through 2D NMR and LC/MS/MS fragmentation pattern (Figure 101 A). Results are confirmed by comparison with the literature with only minor differences in the NMR, due to solvent effects.[272,305] The target signal for fluorine q-NMR analysis is the fluorine on the *N*-pentyl tail with its chemical shift of δ = -220 ppm assigned as a triplet of triplets, $^{2}J_{HF}$ 47.5 Hz coupling to methylene protons on position 5‴ and $^{3}J_{HF}$ 26.0 Hz coupling to methylene at position 4‴. The extraction was evaluated in chloroform, methanol, and acetonitrile.

The signals used for quantification in methanol were the indazole protons 4′ 8.22 ppm, 7′ 7.64 ppm, 6′ 7.46 ppm, and 5′ 7.31 ppm. In acetonitrile, the same protons were used except 6′ due to an overlapping impurity. In chloroform, H-5′ was excluded due to overlap with the residual chloroform H-solvent signal, nevertheless chloroform gave a cleaner spectrum, with fewer impurities and no sugars from the matrix component (as found when methanol was the solvent of extraction) with additional signals available for integration such as the fluoropentyl methylenes 1‴ and 5‴. DMS singlet at δ = 3.0 ppm integrating for six protons, was used as an IS in CDCl$_3$. Additionally, *N*-methyltrifluoroacetamide was evaluated as an IS for ^{19}F q-NMR, resulting in apparently significantly lower amounts of SCA, using Anova two factor analysis, in comparison to its contemporaneous analysis by ^{1}H q-NMR and then by ^{1}H q-NMR using maleic acid (IS) in methanol and acetonitrile, and DMS (IS) in chloroform (Table 23). The reason behind this apparently lower yield is the resonance (chemical shift) of the *N*-methyltrifluoroacetamide ^{19}F signal at δ = -75.9 compared to the ^{19}F of 5F-ADB at δ = -220.2 ppm, resulting in unequal excitation. Uniform excitation across the spectrum has to be achieved in order for all the signals to get the same magnetization in the pulse sequence, thus making the centre point of the spectra (O1P) a crucial parameter when accurate and reproducible quantitative results are to be achieved for ^{19}F q-NMR.

Table 23. Quantitative analysis of a sample of 5F-ADB by ^{1}H NMR in CD$_3$OD, CD$_3$CN, and CDCl$_3$ compared to ^{19}F q-NMR using *N*-methyltrifluoroacetamide (n = 4).

Nucleus, Solvent (IS)	^{1}H in CD$_3$OD (MA)	^{1}H in CD$_3$CN (MA)	^{1}H in CDCl$_3$ (DMS)	^{1}H in CDCl$_3$ (*N*-Me-TFA)	^{19}F in CDCl$_3$ (*N*-Me-TFA)
Amount (mg/g)	11.84 ± 0.28	11.06 ± 0.16	11.03 ± 0.14	11.48 ± 0.12	8.86 ± 0.19
RSD (%)	2.34	1.45	1.30	1.01	2.18

Therefore, 2-chloro-4-fluorotoluene was used as a ^{19}F q-NMR IS with (protio) methanol as the extraction solvent and CD$_3$OD as the NMR solvent, resulting in a good agreement with ^{1}H q-NMR using maleic acid (MA) as the IS. The ^{19}F NMR IS signal has chemical shift δ = -117.8 ppm. As 5F-ADB ^{19}F resonates at δ = -220.2 ppm, the O1P was therefore set at δ = -165 ppm approximately equally between both resonances resulting in equal excitation of both fluorines. Changing the O1P position significantly influenced the accuracy of the quantitative results. The ^{19}F q-NMR results (Table 24) are in agreement with the ^{1}H q-NMR using maleic acid (MA) (10.4 ± 0.2 mg/g, RSD 1.6%) as the IS.

Table 24. Quantitative analysis of 5F-ADB by ^{1}H and ^{19}F NMR (proton coupled) in CD$_3$OD with 2-chloro-4-fluorotoluene as IS at O1P = -160 ppm (n = 5).

Nucleus	^{1}H	^{19}F
Amount (mg/g)	9.8 ± 0.8	9.4 ± 0.7
RSD (%)	7.9	7.3

The effect of changing the O1P was tested using plant material (100.0 mg) containing 5F-ADB with 2-chloro-4-fluorotoluene as the IS, setting the O1P approximately in the middle of the two signals (-165 ppm). This resulted in quantitative results in agreement with ^{1}H q-NMR results, while shifting the O1P to -220 and -117 ppm, resulted in significantly lower and higher integration values respectively and, consequently, significantly altered quantitative results as tested by t-tests ($p < 0.05$). (Figure 110).
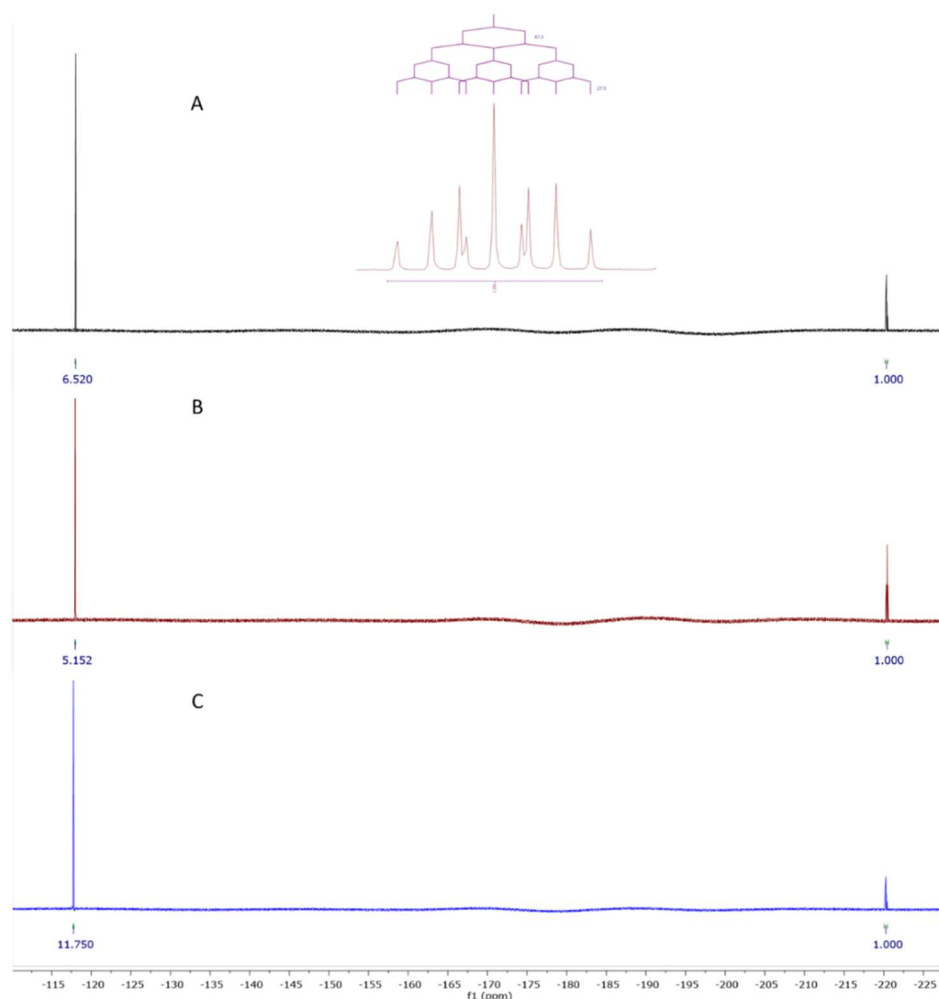
Figure 110. ^{19}F-NMR (^{1}H coupled) stacked spectra of 5F-ADB with its ^{19}F signal at -220.2 ppm and the IS 2-chloro-4-fluorotoluene (-117.8 ppm) with O1P set at: (A) -165 ppm, (B) -220 ppm, (C) -117 ppm, with (inset) expansion of the of 5F-ADB ^{19}F signal.

A seized sample (HN Exodus5) containing 5F-ADB was analysed using inverse-gated decoupling ^{19}F NMR in order to eliminate the Nuclear Overhauser Effect (NOE), and provide the added benefit of an enhanced signal to noise (S/N) ratio. The results were compared with proton-coupled ^{19}F NMR; the results from the ^{19}F proton coupled and ^{19}F proton decoupled methods are in good agreement (Figure 111). ^{1}H NMR q-NMR showed 7.1 ± 0.11 mg/g (RSD of 1.57%), ^{19}F proton-coupled q-NMR showed 6.9 ± 0.02 mg/g (RSD of 0.24%), ^{19}F inverse-gated decoupled q-NMR showed 6.8 ± 0.08 mg/g (RSD of 0.78%).
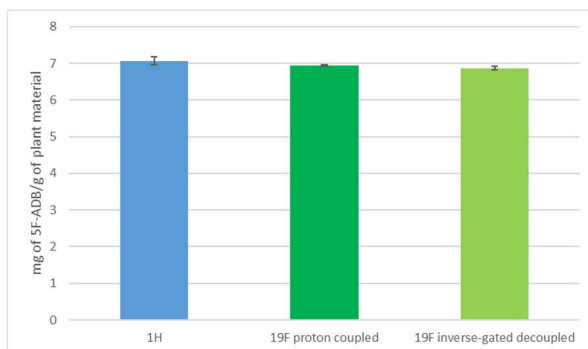
Figure 111. 5F-ADB quantified in a sample using ^{1}H, ^{19}F proton coupled, and ^{19}F inverse-gated decoupled spectroscopy.

Two batches of seized "Exodus" brand, 8 seized in 2016, and 7 seized in 2017, were subjected to quantitative analysis using ^{19}F proton coupled/decoupled and ^{1}H NMR using the IS 2-chloro-4-fluorotoluene, and also by UHPLC. Confirmation of the quantitation by ^{19}F q-NMR was achieved with UHPLC using the purified 5F-ADB as the reference standard to construct a calibration curve (gradient 1), using $\lambda = 298$ nm wavelength where the indazole absorbs strongly, resulting in RT = 6.8 min. Initially, 1-methylindazole-3-carboxylic acid was used as a UHPLC IS, but this was abandoned due to the overlap of the 1-methylindazole-3-carboxylic acid peak with a plant matrix component at RT = 5.6 min (Figure 112). 5F-AKB48 (RT = 7.2 min) was chosen instead as an IS in UHPLC analysis due to its similar chromophore to 5F-ADB (indazole), and the presence of an *N*-adamantanyl substituent provided sufficient hydrophobicity to be separated from the peak of 5F-ADB (Figure 112). 5F-ADB UHPLC calibration curve using 5F-AKB48 as an IS was in the range 1.25-40.00 µg/mL giving excellent linearity $R^2 = 0.9999$ and an IS RSD of 4.8% (Figure 113).

1-Me-indazole-3-carboxylic acid   5F-ADB   5F-AKB48
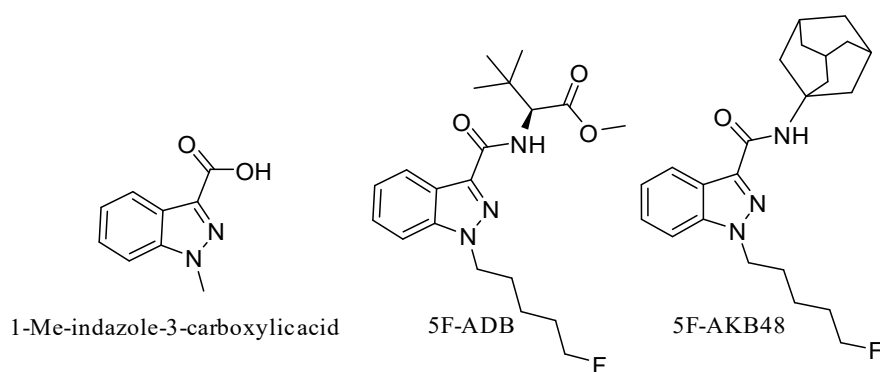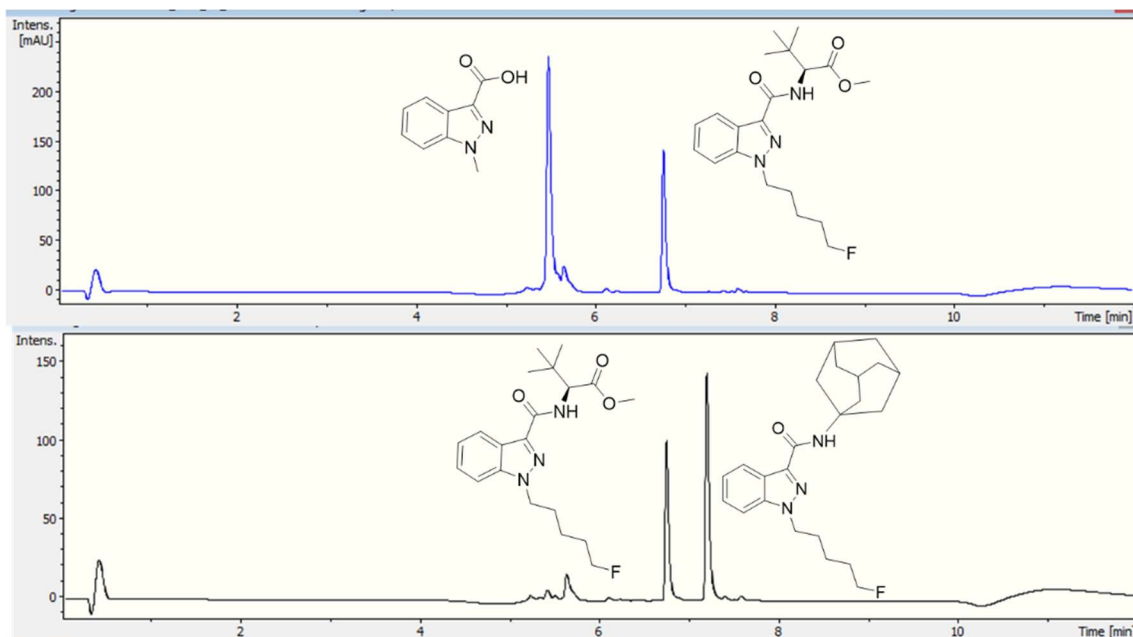
Figure 112. UHPLC chromatograms (λ = 298 nm) for an "Exodus" sample containing 5F-ADB RT = 6.8 min (top) using 1-methylindazole-3-carboxylic acid as IS RT = 5.6 min showing overlap with a matrix component, (bottom) using 5F-AKB48 as IS RT = 7.2 min.
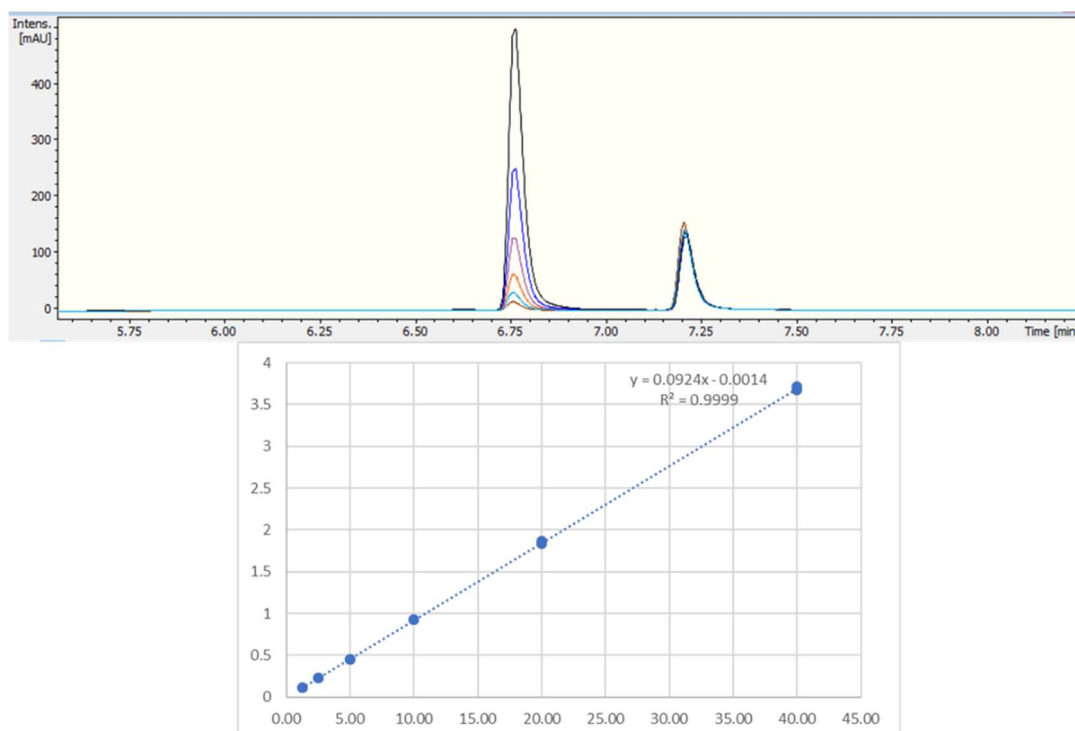
Figure 113. (Top) stacked UHPLC chromatogram concentrations from 1.25-40.0 µg/mL (λ = 298 nm) of 5F-ADB (RT = 6.8 min) and 5F-AKB48 IS (RT = 7.2 min), (bottom) calibration curve of 5F-ADB against 5F-AKB48 (IS), R^2 = 0.9999.

2016 seized "Exodus" samples analyses revealed a consistent dose of 5F-ADB across all 8 samples with an acceptable precision (RSD%) of less than 10% for the analysis of samples in the herbal form (Table 25).[217] Furthermore, using ANOVA two-factor with replication analysis of the four groups (^{19}F coupled, ^{19}F decoupled, ^{1}H NMR and UHPLC) revealed no statistically significant differences ($p > 0.05$).

Table 25. Quantification (mg/g) of SCA in plant material of "Exodus" brand seized in 2016 containing 5F-ADB.

Sample	NMR n = 3						UHPLC n = 4	
	^{1}H	RSD %	^{19}F coupled	RSD %	^{19}F decoupled	RSD %	UHPLC	RSD %
Exodus9	7.39 ± 0.20	2.74	7.34 ± 0.27	3.73	7.12 ± 0.24	3.36	6.96 ± 0.12	1.67
Exodus10	8.04 ± 0.43	5.35	7.87 ± 0.37	4.69	7.87 ± 0.47	5.94	7.92 ± 0.38	4.79
Exodus11	8.24 ± 0.17	2.00	8.01 ± 0.12	1.48	8.05 ± 0.06	0.79	7.87 ± 0.11	1.46
Exodus12	8.04 ± 0.12	1.49	7.89 ± 0.07	0.88	7.93 ± 0.14	1.81	7.97 ± 0.10	1.20
Exodus13	7.78 ± 0.02	0.21	7.71± 0.04	0.54	7.72 ± 0.05	0.65	8.19 ± 0.07	0.79
Exodus14	7.65 ± 0.08	1.00	7.61 ± 0.07	0.90	7.66 ± 0.11	1.45	7.91 ± 0.12	1.52
Exodus15	7.57 ± 0.22	2.93	7.52± 0.24	3.14	7.50 ± 0.17	2.26	7.54 ± 0.09	1.17
Exodus16	7.43 ± 0.18	2.46	7.45± 0.21	2.75	7.48 ± 0.24	3.18	7.94 ± 0.14	1.82

Table 26. Quantification (mg/g) of SCA in plant material of "Exodus" brand seized in 2017 containing 5F-ADB.

Sample	NMR n = 3						UHPLC n = 4	
	^{1}H	RSD %	^{19}F coupled	RSD %	^{19}F decoupled	RSD %	UHPLC	RSD %
Exodus1	10.48 ± 0.29	2.78	10.65 ± 0.11	1.08	10.68 ± 0.12	1.11	12.44 ± 0.63	5.03
Exodus2	7.81 ± 0.12	1.51	7.75 ± 0.07	0.92	7.77 ± 0.16	2.09	8.83 ± 0.03	0.34
Exodus3	9.17 ± 0.13	1.41	9.07 ± 0.19	2.13	9.12 ± 0.23	2.55	11.10± 1.29	11.60
Exodus4	8.69 ± 0.10	1.17	8.66 ± 0.13	1.49	8.60 ± 0.10	1.12	8.35 ± 0.15	1.80
Exodus5	17.50 ± 0.09	0.53	17.48 ± 0.23	1.31	17.71 ± 0.05	0.26	20.22 ± 0.25	1.23
Exodus6	8.70 ± 0.08	0.93	8.57 ± 0.09	1.01	8.59 ± 0.11	1.33	8.78 ± 0.07	0.83
Exodus7	14.35 ± 0.10	0.69	13.88 ± 0.09	0.66	13.45 ± 0.53	3.92	16.08 ± 0.17	1.06

However, 2017 "Exodus" samples containing 5F-ADB revealed different quantitative results (Table 26). 5 packs of the 7 contained a similar dose of 5F-ADB to the 2016 samples, but samples 5 and 7 contained from 1.5 to more than double the dose of 5F-ADB, with good precision in most of the samples. The presence of such a large quantitative variation in the 2017 samples is alarming, especially as this recently identified SCA (5F-ADB) has no pharmacological data, so one can only compare it to similar analogues which have approximately 220-fold the potency of THC, e.g. 5F-ADBICA $EC_{50} = 0.77$ nM compared to

THC EC_{50} = 172 nM.[78] This quantitative analysis is of importance to users/abusers, health professionals and law enforcement to get an idea of how much of the SCA is in the sample. It also clearly demonstrates how there is no quality control of the "Exodus" preparations.

AM-694

[1-(5-Fluoropentyl)-1H-indol-3-yl](2-iodophenyl)-methanone (AM-694) was identified (3.0 g) in seized herbal blends branded as "LOCO elite". Identification was achieved through 2D NMR spectroscopy and its LC/MS/MS fragmentation pattern (Figures 74 and 77). Results are confirmed by comparison with the published literature of the first analytical characterization of AM-694 in illicit seizures.[262] Candidate signals for integration are: 3″, 4″, 5″, and 6″ of the iodophenyl substituent, 2′ and 7′ of the indole core, and 1‴ and 5‴ of the fluoropentyl chain. The impact of relaxation delay in ^{19}F NMR was investigated, and it was found that using only a short relaxation delay (< 15s) significantly affected the quantitative results. 15s and 30s relaxation delays were sufficient to achieve reproducible quantitative results. Moreover, such relaxation delays still allowed fast overall sample run-times of 8 and 10 min respectively. ^{1}H q-NMR and ^{19}F q-NMR showed consistent results using 2-chloro-4-fluorotoluene as the IS (Figure 114). Furthermore, cross-method confirmation was demonstrated using UHPLC with reference standard AM-694 RT = 6.9 min and JWH-018 (IS) RT = 7.3 min, constructing a seven-point calibration curve between 1.25-80.0 μg with R^2 = 0.997 and IS RSD = 4.4% (Figure 115).

Two samples were quantified, with significant differences ($p < 0.05$) in their AM-694 content. Sample 1 analysis using (only) ^{1}H NMR spectroscopy, with maleic acid as IS, showed 57.0 ± 2.9 mg/g of plant material, compared to the value for Sample 2 of 37.5 ± 1.1 mg. That ^{1}H NMR quantification of Sample 2 was shown to be consistent when analysed by ^{1}H NMR spectroscopy against both maleic acid and 2-chloro-4-fluorotoluene as IS, and by ^{19}F q-NMR, and also in agreement with UHPLC results, showing no significant differences between these methods using Anova two-factor analysis ($p > 0.05$) (Table 27).
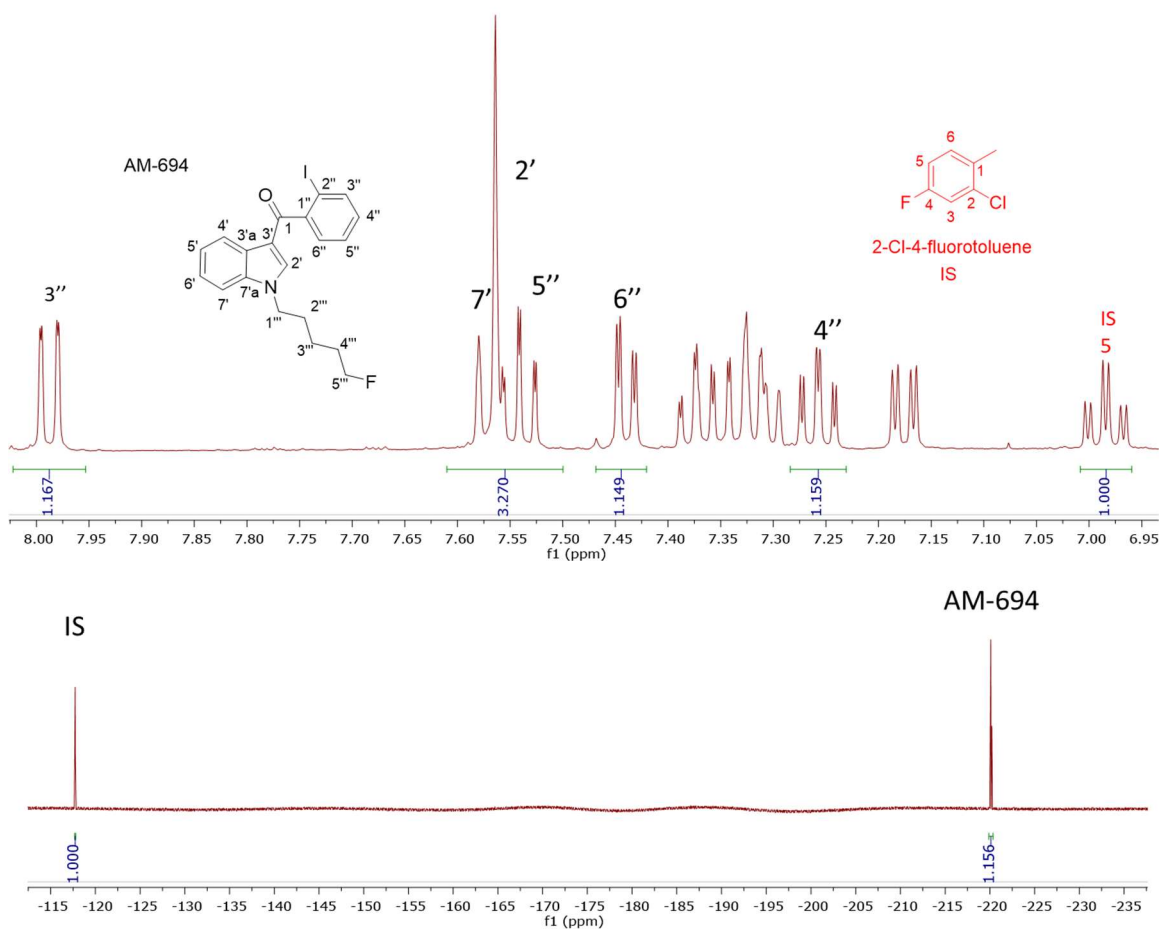
Figure 114. (Top) expansion of ^{1}H NMR aromatic region of AM-694 in CD$_3$OD showing signals used for quantification where the integration of the 2-chloro-4-fluorotoluene IS H5 signal (td) is normalized (1.00 H), (bottom) ^{19}F NMR signals of AM-694 at -220 ppm and the same IS ^{19}F signal at -117 ppm also normalized (1.00 F).

Table 27. Quantitative analysis of AM-694 in Loco elite herbal blends by ^{1}H and ^{19}F NMR, using maleic acid (MA) or 2-chloro-4-fluorotoluene as IS, and UHPLC (against JWH-018).

Analysis method (IS)	^{1}H (MA)	^{1}H (2-chloro-4-fluorotoluene)	^{19}F (2-chloro-4-fluorotoluene)	UHPLC (JWH-018)
Sample 1 (mg/g)[a]	57.0 ± 2.9	n.d.	n.d.	n.d.
RSD (%)	5.2	-	-	-
Sample 2 (mg/g)[a]	37.5 ± 1.1	36.7 ± 2.0	35.4 ± 0.6	38.4 ± 2.6
RSD (%)	3.0	5.4	1.7	6.6

[a] mg of AM-694 per gram of herbal sample.
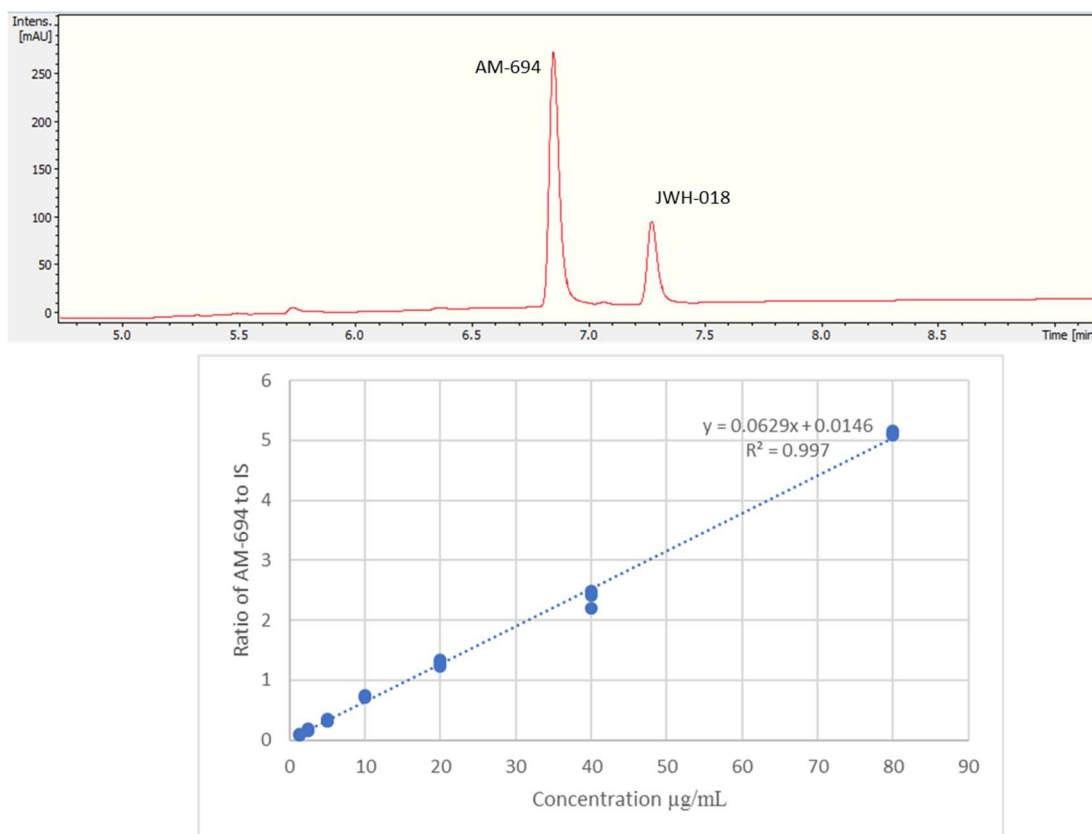
Figure 115. (Top) UHPLC chromatogram (λ = 254 nm) of AM-694 (RT = 6.9 min) and JWH-018 (RT = 7.3 min), (bottom) calibration curve of AM-694 against JWH-018 (IS), R^2 = 0.997.

In the ^{1}H NMR using 2-chloro-4-fluorotoluene as the IS, its H6 signal overlapped with 5′ of the indole and indazole SCA. Nevertheless, other SCA signals such as 4″, 6″, and 7′ were resolved and used as candidate quantitative signals in CD$_3$OD. 5-Fluoropentyl signals 1‴ and 5‴ were resolved when CDCl$_3$ or CD$_3$CN was used as the NMR solvent.

5.3.2 Combustion analysis of SCAs

Combustion analysis resulted in the recovery of all six SCAs tested by UHPLC/TOF-ESI-MS (AB-CHMINACA, AM-694, 5F-ADB, MDMB-CHMICA, MMB-2201, 5F-PB-22) (Figure 116). Three areas of the apparatus were tested for the presence of the SCA, trap 1, trap 2 and the combustion zone (CZ) in the quartz tube where the 200-300 mg cigarettes were fixed.

Most of the SCAs were detected in the first trap (80-90 %), interestingly no to very little SCAs were detected in the CZ, proving that the tested SCAs have a very good volatility. This is supporting evidence for reports of prisoners and prison guards being overcome by smoke inhalation in UK prisons.[136]
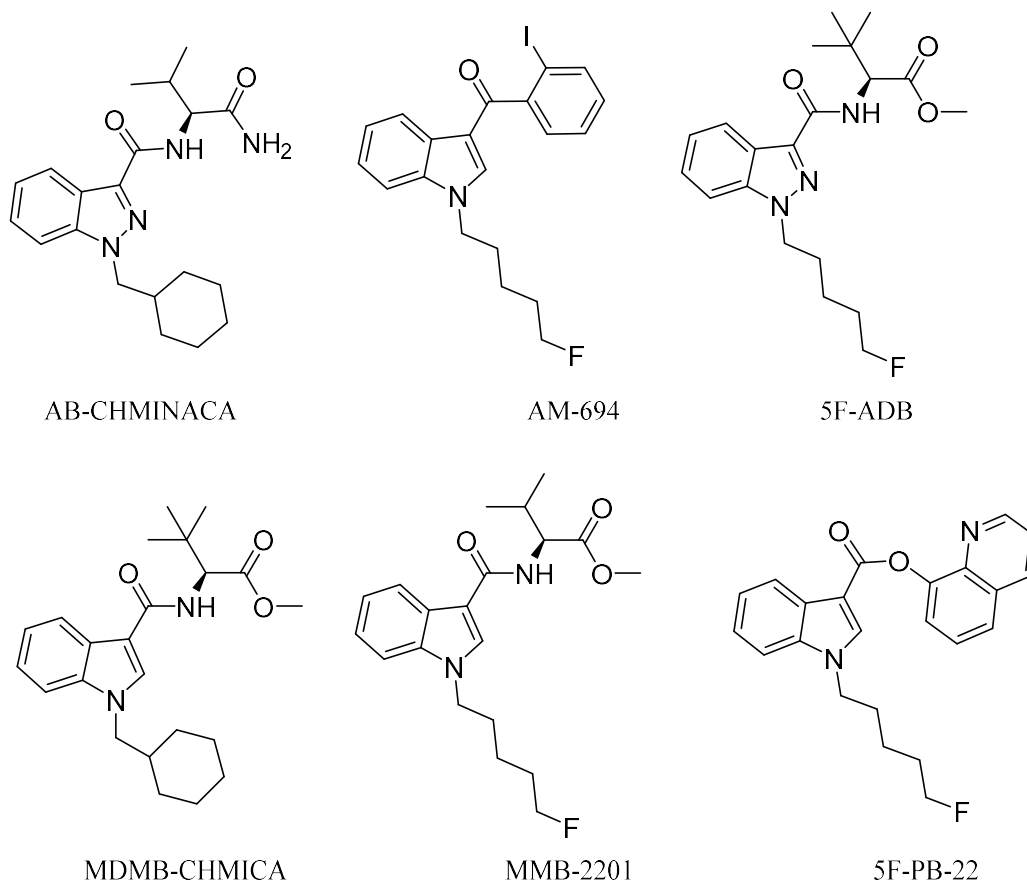
Figure 116. SCAs tested by combustion analysis.

Using gradient 3 for the UHPLC/TOF-ESI-MS/MS analysis resulted in the detection of the combustion samples of AB-CHMINACA, AM-694, 5F-ADB/MMB-2201 mixture, and 5F-PB-22 (Figure 117), with their mass ions and fragmentation pattern assignments confirmed by comparison with our in-house built database. GC/MS analysis resulted in the detection of the SCA in trap 1 as well as some combustion products from some of the SCA tested. 5F-PB-22 GC/MS combustion analysis resulted in the detection of 5F-PB-22 at RT = 8.20 min as well as the combustion products 1-(5-fluoropentyl)-indole (205 m/z) and 1-pentyl-indole (185 m/z) at RT = 5.71 min and RT = 6.15 min respectively (Figure 118).
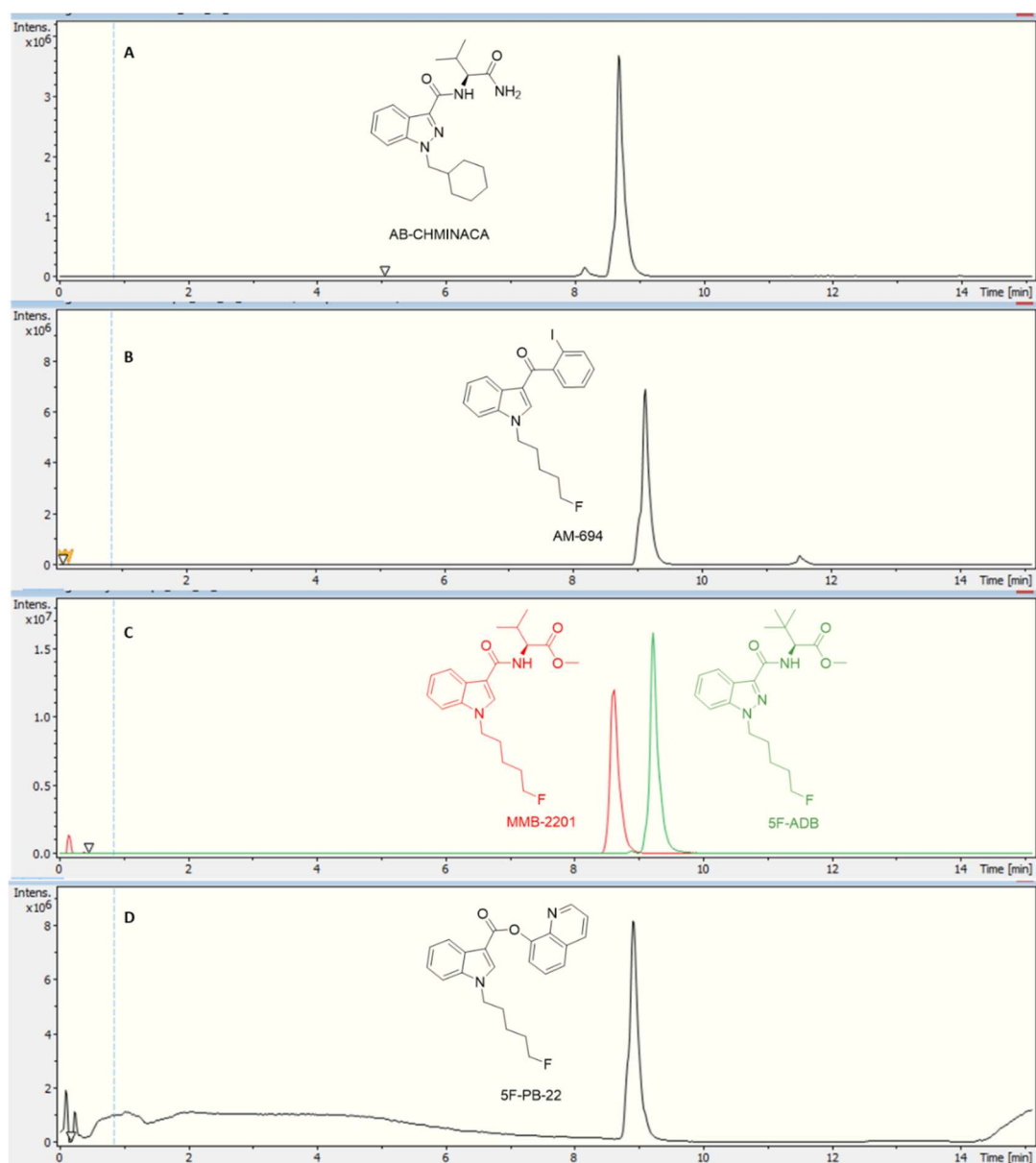
Figure 117. Combustion analysis chromatogram of trap 1 for (A) AB-CHMINACA RT = 8.7 min, (B) AM-694 RT = 9.1 min, (C) MMB-2201 RT = 8.6 min, 5F-ADB RT = 9.2 min, (D) 5F-PB-22 RT = 8.9 min.

MDMB-CHMICA combustion analysis resulted in the formation of a new, not previously reported, combustion product. Two peaks appear on the combustion sample TIC (Figure 119), MDMB-CHMICA RT = 11.74 min, and the novel combustion product (compound **7**) RT = 10.80 min, which was absent in the crude sample of MDMB-CHMICA that has not been subjected to combustion.
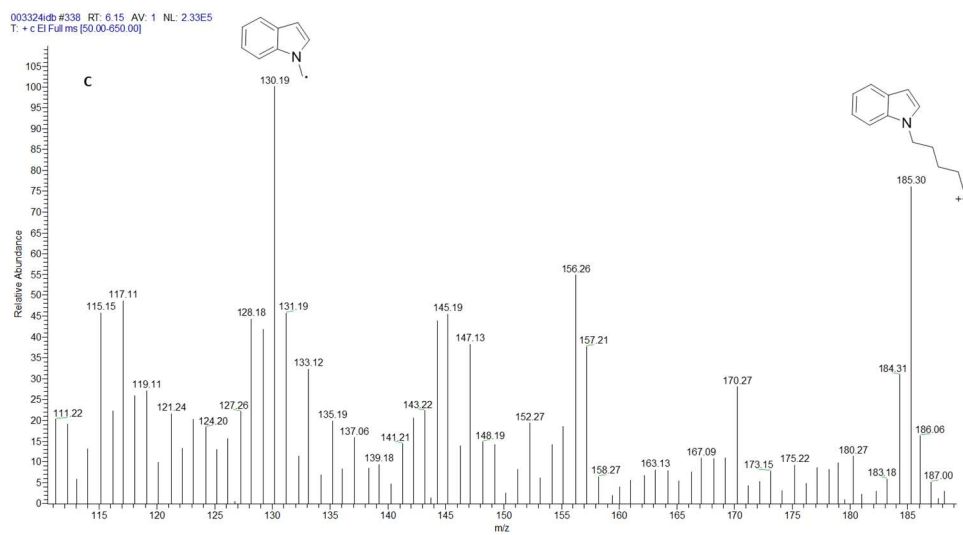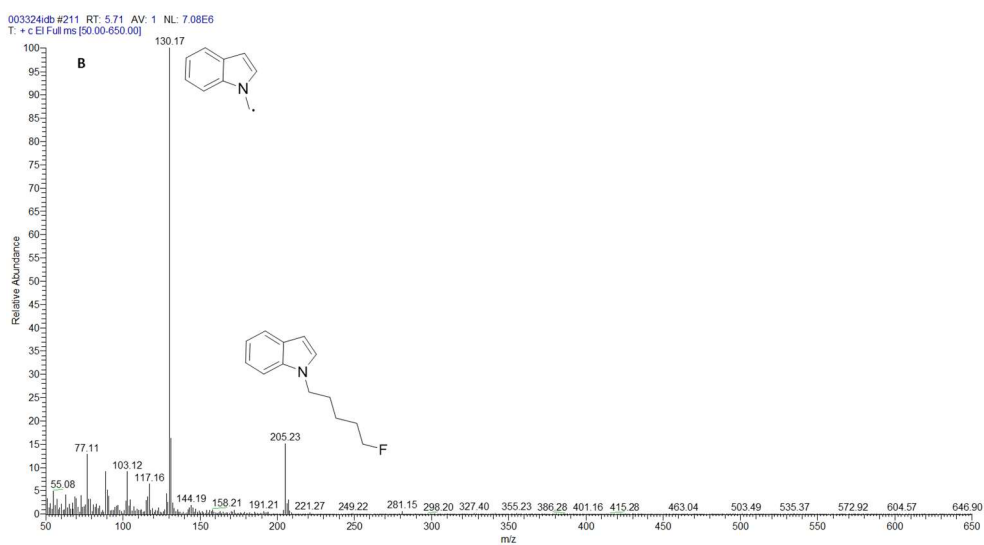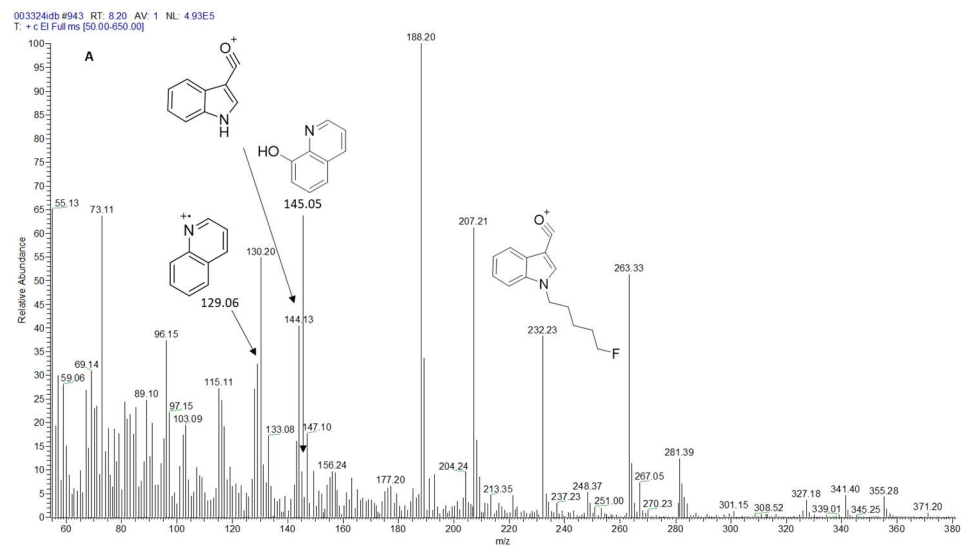
Figure 118. GC/MS EI spectra of (A) 5F-PB-22, (B) 1-(5F-pentyl)-indole, (C) 1-pentyl-

indole.

214
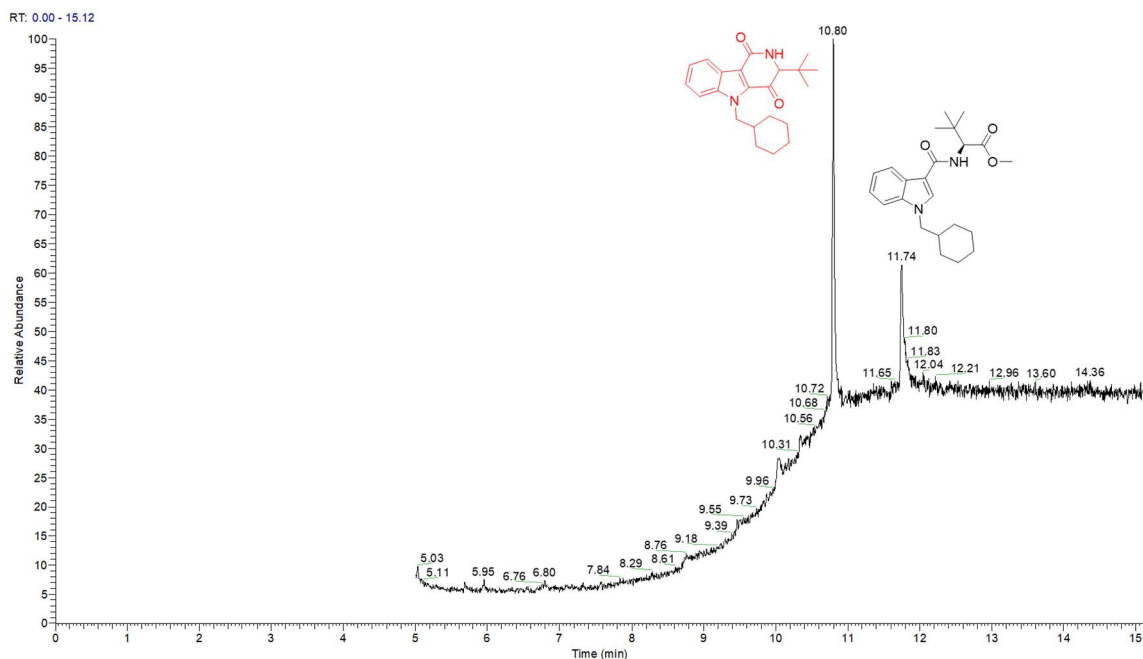
Figure 119. TIC of a combustion sample of MDMB-CHMICA showing the novel combustion product at RT = 10.80 min and MDMB-CHMICA at RT = 11.74 min.

MDMB-CHMICA EI MS afforded a more extensive and slightly different fragmentation than the ESI/MS/MS seen in section 4.3.4 (Figure 101B). The first fragment resulted from the cleavage of the *tert*-butyl side chain (328) rather than the initial loss of methoxy observed in the ESI-MS/MS. In addition to the 240 base peak, also seen in the MS/MS analysis, 245 is concluded to be the result of the loss of the *tert*-butyl side-chain along with the cleavage of the cyclohexyl moiety with the formation of 1-methylidene-indolinium ion (Figure 120). These results are in agreement with those of Langer *et al*.[266] The proposed mechanism for the formation of compound **7** is rearrangement involving intramolecular electrophilic substitution of indole by the terminal methyl ester of MDMB-CHMICA during the combustion process (Figures 120 and 121).

Unlike in the MS fragmentation pattern of MDMB-CHMICA, the 296 m/z peak is more intense and is the result of the formation of an indole-1-cyclohexylmethyl-*N*-propylidene ion, while the rest of the fragments are similar to MDMB-CHMICA with a base-peak fragment of 240 m/z. LC chromatographic separation and HR-MS molecular ion identification of compound **7** were confirmed using UHPLC/TOF-ESI-MS showing a low

intensity peak and [M+H]$^+$ for compound **7** at RT = 10.7 min, 353.2229 found for

C$_{22}$H$_{29}$N$_2$O$_2$ requires 353.2223, and MDMB-CHMICA RT = 9.7 min, [M+H]$^+$ 385.2493

found for C$_{23}$H$_{33}$N$_2$O$_3$ requires 385.2485 (Figure 122).
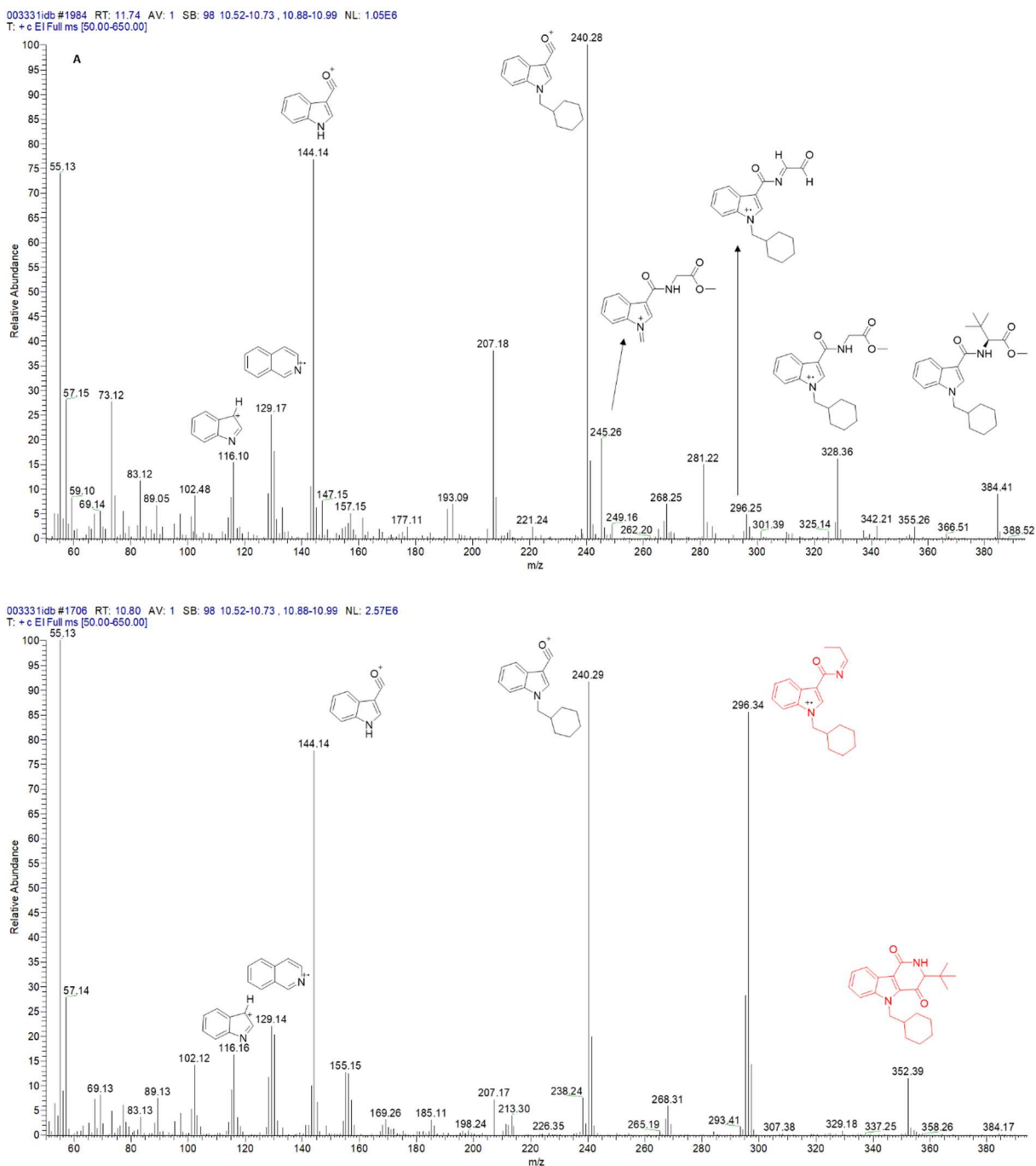
Figure 120. EI spectrum of (A) MDMB-CHMICA showing proposed fragmentation pattern

with assignments, (B) compound **7** with proposed fragmentation pattern and assignments.
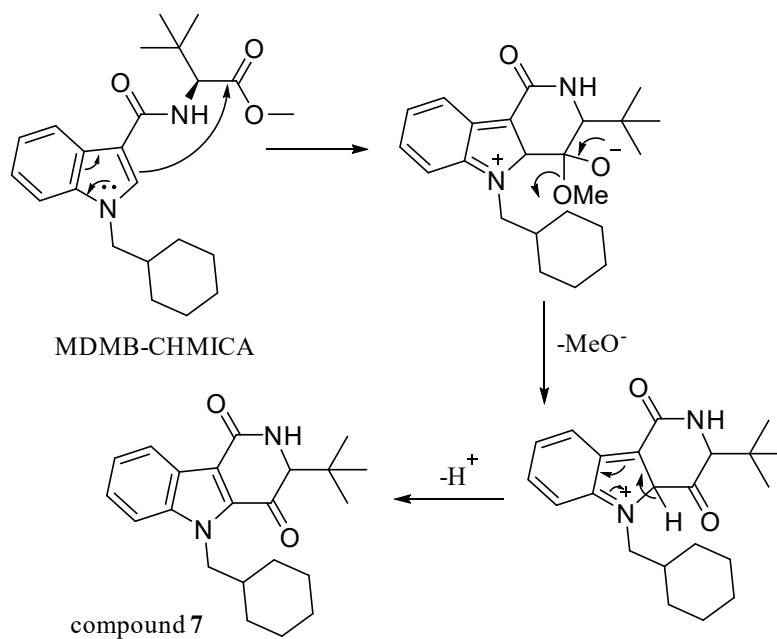
Figure 121. Proposed mechanism for the formation of combustion product compound **7**.
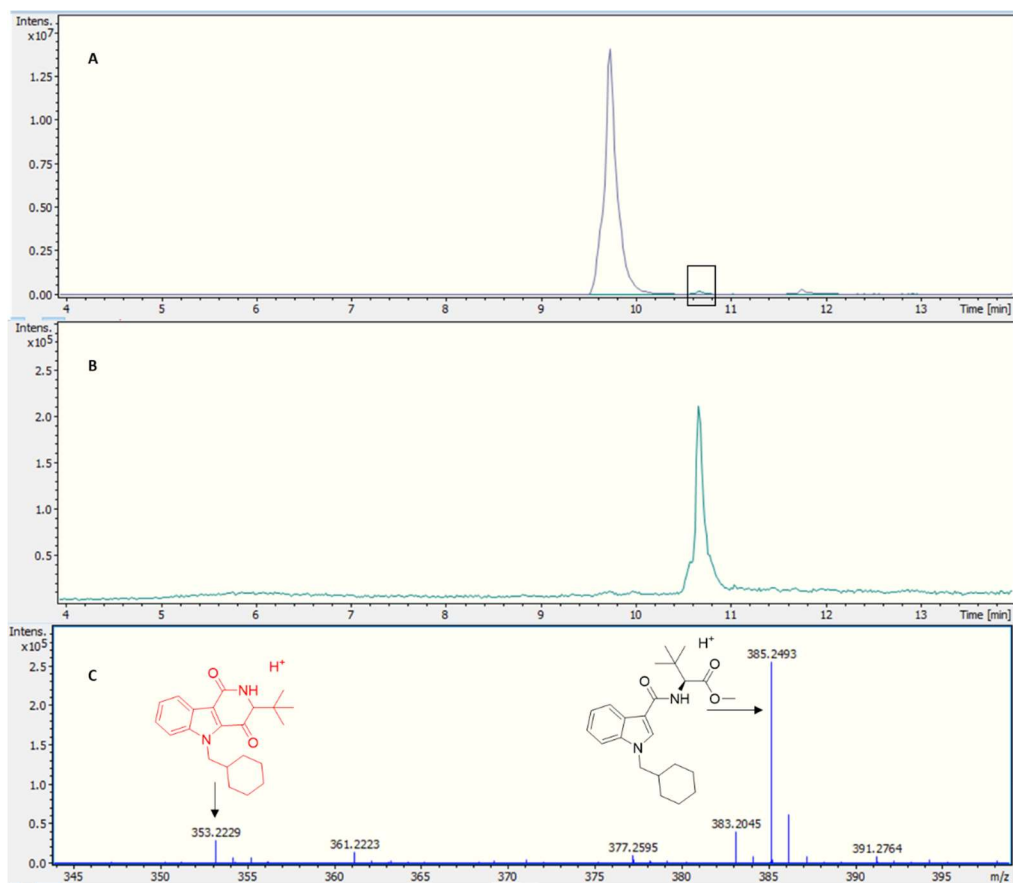
Figure 122. (A) UHPLC TIC of combustion sample of MDMB-CHMICA showing MDMB-CHMICA peak at 9.7 min, (B) expansion of compound **7** peak at 10.7 min, (C) ESI-MS spectrum showing both molecular ions.

5.4 Conclusions

In this chapter, fluorine (^{19}F) NMR spectroscopy has been applied for the first time to seized herbal blends containing fluorinated SCA to provide a fast (~8 min), accurate and robust quantitative analytical method with no background interference from the (plant material) matrix component. This analytical technique requires almost no method development (beyond the NMR acquisition parameters) compared to chromatographic methods. 2-Chloro-4-fluorotoluene was used as an IS in ^{19}F q-NMR, resulting in a method with close agreement to ^{1}H q-NMR results using two different IS, and cross-method confirmation using UHPLC.

Acquisition parameters such as the centre point of the spectra (O1P) and the relaxation delay have to be chosen carefully for accurate and precise outcomes. An inverse-gated decoupling NMR experiment was employed to improve the S/N ratio and to remove any NOE enhancement. This technique has the potential to be applied for the fast analysis of herbal blends sprayed with fluorinated SCA, especially with the recent increase in the occurrence of such fluorinated 3rd generation SCA, and without the need to resort to any lengthy chromatographic analysis. Analysis of packs containing 5F-ADB revealed quantitative differences between 2016 and 2017 seizures in the dose of 5F-ADB, with some packs having double the dose compared to others.

The in-house constructed SCA smoking simulator provided a good method for the recovery of combusted SCAs. SCAs showed good volatility with most of them being captured in the traps with little or no SCA left in the combustion zone (CZ) as tested by UHPLC/MS and GC/MS. GC/MS analysis revealed combustion products for 5F-PB-22. MDMB-CHMICA combustion sample GC/MS and UHPLC/ESI-MS analysis resulted in the detection of a novel combustion product, compound **7**.

This study of combustion products of SCAs provides markers which maybe useful for drug analysts and toxicologists in examining samples obtained from suspected SCA users. Thus, taken together, making reliable methods for the identification and quantification of substituted 3rd generation SCAs.

General Conclusions

In this research project, qualitative and quantitative analytical methods were developed for the chemical characterization and quantification of street-seized illicit drugs with a focus on NPS. All of the major classes of NPS were analysed, e.g. synthetic cannabinoids, cathinones, phenethylamines, arylcyclohexylamines, and phenidates. NPS represent a challenge to drug analysts and toxicologists worldwide, due to the frequent alteration in their chemical structure by the addition or removal of single or multiple substituents. This dynamic evolution makes them a moving target for which drug analysts need to develop new methods of analysis in order to stay ahead of the curve. Further complicating the analysis is the issue of purity. The presence of NPS in multiple components mixed together with benign cutting agents, which are added to make profit, makes for complex analytes. These sample therefore require more than one method for their characterization to obtain definite confirmation of their chemical structures. Drug analysis laboratories rely mainly on chromatographic methods coupled to MS for the daily analysis of seized samples. However, complex samples require the use of other techniques such as high-field NMR spectroscopy to provide assistance in resolving these mixtures and for the structural elucidation of novel compounds.

Multiple analytical techniques were used in these investigations, with a main focus on NMR spectroscopy for the characterization and quantification of street samples. Detailed quantitative NMR (q-NMR) analysis was applied to numerous samples, including complex ones requiring the use of different IS. Fast, accurate, and precise results comparable to those obtained by chromatographic and MS techniques were achieved, without the use of a high purity reference standard of the drug being investigated. Such reference standards are mostly not available in the case of NPS especially for the more recent generations of SCA.

The first part of this research project revolved around the analysis of night-club seizures from different parts of the South west of England especially concerning cathinones and phenethylamines. The analysis revealed a coexistence of MDMA, the most popular night-club drug, with other phenethylamines and cathinones, all of which have potent pharmacological profiles. 1D/2D NMR and q-NMR analysis allowed the structural

elucidation and quantification of complex MDMA/NPS/cutting agent samples. ^{1}H q-NMR

analysis of seized MDMA mixtures has not been reported before. Moreover, the use of a

HILIC column, which is often used for the analysis of high polarity compounds (amino acids)

coupled to MS, proved useful for the separation and identification of MDMA/cathinone

mixtures. A ^{1}H q-NMR-method was developed for the quantitative analysis of MDMA tablets

with confirmation of the method using UHPLC/UV and UHPLC/MS. The developed q-NMR

method resulted in good precision with advantages over chromatographic and MS techniques

such as the ability of applying q-NMR to detect and quantify impurities that lack a

chromophore (for UV/vis detection) or have poor ionization (for MS detection). This

application is the first q-NMR cross-method confirmed analytical study on MDMA tablets.

The quantitative analysis corroborated media accounts of high-dose MDMA tablets in

circulation, where 35% of the tablets were shown to contain double to more than double the

dose of MDMA for an adult, thus adding analytical evidence to media allegations. This

contributes to drug analysis by q-NMR method development for MDMA analysis. It can also

contribute to law enforcement and health officials being aware of the situation in night-club

venues. Cathinone and phenethylamine carbamate derivatives were made and analysed via

chromatographic and MS techniques, revealing an alteration in their polarity that allowed

separation and the formation of distinctive isotopic clusters as the result of the incorporation

of 3 chlorine atoms into their structure by making the trichloroethyl carbamate derivatives.

This analytical study allowed the chromatographic separation and identification of cathinones

and phenethylamines that usually have poor chromatography and non-distinctive MS

fragments, two of which (ethylone a cathinone and 2C-B a phenethylamine) are reported for

the first time.

    The second theme investigated in this research project is the arylcyclohexylamine

and phenidate category of NPS. The analysis revealed much more complex samples with 4-6

component mixtures, some of which were not detected by UHPLC/MS, e.g. dimethyl sulfone

(DMS), which was detected and quantified by NMR. Components of less than 1% in the

sample could not be easily detected by NMR. In these instances, UHPLC/TOF-ESI-MS/MS

proved invaluable for the confirmation of trace impurities that could arise from cross contamination. The presence of multiple samples containing the illicit drug ketamine along with its NPS analogues such as MXE and MXP are reported. Furthermore, NMR analysis of phenidate mixtures resulted in the detection of NPS from different families, MPA from phenethylamines and 5-MeO-DALT from tryptamines, along with compounds used as cutting agents, e.g. the excipient mannitol and the API benzocaine. Using maleic acid as an IS for q-NMR allowed the quantification of a mixture that contains a high polarity component (mannitol) without resorting to chromatographic techniques that require derivatization and the construction of a calibration curve for each component in the mixture.

In the following chapter, SCA characterization, structural elucidation and separation were achieved. SCAs are the number one class of NPS by frequency of seizures in Europe. They present many analytical challenges, mainly due to their structural complexity and the speed at which these NPS drugs are being altered, creating numerous analogues. The development of 3rd generation SCA that possess polar moieties makes their analysis different from the previous JWH and AM-series of low polarity. Therefore, an updated analytical protocol is urgently needed. 1D/2D NMR spectroscopy allowed the profiling of seized samples of SCA in attractively packaged brands. This is the first reported impurity profiling for SCA. Impurities such as propylene glycol, isopropyl alcohol and ethyl acetate were detected in SCA, either as additives or impurities arising from synthesis. The dispersive power of heteronuclear 2D NMR was employed for the characterization of SCA. ^{19}F-HOESY and ^{19}F-HMBC helped in the structural elucidation of fluorinated SCAs. HSQC-TOCSY allowed the separation of the cross-peak signals of each ^{1}H-^{13}C spin system, providing definitive confirmation in assigning the compound along with any impurities present. NMR ambiguities for AM-694 were clarified along with the first reported ^{15}N NMR data for AB-CHMINACA. These data are presented using nitromethane as an external reference standard. Derivatization of the impurities present such as propylene glycol using *p*-toluenesulfonyl isocyanate (PTSI) followed by UHPLC/ESI-MS analysis was achieved with 4 adducts formed, confirming the NMR results. Mislabelling was identified in all the packs of SCAs

analysed. This shows how misleading and how totally devoid of quality control is the illicit SCA market. Qualitative differences among packs seized in 2016 and 2017 were observed, the latter containing a more potent SCA. This could lead to drug user/abuser intoxication or even death due to the unintended intake of one or even 3 or 4 more powerful SCA.

The analytical characterization of prison (HMP) samples is described using ESI-MS for fast detection and confirmation of samples. This revealed that SCAs are popular in this particular prison. There are mixtures of SCAs that have no published pharmacological data, but are presumed to be potent by comparison to known close structural analogues. Analytical characterization of AMB-FUBINACA using 1D/2D NMR is reported using different deuterated solvents. A combination of ^{1}H-^{19}F decoupled and pure shift NMR spectroscopy was used for the first time to study the effects of the fluorine of 4-fluorobenzyl on its neighbouring protons, thus aiding in the structural elucidation of the novel SCA. The separating power of 2D DOSY NMR spectroscopy was employed for the profiling of complex samples of SCAs, based on their self-diffusion coefficient (D) resulting in excellent separation. No study has been published on the use of DOSY NMR for the analysis of SCA.

Six components of SCAs in "K2" packages of herbal blends were detected, separated and characterized using a protocol that was developed and is composed of UHPLC/TOF-ESI-MS/MS, flash column chromatography and 1D/2D NMR spectroscopy. This analytical platform achieved base-line separation of all components in under 8 min on the UHPLC/ESI-MS revealing an acid impurity (compound **2**), a potential by-product or precursor from the synthesis of the amide (compound **1**), reported for the first time, and the NMR characterization of compound **1** also reported for the first time. The developed flash column chromatography method allowed the separation of all detectable components in the mixture, providing drug analysts with a flash column chromatography method for the separation of recent 3rd generation SCAs with close structural similarities, with 1D/2D NMR spectroscopic characterization providing definitive confirmation of the compounds. This analysis also showed how the contents of the infamous "K2" packets evolved from 1st and 2nd generation SCA, to more recent SCAs, some of which have no published pharmacological data.

In the final chapter, the presence of terminally fluorinated SCA in the majority of the seized samples was exploited to develop the first reported quantitative ^{19}F-NMR method using 2-chloro-4-fluorotoluene as an IS for their quantification. This method gave a fast (8-10 min) and accurate analysis, achieving high precision results without any interference from the plant matrix components, *Turnera diffusa* (Damiana) or *Althaea officinalis* (marshmallow). q-^{19}F NMR spectroscopy was compared with the established analytical methods used in the pharmaceutical industry e.g. q-^{1}H NMR and UHPLC and gave results in excellent agreement. Furthermore, packages of similar brands of herbal blends containing 5F-ADB from seizures in different years (2016 and 2017) were quantitatively assayed using q-^{19}F NMR with cross-method confirmation. Some 2017 packages were shown to contain double the dose of 5F-ADB compared with the 2016 samples. The influence of the O1P (centre point of the spectra that defines the transmitter excitation) and of the NMR relaxation delays have been assessed and shown to have significant effects on the quantitative results. This will also provide aid to drug analysts working in NMR spectroscopic quantification of fluorinated compounds.

A smoking simulation apparatus was designed and constructed in-house to simulate the SCA smoking process. This allowed the recovery of SCAs that had been burnt in cigarettes as analysed by UHPLC/TOF-ESI-MS. The capturing of some combustion degradation products was established using GC/MS analysis. Additionally, the structure of a novel combustion product (compound **7**) is proposed, resulting from the combustion of MDMB-CHMICA. This proposed compound was detected by GC/MS and UHPLC/TOF-ESI-MS. Furthermore, little-to-no SCA was detected in the combustion zone, proving its good volatility, and adding weight to media reports of prisoners and prison guards being overcome by SCA smoke inhalation.

In conclusion, robust pharmaceutical analysis of illicit drugs and their cutting agents has been undertaken. This has resulted in new and potentially useful data for pharmaceutical analysts, forensic science, the Police and Prison Services, and for Accident and Emergency Staff of what drugs were in circulation in the South West in recent years.

References

1. The Psychoactive Substance Act (2016). Meaning of psychoactive substances. **2016**, available at: http://www.legislation.gov.uk/ukpga/2016/2/contents/enacted/data.htm. (accessed 24/03/19).

2. E. Wadsworth, C. Drummond, P. Deluca. The adherence to UK legislation by online shops selling new psychoactive substances. *Drugs Educ. Prev. Policy.* **2018**, 1, 97-100.

3. B. P. Smyth. New psychoactive substances in Ireland following the criminal justice (psychoactive substance) act - why all the pessimism? *Addiction*. **2017**, 112, 1686.

4. E. Wadsworth, C. Drummond, A. Kimergard, P. Deluca. A market on both "sides" of the law: The use of the hidden web for the sale of new psychoactive substances. *Psychopharmacol. Clin. Exp.* **2017**, 32, 1-7.

5. The Huffington Post online. Legal high ban is as bad as Tudor ban on Catholics says Ex-government advisor David Nutt. **2015**, available at: http://www.huffingtonpost.co.uk/2015/06/23/legal-high-ban-david-nutt_n_7645644.html. (accessed 24/03/19).

6. European Monitoring Centre for Drug and Drug Addiction (EMCDDA), Monitoring New Drugs. **2006**, available at: http://www.emcdda.europa.eu/system/files/publications/408/Monitoring_new_drugs_72902.pdf (accessed 24/03/19)

7. H. Chung, J. Lee, E. Kim. Trends of novel psychoactive substances (NPSs) and their fatal cases. *Forensic Toxicol.* **2016**, 34, 1-11.

8. European Monitoring Centre for Drug and Drug Addiction (EMCDDA), New Psychoactive Substances in Europe: An update from the EU Early Warning System. **2015,** available at: www.emcdda.europa.eu/system/files/publications/65/TD0415135ENN.pdf. (accessed 24/03/19).

9.   J. P. Smith, O. B. Sutcliffe, C. E. Banks. An overview of recent developments in the analytical detection of New Psychoactive Substances (NPSs). *Analyst*. **2015**, 140, 4932-4948.

10.   C. Soussan, A. Kjellgren. The users of Novel Psychoactive Substances: Online survey about their characteristics, attitudes and motivations. *Int. J. Drug Policy*. **2016**, 32, 77-84.

11.   European Commission Eurobar. Young People and Drugs Report. **2014**, available at: http://ec.europa.eu/public_opinion/flash/fl_401_en.pdf. (accessed 24/03/19).

12.   D. M. Wood, L. Hunter, F. Measham, P. I. Dargan. Limited use of novel psychoactive substances in South London nightclubs. *Q. J. Med*. **2012**, 105, 959-964.

13.   A. Shulgin, A. Shulgin. PIHKAL*:* A Chemical Love Story, Transform Press: Berkeley, California, **1991**.

14.   A. Shulgin, A. Shulgin. TIHKAL, The Continuation, Transform Press: Berkeley, California, **1997**.

15.   UNDOC laboratory and scientific section portal. Synthetic cathinones. **2018**, available at: https://www.unodc.org/LSS/SubstanceGroup/Details/67b1ba69-1253-4ae9-bd93-fed1ae8e6802 (accessed 24/03/19).

16.   J. S. B. Sanchez. Sur un homologue de l'ephedrine. *Bull. Soc. Chim. France*. **1929**, 45, 284-286.

17.   V. Auwarter, S. Dresen, W. Weinmann, M. Muller, M. Putz, N. Ferreiros. Spice and other herbal blends: harmless incense or cannabinoid designer drugs? *J. Mass Spectrom*. **2009**, 44, 832-837.

18.   Scientific Working Group for the Analysis of Seized Drugs (SWGDRUG) recommendations. **2011**, available at: file:///G:/Introduction%20of%20thesis/SWGDRUG%20Recommendations%206.pdf. (accessed 24/03/19).

19.   A. D. Krikorian. Khat and its use: An historical perspective. *J. Ethnopharmacol*. **1984**, 12, 115-178.

20. O. Wolfes. Uber das Vorkommen von d-nor-iso-Ephedrin in *Catha edulis*. *Arch. der Pharmazie*. **1930**, 268, 81-83.

21. D. W. Peterson, C. K. Maitai, S. B. Sparler, Relative potencies of two phenylalkylamines found in the abused plant *Catha edulis*, khat. *Life Sci.* **1980**, 27, 2143-2147.

22. J. F. Hyde, E. Browning, R. Adams. Synthetic homologs of d,l-ephedrine. *J. Am. Chem. Soc.* **1928**, 50, 2287-2292.

23. N. V. Cozzi, K. F. Foley. Methcathinone is a substrate for the serotonin uptake transporter. *Pharmacol. Toxicol.* **2003**, 93, 219-225.

24. J. DeRuiter, L. Hayes, A. Valaer, C. R. Clarke. Methcathinone and designer analogues: synthesis, stereochemical analysis, and analytical properties. *J. Chromatogr. Sci.* **1994**, 32, 552-564.

25. D. Gustavsson, C. Escher. Mephedrone-Internet drug which seems to have come and stay. Fatal cases in Sweden have drawn attention to previously unknown substance. *Lakartidningen*. **2009**, 106, 2769-2771.

26. A. R. Winstock, L. R. Mitcheson, P. Deluca, Z. Davey, O. Corazza, F. Schifano, Mephedrone, new kid for the chop? *Addiction*. **2010**, 106, 154-161.

27. B. Miserez, O. Ayrton, J. Ramsey. Analysis of purity and cutting agents in street mephedrone samples from South Wales. *Forensic Toxicol.* **2014**, 32, 305-310.

28. J. P. Kelly**.** Cathinone derivatives: A review of their chemistry, pharmacology and toxicology. *Drug Test. Anal.* **2011**, 3, 439-453. DOI 10.1002/dta.313.

29. C. Liu, W. Jia, T. Li, Z. Hua, Z. Qian. Identification and analytical characterization of nine synthetic cathinone derivatives *N*-ethylhexedrone, 4-Cl-pentedrone, 4-Cl-alpha-EAPP, propylone, *N*-ethylnorpentylone, 6-MeO-bk-MDMA, alpha-PiHP, 4-Cl-alpha-PHP, and 4-F-alpha-PHP. *Drug Test. Anal.* **2016**. DOI 10.1002/dta.2136.

30. M. R. Alotaibi, S. M. Husbands, I. S. Blagbrough. ^{1}H, ^{13}C, ^{15}N HMBC and ^{19}F NMR spectroscopic characterization of seized flephedrone, cut with benzocaine. *J. Pharm. Biomed. Anal.* **2015**, 107, 535-538.

31. C. Pifl, H. Reither, O. Hornykiewicz. The profile of mephedrone on human monoamine transporters differs from 3,4-methylenedioxymethamphetamine primarily by lower potency at the vesicular monoamine transporter. *Eur. J. Pharmacol.* **2015**, 755, 119-126.

32. Home Office UK. Seizures of Drugs in England and Wales, financial year ending 2017. Statistical bulletin. **2017**, available at: https://www.gov.uk/government/uploads/system/uploads/attachment_data/file/657872/seizures-drugs-mar2017-hosb2217.pdf. (accessed 24/03/19).

33. T. Passie, U. Benzenhöfer. The History of MDMA as an Underground Drug in the United States, 1960-1979. *J. Psychoactive Drugs.* **2016**, 48, 67-75.

34. V. R. Sreenivasan. Problems in identification of methylenedioxy and methoxy amphetamines. *J. Criminal Law*. **1972**, 63, 304-312.

35. N. Vogels, T. M. Brunt, S. Rigter, P. V. Dijk, H. Vervaeke, R. J. M. Niesink. Content of ecstasy in The Netherlands: 1993-2008. *Addiction*. **2009**, 104, 2057-2066.

36. 2006 World Drug Report. United Nations Office on Drugs and Crime, volume 1. **2006**, available at: https://www.unodc.org/pdf/WDR_2006/wdr2006_volume1.pdf. (accessed 24/03/19).

37. The Phenom Penh Post. "Lack of safrole can't stop the menace". **2015**, available at: http://www.phnompenhpost.com/national/lack-safrole-cant-stop-menace (accessed 24/03/19).

38. M. Collins, A. Heagney, F. Cordaro, D. Odgers, G. Tarrant, S. Stewart. Methyl 3-[3',4'-(methylenedioxy)phenyl]-2-methyl glycidate: an ecstasy precursor seized in Sydney, Australia. *J. Forensic Sci.* **2007**, 52, 898-903.

39. EMCDDA. European Drug Report 2017. Trends and developments. available at: http://www.emcdda.europa.eu/system/files/publications/4541/TDAT17001ENN.pdf. (accessed 24/03/19).

40. L. A. King. New phenylethylamines in Europe. *Drug Test. Anal.* **2013**. DOI 10.1002/dta.1570.

41. C. D. Rosenbaum, S. P. Carreiro, K. M. Babu. Here today, gone tomorrow and back again? a review of herbal marijuana alternatives (K2, Spice), synthetic cathinones (bath salts), kratom, *Salvia divinorum*, methoxetamine, and piperazines. *J. Med. Toxicol.* **2012**, 8, 15-32.

42. D. D. Torrance. (2010) MixMag drugs survey. Mix Mag 225, 53.

43   E. F. Domino. Taming the ketamine tiger. *Anesthesiology*. **2010**, 113, 678-684.

44. R. B. Rothman, A. A. Reid, J. A. Monn, A. E. Jacobson, K. C. Rice. The psychotomimetic drug phencyclidine labels two high affinity binding sites in guinea pig brain: Evidence for n-methyl-d-aspartate coupled and dopamine reuptake carrier-associated phencyclidine binding sites. *Mol. Pharmacol.* **1989**, 36, 887-896.

45. V. H. Maddox. The historical development of phencyclidine, in PCP (Phencyclidine): Historical and Current Perspectives. (Ed: E. Domino). NPP Books: Michigan, **1981**, pp. 1-8.

46. G. Corssen and E. F. Domino. Dissociative anaesthesia: further pharmacologic studies and first clinical experience with the phencyclidine derivative CI-581. *Anesth. Analg.* **1966**, 45, 29-40.

47. C. E. Reier. Ketamine-" dissociative agent" or hallucinogen? *New Engl. J. Med.* **1971**, 284, 791-792.

48. G. D. Lundberg, R. C. Gupta, S. H. Montgomery. Phencyclidine: Patterns seen in street drug analysis. *Clin. Toxicol.* **1976**, 9, 503-511.

49. P.S. Chu, S. C. Kwok, K. Lam, T. Chu, S. W. Chan, C. Man, W. Ma, K. Chui, M. Yiu, Y. Chan. Street ketamine'-associated bladder dysfunction: A report of ten cases. *Hong Kong Med. J.* **2007**, 13, 311-313.

50. T. E. Freese, K. Miotto, C. J. Redback. The effects and consequences of selected club drugs. *J. Subst. Abuse Treat*. **2002**, 23, 151-156.

51. Bluelight.com, Welcome to the big and dandy methoxetamine thread. **2010**, available at: http://www.bluelight.org/vb/threads/524290-The-Big-amp-Dandy-

Methoxetamine(2-(3-methoxyphenyl)-2-(ethylamino)cyclohexanone)-Thread.
(accessed 24/03/19).

52. H. Morris, Vice online. Interview with a ketamine Chemist. **2011**, available at:
https://www.vice.com/en_uk/read/interview-with-ketamine-chemist-704-v18n2.
(accessed 24/03/19).

53. P. A. Hays, J. F. Casale, A. L. Berrier. The characterization of 2-(3-methoxyphenyl)-2-
(ethylamino)cyclohexanone (Methoxetamine). *Micro. J.* **2012**, 9, 3-17.

54. P. I. Dargan, H. C. Tang, W. Liang, D. M. Wood, D. T. Yew. Three months of
methoxetamine administration is associated with significant bladder and renal toxicity
in mice. *Clin. Toxicol.* **2014**, 52, 176-180.

55. European Monitoring Centre for Drug and Drug Addiction (EMCDDA). Risk
assessments. Report on the risk assessment of 2-(3-methoxyphenyl)-2-(ethylamino)
cyclohexanone (methoxetamine) in the framework of the Council Decision on new
psychoactive substances. **2014**, available at:
http://www.emcdda.europa.eu/attachements.cfm/att_228264_EN_TDAK14004ENN.p
df. (accessed 24/03/19).

56. R. A. Glennon, M. Titeler, J. D. McKenny. Evidence for 5-HT2 involvement in the
mechanism of action of hallucinogenic agents. *Life Sci*. **1984**, 35, 2505-2511.

57. A. M. Araújo, F. Carvalho, M. L. Bastos, P. G. Pinho, M. Carvalho. The
hallucinogenic world of tryptamines: an updated review. *Arch. Toxicol.* **2015**, 89,
1151-1173.

58. E. Tanaka, T. Kamata, M. Katagi, H. Tsuchihashi, K. Honda. A fatal poisoning with 5-
methoxy-*N*,*N*-diisopropyltryptamine, Foxy. *Forensic Sci. Int*. **2006,** 163,152-154.

59. D. M. Boland, W. Andollo, G. W. Hime, W. L. Hearn. Fatality due to acute alpha-
methyltryptamine intoxication. *J. Anal. Toxicol.* **2005**, 29, 394-397.

60. J. M. Corkery, E. Durkin, S. Elliott, F. Schifano, A. H. Ghodse. The recreational
tryptamine 5-MeO-DALT (*N*,*N*-diallyl-5-methoxytryptamine): a brief review. *Prog.*
Neuropsychopharmacol. Biol. Psychiatry. **2012**, 39, 259-262.

61. S. J. Gatley, D. Pan, R. Chen, G. Chaturvedi, Y. S. Ding. Affinities of methylphenidate derivatives for dopamine, norepinephrine and serotonin transporters. *Life Sci.* **1996**, 58, 231-239.

62. R. C. Spencer, D. M. Devilbiss, C. W. Berridge. The cognition-enhancing effects of psychostimulants involve direct action in the prefrontal cortex. *Biol. Psychiatry.* **2015**, 77, 940-950.

63. J. S. Markowitz, B. K. Logan, F. Diamond, K. S. Patrick. Detection of the novel metabolite ethylphenidate after methylphenidate overdose with alcohol coingestion. *J. Clin. Psychopharm.* **1999**, 19, 362-366.

64. L. Iversen, Advisory Council on the Misuse of Drugs (ACMD). Methylphenidate-based NPS. **2015**. available at: https://www.gov.uk/government/uploads/system/uploads/attachment_data/file/420983/TCDO_methylphenidate_NPS.pdf. (accessed 24/03/19).

65. J. Krueger, H. Sachs, F. Musshoff, T. Dameb, J. Schaeper, M. Schwerer, M. Graw, G. Roider. First detection of ethylphenidate in human fatalities after ethylphenidate intake. *Forensic Sci. Int.* **2014**, 243, 126-129.

66. C. Parks, D. McKeown, H. J. Torrance. A review of ethylphenidate in deaths in East and West Scotland. *Forensic Sci. Int.* **2015**, 257, 203-208.

67. H. Klare, J. M. Neudörfl, S. D. Brandt, E. Mischler, S. M. Giebing, K. Deluweit, F. Westphald. T. Laussmann. Analysis of six 'neuro-enhancing' phenidate analogs. *Drug Test. Anal.* **2017**, DOI 10.1002/dta.2161.

68. D. S. Isenschmid. Cocaine in: Wiley Encyclopedia of Forensic Science, John Wiley and Sons, New York, **2009**.

69. K. C. Lee, B. Ladizinski, D. G. Federman. Complications associated with use of levamisole-contaminated cocaine: an emerging public health challenge. *Mayo Clin. Proc.* **2012**, 87, 581-586.

70. A. M. Valentino, K. Fuentecilla. Levamisole: An analytical profile. *Micro. J.* **2005**, 3, 134-137.

71. J. F. Casale, E. M. Corbeil, P. A. Hays. Identification of levamisole impurities found in cocaine exhibits. *Micro. J.* **200**8, 6, 82-89.

72. U. S. Department of Justice National Drug Intelligence Centre. National drug threat assessment 2011: Impact of drugs on society. Sec 2.25-2.26, available at: https://www.justice.gov/archive/ndic/ndic-moved.html (accessed 24/03/19).

73. N. Fucci. Unusual adulterants in cocaine seizured on Italian clandestine market. *Forensic Sci. Int.* **2007**, 172, 1.

74. S. Schneider, F. Meys. Analysis of illicit cocaine and heroin samples seized in Luxembourg from 2005-2010. *Forensic Sci. Int.*, **2011**, 212, 242-246.

75. A. Larocque, R. S. Hoffman. Levamisole in cocaine: Unexpected news from an old acquaintance. *Clin. Toxicol.* **2012**, 50, 231-241.

76. J. A. Buchanan, J. A. Vogel, A. M. Eberhardt. Levamisole-induced occlusive necrotizing vasculitis of the ears after use of cocaine contaminated with levamisole. *J. Med. Toxicol.* **2011**, 7, 83-84.

77. M. H. Clausen, S. Kneisel, B. Szabo, V. Auwarter. Acute toxicity due to the confirmed consumption of synthetic cannabinoids: Clinical and laboratory findings. *Addiction.* **2013**, 108, 534-544.

78. S. D. Banister, M. Moir, J. Stuart, R. C. Kevin, K. E. Wood, M. Longworth, S. M. Wilkinson, C. Beinat, A. S. Buchanan, M. Glass, M. Connor, I. S. McGregor, M. Kassiou. Pharmacology of indole and indazole synthetic cannabinoid designer drugs AB-FUBINACA, ADB-FUBINACA, AB-PINACA, ADBPINACA, 5F-AB-PINACA, 5F-ADB-PINACA, ADBICA, and 5F-ADBICA. *ACS Chem. Neurosci.* **2015**, 6, 1546-1559.

79. J. W. Huffman, D. Dai, B. R. Martin, D. R. Compton. Design, synthesis, and pharmacology of cannabimimetic indoles. *Bioorg. Med. Chem. Lett.* **1994**, 4, 563-566.

80. V. Auwarter, S. Dresen, W. Weinmann, M. Muller, M. Putz, N. Ferreiros. 'Spice' and other herbal blends: Harmless incense or cannabinoid designer drugs? *J. Mass Spectrom.* **2009**, 44, 832-837.

81. L. Iversen and S. Gibbons, Advisory Council on the Misuse of Drugs (ACMD), Third generation synthetic cannabinoids. **2014**, 1-29, available at: https://www.gov.uk/government/uploads/system/uploads/attachment_data/file/380161/CannabinoidsReport.pdf. (accessed 24/03/19).

82. F. Sjöqvist, M. Garle, A. Rane. Use of doping agents, particularly anabolic steroids, in sports and society. *Lancet*. **2008**, 371, 1872-1882.

83. T. Sobolevsky, G. Krotov, M. Dikunets, M. Nikitina, E. Mochalova, G. Rodchenkov. Anti-doping analyses at the Sochi Olympic and Paralympic Games 2014. *Drug Test. Anal*. **2014**, DOI 10.1002/dta.1734.

84. The Guardian, Russia accused of athletics doping cover-up on German TV. **2014**, available at: https://www.theguardian.com/sport/2014/dec/03/russia-accused-athletics-doping-cover-up-olympics. (accessed 24/03/19)

85. The New York Times, Russian Insider Says State-Run Doping Fuelled Olympic Gold. **2016**, available at: https://www.nytimes.com/2016/05/13/sports/russia-doping-sochi-olympics-2014.html. (accessed 24/03/19).

86. R. H. McLaren. WADA investigation of Sochi allegations. **2016**, available at: https://www.wada-ama.org/sites/default/files/resources/files/mclaren_report_part_ii_2.pdf. (accessed 24/03/19).

87. Olympics International Committee (IOC). IOC sanctions four Russian athletes as part of Oswald Commission findings. **2017**, available at: https://www.olympic.org/news/ioc-sanctions-four-russian-athletes-as-part-of-oswald-commission-findings-2017-11-24. (accessed 24/03/19).

88. BBC. Russian doping: IOC bans Russia from 2018 Winter Olympics. **2017**, available at: https://www.bbc.co.uk/sport/winter-sports/42242007. (accessed 24/03/19).

89. The Guardian. Manchester lab's drug tests may have been manipulated. **2017**, available at: https://www.theguardian.com/uk-news/2017/feb/19/manchester-lab-randox-drink-drug-tests-toxicology-may-have-been-manipulated. (accessed 24/03/19).

90. BBC. Drug-driving cases dropped over forensics. **2017**, available at: http://www.bbc.co.uk/news/uk-42067094. (accessed 24/03/19).

91. Chemistry World. Misconduct scandal hits UK forensics lab. **2017**, available at: https://www.chemistryworld.com/news/misconduct-scandal-hits-uk-forensics-lab/3008372.article. (accessed 24/03/19).

92. The Home Office's oversight of forensic services, Dec 2014. available at: https://www.nao.org.uk/wp-content/uploads/2015/01/The-Home-Office's-oversight-of-forensic-services.pdf. (accessed 24/03/19).

93. BBC. New forensic science service planned. **2016**, available at: http://www.bbc.co.uk/news/uk-35793073. (24/03/19).

94. The Washington Post. True crime. Mass. crime chemist admits daily drug use in lab, sparking a second scandal. **2016**. available at: https://www.washingtonpost.com/news/true-crime/wp/2016/05/05/mass-crime-chemist-admits-daily-drug-use-in-lab-sparking-a-second-scandal/?utm_term=.b421f3b8326a. (accessed 24/03/19).

95. M. J. Brownstein. A brief history of opiates, opioid peptides, and opioid receptors. *Proc. Natl. Acad. Sci.* **1993**, 90, 5391-5393.

96. Erowid. Opium-Poppy Cultivation, Morphine, and Heroin Manufacture. **2005**, available at: https://www.erowid.org/archive/rhodium/chemistry/opium.html. (accessed 24/03/19).

97. United Nations Office on Drugs and Crime (UNODC). World drug report 2010, available at: file:///G:/Introduction%20of%20thesis/opioids/World_Drug_Report_2010_lo-res.pdf. (accessed 24/03/19).

98. United Nations Office on Drug Control and Crime (2003). Global Impact of the Ban on Opium Production in Afghanistan. Vienna: United Nations. Available at: https://www.unodc.org/documents/afghanistan/Counter_Narcotics/The_Opium_Economy_in_Afghanistan_-_2003.pdf. (accessed 24/03/19).

99. BBC. Trump: Opioid 'national shame' a public health emergency. **2017**, available at: http://www.bbc.co.uk/news/world-us-canada-41756705. (accessed 24/03/19).

100. Centre for Disease Control and Prevention (CDC). Drug overdose death data. **2018**, available at: https://www.cdc.gov/drugoverdose/data/statedeaths.html. (accessed 24/03/19).

101. National Institute of Drug Abuse (NIDA). Statement from the NIH director on combating the opioid crisis with scientific solutions. **2017**, available at: https://www.nih.gov/about-nih/who-we-are/nih-director/statements/statement-nih-director-combating-opioid-crisis-scientific-solutions. (accessed 24/03/ 19).

102. The Surgeon General's Report on Alcohol, Drugs and Health, Facing Addiction in America. P 14, **2016**, available at: https://addiction.surgeongeneral.gov/surgeon-generals-report.pdf. (accessed 24/03/19).

103. J. Porter, H. Jick. Addiction rare in patients treated with narcotics. *N. Engl. J. Med.*, **1980**, 302, 123.

104. BBC Opioid crisis: The letter that started it all. **2017**. available at: http://www.bbc.co.uk/news/world-us-canada-40136881. (accessed 24/03/19).

105. P. T. M. Leung, E. M. Macdonald, M. B. Standbrook, I. A. Dhalla, D. M. Juurlink. A 1980 Letter on the risk of opioid addiction. *N. Engl. J. Med.* **2017**, 376, 2194-2195.

106. T. C. Kram, D. A. Cooper, A. C. Allen. Behind the identification of China White. *Anal. Chem.* **1981**, 53 1379A-1386A.

107. T. J. Gillespie, A. J. Gandolfi, T. P. Davis, R. A. Morano. Identification and quantification of alpha-methylfentanyl in post mortem specimens. *J. Anal. Toxicol.*, **1982**, 6, 139-142.

108. J. F. Casale, J. R. Mallette, E. M. Guest. Analysis of illicit carfentanil: Emergence of the death dragon. *Forensic Chem.* **2017**, 3, 74-80.

109. CBS news, fentanyl drives another record year of overdose deaths in Ohio, **2017**, available at: https://www.cbsnews.com/news/fentanyl-drives-another-record-year-of-overdose-deaths-in-ohio/. (accessed 24/03/19).

110. The Independent. 27 people suffers heroin overdose in small West Virginia town in just four hours. **2016**, available at:

http://www.independent.co.uk/news/world/americas/heroin-deaths-virginia-27-overdoses-in-4-hours-huntington-city-fairfax-county-a7197476.html. (accessed 24/03/19).

111. Centre for Disease Control and Prevention (CDC). Opioid Overdose Outbreak - West Virginia, August 2016, available at:

https://www.cdc.gov/mmwr/volumes/66/wr/mm6637a3.htm. (accessed 24/03/19).

112. J. R. Riches, R. W. Read, R. M. Black, N. J. Cooper, C. M. Timperley. Analysis of clothing and urine from Moscow theatre siege casualties reveals carfentanil and remifentanil use. *J. Anal. Toxicol.* **2012**, 36, 647-656.

113. J. Massey, M, Kilkenny, S. Batdorf, S. K. Sanders, D. Ellison, J. Halpin, R. M. Gladden, D. Bixler, L. Haddy, R. Gupta. Opioid Overdose Outbreak - West Virginia, August 2016. *MMWR Morb. Mortal. Wkly. Rep.* **2017**, 66, 975-980.

114. The Times, Drug Caution: Britain must not follow America into an opioid addiction crisis. **2017**, available at: https://www.thetimes.co.uk/article/drug-caution-kb0pvgvwz. (accessed 24/03/19).

115. National Crime Agency (NCA), Recent deaths possibly linked to fentanyl. Apr 2017, available at: http://www.nationalcrimeagency.gov.uk/publications/795-recent-deaths-possibly-linked-to-fentanyl/file. (accessed 24/03/19).

116. The Guardian. Three men jailed for running cannabis factory in ex-nuclear bunker. **2107**, available at: https://www.theguardian.com/uk-news/2017/aug/11/three-men-jailed-cannabis-factory-nuclear-bunker. (accessed 24/03/19).

117. S. T. Wilkinson, S. Yarnell, R. Radhakrishnan, S. A. Ball, D. C. D'Souza. Marijuana legalization: Impact on physicians and public health. *Annu. Rev. Med.* **2016**, 67, 453-466.

118. O. Fernandez. THC:CBD in daily practice: Available data from UK, Germany and Spain. *Eur. Neurol.* **2016**, 75, 1-3.

119. T. J. Nurmikko, M. G. Serpell, B. Hoggart, P. J. Toomey, B. J. Morlion, D. Haines. Sativex successfully treats neuropathic pain characterised by allodynia: A randomised, double-blind, placebo-controlled clinical trial. *Pain.* **2007**, 133, 210-220.

120. G. S. Yacoubian. Assessing the relationship between marijuana availability and marijuana use: a legal and sociological comparison between the United States and the Netherlands. *J. Alcohol Drug Educ.* **2007**, 51, 17-34.

121. C. Cox. The Canadian Cannabis Act legalizes and regulates recreational cannabis use in 2018. *Health Policy.* **2018**, 122, 205-209.

122. A. Woodak. For and against cannabis control: Costs outweigh the benefits. *BMJ.* **2002**, 324, 105-106.

123. C. Palmer. Key themes and research agendas in the sport-alcohol nexus. *J. Sport Soc. Issues*. **211**, 35, 168-185.

124. D. J. Nutt, L. A. King, L. D. Phillip. Drug harms in the UK: a multicriteria decision analysis. *Lancet*. **2010**, 376, 1558-1565.

125. National Institute of Health (NIH). A multi-site phase 3 study of MDMA-assisted psychotherapy for PTSD. **2019**, available at: https://clinicaltrials.gov/ct2/show/NCT03537014. (accessed 24/03/19).

126. B. Sessa. Why MDMA therapy for alcohol use disorder? And why now? *Neuropharmacology*. **2018**, 142, 83-88.

127. A. O'Hagan. Behind Bars: The Truth about Drugs in Prisons. *Forensic Res. Criminol. Int. J.* **2017**, 5, 1-12.

128. S. Fazel, P. Bains, H. Doll. Substance abuse and dependence in prisoners: A systematic review. *Addiction*. **2005**, 101, 181–191.

129. M. Chambers. Policy exchange. Coming clean: Combating drug misuse in prisons. **2010**, available at: https://www.policyexchange.org.uk/wp-content/uploads/2016/09/coming-clean-jun-10.pdf. (accessed 24/03/19).

130. HM Chief Inspector of Prisons in England and Wales, Annual report 2011-2012, available at: http://www.justice.gov.uk/downloads/publications/corporate-reports/hmi-prisons/hm-inspectorate-prisons-annual-report-2011-12.pdf. (accessed 24/03/19).

131. HM Chief Inspector of Prisons in England and Wales, Annual report 2013-2014, available at: https://www.justiceinspectorates.gov.uk/hmiprisons/wp-content/uploads/sites/4/2014/10/HMIP-AR_2013-14.pdf. (accessed 24/03/19).

132. The Centre for Social Justice, Drugs in prisons. **2015**, available at: https://www.centreforsocialjustice.org.uk/core/wp-content/uploads/2016/08/CSJJ3090_Drugs_in_Prison.pdf. (accessed 24/03/19).

133. HM Inspectorate of Prisons in England and Wales Annual Report 2015-16, available at: https://www.justiceinspectorates.gov.uk/hmiprisons/media/press-releases/2016/07/hm-inspectorate-of-prisons-annual-report-201516-prisons-unacceptably-violent-and-dangerous-warns-chief-inspector/. (accessed 24/03/19).

134. BBC. Legal highs' linked to a number of prison deaths. **2015**, available at: http://www.bbc.co.uk/news/uk-33412838. (accessed 24/03/19).

135. BBC. Reporting undercover from the prison front line. **2017**, available at: http://www.bbc.co.uk/news/uk-38931583. (accessed 24/03/19).

136. C. Howgego. The Guardian. Prisoners say spice use has tripled fuelling violence, illness and debt. **2016**, available at: https://www.theguardian.com/society/2016/jun/01/prisoners-reveal-regular-spice-use-tripled-legal-high-violence-illness-debt. (accessed 24/03/19).

137. The Guardian. Two people die in suspected spice-related incidents. **2107**, available at: https://www.theguardian.com/society/2017/apr/27/two-people-die-in-suspected-spice-related-incidents. (accessed 24/03/19).

138. United States Drug Enforcement Agency (DEA). The National Drug Threat Assessment Summery. **2015**, available at: https://www.dea.gov/docs/2015%20NDTA%20Report.pdf. (accessed 24/03/19).

139. R. Ralphs, L. Williams, R. Askew, A. Norton. Adding spice to the porridge: The development of a synthetic cannabinoid market in an English prison. *Int. J. Drug Policy*. **2017**, 40, 57-69.

140. D. Perrone, R. D. Helgesen, R. G. Fischer. United States drug prohibition and legal highs: How drug testing may lead cannabis users to spice. *Drugs Educ. Prev. Polic*. **2013**, 20, 216-224.

141. Mayo Clinic Medical Laboratories. Drug Testing: An Overview of Mayo Clinic Tests Designed for Detecting Drug Abuse. **2016**; 1-29, available at: https://www.mayomedicallaboratories.com/test-info/drug-book/pod/DrugBook.pdf. (accessed 24/03/19).

142. BBC news. Drones seized over HMP Pentonville carrying drugs and phones. **2017**, available at: www.bbc.co.uk/news/uk-england-london-37152665. (accessed24/03/19).

143. K. C. Ninic, K. Jejcic, E. Glavnik, M. Pustoslemsek. Use of new synthetic drugs in Slovenian prisons. *Eur. Psychiatry*. **2017**, 41S, S583-S644.

144. United States Drug Enforcement Agency (DEA). DEA history book 1985-1990. **1990**, available at: https://web.archive.org/web/20060823024931/http://www.usdoj.gov/dea/pubs/history/1985-1990.html. (accessed 24/03/19).

145. United Nations Office on Drugs and Crime (UNODC). Economic and social consequences of drug abuse and illicit trafficking. **1998**. https://www.unodc.org/pdf/technical_series_1998-01-01_1.pdf. (accessed 24/03/19).

146. R. A. Goldstein, C. DesLauriers, A. M. Burda. Cocaine: History, Social Implications, and Toxicity-A Review. *Dis. Mon*. **2009**, 55, 6-38.

147. R. K. Seigel. Cocaine and the privileged class. *Adv. Alcohol Subst. Abuse*. **1984**, 4, 37-49.

148. S. B. Karch. Cocaine: history, use, abuse. *J. R. Soc. Med*. **1999**, 92, 393-397.

149. United Nations Office on Drugs and Crime (UNODC). Coca cultivation in the Andean region. **2008**, at: https://www.unodc.org/documents/crop-monitoring/Andean_report_2008.pdf. (accessed 24/03/19).

150. C. M. Shanti, C. E. Lucas. Cocaine and the critical care challenge. *Crit. Care Med.* **2003**, 31, 1851-1859.

151. D. K. Hatsukami, M. W. Fischman. Crack cocaine and cocaine hydrochloride. Are the differences myth or reality? *JAMA*. **1996**, 276, 1580-1588.

152. E. J. Nestler. Historical review: Molecular and cellular mechanisms of opiate and cocaine addiction. *Trends Pharmacol. Sci*. **2004**, 25, 210-218.

153. United Nations Office for Drug and Crime (UNODC). Cocaine. **2009**, available at: https://www.unodc.org/documents/data-and-analysis/tocta/4.Cocaine.pdf. (accessed 24/03/19).

154. J. Hargraves, K. Smith. Home Office UK. Seizures of drugs in England and Wales year ending 31 March 2016, available at: file:///G:/HAN%20Thesis%20Introduction/cocaine/seizures-drugs-hosb1316.pdf. (accessed24/03/19).

155. BBC. Spain cocaine seizure: Drug disguised as wooden pallets. **2015**, available at: http://www.bbc.co.uk/news/world-europe-35082219. (accessed 24/03/19).

156. BBC. £500m drugs bust in North Sea 'UK's biggest ever. **2015**, available at: http://www.bbc.co.uk/news/uk-scotland-north-east-orkney-shetland-32533478. (accessed 24/03/19).

157. Sky news. Brits Arrested Over Cocaine Disguised as Wood. **2015**, available at: http://news.sky.com/story/1604635/brits-arrested-over-cocaine-disguised-as-wood. (accessed 24/03/19).

158. Daily Mail online. Britons arrested after drugs gang disguised £240 Million haul of cocaine as wood and charcoal 'bound for the UK'. **2015**, available at: http://www.dailymail.co.uk/news/article-3358023/Britons-arrested-drugs-gang-

disguised-240-MILLION-haul-cocaine-wood-charcoal-bound-UK.html. (accessed 24/03/19).

159. L. King. Drug content of powders and other illicit preparations in the UK. *Forensic Sci. Int*. 1997, **85**, 135-147.

160. BBC. Huge cocaine haul seized in tugboat in Atlantic. **2017**, available at: http://www.bbc.co.uk/news/world-europe-41542224. (accessed 24/03/19).

161. Home Office and London Drugs Policy Forum in partnership with Release. Safer Clubbing: Guidance for Licensing Authorities, Club Managers and Promoters. **2002**, available at: https://www.nwleics.gov.uk/files/documents/safer_clubbing_guide/Safer%20Clubbing%20Guide.pdf. (Accessed 24/03/19).

162. BBC news beat. Six UK music festivals are to allow drug testing including Reading and Leeds. **2017**, available at: http://www.bbc.co.uk/newsbeat/article/39996522/six-uk-music-festivals-are-to-allow-drug-testing-including-reading-and-leeds. (accessed 24/03/19).

163. Somerset Live. Glastonbury 2017: Will the festival take part in drugs testing like Secret Garden Party? **2017**, available at: http://www.somersetlive.co.uk/whats-on/whats-on-news/glastonbury-2017-festival-take-part-99669. (accessed 24/03/19).

164. Royal Society for Public Health (RSPH). Let festival-goers and clubbers test their drugs to reduce harm. **2017**, available at: https://www.rsph.org.uk/about-us/news/let-festival-goers-and-clubbers-test-their-drugs-to-reduce-harm.html. (accessed 24/03/19).

165. The Guardian. Secret Garden Party pioneers drugs testing service for festivalgoers. **2016**, available at: https://www.theguardian.com/society/2016/jul/24/secret-garden-party-pioneers-drugs-testing-for-festival-goers. (accessed 24/03/19).

166. S. L. Kenyon, J. D. Ramsey, T. Lee, A. Johnston, D. W. Holt. Analysis for identification in amnesty bin samples from dance venues. *Ther. Drug Monit.* **2005**, 27, 793-798.

167. M. C. Van Hout, E. Hearne. New psychoactive substances (NPS) on cryptomarket fora: An exploratory study of characteristics of forum activity between NPS buyers and vendors. *Int. J. Drug Policy*. **2017**, 40, 102-110.

168. B. J. Longman. BBC. The growing popularity and potency of ecstasy and MDMA. **2016**, available at: http://www.bbc.co.uk/news/uk-37156380. (accessed 24/03/19).

169. D. M. Wood, J. Button, T. Ashraf, S. Walker, S. L. Greene, N. Drake, J. Ramsey, D. W. Holt, P. I. Dargan. What evidence is there that the UK should tackle the potential emerging threat of methamphetamine toxicity rather than established recreational drugs such as MDMA ('ecstasy')? *Q. J. Med*. **2008**, 101, 207-213.

170. BBC. Man dies after taking 'potent' MDMA drug in Oldham. **2107**, available at: http://www.bbc.co.uk/news/uk-england-manchester-40402468. (accessed 24/03/19).

171. BBC. Sheffield student Joana Burns died after taking ecstasy. **2017**, available at: http://www.bbc.co.uk/news/uk-england-south-yorkshire-40473232. (accessed 24/03/19).

172. BBC. Boy dies taking MDMA at Ilfracombe youth disco. 2017, available at: http://www.bbc.co.uk/news/uk-england-devon-40075962. (accessed 24/03/19).

173. A. Nagesh. Metro. Girls, 12, who took ecstasy pills told they were sweets. **2016**, available at: http://metro.co.uk/2016/06/21/girls-12-who-took-ecstasy-pills-told-they-were-sweets-5957954/. (accessed 24/03/19).

174. Office for National Statistics (ONS), Deaths Related to Drug Poisoning, England and Wales. **2017**, available at: https://www.ons.gov.uk/peoplepopulationandcommunity/birthsdeathsandmarriages/deaths/datasets/deathsrelatedtodrugpoisoningenglandandwalesreferencetable. (accessed 24/03/19).

175. Office for National Statistics (ONS), Deaths involving legal highs in England and Wales: between 2004 and 2013. **2016**, available at: https://www.ons.gov.uk/peoplepopulationandcommunity/birthsdeathsandmarriages/dea

ths/articles/deathsinvolvinglegalhighsinenglandandwales/between2004and2013.

(accessed 24/03/19).

176. S. Elliot, J. Evans. A 3-year review of New Psychoactive Substances in casework. *Forensic Sci. Int.* **2014**, 243, 55-60.

177. S. A. Turris, A. Lund. Mortality at Music Festivals: Academic and Grey Literature for Case Finding. *Prehosp. Disaster. Med.* **2017**, 32, 58-63.

178. J. J. Palamar, P. Acosta, S. Sherman, D. C. Ompad, C. M. Cleland. Self-reported use of novel psychoactive substances among attendees of electronic dance music venues. *Am. J. Drug Alcohol Abuse*. **2016**, 42, 624-632.

179. A. Ridpath, C. R. Driver, M. L. Nolan, A. Karpati, D. Kass, D. Paone, A. Jakubowski, R. S. Hoffman, L. S. Nelson, H. V. Kunins. Illnesses and deaths among persons attending an electronic dance-music festival - New York City, 2013. *Morb. Mortal. Wkly. Rep*. **2014**, 63, 1195-1198.

180. A. L. A. Mohr, M. Friscia, J. K. Yeakel, B. K. Logan. Use of synthetic stimulants and hallucinogens in a cohort of electronic dance music festival attendees. *Forensic Sci. Int.* **2018**, 282, 168-178.

181. D. Lee, C. W. Chronister, J. Hoyer, B. A. Goldberger. Ethylone-related deaths: Toxicological findings. *J. Anal. Toxicol*. **2015**, 39, 567-571.

182. Cancer Research UK. Lung cancer statistics. **2017**, available at: http://www.cancerresearchuk.org/health-professional/cancer-statistics/statistics-by-cancer-type/lung-cancer#heading-One. (accessed 24/03/19).

183. Office for National Statistics (ONS). Adult smoking habits in the UK 2015. **2015**, available at: https://www.ons.gov.uk/peoplepopulationandcommunity/healthandsocialcare/healthand lifeexpectancies/bulletins/adultsmokinghabitsingreatbritain/2015. (accessed 24/03/19).

184. C. Callum, S. Boyle, A. Sandford. Estimating the cost of smoking to the NHS in England and the impact of declining prevalence. *Health Econ. Policy Law.* **2011**, 6, 489-508.

185. HM Archives. HM revenues and Customs receipts. **2014**, available at: http://webarchive.nationalarchives.gov.uk/20140111082948/http://www.hmrc.gov.uk/statistics/receipts/receipts-stats.pdf (accessed 24/03/19).

186. Drinkaware. Consequences: Adult drinking in the UK. **2017**, available at: https://www.drinkaware.co.uk/research/data/consequences/ (accessed24/03/19).

187. Alcohol Concern. Alcohol statistics. **2016**, available at: https://www.alcoholconcern.org.uk/alcohol-statistics. (accessed 24/03/19).

188. Office for National Statistics (ONS). Crime statistics: Nature of crime tables, 2015/16 - violent crime. **2016**, available at: https://www.ons.gov.uk/file?uri=/peoplepopulationandcommunity/crimeandjustice/datasets/natureofcrimetablesviolence/yearendingmarch2016/natureofcrimetablesyearendingmarch2016violence.xls. (accessed 24/03/19).

189. R. Williams, R. Aspinall, M. Bellis, G, Campus-walsh, M. Cramp, A. Dhawan, J. Ferguson, D. Forton, G. Foster, I. Gilmore, M. Hickman, M. Hudson, D. Kelly, A. Langford, M. Lombard, L. Longworth, N. Martin, K. Moriarty, P. Newsome, J. O'Grady, R. Pryke, H. Rutter, S. Ryder, N. Sheron, T. Smith. Addressing liver disease in the UK: a blueprint for attaining excellence in health care and reducing premature mortality from lifestyle issues of excess consumption of alcohol, obesity, and viral hepatitis. *Lancet.* **2014**, 384, 1953-1997.

190. D. J. Nutt. Equasy - An overlooked addiction with implications for the current debate on drug harms. *J. Psychopharmacol.* **2009**, 23, 3-5.

191. Australian National Council on Drugs (ANCD). Young people's opinions on alcohol and other drug issues. Drug policy modelling program, national drug and alcohol research centre University of New South Wales. **2013**, available at: https://ndarc.med.unsw.edu.au/sites/default/files/newsevents/events/RP27-young-peoples-opinions.pdf. (accessed 24/03/19).

192. J. Schneider, P. Galettis, M. Williams, C. Lucas, J. H. Martin. Pill testing at music festivals: can we do more harm? *Intern. Med. J.* **2016**, 46, 1249-1251.

193. European Monitoring Centre for Drug and Drug Addiction (EMCDDA). European drug report trends and developments. **2018**. Available at http://www.emcdda.europa.eu/system/files/publications/8585/20181816_TDAT18001 ENN_PDF.pdf. (accessed 24/03/19).

194. L. J. De Felice, R. A. Glennon, S. S. Negus. Synthetic cathinones: chemical phylogeny, physiology, and neuropharmacology. *Life Sci*. **2014**, 97, 20-26.

195. M. L. Banks, T. J. Worst, D. E. Rusyniak, J. E. Sprague. Synthetic cathinones ("bath salts"). *J. Emerg. Med*. **2014**, 46, 632-642.

196. P. Armenian, T. M. Mamantov, B. T. Tsutaoka, R. R. Gerona, E. F. Silamn, A. H. Wu, K. R. Olson. Multiple MDMA (Ecstasy) overdoses at a rave event: A case series. *J. Intensive Care Med*. **2012**, 28, 252-258.

197. D. Zuba, B. Byrska. Analysis of the prevalence and coexistence of synthetic cannabinoids in "herbal high" products in Poland. *Forensic Toxicol*. **2013**, 31, 21-30.

198. P. A. Hays. Proton nuclear magnetic resonance spectroscopy (NMR) methods for determining the purity of reference drug standards and illicit forensic drug seizures. *J. Forensic Sci*. **2005**, 50, 1342-1360.

199. F. Malz, H. Jancke. Validation of quantitative NMR. *J. Pharm. Biomed. Anal*. **2005**, 38, 813-823.

200. U. Holzgrabe. Quantitative NMR spectroscopy in pharmaceutical applications. *Prog. Nucl. Magn. Reason. Spectrosc*. **2010**, 57, 229-240.

201. J. L. Jungnickel, J. W. Forbes. Quantitative measurement of hydrogen types by integrated nuclear magnetic resonance intensities. *Anal. Chem.***1963**, 35, 938-942.

202. D. P. Hollis. Quantitative analysis of aspirin, phenacetin, and caffeine mixtures by nuclear magnetic resonance spectrometry. *Anal. Chem.***1963**, 35, 1682–1684.

203. L. Barantin, A. L. Pape, S. Akoka. A new method for absolute quantitation MRS metabolites. *Magn. Reson. Med*. **1997**, 38, 179-182.

204. S. Akoka, L. Barantin, M. Trierweiler. Concentration measurement by proton NMR using the ERETIC method. *Anal. Chem*. **1999**, 71, 2554-2557.

205. S. Akoka, M. Trierweiler. Improvement of the ERETIC method by digital synthesis of the signal and addition of a broadband antenna inside the NMR probe. *Instrum. Sci. Technol.* **2002**, 30, 21-29.

206. M. Bernstein. What is qNMR and why is it important? **2012**. https://resources.mestrelab.com/what-is-qnmr/.

207. R. D. Farrant, J. C. Hollerton, S. M. Lynn, S. Provera, P. J. Sidebottom, R. J. Upton. NMR quantification using an artificial signal. *Magn. Reson. Chem.* **2010**, 48, 753-762.

208. I. B. Muller, C. N. Windberg. Validation of an HPLC method for quantitation of MDMA in tablets. *J. Chromatogr. Sci*. **2005**, 43, 434-437.

209. G. Frison, M. Gregio, L. Zamengo, F. Zancanaro, S. Frasson, R. Sciarrone. Gas chromatography/mass spectrometry determination of mephedrone in drug seizures after derivatization with 2,2,2-trichloroethyl chloroformate. *Rapid Commun. Mass Spectrom*. **2011**, 25, 387-390.

210. G. Frison, S. Odoardi, S. Frasson, et al. Characterization of the designer drug bk-2C-B (2-amino-1-(bromo-dimethoxyphenyl)ethan-1-one) by gas chromatography/mass spectrometry without and with derivatization with 2,2,2-trichloroethyl chloroformate, liquid chromatography/high-resolution mass spectrometry, and nuclear magnetic resonance. *Rapid Commun. Mass Spectrom*. **2015**, 29, 1196-1204.

211. Y. P. G. Chandra, A. R. Shetty, S. H. Jayanth, B. S. Hugar, S. Praveen, S. Harish. A death due to ecstasy - a case report. *Med. Legal J*. **2016**, 84, 46-48.

212. R. C. Cookson, T. A. Crabb. Geminal coupling constants in methylene groups alpha to nitrogen and oxygen atoms in 5- and 6-membered ring compounds. *Tetrahedron*. **1967**, 24, 2385-2397.

213. L. Bijlsma, J. V. Sancho, F. Hernández, W. M. A. Niessen. Fragmentation pathways of drugs of abuse and their metabolites based on QTOF MS/MS and MSE accurate-mass spectra. *J. Mass Spectrom*. **2011**, 46, 865-875.

214. L. A. Reitzel, P. W. Dalsgaard, I. B. Müller, C. Cornett. Identification of ten new designer drugs by GC-MS, UPLC-QTOF-MS, and NMR as part of a police investigation of a Danish Internet company. *Drug Test. Anal*. **2011**, 4, 342-354.

215. S. Elliott, C. Smith. Investigation of the first deaths in the United Kingdom involving the detection and quantitation of the piperazines BZP and 3-TFMPP. *J. Anal. Toxicol*. **2008**, 32, 172-177.

216. M. Johansson, D. Fransson, T. Rundlof, N. H. Huynh, T. Arvidsson. A general analytical platform and strategy in search for illegal drugs. *J. Pharm. Biomed. Anal*. **2014**, 100, 215-229.

217. European Network of Forensic Science Institutes-Drug Working Group. Guidelines on sampling of illicit drugs for quantitative analysis. **2014**. Available at file:///G:/HAN%20Thesis%20Introduction/guidelines_quant_sampling_dwg_printing_vf4.pdf (accessed 24/03/19).

218. G. Maniara, K. Rajamoorthi, S. Rajan, G. W. Stockton. Method performance and validation for quantitative analysis by ^{1}H and ^{31}P NMR spectroscopy. Applications to analytical standards and agricultural chemicals. *Anal. Chem*. **1998**, 70, 4921-4928.

219. H. H. Gadape, K. S. Parikh. Quantitative determination and validation of Metformin hydrochloride in pharmaceutical using quantitative nuclear magnetic resonance Spectroscopy. *E. J. Chem*. **2011**, 8, 767-781.

220. P. Gimeno, F. Besacier, M. Bottex, L. Dujourdy, H. Chaudron-Thozet. A study of impurities in intermediates and 3,4-methylenedioxymethamphetamine (MDMA) samples produced via reductive amination routes. *Forensic Sci. Int*. **2005**, 155, 141-157.

221. SWGDRUG monograph. MDDMA. **2014**. Available at http://www.swgdrug.org/Monographs/mddma.pdf. (accessed 24/03/19).

222. L. R. Togni, R. Lanaro, R. R. Resende, J. L. Costa. The variability of ecstasy tablets composition in Brazil. *J. Forensic Sci*. **2014**, 60, 147-151.

223. K. Kanai, K. Takekawa, T. Kumamoto, T. Ishikawa, T. Ohmori. Simultaneous analysis of six phenethylamine-type designer drugs by TLC, LC-MS, and GC-MS. *Forensic Toxicol*. **2008**, 26, 6-12.

224. L. Hermle, M. Spitzer, D. Borchardt, K.-A. Kovar, E. Gouzoulis. Psychological Effects of MDE in Normal Subjects. Are entactogens a new class of psychoactive agents? *Neuropsychopharmacol*. **1993**, 8, 171-176.

225. I. B. Müller, C. N. Windberg. Validation of an HPLC method for quantitation of MDMA in tablets. *J. Chromatogr. Sci*. **2005**, 43, 434-437.

226. N. S. Almeida, L. E. C. Benedito, A. O. Maldaner, A. L. d. Oliveira. A validated NMR approach for MDMA quantification in ecstasy tablets. *J. Braz. Chem. Soc.* **2018**, 29, 1944-1950.

227. S. Wang, M. Cyronak, E. Yang. Does a stable isotopically labelled internal standard always correct analyte response? A matrix effect study on a LC/MS/MS method for the determination of carvedilol enantiomers in human plasma. *J. Pharm. Biomed. Anal*. **2007**, 43, 701-707.

228. A. S. Davison, A. M. Milan, J. J. Dutton. Potential problems with using deuterated internal standards for liquid chromatography-tandem mass spectrometry. *Ann. Clin. Biochem*. **2013**, 50, 274-274.

229. Sigma-Adrich. Quantitative NMR: Technical details and TraceCERT certified reference materials. **2017**. Available at https://www.sigmaaldrich.com/content/dam/sigma-aldrich/docs/Sigma-Aldrich/Brochure/1/qnmr-brochure-rjo.pdf (accessed 24/03/19)

230. European monitoring Centre for Drug and Drug Addiction (EMCDDA). Recent changes in Europe's MDMA/ecstasy market. **2016**. Available at http://www.emcdda.europa.eu/system/files/publications/2473/TD0116348ENN.pdf (accessed 24/03/19).

231. European monitoring Centre for Drug and Drug Addiction (EMCDDA). Methylenedioxymethamphetamine (MDMA or 'Ecstasy') drug profile. **2015**. Available at http://www.emcdda.europa.eu/publications/drug-profiles/mdma (accessed 24/03/19).

232. J. Sitkowski, L. Stefaniak, L. Nicol, M. L. Martin, G. J. Martin, G. A. Webb. Complete assignments of the 1H, 13C and 15N NMR spectra of caffeine. *Spectrochim. Acta.* **1995**, 51, 839-841.

233. S. Kerrigan, M. Savage, C. Cavazos, P. Bella. Thermal degradation of synthetic cathinones: Implications for forensic toxicology. *J. Anal. Toxicol.* **2016**, 40, 1-11.

234. L. T. Sein. Using Punnett squares to facilitate students understanding of isotopic distributions in mass spectrometry. *J. Chem. Educ.* **2006**, 83, 228.

235. C. Giroud, M. Augsburger, L. Rivier, P. Mangin, F. Sadeghipour, E. Varesio, J. L. Veuthey. P. Kamalaprija. 2C-B: A new psychoactive phenylethylamine recently discovered in ecstasy tablets sold on the Swiss black market. *J. Anal. Toxicol.* **1998**, 22, 345-354.

236. D. Zuba. Identification of cathinones and other active components of 'legal highs' by mass spectrometric methods. *Trends Analyt. Chem.* **2012**, 32, 15-30.

237. G. Frison, L. Tedeschi, D. Favretto, A. Reheman, S. D. Ferrara. Gas chromatography/mass spectrometry determination of amphetamine-related drugs and ephedrines in plasma, urine and hair samples after derivatization with 2,2,2-trichloroethyl chloroformate. *Rapid Commun. Mass. Spectrom.* **2005**, 19, 919-927.

238. S. Thornton, D. Lisbon, T. Lin, R. Gerona. Beyond ketamine and phencyclidine: Analytically confirmed use of multiple novel arylcyclohexylamines. *J. Psychoactive Drugs.* **2017**, 49. 289-293.

239. D. M. Wood, S. Davies, M. Puchnarewicz, A. Johnston, P. I. J. E. J. o. C. P. Dargan. Acute toxicity associated with the recreational use of the ketamine derivative methoxetamine. *Eur. J. Clin. Pharmacol.* **2012**, 68, 853-856.

240. J. E. Shields, P. I. Dargan, D. M. Wood, M. Puchnarewicz, S. Davies, W. S. Waring. Methoxetamine associated reversible cerebellar toxicity: Three cases with analytical confirmation. *Clin. Toxicol*. **2012**, 50, 438-440.

241. S. Chiappini, H. Claridge, J. M. Corkery, C. Goodair, B. Loi, F. Schifano. Methoxetamine-related deaths in the UK: an overview. *Hum. Psychopharmacol*. **2015**, 30, 244-248.

242. G. McLaughlin, N. Morris, P. V. Kavanagh, J. D. Power, J. O'Brien, B. Talbot, S. P. Elliot, J. Wallach, K. Hoang, H. Morris, S. D. Brandt. Test purchase, synthesis, and characterization of 2-methoxydiphenidine (MXP) and differentiation from its meta- and para-substituted isomers. *Drug Test. Anal.* **2016**, 8, 98-109.

243. J. Casale, P. A. Hays. Ethylphenidate: An Analytical Profile. *Micro J.* **2011**, 8, 58-61.

244. B. Pagano, I. Lauri, S. De Tito, et al. Use of NMR in profiling of cocaine seizures. *Forensic Sci Int*. **2013**, 231, 120-124.

245. SWGDRUG monograph. Methoxphenidine. **2016**, available at: http://www.swgdrug.org/monographs/methoxphenidine.pdf. (accessed 24/03/19).

246. O. I. G. Khreit, C. Irving, E. Schmidt, J. A. Parkinson, N. N. Daeid, O. B. Sutcliffe. Synthesis, full chemical characterisation and development of validated methods for the quantification of the components found in the evolved "legal high" NRG-2. *J. Pharm. Biomed. Anal*. **2012**, 5, 122-135.

247. J. Casale, P. A. Hays. Methiopropamine: An Analytical Profile. *Micro J.* **2011**, 8, 53-57.

248. S. D. Brandt, P. V. Kavanagh, G. Dowling, B. Talbot, F. Westphal, M. R. Meyer, H. H. Maurer, A. L. Halberstadt. Analytical characterization of *N,N*-diallyltryptamine (DALT) and 16 ring-substituted derivatives. *Drug Test. Anal*. **2017**, 9, 115-126.

249. SWGDRUG monograph. Alpha-ethyltryptamine. **2017**, available at: http://www.swgdrug.org/Monographs/alpha-Ethyltryptamine.pdf. (accessed 24/03/19).

250. R. G. Pertwee. Cannabinoid pharmacology: the first 66 years. *Br. J. Pharmacol*. **2006**, 147, 163-171.

251. E. J. Brand, Z. Zhao. Cannabis in Chinese medicine: Are some traditional indications referenced in ancient literature related to cannabinoids? *Front. Pharmacol*. **2017**, 8, 108. DOI 10.3389/fphar.2017.00108.

252. I. Vardakou, C. Pistos, C. Spiliopoulou. Spice drugs as a new trend: Mode of action, identification and legislation. *Toxicol. Lett*. **2010**, 197, 157-162.

253. S. D. Banister, J. Stuart, R. C. Kevin, A. Edington, M. Longworth, S. M. Wilkinson, C. Beinat, A. S. Buchanan, D. E. Hibbs, M. Glass, M. Connor, I. S. McGregor, M. Kassiou. Effects of bioisosteric fluorine in synthetic cannabinoid designer drugs JWH-018, AM-2201, UR-144, XLR-11, PB-22, 5F-PB-22, APICA, and STS-135. *ACS Chem. Neurosci*. **2015**, 6, 1445-1458.

254. EMCDDA–Europol. Annual Report on the implementation of Council Decision 2005/387/JHA. **2008**, available at http://www.emcdda.europa.eu/attachements.cfm/att_132902_EN_2008_Implementation%20report.pdf. (accessed 24/03/19).

255. A. Makriyannis, H. Deng, Inventors; University of Connecticut assignee. Cannabimimetic indole derivatives. **2005**. Patent US6900236B1. Available at: https://patentimages.storage.googleapis.com/9d/ec/b4/ea8af239e287da/US6900236.pdf . (accessed 24/03/19).

256. T. Doi, A. Asada, A. Takeda, T. Tagami, M. Katagi, H. Kamata, Y. Sawabe. Enantioseparation of the carboxamide-type synthetic cannabinoids *N*-(1-amino-3-methyl-1-oxobutan-2-yl)-1-(5-fluoropentyl)-1H-indazole-3-carboxamide and methyl [1-(5-fluoropentyl)-1H-indazole-3-carbonyl]-valinate in illicit herbal products. *J. Chromatogr. A*. **2016**, 1473, 83-89.

257. A. Westin, J. Frost, W. Brede, P. O. Gundersen, S. Einvik, H. Aarset, L. Slordal. Sudden cardiac death following use of the synthetic cannabinoid MDMB-CHMICA. *J. Anal. Toxicol*. **2016**, 40, 86-87.

258. L. Schep, R. Slaughter, S. Hudson, R. Place, M. Watts. Delayed seizure-like activity following analytically confirmed use of previously unreported synthetic cannabinoid analogues. *Hum. Exp. Toxicol*. **2015**, 34, 557-560.

259. K. Hasegawa, A. Wurita, K. Minakata, K. Gonmori, I. Yamagishi, H. Nozawa, K. Watanabe, O. Suzuki. Identification and quantitation of 5-fluoro-ADB, one of the most dangerous synthetic cannabinoids, in the stomach contents and solid tissues of a human cadaver and in some herbal products. *Forensic Toxicol*. **2015**, 33, 112-121.

260. EMCDDA–EU early warning update. Fentanils and synthetic cannabinoids: Driving greater complexity into the drug situation. **2018**, available at: http://www.emcdda.europa.eu/system/files/publications/8870/2018-2489-td0118414enn.pdf. (accessed 24/03/19).

261. A. Frinculescu, C. L. Lyall, J. Ramsey, B. Miserez. Variation in commercial smoking mixtures containing third-generation synthetic cannabinoids. *Drug Test. Anal*. **2017**, 9, 327-333.

262. J. I. Nakajima, M. Takahashi, T. Seto, C. Kanai, J. Suzuki, M. Yoshida, T. Hamano. Identification and quantitation of two benzoylindoles AM-694 and (4-methoxyphenyl)(1-pentyl-1H-indol-3-yl)methanone, and three cannabimimetic naphthoylindoles JWH-210, JWH-122, and JWH-019 as adulterants in illegal products obtained via the internet. *Forensic Toxicol*. **2011**, 29, 95-110.

263. T. W. Lefever, J. A. Marusich, B. F. Thomas, D. G. Barrus, N. C. Peiper, R. C. Keven, J. L. Wiley. Vaping synthetic cannabinoids: A novel preclinical model of E-cigarette use in mice. *Subst. Abuse*. **2017**, 11, 1-8.

264. T. Zhou, H. Zhang, G. Duan. Simultaneous determination of diethylene glycol and propylene glycol in pharmaceutical products by HPLC after precolumn derivatization with *p*-toluenesulfonyl isocyanate. *J. Sep. Sci*. **2007**, 30, 2620-2627.

265. I. P. Buchler, M. J. Hays, S. G. Hegde, S. L. Hockerman, D. E. Jones, S. W. Kortum, J. G. Rico, R. E. Tenbrink, K. K. Wu. Inventors. Indazole derivatives as CB1 receptor modulators and their preparation and use in treatment of diseases. **2009**. Patent

WO/2009/106980. https://patents.google.com/patent/WO2009106980A3. (accessed 24/03/19).

266. N. Langer, R. Lindigkeit, H.-M. Schiebel, U. Papke, L. Ernst, T. Beuerle. Identification and quantification of synthetic cannabinoids in "spice-like" herbal mixtures: update of the German situation for the spring of 2015. *Forensic Toxicol*. **2015**, 34, 94-107.

267. EMCDDA-Europol 2015. Annual report on the implementation of council decision 2005/387/JHA. **2015**, available at http://www.emcdda.europa.eu/system/files/publications/2880/TDAS16001ENN.pdf. (accessed 24/03/19).

268. M. J. Bowden, J. P. B. Williamson, Inventors. Cannabinoid compounds. **2014**. Patent WO/2014/167530. Available at: https://patentscope.wipo.int/search/en/detail.jsf?docId=WO2014167530. (accessed 24/03/19).

269. J. Hahn, Y. B. Monakhova, J. Hengen, M. Kohl-Himmelseher, J. Schussler, H. Hahn, T. Kuballa, D. W. Lachenmeier. Electronic cigarettes: overview of chemical composition and exposure estimation. *Tob. Induc. Dis*. **2014**, 12, 23.

270. BBC. Drugs smuggled into Guys Marsh prison in dead rats. **2019**, available at: https://www.bbc.co.uk/news/uk-england-dorset-47670309. (accessed 26/03/19).

271. S. M. Wilkinson, S. D. Banister, M. Kassiou. Bioisosteric fluorine in the clandestine design of synthetic cannabinoids. *Aust. J. Chem*. **2015**, 68, 4-8.

272. V. Shevyrin, V. Melkozerov, A. Nevero, O. Eltsov, Y. Shafran, Y. Morzherin, A. T. Lebedev. Identification and analytical characteristics of synthetic cannabinoids with an indazole-3-carboxamide structure bearing a *N*-1-methoxycarbonylalkyl group. *Anal. Bioanal. Chem*. **2015**, 407, 6301-6315.

273. M. Foroozandeh, R. W. Adams, N. J. Meharry, D. Jeannerat, M. Nilsson, G. A. Morris. Ultrahigh-resolution NMR spectroscopy. *Angew. Chem*. **2014**, 53, 6990-6992.

274. D. Williams, I. Fleming. Spectroscopic methods in organic chemistry. 6th ed: Mcgraw-Hill Higher Education, **2008**.

275. J. L. Wiley, J. A. Marusich, T. W. Lefever, K. R. Antonazzo, M. T, Wallgren, R. A. Cortes, P. R. Patel, M. Grabenauer, K. N. Moore, B. F. Thomas. AB-CHMINACA, AB-PINACA, and FUBIMINA: Affinity and potency of novel synthetic cannabinoids in producing Δ^9 Tetrahydrocannabinol-like effects in mice. *J. Pharmacol. Exp. Ther*. **2015**, 354, 328-339.

276. U. Holzgrabe, M. Malet-Martino. Analytical challenges in drug counterfeiting and falsification-The NMR approach *J. Pharm. Biomed. Anal*. **2011**, 55, 679-687.

277. E. O. Stejskal, J. E. Tanner. Spin diffusion measurements: Spin echoes in the presence of a time-dependent field gradient. *J. Chem. Phys*. **1965**, 42, 288-292.

278. A. Becht, C. Schollmayer, J. Wiest, D. Heller, W. Baumann, U. Holzgrabe. Diffusion ordered NMR spectroscopy measurements as screening method of potential reactions of API and excipients in drug formulations. *J. Pharm. Biomed. Anal*. **2019**, 162, 41-46.

279. S. Trefi, V. Gilard, S. Balayssac, M. Malet-Martino, R. Martino. The usefulness of 2D DOSY and 3D DOSY-COSY 1H NMR for mixture analysis: application to genuine and fake formulations of sildenafil (Viagra). *Magn. Reson. Chem*. **2009**, 47, 163-173.

280. S. Balayssac, E. Retailleau, G. Bertrand, M. P. Escot, R. Martino, M. Malet-Martino, V. Gilard. Characterization of heroin samples by 1H NMR and 2D DOSY 1H NMR. *Forensic Sci. Int*. **2014**, 234, 29-38.

281. G. Merola, Z. Aturki, G. D'Orazio, R. Gottardo, T. Macchia, F. Tagliaro, S. Fanali. Analysis of synthetic cannabinoids in herbal blends by means of nano-liquid chromatography. *J. Pharm. Biomed. Anal*. **2012**, 71, 45-53.

282. B. K. Logan, L. E. Reinhold, A. Xu, F. X. Diamond. Identification of synthetic cannabinoids in herbal incense blends in the United States. *J. Forensic Sci*. **2012**, 57,1168-1180.

283. B. Moosmann, S. Kneisel, A. Wohlfarth, V. Brecht, V. Auwärter. A fast and inexpensive procedure for the isolation of synthetic cannabinoids from 'Spice' products using a flash chromatography system. *Anal. Bioanl. Chem*. **2013**, 405, 3929-3935.

284. V. Shevyrin, V. Melkozerov, A. Nevero, O. Eltsov, A. Baranovsky, Y. Shafran. Synthetic cannabinoids as designer drugs: new representatives of indol-3-carboxylates series and indazole-3-carboxylates as novel group of cannabinoids. Identification and analytical data. *Forensic Sci. Int*. **2014**, 244, 263-275.

285. SWGDRUG monograph. PX-1. **2016**, available at: http://swgdrug.org/Monographs/PX-1.pdf. (accessed 24/03/19).

286. N. Uchiyama, Y. Shimokawa, R. Kikura-Hanajiri, Y. Demizu, Y. Goda, T. Hakamatsuka. A synthetic cannabinoid FDU-NNEI, two 2H-indazole isomers of synthetic cannabinoids AB-CHMINACA and NNEI indazole analog (MN-18), a phenethylamine derivative N-OH-EDMA, and a cathinone derivative dimethoxy-alpha-PHP, newly identified in illegal products. *Forensic Toxicol*. **2015**, 33, 244-259.

287. N. Langer, R. Lindigkeit, H. M. Schiebel, L. Ernst, T. Beuerle. Identification and quantification of synthetic cannabinoids in 'spice-like' herbal mixtures: A snapshot of the German situation in the autumn of 2012. *Drug. Test. Anal*. **2014**, 6, 59-71.

288. G. Behonick, K. G. Shanks, D. J. Firchau, G. Mathur, C. F. Lynch, M. Nashelsky, D. J. Jaskierny, C. Meroueh. Four postmortem case reports with quantitative detection of the synthetic cannabinoid, 5F-PB-22. *J. Anal. Toxicol*. **2014**, 38, 559-562.

289. F. Gaunitz, S. Lehmann, A. Thomas, M. Thevis, M. A. Rothschild, K. Mercer-Chalmers-Bender. Post-mortem distribution of the synthetic cannabinoid MDMB-CHMICA and its metabolites in a case of combined drug intoxication. *Int. J. Legal. Med*. **2018**, 132, 1645-1657.

290. S. Tai, W. E. Fantegrossi. Synthetic cannabinoids: Pharmacology, behavioral effects, and abuse potential. *Curr. Addict. Rep*. **2014**, 1, 129-136.

291. European Monitoring Centre for Drug and Drug Addiction (EMCDDA). Perspective on drugs: Synthetic cannabinoids in Europe. **2017**, available at: http://www.emcdda.europa.eu/system/files/publications/2753/POD_Synthetic%20cannabinoids_0.pdf. (accessed 24/03/19).

292. H. Chung, H. Choi, S. Heo, K. Eunmi, J. Lee. Synthetic cannabinoids abused in South Korea: Drug identifications by the National Forensic Service from 2009 to June 2013. *Forensic Toxicol*. **2014**, 32, 82-88.

293. F. Fowler, B. Voyer, M. Marino, J. Finzel, M. Veltri, N. M. Wachter, L. Huang. Rapid screening and quantification of synthetic cannabinoids in herbal products with NMR spectroscopic methods. *Anal. Methods*. **2015**, 7, 7907-7916.

294. S. J. Dunne, J. P. Rosengren-Holmberg. Quantification of synthetic cannabinoids in herbal smoking blends using NMR. *Drug Test. Anal*. **2017**, 9, 734-743.

295. G. F. Pauli, B. U. Jaki, D. C. Lankin. Quantitative 1H NMR: Development and Potential of a Method for Natural Products Analysis. *J. Nat. Prod*. **2005**, 68, 133-149.

296. R. Martino, V. Gilard, F. Desmoulin, M. Malet-Martino. Fluorine-19 or phosphorus-31 NMR spectroscopy: A suitable analytical technique for quantitative in vitro metabolic studies of fluorinated or phosphorylated drugs. *J. Pharm. Biomed. Anal*. **2005**, 38, 871-891.

297. S. J. Barry, T. N. Pham, P. J. Borman, A. J. Edwards, S. A. Watson. A risk-based statistical investigation of the quantification of polymorphic purity of a pharmaceutical candidate by solid-state 19F NMR. *Analytica Chimica Acta*. **2012**, 712, 30-36.

298. E. W. Gunderson, H. M. Haughey, N. Ait-Daoud, A. S. Joshi, C. L. Hart. A survey of synthetic cannabinoid consumption by current cannabis users. *Subst. Abuse.* **2014**, 35, 184-189.

299. R. R. Baker. Temperature distribution inside a burning cigarette. *Nature*. **1974**, 247, 405-406.

300. R. R. Baker. Product formation mechanisms inside a burning cigarette. *Prog. Energy Combust. Sci.* **1981**, 7, 135-153.

301. C. Darquenne. Aerosol deposition in health and disease. *J. Aerosol Med. Pulm. Drug Deliv*. **2012**, 25, 140-147.

302. P. Kavanagh, A. Grigoryev, S. Savchuk, I. Mikhura, A. Formanovsky. UR-144 in products sold via the Internet: Identification of related compounds and characterization of pyrolysis products. *Drug Test. Anal*. **2013**, 5, 683-692.

303. S. Raso, S. Bell. Qualitative analysis and detection of the pyrolytic products of JWH-018 and 11 additional synthetic cannabinoids in the presence of common herbal smoking substrates. *J. Anal. Toxicol*. **2017**, 41, 551-558.

304. R. C. Kevin, A. L. Kovach, T. W. Lefever, T. F. Gamage, J. L. Wiley, I. S. McGregor, B. F. Thomas. Toxic by design? Formation of thermal degradants and cyanide from carboxamide-type synthetic cannabinoids CUMYL-PICA, 5F-CUMYL-PICA, AMB-FUBINACA, MDMB-FUBINACA, NNEI, and MN-18 during exposure to high temperatures. *Forensic Toxicol*. **2019**, 37, 17-26.

305. S. Akamatsu, M. Yoshida. Fragmentation of synthetic cannabinoids with an isopropyl group or a tert-butyl group ionized by electron impact and electrospray. *J. Mass Spectrom*. **2016**, 51, 28-32.

Appendices

Appendix 1. X-ray data of MXE

Table 1. Crystal data and structure refinement for MXE.

Identification code	s16phar1
Empirical formula	C15 H22 Cl N O2
Formula weight	283.78
Temperature	150.01(10) K
Wavelength	1.54184 Å
Crystal system	Monoclinic
Space group	P21
Unit cell dimensions	a = 8.51600(10) Å
	b = 9.88100(10) Å
	c = 8.7487(2) Å
Volume	724.01(2) Å3
Z	2
Density (calculated)	1.302 Mg/m3
Absorption coefficient	2.316 mm-1
F(000)	304
Crystal size	0.200 x 0.200 x 0.120 mm3
Theta range for data collection	5.141 to 73.336°.
Index ranges	-10<=h<=10, -12<=k<=7, -10<=l<=10
Reflections collected	6389
Independent reflections	2121 [R(int) = 0.0207]
Completeness to theta = 67.684°	99.90%
Absorption correction	Semi-empirical from equivalents
Max. and min. transmission	1.00000 and 0.92993
Refinement method	Full-matrix least-squares on F2
Data / restraints / parameters	2121 / 1 / 182
Goodness-of-fit on F2	1.054
Final R indices [I>2sigma(I)]	R1 = 0.0215, wR2 = 0.0577
R indices (all data)	R1 = 0.0216, wR2 = 0.0579
Absolute structure parameter	0.014(10)
Extinction coefficient	n/a
Largest diff. peak and hole	0.173 and -0.164 e.Å-3

Table 2. Atomic coordinates (x 104) and equivalent isotropic displacement

parameters (Å2x 103) for MXE. U(eq) is defined as one third of the trace of the

orthogonalized Uij tensor.

Atom	x	y	z	U(eq)
C(1)	2221(2)	4360(2)	7315(2)	30(1)
C(2)	2983(2)	4992(2)	6063(2)	26(1)
C(3)	2398(2)	5998(2)	3346(2)	17(1)
C(4)	1071(2)	5961(2)	1892(2)	19(1)
C(5)	1389(2)	6803(2)	554(2)	23(1)
C(6)	1608(2)	8281(2)	1092(2)	26(1)
C(7)	2968(2)	8396(2)	2488(2)	26(1)
C(8)	2669(2)	7493(2)	3817(2)	20(1)
C(9)	3883(2)	5259(2)	3012(2)	18(1)
C(10)	5416(2)	5734(2)	3576(2)	21(1)
C(11)	6732(2)	5000(2)	3296(2)	24(1)
C(12)	6543(2)	3817(2)	2457(2)	23(1)
C(13)	5003(2)	3337(2)	1883(2)	21(1)
C(14)	3674(2)	4051(2)	2167(2)	20(1)
C(15)	3375(2)	1593(2)	525(2)	30(1)
N	1764(2)	5249(2)	4627(2)	18(1)
O(1)	-152(1)	5348(2)	1906(2)	26(1)
O(2)	4923(1)	2150(2)	1076(2)	30(1)
Cl	668(1)	2148(1)	3940(1)	24(1)

Table 3. Bond lengths [Å] for MXE.

C(1)-C(2)	1.506(3)
C(1)-H(1C)	0.98
C(1)-H(1D)	0.98
C(1)-H(1E)	0.98
C(2)-N	1.500(2)
C(2)-H(2A)	0.99
C(2)-H(2B)	0.99
C(3)-N	1.521(2)
C(3)-C(9)	1.534(2)
C(3)-C(8)	1.540(2)
C(3)-C(4)	1.541(2)
C(4)-O(1)	1.207(2)
C(4)-C(5)	1.501(2)
C(5)-C(6)	1.535(3)
C(5)-H(5A)	0.99
C(5)-H(5B)	0.99
C(6)-C(7)	1.527(2)
C(6)-H(6A)	0.99
C(6)-H(6B)	0.99
C(7)-C(8)	1.523(2)
C(7)-H(7A)	0.99
C(7)-H(7B)	0.99
C(8)-H(8A)	0.99
C(8)-H(8B)	0.99
C(9)-C(10)	1.391(2)
C(9)-C(14)	1.398(3)
C(10)-C(11)	1.393(3)
C(10)-H(10)	0.95
C(11)-C(12)	1.374(3)
C(11)-H(11)	0.95
C(12)-C(13)	1.399(2)
C(12)-H(12)	0.95
C(13)-O(2)	1.364(2)

Table 4. Bond angles [°] for MXE.

C(2)-C(1)-H(1C)	109.5
C(2)-C(1)-H(1D)	109.5
H(1C)-C(1)-H(1D)	109.5
C(2)-C(1)-H(1E)	109.5
H(1C)-C(1)-H(1E)	109.5

H(1D)-C(1)-H(1E)	109.5
N-C(2)-C(1)	110.81(14)
N-C(2)-H(2A)	109.5
C(1)-C(2)-H(2A)	109.5
N-C(2)-H(2B)	109.5
C(1)-C(2)-H(2B)	109.5
H(2A)-C(2)-H(2B)	108.1
N-C(3)-C(9)	108.87(14)
N-C(3)-C(8)	108.98(13)
C(9)-C(3)-C(8)	114.78(14)
N-C(3)-C(4)	106.95(12)
C(9)-C(3)-C(4)	109.77(13)
C(8)-C(3)-C(4)	107.20(14)
O(1)-C(4)-C(5)	124.31(15)
O(1)-C(4)-C(3)	120.60(15)
C(5)-C(4)-C(3)	114.97(14)
C(4)-C(5)-C(6)	108.47(14)
C(4)-C(5)-H(5A)	110
C(6)-C(5)-H(5A)	110
C(4)-C(5)-H(5B)	110
C(6)-C(5)-H(5B)	110
H(5A)-C(5)-H(5B)	108.4
C(7)-C(6)-C(5)	110.38(15)
C(7)-C(6)-H(6A)	109.6
C(5)-C(6)-H(6A)	109.6
C(7)-C(6)-H(6B)	109.6
C(5)-C(6)-H(6B)	109.6
H(6A)-C(6)-H(6B)	108.1
C(8)-C(7)-C(6)	111.09(15)
C(8)-C(7)-H(7A)	109.4
C(6)-C(7)-H(7A)	109.4
C(8)-C(7)-H(7B)	109.4
C(6)-C(7)-H(7B)	109.4
H(7A)-C(7)-H(7B)	108
C(7)-C(8)-C(3)	113.26(14)
C(7)-C(8)-H(8A)	108.9
C(3)-C(8)-H(8A)	108.9
C(7)-C(8)-H(8B)	108.9
C(3)-C(8)-H(8B)	108.9
H(8A)-C(8)-H(8B)	107.7
C(10)-C(9)-C(14)	119.80(16)
C(10)-C(9)-C(3)	121.66(16)
C(14)-C(9)-C(3)	118.50(14)
C(9)-C(10)-C(11)	119.66(18)
C(9)-C(10)-H(10)	120.2

C(11)-C(10)-H(10)	120.2
C(12)-C(11)-C(10)	121.11(16)
C(12)-C(11)-H(11)	119.4
C(10)-C(11)-H(11)	119.4
C(11)-C(12)-C(13)	119.45(16)
C(11)-C(12)-H(12)	120.3
C(13)-C(12)-H(12)	120.3
O(2)-C(13)-C(14)	124.14(16)
O(2)-C(13)-C(12)	115.67(15)
C(14)-C(13)-C(12)	120.18(17)
C(13)-C(14)-C(9)	119.79(15)
C(13)-C(14)-H(14)	120.1
C(9)-C(14)-H(14)	120.1
O(2)-C(15)-H(15A)	109.5
O(2)-C(15)-H(15B)	109.5
H(15A)-C(15)-H(15B)	109.5
O(2)-C(15)-H(15C)	109.5
H(15A)-C(15)-H(15C)	109.5
H(15B)-C(15)-H(15C)	109.5
C(2)-N-C(3)	114.54(13)
C(2)-N-H(1A)	106.6(14)
C(3)-N-H(1A)	110.3(16)
C(2)-N-H(1B)	106.8(14)
C(3)-N-H(1B)	109.3(14)
H(1A)-N-H(1B)	109(2)
C(13)-O(2)-C(15)	117.57(15)

Table 5. Anisotropic displacement parameters (Å2x 103) for MXE. The anisotropic

displacement factor exponent takes the form: $-2\pi2[\,h^2\,a^{*2}U^{11} + \; + 2\,h\,k\,a^*\,b^*\,U^{12}\,]$

	U11	U22	U33	U23	U13	U12
C(1)	36(1)	32(1)	22(1)	5(1)	8(1)	1(1)
C(2)	22(1)	31(1)	22(1)	5(1)	1(1)	2(1)
C(3)	17(1)	18(1)	17(1)	2(1)	4(1)	1(1)
C(4)	17(1)	19(1)	20(1)	3(1)	4(1)	2(1)
C(5)	23(1)	29(1)	17(1)	2(1)	4(1)	1(1)
C(6)	29(1)	25(1)	23(1)	5(1)	6(1)	3(1)
C(7)	32(1)	19(1)	27(1)	2(1)	7(1)	5(1)
C(8)	23(1)	16(1)	21(1)	2(1)	5(1)	1(1)
C(9)	17(1)	19(1)	16(1)	2(1)	5(1)	0(1)
C(10)	20(1)	24(1)	21(1)	0(1)	4(1)	5(1)
C(11)	16(1)	34(1)	23(1)	5(1)	4(1)	4(1)
C(12)	19(1)	31(1)	21(1)	6(1)	7(1)	5(1)
C(13)	24(1)	20(1)	19(1)	2(1)	6(1)	2(1)
C(14)	17(1)	22(1)	20(1)	2(1)	4(1)	1(1)
C(15)	41(1)	19(1)	30(1)	4(1)	8(1)	4(1)
N	18(1)	18(1)	18(1)	0(1)	4(1)	1(1)
O(1)	19(1)	31(1)	27(1)	0(1)	2(1)	4(1)
O(2)	30(1)	25(1)	35(1)	7(1)	8(1)	6(1)
Cl	25(1)	21(1)	28(1)	2(1)	7(1)	4(1)

Table 6. Hydrogen coordinates (x 104) and isotropic displacement parameters

(Å2x 10 3) for MXE.

	x	y	z	U(eq)
H(1C)	3021	4263	8266	45
H(1D)	1798	3467	6971	45
H(1E)	1349	4939	7522	45
H(2A)	3496	5857	6446	31
H(2B)	3822	4382	5810	31
H(5A)	482	6731	-327	27
H(5B)	2364	6478	202	27
H(6A)	1848	8848	231	31
H(6B)	606	8617	1381	31
H(7A)	3984	8130	2173	31
H(7B)	3068	9348	2845	31
H(8A)	1721	7831	4207	24
H(8B)	3597	7556	4679	24
H(10)	5565	6555	4149	26
H(11)	7777	5323	3691	29
H(12)	7450	3330	2267	28
H(14)	2630	3719	1787	23

H(15A)	3485	724	15	45
H(15B)	2757	2218	-222	45
H(15C)	2822	1455	1402	45
H(1A)	910(30)	5760(30)	4950(30)	35(7)
H(1B)	1370(30)	4400(30)	4250(30)	27(6)

Table 7. Torsion angles [°] for MXE.

N-C(3)-C(4)-O(1)	-3.7(2)
C(9)-C(3)-C(4)-O(1)	114.30(18)
C(8)-C(3)-C(4)-O(1)	-120.42(18)
N-C(3)-C(4)-C(5)	172.54(14)
C(9)-C(3)-C(4)-C(5)	-69.51(19)
C(8)-C(3)-C(4)-C(5)	55.77(17)
O(1)-C(4)-C(5)-C(6)	116.78(19)
C(3)-C(4)-C(5)-C(6)	-59.25(19)
C(4)-C(5)-C(6)-C(7)	57.67(18)
C(5)-C(6)-C(7)-C(8)	-57.1(2)
C(6)-C(7)-C(8)-C(3)	55.7(2)
N-C(3)-C(8)-C(7)	-167.91(14)
C(9)-C(3)-C(8)-C(7)	69.71(18)
C(4)-C(3)-C(8)-C(7)	-52.50(17)
N-C(3)-C(9)-C(10)	-102.09(19)
C(8)-C(3)-C(9)-C(10)	20.4(2)
C(4)-C(3)-C(9)-C(10)	141.15(16)
N-C(3)-C(9)-C(14)	75.52(18)
C(8)-C(3)-C(9)-C(14)	-162.04(14)
C(4)-C(3)-C(9)-C(14)	-41.2(2)
C(14)-C(9)-C(10)-C(11)	-0.1(3)
C(3)-C(9)-C(10)-C(11)	177.44(15)
C(9)-C(10)-C(11)-C(12)	0.6(3)
C(10)-C(11)-C(12)-C(13)	-0.5(3)
C(11)-C(12)-C(13)-O(2)	-179.39(16)
C(11)-C(12)-C(13)-C(14)	-0.2(3)
O(2)-C(13)-C(14)-C(9)	179.81(16)
C(12)-C(13)-C(14)-C(9)	0.7(3)
C(10)-C(9)-C(14)-C(13)	-0.5(3)
C(3)-C(9)-C(14)-C(13)	-178.18(15)
C(1)-C(2)-N-C(3)	174.99(16)
C(9)-C(3)-N-C(2)	52.42(19)
C(8)-C(3)-N-C(2)	-73.46(18)
C(4)-C(3)-N-C(2)	170.96(15)
C(14)-C(13)-O(2)-C(15)	-1.7(3)
C(12)-C(13)-O(2)-C(15)	177.48(16)

Appendix 2. X-ray data of AM-694

Table 1. Crystal data and structure refinement for AM-694.

Identification code	s17phar10
Empirical formula	C20 H19 F I N O
Formula weight	435.26
Temperature	150.00(10) K
Wavelength	1.54184 Å
Crystal system	Triclinic
Space group	P-1
Unit cell dimensions	a = 9.1798(3) Å α = 115.538(3)°.
	b = 10.4887(4) Å β = 97.804(3)°.
	c = 11.2304(4) Å γ = 106.811(3)°.
Volume	890.49(6) Å3
Z	2
Density (calculated)	1.623 Mg/m3
Absorption coefficient	14.259 mm-1
F(000)	432
Crystal size	0.277 x 0.210 x 0.030 mm3
Theta range for data collection	4.577 to 73.169°.
Index ranges	-10<=h<=11, -12<=k<=12, -13<=l<=13
Reflections collected	18642
Independent reflections	3540 [R(int) = 0.0630]
Completeness to theta = 1.000°	100.00%
Absorption correction	Gaussian
Max. and min. transmission	1.000 and 0.729
Refinement method	Full-matrix least-squares on F2
Data / restraints / parameters	3540 / 0 / 217
Goodness-of-fit on F2	1.053
Final R indices [I>2sigma(I)]	R1 = 0.0355, wR2 = 0.0942
R indices (all data)	R1 = 0.0372, wR2 = 0.0971
Extinction coefficient	n/a
Largest diff. peak and hole	1.280 and -0.980 e.Å-3

Table 2. Atomic coordinates (x 10⁴) and equivalent isotropic displacement parameters (Å²x 10³) for AM-694. U(eq) is defined as one third of the trace of the orthogonalized Uij tensor.

Atom	x	y	z	U(eq)
C(1)	202(4)	1721(4)	1752(3)	35(1)
C(2)	90(4)	3175(4)	2767(3)	33(1)
C(3)	1023(4)	4572(4)	2683(3)	30(1)
C(4)	840(4)	6012(4)	3677(4)	32(1)
C(5)	1860(4)	7446(4)	3685(4)	33(1)
C(6)	4202(4)	8800(3)	5843(3)	27(1)
C(7)	3472(4)	9375(4)	6842(4)	34(1)
C(8)	4409(5)	10202(4)	8205(4)	39(1)
C(9)	6036(5)	10445(4)	8554(3)	38(1)
C(10)	6752(4)	9857(4)	7548(3)	31(1)
C(11)	5814(4)	8998(3)	6157(3)	25(1)
C(12)	6109(4)	8220(3)	4855(3)	24(1)
C(13)	4674(4)	7628(3)	3837(3)	26(1)
C(14)	7549(4)	8025(3)	4599(3)	25(1)
C(15)	7485(4)	7074(3)	3116(3)	24(1)
C(16)	6678(4)	5483(4)	2334(3)	29(1)
C(17)	6680(5)	4690(4)	981(4)	44(1)
C(18)	7486(5)	5471(5)	396(4)	54(1)
C(19)	8315(5)	7054(5)	1162(4)	44(1)
C(20)	8326(4)	7836(4)	2510(3)	30(1)
N	3549(3)	7969(3)	4406(3)	26(1)
O	8820(3)	8624(3)	5518(2)	33(1)
I	5614(1)	4188(1)	3206(1)	41(1)
F	-502(3)	1369(3)	408(2)	51(1)

Table 3. Selected bond lengths [Å] and angles [°] for AM-694.

C(1)-F	1.395(4)
C(1)-C(2)	1.503(5)
C(1)-H(1A)	0.99
C(1)-H(1B)	0.99
C(2)-C(3)	1.519(5)
C(2)-H(2A)	0.99
C(2)-H(2B)	0.99
C(3)-C(4)	1.516(4)
C(3)-H(3A)	0.99
C(3)-H(3B)	0.99
C(4)-C(5)	1.521(5)
C(4)-H(4A)	0.99
C(4)-H(4B)	0.99

C(5)-N	1.465(4)
C(5)-H(5A)	0.99
C(5)-H(5B)	0.99
C(6)-C(7)	1.388(4)
C(6)-N	1.395(4)
C(6)-C(11)	1.405(5)
C(7)-C(8)	1.379(5)
C(7)-H(7)	0.95
C(8)-C(9)	1.409(6)
C(8)-H(8)	0.95
C(9)-C(10)	1.387(5)
C(9)-H(9)	0.95
C(10)-C(11)	1.402(4)
C(10)-H(10)	0.95
C(11)-C(12)	1.444(4)
C(12)-C(13)	1.390(4)
C(12)-C(14)	1.442(5)
C(13)-N	1.342(4)
C(13)-H(13)	0.95
C(14)-O	1.230(4)
C(14)-C(15)	1.510(4)
C(15)-C(16)	1.396(4)
C(15)-C(20)	1.397(4)
C(16)-C(17)	1.383(5)
C(16)-I	2.097(3)
C(17)-C(18)	1.377(6)
C(17)-H(17)	0.95
C(18)-C(19)	1.391(6)
C(18)-H(18)	0.95
C(19)-C(20)	1.373(5)
C(19)-H(19)	0.95
C(20)-H(20)	0.95

Table 4. Bond angles [°] for AM-694.

F-C(1)-C(2)	109.2(3)
F-C(1)-H(1A)	109.8
C(2)-C(1)-H(1A)	109.8
F-C(1)-H(1B)	109.8
C(2)-C(1)-H(1B)	109.8
H(1A)-C(1)-H(1B)	108.3
C(1)-C(2)-C(3)	113.6(3)
C(1)-C(2)-H(2A)	108.9
C(3)-C(2)-H(2A)	108.9
C(1)-C(2)-H(2B)	108.9
C(3)-C(2)-H(2B)	108.9
H(2A)-C(2)-H(2B)	107.7
C(4)-C(3)-C(2)	112.6(3)
C(4)-C(3)-H(3A)	109.1
C(2)-C(3)-H(3A)	109.1
C(4)-C(3)-H(3B)	109.1
C(2)-C(3)-H(3B)	109.1
H(3A)-C(3)-H(3B)	107.8
C(3)-C(4)-C(5)	113.4(3)
C(3)-C(4)-H(4A)	108.9
C(5)-C(4)-H(4A)	108.9
C(3)-C(4)-H(4B)	108.9
C(5)-C(4)-H(4B)	108.9
H(4A)-C(4)-H(4B)	107.7
N-C(5)-C(4)	111.8(3)
N-C(5)-H(5A)	109.3
C(4)-C(5)-H(5A)	109.3
N-C(5)-H(5B)	109.3
C(4)-C(5)-H(5B)	109.3
H(5A)-C(5)-H(5B)	107.9
C(7)-C(6)-N	128.8(3)
C(7)-C(6)-C(11)	123.4(3)
N-C(6)-C(11)	107.8(3)
C(8)-C(7)-C(6)	117.2(3)
C(8)-C(7)-H(7)	121.4
C(6)-C(7)-H(7)	121.4
C(7)-C(8)-C(9)	120.8(3)
C(7)-C(8)-H(8)	119.6
C(9)-C(8)-H(8)	119.6
C(10)-C(9)-C(8)	121.6(3)
C(10)-C(9)-H(9)	119.2
C(8)-C(9)-H(9)	119.2
C(9)-C(10)-C(11)	118.4(3)

C(9)-C(10)-H(10)	120.8
C(11)-C(10)-H(10)	120.8
C(10)-C(11)-C(6)	118.6(3)
C(10)-C(11)-C(12)	134.6(3)
C(6)-C(11)-C(12)	106.7(3)
C(13)-C(12)-C(14)	125.0(3)
C(13)-C(12)-C(11)	105.8(3)
C(14)-C(12)-C(11)	129.2(3)
N-C(13)-C(12)	110.7(3)
N-C(13)-H(13)	124.6
C(12)-C(13)-H(13)	124.6
O-C(14)-C(12)	123.4(3)
O-C(14)-C(15)	119.0(3)
C(12)-C(14)-C(15)	117.6(3)
C(16)-C(15)-C(20)	118.4(3)
C(16)-C(15)-C(14)	123.9(3)
C(20)-C(15)-C(14)	117.6(3)
C(17)-C(16)-C(15)	120.6(3)
C(17)-C(16)-I	117.4(3)
C(15)-C(16)-I	121.8(2)
C(18)-C(17)-C(16)	119.9(3)
C(18)-C(17)-H(17)	120
C(16)-C(17)-H(17)	120
C(17)-C(18)-C(19)	120.4(3)
C(17)-C(18)-H(18)	119.8
C(19)-C(18)-H(18)	119.8
C(20)-C(19)-C(18)	119.5(4)
C(20)-C(19)-H(19)	120.2
C(18)-C(19)-H(19)	120.2
C(19)-C(20)-C(15)	121.1(3)
C(19)-C(20)-H(20)	119.5
C(15)-C(20)-H(20)	119.5
C(13)-N-C(6)	108.9(3)
C(13)-N-C(5)	127.0(3)
C(6)-N-C(5)	123.8(3)

Table 5. Anisotropic displacement parameters (Å^2x 10^3) for AM-694. The

anisotropic displacement factor exponent takes the form: $-2\pi^2[\, h^2\, a^{*2}U^{11} + ... + 2\, h\, k\, a^*\, b^*$

$U^{12}\,]$

	U^{11}	U^{22}	U^{33}	U^{23}	U^{13}	U^{12}
C(1)	39(2)	31(2)	32(2)	13(1)	10(1)	14(1)
C(2)	36(2)	30(2)	34(2)	15(1)	13(1)	13(1)
C(3)	28(2)	28(2)	33(1)	13(1)	14(1)	12(1)
C(4)	26(2)	30(2)	40(2)	16(1)	14(1)	14(1)
C(5)	26(2)	31(2)	45(2)	17(1)	10(1)	17(1)
C(6)	31(2)	20(1)	33(1)	14(1)	14(1)	12(1)
C(7)	39(2)	26(2)	42(2)	16(1)	21(2)	18(1)
C(8)	50(2)	31(2)	41(2)	16(1)	25(2)	20(2)
C(9)	50(2)	26(2)	32(2)	10(1)	12(2)	14(2)
C(10)	35(2)	23(1)	32(2)	12(1)	8(1)	12(1)
C(11)	28(2)	21(1)	29(1)	14(1)	12(1)	12(1)
C(12)	24(2)	20(1)	29(1)	12(1)	9(1)	9(1)
C(13)	27(2)	23(1)	29(1)	13(1)	9(1)	11(1)
C(14)	27(2)	20(1)	30(1)	12(1)	10(1)	9(1)
C(15)	22(1)	21(1)	29(1)	12(1)	8(1)	10(1)
C(16)	23(2)	26(2)	35(2)	13(1)	9(1)	8(1)
C(17)	39(2)	33(2)	39(2)	4(2)	12(2)	8(2)
C(18)	53(2)	52(2)	32(2)	6(2)	19(2)	8(2)
C(19)	38(2)	54(2)	42(2)	28(2)	18(2)	12(2)
C(20)	26(2)	31(2)	38(2)	18(1)	10(1)	13(1)
N	23(1)	23(1)	34(1)	14(1)	9(1)	11(1)
O	25(1)	34(1)	31(1)	12(1)	5(1)	10(1)
I	38(1)	29(1)	64(1)	27(1)	22(1)	13(1)
F	64(2)	42(1)	33(1)	12(1)	7(1)	18(1)

Table 6. Hydrogen coordinates (x 104) and isotropic displacement parameters (Å2x 10 3) for

AM-694.

	x	y	z	U(eq)
H(1A)	1336	1854	1883	42
H(1B)	-351	871	1908	42
H(2A)	492	3362	3716	40
H(2B)	-1046	3037	2598	40
H(3A)	2167	4740	2892	36
H(3B)	651	4374	1727	36
H(4A)	1133	6162	4624	38
H(4B)	-294	5868	3423	38
H(5A)	1740	7229	2719	40
H(5B)	1478	8273	4144	40
H(7)	2374	9205	6597	40
H(8)	3951	10613	8918	47
H(9)	6658	11025	9501	46
H(10)	7852	10032	7796	37
H(13)	4513	7059	2871	31
H(17)	6125	3608	456	53
H(18)	7475	4926	-537	65
H(19)	8871	7590	756	53
H(20)	8916	8913	3040	36

Table 7. Torsion angles [°] for AM-694.

F-C(1)-C(2)-C(3)	-64.2(4)
C(1)-C(2)-C(3)-C(4)	177.8(3)
C(2)-C(3)-C(4)-C(5)	175.8(3)
C(3)-C(4)-C(5)-N	-74.2(4)
N-C(6)-C(7)-C(8)	-178.2(3)
C(11)-C(6)-C(7)-C(8)	1.1(5)
C(6)-C(7)-C(8)-C(9)	0.0(5)
C(7)-C(8)-C(9)-C(10)	-0.5(6)
C(8)-C(9)-C(10)-C(11)	-0.3(5)
C(9)-C(10)-C(11)-C(6)	1.4(5)
C(9)-C(10)-C(11)-C(12)	-179.9(3)
C(7)-C(6)-C(11)-C(10)	-1.9(5)
N-C(6)-C(11)-C(10)	177.6(3)
C(7)-C(6)-C(11)-C(12)	179.1(3)
N-C(6)-C(11)-C(12)	-1.5(3)
C(10)-C(11)-C(12)-C(13)	-177.7(3)
C(6)-C(11)-C(12)-C(13)	1.1(3)

C(10)-C(11)-C(12)-C(14)	3.8(6)
C(6)-C(11)-C(12)-C(14)	-177.4(3)
C(14)-C(12)-C(13)-N	178.2(3)
C(11)-C(12)-C(13)-N	-0.4(4)
C(13)-C(12)-C(14)-O	176.5(3)
C(11)-C(12)-C(14)-O	-5.3(5)
C(13)-C(12)-C(14)-C(15)	-1.5(5)
C(11)-C(12)-C(14)-C(15)	176.7(3)
O-C(14)-C(15)-C(16)	110.3(4)
C(12)-C(14)-C(15)-C(16)	-71.6(4)
O-C(14)-C(15)-C(20)	-67.7(4)
C(12)-C(14)-C(15)-C(20)	110.4(3)
C(20)-C(15)-C(16)-C(17)	-1.7(5)
C(14)-C(15)-C(16)-C(17)	-179.7(3)
C(20)-C(15)-C(16)-I	172.3(2)
C(14)-C(15)-C(16)-I	-5.7(4)

Appendix 3. Outputs arising from this work

Refereed Publications:

1. Analysis of synthetic cannabinoid agonists and their degradation products after combustion in a smoking simulator. Husain A. Naqi, Christopher R. Pudney, Stephen M. Husbands and Ian S. Blagbrough. *Anal. Methods.* .**2019**, 11, 3101-3107. DOI: 10.1039/c9ay00814d.

2. ^{19}F and ^{1}H quantitative-NMR spectroscopic analysis of fluorinated third-generation synthetic cannabinoids. Husain A. Naqi, Timothy J. Woodman, Stephen M. Husbands and Ian S. Blagbrough. *Anal. Methods.* .**2019**, 11, 3090-3100. DOI: 10.1039/c9ay00814d.

Oral Presentations:

1. "Pharmaceutical analysis of seized ethylone-ecstasy mixtures", APS PharmSci, 5th of September 2016, Glasgow, UK.

2. "Pharmaceutical analysis of seized ethylone–ecstasy mixtures using quantitative NMR spectroscopy and ESI-MS", Early Career Researcher Meeting in Analytical Biosciences,15th March 2017, University of Warwick, UK.

3. "Analysis of Novel Psychoactive Substance (NPS)/illicit drug mixtures by NMR and LC/MS/MS" Emerging Analytical Professionals (EAP), 12th of May 2017, Kettering, UK.

4. "Pharmaceutical analysis of police seizures and amnesty bins in the Southwest of England", 254th ACS national meeting and exposition, 20th of August, Washington D.C, USA.

Poster Presentations:

1. "Pharmaceutical analysis of seized ethylone-ecstasy mixtures", APS PharmSci, 5th of September 2016, Glasgow, UK.

2. "Carbamate derivatization studies of MDMA, ethylone, and mephedrone", APS PharmSci, 5th of September 2016, Glasgow, UK.

3. "Pharmaceutical analysis of seized ethylone-ecstasy mixtures using quantitative NMR spectroscopy and ESI-MS", Early Career Researcher Meeting in Analytical Biosciences, 15th March 2017, University of Warwick, UK.

4. "Analysis of multicomponent NPS/illicit drug mixtures", APS PharmSci, 5th of September 2017, Hertfordshire, UK.

5. "Analysis of Multicomponent NPS/Illicit Drug Mixtures", AAPS annual meeting and exposition, 12th of November 2017, San Diego, USA.

6. "Carbamate Derivatization Studies of MDMA, Ethylone, and Mephedrone" AAPS annual meeting and exposition, 12th of November 2017, San Diego, USA.

7. "Pharmaceutical Analysis of Seized ethylone–ecstasy Mixtures", AAPS annual meeting and exposition, 12th of November 2017, San Diego, USA.

8. "Analysis of multicomponent NPS/illicit drug mixtures" 25th meeting of GP2A, September 2017, Liverpool, UK.

9. "A validated ^{19}F NMR technique to assay quantitatively fluorinated synthetic cannabinoids agonists", AAPS annual meeting and exposition, 3rd of November 2018, Washington D.C, USA.

10. "Characterization and quantification of five Synthetic Cannabinoid Agonists (SCA) using NMR and UHPLC-QTOF/MS/MS", AAPS annual meeting and exposition, 3rd of November 2018, Washington D.C, USA.
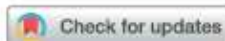
Check for updates

Analysis of synthetic cannabinoid agonists and their degradation products after combustion in a smoking simulator†

Husain A. Naqi,[a] Christopher R. Pudney,[b] Stephen M. Husbands[a] and Ian S. Blagbrough [orcid] *[a]

Synthetic cannabinoids are a major class of NPS with a high impact on analytical, forensic and toxicological fields. The main route of administration of synthetic cannabinoids is through inhalation, delivered by smoking a conventional or electronic cigarette, pyrolysis possibly altering the nature of these compounds and resulting in unknown combustion products with unknown biological activity/toxicology. In this study, a twin-trap smoking inhalation model that simulates human inhalation has been developed. The smoking simulator allows the efficient trapping of the combustion products. Analysis using UHPLC-TOF-ESI-MS and GC-MS allowed the detection of all six synthetic cannabinoids tested in the smoking simulator. A novel combustion product of MDMB-CHMICA was identified, a dihydro-1H-pyridoindole-dione with its structure and mechanism of formation proposed. This study of SC combustion products provides markers which may be useful for drug analysts and toxicologists in examining samples obtained from suspected SC users/abusers.

1. Introduction

Synthetic cannabinoids (SCs) act as agonists at the same receptors as the natural product cannabinoids, but they do so with much higher potency for both CB_1 and CB_2 receptor subtypes. The original SC drugs, e.g. the Hebrew University compound HU-210, Pfizer compounds CP 47,497 and CP 59,540, have been further developed into second and now third generation analogues.[1] In the early 1990s, John W. Huffman from Clemson University synthesized a series of SCs with a core structure of naphthoylindole, most notably JWH-018 (Fig. 1) which, along with CP 47,497, constituted the first wave of illicitly synthesized SCs that started emerging on the streets in 2008, with the help of internet vendors that promoted these compounds as apparent research chemicals, herbal incense and so called legal highs, at least before the 2016 Psychoactive Substance Act.[3–4] Later SCs, illicitly manufactured, retained the indole core, but with different functional group modifications to the head, tail and linker moieties (Fig. 1), resulting in hundreds of compounds in this second generation. Some of these were also based on published medicinal chemistry compounds, including the AM series developed by Prof. A. Makríyannis at the University of

Connecticut, CT, USA.[5] Continuous banning of SCs by Governments worldwide resulted in further developments, including compounds that possess the indazole core structure instead of the indole, and amino acids such as alanine and phenylalanine in the head components, replacing the naphthalene and substituted aromatic moiety. Most of these newer generation SCs are novel compounds.[6]

These SCs are still known by the street name "spice" due to the first brands promoted over the internet and sold on the street, e.g. Spice and K2. They are still sold in the form of herbal blends of potpourri, Damiana (Turnera diffusa), Marshmallow plant (Althaea officinalis) and other herbal blends soaked or sprayed with the SC. SC analysis involves the characterization and quantification, using GC- and LC-hyphenated techniques, of seized powders or often herbal blends containing SCs and also toxicological samples, the latter relying on MS techniques for analysis. Analytical methods that can be applied to crude samples are of great value to drug analysts, but due to the fact that SCs in herbal blends are mostly smoked, analytical studies of combustion products are required.[7] Simulation of smoking is challenging for a number of reasons, mainly relating to the temperature and the flow rate. Temperature in cigarette smoking can routinely reach 700 °C and even goes up 900 °C at some hot spots.[8] Potentially toxic pyrolysis compounds are released from herbal materials when temperatures exceed 200 °C, which is the case in cigarette smoking, e.g. toxic compounds include toluene, benzene, and naphthalene.[9] The presence of several nitrogen atoms in the majority of SCs could potentially result in a number of chemically variable

[a]Department of Pharmacy and Pharmacology, University of Bath, Bath BA2 7AY, UK. E-mail: prsisb@bath.ac.uk; Tel: +44 (0)1225 386795

[b]Department of Biology and Biochemistry, University of Bath, Bath BA2 7AY, UK

† Electronic supplementary information (ESI) available. See DOI: 10.1039/c9ay00722a
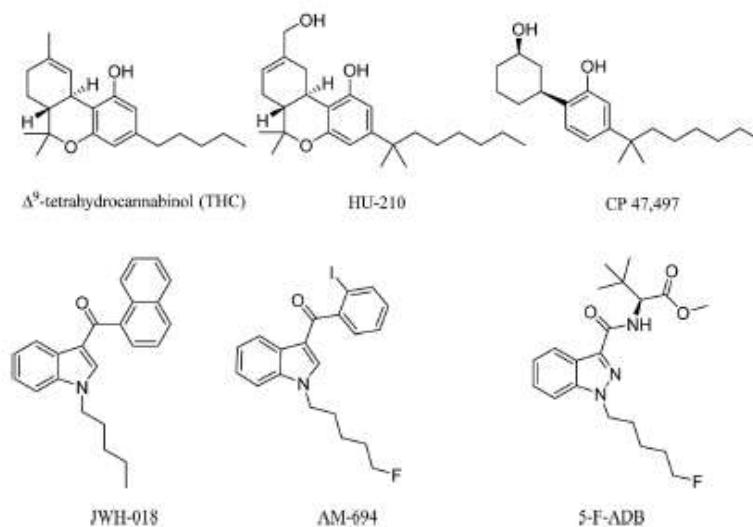
Fig. 1 A natural phytocannabinoid (THC) and five SCs.

combustion products due to the thermal lability of C–N bonds. For an accurate simulation of the smoking process, a flow rate of 30 L min^{-1} needs to be maintained.[10]

The first reported SC pyrolysis analysis was performed on UR-144, an indole tetramethyl-cyclopropyl closely related to JWH-018 using LC-MS/MS.[11] Raso and Bell[12] performed GC-MS analysis, revealing pyrolysis products of first generation (JWH-018, JWH-073) and second generation (AM-694) SC using an in-house built pyrolysis device comprised of a quartz tube inserted into a round-bottom flask, where the sample is combusted using a blow torch. Common and distinctive fragments were revealed for each type of SC, e.g. naphthalene for the JWH family and cinnoline amine for the indazole family. The authors also acknowledged the problem of maintaining a stable temperature.[12] Kevin et al.[13] recently by-passed the issue of fluctuating temperature by conducting a temperature controlled study on six carboxamide type SC at 200, 400, 600, and 800 °C using a pyro-probe coupled to a GC-MS, thus creating temperature-controlled pyrolysis conditions where the degradants were analysed at each temperature.[13]

A focus on the simulation of smoking is the aim of this paper rather than pyrolysis at high temperatures coupled to anaerobic conditions. Work on the combustion and degradation products is an area that requires further investigation due to the generation of potentially harmful products with possible alteration in the target receptor or the affinity for that receptor of any new compounds. In particular, it is essential that we determine the nature of the volatile products resulting from combustion so that there is a better understanding of what ab/users of SCs are actually inhaling.[14] In this study, a SC smoking model was designed and constructed. It was then employed for the analysis of different SCs and the detection of their combustion products. The resulting combustion products may help drug analysts to

uncover markers for SC smoking that will facilitate toxicological drug detection and inform research into the biological effects of SC use.

2. Experimental section

Chemicals and sample preparation

All extraction solvents 99.9% anhydrous (chloroform, methanol, and acetonitrile), were purchased from Fisher Scientific (UK) and ACROS Organics (UK). The samples were in the form of herbal blends (1.0–3.0 g) as commercially packaged brands (Exodus, Loco Elite). *Turnera diffusa* (Damiana) dried herb (illicit-drug free) was purchased from Spiceworks (Hereford, UK).

UHPLC-TOF-ESI-MS and GC-MS

Analysis of the combustion products used UHPLC-TOF-ESI-MS and GC-MS. The UHPLC-QTOF-ESI-MS analysis was conducted using a MaXis HD Quadrupole electrospray ionization Time-of-Flight (ESI-QTOF) mass spectrometer (MS) (Bruker Daltonik GmbH, Bremen, Germany), operated in ESI positive mode. The QTOF was coupled to an Ultimate 3000 UHPLC (Thermo Fisher Scientific, CA, USA). The capillary voltage was set to 4500 V, nebulizing gas at 4 bar, drying gas at 12 L min^{-1} at 220 °C. The TOF scan range was from 75–1000 mass-to-charge ratio (m/z). For LC-MS/MS capabilities, the in-source CID was set to 0.0 eV, with the collision energy for TOF MS acquisition at 3.0 eV. The collision energy was set to a sliding scale from 100 m/z at 14.0 eV, 500 m/z at 20.0 eV and 1000 m/z at 30.0 eV. For the analytes, the actual collision energy was between 15.0–18.0 eV. Liquid chromatography separation was performed using an Acquity UPLC BEH C18, 1.7 μM, 2.1 × 50 mm RP-column (Waters, Milford, MA, USA) with a flow rate of 0.4

mL min⁻¹, and an injection volume of 10 μL at 40 °C column temperature. Mobile phase A consisted of LC-MS grade water 0.1% formic acid v/v, mobile phase B consisted of acetonitrile 0.1% formic acid v/v. For Gradient 1 starting with 1% B for 2 min followed by a linear increase from 2.0 min to 100% B at 5.0 min, held for 3 min, followed by return to 1% B at 8.1 min, where it was held for equilibration for 3.9 min, total run time of 12.0 min. For gradient 2, starting with 1% B for 2 min followed by a linear increase from 2.0 min to 100% B at 10.0 min, held for 3 min followed by return to 1% B at 13.1 min, where it was held for equilibration for 2.9 min, total run time of 16.0 min. Data analysis used Bruker data analysis 4.3. Gradient 3 and mobile phases were: mobile phase A consisted of LC-MS grade water 0.1% FA v/v; mobile phase B consisted of

acetonitrile 0.1% FA v/v. Solvent gradient started from 1% B for 2 min followed by a linear increase from 2.1 min to 100% B at 9.0 min, held for 3 min, followed by a return to 1% B at 12.1 min, where it was held for 2.9 min for equilibration, giving a total run time of 15.0 min.

GC-MS analysis of SC combustion was achieved on a Thermofisher ISQ series GC-MS. Full scan mode 50–650 m/z, injection volume splitless 1 μL, with He as the carrier gas, flow rate 12.0 mL min⁻¹. HP-1 column was used (50 m × 0.32 mm, 0.17 μm thickness) Temperature gradient started at 80 °C, it was increased to 320 °C at 20 °C min⁻¹, then maintained for 3.0 min with a total run time of 15.0 min. Transfer line temperature 310 °C, ion source temperature 310 °C, scan rate of 0.2 s per scan. Data analysis used Xcalibur software.
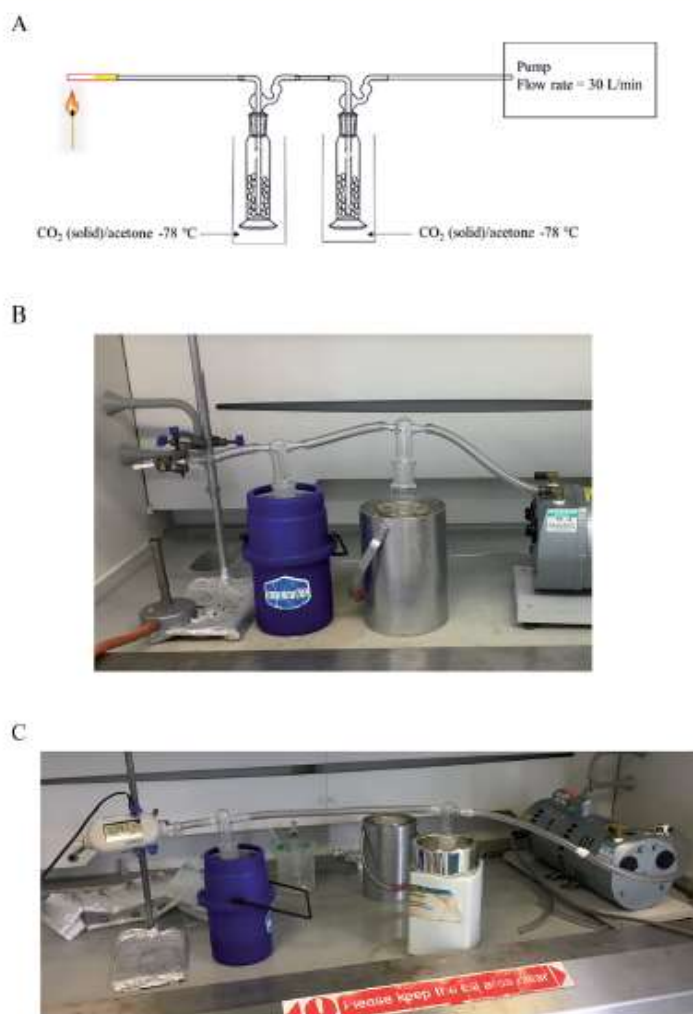

Fig. 2 In-house constructed SC smoking simulation model: (A) graphic, (B) cigarette inserted into the quartz tube, (C) Copley flow rate meter in position.

276

SC smoking simulation apparatus

The smoking model is a two-stage trap rig (Fig. 2), constructed in-house using two 250 mL gas washing bottles Lenz® (VWR, UK), filled to the midpoint with 8 mm glass beads (VWR, UK) to increase the surface area. Volatile products from the combustion were collected in two dry ice/acetone traps. The gas washing bottle heads were without filters, with traps placed in a dry ice/acetone slush-bath allowing the efficient trapping of the volatiles. A quartz tube 8 mm OD × ID 6 mm was purchased from Almath crucibles (Suffolk, UK) where the SC cigarettes were inserted. The traps were connected to a GAST G626X pump (General Electric, USA), the pump dial was used to control the flow rate which was measured using a Copley® DFM 2000 flow regulator (Nottingham, UK). The flow rate was set between 28–30 L min^{-1} and the temperature was monitored using a TENMA thermocouple. SC-doped herb (200 mg with SC concentration between 1–6% by weight)[62] was rolled into a cigarette and inserted into the quartz tube followed by lighting it with a cigarette lighter.

Sample collection

The condensed volatiles were extracted by washing the glass beads in each trap with methanol (3 × 25.0 mL), followed by concentration by solvent evaporation under a stream of nitrogen gas and finally the samples were reconstituted in methanol (1.0 mL) for UHPLC-TOF-ESI-MS and GC-MS analysis.

3. Results and discussion

Analysis of combustion showed the recovery of all six SCs tested by UHPLC-TOF-ESI-MS (AB-CHMINACA, AM-694, 5F-ADB,

MDMB-CHMICA, MMB-2201, 5F-PB-22) (Fig. 3). Three areas of the apparatus were tested for the presence of the SC, trap 1, trap 2 and the combustion zone (CZ) in the quartz tube where the 200–300 mg cigarettes were fixed. Most of the SCs were detected in the first trap (80–90%) and interestingly no to very little SCs were detected in the CZ, proving that the tested SCs have very good volatility. This is supporting evidence for reports of prisoners and prison guards being overcome by smoke inhalation in UK prisons.[15] There was neither visible evidence of the presence of American (Virginian) tobacco mixed with any of the SCs on herbal material tested, *T. diffusa* (Damiana), nor by HR-MS scanning the samples' MS data for any nicotine molecular ions e.g. $C_{10}H_{15}N_2$ requires 163.1229 [M + H]$^+$ and $C_{20}H_{29}N_4Cl$ dimer-HCl salt requires 360.2069 (Fig. S1†).

UHPLC-TOF-ESI-MS/MS analysis resulted in the detection of the combustion samples of AB-CHMINACA, AM-694, 5F-ADB/MMB-2201 mixture, and 5F-PB-22 (Fig. 4), with their mass ions and fragmentation pattern assignments confirmed by comparison with our in-house built database.[16] The total ion current (TIC) chromatograms are shown. Each TIC chromatogram represents the summed intensity across the entire range of masses being detected at every point in the analysis. Then the HR-MS data are shown followed by the extracted-ion chromatograms (EIC) of each analyte *m/z* value that is being sought. That the chromatographic peaks are homogenous, nothing is co-eluting, is seen from the clean HR-MS data. GC-MS analysis resulted in the detection of the parent SC in trap 1 as well as some combustion products from some of the SCs tested. 5F-PB-22 GC-MS combustion analysis resulted in the
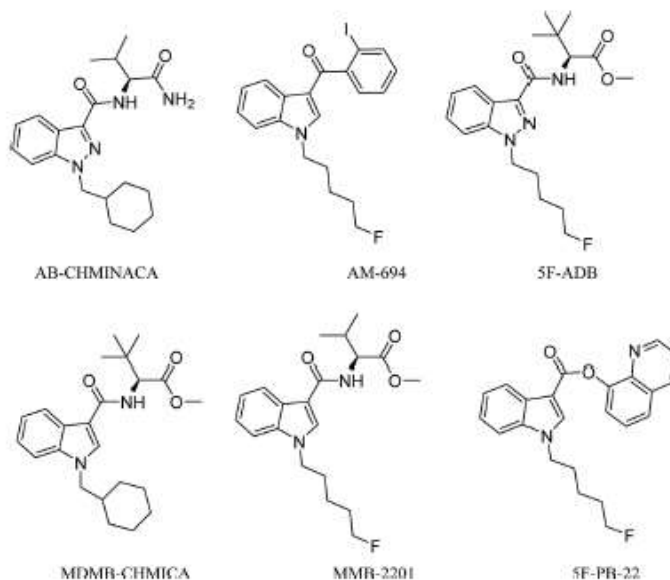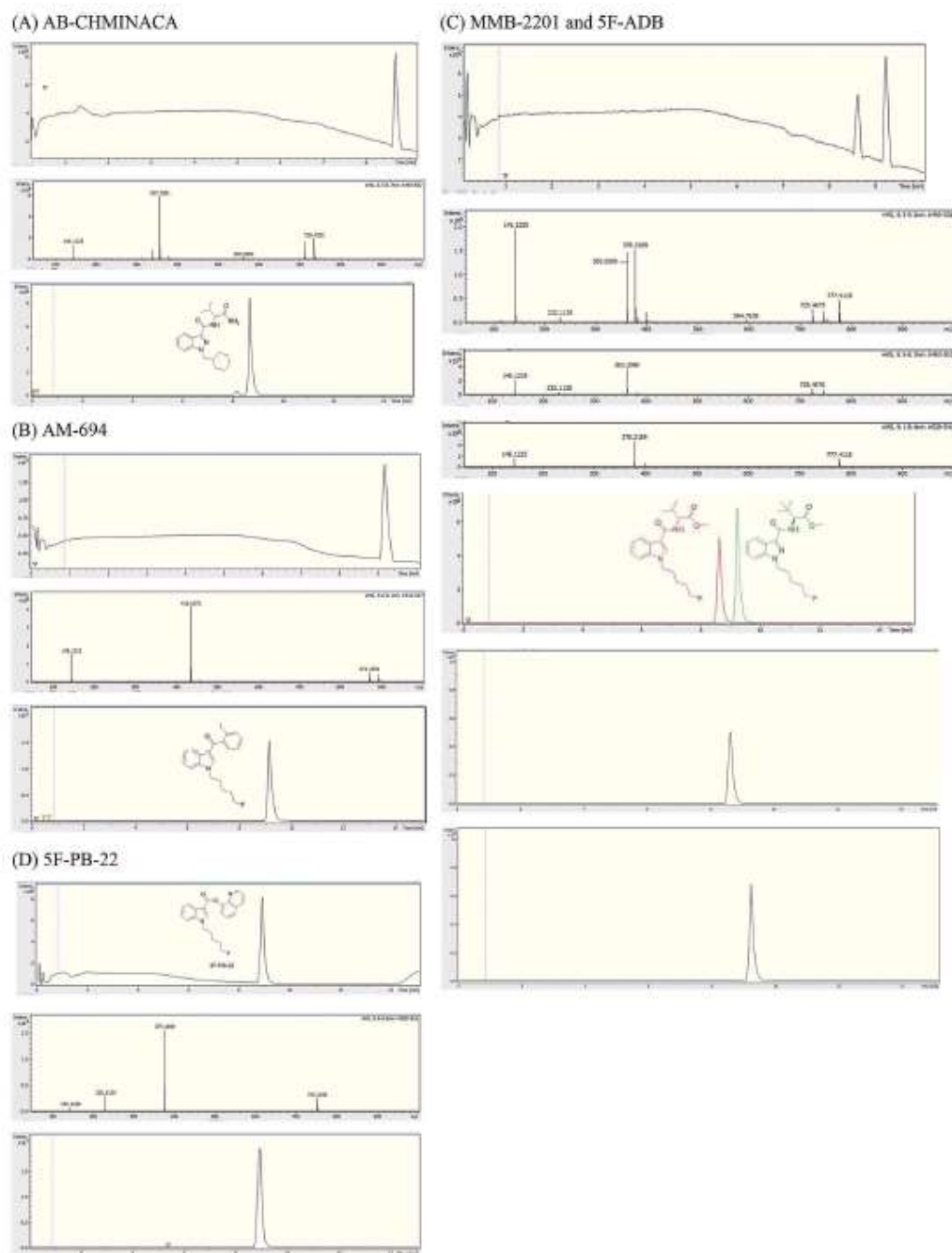

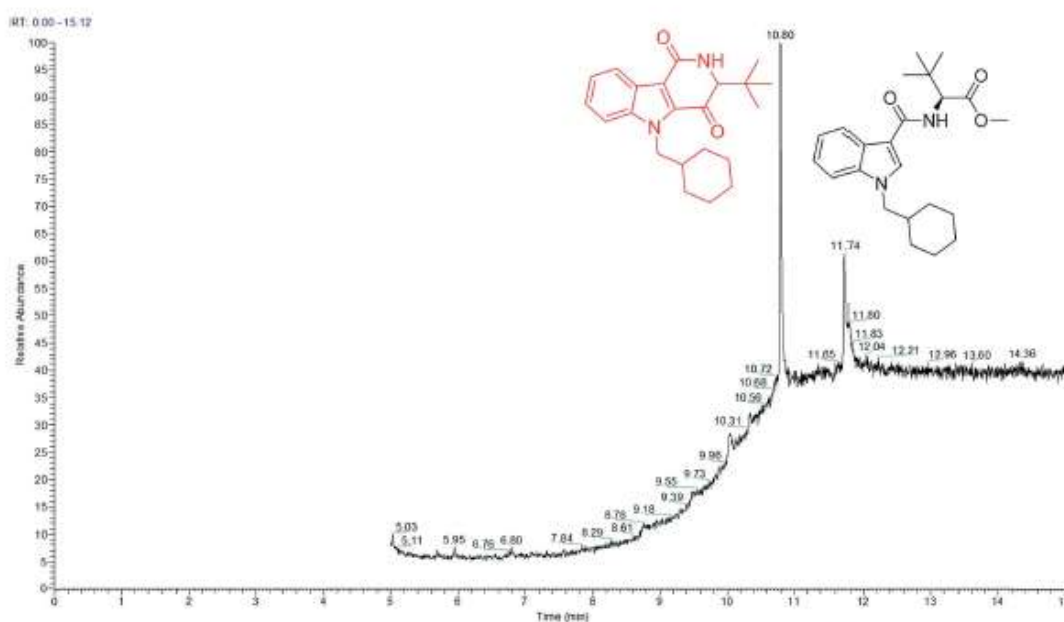Fig. 3 SCs tested by combustion analysis.

277

(A) AB-CHMINACA

(C) MMB-2201 and 5F-ADB

(B) AM-694

(D) 5F-PB-22

Fig. 4 Each TIC chromatogram is shown above the respective HR-MS data followed by the EIC of each specific analyte *m/z* value. Typical UHPLC-TOF-ESI-MS/MS analysis of trap 1 for: (A) AB-CHMINACA RT = 8.7 min, (B) AM-694 RT = 9.1 min, (C) MMB-2201 RT = 8.6 min, 5F-ADB RT = 9.2 min, (D) 5F-PB-22 RT = 8.9 min.

278

Fig. 5 TIC chromatogram of a combustion sample of MDMB–CHMICA showing the novel combustion product at RT = 10.80 min and MDMB–CHMICA at RT = 11.74 min.

detection of 5F-PB-22 at RT = 8.20 min as well as the combustion products 1-(5-fluoropentyl)-indole (205 m/z) and 1-pentyl-indole (185 m/z) at RT = 5.71 min and RT = 6.15 min respectively (Fig. S2†).

MDMB-CHMICA EI MS afforded a more extensive and slightly different fragmentation than the ESI-MS/MS. The first fragment resulted from the cleavage of the *tert*-butyl side chain (328) rather than the initial loss of methoxy observed in the ESI-MS/MS. In addition to the 240 base peak, also seen in the MS/MS analysis, 245 is concluded to be the result of the loss of the *tert*-butyl side-chain along with the cleavage of the cyclo-hexyl moiety with the formation of 1-methylidene-indolinium ion (Fig. S3†). These results are in agreement with those of Langer et al.[17]

Analysis of MDMB-CHMICA combustion showed that there had been the formation of a not previously reported combustion product. Two peaks appear in the combustion sample TIC chromatogram (Fig. 5), MDMB-CHMICA RT = 11.74 min, and the novel combustion product, a keto-δ-lactam (a dihydro-1*H*-pyridoindole-dione) RT = 10.80 min, which was absent in the crude sample of MDMB-CHMICA that had not been subjected to combustion. The proposed mechanism for the formation of the keto-δ-lactam is rearrangement involving intramolecular electrophilic substitution of indole by the terminal methyl ester of MDMB-CHMICA during the combustion process (Fig. S4†). Unlike in the MS fragmentation pattern of MDMB-CHMICA, the 296 m/z peak is more intense and is the result of the formation of an indole-1-cyclohexylmethyl-*N*-propylidene ion, while the rest of the fragments are similar to MDMB-CHMICA with a base-

peak fragment of 240 m/z. UHPLC separation of the two products and their HR-MS molecular ion identification using UHPLC-TOF-ESI-MS showed a low intensity peak and $[M + H]^+$ for the keto-δ-lactam at RT = 10.7 min, 353.2229 found for $C_{22}H_{29}N_2O_2$ requires 353.2223, and MDMB-CHMICA RT = 9.7 min, $[M + H]^+$ 385.2493 found for $C_{23}H_{33}N_2O_3$ requires 385.2485 (Fig. S5†).

4. Conclusions

The in-house constructed SC smoking simulator provided a good method for the recovery of combusted SCs. SCs showed good volatility with parent SCs being captured in the traps with little or no SC left in the combustion zone (CZ) as tested by UHPLC-MS and GC-MS. GC-MS analysis revealed combustion products for 5F-PB-22 that were not detected using the UHPLC method. Combustion of MDMB-CHMICA resulted in the formation of a novel keto-δ-lactam that could be detected by both GC-MS and UHPLC-ESI-MS analysis.

This study of combustion products of SCs provides markers which may be useful for drug analysts and toxicologists in examining samples obtained from suspected SC users. Thus, taken together, making reliable methods for the identification and quantification of substituted 3rd generation SCs.

Conflicts of interest

There are no conflicts of interest to declare.

Acknowledgements

References

1 I. Vardakou, C. Pistos and C. Spiliopoulou, Spice drugs as a new trend: Mode of action, identification and legislation, *Toxicol. Lett.*, 2010, **197**, 157–162.

2 J. W. Huffman, D. Dai, B. R. Martin and D. R. Compton, Design, synthesis, and pharmacology of cannabimimetic indoles, *Bioorg. Med. Chem. Lett.*, 1994, **4**, 563–566.

3 V. Auwarter, S. Dresen, W. Weinmann, M. Muller, M. Putz and N. Ferreiros, 'Spice' and other herbal blends: Harmless incense or cannabinoid designer drugs?, *J. Mass Spectrom.*, 2009, **44**, 832–837.

4 EMCDDA–Europol Annual Report on the implementation of Council Decision 2005/387/JHA, 2008, http://www.emcdda.europa.eu/attachements.cfm/att_132902_EN_2008_Implementation.report.pdf, accessed 05/04/19.

5 A. Makriyannis and H. Deng, Cannabimimetic indole derivatives, USP US 6900236 B1, University of Connecticut, 2005, https://patentimages.storage.googleapis.com/9d/ec/b4/ea8af239e287da/US6900236.pdf, accessed 05/04/19.

6 S. D. Banister, M. Moir, J. Stuart, R. C. Kevin, K. E. Wood, M. Longworth, S. M. Wilkinson, C. Beinat, A. S. Buchanan, M. Glass, M. Connor, I. S. McGregor and M. Kassiou, Pharmacology of indole and indazole synthetic cannabinoid designer drugs AB-FUBINACA, ADB-FUBINACA, AB-PINACA, ADBPINACA, 5F-AB-PINACA, 5F-ADB-PINACA, ADBICA, and 5F-ADBICA, *ACS Chem. Neurosci.*, 2015, **6**, 1546–1559.

7 E. W. Gunderson, H. M. Haughey, N. Ait-Daoud, A. S. Joshi and C. L. Hart, A survey of synthetic cannabinoid consumption by current cannabis users, *Subst. Abuse: Res. Treat.*, 2014, **35**, 184–189.

8 R. R. Baker, Temperature distribution inside a burning cigarette, *Nature*, 1974, **247**, 405–406.

9 R. R. Baker, Product formation mechanisms inside a burning cigarette, *Prog. Energy Combust. Sci.*, 1981, **7**, 135–153.

10 C. Darquenne, Aerosol deposition in health and disease, *J. Aerosol Med. Pulm. Drug Delivery*, 2012, **25**, 140–147.

11 P. Kavanagh, A. Grigoryev, S. Savchuk, I. Mikhura and A. Formanovsky, UR-144 in products sold *via* the Internet: Identification of related compounds and characterization of pyrolysis products, *Drug Test. Anal.*, 2013, **5**, 683–692.

12 S. Raso and S. Bell, Qualitative analysis and detection of the pyrolytic products of JWH-018 and 11 additional synthetic cannabinoids in the presence of common herbal smoking substrates, *J. Anal. Toxicol.*, 2017, **41**, 551–558.

13 R. C. Kevin, A. L. Kovach, T. W. Lefever, T. F. Gamage, J. L. Wiley, I. S. McGregor and B. F. Thomas, Toxic by design? Formation of thermal degradants and cyanide from carboxamide-type synthetic cannabinoids CUMYL-PICA, 5F-CUMYL-PICA, AMB-FUBINACA, MDMB-FUBINACA, NNEI, and MN-18 during exposure to high temperatures, *Forensic Toxicol.*, 2019, **37**, 17–26.

14 A. Kaizaki-Mitsumoto, K. Hataoka, M. Funada, Y. Odanaka, H. Kumamoto and S. Numazawa, Pyrolysis of UR-144, a synthetic cannabinoid, augments an affinity to human CB1 receptor and cannabimimetic effects in mice, *J. Toxicol. Sci.*, 2017, **42**, 335–341, DOI: 10.2131/jts.42.335.

15 C. Howgego, The Guardian, Prisoners say 'spice' use has tripled fuelling violence, illness and debt, 2016, https://www.theguardian.com/society/2016/jun/01/prisoners-reveal-regular-spice-use-tripled-legal-high-violence-illness-debt, accessed 05/04/19.

16 H. A. Naqi, T. J. Woodman, S. M. Husbands and I. S. Blagbrough, ^{19}F and ^{1}H quantitative-NMR spectroscopic analysis of fluorinated third-generation synthetic cannabinoids, *Anal. Methods*, 2019, DOI: 10.1039/c9ay00814d, accompanying paper in this issue.

17 N. Langer, R. Lindigkeit, H.-M. Schiebel, U. Papke, L. Ernst and T. Beuerle, Identification and quantification of synthetic cannabinoids in "spice-like" herbal mixtures: update of the German situation for the spring of 2015, *Forensic Toxicol.*, 2016, **34**, 94–107.

280

Check for updates

^{19}F and ^{1}H quantitative-NMR spectroscopic analysis of fluorinated third-generation synthetic cannabinoids†

Husain A. Naqi, Timothy J. Woodman, Stephen M. Husbands and Ian S. Blagbrough *

Quantitative nuclear magnetic resonance (q-NMR) spectroscopy is a robust and reliable analytical method that possesses many advantages over conventional chromatographic techniques used in drug analysis. In this paper, the application of ^{19}F and ^{1}H NMR spectroscopy to quantify the amounts of synthetic cannabinoids (SCs), AM-694 and 5F-ADB, in herbal incense packages is discussed. These SC samples, seized in the South West of England in the summers of 2016 and 2017, are part of a growing illicit drug problem in the UK. For accurate quantitative analysis using ^{19}F observe, the data acquisition and the NMR processing parameters, such as spectral width, the centre point of the spectrum, nuclear Overhauser effect (NOE) enhancement and relaxation delay, are discussed together with cross-method validation. The reproducibility, simplicity, high speed, and non-destructive nature provide reliable quantitative analysis and, by using ^{19}F NMR, there is essentially no background interference. This quantitation is without resorting to the use of (often unavailable) standards as reference materials or to lengthy sample preparation, which are the norm in many analytical chromatographic techniques. The NMR methods allowed a direct comparison between ^{1}H and ^{19}F NMR, revealing the robustness and the effectiveness of ^{19}F NMR for application as a rapid (~8 min), quantitative analytical method for fluorinated SCs which are now being seized with an increasing frequency and are highly toxic.

Introduction

Synthetic cannabinoids (SCs), also known by their street name "spice", are potent agonists binding to the cannabinoid receptors CB_1 and CB_2 distributed throughout the central nervous system (CNS) and immune system, respectively, producing psychoactive effects similar to, and in most cases more potent than, the mainstream drugs they are mimicking, e.g. Δ^9-tetrahydrocannabinol (THC).[1] Unlike Δ^9-THC, a partial agonist with low affinity for the CB_1 receptor, SCs are full receptor agonists with high affinity binding to CB_1 and moreover they also possess CB_2 receptor affinity.[2] These pharmacological characteristics result in drug users/abusers having severe physical and psychiatric episodes, not present with traditional cannabis smoking. These effects are described as the "cannabinoid tetrad", which are hypothermia, analgesia, catalepsy, and

Department of Pharmacy and Pharmacology, University of Bath, Bath BA2 7AY, UK. E-mail: prsisb@bath.ac.uk; Tel: +44 (0)1225 386795

† Electronic supplementary information (ESI) available: Fig. S1 shows the ^{19}F NMR (^{1}H coupled) stacked spectra of 5F-ADB with its ^{19}F signal at −220.2 ppm and the IS 2-chloro-4-fluorotoluene (−117.8 ppm) with different O1P set at (A) −165 ppm, (B) −220 ppm, and (C) −117 ppm, with (inset) expansion of the of 5F-ADB ^{19}F signal. Fig. S2 shows 5F-ADB quantified in a sample using ^{1}H, ^{19}F proton coupled, and ^{19}F inverse-gated decoupled spectroscopy. See DOI: 10.1039/c9ay00814d

locomotor activities, leading to symptoms ranging from excited delirium to kidney damage.[3]

In 2008, the first generation of synthetic cannabinoids hit the streets,[3] such as the Pfizer compound CP 47,497 and the John W. Huffman designed JWH-018 (Fig. 1). Typically these ligands were designed and developed as medicinal chemistry compounds, intended to exploit the pathological implications of the CB receptors in many diseases, but they were side-tracked to the illicit clandestine designer-drug market.[4,5] The following generations of SC were based initially on JWH-018, but they have evolved with variations of fluoroalkyls (AM-694), indazoles (5F-ADB), quinoline (5F-PB22) and amides (PX-1) integrated into their structures, replacing the naphthoylindole of JWH-018.[6,7] The continuous and rapid change in substituents on the available SCs makes them a moving target posing many analytical challenges. The Korean National Forensic Services reported that from 2008 to 2010 most of the SCs seized were first generation non-fluorinated compounds,[8] e.g. JWH-018, CP 47,497, and UR-144 (Fig. 1). In 2012, fluorinated analogues started emerging such as XLR-11, a fluoropentyl analogue of UR-144, and by 2013 approximately 90% of the SCs seized were fluorinated.[8] It is believed that the growing trend in the bioisosteric fluorine introduction into SCs was inspired by a Makriyannis patent,[9] where he demonstrated a much higher potency of AM-2201 than that of non-fluorinated analogues, e.g.

281

JWH-018 (Fig. 1). Initially, AM-2201 was identified in herbal blends, and this has escalated into many SCs with no precedent in the scientific literature, e.g. 5F-ADB-PINACA, 5F-AB-PICA, and 5F-PB-22.[5] The third-generation SCs include fluorinated AM-694 and 5F-ADB (Fig. 1). Also, besides the enhanced potency of fluorinated analogues, the addition of a fluorine substituent was possibly intended to circumvent legal restrictions imposed on specified SCs.[5,10]

^{1}H-NMR is inherently quantitative, as the integrated functional group signals are directly proportional to the number of spins generated by the signals in question. Nevertheless, NMR is only quantitative if the appropriate acquisition and processing parameters are determined by experiment and then implemented. Early applications of quantitative NMR (q-NMR), using low-field instruments, required considerably large amounts of sample and Internal Standard (IS).[11] The development of high-field NMR spectrometers facilitated improved sensitivity meaning that impurities could be quantified at less than 0.1% of the total sample, demonstrating that NMR is comparable with chromatographic methods for quantitative analysis.[12–15] NMR has more advantages than other analytical approaches such as those that are chromatography based. NMR does not require the use of a high purity reference standard for the construction of the required calibration curve. Such a standard is expensive and often unavailable, especially for newer, more recently identified SCs.[14] NMR also has the advantage of less sample preparation being required. No serial dilution is required to run the sample and no mobile phase has to be prepared. Also, as there is no interaction with a column, no blank samples are required to be chromatographed in order to avoid carry-over that could affect the analysis. NMR is not subject to problems from small compounds and impurities with no chromophore or a different UV response which pose challenges to chromatographic and UV methods.[14,15]

Quantitative analysis of SCs in herbal blends has been reported using some analytical techniques, mostly chromatography and MS-based ones.[16] GC/MS showed qualitative and quantitative variations among SCs in herbal-blend brands in 2014.[17] ^{1}H q-NMR reports on SC quantitation are scarce, but there is a report on purchased herbal blends containing SCs using maleic acid (MA) as an internal standard.[18] A study on the extraction efficiency of common solvents, e.g. acetone, acetonitrile, chloroform, and methanol, using ^{1}H q-NMR with 1,3,5-trimethoxybenzene as an internal standard and GC/MS on seized herbal blends and in-house preparations found no significant difference between the solvents used for the SC extraction.[19]
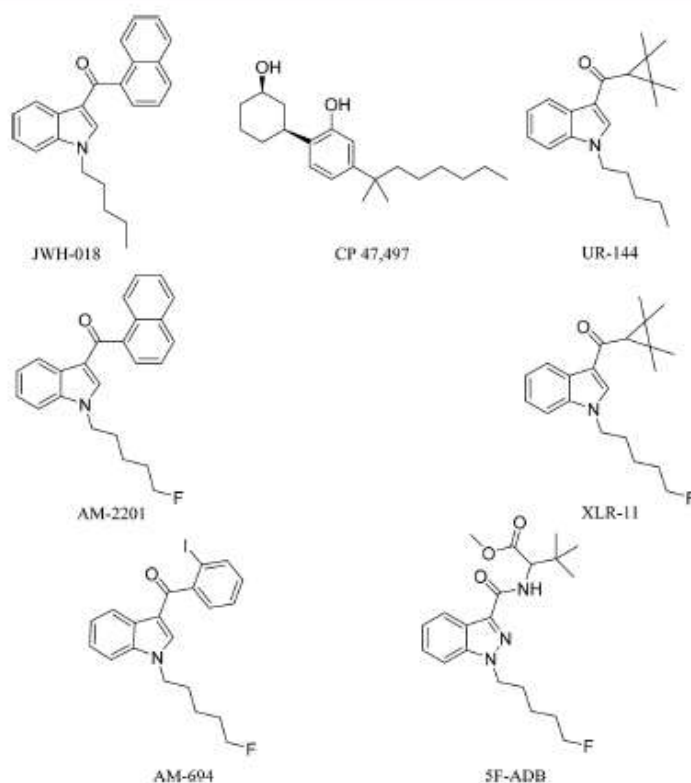

Fig. 1 1st, 2nd, and 3rd generation SCs.

282

The ^{19}F nucleus is attractive for q-NMR spectroscopy, mainly due to the sensitivity of the nucleus (its relative sensitivity is 83.4% of ^{1}H) and its natural abundancy of 100%.[20] Additionally, the wide range of chemical shift (500 ppm) reduces the chance of overlapping signals, and the absence of fluorinated impurities inherently means that there is less background noise.[21] ^{19}F q-NMR has been applied to analyse fluorinated Active Pharmaceutical Ingredients (API).[22] Nevertheless, for quantitative results more NMR parameters have to be addressed than for ^{1}H q-NMR,[21] e.g. equal excitation for the signals across the entire spectral width must be achieved, otherwise the integration values will suffer which in turn affects the analytical results. This is achieved by setting the centre point of the spectral window midway between the signal of the internal standard and the compound, using a 90° pulse angle followed by a sufficient relaxation delay of $5 \times T_1$ to recover the magnetization to 99.3% of its size. The use of a suitable relaxation delay is common with ^{1}H q-NMR. If the ^{19}F spectrum is acquired with broadband ^{1}H decoupling, then NOE enhancement of the signals may arise. In order to avoid this, an inverse-gated decoupling sequence is used.[21]

A validated ^{19}F q-NMR spectroscopic method is reported for the first time to quantify fluorinated SCs, e.g. AM-694 and 5-F-ADB (Fig. 1), in herbal blends recently seized in the South West of England. The technique was compared to both ^{1}H q-NMR and UHPLC for accurate quantification and was shown to be in good agreement. Moreover, quantitative differences between seized sample batches are discussed. This investigation of the acquisition parameters associated with ^{19}F q-NMR will help drug analysts to run a fast and robust quantitative analysis for fluorinated (illicit) drugs with minimal background interference and signal overlap. It is important because such highly toxic SCs are currently being found with increasing frequency and outbreaks of zombification caused by AMB-FUBINACA have been reported in NEJM,[23] and in various UK cities in the popular press.

Experimental section

Chemicals and sample preparation

Extraction solvents (all 99.9% anhydrous) chloroform, methanol, and acetonitrile were purchased from Fisher Scientific (UK) and ACROS Organics (UK). Deuterated solvents (CDCl$_3$, CD$_3$OD, and CD$_3$CN) were purchased from Cambridge Isotope Laboratories (Goss Scientific, UK). NMR internal standards (IS) 2-chloro-4-fluorotoluene, dimethyl sulfone (DMS), and maleic acid (MA) are *TraceCERT* certified reference materials purchased from Sigma-Aldrich (UK). [1-(5-Fluoropentyl)-1*H*-indol-3-yl](2-iodophenyl)-methanone (AM-694) 10.0 mg, *N*-(1-adamantyl)-1-(5-fluoropentyl)-1*H*-indazole-3-carboxamide (5F-AKB-48) 1.0 mg mL^{-1} in a 1.0 mL vial, and (1-pentyl-1*H*-indol-3-yl)-1-naphthalenyl-methanone (JWH-018) 100 μg mL^{-1} in a 1.0 mL vial were purchased from LGC (Teddington, UK). *N*-Methyltrifluoroacetamide (*N*-methyl-TFA) >98.0% was purchased from Tokyo Chemical Industry (TCI, Tokyo, Japan). SC samples were provided by the Drug Expert Action Team (DEAT), Avon and Somerset Constabulary, from recent (2016–2017) seizures.

The samples were in the form of herbal blends (1.0–3.0 g) as commercially packaged brands (Exodus, Loco Elite). *Turnera diffusa* (damiana) dried herb (illicit-drug free) was purchased from Spiceworks (Hereford, UK).

All standards and samples were weighed using a SE2F Sartorius analytical balance, between 1.0 and 2.0 mg mL^{-1} IS was used. Preliminary analysis of non-homogenized herbal-blend samples yielded large variations in the amounts of the SCs sprayed on the carrier plant materials between samples tested by NMR. Therefore, two approaches were employed for the homogenization of the herbal-blend samples. Either they were ground to a fine powder with 100 grit sandpaper[24] or they were frozen in liquid nitrogen, followed by grinding to a fine powder using a mortar and pestle. For sample preparation for UHPLC and NMR analyses, homogenized plant materials (100 mg) were extracted with methanol (2 × 4.0 mL) with sonication (30 min) at 20 °C, centrifuged, and then the supernatant extract was decanted and the pellet (plant material) discarded. The extract was then evaporated to dryness under reduced pressure and reconstituted in deuterated solvent (1.0 mL) containing the IS (DMS, MA or 2-chloro-4-fluorotoluene) for NMR spectroscopic analysis. For UHPLC analysis, samples were diluted 100-fold in UHPLC solvent to bring them within the calibration range. AM-694 was quantified using a 7-point calibration curve between 1.25 and 80 μg mL^{-1} with JWH-018 as the IS. 5F-ADB was quantified using a 6-point calibration curve between 1.25 and 40 μg mL^{-1} with 5F-AKB48 as the IS (10.0 μg mL^{-1}). The response was calculated as the ratio of the area under the curve of the compounds to that of the respective IS. Data analysis was conducted using the Microsoft Excel data analysis tool pack.

Instrumentation

NMR spectroscopy. NMR spectra were recorded on a Bruker AVANCE III 500 MHz spectrometer. [1]H, ^{13}C, and ^{19}F frequencies are 500.13, 125.76, and 470.59 MHz, respectively. The probe was a variable temperature BBFO+ with three channels, and the temperature was 25 °C. Chemical shifts were referenced to 0.0 ppm for TMS or residual (protio) solvent peaks and are reported in ppm. Coupling constants (*J*, line-separations, absolute values) are rounded to the nearest 0.5 Hz. An inversion recovery pulse sequence was performed to measure the longitudinal relaxation time T_1 for the 2-chloro-4-fluoro-toluene IS and 5F-ADB. The T_1 relaxation delay for the IS signal for ^{1}H quantification for H5 ([1]H $\delta = 6.98$ ppm, 1H, td 8.5, 2.5 Hz) was 5.7 s, and T_1 for the indazole 5F-ADB ranged from 2.9–3.5 s. For quantitative ^{1}H NMR, the pulse sequence was composed of 64k data points, an acquisition time of 3.18 s, 16 scans, 50 s delay, and 90° pulse angle; integration was performed manually. All NMR spectra were acquired using Bruker TopSpin 2.1 and processed using either Bruker TopSpin 3.5 or Mestralab Mnova 11.2. The ^{19}F q-NMR proton coupled and inverse gated pulse sequence used a sweep of 241.51 ppm, O1P – 168 ppm, 6k point counts, an acquisition time of 0.7 s, 16 scans, 30 s delay, and 90° pulse angle; phase and baseline correction and integration were performed manually. Structural elucidation was achieved with

283

the use of 2D NMR spectroscopy. Eqn (1) was used for ^{1}H q-NMR quantitation:

$$m(\mathrm{x}) = P(\mathrm{std}) \frac{M_w(\mathrm{x})}{M_w(\mathrm{std})} \frac{A(\mathrm{x})}{A(\mathrm{std})} m(\mathrm{std}) \frac{N(\mathrm{std})}{N(\mathrm{x})} \frac{m(\text{herbal package})}{m(\text{sample used})}$$

(1)

where x is the analyte, std is the IS, m is the mass in mg, P is the purity, M_w is the molecular weight in g mol^{-1}, A is the integral value of the resonance being investigated, N is the number of protons represented by the signal, m(herbal package) is the mass of the herbal package in mg and m(sample used) is the mass of the extracted sample in mg.

UHPLC-ESI-MS/MS. The UHPLC-ESI-QTOF MS analysis was conducted using a MaXis HD quadrupole electrospray ionization time-of-flight (ESI-QTOF) mass spectrometer (MS) (Bruker Daltonik GmbH, Bremen, Germany), operated in ESI positive-mode. The QTOF was coupled to an Ultimate 3000 UHPLC (Thermo Fisher Scientific, Sunnyvale, CA, USA). The capillary voltage was set to 4500 V, nebulizing gas at 4 bar, and drying gas at 12 L min^{-1} at 220 °C. The TOF scan range was from 75 to 1000 mass-to-charge ratio (m/z). For LC-MS/MS capabilities, the in-source CID was set to 0.0 eV, with the collision energy for TOF MS acquisition at 3.0 eV. The collision energy was set to a sliding scale from 100 m/z at 14.0 eV, 500 m/z at 20.0 eV and 1000 m/z at 30.0 eV. For the analytes, the actual collision energy was between 15.0 and 18.0 eV. UHPLC calibration curve construction and sample quantitative analysis were performed on a Dionex Ultimate 3000 UHPLC with a variable wavelength detector (λ = 254, 280, and 298 nm). Liquid chromatography separation was performed using an Acquity UPLC BEH C18, 1.7 μM, 2.1 × 50 mm RP-column (Waters, Milford, MA, USA) with a flow rate of 0.4 mL min^{-1}, and an injection volume of 10 μL at a column temperature of 40.0 °C.

Mobile phase A consisted of MS grade water with 0.1% trifluoroacetic acid (v/v), and mobile phase B consisted of acetonitrile with 0.1% trifluoroacetic acid (v/v). For AM-694 and 5F-ADB calibration curves and quantitation the following solvent gradient 1 was used: the gradient started from 1% B for 2.0 min followed by a linear increase to 100% B at 5.0 min, held for 3 min, followed by a return to 1% B at 8.1 min, where it was held for equilibration for 3.9 min, with a total run time of 12.0 min. For 5F-ADB purity determination, the flow rate was 0.4 mL min^{-1}, and the column temperature was 25.0 °C. Gradient 2 started with 1% B until 2.0 min followed by a linear increase to 100% B at 20.0 min, held for 4.0 min, followed by a return to 10% B at 24.1 min where it was held for 10.9 min with a total run time of 35.0 min. Data analysis used the Bruker data and quant analysis 4.3 package.

Results and discussion

The 5F-ADB reference material was extracted from a seized sample (1.3 g) with CHCl$_3$ (2 × 25.0 mL) with sonication for 30 min each time. The combined extracts were passed through a 0.25 μm syringe filter. The filtrate was evaporated to dryness under reduced pressure yielding ~90 mg of residue which was purified by flash-column normal phase silica chromatography, followed by semi-preparative RP HPLC, resulting in pure 5F-

ADB (38.0 mg). Purity and confirmation of the structure were obtained by NMR, UHPLC, and HRMS (Fig. 2).

^{1}H NMR (500 MHz in CD$_3$OD): δ 8.21 (4′) (1H, dd J = 8.0, 2.0 Hz), 7.83 (NH) (1H, br d J = 9.5 Hz), 7.64 (7′) (1H, dd J = 8.5, 1.5 Hz), 7.46 (6′) (1H, td J = 8.5, 1.5 Hz), 7.29 (5′) (1H, td J = 8.5, 2.0 Hz), 4.62 (2″) (1H, d J = 9.5 Hz), 4.52 (1‴) (2H, t J = 7.5 Hz), 4.40 (5‴) (2H, dt J = 47.5, 6.0 Hz), 3.78 (5″) (3H, s), 2.01 (2″) (2H, quintet J = 7.5 Hz), 1.73 (4‴) (2H, d quintet J = 26.0, 6.0 Hz), 1.41–1.47 (3‴) (2H, m), 1.10 (4″) (9H, s).

^{13}C NMR (125.8 MHz in CD$_3$OD): δ 173.1 (1″), 164.2 (1), 142.5 (7′a), 137.3 (3′), 126.8 (6′), 124.0 (5′), 123.9 (3′a), 123.0 (4′), 111.1 (7′), 84.7 (5‴, d $^1J_{CF}$ = 164.0 Hz), 61.3 (2″), 52.5 (5″), 50.2 (1‴), 35.8 (3″), 31.0 (4‴, d $^2J_{CF}$ = 19.5 Hz), 30.4 (2‴), 27.1 (4″), 23.7 (3‴ d, $^3J_{CF}$ = 5.5 Hz); ^{19}F observe δ −220.3 (5‴F, tt $^2J_{HF}$ = 47.5, $^3J_{HF}$ = 26.0 Hz). HRMS found [M + H]$^+$ 378.2193 m/z for C$_{20}$H$_{29}$FN$_3$O$_3$ requires 378.2187, and found [M + Na]$^+$ 400.2010 m/z for C$_{20}$-H$_{28}$FN$_3$O$_3$Na requires 400.2006 (Fig. 2).

5F-ADB quantified in seized herbal blends

N-[[1-(5-Fluoropentyl)-1H-indazol-3-yl]carbonyl]-3-methyl-ʟ-valine methyl ester (5F-ADB) was identified in seized herbal blend samples branded as "Exodus". Identification was achieved by interpretation of 2D NMR data and the LC-MS/MS fragmentation pattern. Results are confirmed by comparison with the literature with only minor differences in the NMR, due to solvent effects.[23,24] The ^{19}F signal for q-NMR analysis is on the N-pentyl tail with its chemical shift of δ = −220 ppm assigned as a triplet of triplets, $^2J_{HF}$ 47.5 Hz coupling to methylene protons on position 5‴ and $^3J_{HF}$ 26.0 Hz coupling to methylene at position 4‴.

The extraction was evaluated in chloroform, methanol, and acetonitrile. The signals used for quantification in methanol were the indazole protons 4′ at 8.22 ppm, 7′ at 7.64 ppm, 6′ at 7.46 ppm, and 5′ at 7.31 ppm. In acetonitrile, the same protons were used except 6′ due to an overlapping impurity. In chloroform, H-5′ was excluded due to the overlap with the residual chloroform H-solvent signal; nevertheless chloroform gave a cleaner spectrum, with fewer impurities and no sugars from the matrix component (as found when methanol was the solvent of extraction) with additional signals available for integration such as the fluoropentyl methylenes 1‴ and 5‴. The DMS singlet at δ = 3.00 ppm integrating for six protons was used as an IS in CDCl$_3$.

In ^{19}F q-NMR with N-methyltrifluoroacetamide, apparently significantly lower amounts of SC, using Anova two factor analysis, were obtained than in a contemporaneous analysis by ^{1}H q-NMR using maleic acid (IS) in methanol and acetonitrile, DMS (IS) in chloroform, and then N-methyltrifluoroacetamide in chloroform (Table 1). The reason behind this apparently lower assay result is the resonance (chemical shift) of the N-methyltrifluoroacetamide ^{19}F signal at δ = −75.9 compared to the ^{19}F signal of 5F-ADB at δ = −220.2 ppm, resulting in unequal excitation. Uniform excitation across the spectrum has to be achieved in order for all the signals to get the same magnetization in the pulse sequence, thus making the centre point of the spectral window a crucial parameter when accurate and reproducible quantitative results are to be achieved for ^{19}F q-NMR.
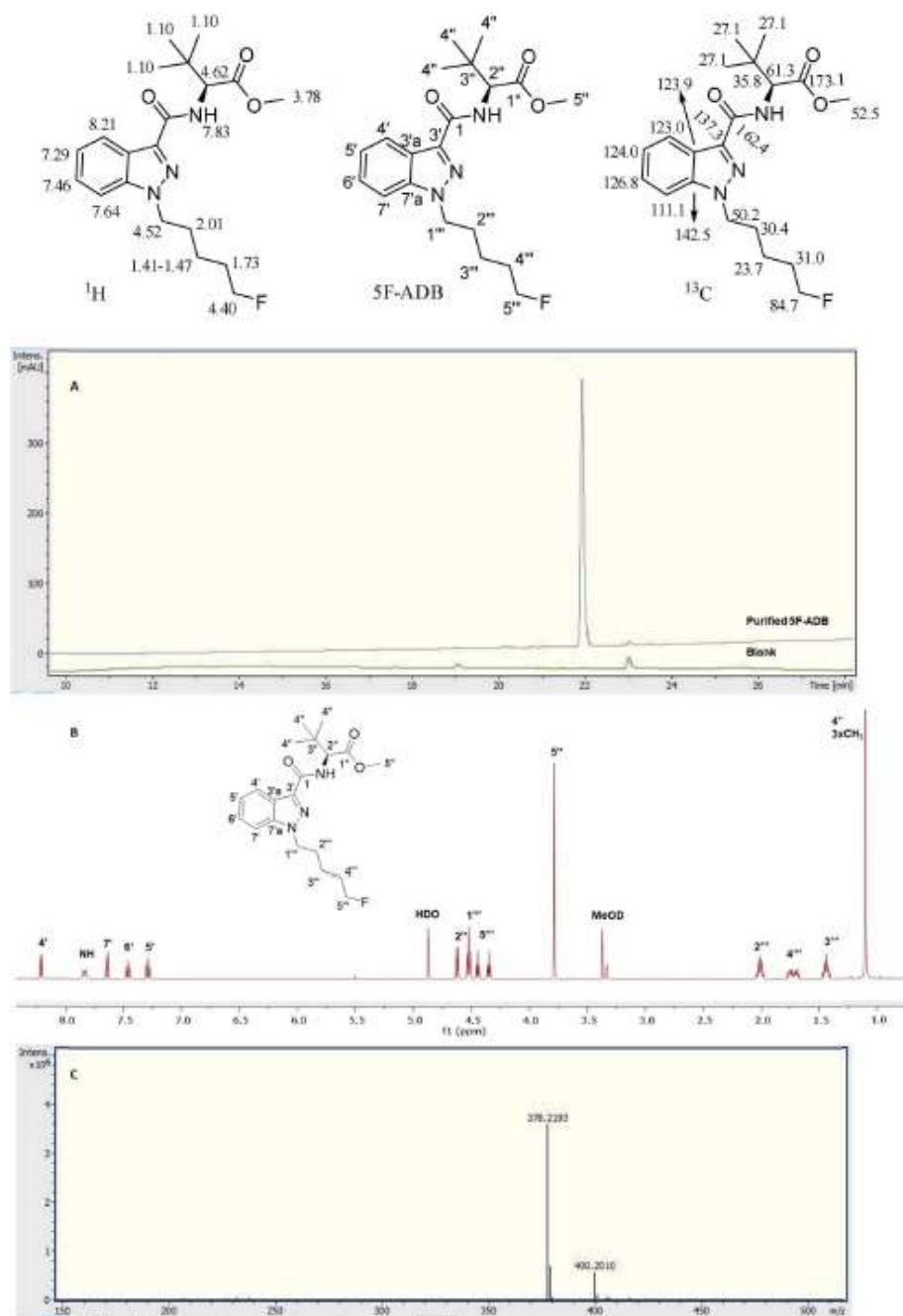
284

Fig. 2 Analytical purity of 5F-ADB as tested by (A) UHPLC with RT = 22.0 min, (B) ¹H-NMR in CD₃OD with assignments, and (C) HRMS showing [M + H]⁺ and [M + Na]⁺.

When N-methyltrifluoroacetamide was evaluated as an IS for ¹H q-NMR it was shown to be as useful an IS as MA or DMS. Although apparently attractive for ¹⁹F NMR with its 3 equivalent fluorine atoms, its wide chemical shift separation from the analyte signal made it a poor choice. Rather, 2-chloro-4-fluorotoluene was used as a ¹⁹F q-NMR IS with (protio) methanol as

285

Table 1 Quantitative analysis of a sample of 5F-ADB by ^{1}H NMR in CD$_3$OD, CD$_3$CN, and CDCl$_3$ compared to ^{19}F q-NMR using N-methyltri-fluoroacetamide ($n = 4$)

Nucleus, solvent (IS)	^{1}H in CD$_2$OD (MA)	^{1}H in CD$_3$CN (MA)	^{1}H in CDCl$_3$ (DMS)	^{1}H in CDCl$_3$ (N-Me-TFA)	^{19}F in CDCl$_3$ (N-Me-TFA)
Amount (mg g^{-1})	11.84 ± 0.28	11.06 ± 0.16	11.03 ± 0.14	11.48 ± 0.12	8.86 ± 0.19
RSD (%)	2.34	1.45	1.30	1.01	2.18

the extraction solvent and CD$_3$OD as the NMR solvent, resulting in a good agreement with the data from ^{1}H q-NMR using maleic acid (MA) as the IS. This ^{19}F NMR IS signal has a chemical shift of $\delta = -117.8$ ppm. As 5F-ADB ^{19}F resonates at $\delta = -220.2$ ppm, the central point (Bruker's O1P) was therefore set at $\delta = -165$ ppm approximately equally between both resonances resulting in equal excitation of both fluorine signals. The ^{19}F q-NMR (proton coupled) results of 5F-ADB are in agreement with the ^{1}H q-NMR results using maleic acid (MA) (10.4 ± 0.2 mg g^{-1}, RSD 1.6%, $n = 5$) as the IS and 9.8 ± 0.8 mg g^{-1} (RSD 7.9%, $n = 5$) was observed with 2-chloro-4-fluorotoluene as the IS, and 9.4 ± 0.7 mg g^{-1} (RSD 7.3%, $n = 5$) with ^{19}F NMR. The effect of changing the O1P was tested using the plant material (100.0 mg) containing 5F-ADB with 2-chloro-4-fluorotoluene as the IS, and setting the O1P approximately in the middle of the two signals (-165 ppm). This resulted in quantitative results in agreement with ^{1}H q-NMR results. Not unexpectedly, shifting the O1P to -220 and -117 ppm resulted in significantly lower

and higher integration values, respectively, and, consequently, significantly altered quantitative results as tested by t-tests ($p < 0.05$) (Fig. S1†). The need to set the spectral midpoint as the excitation frequency is an important parameter.

A seized sample (HN Exodus5) containing 5F-ADB was analysed using inverse-gated decoupling ^{19}F NMR in order to eliminate the nuclear Overhauser effect (NOE), and for providing the added benefit of an enhanced signal to noise (S/N) ratio by collapsing the ^{19}F signals to singlets. The results were compared with proton-coupled ^{19}F NMR; the results from the ^{19}F proton coupled and ^{19}F proton decoupled methods are in good agreement (Fig. S2†). ^{1}H q-NMR showed 7.1 ± 0.11 mg g^{-1} (RSD of 1.57%), ^{19}F proton-coupled q-NMR showed 6.9 ± 0.02 mg g^{-1} (RSD of 0.24%), and ^{19}F inverse-gated decoupled q-NMR showed 6.8 ± 0.08 mg g^{-1} (RSD of 0.78%).

Two batches of seized "Exodus" brand, 8 seized in 2016 and 7 seized in 2017, were subjected to quantitative analysis using ^{19}F proton coupled/decoupled and ^{1}H NMR using the IS 2-chloro-4-

1-Me-indazole-3-carboxylicacid   5F-ADB   5F-AKB48
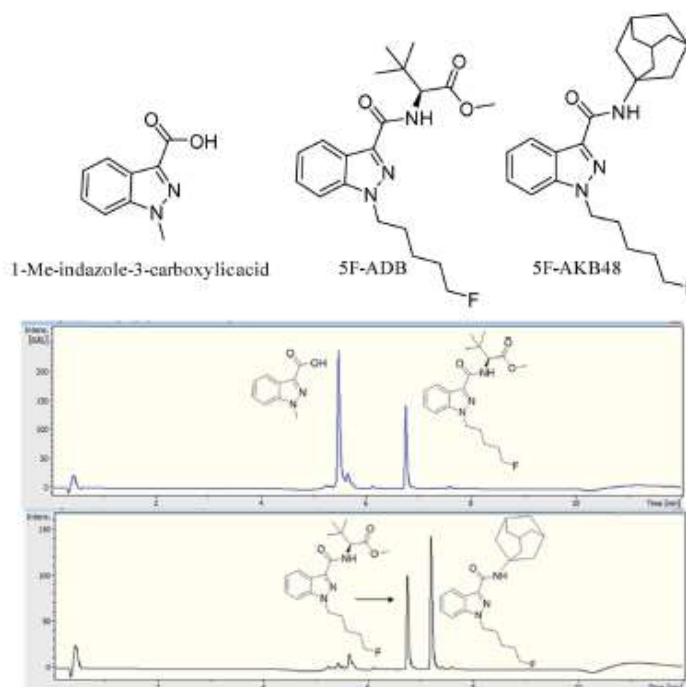
Fig. 3 UHPLC chromatograms ($\lambda = 298$ nm) for an "Exodus" sample containing 5F-ADB, RT = 6.8 min, (upper) using 1-methylindazole-3-carboxylic acid as the IS, RT = 5.6 min, showing overlap with a matrix component, (lower) using 5F-AKB48 as the IS, RT = 7.2 min.

286

fluorotoluene, and also by UHPLC. Confirmation of the quantitation by ^{19}F q-NMR was achieved with UHPLC using the purified 5F-ADB as the reference standard to construct a calibration curve (gradient 1), using $\lambda = 298$ nm wavelength where the indazole absorbs strongly, resulting in RT = 6.8 min. Initially, 1-methylindazole-3-carboxylic acid was used as a UHPLC IS, but this was abandoned due to the overlap of the 1-methylindazole-3-carboxylic acid peak with a plant matrix component at RT = 5.6 min (Fig. 3). 5F-AKB48 (RT = 7.2 min) was chosen instead as an IS in UHPLC analysis due to its similar chromophore to 5F-ADB (indazole), and the presence of an N-adamantanyl substituent provided sufficient hydrophobicity to be separated from the peak of 5F-ADB (Fig. 3). The 5F-ADB UHPLC calibration curve using 5F-AKB48 as an IS was in the range of 1.25–40.00 μg mL^{-1} giving excellent linearity, $R^2 = 0.9999$, and an IS RSD of 4.8% (Fig. 4).

2016 seized "Exodus" sample analyses revealed a consistent dose of 5F-ADB across all 8 samples with an acceptable precision (RSD %) of less than 10% for the analysis of samples in the herbal form (Table 2).[27] Furthermore, analysis using ANOVA

two-factor with replication analysis of the four groups (^{19}F coupled, ^{19}F decoupled, ^{1}H NMR, and UHPLC) revealed no statistically significant differences ($p > 0.05$). However, seven 2017 "Exodus" samples containing 5F-ADB revealed different quantitative results (Table 3). 5 packs of the 7 contained a similar dose of 5F-ADB to the 2016 samples, but samples 5 and 7 contained from 1.5 to more than double the dose of 5F-ADB, with good precision in most of the samples. The presence of such a large quantitative variation in the 2017 samples is alarming, especially as this recently identified SC (5F-ADB) is toxic, being implicated in 10 deaths in Japan,[28,29] and it is comparable to similar analogues which have approximately 220-fold potency of that of THC, e.g. 5F-ADBICA EC$_{50}$ = 0.77 nM compared to THC EC$_{50}$ = 172 nM.[1] The wide deviation and lack of homogeneity of the levels of 5F-ADB both within and between sample packages varied 60 000-fold from 0.8 μg g^{-1} to 49 mg g^{-1}.[20] An easy and robust quantitative analysis of fluorinated SCs is clearly important. This technique has the potential to be applied in the rapid analysis of herbal blends sprayed with fluorinated SCs, gaining in importance with the annual increase
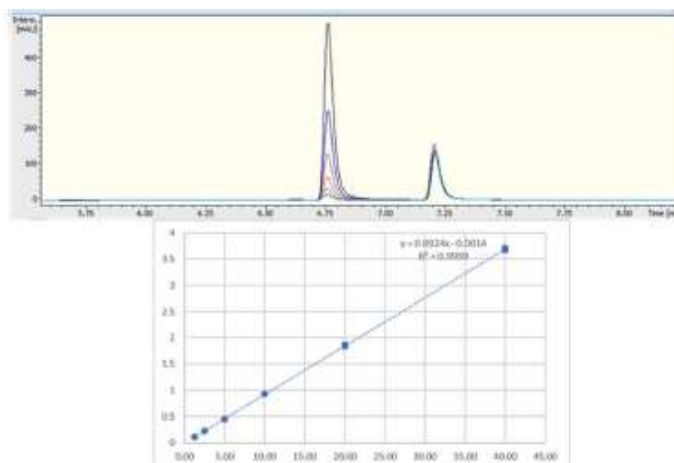

Fig. 4 (Upper) stacked UHPLC chromatogram concentrations from 1.25 to 40.0 μg mL^{-1} (λ = 298 nm) of 5F-ADB (RT = 6.8 min) and 5F-AKB48 IS (RT = 7.2 min); (lower) calibration curve of 5F-ADB against 5F-AKB48 (IS), R^2 = 0.9999.

Table 2 Quantification (mg g^{-1}) of SCs in the plant material of the "Exodus" brand seized in 2016 containing 5F-ADB

| | NMR $n = 3$ | | | | | | UHPLC $n = 4$ | |
Sample	^{1}H	RSD %	^{19}F coupled	RSD %	^{19}F decoupled	RSD %	UHPLC	RSD %
Exodus 9	7.39 ± 0.20	2.74	7.34 ± 0.27	3.73	7.12 ± 0.24	3.36	6.96 ± 0.12	1.67
Exodus 10	8.04 ± 0.43	5.35	7.87 ± 0.37	4.69	7.87 ± 0.47	5.94	7.92 ± 0.38	4.79
Exodus 11	8.24 ± 0.17	2.00	8.01 ± 0.12	1.48	8.05 ± 0.06	0.79	7.87 ± 0.11	1.46
Exodus 12	8.04 ± 0.12	1.49	7.89 ± 0.07	0.88	7.93 ± 0.14	1.81	7.97 ± 0.10	1.20
Exodus 13	7.78 ± 0.02	0.21	7.71 ± 0.04	0.54	7.72 ± 0.05	0.65	8.19 ± 0.07	0.79
Exodus 14	7.65 ± 0.08	1.00	7.61 ± 0.07	0.90	7.66 ± 0.11	1.45	7.91 ± 0.12	1.52
Exodus 15	7.57 ± 0.22	2.93	7.52 ± 0.24	3.14	7.50 ± 0.17	2.26	7.54 ± 0.09	1.17
Exodus 16	7.43 ± 0.18	2.46	7.45 ± 0.21	2.75	7.48 ± 0.24	3.18	7.94 ± 0.14	1.82

287

Sample	NMR $n = 3$						UHPLC $n = 4$	
	^{1}H	RSD %	^{19}F coupled	RSD %	^{19}F decoupled	RSD %	UHPLC	RSD %
Exodus 1	10.48 ± 0.29	2.78	10.65 ± 0.11	1.08	10.68 ± 0.12	1.11	12.44 ± 0.63	5.03
Exodus 2	7.81 ± 0.12	1.51	7.75 ± 0.07	0.92	7.77 ± 0.16	2.09	8.83 ± 0.03	0.34
Exodus 3	9.17 ± 0.13	1.41	9.07 ± 0.19	2.13	9.12 ± 0.23	2.55	11.10 ± 1.29	11.60
Exodus 4	8.69 ± 0.10	1.17	8.66 ± 0.13	1.49	8.60 ± 0.10	1.12	8.35 ± 0.15	1.80
Exodus 5	17.50 ± 0.09	0.53	17.48 ± 0.23	1.31	17.71 ± 0.05	0.26	20.22 ± 0.25	1.23
Exodus 6	8.70 ± 0.08	0.93	8.57 ± 0.09	1.01	8.59 ± 0.11	1.33	8.78 ± 0.07	0.83
Exodus 7	14.35 ± 0.10	0.69	13.88 ± 0.09	0.66	13.45 ± 0.53	3.92	16.08 ± 0.17	1.06

in the occurrence of such fluorinated third-generation SCs seen in 2016–2019.[29–32] This analysis is of importance to users/abusers, health professionals and law enforcement to determine how much SC is in the sample. It also clearly demonstrates how there is no quality control of the "Exodus" preparations.

AM-694 quantified in seized herbal blends

[1-(5-Fluoropentyl)-1H-indol-3-yl](2-iodophenyl)-methanone (AM-694) was isolated from seized herbal blends (3.0 g) branded as "Loco elite". Identification was achieved through 2D NMR spectroscopy and its LC-MS/MS fragmentation pattern. Results were confirmed by comparison with the published literature of the first analytical characterization of illicit AM-694 from seizures.[6] Candidate signals for integration are 3″, 4″, 5″, and 6″ of the 2-iodophenyl substituent, 2′ and 7′ of the indole core, and 1‴ and 5‴ of the fluoropentyl chain. The impact of relaxation delay in ^{19}F NMR was investigated, and it was found that using only a short relaxation delay (<15 s) significantly affected the quantitative results. 15 s and 30 s relaxation delays were sufficient to achieve reproducible quantitative results. Moreover,
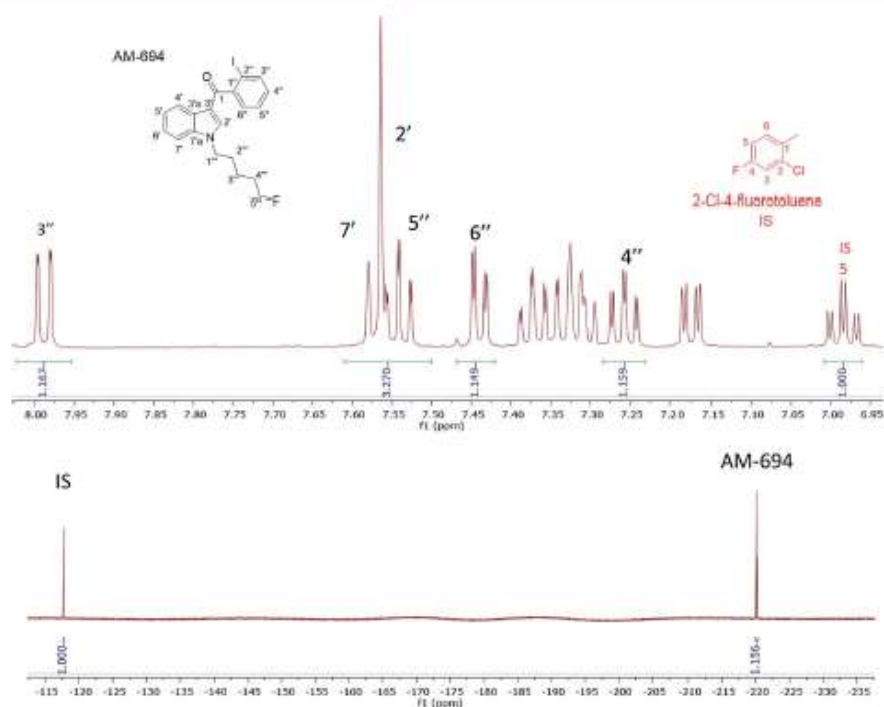

Fig. 5 (Upper) expansion of the ^{1}H NMR aromatic region of AM-694 in CD₃OD showing signals used for quantification where the integration of the 2-chloro-4-fluorotoluene IS H5 signal (td) is normalized (1.00 H); (lower) ^{19}F NMR signals of AM-694 at −220 ppm and the same IS ^{19}F signal at −117 ppm also normalized (1.00 F).
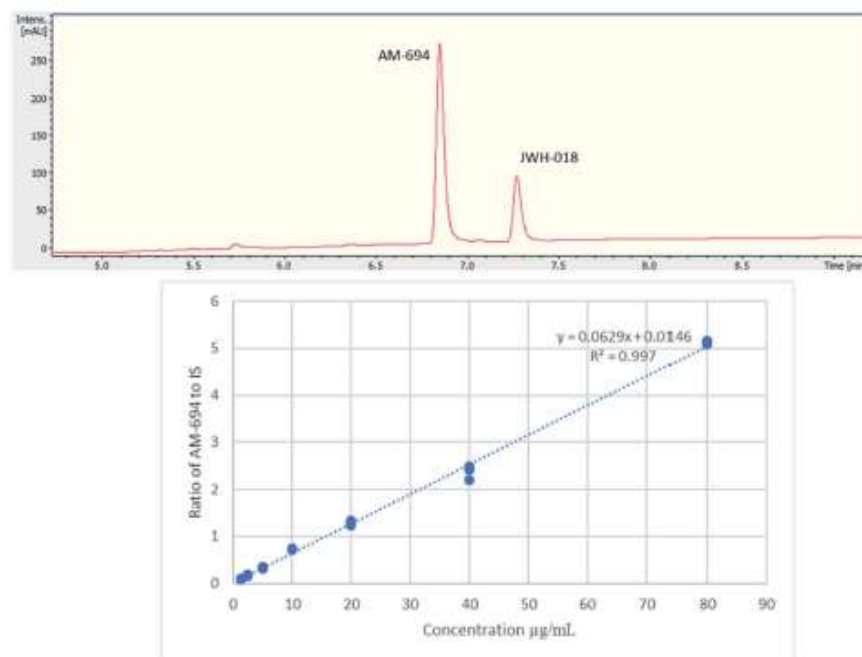
Fig. 6 (Upper) UHPLC chromatogram ($\lambda = 254$ nm) of AM-694 (RT = 6.9 min) and JWH-018 (RT = 7.3 min); (lower) calibration curve of AM-694 against JWH-018 (IS), $R^2 = 0.997$.

Table 4 Quantitative analysis of AM-694 in "Loco elite" herbal blends by ^{1}H and ^{19}F NMR, using maleic acid (MA) or 2-chloro-4-fluorotoluene as the IS, and UHPLC (against JWH-018)

Analysis method (IS)	^{1}H (MA)	^{1}H (2-chloro-4-fluorotoluene)	^{19}F (2-chloro-4-fluorotoluene)	UHPLC (JWH-018)
Sample 1 (mg g^{-1})^a	57.0 ± 2.9	n.d.	n.d.	n.d.
RSD (%)	5.2	—	—	—
Sample 2 (mg g^{-1})^a	37.5 ± 1.1	36.7 ± 2.0	35.4 ± 0.6	38.4 ± 2.6
RSD (%)	3.0	5.4	1.7	6.6

^{a} mg of AM-694 per gram of herbal sample.

such relaxation delays still allowed fast overall sample run-times of 8 and 10 min, respectively. ^{1}H q-NMR and ^{19}F q-NMR showed consistent results when using 2-chloro-4-fluorotoluene as the IS (Fig. 5). Furthermore, cross-method validation was demonstrated using UHPLC with reference standard AM-694, RT = 6.9 min, and JWH-018 (IS), RT = 7.3 min, constructing a seven-point calibration curve between 1.25 and 80.0 µg with R^2 = 0.997 and IS RSD = 4.4% (Fig. 6).

Two samples were quantified, with significant differences ($p < 0.05$) in their AM-694 content. Sample 1 analysis using (only) ^{1}H NMR spectroscopy, with maleic acid as the IS, showed 57.0 ± 2.9 mg g^{-1} of plant material, compared to the value for Sample 2 of 37.5 ± 1.1 mg. The latter ^{1}H NMR quantification of Sample 2 was shown to be consistent when analysed by ^{1}H NMR spectroscopy against both maleic acid and 2-chloro-4-fluorotoluene

as the IS, and by ^{19}F q-NMR, and also in agreement with UHPLC results, showing no significant differences between these methods using Anova two-factor analysis ($p > 0.05$) (Table 4).

In the ^{1}H NMR when using 2-chloro-4-fluorotoluene as the IS, its H6 signal overlapped with 5' of the indole and indazole SC. Nevertheless, other AM-694 signals such as 4″, 6″, and 7' were resolved and used as candidate quantitative signals in CD$_3$OD. 5-Fluoropentyl signals 1‴ and 5‴ were resolved when CDCl$_3$ or CD$_3$CN was used as the NMR solvent, providing further options for q-NMR analysis.

Conclusions

In this study, ^{19}F-NMR spectroscopy has been applied for the first time to seized herbal blends containing fluorinated 3rd

289

generation SCs to provide a fast (~8 min), accurate and robust quantitative analytical method with no background interference from the plant-material matrix. This analytical technique requires almost no method development (beyond the NMR acquisition parameters) compared to chromatographic methods. There is no need to resort to any lengthy chromatographic analysis. 2-Chloro-4-fluorotoluene was used as an IS in ^{19}F q-NMR, resulting in a method with close agreement with ^{1}H q-NMR results using two different ISs, and cross-method validation was performed using UHPLC.

Acquisition parameters such as the centre point of the spectral window and the relaxation delay have to be chosen carefully for accurate and precise outcomes. An inverse-gated decoupling NMR experiment was employed to improve the S/N ratio and to remove any NOE enhancement. That such analytical data are important is underlined by the analysis of packets of the "Exodus" brand containing 5F-ADB which revealed quantitative differences between 2016 and 2017 seizures in the dose of 5F-ADB, with some packets having double the dose compared to others.

Conflicts of interest

There are no conflicts of interest to declare.

Acknowledgements

References

1 S. D. Banister, M. Moir, J. Stuart, R. C. Kevin, K. E. Wood, M. Longworth, S. M. Wilkinson, C. Beinat, A. S. Buchanan, M. Glass, M. Connor, I. S. McGregor and M. Kassiou, Pharmacology of indole and indazole synthetic cannabinoid designer drugs AB-FUBINACA, ADB-FUBINACA, AB-PINACA, ADBPINACA, 5F-AB-PINACA, 5F-ADB-PINACA, ADBICA, and 5F-ADBICA, *ACS Chem. Neurosci.*, 2015, **6**, 1546–1559.

2 S. Tai and W. E. Fantegrossi, Synthetic cannabinoids: Pharmacology, behavioral effects, and abuse potential, *Current Addiction Reports*, 2014, **1**, 129–136.

3 V. Auwärter, S. Dresen, W. Weinmann, M. Muller, M. Putz and N. Ferreiros, 'Spice' and other herbal blends: harmless incense or cannabinoid designer drugs?, *J. Mass Spectrom.*, 2009, **44**, 832–837, DOI: 10.1002/jms.1558.

4 J. W. Huffman, D. Dai, B. R. Martin and D. R. Compton, Design, synthesis, and pharmacology of cannabimimetic indoles, *Bioorg. Med. Chem. Lett.*, 1994, **4**, 563–566.

5 S. D. Banister, J. Stuart, R. C. Kevin, A. Edington, M. Longworth, S. M. Wilkinson, C. Beinat, A. S. Buchanan, D. E. Hibbs, M. Glass, M. Connor, I. S. McGregor and M. Kassiou, Effects of bioisosteric fluorine in synthetic cannabinoid designer drugs JWH-018, AM-2201, UR-144,

XLR-11, PB-22, 5F-PB-22, APICA, and STS-135, *ACS Chem. Neurosci.*, 2015, **6**, 1445–1458.

6 J. I. Nakajima, M. Takahashi, T. Seto, C. Kanai, J. Suzuki, M. Yoshida and T. Hamano, Identification and quantitation of two benzoylindoles AM-694 and (4-methoxyphenyl)(1-pentyl-1*H*-indol-3-yl)methanone, and three cannabimimetic naphthoylindoles JWH-210, JWH-122, and JWH-019 as adulterants in illegal products obtained *via* the internet, *Forensic Toxicol.*, 2011, **29**, 95–110.

7 N. Uchiyama, Y. Shimokawa, R. Kikura-Hanajiri, Y. Demizu, Y. Goda and T. Hakamatsuka, A synthetic cannabinoid FDU-NNEI, two 2*H*-indazole isomers of synthetic cannabinoids AB-CHMINACA and NNEI indazole analog (MN-18), a phenethylamine derivative N-OH-EDMA, and a cathinone derivative dimethoxy-alpha-PHP, newly identified in illegal products, *Forensic Toxicol.*, 2015, **33**, 244–259, DOI: 10.1007/s11419-015-0268-7.

8 H. Chung, H. Choi, S. Heo, K. Eunmi and J. Lee, Synthetic cannabinoids abused in South Korea: drug identifications by the National Forensic Service from 2009 to June 2013, *Forensic Toxicol.*, 2014, **32**, 82–88.

9 A. Makriyannis and H. Deng, University of Connecticut. Cannabimimetic indole derivatives, Patent US6900236B1, 2005, https://patentimages.storage.googleapis.com/9d/ec/b4/ea8af239e287da/US6900236.pdf, accessed 17/04/19.

10 S. M. Wilkinson, S. D. Banister and M. Kassiou, Bioisosteric fluorine in the clandestine design of synthetic cannabinoids, *Aust. J. Chem.*, 2015, **68**, 4–8.

11 A. Zivkovic, J. J. Bandolik, A. J. Skerhut, C. Coesfeld, M. Prascevic, L. Zivkovic and H. Stark, Quantitative analysis of multicomponent mixtures of over-the counter pain killer drugs by low-field NMR spectroscopy, *J. Chem. Educ.*, 2017, **94**, 121–125, DOI: 10.1021/acs.jchemed.6b00105.

12 G. Maniara, K. Rajamoorthi, S. Rajan and G. W. Stockton, Method performance and validation for quantitative analysis by ^{1}H and ^{31}P NMR spectroscopy. Applications to analytical standards and agricultural chemicals, *Anal. Chem.*, 1998, **70**, 4921–4928.

13 U. Holzgrabe, Quantitative NMR spectroscopy in pharmaceutical applications, *Prog. Nucl. Magn. Reson. Spectrosc.*, 2010, **57**, 229–240.

14 P. A. Hays, Proton nuclear magnetic resonance spectroscopy (NMR) methods for determining the purity of reference drug standards and illicit forensic drug seizures, *J. Forensic Sci.*, 2005, **50**, 1342–1360.

15 F. Malz and H. Jancke, Validation of quantitative NMR, *J. Pharm. Biomed. Anal.*, 2005, **38**, 813–823.

16 J. P. Smith, O. B. Sutcliffe and C. E. Banks, An overview of recent developments in the analytical detection of New Psychoactive Substances (NPSs), *Analyst*, 2015, **140**, 4932–4948.

17 A. Frinculescu, C. L. Lyall, J. Ramsey and B. Miserez, Variation in commercial smoking mixtures containing third-generation synthetic cannabinoids, *Drug Test. Anal.*, 2017, **9**, 327–333.

290

Pharmaceutical analysis of seized ethylone–ecstasy mixtures

Husain Naqi, Timothy J. Woodman, Stephen M. Husbands, and Ian S. Blagbrough

Department of Pharmacy and Pharmacology, University of Bath, Bath BA2 7AY, U.K.

Abstract - **Identification and characterization of seized ethylone–ecstasy mixtures follows from 1D/2D nuclear magnetic resonance (NMR) spectroscopy, mass spectrometry, and thin layer chromatography analysis. Maleic acid was used as an NMR internal standard for quantification of the mixtures. Electrospray soft ionization mass spectrometry was used to determine the molecular ions. This is the first analytical report of ethylone–ecstasy mixtures and their quantification.**

INTRODUCTION

3,4-Methylendioxymethamphetamine (ecstasy, E) is a highly popular psychostimulatory, hallucinogenic empathogenic drug which belongs to the phenethylamine class, and exerts its physiological effects through actions on many neurotransmitters, primarily serotonin [1]. Ethylone is β-keto-methylenedioxy-ethylamphetamine. It is a new psychoactive substance (NPS), adding to the hundreds of recent NPS, synthesized as mainstream stimulants e.g. ecstasy, methamphetamine, and cocaine are class A and banned. Ethylone has a pharmacological profile similar to ecstasy and other stimulants [2]. Such mixtures, found in drug samples seized by the Bristol police, might lead to life threatening serotonin (5-HT) toxicity.

MATERIALS AND METHODS

1) Seized samples (20 mg) were dissolved in D_2O (1 mL) and analysed by high-field NMR spectroscopy. ^{1}H, ^{13}C, Distortionless Enhancement by Polarization Transfer (DEPT), and 2D NMR spectra were obtained on a Bruker AVANCE III 500 MHz spectrometer, with data processing using Bruker software (Topspin 2.1).

2) Stock solutions (1 mg/mL in HPLC grade methanol) of the seized samples were prepared. Mass spectra were obtained using electrospray ionization-mass spectrometry (ESI-MS) from Bruker daltonics with positive-ion mode samples (10 µg/mL in HPLC grade methanol).

3) Thin layer chromatography (TLC) was performed on seized samples using TLC silica gel 60 F_{254} plates and a mobile phase of ethyl acetate, methanol, and concentrated ammonia (85:10:5 v/v/v) visualized under UV light and with Dragendorff's reagent.

RESULTS AND DISCUSSION

Complete assignment of the ^{1}H and ^{13}C signals in the mixtures was achieved with the aid of 2D NMR. The ^{1}H NMR data revealed 18 non-coinciding signals for the ethylone–ecstasy mixtures, with molar ratios of 3:1, 2:1, and 1:2. Additionally, the different chemical shifts of the methylenedioxy signals are diagnostic for both drugs in the

mixture, ^{1}H δ 6.03 ppm in ethylone and 5.87 ppm in ecstasy. The splitting patterns of these signals are another distinction. The ethylone methylenedioxy signal appeared as a very fine doublet, while the comparable signal in ecstasy was a sharp singlet. We interpret this difference as an effect of the benzoyl carbonyl functional group in addition to the chiral centre. Maleic acid (alkene ^{1}H signal δ 6.31 ppm) was used as a quantitative internal standard. Initial confirmation of analytes in the mixtures was by TLC showing two resolved spots. The ESI-MS revealed both required molecular ions, *m/z* 194.1184 found for ecstasy and 222.1122 for ethylone.
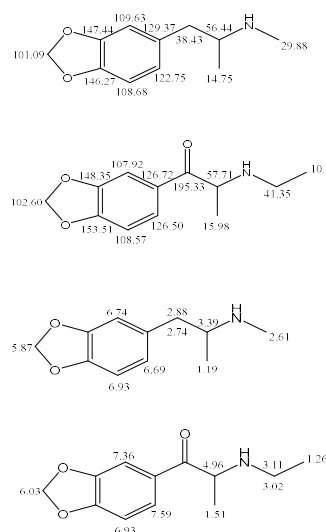

Fig. 1. ^{13}C (above) and ^{1}H (below) assignments of ecstasy (upper) and ethylone (lower) (recorded in D_2O).

CONCLUSIONS

NMR is a powerful tool for the identification of illicit drug mixtures including their quantification against an internal standard (e.g. maleic acid). The methylenedioxy NMR signals are diagnostic for the analysis of these 3:1, 2:1, and 1:2 (molar ratio) mixtures - not previously reported.

ACKNOWLEDGEMENTS

REFERENCES

[1] J.P. Capela *et al*., Molecular and cellular mechanisms of ecstasy-induced neurotoxicity: An overview *Mol. Neurobiol.*, **39** (2009) 210-271.

Carbamate derivatization studies of MDMA, ethylone, and mephedrone

Husain Naqi, Stephen M. Husbands, and Ian S. Blagbrough

Department of Pharmacy and Pharmacology, University of Bath, Bath BA2 7AY, U.K.

Abstract - **Derivatization studies using ethyl chloroformate (ECF) and 2,2,2-trichloroethyl chloroformate (TCF) showed that derivatization is essential for the chromatographic detection of MDMA (ecstasy) and ethylone, changing the polarity and making them more suitable for gas chromatography-flame ionization detection (GC-FID) analysis. However, mephedrone gave sufficiently clean chromatography without any sample derivatization. Both these carbamate derivatizing agents afford reproducible data from consecutive GC injections with enhanced chromatographic properties e.g. increased peak intensity, and non-tailing, sharp peaks.**

INTRODUCTION

The amphetamine analogue 3,4-methylenedioxy-methamphetamine (MDMA, ecstasy, E) is an illicit psychedelic psychostimulant, producing euphoric effects, but with no current medical uses [1]. The term ecstasy began with reference to MDMA, but nowadays it also includes amphetamine derivatives such as 3,4-methylendioxyamphetamine (MDA) and 3,4-methylenedioxy-ethylamphetamine, due to the similar physiological effects induced by this class of illicit drugs. Mephedrone, also known as 4-methyl-methcathinone, is another illicit drug but unlike MDMA and despite the structural similarity of these phenylethylamines, mephedrone is classified as a synthetic cathinone rather than an amphetamine derivative. Another emerging amphetamine derivative is ethylone, also known as MDEC or bk (β-ketone) MDEA. It is important to be able to separate these amphetamine derivatives in pharmaceutical and forensic analysis. To achieve enhanced chromatographic profiles, derivatization is often a routine, but essential step. To produce carbamate derivatives of these amphetamine-like phenylethylamines, two different but related chloroformates have been investigated: ethyl chloroformate (ECF) and 2,2,2-trichloroethyl chloroformate (TCF).

MATERIALS AND METHODS

ECF or TCF (30 μL in ethyl acetate 70 μL) was gently shaken to dissolve the reagent [2]. Aliquots (50 μL) of the solutions were then added to methanolic solutions of the drug samples and heated for 15 min at 80 °C allowing them to concentrate. The residues were dried under a gentle stream of nitrogen followed by redissolving in ethyl acetate (50 μL). Solutions of the derivatized samples (1-1.5 μL of the ethyl acetate) were injected into the GC-FID (CP-9003 Chrompack, Middelburg, Holland) equipped with a ZB-WAX capillary column (polyethylene glycol, 9 m × 0.25 mm × 0.25 μm, Phenomenex), using He carrier gas at a flow rate of 23-27 mL/s. The injector was set at 250 ˚C; different isocratic (e.g. 180 ˚C or 230 ˚C) and gradient (e.g. 180-250 ˚C at 10 ˚C/min) oven temperature programmes were used.

RESULTS AND DISCUSSION

The GC-FID analysis of non-derivatized MDMA yielded only poor chromatography with inconsistent, small broad peaks. Derivatization of MDMA with ECF resulted in better chromatography, with improved peak shape and signal intensity at an isocratic temperature of 230 °C with a typical retention time of 5.08 min.

Ethylone is not detected without derivatization; its chromatography is therefore similar to that of MDMA. Chromatography of the TCF derivative, at an isocratic temperature of 250 °C, resulted in a consistent average retention time of 8.92 min.

The non-derivatized mephedrone gave good GC chromatograms isocratically at 180 ˚C with a retention time of 5.06 min. Derivatization with ECF resulted in a longer retention time of 9.73 min (at 180 ˚C). At a higher temperature, 230 ˚C, the average retention time was both stable and reproducible at 4.08 min. Indeed, these mild reagents, ECF and TCF allowed rapid and efficient switching between the different analytical conditions [3].

CONCLUSIONS

Derivatization is an essential step in the identification of illicit drugs samples. ECF and TCF are reliable derivatizing agents for pharmaceutical analysis that are used for production of more volatile carbamate derivatives with enhanced chromatographic properties. The optimum operating GC-FID oven temperature range for these derivatized samples is between 200-250 °C. Ethylone is similar to ecstasy in the fact that it requires derivatization in order to be detected by GC-FID, while mephedrone was detected without derivatization. Nevertheless, derivatization of mephedrone with TCF produced better chromatography.

ACKNOWLEDGEMENTS

REFERENCES

[1] H.P. Rang, M.M. Dale, J.M. Ritter, R.J. Flower and G. Henderson, CNS stimulants and psychotomimetic drugs in *Rang and Dale's Pharmacology,* London, Elsevier Churchill Livingstone, 2012, ch. 47, pp. 590-591.

[2] G. Frison, L. Tedeschi, D. Favretto, A. Reheman and S.D. Ferrara, Gas chromatography/mass spectrometry determination of amphetamine-related drugs and ephedrines in plasma, urine and hair samples after derivatization with 2,2,2-trichloroethyl chloroformate *Rapid Commun. Mass Spectrom*., **19** (2005) 919-927.

[3] G. Frison *et al*., Gas chromatography/mass spectrometry determination of mephedrone in drug seizures after derivatization with 2,2,2-

Pharmaceutical analysis of seized ethylone–ecstasy mixtures using quantitative NMR spectroscopy and ESI-MS

Husain A. Naqi, Timothy J. Woodman, Stephen M. Husbands, and Ian S. Blagbrough
Department of Pharmacy and Pharmacology, University of Bath, Bath BA2 7AY, UK

Ethylone-ecstasy (MDMA) mixtures were obtained from different Bristol night clubs following Police seizures. NMR spectroscopic analysis allowed identification, structural elucidation, and quantification of these mixtures. Additional confirmation of the structures came from Electrospray Ionization Mass Spectrometry (ESI-MS). Quantitative NMR analysis, using maleic acid as the internal standard, revealed different ratios of the mixtures, e.g. 2:1, 1:2, and 1:3 ethylone:ecstasy.

The different chemical shifts of the methylenedioxy signals are diagnostic for both drugs in the mixture, ^{1}H δ 6.03 ppm in ethylone and 5.87 ppm in ecstasy. The fine splitting patterns of these methylenedioxy signals are another distinction. The ethylone methylenedioxy signal appeared as a very fine doublet, while the comparable signal in ecstasy was a sharp singlet. Maleic acid was used as a quantitative internal standard due to its high solubility and the non-overlapping peak at δ 6.30 ppm. In these mixtures, the majority of the NMR signals of ethylone and ecstasy are suitable candidates for quantification due to the absence of any peak overlap. The ESI-MS revealed both required molecular ions, *m/z* 194.1184 found for ecstasy and 222.1122 found for ethylone. Fragmentation of both [M+H]$^+$ provided further corroboration of the components in the mixture.

Such combinations of illicit drugs, e.g ecstasy with a Novel Psychoactive Substance (NPS), e.g. ethylone, might be aimed at altering the experience for the user. However, the presence of another pharmacologically active substance might result in serious harm, even lethality, especially as the biological activities of NPS are not well understood.

Analysis of multicomponent NPS/illicit drug mixtures

Husain A. Naqi, Stephen M. Husbands, and Ian S. Blagbrough

Department of Pharmacy and Pharmacology, University of Bath, Bath BA2 7AY, U.K.

Abstract – **Multicomponent mixtures of Novel Psychoactive Substances (NPS) and illicit drugs obtained from Bristol night clubs were characterized using NMR Spectroscopy and UPLC/MS with MS/MS to identify NPS with identical [M+H]$^+$, e.g. ethylphenidate and methoxtamine (MXE). The results prove that drug users/abusers cannot be certain of what they are taking.**

INTRODUCTION

Analytical techniques employed to identify mixtures of illicit drugs and Novel Psychoactive Substances (NPS), are mainly based on mass spectrometry (MS) [1]. Recent reports show that different NPSs are being mixed together, e.g. 4-MEC with pentedrone, *N,N*-diallyl-5-methoxytryptamine (5-MeO-Dalt) with ethylphenidate [2]. Our analysis revealed even more complex mixtures with 3-5 components of illicit drugs, NPS, and cutting agents. Additionally, such mixtures could prove challenging for routine analysis using Fourier Transform Infrared spectroscopy (FTIR) and MS, due to the absence of reference standards for new NPS and also poor ionization of some common cutting agents, e.g. creatine.

MATERIALS AND METHODS

Seized samples (10-20 mg) were dissolved and sonicated for 20 min in D_2O or $CDCl_3$ (1 mL) referenced to TSP-d4 or TMS. DEPT and TOCSY-HSQC spectra were obtained on a Bruker AVANCE III 500 MHz NMR spectrometer, with data processing using MNOVA 11.0 software. Stock solutions (1 mg/mL in HPLC grade methanol) of the seized samples were used for QTOF-UPLC/MS analysis using a MaXis HD Quadrupole electrospray Time-of-Flight (ESI-QTOF) mass spectrometer (Bruker Daltonik GmbH, Bremen, Germany), operated in ESI positive mode. For LC/MS/MS the collision energy was 15.0-16.0 eV.

RESULTS AND DISCUSSION

Identification of a complex 5-component mixture of ketamine 57%, dimethyl sulfone (MSM) 33%, creatine 7%, methoxtamine (MXE) 2%, 1% methoxphenidine (MXP) was achieved primarily by 2D NMR, e.g. COSY, HMBC. Additionally, TOCSY-HSQC proved valuable for the identification of complex mixtures with many overlapping signals. Furthermore, creatine had poor ionization in the loop injection method in the ESI-MS, but was detected by LC/MS, while the adulterant MSM, sold in health shops as a dietary supplement, could not be detected by LC/MS.

Another, mixture of 3 NPS was analysed. It was composed of methiopropamine, ethylphenidate and 5-MeO-Dalt, 40%, 39%, and 21% respectively. The two NPS ethylphenidate and MXE are formula isomers ($C_{15}H_{21}NO_2$).

They were easily distinguished by MS/MS on the basis of their individual fragmentation patterns (Fig. 1).
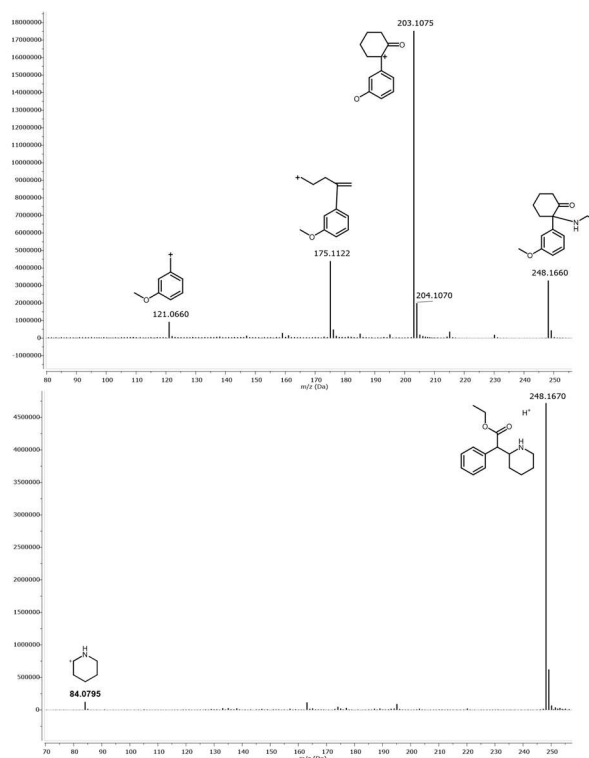

Fig. 1. MS/MS fragmentation of MXE (upper) and ethylphenidate (lower).

CONCLUSIONS

Complex 3- and 5-component mixtures of NPS/illicit drug/cutting agents have been analysed unambiguously. We have employed a range of 2D NMR experiments for the analysis of complex mixtures including TOCSY-HSQC. We also used LC/MS/MS to differentiate between the $C_{15}H_{21}NO_2$ formula isomers ethylphenidate and MXE.
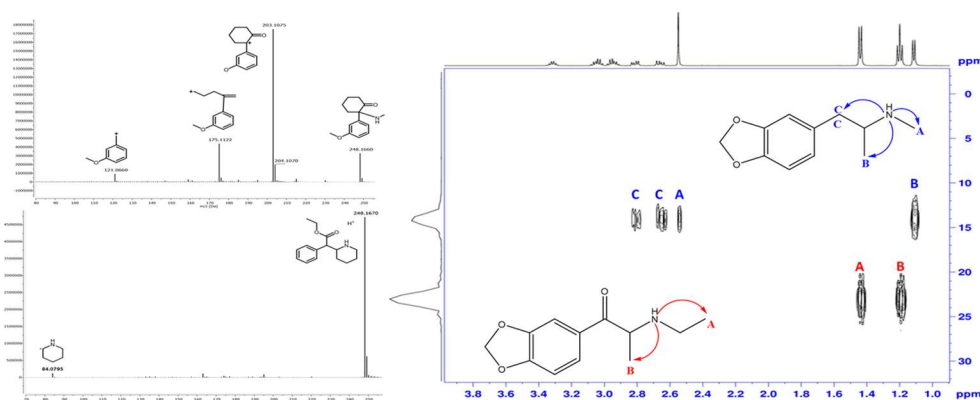
ACKNOWLEDGEMENTS

REFERENCES

[1] J. P. Smith, O. B. Sutcliffe and C. E. Banks, An overview of recent developments in the analytical detection of new psychoactive substances, *Analyst*, **140** (2015) 4932–4948.

Analysis of multicomponent NPS/illicit drug mixtures

Husain A. Naqi, Stephen M. Husbands, and Ian S. Blagbrough

Department of Pharmacy and Pharmacology, University of Bath, Bath BA2 7AY, UK
E-mail: prsisb@bath.ac.uk

Current analytical techniques employed to identify mixtures of illicit drugs and Novel Psychoactive Substances (NPS) are mainly based on mass spectrometry (MS).[1] Recent reports show that different NPS are being mixed together, e.g. 4-MEC with pentedrone, *N,N*-diallyl-5-methoxytryptamine (5-MeO-Dalt) with ethylphenidate.[2,3] Our analysis revealed even more complex mixtures with 3- and 5-components of illicit drugs, NPS, and cutting agents. Identification of a complex 5-component mixture of ketamine 57%, dimethyl sulfone (MSM) 33%, creatine 7%, methoxetamine (MXE) 2%, and methoxphenidine (MXP) 1% was achieved primarily by 2D NMR, e.g. COSY, TOCSY-HSQC, HMBC. Furthermore, creatine has poor ionization in the loop injection method in ESI-MS, but was detected by LC/MS, while the adulterant MSM, sold in health shops as a dietary supplement, could not be detected by LC/MS. The two NPS ethylphenidate and MXE are formula isomers ($C_{15}H_{21}NO_2$). They were easily distinguished by MS/MS on the basis of their individual fragmentation patterns (Fig. 1). Ecstasy (MDMA) was frequently found mixed with the NPS ethylone. Characterization of this mixture was also achieved using 2D NMR spectroscopy including ^{15}N-HMBC (Fig. 1). Complex 3- and 5-component mixtures of NPS/illicit drug/cutting agents have been analysed unambiguously using 2D NMR and LC/MS/MS.

Figure 1. LC/MS/MS fragmentation pathway of MXE and ethylphenidate (left), ^{15}N-HMBC of ethylone and ecstasy mixture (right).

References

1. Smith, J. P.; Sutcliffe, O. B.; Banks, C. E. *Analyst* **2015**, *140*, 4932-4948.
2. Odoradi, S.; Romolo, F. S.; Rossi, S. S. *Forensic Sci. Int.* **2016**, *265*, 116-120.
3. Alotaibi, M. R.; Husbands, S. M.; Blagbrough, I. S. *J. Pharm. Biomed. Anal.* **2015**, *107*, 535-538.

Pharmaceutical analysis of seized ethylone–ecstasy mixtures

Husain A. Naqi, Timothy J. Woodman, Stephen M. Husbands, and Ian S. Blagbrough*
Department of Pharmacy and Pharmacology, University of Bath, Bath BA2 7AY, UK

Purpose
3,4-Methylendioxymethamphetamine (ecstasy, E) is a highly popular psychostimulatory, hallucinogenic empathogenic drug which belongs to the phenethylamine class, and exerts its physiological effects through actions on many neurotransmitters, primarily serotonin (5-HT). Ethylone is β-keto-methylenedioxy-ethylamphetamine with a pharmacological profile similar to ecstasy and other stimulants [1]. Ethylone is a new psychoactive substance (NPS), adding to the hundreds of recent NPS, synthesized as mainstream stimulants. Mixtures of such NPS are found in drug samples seized by the Bristol police; they may well lead to life threatening serotonin toxicity. We aim to identify and characterize seized ethylone–ecstasy mixtures by 1D/2D nuclear magnetic resonance (NMR) spectroscopy and mass spectrometry, using maleic acid as an NMR internal standard for quantification of the mixtures.

Method
Seized samples (20 mg) were dissolved in D_2O (1 mL) and analysed by high-field NMR spectroscopy. ^1H, ^{13}C, Distortionless Enhancement by Polarization Transfer (DEPT), and 2D NMR spectra were obtained on a Bruker AVANCE III 500 MHz spectrometer, with data processing using Bruker software (Topspin 2.1). Mass spectra were obtained using electrospray ionization-mass spectrometry (ESI-MS) from Bruker daltonics with positive-ion mode samples (10 µg/mL in HPLC grade methanol). Maleic acid (alkene ^1H signal δ 6.31 ppm) was used as a quantitative internal standard.

Results
Complete assignment of the ^1H and ^{13}C NMR signals in the mixtures was achieved with the aid of 2D NMR. From three independent samples, the ^1H NMR data revealed 18 non-coinciding signals for the ethylone–ecstasy mixtures, with molar ratios of 3:1, 2:1, and 1:2 respectively, following the ^1H NMR integration. Additionally, the different chemical shifts of the methylenedioxy signals are diagnostic for both the drugs in the mixture, ^1H δ 6.03 ppm in ethylone and 5.87 ppm in ecstasy. The splitting patterns of these signals are another distinction. The ethylone methylenedioxy signal appeared as a very fine doublet, while the comparable signal in ecstasy is a sharp singlet. We interpret this difference as an effect of the benzoyl carbonyl functional group in addition to the chiral centre. ESI-MS revealed both molecular ions, found *m/z* 194.1184 for ecstasy, requires 194.1175 for $C_{11}H_{16}NO_2$ [M+H]$^+$, and *m/z* 222.1122 for ethylone, requires 222.1123 for $C_{12}H_{16}NO_3$ [M+H]$^+$ both within 5 ppm mass accuracy limits.

Conclusion
NMR is a powerful tool for the identification of illicit drug mixtures including their quantification against an internal standard, e.g. maleic acid. The methylenedioxy NMR signals, *inter alia*, are diagnostic for the pharmaceutical analysis of these three 3:1, 2:1, and 1:2 (molar ratio) mixtures.

Reference: 1. D. Lee, C.W. Chronister, J. Hoyer and B.A. Goldberger, *J. Anal. Toxicol.*, 2015, *39*, 567-571.
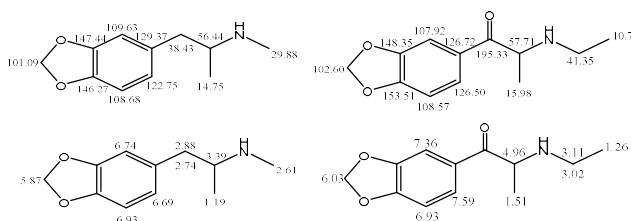
Figure 1. ^{13}C (above) and ^1H (below) assignments of ecstasy (left) and ethylone (right) (D_2O).

Analysis of Multicomponent NPS/Illicit Drug Mixtures

Husain A. Naqi, Stephen M. Husbands, and Ian S. Blagbrough*
Department of Pharmacy and Pharmacology, University of Bath, Bath BA2 7AY, UK

Purpose

Typical pharmaceutical analytical techniques employed to identify mixtures of illicit drugs and Novel Psychoactive Substances (NPS) are mainly based on mass spectrometry (MS). Recent analysis shows that different NPS are being mixed together, e.g. *N,N*-diallyl-5-methoxytryptamine (5-MeO-Dalt) with ethylphenidate, 4-MEC with pentedrone. Complex multicomponent mixtures of NPS and illicit drugs obtained from different Bristol night clubs were characterized using NMR spectroscopy and UPLC/MS, and also analysed with MS/MS to identify unambiguously NPS with identical [M+H]$^+$, e.g. ethylphenidate and methoxetamine (MXE).

Method

Seized samples (10-20 mg) were dissolved and sonicated for 20 min in D_2O or $CDCl_3$ (1 mL) referenced to TSP-d4 or TMS. DEPT and TOCSY-HSQC spectra were obtained on a Bruker AVANCE III 500 MHz NMR spectrometer, with data processing using MNOVA 11.0 software. Stock solutions (1 μg/mL in HPLC grade methanol) of the seized samples were used for QTOF-UPLC/MS analysis using a MaXis HD Quadrupole Electrospray Time-of-Flight (ESI-QTOF) MS (Bruker Daltonik GmbH, Bremen, Germany), in positive-ion mode. For LC/MS/MS, the collision energy was 15.0-18.0 eV.

Results

A mixture of 3 NPS was analysed and shown to be composed of methiopropamine, ethylphenidate, and 5-MeO-Dalt, 40%, 39%, and 21% (molar ratios) respectively. Identification of a complex 5-component mixture of ketamine 57%, dimethyl sulfone (MSM) 33%, creatine 7%, methoxetamine (MXE) 2%, and methoxphenidine (MXP) 1% was achieved primarily by 2D NMR, e.g. COSY, HMBC. TOCSY-HSQC proved valuable for the identification of complex mixtures with many overlapping signals. Furthermore, creatine had poor ionization in the loop injection method in ESI-MS, but was detected by LC/MS, while the adulterant MSM, sold in health shops as a dietary supplement, could not be detected by LC/MS. The two NPS ethylphenidate and MXE are formula isomers ($C_{15}H_{21}NO_2$). They were easily distinguished by MS/MS on the basis of their unique fragmentation patterns (Fig. 1).

Conclusion

Complex 3- and 5-component mixtures of NPS/illicit drug/cutting agents have been analysed unambiguously. We have employed a range of 2D NMR experiments for the analysis of complex mixtures including TOCSY-HSQC. We also used LC/MS/MS to differentiate between the $C_{15}H_{21}NO_2$ formula isomers ethylphenidate and MXE. These results prove that drug users/abusers cannot be certain of what they are taking.

Figure 1. MS/MS fragmentation of MXE (left) and ethylphenidate (right).

Carbamate derivatization studies of MDMA, ethylone, and mephedrone

Husain Naqi, Stephen M. Husbands, and Ian S. Blagbrough*
Department of Pharmacy and Pharmacology, University of Bath, Bath BA2 7AY, U.K.

Purpose: The amphetamine analogue 3,4-methylenedioxy-methamphetamine (MDMA, ecstasy, E) is an illicit psychedelic psychostimulant, producing euphoric effects, but with no current medical uses [1]. The term ecstasy began with reference to MDMA, but nowadays it also includes amphetamine derivatives such as 3,4-methylendioxyamphet-amine (MDA) and 3,4-methylenedioxy-ethylamphetamine, due to the similar physiological effects induced by this class of illicit drugs. Mephedrone, also known as 4-methyl-methcathinone, is another illicit drug but unlike MDMA and despite the structural similarity of these phenylethylamines, mephedrone is classified as a synthetic cathinone rather than an amphetamine derivative. Another emerging amphetamine derivative is ethylone, also known as MDEC or bk (β-ketone) MDEA. It is important to be able to separate these amphetamine derivatives in pharmaceutical and forensic analysis. To achieve enhanced chromatographic profiles, derivatization is often a routine, but essential step. To produce carbamate derivatives of these amphetamine-like phenylethylamines, two different but related chloroformates have been investigated: ethyl chloroformate (ECF) and 2,2,2-trichloroethyl chloroformate (TCF). Derivatization studies using ethyl chloro-formate (ECF) and 2,2,2-trichloroethyl chloroformate (TCF) showed that derivatization is essential for the chromatographic detection of MDMA (ecstasy) and ethylone, changing the polarity and making them more suitable for gas chromatography-flame ionization detection (GC-FID) analysis. However, mephedrone gave sufficiently clean chromatography without any sample derivatization. Both these carbamate derivatizing agents afford reproducible data from consecutive GC injections with enhanced chromatographic properties e.g. increased peak intensity, and non-tailing, sharp peaks.

Method: ECF or TCF (30 µL in ethyl acetate 70 µL) was gently shaken to dissolve the reagent [2]. Aliquots (50 µL) of the solutions were then added to methanolic solutions of the drug samples and heated for 15 min at 80 °C allowing them to concentrate. The residues were dried under a gentle stream of nitrogen followed by re-dissolving in ethyl acetate (50 µL). Solutions of the derivatized samples (1-1.5 µL of the ethyl acetate) were injected into the GC-FID (CP-9003 Chrompack, Middelburg, Holland) equipped with a ZB-WAX capillary column (polyethylene glycol, 9 m × 0.25 mm × 0.25 µm, Phenomenex), using He carrier gas at a flow rate of 23-27 mL/s. The injector was set at 250 °C; different isocratic (e.g. 180 °C or 230 °C) and gradient (e.g. 180-250 °C at 10 °C/min) oven temperature programmes were used.

Results: The GC-FID analysis of non-derivatized MDMA yielded only poor chromatography with inconsistent, small broad peaks. Derivatization of MDMA with ECF resulted in better chromatography, with improved peak shape and signal intensity at an isocratic temperature of 230 °C with a typical retention time of 5.08 min. Ethylone is not detected without derivatization; its chromatography is therefore similar to that of MDMA. Chromatography of the TCF derivative, at an isocratic temperature of 250 °C, resulted in a consistent average retention time of 8.92 min. The non-derivatized mephedrone gave good GC chromatograms isocratically at 180 °C with a retention time of 5.06 min. Derivatization with ECF resulted in a longer retention time of 9.73 min (at 180 °C). At a higher temperature, 230 °C, the average retention time was both stable and reproducible at 4.08 min. Indeed, these mild reagents, ECF and TCF allowed rapid and efficient switching between the different analytical conditions [3].

Conclusion: Derivatization is an essential step in the identification of illicit drugs samples. ECF and TCF are reliable derivatizing agents for pharmaceutical analysis that are used for production of more volatile carbamate derivatives with enhanced chromatographic properties. The optimum operating GC-FID oven temperature range for these derivatized samples is between 200-250 °C. Ethylone is similar to ecstasy in the fact that it requires derivatization in order to be detected by GC-FID, while mephedrone was detected without derivatization. Nevertheless, derivatization of mephedrone with TCF produced better chromatography.

Reference

1. H.P. Rang, M.M. Dale, J.M. Ritter, R.J. Flower and G. Henderson, CNS stimulants and psychotomimetic drugs in Rang and Dale's Pharmacology, London, Elsevier Churchill Livingstone, 2012, ch. 47, pp. 590-591.
2. G. Frison, L. Tedeschi, D. Favretto, A. Reheman and S.D. Ferrara, Gas chromatography/mass spectrometry determination of amphetamine-related drugs and ephedrines in plasma, urine and hair samples after derivatization with 2,2,2-trichloroethyl chloroformate *Rapid Commun. Mass Spectrom*., **19** (2005) 919-927.
3. G. Frison *et al*., Gas chromatography/mass spectrometry determination of mephedrone in drug seizures after derivatization with 2,2,2-trichloroethyl chloroformate *Rapid Commun. Mass Spectrom*., **25** (2011) 387-390.

A validated ^{19}F NMR technique to assay quantitatively fluorinated synthetic cannabinoids agonists

Husain A. Naqi, Timothy J. Woodman, Stephen M. Husbands, Ian S. Blagbrough[*]

Department of Pharmacy and Pharmacology, University of Bath, Bath BA2 7AY, UK.

Purpose

Synthetic Cannabinoid Agonists (SCA), also known by their street name Spice, are potent binders to the CB1 and CB2 receptors, producing psychoactive effects in most cases more potent than the drugs they are trying to mimic. The first generation of SCA were based on medicinal chemistry compounds intended to exploit the pathological implication of the CB receptors in many diseases, but side-tracked into the illicit clandestine design drug market. Fluorinated SCAs are increasingly prevalent, such that in 2013 ~ 90% of seized SCAs were fluorinated in at least one position. The work aims to develop a fast and accurate quantitative analysis method for fluorinated SCA e.g. (5F-ADB, AM-694) in seized samples with cross method validation.

Method

Deuterated solvents were purchased from Cambridge Isotopes Laboratories (UK, Goss Scientific), NMR internal standards 2-chloro-4-fluorotoluene, dimethyl sulfone (DMS), and maleic acid (MA) are TraceCERT purchased from Sigma-Aldrich (UK). 5F-ADB, AM-694, and JWH-018 were purchased from LGC (Teddington, UK). ^{19}F q-NMR pulse sequence: SW of 241 ppm, (O1P) -160 ppm, 6k data points, AQ 0.7s, 16 scans, D1 30s, 90° pulse angle on Bruker AVANCE III 500 MHz spectrometer. UHPLC analyses on a Dionex Ultimate 3000 UHPLC, an Acquity UPLC BEH C18, 1.7 µM, 2.1 x 50 mm RP-column.

Results

5F-ADB ^{19}F-q-NMR analysis using coupled and decoupled inverse-gated methods resulted in agreement with ^{1}H NMR using maleic acid as internal standard. Uniform excitation across the spectrum is essential to ensure that all signals receive the same magnetization in the pulse sequence, thus making the centre point of the spectra (O1P) a critical parameter when quantitative results are required. AM-694 ^{19}F-q-NMR analysis was validated using UHPLC.

Conclusions

Fluorine (^{19}F) NMR spectroscopy has been applied for the first time to seized herbal blends containing fluorinated SCA to provide a fast (~ 8 min), accurate and robust quantitative analytical method with no background interference from the (plant material) matrix component. The analytical technique requires almost no method development (beyond the NMR acquisition parameters) compared to chromatographic methods. 2-Chloro-4-fluorotoluene was used as an IS in ^{19}F q-NMR, resulting in a method with close agreement to ^{1}H q-NMR results using two different IS and cross method validation using UHPLC. We thank the Government of Kuwait for a scholarship (to HAN) and DEAT, the Avon and Somerset Constabulary, for the seized samples.
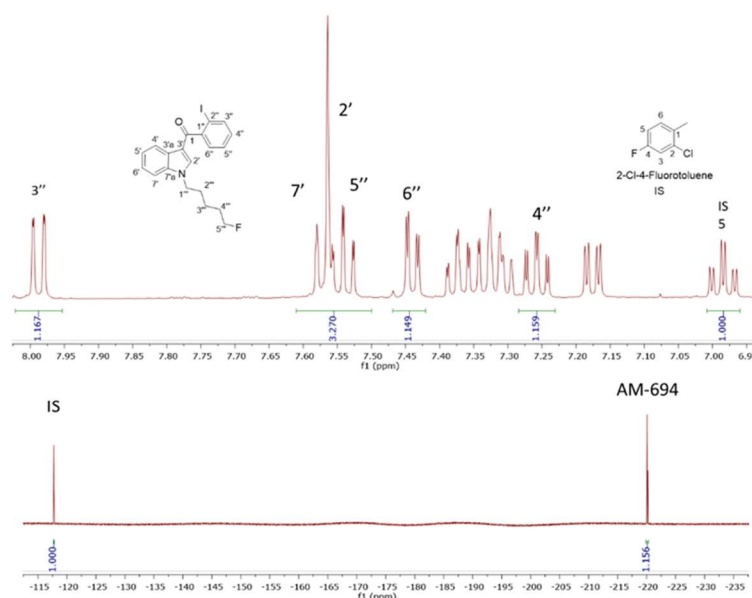

Fig. 1 Expansion of ^{1}H NMR aromatic region showing signals used for quantification where the area of the 2-chloro-4-fluorotoluene IS H5 signal is normalized (1.00 H) (upper); ^{19}F NMR signals of 5-F-ADB at -220 and the same IS ^{19}F signal at -117 also normalized (1.00 F) (lower)

Characterization and quantification of six Synthetic Cannabinoid Agonists (SCA) using NMR and UHPLC-QTOF/MS/MS

Husain A. Naqi, Stephen M. Husbands, and Ian S. Blagbrough[*]

Department of Pharmacy and Pharmacology, University of Bath, Bath BA2 7AY, UK.

Purpose

Synthetic Cannabinoid Agonists (SCA) (Spice) are the most popular class of Novel Psychoactive Substances (NPS) by seizures. They bind with high potency to the CB1 receptor, thus inducing psychoactive effects. They are responsible for many fatalities and severe intoxications. Their analysis is complicated by many factors: many analytes in the sample, present only in sub-milligram amounts, matrix components.

Method

All extraction solvents (methanol, chloroform, and acetonitrile) 99.9% anhydrous, was purchased from Fisher Scientific ACROS Organics, deuterated solvent ($CDCl_3$) was purchased from Cambridge Isotopes Laboratories (UK, Goss Scientific). Herbal blend samples were provided by the Avon and Somerset Constabulary, from recent seizures. The samples were in the form of herbal blends (1.0 g) as commercially packaged brands (K2 black edition). Samples were weighed using a SE2F Sartorius analytical balance. Herbal blends were extracted twice with methanol (2 x 30.0 mL) with sonication (30 min), centrifugation, removal of supernatant extract, the pellet (plant material) was discarded. Then the extract was evaporated to dryness under reduced pressure and reconstituted in deuterated solvent (1.0 mL). NMR spectra were recorded on Bruker AVANCE III 500 MHz spectrometer, ^{1}H, ^{13}C, and ^{19}F frequencies are 500.130, 125.758, and 470.592 respectively. The QTOF-UHPLC-MS analysis was conducted using a MaXis HD Quadrupole electrospray Time-of-Flight (ESI-QTOF) mass spectrometer (Bruker Daltonik GmbH, Bremen, Germany), operated in both ESI positive.

Results

Using UHPLC/TOF/MS/MS six base-line resolved peaks were achieved, five of them are SCA and one is a possible reaction precursor (PX1 acid) for the synthesis of PX1 amide (Figure 1). All $[M+H]^{+}$ are within 5 ppm of mass accuracy limits and have distinctive fragmentation patterns in MS/MS. 1D/2D NMR of the crude extracts resulted in complex spectra. Nevertheless, signals for integration in ^{1}H NMR were identified for each SCA compound, and employed to calculate the molar ratio of each SCA in the herbal blend: 5F-PB-22 6%, MDMB-CHMICA 7%, 5F-AKB-48 9%, PX1 11%, 5F-ADB 23%, and propylene glycol 44%.

Conclusions

We have determined an analytical platform for the separation and characterization of closely related SCA from a seized herbal blend sample containing: PX1, 5-F-PB-22, 5-F-ADB, MDMB-CHMICA, and 5-F-AKB-48 using LC-TOF, LC/MS/MS, 2D NMR, and flash column chromatography. LC/MS/MS allowed the identification of a possible reaction precursor, PX1 acid, not previously reported. This approach will provide drug analysts with methods to tackle complex mixtures of SCA in herbal matrix, health services responders with an idea of the type of mixtures with potent CB1 activities. We thank the Government of Kuwait for a scholarship (to HAN) and DEAT, the Avon and Somerset Constabulary, for the seized samples.
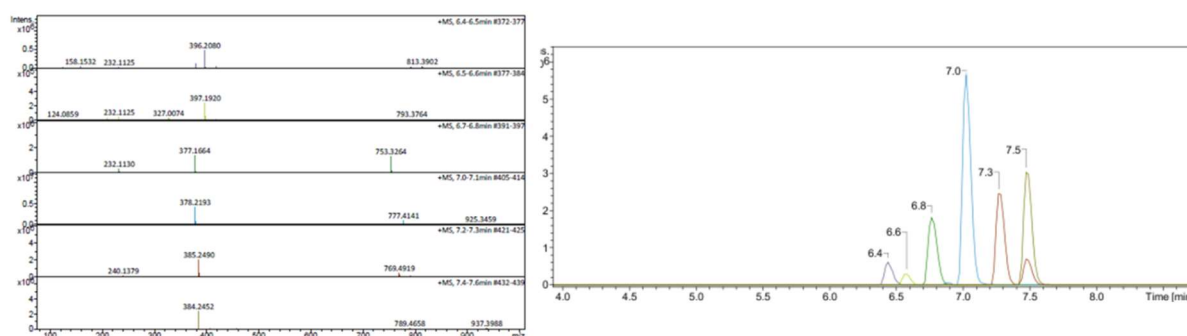

Fig. 1 Extracted ion chromatogram and ESI-QTOF of SCA mixture in K2 product.

Appendix 4. Geoffrey Phillips JPAG Prize